

GEOCHEMISTRY, MINERALOGY AND HYDROGEOCHEMISTRY

OF THE AMBASSADOR MULTI-ELEMENT LIGNITE DEPOSIT, WESTERN AUSTRALIA

G. B. DOUGLAS, D. J. GRAY AND C. R. M. BUTT, MARCH, 1993

WITH ADDITIONAL INVESTIGATIONS ON THE CHARACTERIZATION OF ORGANIC MATTER

D. J. GRAY, APRIL, 1996

FINAL REPORT FOR PNC (EXPLORATION) PTY LTD

VOLUME 1

CSIRO AUSTRALIA

CRCLEME
Cooperative Research Centre for Landscape Evolution & Mineral Exploration

CRC LEME is an unincorporated joint venture between the Australian National University, University of Canberra, Australian Geological Survey Organisation and CSIRO Exploration and Mining

ENERGY AND MINERALS AUSTRALIA

This report was reformatted by Energy and Minerals Australia Limited in 2013 from a scan of the original report

PREFACE

The mid-Eocene lignites in the palaeochannels at Mulga Rock in the south west of the Officer Basin, Western Australia, are strongly enriched in a wide range of chemical elements, including base metals and rare earth elements as well as uranium at potential ore grades. These elements occur as a remarkable number of different minerals, including native metals, sulphides, arsenides, chlorides and oxides; some minerals appear to be previously unknown. The source of the elements and the reason for their concentration at this site is not known. However, their presence has implications for the possibility of primary mineralization in nearby basement rocks, for the genesis of sedimentary sulphide deposits and for the mechanisms and timing of element mobility in the weathering environment of southern Western Australia. The enrichment may be related to processes analogous to those giving rise to high concentrations of base metals in saline groundwaters on the Yilgarn Block, at Lake Maurice and Streaky Bay in South Australia and at Lake Tyrrell in Victoria. However, none of these sites have significant enrichments in the associated sediments. Alternatively, the enrichments may be derived from a specific local source.

The deposits are therefore of considerable research interest, both from a direct exploration viewpoint and for the insight they can provide of the processes involved in element mobility and concentration during weathering (itself of value in interpreting geochemical data). Accordingly, the principal objectives of the research program have been:

1. To provide a thorough geochemical, mineralogical and petrographic description of the deposits.

2. To establish the groundwater geochemistry of the deposits.

3. To interpret the occurrence of the deposits in the context of the geological and weathering history of the region, and to develop models for their formation.

4. To attempt to establish the source(s) of the metals and their prospectivity.

5. To predict environments where further economic mineralization (of any of the metals) may occur.

6. To characterize the organic matter and determine its relationship, if any, with U mineralization.

Following discussions with geologists from PNC Exploration Australia Ltd, it was decided to concentrate the investigations on the Ambassador deposit. This deposit has been extensively drilled and has formed in a more confined drainage system than either the Shogun or the Emperor deposits.

C.R.M. Butt
Project Leader

Cooperative Research Centre for Landscape Evolution and Mineral Exploration
c/- CSIRO Division of Exploration and Mining
Floreat Park, Western Australia

April, 1996

SUMMARY

This report presents a literature review and preliminary results of research into the Ambassador multi-element lignite deposit, Western Australia.

Literature review

(i) *Geological setting:* There are several geological settings in which substantial amounts of U and trace elements have accumulated in organic matter in palaeochannels, active terrestrial channels and/or in marginal marine environments. Deposition or precipitation of the radionuclides and trace metals may be either syngenetic or epigenetic, with no point source necessary, although in several deposits there are possible source rocks with high U abundances. Enrichment at a redox front is a common mechanism by which diffuse, organically associated, accumulations of U and trace elements may be concentrated into narrow high-grade zones of economic significance.

(ii) *Mineralogy:* Uranium and trace element-rich organic deposits commonly have a diverse range of minerals. A significant proportion of the U and trace elements may be directly associated with the organic matter, possibly in ion-exchangeable sites. Organic matter may also catalyse the dissolution of detrital minerals and be integral in the formation of a number of authigenic minerals, especially U and Ti silicates.

(iii) *Complexation by organic matter:* Radionuclides and trace elements in groundwater environments may occur in either true solution or as colloids. At lower pH, (<4) the only species capable of complexing radionuclides and trace elements are silica colloids, which are only protonated in very acid conditions. At moderately acidic pH (*ca.* 4-7), free radionuclides and/or trace elements are complexed via carboxylate functional groups of organic macromolecules or colloidal organic complexes. For actinides (*i.e.*, U and Th), such complexation is probably irreversible, except in waters that have a high ionic strength and, in particular, are dominated by divalent cations such as Ca. In consequence, actinides are probably mostly transported as organic colloids formed by the coagulation of organic matter. At higher pH (>7), carbonate/bicarbonate ligands dominate the complexation, particularly that of U. In the Yilgarn Block, groundwaters associated with calcrete U deposits are alkaline and U is considered to have been mobilized as carbonate/bicarbonate ligands. In the vicinity of Mulga Rock, however, once groundwaters mixed with the organic matter all U and trace elements would have been transported as organic complexes.

Research

(i) *Geochemistry of the lignite horizon:* A geochemical survey of the top two metres of the lignite horizon confirmed that the Ambassador deposit contains a high concentration of a wide range of trace elements in addition to U, *e.g.* Cu: maximum 8550 ppm, Sc: 1090 ppm, Zr: 2770 ppm, La: 1040 ppm, Cr: 1060 ppm). The distribution of several elements, particularly the REE, Zr and V, vary systematically down the length of the palaeochannel, which may indicate the original geochemical structure of the channel or may be a reflection of the preferential dissolution and/or redistribution of particular suites of elements. Statistical analyses of the major and trace element data have demonstrated that a number of coherent associations of elements are present. Uranium is strongly correlated with Sc and Tl; this association has been used as a pathfinder for other

U deposits elsewhere. It is important to recognise that the Ambassador deposit has a sharply reducing environment, because elements not normally associated in oxidizing environments may have a similar geochemical and spatial distribution in reducing conditions.

(ii) ***Mineralogy:*** The Mulga Rock deposit is characterized by a very diverse mineralogy, with over 50 mineral species having been identified. However, these minerals are not the only hosts to the trace elements. Sequential extraction analyses have suggested that significant proportions of many elements are associated with a labile organic phase (*e.g.,* U, 0-90%), whereas other elements are probably associated with authigenic sulphides, either by incorporation into their primary crystal structure or by surface adsorption. The presence of some trace elements in the extraction residue also suggests that primary heavy mineral phases also persist.

(iii) ***Isotopic analysis*****:** Pb-Pb, Rb-Sr and Sm-Nd isotopic analyses have shown that there has been homogenization of Pb, Sr and REE in the Ambassador deposit, possibly due to mobilization and precipitation during weathering and diagenesis. The homogenization of the three isotopic systems precludes determination of the age of the source(s) or mineralization. Preliminary results suggest that an unusual lithology, other than the granites and greenstones of the Yilgarn, is the source of the mineralization. In particular, Pb-Pb isotopic analysis suggests a source of Archaean or Proterozoic age, with a high Th/U ratio. Further isotopic analysis of organic-rich palaeochannel samples from throughout the Yilgarn and analysis of basement samples is required to constrain possible source lithologies.

(iv) ***Groundwater geochemistry*****:** Groundwaters at Mulga Rock differ from those from sites on the Yilgarn block, having low oxidation potentials (Eh) and low concentrations of a number of trace elements. These differences are probably due to the abundance of solid organic matter. Hydrogeochemical investigations suggest that the groundwaters from the Ambassador palaeochannel are distinct from those sampled from the main drainage system, including the Emperor and Shogun deposits, being less saline, enriched in K, Ca and Sr, and depleted in Al, Fe and Mn. Some of the waters from the mineralized zone at Ambassador have particularly low Eh values, with sulphate possibly being reduced to sulphide species; they are also significantly enriched in dissolved HCO_3, PO_4, Ba, U and W, depleted in dissolved Si, and less saline.

(v) ***Basement geology and geochemistry*****:** The basement lithologies of the Ambassador deposit consist of a sequence of predominantly unmineralized quartzites, cherts, shales and dolomites. Although these rocks do locally contain moderately elevated concentrations of the elemental suite found at the redox horizon (*e.g.*, Cu: maximum 440 ppm, Ce: 580 ppm, Zn: 4530 ppm, V: 950 ppm, Ni: 1040 ppm), it is difficult to assess if these lithologies represent either a single source or are even only partly responsible for the palaeochannel mineralization. Further sampling and geochemical analysis (including isotopic analysis) of the basement may resolve this question.

(vi) ***Maceral analysis:*** Maceral analysis of two samples from the Ambassador deposit has shown that the lignites have reached a degree of maturation equivalent to that of brown coals. A small amount of the organic matter may have been derived from Cretaceous sediments upstream of the Ambassador deposit. At least 50% of the identifiable organic matter is derived from plants, with the floral assemblage suggestive of a subaquatic, herbaceous environment. The presence of algal-derived macerals suggests quiescent, low energy conditions,

with relatively clear, nutrient-rich waters, consistent with the regional topography of the eastern margin of the Yilgarn Block.

Genetic model

A tentative genetic model for the formation of the mineralization of the Ambassador deposit suggests that the environment of deposition of the organic matter was likely to have been a lowland area, probably a swamp or marsh, situated on a flat-lying stable platform. Petrographic analysis of the macerals indicate that the dominant flora was low heathland or sub-aquatic plants, devoid of trees or large plants. The presence of abundant algae suggests that the waters were probably well oxygenated, clear and nutrient-rich. The proximity of the Ambassador deposit to possible mid to late-Eocene shorelines (sea levels in the Eocene were approximately 300 m higher than the present day) suggests that interaction with seawater may have occurred. Sulphur concentrations in lignites at Mulga Rock are consistent with a marine environment, although S may have been introduced by later saline groundwaters.

In much of the northern Yilgarn Block, groundwaters are alkaline and U is transported as dissolved carbonate complexes. However, in the mildly acidic, organic rich environment of Mulga Rock, it is postulated that most of the U and trace elements would be associated with colloidal material and only a minor amount with truly dissolved species. At the present pH of the Ambassador deposit (pH 4-8), it is probable that organic colloids will dominate any active transport and enrichment processes in the groundwater. However, if the groundwater pH was also lower in the past, silica colloids may also have been significant. The preferential association of some of the radionuclides with, and transport by, certain colloid types may also explain the U-series disequilibrium observed in the Ambassador deposit.

Post-depositional diagenetic changes within the Ambassador deposit have resulted in a unique suite of minerals and organic-trace element associations. The systematic change in the ratio of light REE to heavy REE laterally along the main mineralized zone and the marked vertical variation in the abundances of many elements, including Ti, U, Th and S, indicate that there has been appreciable element redistribution in response to the different Eh-pH conditions imposed by the redox front. Furthermore, the presence of elevated levels of Ca in the main mineralized zone may indicate a period during which mobile humic matter has been influenced by groundwater movement and composition. Evidence of diagenesis has been identified by U, Pb, Sr and Nd isotopic studies and includes the development of U-daughter disequilibria in the organic matter, and the homogenization of Pb, Sr and Nd isotopes over a large area of the mineralization. Estimates of the enrichment of U by organic matter based on solid and groundwater geochemistry have shown that the enrichment factor for the Ambassador organic matter is consistent with other U-trace element organic matter deposits, with the concentration of Ca in the groundwaters possibly being a strong influence in the distribution of U.

There are two potential sources for the elemental suite that forms the mineralization of the organic matter at Mulga Rock.

1. The Archaean and Proterozoic basement rocks of the Yilgarn Block and Albany-Fraser Province represent a diffuse, non-point source via the extensive palaeochannel system that has existed since at least the Permian. Organic matter in major river systems draining large continental areas may be significantly enriched in trace metals. Although this organic matter accounts for only a small proportion of the total

load, if it is preferentially removed from a fluvial system at one location (*e.g*., estuarine mixing), an accumulation of highly mineralized organic matter may develop. If the enormous area of the Precambrian Craton, with its diversity of lithologies, coupled with the expansive palaeochannel system and the extensive weathering profile is considered, it is reasonable to assume that the multi-element suite observed at the Ambassador deposit could be produced at suitable trap sites.

2. The second possibility for a source of mineralization is an unusual lithology, suggested by isotopic analysis. In particular, the Pb-Pb isotopic data suggest that a very distinctive lithology, Archaean or Proterozoic in age, with a high Th/U ratio, probably lamproites, kimberlites or carbonatites is the likely source for the mineralization. Additional studies using the Rb-Sr and Sm-Nd isotopic systems also support this hypothesis; however, these isotopic signatures are also compatible with many granites and greenstones from the Yilgarn block. The source rocks could thus represent a point source of mineralization located either within the basement proximal to the palaeochannel or directly linked via one of the branches of the Minigwal palaeochannel system.

TABLE OF CONTENTS

1.0 Description of the Mulga Rock Deposit 1

1.1 Location and Regional Geology 1
1.2 Local Geology 1

2.0 Literature Review 3

2.1 An investigation of organic matter hosted U-trace element deposits and modern analogues to the Ambassador deposit 3
2.1.1 Introduction 3
2.1.2 Coutras deposit, southwestern France 3
2.1.3 Streaky Bay palaeochannel system, South Australia 4
2.1.4 Flodelle Creek U deposit, northeastern Washington, USA 5
2.1.5 Magela Creek system, Alligator Rivers region, Northern Territory 6
2.1.6 Henkries deposit, Namaqualand District, South Africa 6
2.1.7 Lake Tyrrell system, Murray Basin, southeastern Australia 7
2.1.8 Other U-trace element organic matter rich deposits 8
2.1.9 Conclusion 8
2.2 Mineralogy and diagenesis of organic rich U and trace metal deposits 8
2.2.1 Introduction 8
2.2.2 Mineralogy of organic rich U-trace element deposits 8
2.2.3 Conclusions 15
2.3 Transport and complexation of U and trace elements in organic rich groundwaters 16
2.3.1 Introduction 16
2.3.2 Colloid formation and transport of U and trace elements 16
2.3.3 Radionuclide and trace element complexation by organic matter 19
2.3.4 Conclusion 23

3.0 Major and Trace Element Distribution in the Ambassador Deposit 25

3.1 Introduction 25
3.2 Sampling and analysis 25
3.2.1 Sample selection 25
3.2.2 Sample Preparation and analysis 25
3.3 Statistical analysis of Ambassador geochemistry 26
3.3.1 Introduction 26
3.3.2 Statistical methods 26
3.3.3 Result and Discussion 26
3.3.4 Conclusion 33

4.0 A Sequential Extraction Study of the Ambassador Deposit 34

4.1 Introduction 34
4.2 Sequential extraction method 34
4.3 Results and Discussion 35
4.4 Conclusion 39

5.0 Isotopic Geochemistry of the Ambassador Deposit 40

5.1 Introduction 40
5.2 Summary of the theory of radiogenic isotopic systems 40
5.3 Analysis, Results and Discussion 41
5.4 Source rock age 46
5.5 Conclusion 46

6.0 Groundwater Investigations 47

6.1 Introduction 47
6.2 Sampling and analysis 47
6.3 Results and discussion 49
6.3.1 Compilation of results 49
6.3.2 Oxidation potential and acidity of Mulga Rock groundwaters 49
6.3.3 Isotope chemistry of Mulga Rock groundwaters 51
6.3.4 Major ion chemistry of groundwaters at Mulga Rock 53
6.3.5 Trace element chemistry of Mulga Rock groundwaters 55
6.3.6 Uranium chemistry of Mulga Rock groundwaters 57
6.3.7 Summary 57
6.4 Hydrogeochemical mapping 57
6.4.1 Description of mapping 57
6.4.2 Isotope and water quality parameters 58
6.4.3 Barium and pH controlled major elements 58
6.4.4 Trace elements 59
6.4.5 Summary 59
6.5 Conclusion 59

7.0 Basement Geology and Geochemistry 60

7.1 Introduction 60
7.2 Results and Discussion 60
7.3 Conclusion 61

8.0 Characterization of Organic Matter from the Ambassador Deposit 62

8.1 Introduction 62
8.2 Maceral characterization 62
8.3 Analytical Techniques 63
8.3.1 ^{13}C NMR 63
8.3.2 C,H,O,N Analyses 65
8.3.3 Petrography 67
8.3.4 Multiple linear regression analysis 67
8.4 Materials and methods 67
8.4.1 Samples 67
8.4.2 ^{13}C NMR procedure 67
8.4.3 C,H,O,N analytical procedure 67
8.4.4 Petrographic analyses 70

8.5 Results 70
8.5.1 ^{13}C NMR 70
8.5.2 C,H,O,N Analyses 73
8.5.3 Petrographic Analysis 76
8.5.4 Multiple linear regression analysis 78
8.5.5 Mapping of the data 94
8.6 Discussion 100
8.7 Conclusions 101

9.0 A U-Th Disequilibrium Study of the Ambassador Deposit 102

9.1 Introduction 102
9.2 Experimental 103
9.3 Results and discussion 103
9.4 Conclusion 111

10.0 Genesis of the Ambassador Deposit 112

10.1 Introduction 112
10.1.1 Environment of deposition 112
10.1.2 Sources of U and trace elements 112
10.1.3 Diagenesis and enrichment 113
10.2 Recommendations for future research 115
10.2.1 Organic matter and element enrichment 115
10.2.2 Origin of mineralization 115
10.2.3 Element speciation 116
10.2.4 Regional studies 116
10.2.5 Benefits 116

Acknowledgements 117

References 118

LIST OF FIGURES

Figure 1.1 Location of the Mulga Rock deposit 2

Figure 1.2 Stratigraphy of the Mulga Rock deposit 2

Figure 2.1 Speciation of the uranyl (UO_2^{2+}) ion in the system UO_2^{2+}-humic acid [HA]-CO_3^{2-} 20

Figure 3.1 Cluster diagram of Ambassador major and trace element geochemistry 30

Figure 5.1 (a) Nd-Sr diagram for the Ambassador organic matter. Also depicted are fields of isotopic ratios for Western Australian lamproites and kimberlites and a number of other basic and ultrapotassic lithologies from around the world 42

Figure 5.1 (b) and (c): Pb Isochron diagrams for Ambassador organic matter. The error of the isotopic measurements is depicted as a small solid symbol in the top left-hand corner of each isochron diagram 43

Figure 5.2 (a)-(e): Histograms of Sr, Nd and Pb isotopic ratios for lithologies from the Yilgarn Block 44

Figure 6.1 Water sampling sites at Ambassador (with Emperor and Shogun holes shown in the insert) 48

Figure 6.2 Eh vs. pH for groundwaters from Minigwal, Ambassador and other sites 52

Figure 6.3 HCO_3- vs. pH for groundwaters from Minigwal, Ambassador and other sites 52

Figure 6.4 Fe vs. Eh for groundwaters from Minigwal, Ambassador and other sites 52

Figure 8.1 ^{13}C NMR spectra of (a) alginites, (b) sporinites, (c) vitrinites and (d) fusinite. (Modified from Wilson, 1987) 64

Figure 8.2 H/C vs. O/C development lines of the macerals (modified from van Krevelen, 1963) 66

Figure 8.3 Samples used for organic matter characterization at Ambassador 68

Figure 8.4 Estimated %Noise vs. LOI for ^{13}C NMR 71

Figure 8.5 Organic matter content vs. LOI 73

Figure 8.6 Atomic H/C percentage error vs. LOI 75

Figure 8.7 H/C vs. O/C data for Ambassador superimposed on van Krevelen development lines of the macerals 76

Figure 8.8 MLRA for vitrinite, for Ambassador samples 88

Figure 8.9 MLRA for mineral/organic matrix, for Ambassador samples 88

Figure 8.10 MLRA for atomic H/C, for Ambassador samples 89

Figure 8.11 MLRA for aliphatic content, for Ambassador samples 90

Figure 8.12 MLRA for aliphatic content, for Ambassador samples 91

Figure 8.13 MLRA for carboxylic content, for Ambassador samples 92

Figure 8.14 MLRA for Aliphatic peak position, for Ambassador samples 92

Figure 8.15 Linear regression for Aliphatic peak position vs. logU, for Ambassador samples 93

Figure 8.16 Linear regression for logU vs. Aliphatic peak position, for Ambassador samples 94

Figure 8.17 Distribution of calculated vitrinite concentration for the Ambassador deposit, Mulga Rock 95

Figure 8.18 Distribution of calculated mineral/organic matter concentration for the Ambassador deposit, Mulga Rock 96

Figure 8.19 Distribution of the Aliphatic Peak Position for the Ambassador deposit, Mulga Rock 97

Figure 8.20 Distribution of the Aromatic Peak Position for the Ambassador deposit, Mulga Rock 98

Figure 8.21 Distribution of U for samples used for organic matter characterization at the Ambassador deposit, Mulga Rock 99

Figure 9.1 Down hole disequilibrium profile of hole 6096 106

Figure 9.2 Down hole disequilibrium profile of hole 6184 107

Figure 9.3 Down hole disequilibrium profile of hole 6221 108

LIST OF PLATES

Plate 2.1: SEM photomicrographs of Ambassador samples (1) 11

Plate 2.2: SEM photomicrographs of Ambassador samples (2) 12

Plate 8.1A: Petrographic Analysis of Sample 00-6037 79

Plate 8.1B: Petrographic Analysis of Sample 00-6037 continued 80

Plate 8.2A: Petrographic Analysis of Sample 00-6054 81

Plate 8.2B: Petrographic Analysis of Sample 00-6054 continued 82

Plate 8.3: Petrographic Analysis of Sample 00-6056 83

Plate 8.4A: Petrographic Analysis of Sample 00-6061 84

Plate 8.4B: Petrographic Analysis of Sample 00-6061 continued 85

Plate 8.5: Petrographic Analysis of Sample 00-6074 86

Plate 8.6: Petrographic Analysis of Sample 00-6089 87

LIST OF TABLES

Table 2.1: Mineralogy of the Shogun and Ambassador deposits 9

Table 3.1: Mean concentrations and standard deviations of elements analysed from the Ambassador redox front 27

Table 3.2: Correlation matrix of Ambassador major and trace element geochemistry 28

Table 4.1: Results of the sequential extraction analysis 36

Table 5.1: Rb-Sr, Sm-Nd and Pb-Pb isotopic composition of Ambassador organic matter 41

Table 6.1: Mulga Rock water samples 48

Table 6.2: Averaged elemental compositions of Minigwal and Ambassador waters, with results from other sites given for comparison 50

Table 6.3: Averaged elemental compositions (mg/L) of Ambassador waters 51

Table 6.4: Range in SI values for groundwaters at Mulga Rock, relative to the least soluble phase for each element tested 56

Table 8.1: ^{13}C NMR parameters of geochemically important C groups 65

Table 8.2: Compositions of selected samples 69

Table 8.3: Calculated proportions of functional C groups, using ^{13}C NMR 72

Table 8.4: Organic matter elemental analysis 74

Table 8.5: Petrographic results (% of organic and mineral groups) for duplicate analyses of samples from the Ambassador deposit 77

Table 8.6: Compiled petrographic results (% of organic and mineral groups) for Ambassador samples 78

Table 9.1: Results of y-spectroscopy of Ambassador samples. All daughter product concentrations are expressed as equivalent U (eU) concentrations 104

Table 9.2: Interpretation of U-Th disequilibrium of Ambassador samples 105

1.0 DESCRIPTION OF THE MULGA ROCK DEPOSIT

1.1 Location and Regional Geology

Mulga Rock is about 240 km NE of Kalgoorlie, on the SW margin of the Great Victoria Desert. (Figure 1.1). The area is an undulating sandy plain at an elevation of 325-400 m, crossed by ESE-trending sand dunes. The vegetation consists of an open spinifex-eucalypt association. The climate is semi-arid to arid, with an erratic rainfall averaging about 200 mm p.a., with hot summers and mild winters.

The deposit is on the SW extremity of the Officer Basin, where sediments of the Lower Permian Paterson Formation overlie the Precambrian basement, predominantly Archaean and Proterozoic granitoids of the Yilgarn Block and Albany-Frazer Range Province, respectively. Permian rocks rarely outcrop but are overlain by a variety of Mesozoic (Lower Cretaceous) and Cainozoic sediments. The region has been subjected to continental conditions since the Cretaceous, and planation and sedimentation have continued under humid and then arid conditions.

The Mulga Rock lignites lie in a buried palaeochannel 5-15 km wide that has been traced for over 100 km (Fulwood and Barwick, 1988). The palaeochannel connects to the present day Lake Raeside-Ponton Creek drainage system in the west but has not been traced to the south. Originally, the headwaters of the palaeochannel may have been the Lake Minigwal drainage system, but this has since been captured by the Lake Rason system. The main channel is confined to a valley underlain by Permian mudstones, thought to have been eroded during the late Cretaceous and early Tertiary. However, in common with similar channels on the Yilgarn Block, it is possible that it follows even earlier channels that were widened and subsequently infilled during glaciation in the Permian. Some disturbance to the channel may have been caused by seismic activity along the margin of the Yilgarn Block.

1.2 Local Geology

The palaeovalley contains up to 100 m of non-marine Tertiary sediments (Figure 1.2) overlying the Permian, in the following broad units:

1. Fluviatile sands and interbedded lacustrine sediments.
2. Lacustrine to paludal sediments, including lignites (peats), clay-rich lignites and carbonaceous sands and clays.
3. Basal fluviatile sands and gravels.

The lignites have been dated as being Middle Eocene (Islam, 1983) and the whole sequence is covered by a veneer of 2-10 m of aeolian sand. The upper units have been weathered and are variably ferruginized and silicified; silcrete formation is locally intense in some sandy units, usually within 10 m of the surface. The depth of weathering usually exceeds 20 m, with a sharp weathering front at a redox boundary at the contact between kaolinitic clay and the lignite, commonly close to the water-table. The weathering is presumably equivalent to that which affected the Yilgarn Block, estimated as occurring during humid, tropical climates during the Oligocene to mid-Miocene. However, some of the sediments could themselves be eroded products of such weathering, *e.g.,* some kaolinitic and quartz units, and the sequence has undoubtedly been affected by later weathering under the more arid environment that has prevailed since the mid-Miocene.

Figure 1.1 Location of the Mulga Rock deposit

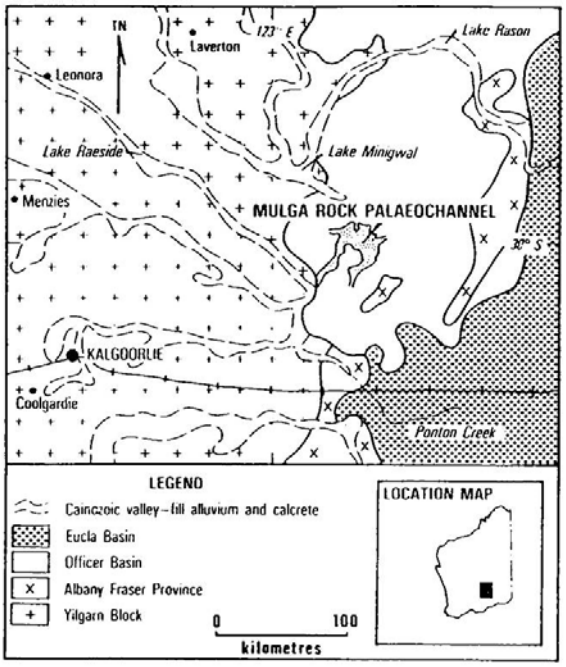

Figure 1.2 Stratigraphy of the Mulga Rock deposit

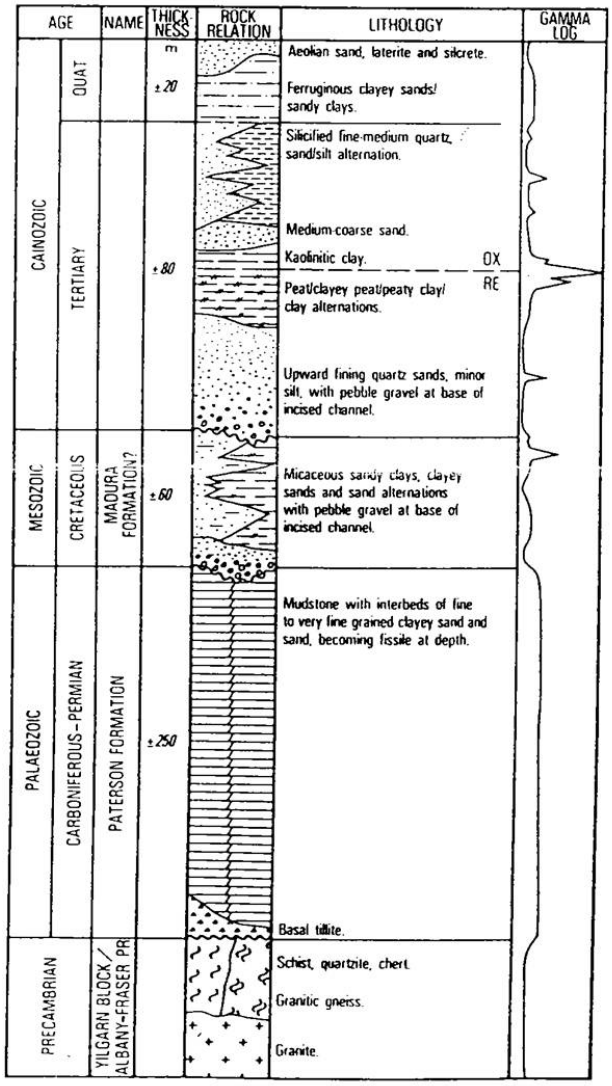

2.0 LITERATURE REVIEW

This literature review deals with important aspects of U-trace element organic matter associations is divided into three sections. Section 2.1 compares the Mulga Rock mineralization to a number of other similar deposits and analogues from around the world. Section 2.2 examines the mineralogy and diagenesis observed in mineralized organic matter[1] rich deposits, and section 2.3 investigates the methods of complexation and transport of U and trace elements in organic matter rich environments.

2.1 An investigation of organic matter hosted U-trace element deposits and modern analogues to the Ambassador deposit

2.1.1 Introduction

By investigating other organic matter hosted multi-element deposits and modern analogues, further insights can be gained into the genesis of the Ambassador deposit and possibly give indications to likely future palaeochannel exploration targets. Many U-trace element occurrences in organic matter occur in lowland "bog" type environments. The general characteristics of uraniferous "bogs" are given in Zielinski *et al*. (1987) and a summary of those points is given here. Uraniferous "bogs" have been identified worldwide and are characterized by a near-surface association of U with organic matter, small size (generally <250 tonnes of U), highly variable grade, a spatial association with granitic terrains and marked radioactive disequilibria (U>> daughters) due to the youth of the deposits. Many of these aspects are common to the U-bearing, organic matter-rich deposits discussed below. A literature review has identified a significant number of organic matter hosted multi-element deposits from around the world, and a representative selection of these are described briefly below-In addition, other organic poor systems, that may have groundwater systems that may be analogues to the original source at this site, are discussed.

2.1.2 Coutras deposit, southwestern France

This deposit occurs in a sedimentary basin containing unconsolidated arenaceous sediments of mid-Eocene age and contains reserves of 20,000 tons of U metal at 0.1% U. The sediments occur as black tabular lenses of reduced material that contain abundant coalified plant debris and were deposited in a palaeodeltaic environment with sediments derived from granitic and metamorphic terranes. An active redox front is present, at which the deposition of U occurs. The redox stratigraphy consists of an upper oxidized sand layer overlying a bleached clay layer in contact with the redox front. There is marked U-series disequilibrium within the bleached clay layer, indicating recent redistribution of U, but the sediments below the redox front are at radioactive equilibria, due to the comparatively recent accumulation of the orebody within the last 500,000 years (Meunier, *et al.*, 1989). There is little or no structural deformation of the sequence. The U distribution is apparently not controlled by sedimentary structures although it has been observed that the major U ore zone parallels the neritic (transition) zone of a marine transgression that occurred during the Lutetian (lower-mid Eocene).

1 Note the terms humic materials, humic matter and organic matter are equivalent and will be used interchangeably in the text. Humic and fulvic acids per se can be classified as fractions of humic (organic) materials, with the insolubility of humic acid at pH <2 used to separate it from fulvic acid.

Uranium (up to 4 % maximum) is mainly concentrated in the deltaic plain sediments where organic matter (classified as a lignite) is most abundant (up to 2.1% total carbon, *i.e.* approximately 4% organic matter).

The mineralogy of the Coutras deposit indicates that the majority of the U is present as fine disseminations in the organic matrix or as rare spherules (microspheres) of pitchblende and coffinite on the surface of detrital minerals. Both euhedral and framboidal pyrite are present throughout the matrix and rare arsenopyrite is associated with organic fragments. Needles of authigenic Se and a possible V oxide/hydroxide have also been recognized. Although little information is available on the geochemistry of the Coutras deposit it seems that the assemblage is similar to that observed in other types of U deposits, in that it is enriched in U, V, Se and Mo. The occurrence of these elements together is due to the formation of similar oxy-ion aqueous complexes and will be discussed further in a review of the geochemistry of organic-matter-trace element interactions (Section 2.3.3).

There are many parallels between the Coutras and the Ambassador deposits. Both occur in a palaeochannel or basin of mid-Eocene age that contains sediments with abundant organic matter and plant remains. An active redox front beneath an upper bleached clay layer is also present in both deposits, with marked radioactive disequilibrium in the clay layer, delineating previous redox front positions. In contrast to the Ambassador deposit, the Coutras deposit has at least an order of magnitude less organic carbon. The size of both deposits is quite similar, with the Coutras deposit containing 20,000 tonnes of U and the entire Mulga Rock deposit approximately 13,000 tonnes of U.

2.1.3 Streaky Bay palaeochannel system, South Australia

This deposit is located on the South Australian coast, to the west of the Gawler Ranges and to the east of the Eucla Basin. The Streaky Bay system consists of Eocene fluviatile sediments that fill palaeochannels incised into Proterozoic basement. The sediments contain acid saline groundwaters and redox fronts with widespread U mineralization, with the entire Proterozoic and Tertiary sequence covered by recent sediments (Binks and Hooper, 1984). Numerous redox fronts may be present and, within the reduced palaeochannel stratigraphy, sediments may contain abundant pyrite, carbonaceous wood fragments and humic staining. Marked U-series disequilibrium occurs within the mineralization, indicative of the redistribution of U within the deposit. No petrographic studies have been performed on the deposit although it is likely that in light of the redistribution of the U and its daughter products that mineralization is associated as adsorbed species on the humic and sulphide phases. The grade of mineralization is low, with U concentrations generally in the range 100-200 ppm and only rarely up to a few thousand ppm. Thorium (<30 ppm), base metal, V, Mo and precious metal concentrations are also low.

Although the environment of deposition of the Streaky Bay palaeochannel has not been described, its spatial association with an escarpment and the presence of fluvial and lacustrine sediments indicates a low relief, perhaps marginal marine, environment. The presence of sponge spicules and glauconite coated sand grains in some of the Streaky bay palaeochannels indicates that the area was probably subject to minor marine incursions or estuarine conditions. The mineralization is thought to have formed due to the lateral movement of oxidized U-bearing groundwaters derived from overlying Pliocene sands intersecting islands of reduced Eocene sediments. The ultimate source of the U is thought to be the mid-Proterozoic Hiltaba Granite. This granite has an above average U content (mean 7 ppm U, maximum 15 ppm U) and is known to occur at shallow depths near some of the palaeochannels.

The groundwaters within the Streaky Bay palaeochannel system are highly reduced (Eh minimum -360 mV), acidic (pH minimum 2.8) and have high salinities (up to 82,500 mg/L, approximately three times seawater). The concentration of dissolved U is very high in the Streaky Bay palaeochannel system, ranging up to 12.3 mg/L. The reason for such high dissolved U concentrations is probably due to two factors. Firstly, the very low pH of the system means that all the carboxylic functional groups on the organic matter which are the main complexing group (Section 2.3.3) are effectively protonated, and therefore will not bind U. Secondly, the relative paucity of reduced sediments compared to the massive lignites of other similar deposits may mean that all available adsorption sites at the prevailing pH may have been complexed, resulting in substantial concentrations of uranyl (UO_2^{2+}) ions remaining dissolved in solution.

The Streaky Bay deposit may represent the closest known analogue to the Mulga Rock deposit in terms of age, geological setting and style of mineralization. Both deposits are in Eocene fluviatile palaeochannel sediments which contain organic matter, redox fronts and acid saline groundwaters. In contrast to Mulga Rock, at Streaky Bay, a probable source rock has been identified, organic matter is not as abundant, significantly higher uranium is present in the groundwaters and the mineralization is significantly lower grade.

2.1.4 Flodelle Creek U deposit, northeastern Washington, USA

This deposit was the first surficial U deposit to be mined in the United States, and is located in a series of organic matter-rich ponds formed by beavers on a glacially scoured granitic terrane. The Flodelle Creek deposit and contains abundant organic matter (in excess of 50%) and reduced authigenic sulphide species, possibly produced by the action of sulphate-reducing bacteria. The U is sourced from the granitic bedrock, with the source likely to be a local granite which is anomalous in U (mean 12 ppm, range 4-80 ppm).via ground, spring and surface waters (Johnson *et al*., 1987) and is still accumulating. Due to the very young age of the deposit (<5,000 years), few daughter products are present, the deposit having been discovered by a regional geochemical survey. Uranium enrichment in the Flodelle ranges up to approximately 9,000 ppm. A similar deposit to Flodelle creek also occurs in peats in northern Finland, associated with glacial sediments and a granite containing anomalous U concentrations (8 ppm) (Peuraniemi and Aario, 1991).

The aqueous geochemistry of the Flodelle Creek deposit is neutral to acidic (pH 5.9-7.6), with low Eh values, and low dissolved U concentrations (Zielinski, *et al*., 1987). The waters of Flodelle Creek are also very fresh (TDS approximately 100 mg/L).

The Flodelle Creek deposit may be compared to the Mulga Rock deposit in a number of ways

1. it may represent a modern analogue of the method of enrichment of U at Mulga Rock, prior to further concentration by a redox front;
2. it is one of the few deposits with organic matter concentrations as high as that at Mulga Rock,
3. it is a surface deposit located in a glacially scoured depression;
4. it demonstrates that humic materials may have been able to concentrate U (and potentially other trace elements) in relatively fresh waters from a large low grade U anomaly, without the need of a primary high-grade deposit within the catchment.

2.1.5 Magela Creek system, Alligator Rivers region, Northern Territory

The Magela Creek system, located adjacent to the Ranger Uranium mine at Jabiru, may provide a modern analogue in terms of geological setting and a mechanism of syngenetic enrichment that could have occurred in palaeochannel environments. Although unlike at Mulga Rock, the enrichment of the Magela Creek sediments is from a clearly defined source, the mechanism of accumulation of U and trace elements is relevant. Magela Creek consists of a narrow creek and billabong system that flows out onto a large, low gradient marsh-floodplain system locally up to a 5 km wide. Abundant sediments rich in organic matter (up to 16.8% organic carbon, *i.e.* approximately 34 % total organic matter) are known to accumulate within the billabongs and floodplain sediments of the Magela Creek system. Uranium (up to 16.5 ppm, dry weight) and organic matter concentrations are highly correlated, with a significant proportion of the U directly associated with the organic matter (Noller and Hart, 1992). Because of the low concentrations of divalent cations, particularly Ca and Mg, in the headwaters of the Magela Creek system, the fine organic matter, principally humic materials, remains in suspension (Hart *et al*., 1992). The Ca and Mg concentrations are substantially higher in the quiescent waters of the floodplain, possibly due to interaction with seawater from tidal or groundwater incursion. Thus, when the creekwaters reach the floodplain, the organic colloids coagulate and settle. This mechanism concentrates U and trace elements that have been strongly complexed to the organic matter during transport in the upper reaches of the Magela Creek system. The resultant organic rich sediments contain a mixture of organic debris, derived directly from coagulated humic matter, and aquatic and terrestrial plant materials. Most of the plant material decays or undergoes humification during the dry season. This process has continued for over 10,000 years and a thick accumulation of organic-rich sediments enriched in radionuclides and trace metals has developed. Authigenic sulphide minerals have also been observed in the sedimentary sequence of the floodplain, formed during anoxic periods that occur in the dry season; these may also be a site of radionuclide and trace element accumulation.

The Magela Creek system potentially represents a modern depositional analogue to the Mulga Rock deposit. It demonstrates that substantial accumulations of organic matter may develop in a terrestrial setting and that this organic matter may be syngenetically enriched in U and trace elements where there is a suitable source present.

2.1.6 Henkries deposit, Namaqualand District, South Africa

The Henkries deposit occurs in an inland channel system developed on a granitic basement. The host sediments for the Henkries deposit are a series of lacustrine clays and sands containing a large amount of diatomaceous earth and carbonaceous material that were deposited within a sinuous, locally ponded channel system. The majority of the deposit is covered by recent aeolian sands. The channel sediments are probably Quaternary, with estimates of the age, derived from U-disequilibria studies, of about 40,000 years. The total reserves of the deposit are approximately 1,450 tons of U_3O_8 (Ralston *et al*., 1986) with the ore patchily distributed throughout the channel sediments. Unfortunately, no trace element concentrations are available. Enrichment of the orebody is thought to have occurred by adsorption from U-rich groundwaters, possibly derived from the granitic basement with uraniferous pegmatites that may contain up to 50 ppm U_3O_8. Although no formal redox fronts are active in the Henkries deposit, it is at present a dynamic system accumulating U. Previous groundwater movements are implicated from palaeoclimatic studies, with evidence from U-disequilibria studies of both leaching and accumulation of U. Palaeoclimatological studies have shown that the Henkries region probably had a considerably cooler climate, with increased rainfall. Such conditions promote the accumulation of organic

matter in a lowland setting. The recent aeolian sands which cover the deposit have protected the organic matter within the channel system.

The Henkries deposit shares a number of similarities to the Mulga Rock deposit:

1. the environment of deposition involving lacustrine sediments that were probably deposited in a low energy, shallow water environment (*e.g.* marsh or swamp) in an area of impeded drainage bounded by a prominent barrier dune (also inferred for the Mulga Rock palaeochannel system);
2. crystalline basement consisting of weathered Proterozoic granites and pegmatites;
3. very low regional gradients in the hinterland, being 1:100-1:200 in the Henkries (*c.f.* Yilgarn Block);
4. the uneven distribution of the ore, due to the influence of groundwaters.

2.1.7 Lake Tyrrell system, Murray Basin, southeastern Australia

Sediments in the Lake Tyrrell system do not contain significant organic matter, but may provide an active, modern analogue to Mulga Rock with respect to the source of trace elements in channel-hosted organic-rich deposits. It is an active system comprising an inland playa that interacts with acid, saline groundwaters to produce a sequence of evaporites, redbeds and syngenetic sulphides (Macumber, 1992). Acidification of the system is related to the oxidation of pyrite and is maintained due to the lack of an appropriate buffer in the aquifer sediments. Salinities within the Lake Tyrrell system may reach in excess of 250,000 ppm, with precipitation of salts in the lake system itself. The groundwater brines may contain up to 700 ppb total REE, 3,500 ppb Cu, 38,500 ppb Pb, 1,300 ppb Zn and 66 ppb U, with U concentrations at or below detection limits, 0.1-0.5 ppb, for most samples. Laboratory studies indicate that the metals were probably derived from local sedimentary sequences (Giblin and Dickson, 1992). These trace metal concentrations are not surprising, given the pH of the system which may be as low as 3.2 in groundwaters and even lower in surface waters (Fee et al., 1992).

Elevated concentrations of radionuclides are also present within the groundwater system. Although U and Th are relatively immobile, even in waters with pH<3, (possibly due to the lack of a suitable complexing agent such as humic materials, a lack of an enriched source, and/or to the oxic, hypersaline conditions in the upper aquifer), many of the daughter radionuclides are highly mobile, display elevated concentrations and are concentrated in a relatively restricted zone of reduced black muds in the north of the Lake Tyrrell system. This accumulation of daughter radionuclides results in a significant radiometric anomaly (Dickson and Herczeg, 1992). However, the lack of a significant body of reduced (organic) material within the sediments of Lake Tyrrell to adsorb the radionuclides differentiates this site from other deposits outlined in this review. Significant trace metal accumulation only occurs in the system at alkaline pH, due coprecipitation with Fe-hydroxide species (Dickson and Herczeg, 1992).

The relevance of the Lake Tyrrell system to the Mulga Rock deposit is that it demonstrates that no point source of primary mineralization is necessary to generate brines enriched in U and trace elements and, although acidic reduced groundwaters conducive to the movement of U may be present, a suitable depositional area (*e.g.* organic matter) is also required. Studies of the geological setting and hydrogeochemical regime of presently active systems such as Lake Tyrrell, and the recognition of the factors relating to the generation of source and depositional areas, are crucial in recognizing potential areas of mineralization similar to that of the Mulga Rock deposit.

2.1.8 Other U-trace element organic matter rich deposits

Numerous other organic matter-trace element rich deposits from a variety of geological settings have also been identified from the literature review. These studies (*e.g.* Vassiliou, 1980; Toens, 1981; Ilger *et al*., 1987; Culbert and Leighton, 1988; Parnell, 1988; Pointer *et al*, 1989; Hooker, 1990; Hansley and Spirakis, 1992) have been listed in the bibliography for future reference.

2.1.9 Conclusion

It has been observed in the Coutras deposit and in the more modern settings of the Henkries Flodelle Creek and Magela Creek that it is possible to accumulate substantial amounts of organic matter (and in some cases authigenic sulphide species) in an active terrestrial channel or palaeochannel and/or in a marginal marine environment. Deposition or precipitation of the radionuclides and trace metals may be either syngenetic or epigenetic, and no particular point source is necessary, although in a number of cases a large low grade U anomaly is present. Enrichment in a redox front (*e.g.* Coutras, Streaky Bay) is a common mechanism by which diffuse, organically associated, accumulations of U and trace elements may be concentrated into narrow high-grade zones of economic significance.

2.2 Mineralogy and diagenesis of organic rich U and trace metal deposits

2.2.1 Introduction

It has been widely recognized for over a century that there is a close association between U and trace element accumulation and natural organic matter (*e.g*. Ellsworth, 1928; Szalay, 1954; Wellin, 1966; Vassiliou, 1986, Ilger et al. 1987, Parnell, 1988, Raymond et al., 1990 and numerous references contained therein). Enrichments of U in solid hydrocarbons (bitumens), shales, lignites and coals have also been extensively documented (*e.g*. reviews in Boyle, 1982 and Landais, 1986) with U-ores associated with carbonaceous material representing some of the largest commercially exploitable deposits. Several mechanisms of enrichment of the organic matter in U and trace metals have been proposed, but most involve U transport as the aqueous, carbonate or organic (humic) UO_2^{2+} complexes. The method of complexation and/or reduction of U and the subsequent formation of uraniferous minerals is however, the subject of a deal of conjecture (*e.g*. Nakashima *et al*., 1984; Vassiliou, 1986; Ilger *et al*., 1987; Meunier *et al*., 1987; Petrova and Ye Chistilin, 1987) and is examined in detail here.

2.2.2 Mineralogy of organic rich U-trace element deposits

An SEM investigation conducted in-house at CSIRO has demonstrated that a wide range of elemental associations may occur in the organic-rich sediments. The following summary is intended to be mainly petrographic in nature, using information obtained in the literature review and previous mineralogical studies of the Mulga Rock deposit. The actual mechanism of fixation of trace elements and radionuclides is discussed in Section 2.3.3. The mineralogy of U-trace element-organic matter deposits may be summarized in terms of five mineral associations, three associations being authigenic and two detrital. More than 50 mineral phases other than the common rock-forming minerals have been recognized in the Shogun deposit (Just, 1988), so that these five mineral associations are somewhat arbitrarily defined since some element-organic matter associations may not be true minerals *e.g.* the U-organic phase "thucholite" (Ellsworth, 1928) whereas other associations may be a combination *e.g.* trace metals complexed by organic matter which is in turn adsorbed onto a clay substrate.

Although the mineralogical description of Just, (1988) relates to the Shogun deposit, many parallels can be drawn with other U-trace element organic-matter deposits and hence is included here in the discussion for reference. A compilation of the minerals and elemental groupings identified the Shogun and Ambassador deposits is presented in Table 2.1. This list is incomplete, particularly for the Ambassador deposit, and will be the subject of further mineralogical analysis using SEM. Many of the minerals or elemental associations listed in the table may have been placed in one or more categories (*e.g*. zircon, heavy minerals/oxide). Where possible, common mineral names have been used in the table. A selection of minerals from the redox front of the Ambassador deposit are shown in SEM photomicrographs in Plates 2.1 and 2.2.

Table 2.1: Mineralogy of the Shogun and Ambassador deposits

Mineral / Element	Shogun Deposit	Ambassador Deposit
Organic	U, Ti, V, Cr, REE	U, Ti, V, Fe-Ti, REE
Sulfide / Sulfate	Pyrite, Galena, Sphalerite, Covellite, Chalcocite, Polydymite, Anglesite, Gypsum, Barite, U-S, CoNiCoMoU-S, REE-Ca-S	Pyrite, Galena, Sphalerite, FeNiCo-S, FeZnCd-S, FeTi-S, ZnNiCoFe-S, CeSmNd-S, CaCeSmNd-S, UFeZnCoNi-S, U-S, UFeZnNi-S, FeTiVSe-S, CaCdCeFeNiZn-SO_4,
Silicate / Oxide / Native	Coffinite, Rutile, Ilmenite, Se, Pb-Se, Hg-Se, Cu-Se, PbAg-Se, PbCu-Cl	PbTiV, Se, CeSmNd-Si, CaCeSmNd-Si, S, Au-Te, Au
Detrital	Quartz, Kaolinite	Quartz, Kaolinite
Heavy Minerals	Baddelyite, Leucoxene, Oyamalite, Apatite, Ilmenite, Xenotime, Rutile, Zircon, Cassiterite, Hematite, Magnetite, Monazite, Columbite	Zircon, Ilmenite

(i) Organically complexed trace elements and radionuclides

Complexation by amorphous organic (humic) matter and subsequent diagenesis to form a suite of authigenic minerals accounts for the majority of minerals encountered in many U-trace element-organic matter deposits. Uranium associated with organic matter generally occurs as a diffuse impregnation within the organic matrix. The association of diffusely distributed U in organic matrices has been recognized from many organic-hosted U deposits including black shales and coals (Ahmad and Finlay, 1987), lignites (Ilger *et al*., 1987) and bitumens (Parnell, 1988, Eakin and Gize, 1992). The morphology of the U-organic matter association has been the subject of numerous studies to determine the exact association (*e.g.* Vassiliou, 1980, Ilger *et al*., 1987, Finkelman, 1982).

Plates 2.1 and 2.2: SEM photomicrographs of Ambassador samples

(a) Sample 6037, "Cubic" pyrite ringing quartz grains in a framboidal pyrite matrix

(b) Sample 6037, Bright patches in kaolinite/organic matrix are Ti-rich zones

(c) Sample 6101, ZnCdNiFeUS grains (teeth shape), bright blotches are $CaCdCeFeNiZnSO_4$ crystals

(d) Sample 6081, Detrital zircon showing evidence of dissolution along cleavages

(e) Sample 6081, Amorphous Ti-Fe oxide (RHS) and detrital zircon (LHS)

(f) Sample 6070, Grain of Ce(SmNd)CaSi surrounded by quartz grains

(g) Sample 6101, "Plate" of UFeCoNiZnS and US (?) (centre field) on $FeNiCoSO_4$ (?) (bright background) and $ZnNiCoFeSO_4$ (?) (crystal aggregate)

(h) Sample 6037, Irregular patch of FeTiS set in a Ti-rich kaolinite/lignite matrix

(i) Sample 6101, Grain of UFeNiZnS growing crystals of $CoNiZnFeSO_4$ (?) in its centre

(j) Sample 6117: Composite grain of CeNdSmGdS (bright) and clay (dark) in kaolinite/lignite matrix

(k) Sample 6117: Grains of FeTiVSeS in kaolinite/lignite matrix

(l) Sample 6099: Small (<1 m) spherules of CeNdSmGdS in between quartz grains (grey) and kaolinite/lignite matrix (black)

Plate 2.1: SEM photomicrographs of Ambassador samples (1)

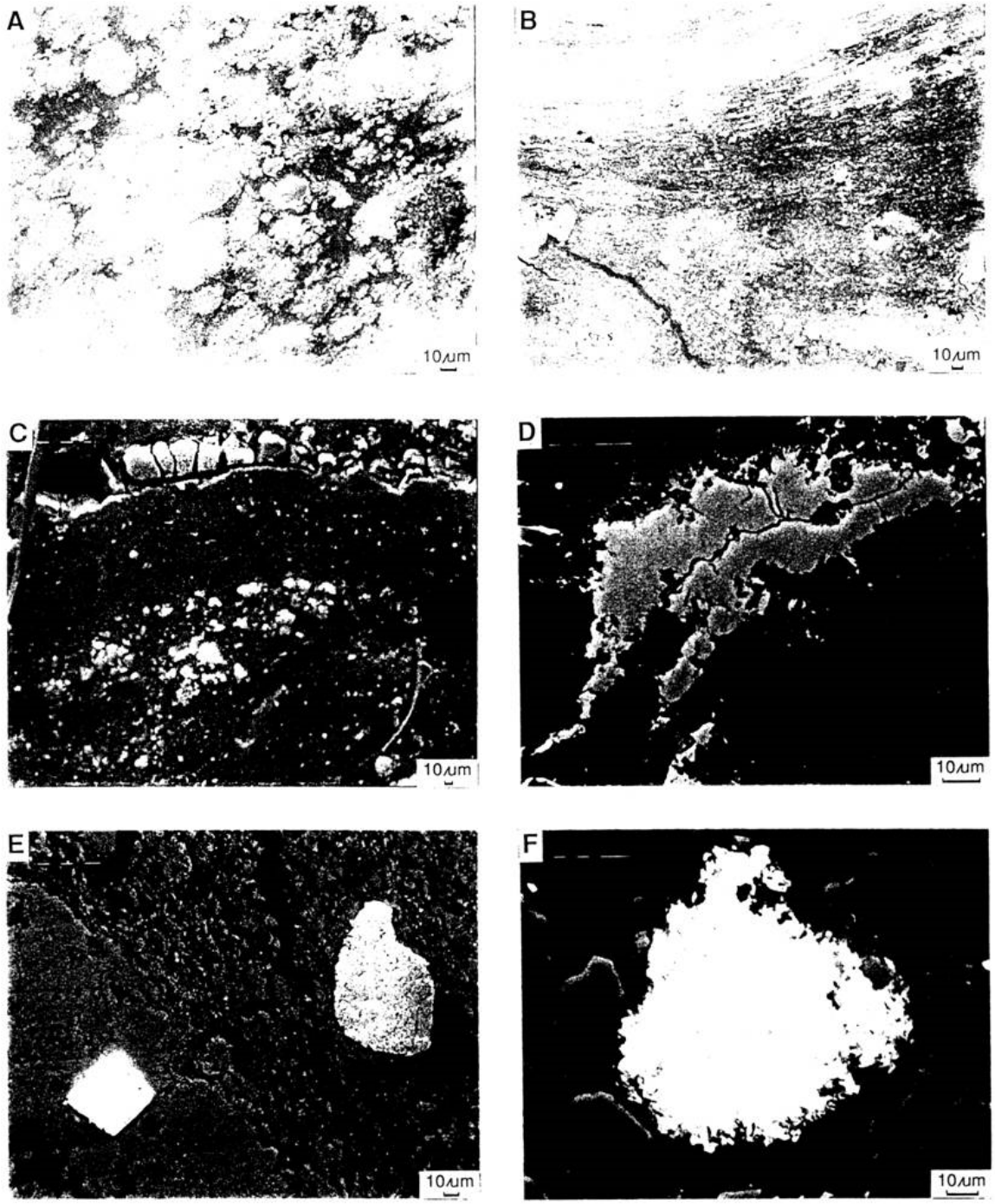

Plate 2.2: SEM photomicrographs of Ambassador samples (2)

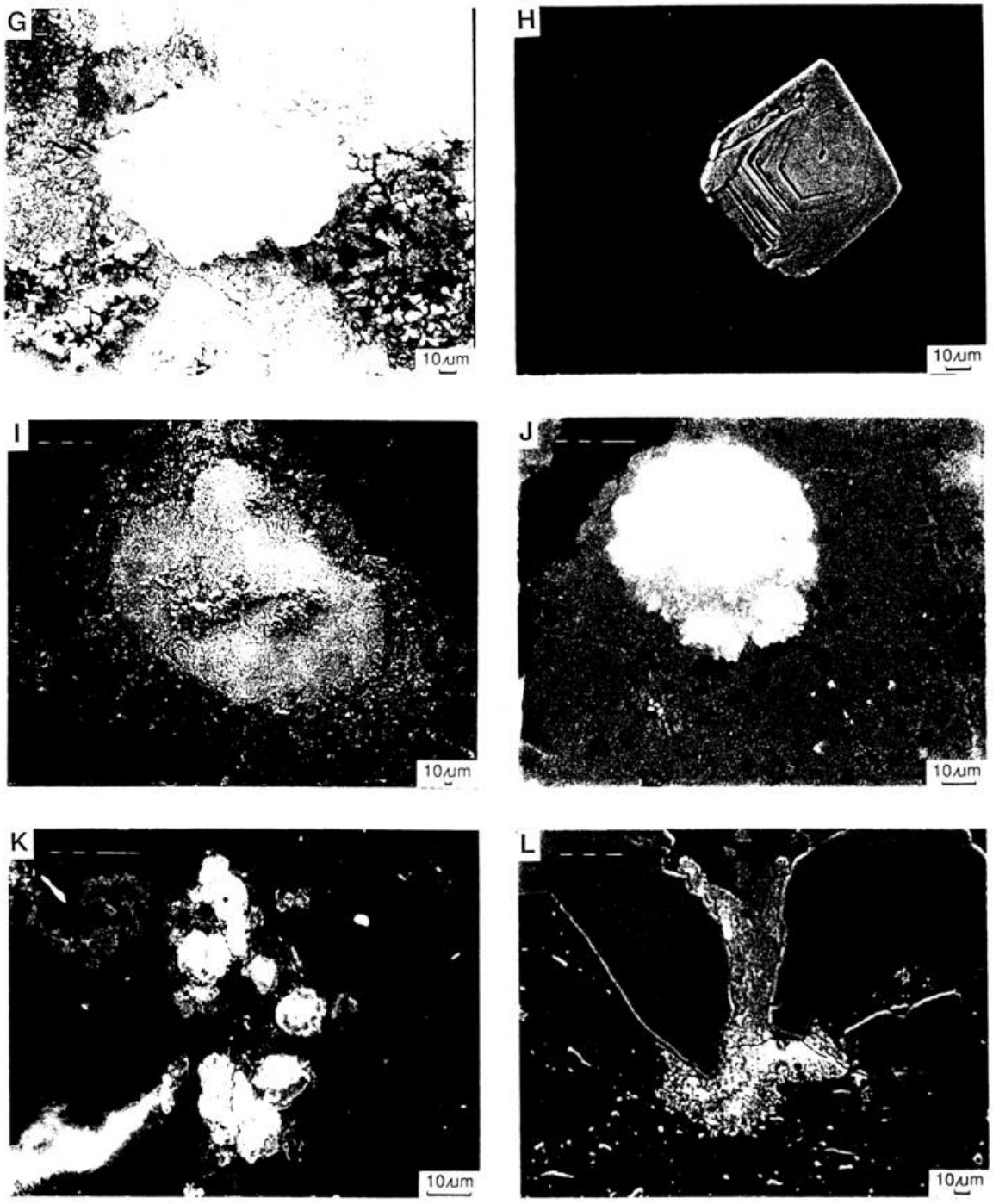

It has been demonstrated in a number of instances that the distribution of U in organic matter probably occurs in optically unresolvable microcrystalline phases or is truly amorphous in nature, with no U-minerals recognizable using X-ray diffraction (XRD), autoradiography or electron microprobe techniques. The presence of U-and REE-sulphide grains as spherules is common in a number of organic-hosted U deposits *e.g.* Petrova and Chistilin, (1987) and Meunier, *et al*., (1989), but the origin or significance (relevance) of these spherules is not known. Based on microprobe analysis (*e.g.* Parnell, 1988), Th, REE and some non-metals, particularly P, S and Se, are also thought to be associated with amorphous organic matter, but little work has been done on identifying the exact mode of the association.

In the Ambassador deposit, extraction of humic substances from samples in the present study suggests that significant proportions of U and other trace elements are bound directly to organic, matter probably in an ion-exchangeable form (Section 4.3). This finding is similar to other studies, which have extracted organic matter from U-rich organic samples.

(ii) Sulphide phases

Authigenic sulphide minerals are another common constituent of organic-hosted U deposits. The abundance of S is probably a legacy of the organic-rich material deposited in the palaeochannels, though later sulphate-rich groundwaters or marine aerosols may also be a potential source. Organic materials may contain a wide concentration of S, up to 0.1%, with peats commonly containing up to 0.5% (Aitken *et al*., 1985). Although the S is chemically bound to the organic material, it may be remobilized by a number of mechanisms, including the action of S-reducing bacteria (Nissenbaum and Kaplan, 1972; Bouska, 1981; McMahon and Chapelle, 1991), clay catalysis (Theng, 1974), thermal degradation (Hansley and Spirakis, 1992) and cleavage of S-functional groups via condensation reactions. Furthermore, the presence of framboidal pyrite in many deposits may indicate the action of micro-organisms in the reduction of S, and if H_2S was formed, (often as a result of microbial degradation of organic matter) this is known to have the capacity to directly reduce U (*e.g.* Meunier, 1991). The action of micro-organisms has also been shown to enrich the residual organic matter preferentially in N, S and O compounds (Landais, 1991), thus potentially increasing their complexing capacity. A consequence of the action of micro-organisms is the reduction in the amount of organic matter by up to 50% (Tissot and Welte, 1984).

In the Ambassador deposit, a number of different sulphide minerals occur as discrete crystalline grains spherules or irregular masses in the matrix, adjacent to quartz grains or infilling voids. The sulphide phases include pyrite (FeS_2), galena (PbS) and sphalerite (ZnS), but other transition metals (*e.g.* Co, Ni, Cd, Mo) and U are commonly present. Furthermore, discrete grains of U-sulphides and REE-sulphides are also present. Although sulphide minerals are ubiquitous in organic matter-rich deposits, *e.g.* Coutras, France, (Meunier *et al*., 1989), Morrison Formation, USA, (Hansley and Spirakis, 1992) and Streaky Bay, Australia, (Binks and Hooper, 1984), no other deposits have been documented that have as a diverse an assemblage of elements and minerals as that in the Shogun and Ambassador deposits. In this aspect these deposits are unique and should be the subject of further SEM and geochemical studies.

(iii) Silicate, oxide and native element phases

Authigenic silicate, oxide and native element associations are common in U-rich organic matter deposits; the native elements in particular are a consequence of the reduced environment. One of the major mineral groups

of interest are U- and Ti- bearing silicate and oxide minerals *e.g.*, coffinite ($USiO_4$), U-Ti phases (*e.g.* brannerite, $UTiO_6$) and authigenic FeTi and Ti oxides (*e.g.* ilmenite, $FeTiO_3$; rutile and anatase, TiO_2). The close mineralogical and spatial association of secondary U-Ti minerals commonly observed in U-rich organic matter deposits suggests a common paragenesis.

The U-Ti association is quite common in sandstone type U-deposits (*e.g.* Reynolds and Goldhaber, 1978; Pointer *et al*., 1989) and occurs by a series of interrelated reactions-

$$UO_2 + 2TiO_2 \longrightarrow UTi_2O_6$$

$$UO_2 + 3SiO_2 \longrightarrow USiO_4$$

$$USiO_4 + 2TiO_2 \longrightarrow UTi_2O_6 + SiO_2$$

Coffinite probably forms as the result of precipitation of a solution supersaturated in silica (possibly due to increased solubilization by organic matter) and U, with U simultaneously adsorbing on a SiO_2 precipitate: the maximum adsorption occurring at neutral to acid pH (Nguyen-Trung, 1985, Goldhaber, *et al*. 1987). TiO_2,although requiring very low pH for dissolution, is probably solubilized in a similar way to SiO_2, resulting in the formation of a U-Ti-Si association.

The method of paragenesis for U-Si-Ti phases outlined above may explain the mineralogical relationships observed in the Mulga Rock deposits, particularly the presence of authigenic needles of Fe-Ti or Ti oxides due to remobilization of Ti and the precipitation of U as oxides and coffinite in leucoxenised ilmenite pseudomorphs. Additionally, the stability field for coffinite has been demonstrated to overlap the sulphide-sulphate reduction boundary at a pH between 7 and 8, resulting in the formation of cogenetic coffinite and pyrite. This has been observed in other deposits (Brookins, 1988) and may explain the presence of U sulphide minerals identified by SEM studies of the Ambassador deposit.

The presence of Se as native Se as Se needles (Meunier *et al*. 1989) or as selenides in U-trace element-rich organic matter deposits is indicative of the redistribution of Se, probably sourced from the organic matter. Selenium in low rank coals is often associated with pyrite and may reach concentrations of several tens of ppm (Swaine, 1990). Selenium has a large stability field under transitional to reducing conditions, especially at low pH (Brookins, 1988) and is a common constituent of sandstone-type U deposits. Native Se needles have also been observed at the Shogun deposit.

An assemblage of unusual silicate minerals may also be found in organic-rich deposits, presumably due to the enhanced solubility of Si and trace elements in these environments. In the Shogun deposit, there is a phase mostly containing Ca, Ce, Sm and Nd with traces of S, Si and U occurring as acicular crystals (Just, 1988). The paragenesis of this mineral is difficult to explain, but may possibly be due to the saturation of solutions/colloids enriched in REE at the redox front. Similar Ca-REE -Si mineral assemblages have been identified at the Mary Kathleen U-REE skarn in Queensland, *e.g.* Stillwellite-(REE, Ca) $BSiO_5$ (Kwak and Abeysinghe, 1987), but these minerals are hydrothermal in origin and thus cannot be directly equated with those of low temperature organic-rich deposits.

Studies of the Ambassador deposit also show that it contains of a number of unique silicate minerals, many of which have not been previously identified. One of the most interesting minerals is an assemblage of composite grains up to 50 microns in size which are composed of a Ca-light rare earth element (LREE) silicate, containing Ca, Ce, Sm, Nd and Si, which occurs infilling spaces in the kaolinite/lignite matrix (Pascoe, 1991).

(iv) Detrital silicate minerals (e.g. clays and quartz)

The mineral association involving detrital silicate minerals may constitute a major proportion of the mineralized palaeochannel sediments in U-trace element enriched organic deposits. The two major silicate phases are commonly quartz, which occurs as detrital grains, and kaolinite, which occurs as fine particles intimately associated with organic matter. The relatively low cation exchange capacities (CEC) of quartz (0 meq/100g) and kaolinite (3-5 meq/100g), compared to that of organic matter (up to 300 meq/100g) (Stevenson, 1985), indicates that the detrital silicate phases are probably not important in terms of geochemical enrichment. In organic-rich systems, however, the function of clays such as kaolinites may be two-fold, namely as a *catalyst* for the degradation of organic matter, and as a *substrate* to which organic matter may attach or intercalate, thereby restricting the mobility of the organic matter and increasing the CEC of the clay. It is well established that the surface properties of clays and quartz can be modified by the presence of even a monolayer of natural organic (humic) matter, such that they have similar surface charge characteristics and complexing capacity to the organic matter (Beckett and Le, 1990). This has important consequences for the distribution of elements such as U, which are observed to be diffusely distributed within the kaolinite/organic matter matrix and thus may be complexed either by organic matter which is associated with kaolinite or by free organic matter.

(v) Heavy mineral associations

Heavy minerals are not a common constituent of organic deposits, as they tend to be separated from the less dense organic matter during sedimentation. The heavy minerals in the organic matter of the Shogun deposit are predominantly zircon, rutile, ilmenite, anatase, cassiterite, monazite and xenotime. Many of these minerals are etched or show evidence of partial dissolution, which indicates that they could be a partial source of the REE in the deposit. However, the abundance is insufficient to account for the total observed REE concentrations (Just, 1989). In other organic deposits, many elements normally found in these heavy minerals are thought to be associated with the organic matter: *e.g.* Zr (Ward, 1980) and Ti, (Mc Intyre *et al*., 1985). This is a further indication of the function of organic matter in the solubilization and redistribution of elements originally associated with detrital heavy mineral phases.

The heavy mineral assemblage in the Ambassador deposit appears to be similar to that observed in the Shogun deposit. However, SEM observations and the results of sequential extraction experiments suggest that a significant proportion of the REE and Th are associated with both organic matter and sulphides (Section 4.3), whereas in Shogun, the REE occur in phosphates (monazite and xenotime). This suggests that these minerals have been destroyed in the organic-rich environment.

2.2.3 Conclusions

The study of a number of U and trace element-rich organic deposits has shown that they have a diverse and unique range of minerals. Additionally, a significant proportion of the U and trace elements may be directly associated with the organic matter, probably in ion-exchangeable sites. The ubiquitous presence of organic

matter may also catalyse the dissolution of detrital minerals and be integral in the formation of a number of new minerals, especially U and Ti silicates. The abundance of S, in combination with a reducing, low temperature environment, also results in the formation of a suite of REE-U-trace element sulphides, an assemblage that may be unique to the Ambassador deposit.

2.3 Transport and complexation of U and trace elements in organic rich groundwaters

2.3.1 Introduction

Characterization of the mechanisms of complexation, transport and enrichment of U and trace elements is essential to determining the genesis of metal-rich organic deposits. It is particularly important in deposits such as Mulga Rock, where a primary point source of U and trace elements has not been identified and it is probable that diagenetic groundwater processes have been crucial to the formation of a narrow zone of high grade mineralization. In this section the principal mechanisms of complexation, transport and precipitation of U and trace elements in environments rich in organic matter are reviewed and discussed in terms of their significance to the genesis of the Mulga Rock deposits.

2.3.2 Colloid formation and transport of U and trace elements

Over the last decade colloids have been recognized as one of the major mechanisms for the aqueous transport of trace elements and radionuclides (Mc Carthy and Zachara, 1989 and references contained therein). Numerous studies have examined the dispersion of radionuclides from model nuclear waste disposal sites and mining operations (*e.g.* Choppin, 1988; Short *et al*., 1988; Bates *et al*., 1992; Moulin and Ouzounian, 1992). Colloids may be composed of both inorganic and organic (humic) substances and are classified on the basis of their size (1-0.001 µm) rather than chemical composition. As a consequence of their small size and their surface properties, colloids posses an enormous theoretical surface area (*e.g.* >1000 m^2/g) and a high specific surface energy and thus may have a high sorption capacity for dissolved species. Furthermore, the generally negative surface charge of aqueous colloids means that aggregation only occurs under specific circumstances; colloids thus may remain in suspension for extended periods and be transported appreciable distances. Colloidal material in groundwater may undergo a number of reactions which, due to their inherently high surface areas, may proceed at substantially faster rates than for larger particles and thus may be particularly sensitive to changes in groundwater parameters such as Eh and pH. These reactions include aggregation, coagulation, dissolution and adsorption to aquifer surfaces, migration and filtration; the last two processes being functions of the porosity and permeability of the aquifer system (Avogadro and De Marsily, 1984; Moulin and Ouzounian, 1992).

Numerous studies have demonstrated that for many elements and, in particular, members of the actinide series (*e.g.,* Th and U), colloidal transport is the dominant mechanism for redistribution and concentration. Colloidal species may also accelerate the transport of radionuclides (particularly actinides) in groundwater (Nutall *et al*., 1992), and hence may be responsible for the concentration of adsorbed radionuclides and trace elements in zones of aggregation or low colloid mobility, or in geochemical environments where desorption of actinide species from the colloid surface occurs.

There are four principal mechanisms of colloidal formation, and each of these may have been responsible at Mulga Rock for the transport to, and the deposition of, U and trace elements at the redox front. The relative

amount of each colloidal species involved will however, be a function of the prevailing physiochemical (micro) environment. The mechanisms of colloid formation are-

(i) Coagulation of organic (humic) materials

Organic (humic) materials form the major component of organic-C in natural waters (Thurman, 1985). They may be thought of as complex polyelectrolytes (macromolecules), of high molecular weight, that contain a complex array of organic functional groups (ligands) including carboxylic acids, aliphatic and aromatic alcohols, aldehydes, ketones and methoxy groups (Aitken *et al*., 1985). Humic materials remain soluble over a wide pH range, although the degree of protonation or, the complexation of functional groups by metals, may vary. Humic materials may also function as multidentate ligands where the metals have a charge greater than one. Where metal concentrations are significant and have a charge greater than one, the degree of complexation by humic materials may be also high, thereby reducing the effective surface charge of the humic matter and changing the conformational characteristics of the humic (macro) molecule. This process of charge neutralization, coupled with conformational changes and the possibility of bridging of individual humic (macro) molecules by metal ions, may cause a reduction in solubility and result in the formation of an organic colloid or the precipitation of the humic-metal complex. This is an important mechanism by which the organic fraction of sediments becomes enriched in trace metals and radionuclides as metals ions involved in this complexation process may become irreversibly bound. It has also been demonstrated that the sorption of humic materials confers a negative surface charge on substrates as diverse as clays and iron oxides irrespective of their original surface charge (*e.g.* Ho and Miller, 1985). This has important implications for the subsequent uptake of trace elements and radionuclides because it is the humic materials rather than the substrates that determine the sorption capacity of the particle [Section 2.2.2 (iv)].

The mobility of colloidal particles is determined by the relative ionization of the humic materials, which will be a function of the degree of protonation (*i.e.,* pH) and the amount of complexed species. At pH greater than 7, most of the humic functional groups are ionized, interparticle electrostatic repulsion is high and the particles will be highly mobile. At intermediate pH values (approximately 4-7), complexation by humic materials is at a maximum for most dissolved species and particle mobility is intermediate due to a moderate degree of complexation of the functional groups. At pH less than 4 complexation of dissolved species is at a minimum and the degree of functional group complexation by protons is high, and mobility of the particles is low, due to charge neutralization leading to aggregation and/or coagulation.

(ii) Formation of silica-rich organic colloids

At the pH values between 4 and 8, which matches that of the Ambassador groundwaters, silica may be readily dissolved where humic material is abundant and be transported as a humic complex. Numerous studies have demonstrated the increased solubility of silicate materials in the presence of natural organic matter (*e.g.* Iler, 1979, Bennett and Siegel, 1987) and the redistribution of silica in organic rich deposits (Hansley and Spirakis, 1992). The mobility of silica colloids is particularly sensitive to changes in pH and ionic strength (Iler, 1979), with the maximum mobility in the range 5-7 in the presence of cationic species. This is also the pH range that corresponds to the maximum uptake capacity for most metals, because there is little competition from protons for adsorption sites and no tendency for metals to form insoluble hydroxyl species. In addition metal coatings are known to form on silica colloids (*e.g.* Al, Cr, Ga, Ti and Zr) and may form a positively charged

interface between the negative surfaces of silica colloids and dissolved humic species. Below approximately pH 5, silica colloids become protonated, lose the majority of their surface charge, and hence their mobility. Above pH 7, silica colloids precipitate as gels; this process may be enhanced by the presence of organic matter which may, through hydrogen bonding, link individual silica colloids.

Actinide species, specifically UO_2^{2+} and Th^{4+}, may also be adsorbed at low pH by SiOH groups that are not normally ionized and hence this is a further mechanism by which actinide species, even at low pH, may be redistributed and concentrated by colloidal species. Humic-silica colloids that have the ability to bind actinides (*e.g.* Th) strongly are known to occur in groundwaters (Lieser and Hill, 1992). Similarly, the presence of coffinite indicates coprecipitation of U and Si probably following remobilization as organic complexes (*e.g.* Pointer *et al*., 1989; Eakin and Gize, 1992).

(iii) Formation of pseudo colloids

Pseudo-colloids are a subset of the previous colloid types described, and form when elements in a dissolved or colloidal form become bound to existing colloidal species in the groundwater (Bates *et al*., 1992). These colloids may be important in an environment where perturbations to the physiochemical state of groundwater systems *e.g.* changes in pH, Eh and ionic strength may cause aggregation/dissolution and/or adsorption reactions to occur and thus may alter the speciation of trace metals and radionuclides.

(iv) Intrinsic or eigencolloids

Intrinsic or eigencolloids are a type of colloid that forms due to the precipitation (aggregation) from solution of a solid phase containing a single cation species (Lieser and Hill, 1992). Such colloids frequently form by hydrolysis reactions of actinide species (*e.g.* U, Th) (Moulin and Ouzounian, 1992) although Fe and Al eigencolloids are also known. Intrinsic colloids (termed radiocolloids when composed of a single actinide species only) have been the

subject of many investigations, especially in regards to the modelling of dispersion of nuclear wastes in groundwaters (Short, *et al*., 1988; Maiti *et al*., 1989; Bates, 1992), because they may be present in relatively actinide-rich groundwaters.

All of the colloid types discussed above may have participated in the formation of the Ambassador deposit. Although U was probably transported throughout the Yilgarn as dissolved carbonate complexes, once they reached the mildly acidic, organic rich environment of Mulga Rock, most of the U and trace elements would have been associated with colloidal material and only a minor amount with truly dissolved species. At the present pH of the Ambassador deposit (pH 4-8) it is likely that organic colloids will dominate any active transport and enrichment processes in the groundwater. However, if the groundwater pH was lower in the past, silica colloids may have also been significant. The preferential association of some of the radionuclides with, and transport by, certain colloid types may also explain the U-series disequilibrium observed in the Ambassador deposit. Additionally, sampling of groundwater colloidal material on both a local and regional scale may be a valuable exploration tool in the search for other concealed palaeochannel deposits (Section 10.2).

2.3.3 Radionuclide and trace element complexation by organic matter

The importance of organic matter as a complexing agent for radionuclides and trace elements has already been highlighted in the study of the mineralogy of the Ambassador deposit and in the study of numerous geological analogues. In this section, the affinity of U, other radionuclides (*e.g*. Th) and trace elements (*e.g.*, V, Mo Se) for organic (humic) matter will be reviewed.

Numerous studies have examined the affinity of the UO_2^{2+} (uranyl) ion for organic matter (*e.g.* Li *et al*., 1980; Nash *et al*., 1981; Shanbag and Choppin, 1981b; Nakashima *et al.*, 1984; Van der Weijden and Van Leeuwen, 1985; Giesy *et al*., 1986), with the consensus being that the optimal pH range for the adsorption for the UO_2^{2+} ion is approximately 4-6 (*e.g.* Disnar, 1981; Idiz *et al.*, 1986; Noller and Hart, 1992). As discussed in Section 2.3.2, neutral to slightly acidic conditions are optimal for the adsorption of trace metals by a number of inorganic and organic surfaces because at low pH, there is competition for adsorption sites by protons, whereas, at higher pH values soluble metal hydroxides may form. Studies of the speciation of U *in vitro* and its transport in natural waters indicate that where organic matter is present a significant amount of the U will be transported as a organic matter complex (*e.g.* Giesy *et al.*, 1986). Estimates of the U transported as organic matter complexes varies between approximately 5 and 95 %, dependent on factors such as pH, ionic strength, organic matter concentration and competition from other strong complexing species such as bicarbonate. At high pH, carbonate/bicarbonate species form extremely stable ligands, especially in the case of uranyl ions (*e.g.* Langmuir, 1978) and thus remain as dissolved species. Uranyl di- and tri- carbonate complexes are considered to be the dominant species responsible for U mobility in the northern Yilgarn Block and are associated with the formation of calcrete U deposits in that area (Mann and Deutsher, 1978). Little U is complexed by organic matter above pH 7.5 (Read *et al.*, 1992), because of the competition from carbonate species for the complexation (Zielinski and Meier, 1988). A schematic speciation diagram of the UO_2^{2+}-humic acid-carbonate system is shown in Figure 2.1.

Figure 2.1 Speciation of the uranyl (UO_2^{2+}) ion in the system UO_2^{2+}-humic acid [HA]-CO_3^{2-}

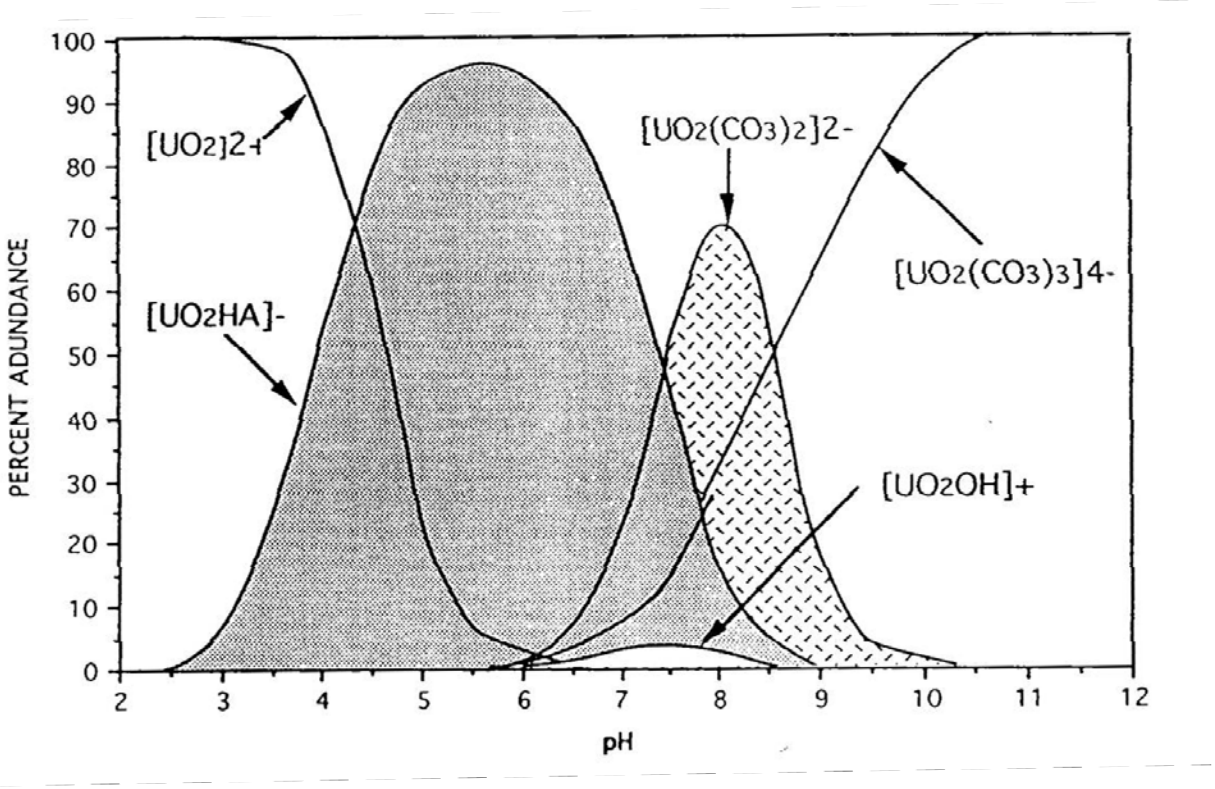

Studies of the complexation of U by peats have shown that peat-derived humic acids may commonly concentrate U in excess of 10,000 times over associated waters (Szalay, 1964, Van der Weijden and Van Leeuwin, 1985)

The mechanism of bonding of the UO_2^{2+} ion to organic matter has also been investigated extensively, with the conclusion that the carboxylate (-COOH) functional group is the dominant binding species at low to intermediate acidic pH, although multiple and/or continuous bonding site behaviour has been observed (Li *et al*., 1980, Giesy *et al.*, 1986) over a wide range of pH. This is consistent with the fact that most carboxylate functional groups are ionized within the low to intermediate acidic pH range, with the degree of ionization and hence the strength of the complexation being dependant on substituent effects from the parent organic macromolecule to which the functional group is attached. Stability constants for the UO_2^{2+}-humate bond also indicate that, once this bond is formed, it is very stable (Nash *et al*., 1981, Shanbhag and Choppin, 1981b) and is not easily displaced by competition from other cationic species. This stability of the uranyl (UO_2^{2+})-humate bond may be due to two factors-

1. dehydration of the cationic uranyl ion is associated with a large positive entropy change (Shanbhag and Choppin, 1981b), and
2. because of the number of potential formal and van der Waals binding sites on the uranyl ion, conformational changes in the organic matter that occur during the bonding process may sterically and electrostatically hinder approaches from other cationic species. This type of strong and weak bonding interaction is supported by a two step binding mechanism advocated by Gaffney *et al.,* (1992)

who propose that there is an initial rapid uptake step (strong complexation), followed by conformational folding of the humic macromolecule (weak interaction).

The uranyl-organic complex is more than 1,000 times stronger than the equivalent Ca-organic complex (Shanbhag and Choppin, 1981a, b). If Ca is the main coagulant of the organic matter (Douglas unpubl. data), this may be subsequently displaced by the uranyl ion, which is essentially irreversibly bound to the organic matter. This mechanism assumes, however, that the Ca is relatively easily displaced after complexation. Alternatively, it has been suggested that the molar Ca/U ratio in groundwaters (as a measure of the relative abundance of U to the total dissolved salts in the groundwater) may be the critical factor in explaining why there are sporadic occurrences of anomalously high concentrations of U in organic matter-rich non-marine sediments and peat bogs (Idiz *et al.,* 1986). It is thought that unless elevated concentrations of U relative to Ca, in addition to low pH, are present in percolating groundwaters, significant mineralization will not occur because all binding sites within the organic matter will have been sequestered by Ca.

The distribution (speciation) of U as a function of molecular weight of the organic matter extracted from solid materials indicates that there is a significant amount of U associated with nominally "dissolved" low molecular weight organic material (Zielinski *et al*., 1988), in some cases <2,000MW (Read *et al*., 1992). Furthermore, it has been recognised that a pH dependency may exist in terms of the distribution of the uranyl species between different molecular weight size fractions (Li *et al*., 1980).

Studies by Nash *et al.,* (1981), Vassiliou (1986), Zielinski and Meunier (1988) and Read *et al.*, (1992), indicate that no formal reduction of the uranyl ion occurs after bonding to organic matter. The lack of reduction may be due to an exceedingly slow kinetics. However, if there is sustained low Eh during diagenesis or metamorphism, reduction of the uranyl ion may occur. The mechanism by which the uranyl ion may be reduced in the presence of organic matter during post-depositional (diagenetic) processes usually involve changes in the structure of the organic matter via maturation (oxidation) of organic functional groups such as carboxylic acids or aldehydes as below (*e.g.* Nakashima *et al*., 1984)

$$\underset{\text{ALDEHYDE}}{UO_2^{2+} + RCHO} + H_2O \longrightarrow UO_2 + \underset{\text{CARBOXYLIC ACID}}{RCOOH} + 2H^+$$

or aliphatic chains (Leventhal, *et al*., 1986)

$$\underset{\text{ALKANE}}{UO_2^{2+} + RCH_2CH_3} \longrightarrow UO_2 + \underset{\text{ALKENE}}{RCH{=}CH_2} + 2H^+$$

where R is an organic macromolecule.

This mechanism is also consistent with the findings of Doi *et al*., (1975), who demonstrated that the higher the rank of the organic matter (coal), the fewer the functional groups and hence the lower the binding capacity. Degradation of organic matter and reduction of the uranyl ion may also occur via radiation damage. This, however, is generally only recognizable in older organic deposits, in which features such as radiation haloes around U-bearing minerals can be seen (Eakin and Gize, 1992).

The assumption that actinide elements such as Th, have extremely low solubilities in aqueous systems (Lieser and Hill, 1992), and are predominantly associated with so-called residual minerals such as monazite, does not apply in organic-rich systems. Nevertheless this assumption still persists in the literature (*e.g.* Coutras deposit, Meunier *et al*., 1992). Thorium may be highly mobile in organic-rich surface and groundwater environments (Short *et al.*, 1988, Gaffney *et al*., 1992). Experiments have shown that Th forms strong complexes with organic matter (Bertha and Choppin, 1978). As with U, Th may be transported as organo-colloid species (Short *et al.*, 1988; Gaffney *et al*., 1992; Lieser and Hill, 1992) and hence behaves similarly to U and REE in organic rich-environments (Read *et al*., 1992). Furthermore, it has also been shown that once complexed by organic matter, Th has limited aqueous chemical reactivity, and becomes effectively decoupled from other Th species. If transport of the Th-humic complex occurs this leads to marked disequilibria in the Th decay series over time (Gaffney *et al*., 1992). This has a detrimental effect on attempts to date or determine the origin of groundwaters or aquifer systems using U-Th isotopic systems.

A geochemical association of a wide range of metallic and non-metallic cationic and anionic species is frequently observed in areas of sediment-hosted U mineralization, and in particular roll-front U deposits. The interest the elemental associations is due to the ostensibly different geochemical characteristics of these elements. The most common association includes the metals U, V, Mo and W, together with the non-metals As P and Se. The geochemistry of these elements in the sedimentary environment is complicated for two main reasons -

1. all have a wide range of oxidation states and hence highly variable redox chemistry and,
2. all form stable complexes with organic materials, the fundamental properties of which, such as stability constants or the pH dependency on formation of complexes are poorly known.

The only real exception is the extensive research undertaken on the geochemical properties of the uranyl UO_2^{2+} ion with organic matter, whereas for other elements only simple organic analogues such as salicylic acid have been used to model behaviour (Briet and Wanty, 1991). However, the geochemistry of these elements has a unifying property in that they form hydrated oxo-anion or cation species of the type ZO_x^{n+} with the trace element (Z) in a high oxidation state, usually +5 or +6. In contrast to organic complexes, the formation and properties of these hydrated oxo-cationic or anionic species have been studied extensively (Cotton and Wilkinson, 1980, Brookins, 1988, and the numerous references contained therein). The fact that many of the hydrated oxo-species are cationic, whereas others are anionic, may explain the intimate association of the elements in solid phase U minerals (*e.g.* autinite U-P, carnotite U-V). Furthermore, at intermediate pH (4-7.5), in the absence of organic matter, $UO_2(HPO_4)_2^{2-}$ has been demonstrated to be the dominant species (Langmuir, 1978). The complexation of both cationic and anionic species has been studied by Disnar (1981), who demonstrated strong complexation by algal organic matter of cationic species such as UO_2^{2+}, whereas anionic species such as MoO_4^{2-} were only weakly complexed.

Bioaccumulation by algae and bacteria is a well documented mechanism for the enrichment of radionuclides and trace elements in organic-rich environments such as bogs and peats where there is appreciable microbial activity (Sikora and Keeney, 1983). Bacterial species such as *Citrobacter sp*. can accumulate up to 9 grams of U per unit gram of dry weight of cellular biomass (Macaskie, *et al*., 1992). Other bacteria have been demonstrated to

concentrate U using a sulphate reduction mechanism (Monagheghi *et al*., 1985), and fungal species may also be efficient in the uptake of dissolved U (Tsezos and Volesky, 1982).

On the basis of the review of the complexation and transport of radionuclides and trace metals in organic-rich environments, a number of conclusions may be made regarding the mineralization of the Ambassador deposit. The pH of the groundwaters in the Ambassador deposit are moderately acidic, which is ideal for the complexation of U and trace elements by humic matter. Based on the relatively small data set available for the Ambassador groundwaters (Appendix 5), estimates of the U enrichment factor of the organic matter and the influence of Ca can be made. Uranium would be expected to be complexed by the solid organic matter some thousand times more than Ca, relative to the abundance of these elements in the groundwater. Assuming the concentration of U in groundwater is in the range 1-60 µg/L (ppb) and the average concentration in the solid is approximately 60 ppm, the solid/solution ratio is between 1,000 and 60,000, which is in broad agreement with the >10,000 concentration factor of U by peat estimated by Szalay (1964). Similarly, based on the very small data set available for groundwaters for the Ambassador deposit, it is estimated that the solid molar Ca/U ratio should be in the order of 10^2 which is in good agreement with the actual solid molar Ca/U ratio for the entire Ambassador area is approximately 150. If however, only the main mineralized zone is considered (for U concentrations >200 ppm), the solid molar Ca/U ratio (17) is approximately an order of magnitude too low. This significant enrichment of U may be due to either-

1. at the redox front, saturation of the groundwater in U species may have resulted in the formation of meta-stable solid U-bearing phases (*i.e.,* not organically bound), or
2. a degree of irreversibility of the organic matter-uranyl bond at elevated uranyl concentrations due to the aggregation of the organic matter. This has been demonstrated in Holocene peats, where U is not displaced by Cu (Zielinski and Meier, 1988), even though the Cu-organic complex is known to be extremely strong, in fact stronger than that of Ca to organic matter (*e.g.* Disnar, 1981).

2.3.4 Conclusion

A literature review has shown that the majority of radionuclides and trace elements in groundwater environments with pH<7 are transported as colloidal rather than dissolved species, particularly where the system contains abundant organic matter. The pH of the system is a strong determinant over the type of complexation. At moderately acidic pH (*ca.* 4-7), free organic macromolecules or colloidal organic complexes radionuclides and/or trace elements via carboxylate functional groups. For actinides (*i.e.* U and Th), this complexation is probably irreversible except in waters that have a high ionic strength, and in particular, are dominated by divalent cations such as Ca. At low pH, the only species capable of complexing radionuclides and trace elements are silica colloids, which are only protonated in very acid conditions. At high pH, carbonate/bicarbonate ligands dominate the complexation, particularly that of U. In addition, low molecular weight (<2,000 MW) organic matter is preferentially enriched in U, although pH may also determine the speciation between different organic matter molecular size fractions. Bioaccumulation by algal, fungal and bacterial species has been demonstrated to be a good mechanism for the concentration of U in organic environments and thus may represent an additional pathway of elemental enrichment.

Simple estimates of the enrichment of U by organic matter based on solid and groundwater geochemistry has shown that the enrichment factor for the Ambassador organic matter is consistent with other studies and that the concentration of Ca in the groundwaters may have a strong influence in the distribution of U. Furthermore, Th may be highly mobile in groundwaters in the presence of organic matter, and the association of a number of elements in U deposits (*e.g.* U, Se, Mo, V, W, P, As) may be due to the formation of similar hydrated oxo-cationic or anionic species that are complexed by organic matter.

3.0 MAJOR AND TRACE ELEMENT DISTRIBUTION IN THE AMBASSADOR DEPOSIT

3.1 Introduction

A geochemical and statistical study of the Ambassador deposit was undertaken in order to characterize the deposit in terms of the abundances, spatial distribution and the statistical relationships of the major and trace elements. This type of approach may assist in identifying elements or suites of elements that may be characteristic of palaeochannel mineralization and hence may be used as pathfinders in geochemical exploration. Furthermore, a study of inter-element relationships may potentially give an insight into the formation of, and the diagenetic processes operative in, organic-rich deposits. In addition, the Mulga Rock deposits appear to be unique in the high abundances and wide range of elements and in the diversity of the mineralogy, and this alone is sufficient justification for an extensive geochemical study.

3.2 Sampling and analysis

3.2.1 Sample selection

The initial objective has been to establish the areal distribution of a range of major and trace elements in the Ambassador channel, based on a constant comparable sample type. Samples were collected from drill holes on each alternate drill line and along the length of the channel, selecting the first metre below the redox front (as logged by PNC) for analysis. This 'ideal' sample was not always available, due to differences in sample selection and recovery. The analysed samples could thus include either:

(a) drill cuttings representing the first metre below the redox front;

(b) drill cuttings representing the first two metres below the redox front;

(c) composites of five 20 cm intervals of drill core.

In some rotary-drilled holes, the sample interval crossed the redox front; in such cases, the underlying sample was also analysed. In some core holes the recovery was poor and the one metre composite is incompletely represented; in one case only 8 cm was recovered. In hole CD 1577, ten 20 cm samples from the first two metres below the redox front were analysed, mean values for the upper (U-rich) metre were calculated.

3.2.2 Sample Preparation and analysis

Only very small quantities (8-70 g) were available for most samples. A representative reference was retained and the remainder disaggregated. Composites of the core samples were made by combining equal masses or equal volumes of the sub-samples. The disaggregated samples were pulverised in a manganese-steel ring mill to less than 75 microns. Over 230 samples were produced and were analysed as follows:

Neutron activation analysis (NAA), (Bequerel Laboratories Pty. Ltd.),
(As, Au, Br, Ce, Co, Cr, Cs, Hf, La, Lu, Sb, Sc, Se, Sm, Ta, Th, U, W, Yb, Zn)

X-ray fluorescence (XRF) using pressed powders, Phillips PW1220C instrument (CSIRO); by the methods of Norrish and Chappell, (1977) and Hart (1989).
(Ba, Bi, Cd, Cu, Ga, Ge, In, Mo, Nb, Ni, Pb, Rb, S, Sr, Tl, V, Y, Zn, Zr)

X-ray fluorescence (XRF) using fused glass discs, Phillips PW1480 instrument (CSIRO), The sample weight used was 1.6 g with Li borate used as the flux.
(SiO_2, Al_2O_3, Fe_2O_3, MnO, MgO, CaO, Na_2O, K_2O, TiO_2, P_2O_5, Cl)

Ignition of samples in porcelain crucibles in a muffle furnace at 1,000^{0}C (2 hours) to determine the concentration of organic matter as loss on ignition, (LOI)

The small quantities of material available necessitated the use of 10 g (rather than 30 g) for NAA, and for a few samples even smaller amounts were used. The high concentration of U in many of the samples caused some analytical interferences, particularly in NAA, and raised the detection limit of some elements.

Maps showing element distributions over the entire Ambassador channel and the main mineralized zones (referred to as the large and small areas respectively) are listed in the order in Table 3.1 and are contained in Appendix 1. Element distributions are shown as symbol plots. Histograms and cumulative frequency plots were used to determine the principal populations and hence the values of the intervals on the symbol plots.
The results of the geochemical analysis are tabulated in Appendix 2. The method of analysis of each of the elements tabulated in Appendix 2 is designated by the suffix .n for NAA, .p for XRF using pressed powders and .f for XRF using fused glass discs.

3.3 Statistical analysis of Ambassador geochemistry

3.3.1 Introduction

Statistical analysis of the Ambassador deposit was performed in an attempt to investigate the relationship between the 51 elements analysed. Niobium, In and Bi were not included in this analysis because only a few of the 149 redox front samples were above detection limits. A summary of the mean concentrations and standard deviations of the 51 elements analysed from the redox front of the Ambassador deposit are given in Table 3.1.

3.3.2 Statistical methods

Three methods of statistical analysis were used; linear regression (correlation coefficients) and two forms of cluster analysis. The first type of cluster analysis sought to group elements on the basis of inter-element relationships independent of location, a similar exercise to that performed in linear regression analysis. The second type of cluster analysis sought to group together sample locations (drillholes) as a result of geochemical similarities calculated on the basis of five groups of up to 20 elements.

3.3.3 Result and Discussion

(a) Linear regression analysis

Results of the linear regression analysis of the 49 elements is presented as a correlation matrix, with confidence levels >95%, >99% and >99.9% highlighted separately (Table 3.2).

Table 3.1: **Mean concentrations and standard deviations of elements analysed from the Ambassador redox front**

Suffix indicates analytical method: .n for NAA, .p for XRF using pressed powders and .f for XRF using fused glass discs

Element	Mean	Std. Dev.	Element	Mean	Std. Dev.
SiO_2.f	56.64	26.71	**Ge.x**	2	1
Al_2O_3.f	10.62	8.30	**Hf.n**	13	12
Fe_2O_3.f	1.62	1.54	**In.x**	3	0
MnO.f	0.01	0.01	**La.x**	123	183
MgO.f	0.41	0.35	**Lu.x**	1	2
CaO.f	0.35	0.43	**Mo.x**	16	15
Na_2O.f	0.82	0.65	**Nb.x**	59	128
K_2O.f	0.64	1.12	**Ni.x**	506	1593
TiO_2.f	1.29	1.09	**Pb.x**	88	144
P_2O_5.f	0.04	0.04	**Rb.x**	26	50
S.x	2.18	3.41	**Sb.x**	1	2
LOI	24.84	24.00	**Sc.x**	54	126
MAJORS	74.89	24.39	**Se.n**	44	168
As.n	12	16	**Sm.n**	43	67
Au.n	22	73	**Sr.x**	67	105
Ba.x	208	272	**Ta.n**	3	4
Bi.x	3	0	**Th.n**	23	27
Br.n	14	12	**Tl.n**	10	18
Cd.x	10	21	**U.n**	473	1035
Ce.n	325	507	**V.x**	158	161
Cl.f	6	11	**W.n**	12	31
Co.n	219	860	**Y.x**	102	148
Cr.n	131	187	**Yb.n**	9	12
Cs.n	2	3	**Zn.n**	1157	3105
Cu.x	483	1071	**Zr.n**	525	511
Eu.n	10	15	**TRACES**	4963	6280
Ga.x	17	16			

Uranium is significantly correlated with a number of elements at the 95% (Ca, S, LOI, Nb, Th), 99% (Ti, Ce, Cr, Lu, Ni, Sm, Y) and 99.9% (As, Co, Cu, Eu, La, Mo, Sc, Sm, Yb) confidence levels. Broadly, it appears that U is highly correlated with REE, elements associated with organic matter (LOI) *i.e.,* Ca, S and a number of trace elements, *e.g.,* Cu, Cr, Ti, Ni, As, Mo, many of which are common in other types of U deposits, especially roll front sandstone types. Additionally, the strong linear association of Nb and Th suggests that these elements may have been redistributed with U in the Ambassador deposit after the Nb and Th were derived from heavy minerals either within the Ambassador deposit or elsewhere.

Table 3.2: Correlation matrix of Ambassador major and trace element geochemistry

Significance of the correlations are shown at the 95-99% (outlined box), 99-99.9% (bold outlined box) and >99.9% (shaded box) confidence levels

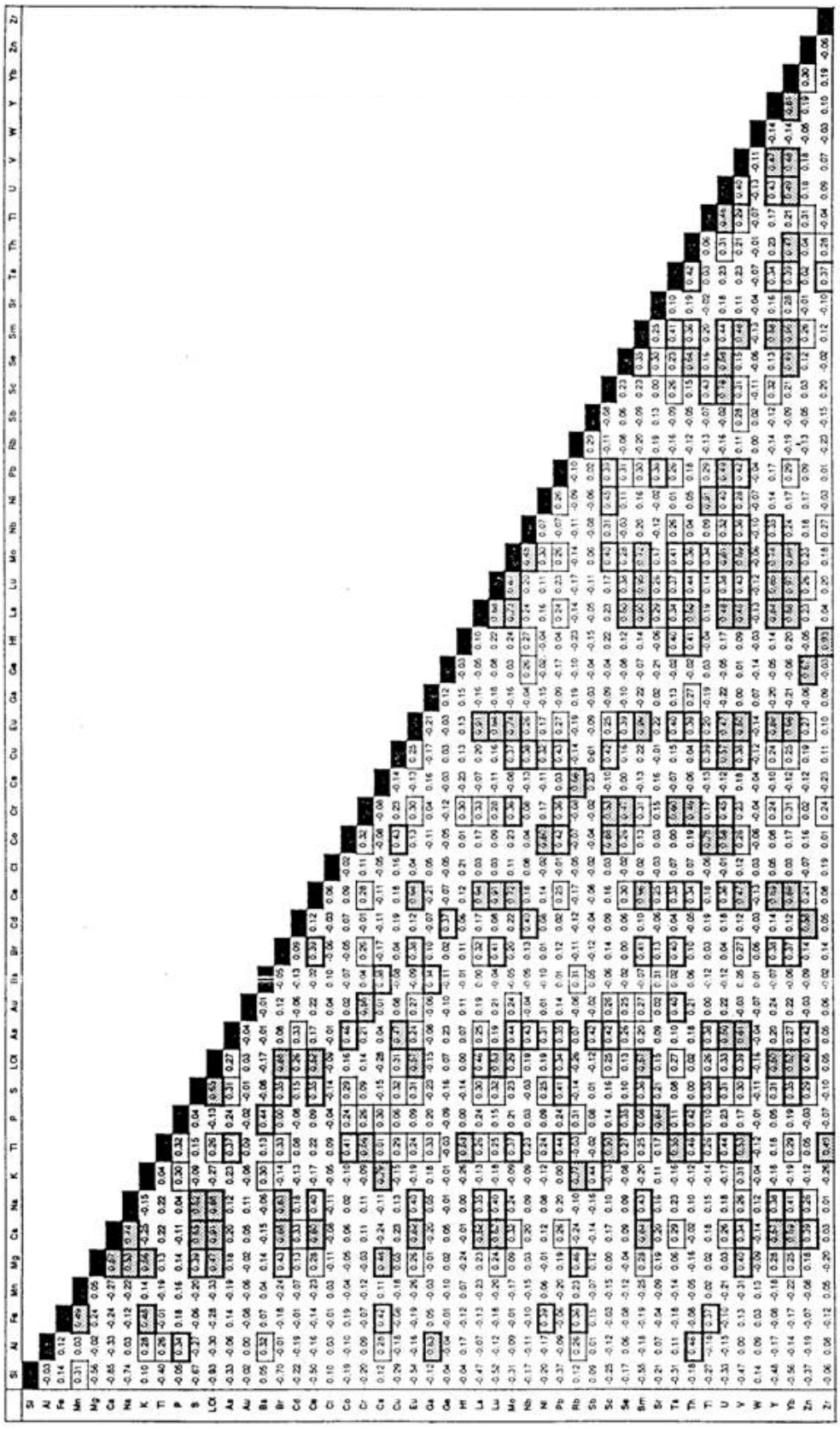

Some alkali and alkaline earth elements (Ca, Na) are highly correlated with LOI, probably being present as complexes in ion-exchangeable sites in organic matter. In contrast, the other alkalis (K, Cs, Rb) are correlated as with Al, Ba, Fe, Sb and V, suggesting that they are at least in part associated with a clay fraction. Some of the elements (*e.g*. Mg) appear to be associated with both organic matter and clays.

The strong association of LOI with a number of the REE and metals (Cd, Cu, Mo, Nb, Ni, Pb, Sc, Ta, Tl, U, V, Zn) suggests that a proportion of these elements are present as true organic complexes rather than in heavy minerals. Elements such as Zr, Ti, Cr, Hf, Nb, Ta and Th that are usually bound in resistant mineral phases are strongly associated with each other. No significant heavy mineral phases have been identified from mineralogical studies of the Ambassador deposit (Section 2.2.2) except for diffuse accumulations of Ti in the organic matter, so that the association may be due to similar geochemical behaviour of these elements in organic environments.

(b) Cluster analysis: inter-element associations

This cluster analysis technique was used to group elements on the basis of inter-element relationships independent of location, a similar exercise to that performed in linear regression analysis. The clustering algorithm (complete linkage cluster analysis) joins individual clusters as late as possible, in order to create a number of well-defined elemental groupings that are associated (clustered) as a result of geological or geochemical influences. The difference between this analysis and linear regression analysis is that the *average* Euclidian distance between *groups* of elements in n-dimensional space defines the association between the clusters. This has a distinct advantage over linear regression analysis which may yield a highly significant correlation score on the basis of one outlying data point.

The cluster analysis of the Ambassador deposit on the basis of major and trace element geochemistry has clearly defined seven clusters (Figure 3.1). In the discussion the term main mineralized zone is used to refer to the intensively drilled area immediately to the south of the confluence of the two south-western trending palaeochannels.

Cluster 1 (REE, As, V, Mo)
This cluster highlights the strong association between these elements, usually at the 99.9% confidence level, identified in the correlation matrix. The cause of the association between As, V, Mo and the REE is not clear, but their extensive hydrous chemistry (see Section 2.3.3) may be a factor. The spatial distribution of this cluster indicates that there is a relative enrichment of heavy REE down channel (west), which is paralleled by a similar distribution of V and to a lesser extent As. The spatial distribution of Mo appears to be similar to that of the light REE.

Cluster 2 (Pb, Cu, Ni, Co, Tl, Zn, U, Sc, Cr and Se)
This cluster defines a strong association between trace metals Se and U. Plots of the elements in this cluster (Appendix 1) show a close association between Cr with Se, and Cu with Pb and Ni, and Co with Zn and Tl in the main mineralized zone. Scandium has the closest association with U, and their distributions are almost identical, with Sc slightly more enriched in the western end of the channel. Both Sc (Ferguson and Winer, 1980) and Tl (Ikramuddin *et al*., 1983) have been identified as potential pathfinder elements in other U deposits. These close relationships are also evident in the adjacent clustering of these elements.

Figure 3.1 **Cluster diagram of Ambassador major and trace element geochemistry**

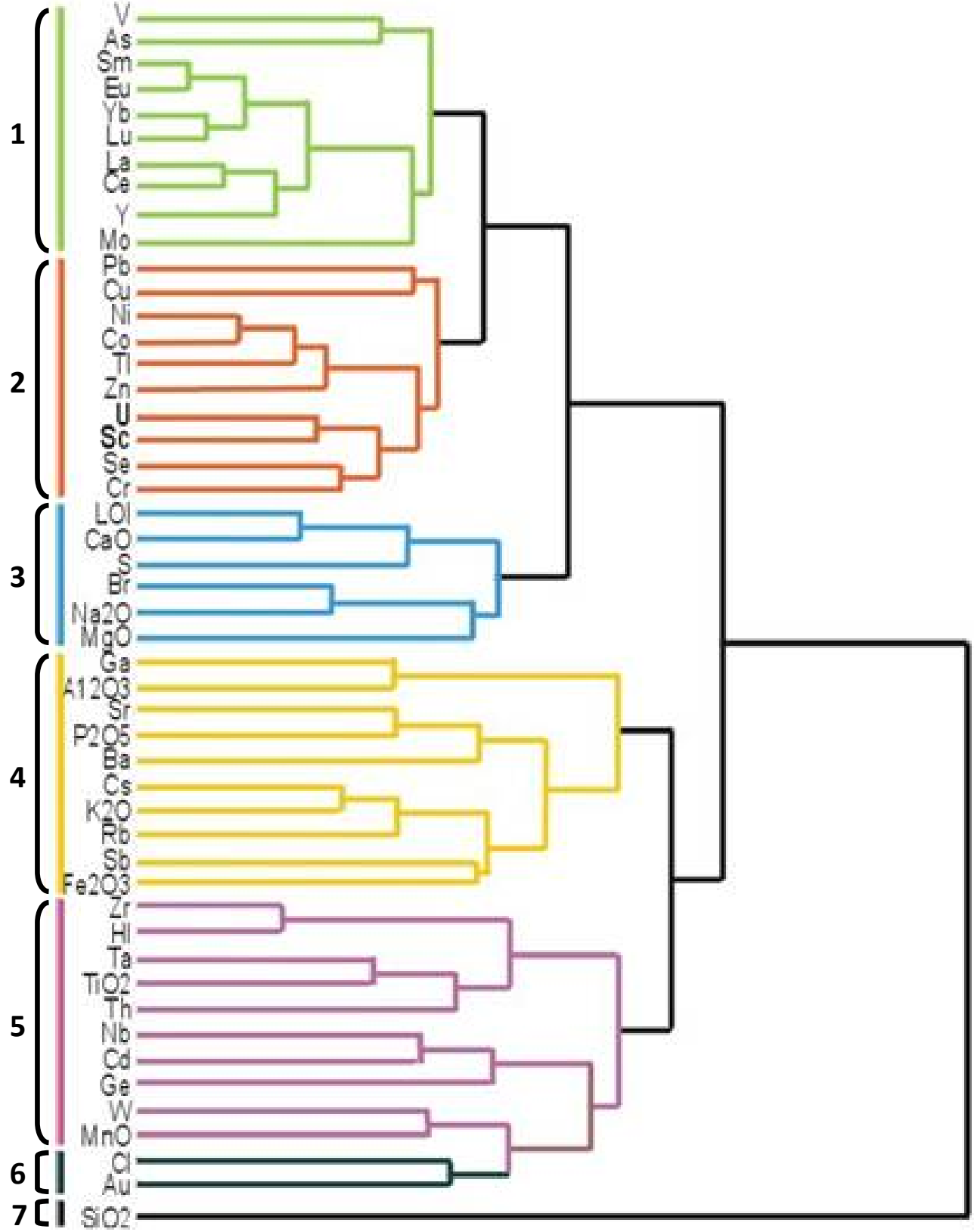

The close association of U and Sc may be a function of the similar ionic radii of Sc^{3+} and U^{6+} and their ability to form hydrous oxo salts (Cotton and Wilkinson, 1980) and hence they may be incorporated into similar structural sites in the organic matter. The geochemistry of Tl is poorly known, particularly in organic environments, however, Tl is known to form soluble aqua and chloride complexes (Cotton and Wilkinson, 1980).

Cluster 3 (LOI, CaO, Na_2O, MgO, S, Br)

This cluster defines a group of elements that are naturally associated with organic matter, either present as cations bonded to functional groups (CaO, Na_2O, MgO) or as a mostly structural (functional group) component (S, Br). Some of the sulphur that was probably originally associated with the organic matter has been reduced to form authigenic sulphides (Section 2.2.2), and some of the S and Br may have been introduced via groundwaters (Section 10.1.1). The spatial distribution of CaO and LOI are almost identical and clearly define the presence of organic matter in the palaeochannel. The distribution of S, Br and Na_2O are less well defined but still show a close relationship to the organic matter.

Cluster 4 (Ga, Al_2O_3, Sr, P_2O_5, Ba, Cs, K_2O, Sb, Rb, Fe_2O_3)

This cluster contains elements that comprise the structural components of clay minerals and as such these elements can be considered to be predominantly inorganically associated. Interestingly, Sb is associated with this group; little is known of the aqueous chemistry of Sb except that it forms a 3+ cation and has an ionic radius slightly larger than that of other 3+ cations. The weak association with Fe in the cluster suggests that it may form an analogue to ferrous iron, Fe^{2+}, perhaps due to the similar ionic radii. This relationship with Fe is also apparent in the close spatial association of Sb and Fe (Appendix 1). All the elements in this cluster are distinctive in that they display a wide spatial distribution and have a particularly low abundance in the main mineralized zone. Potassium, Rb and Cs are also distinctive in that they are associated with basement highs within the palaeochannel, which are predominantly composed of felsic schists; these elements thus probably indicate the presence of detrital micas (muscovite/biotite) in the sediments.

Cluster 5 (Zr, Hf, Ta, TiO_2, Th, Nb, W, MnO, Ge, Cd)

This cluster consists of elements that are usually associated with heavy minerals such as zircon, rutile and ilmenite. The presence of the metals Ge and Cd is surprising, as Cd is a chalcophile element usually associated with Zn. Germanium (as Ge^{2+}), however, has an ionic radius similar to that of Ta, Nb, W and Mo, whereas Cd^{2+} has an ionic radius similar to that of Ti^{2+} and Th^{4+}. The unusual association of these elements is also an indication of the complexity of the chemistry in the Ambassador deposit, which is primarily dictated by organic matter complexation and the chemistry of elements in reduced oxidation states. The distribution of Zr and Hf is almost identical, with a strong enrichment in the western portion of the palaeochannel. This distribution is also similar to that of the heavy REE and hence suggests either an accumulation of detrital zircon (which is normally enriched in Hf and HREE), or preferential redistribution of Zr, Hf and HREE during weathering or diagenesis. Titanium, Nb and Ta all have a similar, even distribution, but may show a small degree of enrichment in the west of the palaeochannel. Thorium, Ge, Cd and W all have a widespread, somewhat erratic distribution, both within and outside the main mineralized zone and are not indicative of a specific source (accumulation).

Cluster 6 (Au, Cl)

This cluster is of particular interest as it highlights the association between Au and Cl, suggesting that Au has been transported in the palaeochannel as a chloride complex, a common occurrence in oxidized environments in

the Yilgarn Block (*e.g.* Gray, 1991). The mobility of Au in groundwaters is further discussed in Section 6.3. Although there is a widespread distribution of Cl throughout the entire Ambassador area, marginally higher Cl concentrations (>5ppm) generally correspond to elevated Au concentrations (>100 ppb).

Cluster 7 (Si)
This cluster consists only of Si. Although Si-colloids may be involved in the complexation and transport of radionuclides and trace elements (Section 2.3.2) this is probably only minor until very low pH conditions prevail. Furthermore, probably only a very small percentage of the Si is present as colloids, while the majority is probably present as detrital quartz, which has a very low cation adsorption capacity compared to the abundant organic matter. Silicon is not associated with Ge, which also occurs in Group IVA, as it is not metallic and does not possess a reduced 2+ oxidation state.

(c) Cluster analysis: spatial association of element groups

Cluster analysis was performed using 5 different elemental suites of up to 20 elements each in order to elucidate spatial and geochemical relationships present within the redox front at the Ambassador Deposit. The five different suites of elements chosen are as follows -

Group A. Cr, La, Sc, Sm, Th, U, Yb, Cu, Mo, Nb, Ni, Pb, S, Zn, Zr, Al_2O_3, CaO, K_2O, TiO_2, LOI

Group B. Lu, La, Sc, Sm, Th, U, Yb, Cu, Eu, Nb, Ni, Pb, S, Zn, Zr, Al_2O_3, V, TiO_2, LOI

Group C. Lu, La, Sc, Sm, Th, U, Yb, Ce, Eu

Group D. Cr, As, Br, Co, W, Ba, Ga, Cu, Mo, Ni, Pb, S, Zn, Mn, Rb, Th, U, Sr, V

Group E. Au, Cr, As, Br, Co, W, Cl, Cu, Mo, Ni, Pb, S, Zn, Tl, Se, Th, U, Ta, V

Each element suite were clustered into 10 groups according to hole number, with all elemental concentrations expressed in ppm (except Au, ppb, Al_2O_3, CaO, K_2O, TiO_2, LOI, %). An extensive description of the geochemical and geological significance of the individual clusters and dendrograms is given in Appendix 3. Where possible U/Th and $(La/Yb)_n$ (chondrite normalized) ratios have been included to assist in the interpretation of the results.

A number of important points may be made concerning the clustering of elements. In each analysis, the 10 clusters are split broadly into three subgroups. The first subgroup, usually accounting for <10% of the samples, is made up of clusters that contain holes that are highly anomalous in one or more elements. The second subgroup generally accounts for between 20 and 40% of samples and comprises holes that are usually within or close to the main mineralized zone and have moderately elevated concentrations of a number of trace elements. The final subgroup, which may account for over 50% of the samples, consists of holes that are predominantly unmineralized and occur throughout the entire palaeodrainage channel network and its surrounding lithologies. Interestingly, cluster Groups D and E give identical groupings even though there are 5 different elements out of 20 in each cluster group.

3.3.4 Conclusion

Statistical analysis of the major and trace element geochemistry of the Ambassador deposit has demonstrated that a number of coherent associations of elements are present both within and outside the main mineralized zone. The influence of redox state has also been highlighted, where elements not normally associated in oxidizing environments may have a similar geochemical and spatial distribution in the reducing environments (*e.g.,* Nb, Ge, Cd). Furthermore, it has been shown that a number of elements are predominantly inorganically associated (*e.g.*, alkalis, Al_2O_3, Fe_2O_3), probably adsorbed onto the surfaces of the clay minerals. A number of elements, particularly the REE, Zr and Hf, vary in a systematic way down the length of the palaeochannel, which may indicate the original geochemical structure of the channel (*e.g.,* the accumulation of heavy minerals) or may be a reflection of the preferential dissolution and/or redistribution of particular suites of elements.

4.0 A SEQUENTIAL EXTRACTION STUDY OF THE AMBASSADOR DEPOSIT

4.1 Introduction

Sequential extraction analysis has been used to investigate the speciation of elements in a range of Ambassador redox front samples. The samples selected were chosen from a collection that formed part of a previous SEM study (Pascoe, 1991) which had demonstrated that a number of elements were not associated with discrete mineral phases, but appear to be associated with either amorphous organic matter and/or to be adsorbed on authigenic and/or clay mineral surfaces. Furthermore, several element associations were recognized as being highly unusual, especially those containing REE-U-S assemblages. The samples selected for sequential extraction analysis contained elevated trace element concentrations as determined from the bulk geochemical analysis (Appendix 2). The samples used in sequential extraction analysis and the elements present in high concentrations are outlined below:-

PNC hole no.	CSIRO sample no.	Elements enriched in sample
1488	6029	Zr, Hf
1490	6037	Ti, V, Se, S, Zn, Mo, Cu, Pb, Co, Fe, Ni, U, Tl, Th
1310	6070	Au
1370	6072	Zr, Hf
1493	6081	Yb, Sm, La, Lu, Eu, Ce, Au
1577	6101	Zn, Mo, Cu, Pb, Co, Fe, Ni, U, Tl
1577	6105	Zn, Mo, Cu, Pb, Co, Fe, Ni, U, Tl
1323	6138	Ti, V

4.2 Sequential extraction method

A two step sequential extraction technique was developed in order to determine the speciation of elements from selected samples within the Ambassador deposit.

(i) Potassium hydroxide (KOH)/ethylenediaminetetra-acetic acid (EDTA) extraction

These reagents extract metals bound to organic matter. Potassium hydroxide (KOH) was used to raise the pH and desorb organic/humic matter, while ethylenediaminetetra-acetic acid (EDTA), a chelating agent, was used to bind free metal ions released during the extraction. Samples were extracted in a solution containing 0.5 M KOH and 0.1 M EDTA. using a solid-solution ratio of 1:20. The samples were extracted under nitrogen with constant stirring over a 24 hour period, ultracentrifuged (40,000 x g) and the supernatant decanted and diluted for analysis.

(ii) Nitric acid/aqua regia extraction

This extraction step determines elements associated with reduced and/or sulphide phases. The extraction involved three additions of concentrated nitric acid to the residue from extraction step (i), with the samples taken to dryness over a waterbath after each reagent addition. After the nitric acid extraction steps the samples were further digested using concentrated aqua regia. The samples were then ultracentrifuged (40,000 x g) and the supernatant decanted and diluted for analysis.

4.3 Results and Discussion

The results of the sequential extraction experiment are given in Table 4.1. It must be stressed that the results for the sequential extraction analysis must be interpreted in broad terms of elemental speciation, *i.e*., the trends rather than specific percentages of the element extracted by each step. There are a number of reasons for this general interpretation. Firstly although the extraction techniques used are thought to be the most applicable to the study of elemental speciation in the Ambassador samples, they are still at best somewhat arbitrary, as there may be a lack of selectivity for the particular phase of interest. This may occur, for example, when colloidal material is released when the organic matrix with which it is associated is dissolved, or when species that are adsorbed onto the surface of sulphides are complexed by EDTA and removed. Secondly, oxidation of the samples subsequent to sampling (*e.g.* formation of metal sulphates) may have significantly altered the speciation of a number of elements. Additionally, the kinetics of dissolution of many mineral species may be extremely slow and thus the extractions used here only apply to elements that are labile in a relatively short time; this may be in considerable contrast to natural conditions. Thirdly, most sequential extraction analyses have been applied to well characterized oxidized, mainly inorganic systems (*e.g.*, Fe-oxides in soils). Little is known about reduced systems rich in organic matter, and thus interpretation of results needs to be treated with due caution. Finally, the paucity of trace element information for comparable organic deposits, combined with the limited knowledge of trace element-organic interactions compared to more conventional inorganic geochemistry, also serves to hinder the interpretation of results. Thus, there is ample justification in treating the interpretation of the elemental speciation with caution: nonetheless a number of significant interpretations can be made.

Organic matter

One of the most important results of the sequential extraction analyses is the highly mobile nature of the organic matter. Between 9 and 35% of the organic matter is extracted over the 24 hour period of the first extraction step. The remainder of the organic matter is consumed in the second digestion step. Varying proportions of a number of elements are also extracted concurrently with the organic matter and their speciation is discussed below.

Transition metals

The two extraction steps have shown that the transition metals (Fe, Mn, Ti, Co, Cr, Cu, Ni, Pb, Zn) in all samples may have a broad range of associations. Titanium is distinctive in that only a relatively small proportion is extracted by each reagent. SEM examination has shown that a number of the samples may contain both Ti and Fe-Ti rich needles and diffuse patches of Ti in the organic matrix. The Ti is probably present as amorphous or crystalline oxides, hence it is not released from the organic matter and complexed by EDTA in the first extraction step. Similarly, TiO_2 is stable in oxidizing low pH solutions (*i.e.,* the HNO_3/aqua regia digestion used in this study)(Brookins, 1988).

In contrast to Ti, Pb is completely extracted by KOH/EDTA extraction step, except in one sample (6138). This implies that the Pb is probably entirely organic bound and hence highly labile. This is confirmed by evidence from Pb-Pb isotopic studies (Section 5.2) that have shown that different isotopes of the Pb have been homogenized by the redox front in the Ambassador deposit. Nevertheless, reduced Pb phases such as galena have been recognized and these too may be dissolved by the KOH/EDTA extraction. In sample 6138, in which most Pb remains after the first extraction step, total extraction occurs in the HNO_3/aqua regia digestion (sulphide oxidation).

Table 4.1: Results of the sequential extraction analysis

KOH / EDTA EXTRACTION - % EXTRACTED

Sample	Mg	Fe	Mn	Ti	S	As	Ce	Co	Cr	Cu	Eu	Hf	La	Ni	Pb	Sc	Se	Sm	Th	U	Y	Yb	Zn	Zr
6029	50	100	9	0	19	46	0	1	43	68	100	27	0	56	100	11	0	26	44	76	24	9	28	0
6037	58	55	69	0	30	56	0	62	8	41	72	0	0	65	100	15	0	22	33	32	72	50	100	1
6070	53	100	44	0	29	0	41	83	22	39	95	0	49	59	100	18	0	57	0	51	52	63	71	1
6072	52	100	52	1	28	100	53	100	13	48	100	16	45	72	100	21	0	72	33	60	28	48	70	1
6081	59	100	100	10	20	100	100	83	57	47	93	0	82	61	100	72	0	100	100	87	62	100	62	27
6101	43	100	100	7	37	100	42	76	24	20	48	100	49	75	100	6	59	52	54	20	69	75	100	7
6105	46	100	100	4	33	42	67	94	35	3	87	100	62	43	100	34	0	76	0	85	63	100	55	14
6138	16	35	36	1	55	0	11	0	0	35	100	100	0	42	20	0	0	9	100	0	18	0	58	2

AQUA REGIA EXTRACTION - % EXTRACTED

Sample	Mg	Fe	Mn	Ti	S	As	Ce	Co	Cr	Cu	Eu	Hf	La	Ni	Pb	Sc	Se	Sm	Th	U	Y	Yb	Zn	Zr
6029	20	0	53	7	6	54	16	0	56	12	0	38	34	12	0	84	0	12	56	24	24	0	14	3
6037	37	0	23	2	28	28	93	32	75	57	28	0	42	35	0	71	71	78	67	68	24	19	0	10
6070	29	0	55	3	28	0	59	33	62	49	5	0	51	41	0	82	0	40	100	49	22	35	13	3
6072	22	0	15	4	12	0	0	0	20	38	0	0	40	14	0	67	0	17	56	40	38	1	3	3
6081	16	0	0	6	12	0	26	2	0	24	7	100	18	7	0	26	0	0	0	13	8	0	7	12
6101	46	0	0	11	37	0	31	14	0	72	46	0	18	25	0	67	0	12	0	73	31	25	0	46
6105	28	0	0	8	18	58	37	6	62	45	13	0	0	13	0	47	0	24	0	15	12	0	10	14
6138	32	31	36	1	35	100	66	0	50	47	0	0	0	42	80	51	0	55	0	100	36	45	17	21

TOTAL EXTRACTED - %

Sample	Mg	Fe	Mn	Ti	S	As	Ce	Co	Cr	Cu	Eu	Hf	La	Ni	Pb	Sc	Se	Sm	Th	U	Y	Yb	Zn	Zr
6029	70	100	62	8	26	100	16	1	99	81	100	65	34	68	100	95	0	38	100	100	47	9	43	4
6037	94	55	92	2	58	84	93	94	82	99	100	0	42	100	100	86	71	100	100	100	96	69	100	12
6070	82	100	98	3	57	0	100	116	84	89	100	0	100	100	100	100	0	97	100	100	74	98	84	4
6072	73	100	66	5	40	100	53	100	33	86	100	16	86	86	100	88	0	89	89	100	66	49	73	4
6081	75	100	100	15	32	100	126	85	57	71	100	100	100	69	100	98	0	100	100	100	71	100	69	39
6101	89	100	100	18	74	100	72	90	24	92	94	100	67	100	100	72	59	65	54	93	100	100	100	52
6105	74	100	100	11	51	100	104	100	97	48	100	100	62	56	100	81	0	100	0	100	76	100	65	28
6138	49	66	71	2	90	100	77	0	50	82	100	100	0	83	100	51	0	64	100	100	53	45	75	23

Iron is almost always completely extracted from all samples by the first extraction step, implying that the Fe is almost totally present as organically-bound ferrous (Fe^{2+}) form. This is not unexpected, since highly reducing conditions have been present over a sustained period at Ambassador. SEM investigation has shown that the two samples (6037, 6138) from which Fe was not extracted by KOH/EDTA, are both rich in sulphide minerals, mostly pyrite. In the second extraction step, a significant amount of Fe is further extracted from one of the samples (6138) and not the other (6037). The remaining Fe in these two samples is thus likely to be present in residual heavy minerals or other phases not attacked by aqua regia. The total amount of S extracted by both steps ranges between 26% and 90%. Samples were dried between each addition of nitric acid in order to dissolve the sulphides, and this may have resulted in the evolution and loss of gaseous oxides of sulphur and hence reduced the recovery.

The remainder of the transition metals (Mn, Co, Cr, Cu, Ni and Zn) all show a high degree of variability in the relative amount extracted by each reagent. This variability may arise from the large range of mineral and organic-mineral associations identified by SEM. Furthermore, SEM results show that there may be partitioning of certain metals into particular mineral phases (*e.g.,* ZnNiCoU sulphides, sample 6101). These elements may also be possibly be present as an adsorbed form on the surface of sulphide phases or as diffuse concentrations of elements in the organic matrix (similar to Ti-rich zones in the organic matrix) which may either represent dissolution of primary (?detrital) minerals or the initial stages of accumulation prior to authigenic mineral growth.

Zirconium and Hafnium

Zirconium and Hf both display a wide degree of speciation in the sample extractions. Zirconium is significantly extracted by the KOH/EDTA extraction in one sample (6081), this probably due to the presence of diffuse patches of Zr in the matrix seen by SEM. SEM also showed that there was no Hf associated with the diffuse Zr and this is confirmed by the results of the first extraction step in which no Hf was extracted. Although the geochemical differences between Zr and Hf are assumed to be small, the fractionation of these elements relative to each other may be enhanced by complexation by organic matter. Similar observations can be made for other apparently coherent element groupings such as the REE, which fractionate markedly due to organic complexation in similar organic-rich geochemical systems (Douglas, unpubl. data). The geochemical decoupling (fractionation) of Zr and Hf at Ambassador is also confirmed by the wide range of Zr/Hf ratios observed for a number of samples throughout the redox front. The mobility of both Zr and Hf is also supported by the presence of corroded zircons seen by SEM, which attest to the enhanced dissolution of zircons in an organic environment. In addition, zircon crystals with little or no Hf have been observed by SEM and may be authigenic. Although the differences in the speciation of both Zr and Hf are somewhat erratic, in most cases significantly more Hf is associated with organic and/or sulphide/reduced or phases than Zr, with complete extraction of Hf occurring for a number of samples.

Rare earth elements

In a similar way to Zr and Hf, the REE (La, Ce, Eu, Sm, Yb and Y) also may show a wide range of speciation. Extraction of the samples with KOH/EDTA suggests that significant amount of the REE are associated with organic matter. The HREE in particular are generally associated with Zr which also has highly variable solubility in KOH/EDTA, as described above. Thus, the irregular distribution of the rare earth elements in the extracts may

be due to a dissolution of a number of different phases (with different REE ratios) associated with the organic matrix as well as potential desorption from other non-organic phases such as sulphides. (Abundant REE sulphides have been observed by SEM studies in some samples, Section 2.2.2).

Europium is nearly or totally extracted from several samples by KOH/EDTA. Under reducing conditions, Eu^{3+} is commonly reduced to Eu^{2+} and has a geochemical behaviour similar to that of Ca^{2+}. Calcium is known to be strongly associated with organic matter, being complexed to carboxylate functional groups. Thus a high proportion of the Eu^{2+} may be associated with organic matter in a manner similar to Ca and hence may be complexed by the EDTA in the first extraction step.

The extraction behaviour of the LREE La, Ce and, to a lesser extent, Sm is similar in both steps. Little or no extraction of the light REE suggests that monazite may be the phase that controls the speciation of these elements. However, Th, which may also occur in monazite, does not have a strong relationship with the LREE recovered in the two extraction steps, but this may be due to the enhanced mobility of Th in organic rich environments (Section 2.3.3). Examination of a number of samples by SEM has also shown that unusual REE phases such as Ce(Sm,Nd)Ca silicates and REE trace metal sulphides are also present, further complicating the interpretation of the speciation of these elements.

Arsenic

Arsenic is variably distributed between the alkali extractable organic, sulphide/reduced and residual phases. In a number of samples, As may be quantitatively removed by the KOH/EDTA extraction step, whereas in others a significant proportion of the As may be associated with a sulphide phase. This is not unexpected as As is known to form stable sulphide species over a wide range of pH and low to intermediate Eh (Brookins, 1988). Overall, however, in six of the eight samples, As is totally extracted, whereas in sample (6037) the majority is extracted. In one sample (6070) no As is extracted; the reason for this is not known.

Magnesium

Magnesium is in general distributed fairly evenly between the KOH/EDTA extractable, aqua regia extractable and the residual phases. The reason for the presence of Mg in the residual phase is not known, as it would be expected that the extensive acid digestion procedure would have removed the majority of the Mg from either organic matter or residual clay minerals. This suggests that residual phases such as Mg-rich chromite may be present in a number of the samples. This is also supported by the fact that the average concentration of Cr in the sequential extraction samples (288 ppm), is over 100% greater than the mean concentration for the entire Ambassador deposit (140 ppm).

Uranium and Thorium

There is a large variation in the relative speciation of both U and Th in the different samples. Except for one sample (6138), a moderate to large (*ca.* 20-90%) proportion of the U is extracted with the labile organic component. The U released by the KOH/EDTA extraction step may potentially be present in four forms;

1. as a truly organic associated metal-ligand complex;
2. as surface adsorbed U on clay minerals and/or sulphides; or
3. as authigenic minerals
4. as secondary U minerals formed by the oxidation of authigenic minerals or organic matter.

Aqua regia extraction suggests that a significant proportion of the U is probably present as authigenic sulphide minerals. This is confirmed by previous SEM investigations, which identified authigenic grains of complex U-transition metal sulphide minerals, especially in sample 6101, in which discrete grains and crystal aggregates of ZnCdNiFeUS and UFeCoNiZnS are abundant (Section 2.2.2). This sample is the only one in which U is not completely removed by the two extraction steps, suggesting that residual sulphide minerals may persist. The implication is that the distribution and speciation of U is partly dependant on the degree of diagenesis and authigenic mineral growth in the samples.

The presence of significant amounts, or all (samples 6081, 6138) of the Th, in the extractable organic phase suggests that Th is not present as residual minerals such as monazite. The poor association with Ce extracted in the first step confirms this conclusion and indicates that Ce and Th have different speciation characteristics in both the organic matter and sulphide phases. This is also suggested by SEM studies that indicate that secondary REE-bearing silicate (CeSmNdCaSi sample 6070) and sulphide (NiZnCeCaS sample 6101) minerals do not contain any Th. Nevertheless, in four samples (6029, 6037, 6070, 6072) most or all of the Th is dissolved by the nitric acid/aqua regia digestion and presumably occurs in an S-poor reduced phase. The apparently high mobility of Th in the presence of organic matter has already been discussed previously above and Section 2.3.3 and the wide range of speciation of Th in the Ambassador deposit only serves to confirm this observation. No Th is extracted from one sample (6105). This sample will be investigated further with scanning electron microscopy to in an attempt determine the geochemical association of Th.

4.4 Conclusion

Sequential extraction analysis has suggested that significant proportions of many elements are associated with a labile organic phase, whereas others are probably associated with authigenic sulphides either by incorporation into their primary crystal structure or by surface adsorption. The presence of some trace elements in the extraction residue also suggests that primary heavy mineral phases may also persist (as confirmed in SEM studies). Results can, however, only be interpreted in broad terms due to unknown factors affecting the speciation such as post sampling oxidation, dissolution kinetics and reagent selectivity during the two extraction steps.

5.0 ISOTOPIC GEOCHEMISTRY OF THE AMBASSADOR DEPOSIT

5.1 Introduction

Isotopic analysis is commonly used in geochemical studies for age determinations of rocks or mineralization, to trace source rocks, as an indicator of cogenesis between different lithologies and in the study of disequilibria or disturbance in isotopic systems. In the present study, Pb-Pb, Rb-Sr and Sm-Nd isotope geochemistry has been used to investigate the origin (source) of U-trace element mineralization at Mulga Rock.

The usefulness of isotopic systems in such studies is that they may potentially identify a unique isotopic "fingerprint" which will be diagnostic of a particular rock type. However, events such as metamorphism may alter the original isotopic signature by redistribution of isotopes throughout the rock, and weathering may influence the isotopic ratio of the regolith or the derived sedimentary material through the differential weathering of constituent minerals.

In genetic or chronological systems, it is assumed that the systems are closed, *i.e.,* there is no transfer of radiogenic or stable isotopes in or out of the system. If open system behaviour occurs to a significant extent, the isotopic system will be disturbed and the data require careful interpretation.

5.2 Summary of the theory of radiogenic isotopic systems

The Rb-Sr and Sm-Nd isotopic systems consist of a number of isotopes, both stable and unstable. Those used in geochronological and isotopic tracing studies are ^{87}Rb, ^{87}Sr, ^{86}Sr and ^{147}Sm, ^{144}Nd and ^{143}Nd. The half lives ($t_{1/2}$) for the respective decay series are as follows-

$^{87}Rb \longrightarrow {}^{87}Sr$ $\quad$ $(t_{1/2})=4.88 \times 10^{10}$ years

$^{147}Sm \longrightarrow {}^{143}Nd$ $\quad$ $(t_{1/2})=1.06 \times 10^{11}$ years

The Rb-Sr and Sm-Nd isotopic systems are expressed in terms of isotopic ratios (i.e., $^{87}Sr/^{86}Sr$, $^{143}Nd/^{144}Nd$), with the stable isotopes (^{86}Sr and ^{144}Nd) being a measure of the initial Sr and Nd present in the system at the time of formation.

The Pb isotopic system is comprised of three radiogenically derived isotopes of Pb (^{208}Pb, ^{207}Pb, ^{206}Pb) and one stable isotope (^{204}Pb) not contributed to by radioactive decay. One of the Pb isotopes (^{208}Pb) is derived from the decay of ^{232}Th and hence the relative abundance of ^{208}Pb and ^{206}Pb is a measure of the initial Th/U elemental ratio, assuming a closed isotopic system (i.e., no migration of U, Th or Pb in or out of the system during decay). The half lives ($t_{1/2}$) of the respective decay series are as follows-

$^{238}U \longrightarrow {}^{206}Pb$ $\quad$ $t_{1/2}=4.5 \times 10^{9}$ years

$^{235}U \longrightarrow {}^{207}Pb$ $\quad$ $t_{1/2}=0.7 \times 10^{9}$ years

$^{232}Th \longrightarrow {}^{208}Pb$ $\quad$ $t_{1/2}=14.0 \times 10^{9}$ years

Lead isotopic data are also expressed as ratios (*i.e.,* $^{208}Pb/^{206}Pb$, $^{207}Pb/^{206}Pb$, $^{206}Pb/^{204}Pb$, and $^{207}Pb/^{204}Pb$, $^{208}Pb/^{204}Pb$), with the stable isotope (^{204}Pb) being a measure of the initial non-radiogenic Pb present in the system at the time of formation.

5.3 Analysis, Results and Discussion

Six samples from the redox front (6040, 6056, 6068, 6079, 6088, 6096) at the Ambassador deposit were analysed. The isotopic ratios for the Rb-Sr and Sm-Nd systems were determined after total dissolution and analysis on a VG 354 mass spectrometer, according to the methods of Korsch and Gulson (1986). The Pb-Pb isotopic ratios were determined after a Na acetate leaching procedure was used to extract exchangeable Pb, and were analysed on a mass spectrometer, according to the methods of Gulson and Mizon (1980) (N.B., the use of extractable Pb, rather than a total digest as in the case for Sr and Nd isotopes, is adequate as the inorganic constituents of the samples, i.e., quartz and kaolinite, are unlikely to contain significant Pb, and hence will have little influence on the isotopic ratio).

The most significant aspect of the results is the homogeneity of the data for the Rb-Sr, Sm-Nd and Pb-Pb isotopic systems (Table 5.1, Figures 5.1 a, b and c). Histograms of Sr (n=69, Figure 5.2 a), Nd (n=84, Figure 5.2 b) and Pb (n=108, Figures 5.2 c-e) isotopic ratios of rocks from the Yilgarn Block suggest that if considered individually, the isotopic ratios of the Ambassador deposit are not atypical. Unfortunately, there are few lithologies that have been analysed for the combination of Sr and/or Nd and Pb isotopes and thus, it is not possible to depict fields of typical Yilgarn lithologies reliably on Figures 5.1 a, b and c. In broad terms, however, it is the combination of the Sr, Nd and Pb isotopic ratios, especially the high $^{208}Pb/^{204}Pb$ vs. $^{206}Pb/^{204}Pb$ and low $^{87}Sr/^{86}Sr$ vs. $^{143}Nd/^{144}Nd$, that are considered to suggest a distinctive source rock is responsible for the mineralization:-

(a) Homogeneous isotope ratios generally indicate either a single, very homogeneous source of Sr, Nd and Pb and/or homogenization during transport, deposition and/or diagenesis. It is most unlikely that the complex Archaean-Proterozoic source terrain (the Yilgarn Block and the Albany-Fraser Province) was homogeneous, so that homogenization during the later processes of remobilization and deposition is implicated. This is not surprising, given the redox contrasts in the deposit, the presence of authigenic galena, REE-bearing sulphides, and the strong associations of Pb and, to a varying extent, REE, with organic matter, as identified by sequential extraction analysis.

Table 5.1: Rb-Sr, Sm-Nd and Pb-Pb isotopic composition of Ambassador organic matter

Sample	$^{208}Pb/^{206}Pb$	$^{207}Pb/^{206}Pb$	$^{206}Pb/^{204}Pb$	$^{207}Pb/^{204}Pb$	$^{208}Pb/^{204}Pb$	$^{147}Sm/^{144}Nd$	$^{143}Nd/^{144}Nd$	$^{87}Sr/^{86}Sr$
6040	2.2093	0.9032	17.196	15.531	37.991	0.1605	0.511847±19	0.720141±14
6056	2.1825	0.8945	17.338	15.554	37.949	0.1111	0.511459±19	0.721370±16
6068	2.2023	0.9019	17.217	15.529	37.916	0.1446	0.511537±21	0.720446±15
6079	2.1908	0.8957	17.372	15.560	38.059	0.1181	0.511428±18	0.721094±18
6088	2.0962	0.8646	18.031	15.589	37.797	0.1759	0.511518±22	0.721564±36
6096	2.2057	0.9079	17.177	15.594	37.887	0.1367	0.511477±14	0.722442±12

(b) The combination of low $^{87}Sr/^{86}Sr$ and intermediate $^{143}Nd/^{144}Nd$ isotopic ratios suggest a distinctive source and, in particular, precludes a number of radiogenic granites.

(c) The high $^{208}Pb/^{204}Pb$ ratios suggest the source has a high Th/U ratio in the range 10-15. In comparison, the usual Th/U ratio for granites is in the range 2-3.

Figure 5.1 **(a) Nd-Sr diagram for the Ambassador organic matter. Also depicted are fields of isotopic ratios for Western Australian lamproites and kimberlites and a number of other basic and ultrapotassic lithologies from around the world (see description below). Modified after Mitchell, (1989)**

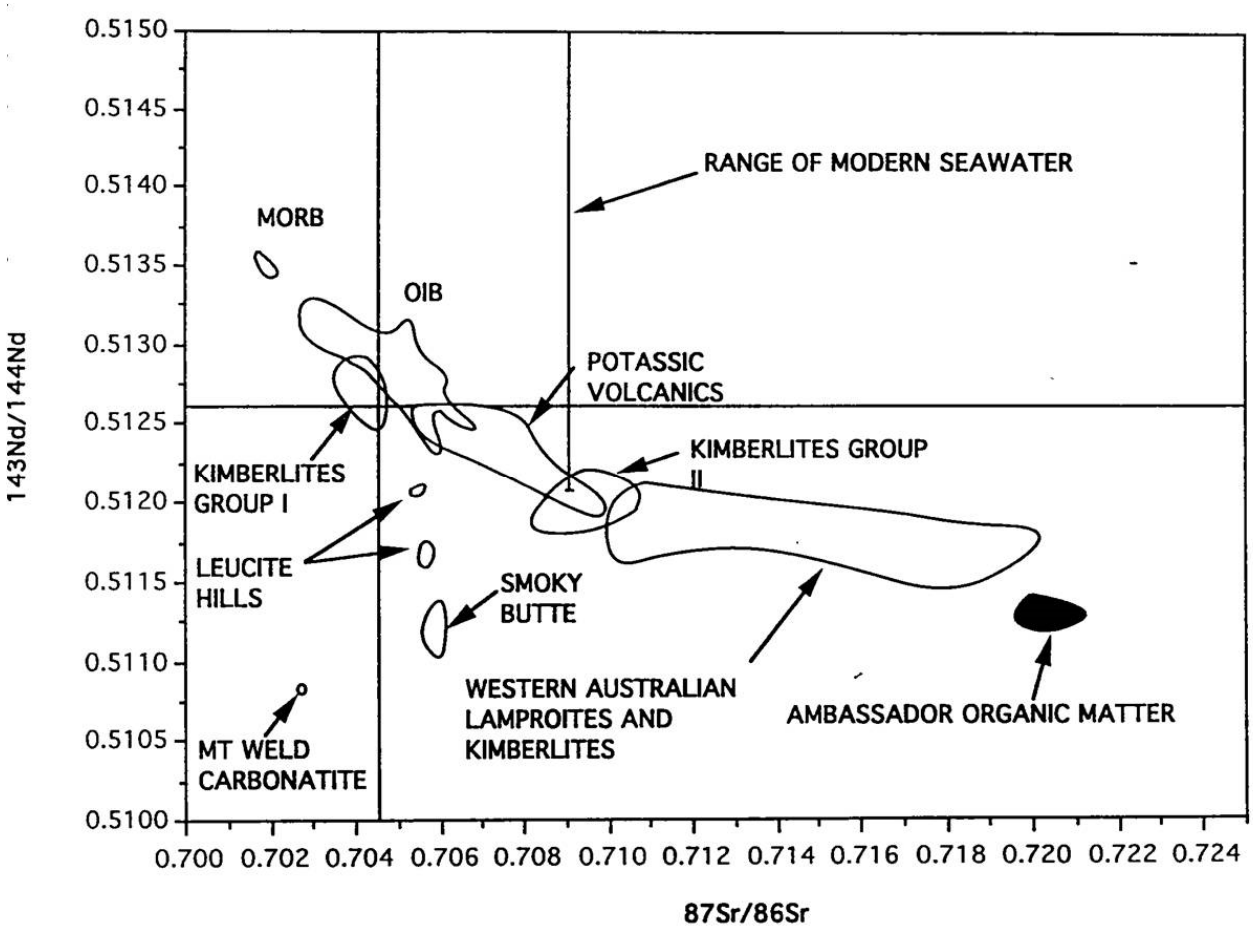

Western Australia lamproites and kimberlites occur exclusively in the Kimberley region, and range in age from Proterozoic (1200 Ma for the diamond bearing Argyle lamproite) to mid-Miocene(20-22 Ma).

Group I (basaltic, 90-1600Ma) kimberlites and Group II (micaceous, 100-200Ma) kimberlites occur in Southern Africa and are distinguished by age, petrography, isotopic characteristics, and distribution.

Smoky Butte lamproites are Oligocene in age (27±3Ma) and occur as a series of thin dykes and plugs in Montana, USA

Leucite Hills lamproites, are (1Ma) in age and occur as 22 exposures of volcanic and sub-volcanic rocks over an area of 2,500 km^2 in Wyoming USA.

Potassic volcanics defines a worldwide field of potassic to ultrapotassic continental volcanics.

MORB defines a field of compositions for mid ocean ridge basalts

OIB defines a field of ocean island basalts

Additional information is contained in Fraser et al., (1985) and Mitchell, (1989).

Figure 5.1 **(b) and (c): Pb Isochron diagrams for Ambassador organic matter. The error of the isotopic measurements is depicted as a small solid symbol in the top left-hand corner of each isochron diagram**

Also depicted are approximate fields of isotopic ratios for Western Australian lamproites and kimberlites and a number of other basic and ultrapotassic lithologies from around the world.

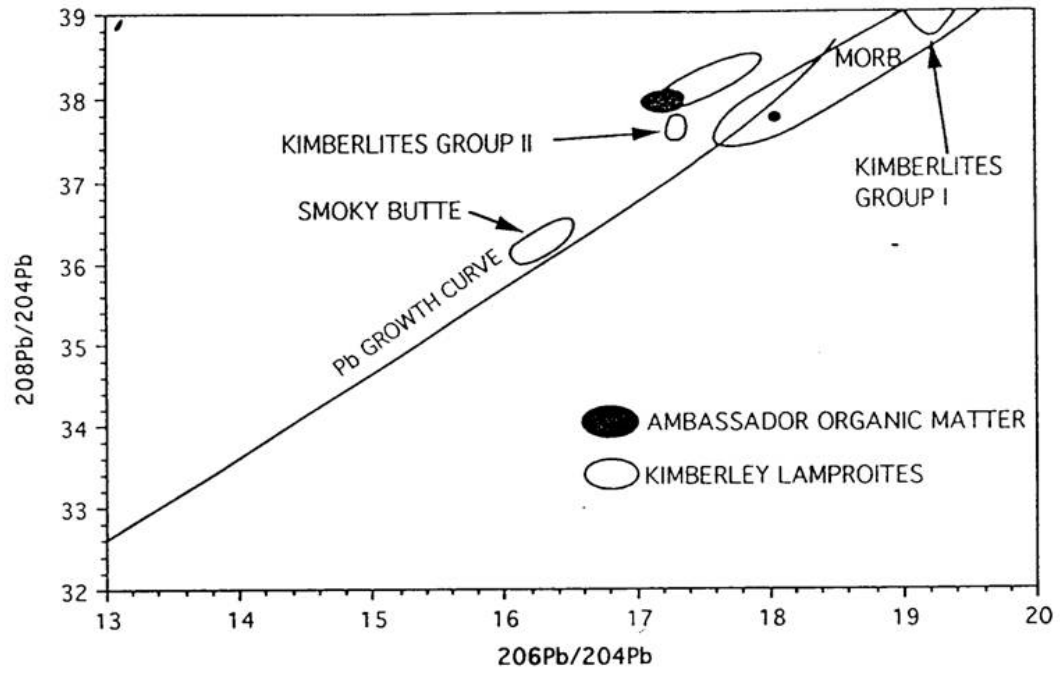

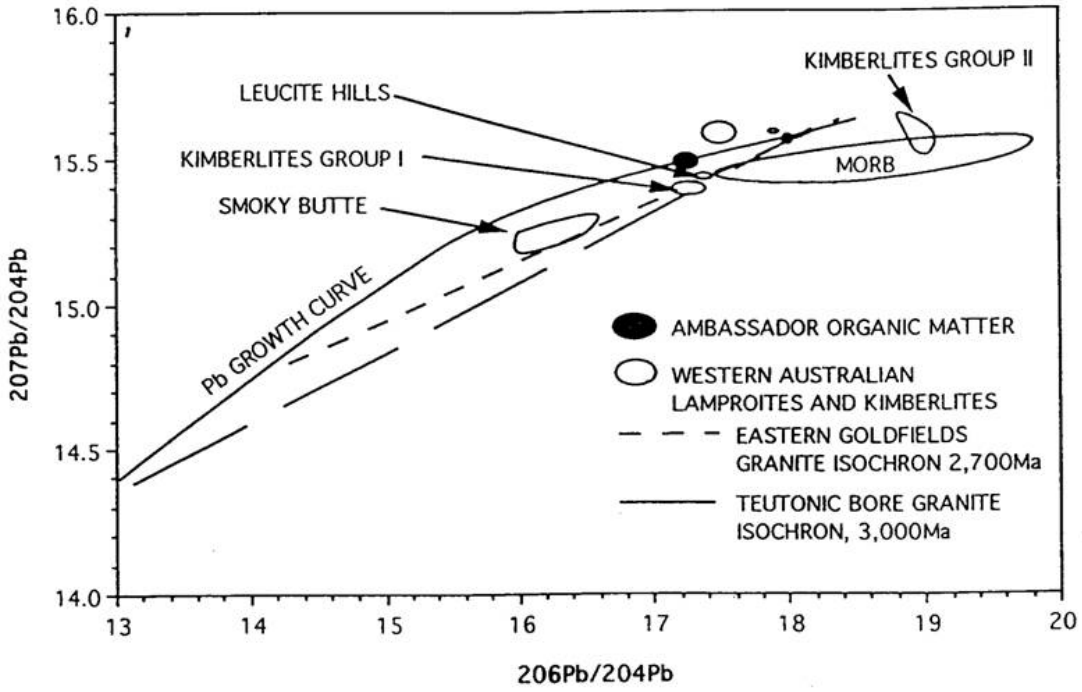

Figure 5.2 (a)-(e): Histograms of Sr, Nd and Pb isotopic ratios for lithologies from the Yilgarn Block

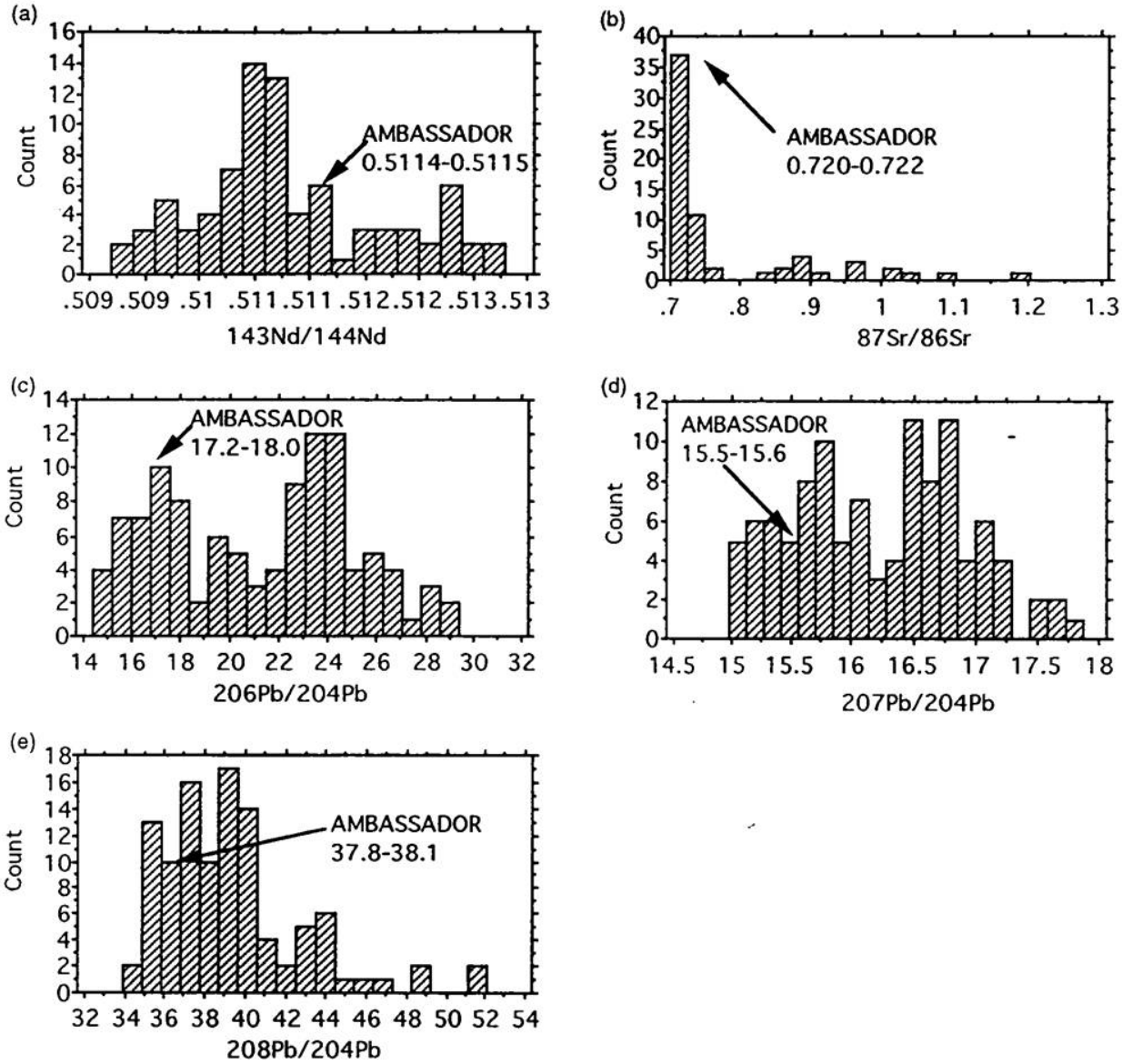

(d) The waters that transported the Pb did not encounter significant U during transport, as this would have decreased the Th/U ratio. Hence, the Pb (and U) source may be close to the Ambassador mineralization.

Possible source rocks for the mineralization are tightly constrained by the requirement that they have a high Th/U ratio (*i.e.,* high $^{208}Pb/^{204}Pb$ ratio). There are three main potential sources for the mineralization:-

1. High grade metamorphic rocks (*e.g.*, granulites)

Rocks are commonly depleted in U by high grade metamorphism. If this occurred in the Archaean or Proterozoic, a sufficient increment of radiogenic Pb would be produced from the decay of Th to give $^{208}Pb/^{204}Pb$ ratios comparable to those seen in the Ambassador mineralization. Ingeneral, the lithologies in the Yilgarn and Albany-Fraser Province have a lower metamorphic grade (greenschist to amphibolite), although granulite metamorphism has been identified in a number of isolated localities, particularly in the Albany-Fraser Province (Griffin, 1990).

The results obtained from Rb-Sr and Sm-Nd isotopic analysis, however, tend to preclude old granulite lithologies from being the possible source because many $^{87}Sr/^{86}Sr$ and $^{143}Nd/^{144}Nd$ ratios would be likely to be higher than that found in the Ambassador organic matter. Nevertheless, differential weathering of minerals, particularly plagioclase feldspar, could produce similar $^{87}Sr/^{86}Sr$ isotopic ratios to that measured in the Ambassador organic matter.

2. Lamproites, kimberlites and carbonatites

The cluster of homogenized Pb-Pb, Sm-Nd and Rb-Sr ratios for the Ambassador mineralization plot in a distinctive area of $^{143}Nd/^{144}Nd$ vs. $^{87}Sr/^{86}Sr$ (Figure 5.1 a), $^{208}Pb/^{204}Pb$ vs. $^{206}Pb/^{204}Pb$ (Figure 5.1 b) and $^{207}Pb/^{204}Pb$ vs. $^{206}Pb/^{204}Pb$ (Figure 5.1 c) diagrams that corresponds to the field of Western Australian lamproites and kimberlites. In particular, on the Nd-Sr diagram (Figure 5.1a), the Ambassador organic matter continues the arcuate trend defining the Nd-Sr isotopic composition of basic-potassic and ultra-potassic rocks from around the world. A brief description of the lithologies in Figures 5.1 a, b, and c are given below. The Leucite Hills and Smoky Butte lamproites from the USA are depicted as examples of lamproites with distinctly different isotopic compositions, but the former share a number of geochemical similarities with the Western Australian lamproite suite (Sahama, 1974).

Lamproites may have a wide range of Th/U ratios, but they are one of the few lithologies in which the ratio can be sufficiently high to satisfy the source rock Th/U ratio required by the Pb-Pb isotopic studies. Additionally, lamproites (and associated kimberlites and carbonatites) have a distinctive geochemistry, being enriched in a number of compatible and incompatible elements, especially Rb, Ba, Ti, Zr Co, Ni, Cr Sc and REE (Mitchell, 1989, Nelson and McCulloch, 1989), an element suite similar to that found in the Ambassador deposit. Nevertheless, the Mt. Weld carbonatite, which is situated approximately 200 km NE of Mulga Rock, is precluded from being a source for the trace elements because its Nd-Sr isotopic ratios are too low and Pb isotopic ratios too high (Nelson *et al.*, 1988) to be compatible with the observed isotopic signature at Mulga Rock. Although only rudimentary geophysical data are available, carbonatites have been discovered near Queen Victoria spring, south of Mulga Rock, and numerous bodies with distinctive magnetic signatures that have been interpreted to be carbonatites, ultramafic bodies or other pipe-like intrusives have been identified close to the Mulga Rock deposit. Further investigation of these magnetic anomalies and additional Pb-Pb, Sm-Nd and Rb-Sr isotopic analysis may potentially identify the source of mineralization. These investigations will include isotopic analysis of organic matter from other regional palaeochannels to assess whether the isotopic ratios of the Ambassador organic matter are diagnostic of lamproite/kimberlite/carbonatite mineralization. Groundwaters in the Ambassador deposit, are, however, isotopically light in ^{18}O, which is in contrast to that expected from a lamproite-kimberlite-carbonatite source. Dilution with other sources of ^{18}O such as meteoric waters or interaction with organic matter may, however, explain this apparent discrepancy.

3. Heavy mineral accumulation

If heavy minerals, such as monazite enriched in Th, had accumulated in the Mulga Rock palaeochannel system, the leaching and transport of Pb derived from the decay of Th in monazite could result in the ^{208}Pb isotopic enrichment observed in the isochron diagram (Figure 5.1b). This scenario is, however, unlikely because no monazite has been identified in the Ambassador deposit, although some is present in the Shogun deposit. Furthermore, an extremely large amount of monazite-derived ^{208}Pb would be required to increase the $^{208}Pb/^{204}Pb$ isotopic ratio. Studies of the U-Th disequilibria patterns, at and below the redox front (Section 9.3),

indicate that monazite-derived Th is not distributed evenly (*i.e.,* the organic matter has a variable $^{230}Th/^{232}Th$ isotopic ratio), and thus is unlikely to have been a significant or unique source of the mineralization.

5.4 Source rock age

It is not possible to obtain an age of the source rock for the Ambassador mineralization. The Pb-Pb isotope data, however, do plot close to the average crustal (growth) evolution curve on a $^{207}Pb/^{204}Pb$ vs. $^{206}Pb/^{204}Pb$ diagram (Figure 5.1a) and give a source rock model age of Upper Proterozoic to Lower Palaeozoic. Due to homogenization of the Pb-Sr and Nd isotopes, the data are tightly clustered and produce what is essentially a single point isochron. Because of the small spread of data, the model age has little or no geological meaning. Furthermore, there is a strong possibility that open system behaviour has occurred, such that even without the homogenizing action of the redox front geologically fictitious isochrons would have been obtained.

Although the homogenization of the Ambassador samples obscures the primary Pb-isotopic signatures, it is possible that the Ambassador samples lie on a mixing line between Archaean granites (shown as isochrons on Figure 5.1b) and a postulated lamproite/kimberlite/carbonatite source. One sample (6088) lies directly on the granite isochrons and hence its Pb isotopic signature is likely to have been directly derived from granitic source. Figure 5.1c also illustrates the close relationship between the Ambassador samples and the Kimberley lamproites and exemplifies the high Th/U ratio which is expressed in the high $^{208}Pb/^{204}Pb$ ratio. The same Ambassador sample in Figure 5.1b also plots on the crustal growth curve and implies that its isotopic composition is derived at least in part from a granitic source, which is not surprising given the ubiquitous presence of granitoids in the Yilgarn block.

5.5 Conclusion

Isotopic analyses indicate that there has been homogenization of Pb, Nd (REE), Sr and possibly other elements in the Ambassador deposit, probably due to mobilization and precipitation during weathering, transport and/or diagenesis. The homogenization of the three isotopic systems (Rb-Sr, Sm-Nd and Pb-Pb) precludes determination of the age of the source(s). The high $^{208}Pb/^{204}Pb$ ratio, however, suggests that rocks with a high Th/U ratio, probably lamproites, kimberlites or carbonatites, are the source of the mineralization. Additional studies using the Rb-Sr and Sm-Nd isotopic systems also support this hypothesis; however, these isotopic signatures are also compatible with many granites and greenstones from the Yilgarn block. Further isotopic analysis of organic matter from other palaeochannels, both unmineralized and mineralized, and basement and regional lithologies is required to confirm the apparently unique isotopic signature present in the Ambassador organic matter and to discount the possibility of weathering, transport and/or diagenesis producing the observed isotopic signature.

6.0 GROUNDWATER INVESTIGATIONS

6.1 Introduction

Water sampling was carried out at Mulga Rock with the following objectives:

(i) to obtain further understanding of the chemical and geological factors influencing the chemistry of groundwaters at Mulga Rock;

(ii) to determine the potential of hydrogeochemistry as an exploration tool;

(iii) to determine which complexing ligands cause element mobility, and how these ions are influenced by groundwater chemistry and water-rock interactions;

(iv) to develop of techniques for study of groundwater data in organic-rich palaeodrainages;

(v) to compare results with data from other sites, principally gold-rich areas in the Yilgarn Block (Gray, 1990,1991), enabling studies at Mulga Rock to be placed in a regional context.

6.2 Sampling and analysis

Water sampling was done in late 1990 and mid 1991. Twenty samples were taken, and were designated as MR1 - 20 for the purposes of this report. The hole number and position of each sample are given in Table 6.1, and shown in Figure 6.1. The various holes are positioned at specific areas:

(i) MR4 and MR6 were sampled from the Emperor deposit;

(ii) MR3 and MR5 were sampled from the Shogun deposit;

(iii) MR1, MR7 and MR8 were sampled south of the Ambassador deposit;

(iv) MR2 and MR9 - MR20 were sampled from the channel containing the Ambassador deposit.

Waters were analysed for pH, temperature, conductivity and oxidation potential (Eh) at the time of sampling. A 125 millilitre (mL) water sample was collected in a polythene bottle (with overfilling to remove all air) for later HCO_3^- analysis by alkalinity titration in the laboratory. About 2.5 litres (L) of water was filtered through a 0.45µm membrane filter in the field. About 100 mL of the filtered solution was acidified [0.1 mL 15 M nitric acid (HNO_3)], and analysed for Na, Mg, Ca and K by atomic absorption spectrophotometry and for Cu, Zn, Pb and Cd by anodic stripping voltammetry at CSIRO Floreat Park Laboratories, and for Co, Al, Fe, Mn, Ba, Cr, Ni, Sr and Si by inductively coupled plasma - atomic emission spectroscopy at CSIRO North Ryde Laboratories. Samples MR12 - MR20 were analysed for PO_4 by the phospho-molybdate method (Murphy and Riley, 1962) at CSIRO Floreat Park Laboratories and samples MR10, MR12, MR13, MR15 and MR19 were analysed for Y, Cs, La, Ce, Pr, Nd, Sm, Eu, Gd, Tb, Dy, Ho, Er, Tm, Yb, Lu, Tl, Th and U by inductively coupled plasma - mass spectroscopy at the Mineral Science Laboratory, Chemistry Centre, WA.

Table 6.1: Mulga Rock water samples

Sample No.	PNC Code	Easting (m)	Northing (m)
MR1	Water Bore #1	76894	76049
MR2	1148	75596	80272
MR3	Water Bore #3	62911	87292
MR4	Water Bore #4	57157	91735
MR5	Water Bore #5	62962	87565
MR6	Water Bore #6	56572	91446
MR7	Water Bore #7 - Shallow	75070	79915
MR8	Water Bore #7 - Deep	"	"
MR9	1213	75279	81446
MR10	1152	75614	81244
MR11	1151	75960	81036
MR12	1419	85380	86347
MR13	1500	82711	84258
MR14	1498	79628	83151
MR15	1247	79548	82917
MR16	1515	78991	82602
MR17	1216	78226	83063
MR18	1177	77866	82796
MR19	1409	78304	82526
MR20	1366	77012	82584

Figure 6.1 Water sampling sites at Ambassador (with Emperor and Shogun holes shown in the insert)

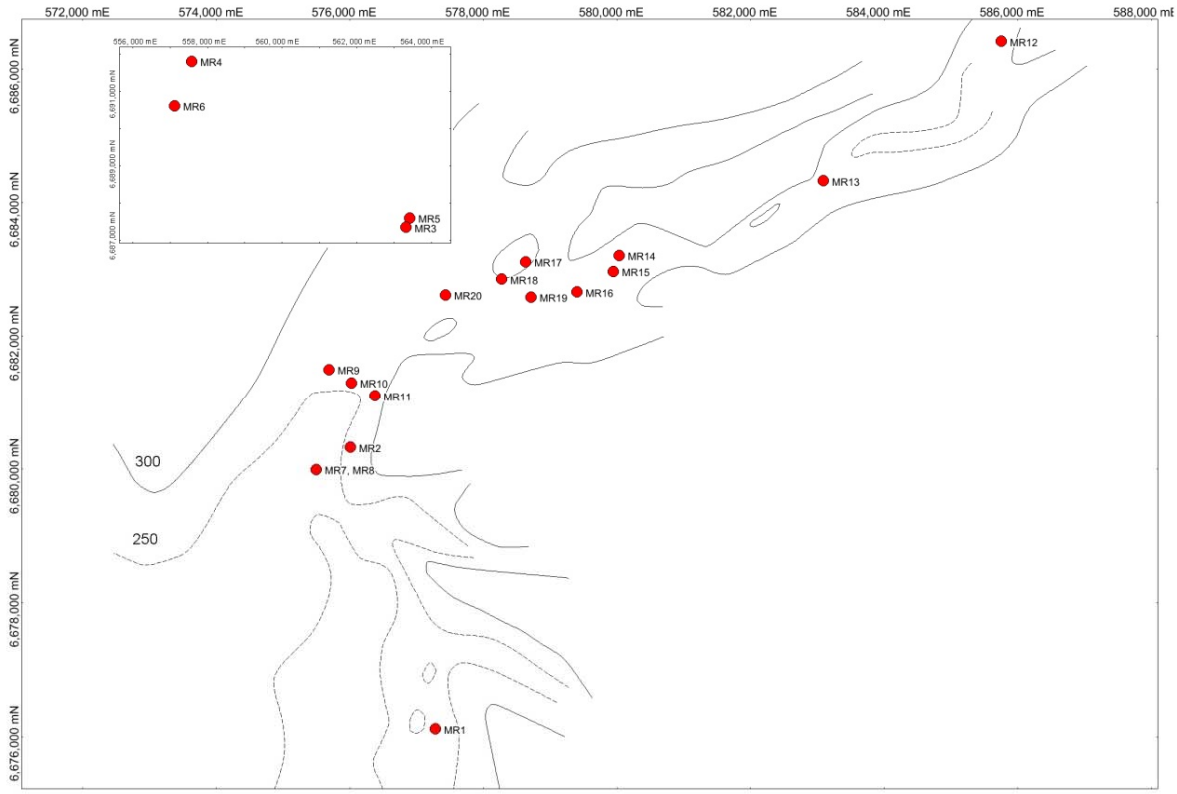

A further 50 mL sample of the filtered water was analysed by ion chromatography at CSIRO Floreat Park Laboratories, for Cl, Br and SO_4, using a DIONEX AS4A column under standard eluent conditions (Dionex, 1985) with a conductivity detector, and for I using a DIONEX AS5 column under standard eluent conditions (*ibid*.) with an electrochemical detector.

Two 1 L sub-samples of the filtered water were mixed with 1 mL 15 M HNO_3 and a 1 g sachet of activated carbon. The bottles were rolled for eight days in the laboratory and the water then discarded. The activated carbon was then analysed for Sb, As, W, U and Au by neutron activation analysis at Becquerel Laboratories and for Sb, Ag, Bi, Hg and V by X-ray fluorescence at CSIRO Floreat Park Laboratories. Laboratory investigations have indicated that this pre-concentration system permits successful analyses of waters for these elements at low concentrations and high salinities. Calibration of the method was obtained by shaking standards of varying concentrations, and in varying salinities, with activated carbon.

The accuracy of the total analyses was confirmed by measuring the cation/anion balance (*i.e.*, total cationic charge less total anionic charge, all divided by total charge). The balances were better than 2%, indicating good analytical accuracy for the major elements.

Selected waters from the Ambassador channel (MR9, MR13 - MR20) were analysed for hydrogen and oxygen isotope abundances, using a VG ISOGAS SIRA 9 Stable Isotope Gas Analyser, standardised for SMOW (Standard Mean Ocean Water).

6.3 Results and discussion

6.3.1 Compilation of results

Isotopic and elemental data for the samples are listed in Appendix 5, Tables A5.1 and A5.2 and plotted in Figures A5.1 - A5.27, with averages given in Table 6.2. Samples were described as "Minigwal" (Samples MR1 and MR3-8) or "Ambassador" (MR2 and MR9-20) so as to indicate differences between water in the main Mulga Rock drainage and water in the smaller Ambassador channel. The total dissolved solids (TDS), a measure of groundwater salinity, were calculated from the major element contents. Also listed in Table 6.2 are data for sea water (taken from Weast *et al.*, 1984) and the averaged data for three other sites previously investigated: Bakers Hill, a non-mineralized area which lies some 50 km east of the western edge of the Yilgarn Block; Mount Gibson, a gold deposit about 100 km north-east of Dalwallinu (central-west Yilgarn; Gray, 1991); and Panglo, a gold deposit some 30 km north of Kalgoorlie (south Yilgarn; Gray, 1990). Averaged results for analyses conducted on Ambassador waters alone are listed in Table 5.3.

6.3.2 Oxidation potential and acidity of Mulga Rock groundwaters

An Eh-pH plot of waters from Mulga Rock and other sites is shown in Figure 6.2. The Mulga Rock waters are all reduced, relative to other sites, and most of the samples are at or below the Eh for reduction of iron oxides (middle dashed line in Figure 6.2). A particularly low Eh was measured for MR19 (CD-1409), which lies within the Ambassador mineralized zone (Figure 6.1). This sample is highly SO_4 depleted, and has an extremely high alkalinity (Figure 5.3). The Eh value locates it on the boundary between H_2S and SO_4 (Figure 6.2), which implies that conditions are sufficiently reducing to enable SO_4 reduction. Thus, the low SO_4 content of MR19 may reflect active reduction of sulphate.

Table 6.2: Averaged elemental compositions of Minigwal and Ambassador waters, with results from other sites given for comparison

Sample	Minigwal (7)#		Ambassador (13)		Bakers Hill (3)		Mt. Gibson (50)		Panglo (50)		Sea water
	Mean	Sd Dv@	Mean	Sd Dv	Mean	Sd Dv	Mean	Sd Dv	Mean	Sd Dv	
pH	6.0	0.9	6.2	0.7	4.7	0.8	6.5	0.7	4.9	1.2	nd
Eh (mV)	123	30	140	124	300	50	310	100	490	180	nd
Na *	0.31	0.01	0.30	0.01	0.28	0.01	0.32	0.02	0.32	0.01	0.31
Mg *	0.033	0.001	0.033	0.003	0.057	0.002	0.033	0.007	0.032	0.003	0.040
Ca *	0.012	0.005	0.025	0.009	0.020	0.004	0.009	0.010	0.008	0.003	0.012
K *	0.0067	0.0005	0.0107	0.0017	0.0030	0.0002	0.0112	0.0018	0.0008	0.0003	0.0112
Cl *	0.54	0.01	0.52	0.01	0.60	0.01	0.53	0.03	0.59	0.01	0.56
SO_4 *	0.101	0.008	0.103	0.030	0.045	0.001	0.075	0.016	0.053	0.005	0.065
Br *	0.0006	0.0001	0.0008	0.0003	0.0016	0.0001	0.0017	0.0002	0.0005	0.0001	0.0019
HCO_3-	70	60	260	330	nd	nd	260	240	50	60	142
TDS	55000	26000	21000	9000	8100	2800	24000	46000	84000	27000	34000
Al	0.5	0.7	0.00	0	1.2	1.3	0.3	2.1	8	14	0.01
Si	8	5	9	8	28	3	30	11	8	12	3
V	<0.002	-	<0.002	-	nd	nd	nd	nd	nd	nd	0.002
Cr	0.014	0.028	0.002	0.001	0.003	0.002	0.004	0.030	0.04	0.09	0.00005
Mn	1.6	0.7	0.3	0.3	1.2	0.7	1	4	3	4	0.002
Fe	30	20	2	3	0.7	0.3	3	10	0.5	1.4	0.01
Co	0.004	0.003	0.010	0.014	0.012	0.006	0.01	0.04	0.19	0.19	0.0003
Ni	0.028	0.029	0.026	0.020	0.01	0.01	0.01	0.05	0.26	0.27	0.005
Cu	0.007	0.004	0.04	0.11	nd	nd	0.01	0.03	0.08	0.06	0.003
Zn	0.06	0.08	0.07	0.08	nd	nd	0.06	0.20	0.3	0.8	0.01
As	<0.02	-	<0.02	-	nd	nd	0	0.3	0.04	0.30	0.003
Sr	8.9	1.9	5.1	2.7	1.6	0.5	2.4	2.7	7	4	8
Ag	<0.005	-	<0.005	-	nd	nd	0.005	0.030	0.02	0.03	0.0003
Cd	<0.002	-	<0.002	-	nd	nd	0.004	0.014	0	0.005	0.0001
Sb	<0.005	-	<0.005	-	nd	nd	0.00	0.02	0	0.02	0.0003
I	0.54	0.21	0.30	0.23	0.05	0.06	0.5	0.9	0.5	0.4	0.06
Ba	0.025	0.005	0.05	0.04	0.053	0.004	0.06	0.12	0	0.01	0.03
W	<0.001	-	0.002	0.002	nd	nd	nd	nd	nd	nd	0.0001
Hg	<0.002	-	<0.002	-	nd	nd	nd	nd	nd	nd	0.00003
Pb	0.010	0.008	0.017	0.017	nd	nd	0.13	0.28	0	0.05	0.00003
Bi	<0.002	-	<0.002	-	nd	nd	0	0.25	0.06	0.25	0.00002
U	<0.002	-	0.008	0.013	nd	nd	nd	nd	nd	nd	0.003
Au	0.004	0.004	0.005	0.007	nd	nd	0.13	0.21	0.3	0.6	0.01

All concentrations in mg/L, except Au in µg/L

Numbers in brackets denote the number of samples taken at each site

@ Standard Deviation or detection limit (whichever is the larger)

* For the elements Na, Mg, Ca, K, Cl, SO_4 and Br, the ratio of the element concentration divided by TDS is used rather than the concentration

nd not determined

- not applicable

Table 6.3: Averaged elemental compositions (mg/L) of Ambassador waters

	Mean	Standard Deviation
PO_4	0.8	1.6
Y	0.0041	0.0021
Cs	0.011	0.008
La	0.0013	0.0006
Ce	0.004	0.003
Pr	0.0005	0.0002
Nd	0.0023	0.0009
Sm	0.0010	0.0003
Eu	0.0005	0.0005
Gd	0.0010	0.0003
Tb	0.0002	0.0001
Dy	0.0006	0.0002
Ho	0.0002	0.0001
Er	0.0005	0.0001
Tm	0.0002	0.0001
Yb	0.0005	0.0000
Lu	0.0002	0.0001
REE (total)	0.013	0.005
Tl	0.0004	0.0002
Th	0.0004	0.0003

The high dissolved Fe concentrations for the Mulga Rock samples are similar to concentrations observed at other sites at low oxidation potentials (Figure 6.4). This dissolved Fe may be derived from the first stage of the oxidation of pyrite and other sulphide minerals:

$$2FeS_2 + 7O_2 + 2H_2O \Rightarrow 2Fe^{2+} + 4SO_4^{2-} + 4H^+ \quad \text{...(1)}$$

(Pyrite)

6.3.3 Isotope chemistry of Mulga Rock groundwaters

Isotope determinations can expand understanding of specific hydrological processes occurring at a site. The isotopes examined, ^2H and ^{18}O , are constituents of the water molecule and their abundances are a specific property of the groundwater. The isotope abundances are expressed in ‰ difference from the SMOW (standard mean ocean water) standard and are examined by plotting ^2H *versus* ^{18}O (Figure A5.1a). A higher δ^2H indicates enrichment of the water in deuterium, the heavy isotope of hydrogen, and a higher $\delta^{18}O$ indicates enrichment in ^{18}O, the heavy isotope of oxygen. Such enrichments occur during evaporation, due to preferential loss of lighter water molecules.

Meteoric water will show a linear relationship between ^2H and ^{18}O (Gat and Gonfiantini, 1981), shown for rain waters at Kalgoorlie (J. Turner, CSIRO, pers. comm., 1992) as the dotted line in Figure A5.1a. Samples previously analysed from Mt. Gibson (Gray, 1991) showed a linear trend distinct from this line. This trend is related to evaporation of the groundwater at this site, as indicated by the linear trend for both isotopes with salinity (Figures A5.1b and A5.1c): *i.e.*, as waters evaporate they become more saline and are proportionally enriched in the heavier isotopes.

Figure 6.2 **Eh vs. pH for groundwaters from Minigwal, Ambassador and other sites**

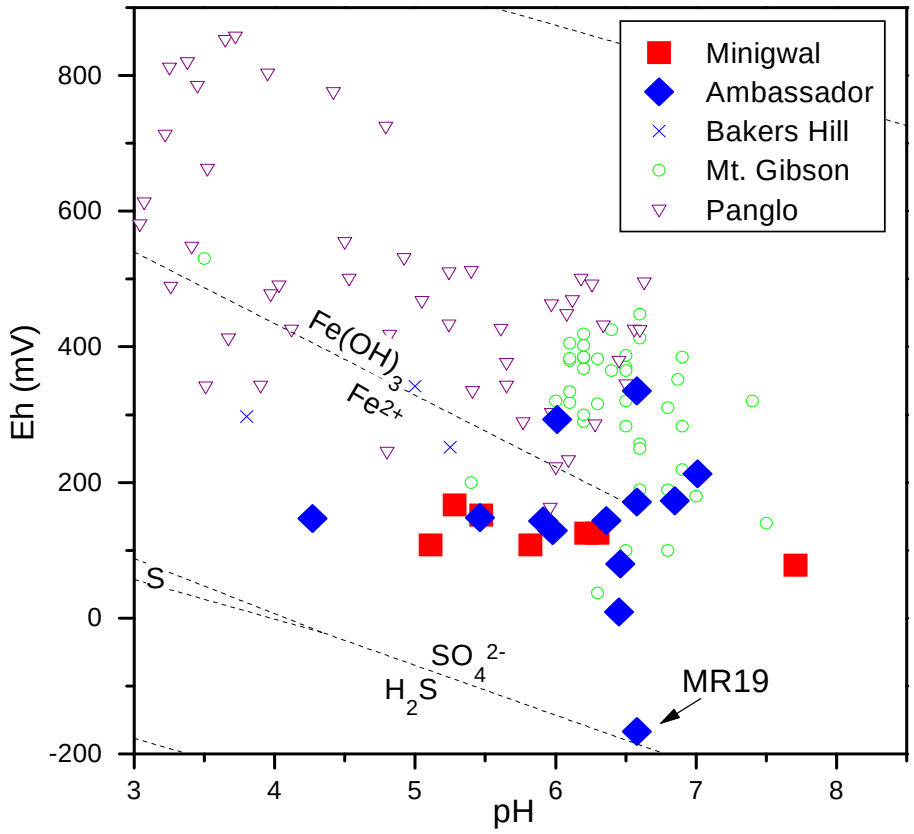

Figure 6.3 **HCO_3- vs. pH for groundwaters from Minigwal, Ambassador and other sites**

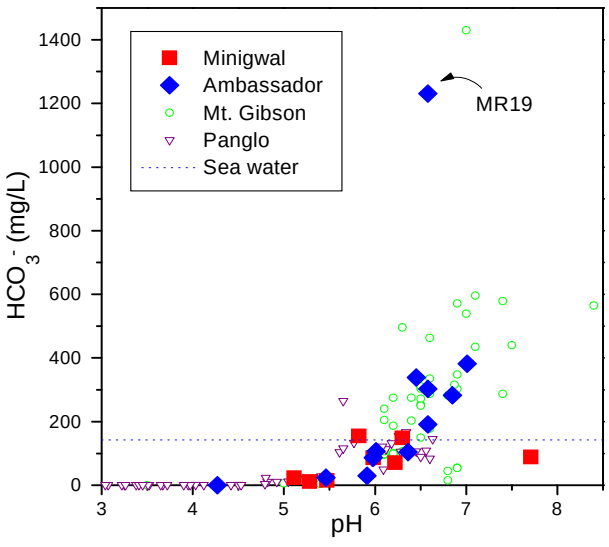

Figure 6.4 **Fe vs. Eh for groundwaters from Minigwal, Ambassador and other sites**

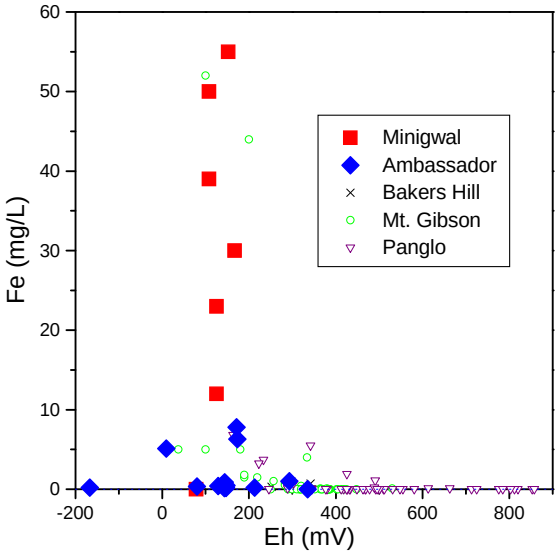

The Mt. Gibson sample lying away from this line is thought to represent a sample that has been contaminated by recent rainfall. Results by other workers in the Yilgarn block (Turner *et al.*, 1992) and elsewhere (Gat and Gonfiantini, 1981) support this hypothesis.

The waters from Ambassador do not fit this model, but instead show complex behaviour not yet clearly understood. The waters are divided into 4 groups, as follows.

1. Samples MR13 and MR14, which are up-gradient of the mineralized area, are strongly depleted in ^{18}O and ^{2}H, relative to the expected ^{2}H and ^{18}O compositions at the observed salinities (Figures A5.1a-c)
2. Samples MR15, MR17 and MR18, which lie on the northern and eastern edge of the mineralization (Figure 6.1), are more strongly depleted in^{2}H than Group 1(Figure A5.1b), although with a smaller ^{18}O depletion (Figures A5.1c)
3. Samples MR9, MR16 and MR19, which lie in and down-gradient of the mineralized area, lie on the evaporative lines, *i.e.*, show standard groundwater behaviour
4. Sample MR20 shows virtually identical isotope abundances and salinity to the Mt. Gibson outlier, and is therefore assumed to be contaminated by fresh water. As this hole was sampled 2 days after prolonged rain in the region, and only had 1 metre of water at the bottom of the hole, this is a sensible hypothesis.

The spatial location of these groups are shown in Figure A5.53 and discussed in Section 6.4.2.

In summary, the waters in Groups 3 and 4 had isotope relationships similar to those at other sites, whereas Groups 1 and 2 are highly anomalous, with $\delta^{2}H$ values lower than at the fresh water end of the evaporative line (Figure A5.1b). Such effects might be hypothesized to be due to isotopic exchange by organic matter, but they occur up-gradient of the organic-rich mineralized zone (which is not ^{2}H or ^{18}O depleted). There might also be active weathering of a light-isotope enriched phase in this region, though there is no supporting evidence for this. Carbonitites, which are suggested as a possible source for the mineralization (Section 6.2), are not depleted in these isotopes, and are therefore unlikely to be the cause of this anomaly.

Thus, the isotope determinations indicate that waters in, and down-gradient of, the main mineralized area at Ambassador have similar isotope abundances to those at other sites, whereas groundwaters up-gradient of the mineralized area show strong depletions in ^{2}H and ^{18}O for reasons not clearly understood. This phenomenon may be of relevance in understanding the hydrogeochemistry and, potentially, the genesis of this deposit.

6.3.4 Major ion chemistry of groundwaters at Mulga Rock

In Table 6.2, the results for the species Na, Mg, Ca, K, Cl, SO_4 and Br are given as the ratio of the ion over TDS, hereafter described as the TDS ratio. The rationale for the use of TDS ratios is demonstrated in Figure A5.2, which shows Na concentration plotted vs. TDS. The sea water data are used to derive the line of possible values if seawater were diluted with freshwater or concentrated by evaporation, hereafter denoted as the seawater line, and shown in Figures A5.2 - A5.9. At all sites studied, Na content and TDS are closely correlated, and the points tend to fall on the seawater line. However, many of the other elements significantly deviate from the sea water line, indicating major regional groundwater processes.

The Minigwal and Ambassador waters have distinct major element properties. Potassium abundances of the Ambassador waters closely follow the sea water line (Figure A5.4), whereas the Minigwal waters have a relative K abundance about 65% that of sea water. Similar differences between the Ambassador and Minigwal groundwater systems are also observed for Ca, Sr, Ba and, to a lesser extent, Br (Figures A5.6 - A5.9), and suggest that these waters have different sources. The data are consistent with the interpretation that the Ambassador channel is a tributary to the main Minigwal system.

The waters in holes MR19 and MR20, from the centre of the mineralized zone at Ambassador, have distinctly lower salinities than other waters (Figure A5.52), implying influx of fresher groundwater in this area, and are strongly enriched in Ba. [Note, however, that isotope studies (Section 6.3.3) suggest that the lower salinity of MR20, but not MR19, may be due to rainwater contamination.] In addition, MR19 is highly reducing (Figure 6.2), with an anomalously high alkalinity (Figure 6.3), enriched in Ca (Figure A5.7) and depleted in SO_4 (Figure A5.5). These observations are consistent with reducing conditions in the mineralized zone leading to SO_4 reduction, with Ca and Ba enrichment due to the higher solubility of the relative sulphate minerals gypsum ($CaSO_4.2H_2O$) and barite ($BaSO_4$) in SO_4 depleted waters (see below).

The solubility of various minerals in contact with the Mulga Rock groundwaters can be determined by speciation analysis. This is commonly done using the program PHREEQE (Parkhurst *et al.,* 1980), which is described in detail in Gray (1990) and Gray (1991), with additional use of the programs PHRQPITZ (courtesy USGS) and PC-PHREEQEP (Crowe and Longstaffe, 1987) to correct for ion pairing effects in the more saline samples. Use of these programs gives information on the speciation of elements in solutions, and calculates the solubility index (SI) for a number of mineral phases for each water sample. If the SI for a particular mineral phase equals zero (empirically from -0.5 to 0.5), then that particular water sample is in equilibrium with the solid phase, under the conditions specified. Where the SI is less than zero (say < -0.5), the solution is under-saturated with respect to the phase, so that, if present, the phase may dissolve. If the SI is greater than zero (say > 0.5), the solution is over-saturated with respect to this phase and the phase can precipitate. This analysis specifies possible reactions, but kinetic constraints may rule out reactions that are thermodynamically allowed. Thus, for example, waters are commonly in equilibrium with calcite, but may become over-saturated with respect to dolomite (as observed here; Table 6.4), due to the slow rate of solution equilibration with this mineral (Drever, 1982).

Trace element and U bonding to organic matter (Section 2.3.3) is not accounted for in this analysis. Thus, complexation of metals by dissolved/suspended organic matter may increase solubility, whereas sorption onto solid humate may decrease the solubility from that calculated. These effects are important for trace elements, such as U, Pb and Cu and other transition metals, which are present at low concentrations and have high affinities for organic matter (Disnar, 1981; Giesy *et al.*, 1986).

The SI values of the water samples for a number of relevant solid phases are given in Appendix 5, Table A5.3 and plotted in Figures A5.28 - A5.51. The Mulga Rock groundwaters are undersaturated with respect to halite (NaCl; Figure A5.28). The more saline Minigwal waters are at equilibrium with gypsum ($CaSO_4.2H_2O$) and celestine ($SrSO_4$; Figures A5.29 and A5.30). All waters are in equilibrium with barite ($BaSO_4$; Figure A5.31), in similarity with other sites (Gray, 1990, 1991), although some water samples in the mineralized zone at Ambassador appear to be over-saturated. The neutral to alkaline waters approach saturation with calcite ($CaCO_3$) and magnesite ($MgCO_3$; Figures A5.32 and A5.33)

Silicon concentration is controlled by lithology, pH and salinity and the Mulga Rock waters have comparable Si contents to the other sites (Table 6.2; Figure A5.12). The waters are generally oversaturated with respect to quartz (the least soluble Si phase) and undersaturated with respect to amorphous silica (Table 6.4; Figure A5.35), indicating complex controls, possibly involving reactions with quartz, amorphous silica and/or Si minerals with intermediate solubility (*e.g.*, chalcedony). The Al concentration in groundwater is controlled by the pH, and in most waters Al concentration is below the detection limit (Figure A5.13). At pH 6, Al solubility appears to be controlled by equilibration with amorphous alumina [$Al(OH)_3$; Figure A5.36), whereas at lower pH values the controlling solid phase appears to be jurbanite [$Al(OH)SO_4$; Figure A5.37].

As discussed in Section 6.3.2 (Figure 6.4), Fe concentrations are high for Minigwal waters and moderate for the Ambassador waters, relative to sites in the Yilgarn. Speciation analyses suggest very complex controls on Fe mobility. In the Ambassador channel, sample MR19 (CD-1409), which is highly reduced (Section 6.3.2), is saturated with respect to pyrite (FeS_2; Figure A5.38), whereas other Ambassador waters reach siderite ($FeCO_3$) saturation (Figure A5.39) and are oversaturated with respect to ferrihydrite [a high solubility Fe(III) phase; Table 6.4; Figure A5.40] at higher pH values. In comparison, despite having high dissolved Fe concentrations, the Minigwal waters are all undersaturated with respect to the Fe minerals discussed above, primarily because they have lower pH and/or Eh values than at Ambassador.

Dissolved Mn concentrations at Mulga Rock are low, relative to other sites (Table 6.2: Figure A5.15), with the Minigwal waters generally having greater Mn contents than at Ambassador. Most of the waters are undersaturated with respect to rhodochrosite ($MnCO_3$; the least soluble Mn mineral at this site; Figure A5.41), with the exception of MR19, which has anomalously high bicarbonate (Figure 6.3), and MR1, which is the most alkaline Minigwal water.

6.3.5 Trace element chemistry of Mulga Rock groundwaters

The concentrations of Cr, Co, Ni, Cu, Zn, REE, Au and Pb are generally low, relative to other sites investigated (Table 6.2; Figures A5.14, A5.17 - A5.21, A5.23 - A5.25). These elements are undersaturated with respect to the pertinent least soluble mineral phase (Figures A5.42 - A5.48), with the exception of Cr, which is oversaturated with respect to Cr_2O_3 (Figure A5.49), indicating slow equilibration with this phase. The pH of the groundwater may, however, control the distribution of the REE, with higher pH (and total alkalinity) corresponding to increased concentrations of HREE relative to LREE (Table A 5.2). Increased HREE enrichment is consistent with bicarbonate and/or organic matter complexation of REE (Douglas, unpubl. data). The undersaturation of the other elements may reflect control by other reactions such as adsorption on organic or mineral surfaces, or simply that the elements are not been dissolved during weathering at a fast enough rate to reach saturation.

Table 6.4: Range in SI values for groundwaters at Mulga Rock, relative to the least soluble phase for each element tested

Mineral	Solution Variable / Mineral Formula	Minigwal Groundwaters				Ambassador Groundwaters			
		Min.	Max.	Mean	Stand. Dev.	Min.	Max.	Mean	Stand. Dev.
	pH	5.1	7.7	6.0	0.9	4.3	7.0	6.2	0.7
	Eh (mV)	80	170	120	30	-170	340	140	120
	TDS (mg/L)	25000	95000	55000	26000	8000	36000	21000	9000
Halite	NaCl	-2.8	-1.8	-2.3	0.4	-3.8	-2.6	-3.1	0.4
Calcite	$CaCO_3$	-3.0	0.1	-1.7	1.2	-2.7	0.3	-0.8	0.9
Gypsum	$CaSO_4.2H_2O$	-0.8	-0.3	-0.4	0.2	-2.2	-0.2	-0.6	0.5
Dolomite	$CaMg(CO_3)_2$	-5.0	1.0	-2.6	2.3	-4.9	1.1	-1.1	1.8
Magnesite	$MgCO_3$	-2.6	0.3	-1.4	1.1	-2.8	0.2	-0.9	0.9
Celestine	$SrSO_4$	-0.8	-0.1	-0.4	0.2	-2.5	-0.3	-0.9	0.5
Barite	$BaSO_4$	-0.3	0.4	0.1	0.2	-0.5	0.7	0.1	0.3
Quartz	SiO_2	-1.0	0.7	0.3	0.6	-0.3	0.9	0.3	0.4
amorphous and silica	SiO_2	-2.3	-0.5	-1.0	0.6	-1.5	-0.4	-0.9	0.4
Gibbsite	$Al(OH)_3$	1.4	3.0	2.0	0.8	-	-	-	-
amorphous alumina	$Al(OH)_3$	-0.9	0.7	-0.3	0.8	-	-	-	-
Siderite	$FeCO_3$	-2.6	-0.6	-1.5	0.9	-3.5	0.1	-1.7	1.2
Goethite	FeOOH	1.2	4.7	3.3	1.3	-2.9	7.0	3.1	3.0
Ferrihydrite	$Fe(OH)_3$	-3.8	-0.3	-1.7	1.3	-7.9	2.0	-1.9	3.0
Rhodochrosite	$MnCO_3$	-3.3	0.4	-1.9	1.4	-3.4	-0.2	-1.9	0.9
Tenorite	$Cu(OH)_2.H_2O$	-10.9	-5.5	-8.7	1.8	-8.6	-4.2	-6.0	2.0
Smithsonite	$ZnCO_3$	-6.2	-4.5	-5.2	0.6	-5.3	-2.5	-3.9	1.1
Otavite	$CdCO_3$	-5.5	-1.8	-4.1	1.5	-3.5	-2.1	-2.8	1.0
Cerussite	$PbCO_3$	-5.5	-1.2	-3.7	1.4	-3.7	-0.6	-2.2	0.9
$Ni(OH)_2$	$Ni(OH)_2$	-7.5	-5.7	-6.7	0.7	-9.2	-4.0	-5.6	1.5
Iodyrite	AgI	-2.8	-2.4	-2.6	0.2	-1.4	-1.4	-1.4	-
$CoCO_3$	$CoCO_3$	-6.5	-6.5	-6.5	-	-5.7	-3.3	-4.1	0.8
Cr_2O_3	Cr_2O_3	-0.9	7.0	1.8	3.2	-6.1	4.8	1.3	4.1
Au Metal	Au	6.6	7.9	7.2	0.5	4.9	7.7	6.4	1.2
Uraninite	UO_2	-	-	-	-	-9.7	-4.0	-7.0	2.8
Rutherfordine	UO_2CO_3	-	-	-	-	-5.1	-4.2	-4.5	0.5
CO_2 (gas)	partial pressure (log atmosphere)	-3.0	-0.9	-1.5	0.7	-1.6	-0.6	-1.3	0.3

\- not applicable (at least one of the mineral components below detection limits in the groundwater) am. amorphous

Iodide concentrations are considerably enhanced, relative to seawater (Figure A5.22), as at the other mineralized sites (Gray, 1990, 1991). High I levels in groundwater are postulated to indicate the enrichment of I within mineralized areas, as I is a chalcophile element, extensively enriched in sulphide environments (Fuge and Johnson, 1984, 1986; Fuge *et al.,* 1988) which may be a useful pathfinder for mineralization (Xuejing *et al.,* 1981; Andrews *et al.,* 1984).

6.3.6 Uranium chemistry of Mulga Rock groundwaters

Uranium concentrations in the Mulga Rock groundwaters are generally low (< 0.002 mg/L; Figure A5.27), and undersaturated with respect to both U(IV) (uraninite) and U(VI) (rutherfordine) minerals (Figures A5.50 and A5.51). However, these speciation calculations do not take account of soluble organic phases. In neutral to acid conditions, and in organic-rich environments, the major aqueous U species would be expected to be UO_2^{2+} bound to dissolved humic acid (Section 2.3.3; Figure 2.1). Therefore, U solubility would be expected to be higher than calculated in the speciation analysis, so that the calculated SI are likely to be over-estimates, and the undersaturation with respect to inorganic minerals (Figures A5.50 and A5.51) is significant. Presumably, the controlling phase is U bound to solid organic matter, which is maintaining very low dissolved U concentrations.

6.3.7 Summary

The Mulga Rock waters have low redox potentials, with one hole having an Eh close to the value for sulphate reduction (Figure 6.2). Dissolved Fe, commonly observed in reduced waters, is particularly high in the Minigwal waters (Figure 6.4). Other major ion determinations (Section 6.3.4) indicate several hydrogeochemical differences between the Ambassador and Minigwal waters, indicating them to be hydrologically distinct. This is consistent with the supposition that the Ambassador waters flow into the Minigwal system. In addition, ^{2}H and ^{18}O isotope investigations (Section 6.3.3) indicate that the Ambassador waters up-gradient of the main mineralized area are anomalously "light", for reasons not clearly understood.

Speciation analysis indicated that the waters are undersaturated with respect to most salts, except for the alkaline earth sulphates (*i.e.*, gypsum, celestine and barite). Aluminium, Si and Fe appeared to have complex controls on solubility, and all the trace elements (including U) except Cr are undersaturated with respect to their inorganic mineral phases. Indeed, trace element concentrations are low relative to other sites, suggesting strong trace metal sorption on organic matter.

Groundwaters from holes MR19 (CD-1409) and MR20 (CD-1366) are particularly anomalous in terms of low Eh, reduced SO_4, high alkalinity, Ca and Ba. These effects will be discussed further in Section 6.4

6.4 Hydrogeochemical mapping

6.4.1 Description of mapping

The spatial distributions of the elements and ions are mapped in Appendix 5, Figures A5.52 - A5.78. The Ambassador mineralized area is indicated, distinguishing between low grade mineralization (100 - 1500 ppm U) and high grade mineralization (> 1500 ppm U). The distributions of Na, Mg, Ca, K, Cl, SO_4 and Sr are not shown because their concentrations are controlled by salinity or salt precipitation. Although in most samples its concentration appears to be controlled by barite equilibration, Ba is included because samples within the mineralized zones have higher Ba concentrations, and one hole (MR20) is oversaturated with respect to barite (Figure A5.31). The distributions of several elements appear to show specific effects within the mineralized area at Ambassador, as are discussed below.

6.4.2 Isotope and water quality parameters

Total dissolved solids (Figure A5.52): The Minigwal groundwaters contain up to 9.5% TDS, which is about 3 x the salinity of sea water. The Ambassador system has lower salinities than the main Minigwal system. Of interest is the apparent increase in salinity going from the eastern edge of the Ambassador channel to the main Minigwal system, with the sharp decrease in the mineralized area. Given that the waters were sampled by bailer rather than by dewatering of the hole, this could be due to contamination by rain water. Isotope analysis (Section 6.3.3) indicate that hole MR20 may be contaminated, but not MR19.

^{2}H and ^{18}O Isotopes (Figure A5.53): The four isotope groups distinguished in Section 6.3.3 have a clear spatial distribution. MR20 is in Group 4, which is assumed to represent a sample diluted by rain water, whereas groundwater in the main mineralized area (Group 3) has similar isotope composition to saline groundwater at other sites. Up-gradient of the mineralized area, the groundwater (Groups 1 and 2) is depleted in the heavy isotopes.

pH (Figure A5.54): The pH distribution is very irregular, indicating localized effects, possibly due to degree of oxidation, presence of sulphides in the solids, buffering capacity of the organic matter or other factors.

Oxidation potential (Figure A5.55): The Eh distribution is also irregular, although the most reduced waters occur within the Ambassador mineralized zone.

Bicarbonate (Figure A5.56): Bicarbonate is clearly enriched in the Ambassador mineralized zone, with sample MR19 measuring more than 1200 mg/L.

Phosphate (Figure A5.57): Only Ambassador samples were analysed, with the main mineralized area being clearly enriched in dissolved PO_4.

6.4.3 Barium and pH controlled major elements

Barium (Figure A5.58): The highest Ba concentrations occur within the Ambassador mineralized zone.

Aluminium (Figure A5.59): Unlike sites in the Yilgarn (Gray, 1990, 1991), dissolved Al concentration at Mulga Rock is poorly correlated with acidity (Figure A5.13). There is a distinct spatial effect, with the waters at Shogun and Emperor having measurable Al, and all of the Ambassador waters being below the detection limit.

Silicon (Figure A5.60): The Ambassador channel has low dissolved Si concentrations, with the greatest depletion occurring within the main mineralized zone.

Iron (Figure A5.61): The Minigwal waters have particularly high Fe concentrations, but there is no clear distribution pattern in the Ambassador channel.

Manganese (Figure A5.62): Dissolved Mn shows a similar distribution to Fe, with enrichment in the Minigwal waters, and no clear distribution pattern in the Ambassador channel.

6.4.4 Trace elements

Most of the trace elements, including the base metals (*Cr, Co, Ni, Cu, Zn and Pb*; Figures A5.53 - A5.68), the rare earth elements (*Y, La, Ce*, *total REE*; Figures A5.69 - A5.72), other chalcophile elements (*I, Au*; Figures A5.73 - A5.74), *Cs* (Figure A5.75) and *Th* (Figure A5.76), do not show any clear spatial distribution. *Uranium* (Figure A5.77) and *tungsten* (Figure A5.78) are relatively enriched in water samples from the main mineralized zone at Ambassador.

6.4.5 Summary

The Minigwal waters are more saline, and are enriched in Al, Fe and Mn, relative to waters at Ambassador. The Ambassador mineralized zone has lower groundwater Eh values, enrichments in dissolved HCO_3, PO_4, Ba, U and W and depletion in dissolved Si. The ^{2}H and ^{18}O isotope behaviours of the water are particularly anomalous up-gradient of the main mineralized zone.

6.5 Conclusion

Groundwaters at Mulga Rock differs from those from Yilgarn sites, having low oxidation potentials (Section 6.3.2), with anomalous isotope effects (Section 6.3.3) and low concentrations of a number of trace elements (Sections 6.3.5 and 6.3.6). All of these differences may be principally due to the high organic matter concentrations at this site.

Hydrogeochemical investigations suggested that the groundwaters at Ambassador are distinct from those sampled from the main drainage system, including the Emperor and Shogun deposits, which is classified here as the Minigwal system. The Minigwal groundwaters were more saline, depleted in K, Ca and Sr (Section 6.3.4), and enriched in Al, Fe and Mn (Section 6.3.5), relative to Ambassador. This is consistent with present-day groundwaters flowing down the Ambassador channel into the larger Minigwal drainage system.

The main mineralized zone at Ambassador has specific groundwater characteristics, that are not observed for the waters samples at Emperor and Shogun. Some of the waters from the mineralized zone at Ambassador have particularly low Eh values, with SO_4 possibly being reduced to sulphide in MR19 (Section 6.3.2). They are significantly enriched in dissolved HCO_3, PO_4, Ba, U and W, depleted in dissolved Si, and less saline (Section 6.4). In addition, anomalous ^{2}H and ^{18}O isotope behaviours are observed just up-gradient of the mineralized zone.

The specific hydrogeochemistry of the Ambassador mineralized zone may relate to interactions between groundwater and solid organic matter, and/or could reflect inflow of water from an additional source. The latter possibility clearly has implications for the genesis of this deposit, and is supported by the apparently reduced salinity in the mineralized zone. However, isotope determinations suggest that one of the two less saline samples is contaminated with rain water, so that this feature requires confirmation by additional sampling.

7.0 BASEMENT GEOLOGY AND GEOCHEMISTRY

7.1 Introduction

Rocks from three core holes from the basement of the Ambassador deposit were examined both petrographically and geochemically to ascertain if basement lithologies were a possible source for the overlying palaeochannel mineralization. Additionally, due to the paucity of outcrop in the Ambassador area, this provided an opportunity to study the local geology. Preliminary results from mapping of the basement geology also suggests that there is a strong structural control on the direction of the palaeochannel, which is similar to the strike of the Proterozoic basement.

7.2 Results and Discussion

Basement samples from the Ambassador area, adjacent to and beneath the palaeochannel, range in age from Proterozoic to Permian. Optical microscopy and XRD analyses have shown that the basement lithologies consist predominantly of quartzites, cherts, (carbonaceous, pyritic) shales and dolomites. Further studies investigating the mineralogy are continuing using SEM in an attempt to relate mineralogical-trace element associations and to determine the accessory mineralogy in rocks such as the carbonaceous shales from hole CD-1594, where identification by optical microscopy proved difficult due to the abundant amorphous organic matter. The basement samples have also been analysed for their major and trace element geochemistry by XRF and NAA with the method of analysis identical to that described in Section 3.2.2 for the palaeochannel samples. The results of the basement geochemical analysis are presented in Appendix 4. The majority of samples are not significantly mineralized, however, a few samples may be anomalous with maximum concentrations of 31 ppm U, 576 ppm Ce, 5 ppm Tl and transition metals (433 ppm Cu, 4533 ppm Zn, 1037 ppm Ni, 947 ppm V). As in the palaeochannel, Sc and U also highly correlated, although abundances are generally much lower.

The dolomites in hole CD-1595 are enriched in Ca, Mg and Mn and may contain moderate concentrations of REE, but have low abundances of all other elements, especially transition metals, relative to other basement rocks. The cherts overlying the dolomites also display similar trace elemental trends, while SiO_2 may constitute in excess of 97% of the major element analysis. Elements that may indicate heavy mineral enrichment such as Zr, Hf, Nb, Ta and Cr occur only in low concentrations. One sample (1595-5, 62.30-62.40 m) is strongly pyritic at the chert and dolomite contact and thus is enriched in Fe (30.69%) and S (33.15%) and has high concentrations of a range of chalcophile elements. Gold, U and Th are at normal crustal abundances.

The basement rocks in hole CD-1594 consist mainly of carbonaceous shales; they contain abundant Si and may have organic contents up to 8% as loss on ignition (LOI). All other major element concentrations are low except for Ti which may constitute up to 2.7% (as TiO_2) of the sample. This hole also contains the highest U (7-31 ppm), moderate Th (6-10 ppm) concentrations and elements consistent with the presence of heavy minerals (*e.g.* Zr, maximum 261 ppm, Hf, maximum 6.5 ppm and elevated REE). Deeper samples (69.62-80.33 m) contain approximately 10 to 20 ppb Au, and elevated concentrations of REE Sb, Se and transition metals (Co, Cr, Cu, Mo, Ni, Pb, Sc, V, Zn). Interestingly, Se, Mo and V enrichment, is a common element suite that accompanies roll-front U mineralization. This hole also contains the consistently highest total concentrations of trace elements (7300 ppm) with the highest total concentrations occurring in the deepest, sulphide-rich, section.

The basement hole CD-1596 consists of a geochemically monotonous sequence of clay rich to almost pure quartzites (up to 99.1% silica), with minor kaolinite and muscovite identified by XRD and confirmed by the presence of increased Al, alkali (*e.g.,* K, Rb, Cs) and alkaline earth element (Ba) concentrations. There are no significant concentrations of Au, U, or trace metals, although V and Zn may be slightly elevated in some samples. The presence of accessory heavy minerals is indicated by increased concentrations of Ti (maximum 0.8%), Zr (maximum 245 ppm), Th (maximum 22 ppm) and REE (*e.g.,* La, maximum 93 ppm).

7.3 Conclusion

The basement lithologies of the Ambassador deposit drill holes examined here consist of a sequence of predominantly unmineralized quartzites, cherts, shales and dolomites. Although these rocks do locally contain moderately elevated concentrations of the elemental suite seen in the redox horizon, it is difficult to assess if these lithologies represent either a single source or are even only partly responsible for the palaeochannel mineralization. Further sampling and geochemical analysis (including isotopic analysis) of the basement may resolve this question. Alternative scenarios for the possible mode of origin of the mineralization of the Ambassador deposit that do not specifically involve the basement rocks are presented in Section 10.1.2.

8.0 CHARACTERIZATION OF ORGANIC MATTER FROM THE AMBASSADOR DEPOSIT

8.1 Introduction

The Mulga Rock lignites may represent a geochemical trap for metals carried by acid brines, either now or in the past. Specific questions are:

(i) are there significant differences in the type of organic matter (OM), either regionally or, specifically, close to mineralization;

(ii) has the type of OM had a fundamental influence on the distribution of the mineralization;

(iii) what is the nature of the association of the trace elements, particularly radionuclides, with the OM.

The project described here involves the characterization of lignites in the Ambassador U deposit, to obtain:

(i) an enhanced understanding of the type and distribution of organic matter;

(ii) information on whether the mineralized zone at Ambassador can be related to specific organic matter properties, or is instead related to other factors such as geomorphological position and/or vicinity of a basement source.

Investigations have involved C,H,O,N elemental analysis, ^{13}C NMR and petrographic analyses of 63 samples selected by PNC staff. These samples were selected to provide information on OM throughout the Ambassador area and to observe if measured characteristics could be correlated with form or distribution of mineralization.

8.2 Maceral characterization

Coals are defined in terms of their petrological components, called *macerals* (van Krevelen, 1963). There are three defined Maceral Groups:

(i) *EXINITE* includes the remainders of waxy and corky products which, on heating, are largely transformed into gas and tar. They include the macerals *resinite* (from resins, waxes and oils), *sporinite* (cell walls of pollen and spores), *cutinites* (leaf cuticles) and *alginite* (algae). This maceral group is equivalent to *LIPTINITE*, a term still used by some analysts. Organic matter containing large amounts of exinite appears to have formed in wet sites with standing water, where plant debris has been destroyed and decomposed to a high degree, so that only the more resistant fragments remain. This group is geochemically the most heterogeneous.

(ii) *VITRINITE* consists predominantly of the remains of plant and wood tissue that on heating, normally leave a fused coke button as the main product. This group is now divided into *telovitrinite* [large (> 0.02 mm) intact clasts of plant tissue], *detrovitrinite* [fine-grained (< 0.02 mm) fragmented clasts of tissue that commonly form a groundmass for all the other coal macerals], and *gelovitrinite* (minor amounts of remobilized vitrinitic gel material). Previously, vitrinite was divided into *telinite* (woody tissue in which the lumens are filled with colloidal humic matter or resin) and *collinite* (woody tissue that has lost its structure during coalification processes, but remains translucent). It appears that

vitrinite was formed under only partly saturated conditions, such as in a swamp where the groundwater level was only slightly below the surface, with stagnant conditions ensuring mummification of plant structures.

(iii) *INERTINITE* includes all chemical, practically inert, macerals that do not soften or cake on heating and cannot be hydrogenated. It includes *micrinite* (woody tissue that has lost its structure, but is completely opaque under transmitted light) and *fusinite* (woody tissue in which the lumens are either empty or filled with mineral constituents). Fusinite resembles charcoal and appears to have been formed under "very dry" conditions, such as during forest fires or other exothermic processes.

The three maceral groups are, to a certain degree, characterized by their chemical composition (Stach *et al*., 1982): vitrinite contains relatively more O, exinite more H and inertinite more C. In this report, the primary categories discussed will be exinite/liptinite and vitrinite.

8.3 Analytical Techniques

8.3.1 ^{13}C NMR

Nuclear magnetic resonance (NMR) is a spectroscopic technique, but it differs from most other such techniques in that it is dependent on nuclear phenomena, rather than electronic effects (for further information see Wilson, 1987). NMR can only be used on a magnetically active nucleus. For example, the ^{1}H nucleus is NMR-active, whereas ^{12}C, which comprises 98.9% of total C, is NMR-inactive. However, ^{13}C (1.1% of total C) is NMR-active and ^{13}C NMR is commonly used in organic matter investigations. Because of the low relative abundance of ^{13}C, there can be detection problems if the organic matter content is low and/or there are significant concentrations of paramagnetic elements. The main paramagnetic element is generally Fe^{III}, though in the complex elemental suite at Ambassador, other elements (such as Cr, Co, Mn, REE and U) may also interfere.

Examples of spectra of different coal types are shown in Figure 8.1. Peaks are observed in positions (measured as chemical shift, in ppm) that are dependent on the chemical environment in which the C occurs, particularly the functional group, but with minor shifts due to other groups nearby. The sharpness of the peaks reflect the homogeneity of the particular functional group and the peak area is approximately proportional to the fraction of the C in specific groups. Geochemically important C groups relevant to this study are shown in Table 8.1. Carboxylic groups would most likely be the ligands for complexed U.

On this basis, various C groups should be identifiable by this method. ^{13}C NMR identifies the proportions of different functional groups but, as several groups can be present on the same molecule, it cannot directly identify molecules themselves. However, the spectra in Figure 8.1 show that various macerals have differing proportions of functional groups so that tentative designations can be made. Thus, the spectra of alginite indicate that it is rich in aliphatic groups, which are very homogenous (hence the small peak width), with only small amounts of aromatic C. In comparison, sporinite has roughly equal amounts of aliphatic and aromatic carbons, whereas vitrinite and fusinite have greater proportions of aromatics. These macerals have broader aliphatic peaks, suggesting more heterogeneous chemistry (such as branching of the aliphatic chain or substitution by other C-groups).

Figure 8.1 **^{13}C NMR spectra of (a) alginites, (b) sporinites, (c) vitrinites and (d) fusinite. (Modified from Wilson, 1987)**

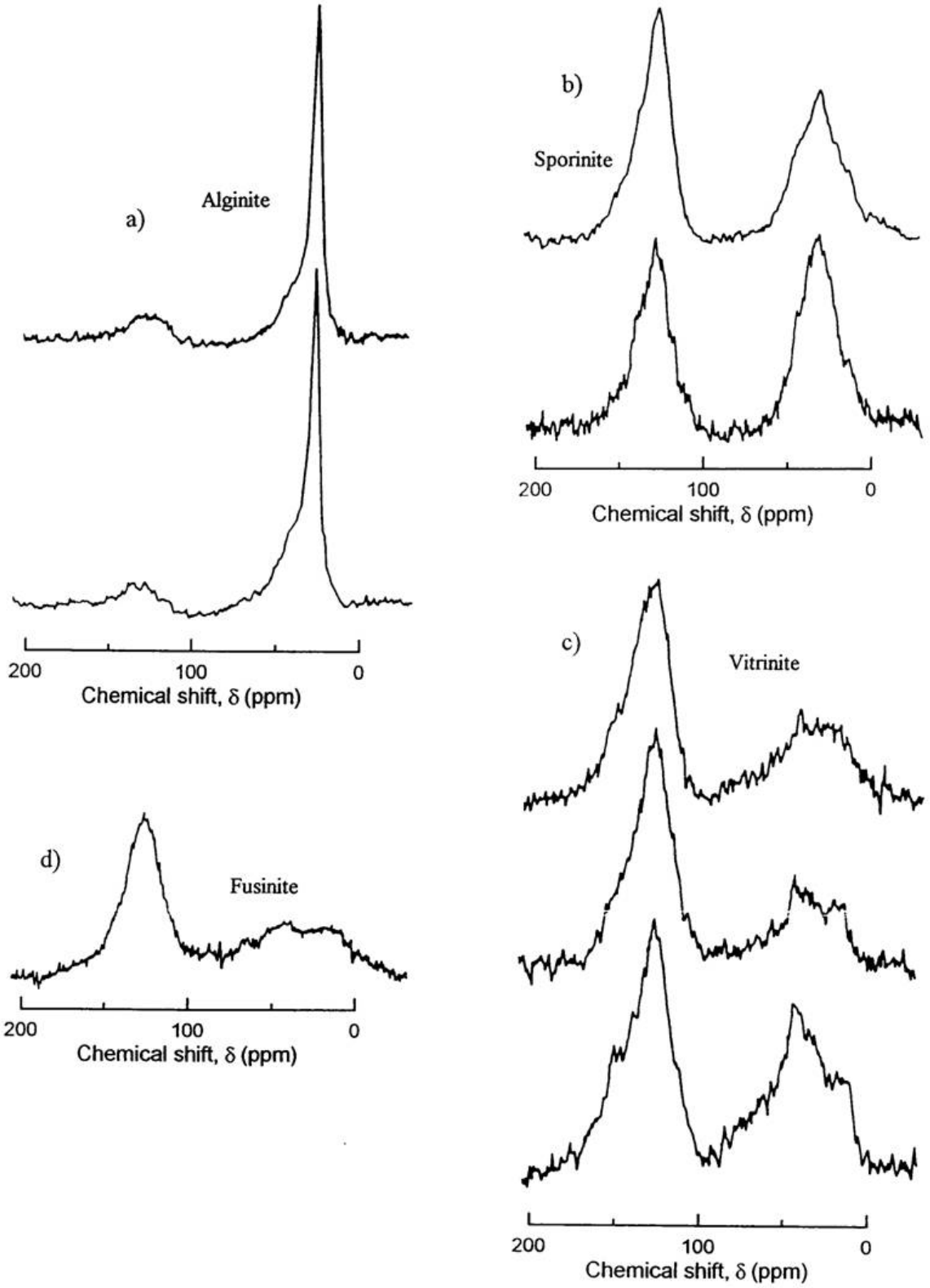

Table 8.1: **^{13}C NMR parameters of geochemically important C groups**

C group	Structure (R denotes either H or C)	Approximate chemical shift (ppm)
Aliphatic	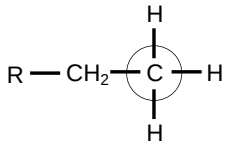	15
	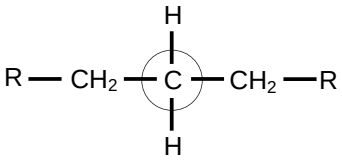	30
Carbohydrate	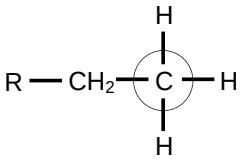	60 - 80
Aromatic	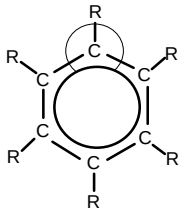	125 - 135
Phenolic	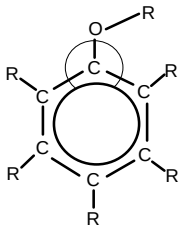	145 - 160
Carboxylic	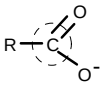	170 - 185
Carbonyl	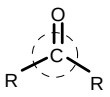	200 - 220

8.3.2 C,H,O,N Analyses

Further information on the geochemistry of organic matter can be obtained by determining its elemental composition, most conveniently expressed in terms of an atomic ratio to C. Thus an atomic H/C ratio of 2 indicates 2 H atoms for every C, suggesting that the organic matter is primarily aliphatic (Table 8.1), whereas a H/C ratio of 1 would suggest aromatic character. High O/C ratios indicate O-containing functional groups, such as carboxylic and carbonyl groups, whereas N could be present as amines (*e.g.*, $-NH_3$) or as part of complex aromatic molecules. These ratios are strongly influenced by the origin of the organic material (*e.g.*, from algae, spores or wood) and also by the degree of maturation (effectively the 'coalification' process), which tends to

result in loss of both O and H. Data was summarized by van Krevelen (1963), in terms of maturation lines for various organic materials (Figure 8.2).

In this diagram, the composition of the macerals at any point of the development line is shown. The final product of coal maturation is a material having negligible H or O (anthracite). Thus, for vitrinite, the primary coalification reaction appears to occur in three phases, as numbered in Figure 8.2:

1. dehydration (loss of H_2O);
2. decarboxylation (loss of C and O);
3. demethanation (loss of C and H).

Figure 8.2 H/C vs. O/C development lines of the macerals (modified from van Krevelen, 1963) Numbers refer to the three phases of coalification discussed in Section 8.3.2.

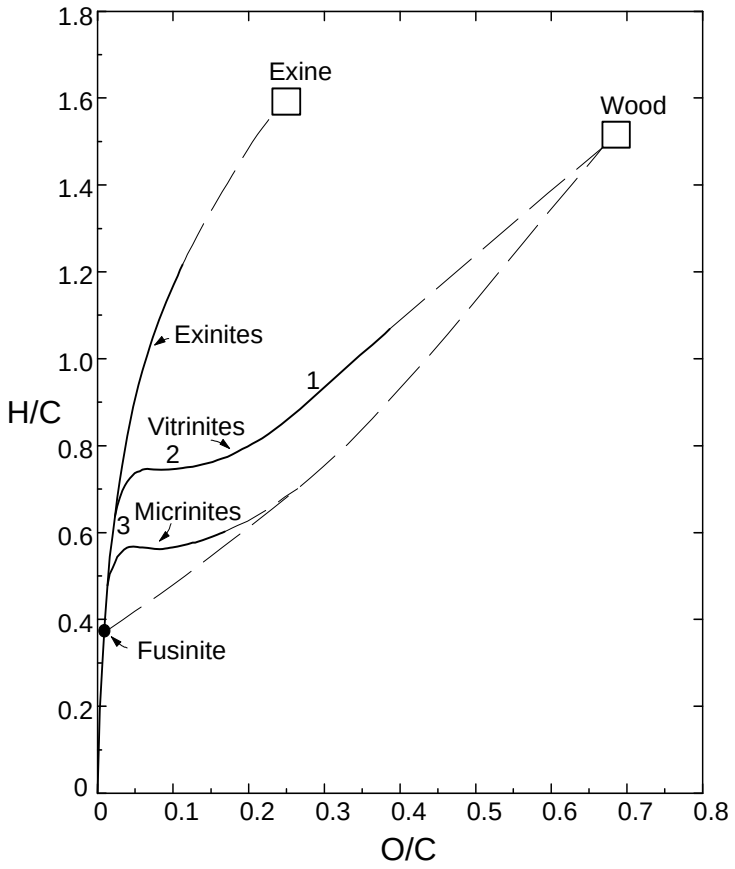

The purest maceral, fusinite, has a constant composition (H/C = 0.38; O/C = 0.01). The compositions of the various micrinites are located in a band parallel to the vitrinization band, but with lower H/C ratios. In contrast, the exinites are considerably richer in H, consistent with the viewpoint that these materials have high proportions of wax alcohol and aliphatic groups. In the vicinity of bituminous coal (H/C < 0.7), the differences in composition between vitrinite and exinite diminish steadily. Beyond this stage, it becomes increasingly difficult to distinguish between these two macerals.

8.3.3 Petrography

The maceral content of lignite material can be analysed petrographically. The purpose was to classify the organic matter in terms of its source(s), degree of degradation and maturation (rank) and environment of deposition. This technique is a useful adjunct to the other methods, because it allows direct examination for each maceral type, whereas the other technique will give a bulk result, which could be the averaged result for a number of different maceral mixtures. However, this analysis can only be performed on unpulverized material and, for the material investigated here, appears to be very operator dependant.

8.3.4 Multiple linear regression analysis

Organic matter at Ambassador was analysed using 3 separate techniques (Sections 8.3.1 - 8.3.3). Results from each of these techniques were compared using Multiple linear regression analysis (MLRA), using the computer program STATISTICA (® Statsoft). The variable of interest was regressed against a suite of other variables, with variables that did not give statistically significant contributions sequentially removed from the regression until an entirely significant MLRA result was achieved for the variable.

8.4 Materials and methods

8.4.1 Samples

The compositions of the 63 samples selected for these preliminary investigations are detailed in Table 8.2 and their locations are shown in Figure 8.3. The samples were selected to represent a range of sites across the mineralized zone, and into areas with little U content.

8.4.2 ^{13}C NMR procedure

^{13}C CPMAS NMR spectra were obtained at ambient temperatures on a Bruker CXP90 Spectrometer operating at the ^{13}C frequency of 22.63 MHz. These experiments were implemented on a Doty 7 mm single-air-bearing probe in which MAS frequencies of 4 kHz were achieved. A recycle delay of 2 s, contact period of 10 ms and ^{1}H $\pi/2$ pulse length of 4 µs were common to all spectra. No spectral smoothing was employed prior to Fourier transformation, and ^{13}C chemical shifts were externally referenced to tetramethylsilane (TMS).

8.4.3 C,H,O,N analytical procedure

The water of hydration (H_2O^-) was determined by heating a weighed sample (up to 5 g, depending on material available) to 105°C. Following this, the sample was heated to 815°C, to give loss on ignition (LOI). This LOI measured at the Chemistry Centre agreed very well with previous LOI determinations during earlier X-ray fluorescence (XRF) analyses.

Elemental analyses were conducted at the WA Chemistry Centre. Approximately 2 mg of sample was weighed and encapsulated in pure Sn metal. The capsule was loaded into a LECO CHNS-932 determinator and the analysis cycle commenced. The sample capsule was dropped into a furnace heated at 1000°C and a precise amount of ultra-high purity O_2 injected. The sample was combusted and any gaseous products swept with the He carrier gas into three infra-red detector cells to determine C, H and S. The gas mixture exiting these detectors was then passed through a series of adsorbent trains to remove CO_2, H_2O and SO_2. The resultant gas

mixture containing He and any N evolved from the sample was passed through a thermal conductivity cell for N determination. The O content was calculated by subtracting C, H, N and S from the total loss on ignition (LOI).

The raw C,H,O,N analyses were corrected and processed as follows:

(i) H and O from separate-phase water (H_2O^-) were subtracted from the raw H and O data;

(ii) H and O contents were corrected for the calculated H and O lost from kaolinite (assumed to be the dominant clay mineral) during ignition
(for H = 2/51 x %Al_2O_3; for O = 16/51 x %Al_2O_3)

Figure 8.3 Samples used for organic matter characterization at Ambassador

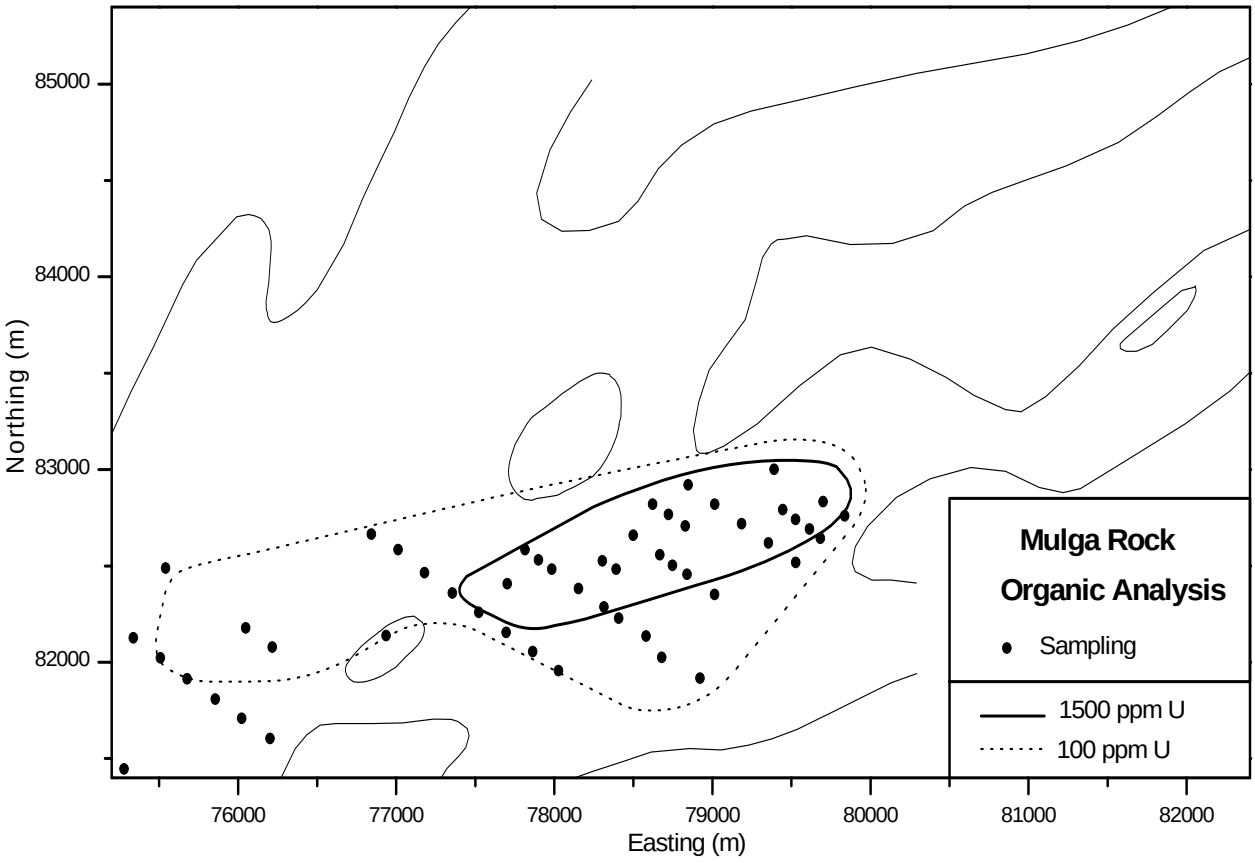

Table 8.2: Compositions of selected samples

CSIRO 00-	Hole No.	East (m)	North (m)	Depth (m)	SiO_2 (%)	Al_2O_3 (%)	Fe_2O_3 (%)	MgO (%)	CaO (%)	Na_2O (%)	TiO_2 (%)	S (%)	LOI (%)	U (ppm)	Analyses		
															CHNO	NMR	Pet
6028	1489	75337	82127	39.4 - 39.8	34.5	1.7	1.5	0.5	0.9	1.1	1.9	3.7	54.4	1	X	X	
6029	1488	75508	82023	39.8 - 40.4	64.9	17.6	1.1	0.1	0.1	0.5	2.3	0.8	12.8	191	X	X	
6030	1387	75678	81914	38.5 - 38.7	10.2	3.1	0.1	0.6	0.9	0.9	1.1	3.1	79.9	53	2	X	X
6031	1360	75855	81809	37.8 - 38.7	29.9	1.3	0.1	0.6	0.8	1.2	2.5	2.5	60.6	99	X	X	
6034	1388	76022	81709	39.2 - 39.3	39.2	15.8	0.9	0.5	0.6	0.7	2.1	1.2	38.6	28	X	X	
6035	1487	76201	81604	49.5 - 50.5	23.9	3.4	0.5	0.6	0.7	1.7	2.6	1.7	63.0	49	X	X	
"	"	"	"	49.8 - 50.0	nd	nd	nd	nd	nd	nd	nd	nd	nd	nd	X		X
"	"	"	"	50.2 - 50.4	nd	nd	nd	nd	nd	nd	nd	nd	nd	nd	X		X
6037	1490	75541	82489	41.3 - 41.4	27.2	5.4	4.1	0.1	0.2	0.4	6.4	10.6	40.3	5870	2	X	X
6039	1412	76048	82178	39 - 41	52.9	3.3	0.5	0.4	0.5	1.5	2.0	2.3	36.6	581	X	X	
6040	1362	76216	82079	41.0 - 41.8	7.1	2.8	0.1	0.6	0.7	1.1	1.5	4.6	81.4	222	X	X	
6043	1298	76935	82138	25 - 27	nd	nd	nd	nd	nd	nd	nd	nd	nd	nd	X		
6054	1365	76843	82665	41 - 42	38.2	8.7	0.3	0.5	0.8	0.8	5.4	1.8	42.1	376	X	X	
"	"	"	"	41 - 41.2	nd	nd	nd	nd	nd	nd	nd	nd	nd	nd	X		X
6056	1366	77012	82584	41.9 - 42.9	9.1	3.4	3.8	1.2	2.0	2.2	2.2	10.1	64.0	136	X	X	
"	"	"	"	41.9 - 42.1	nd	nd	nd	nd	nd	nd	nd	nd	nd	nd	X		X
6058	1367	77179	82464	37.3 - 38.0	64.9	8.4	1.0	0.2	0.3	0.6	2.8	1.1	19.8	222	X	X	
6059	1305	77355	82359	33 - 35	50.3	10.7	1.3	0.5	0.5	1.8	1.6	2.8	29.6	1700	X	X	X
6061	1306	77522	82259	39 - 41	37.9	18.5	0.6	0.7	0.6	2.5	1.4	2.0	36.2	64	2	X	X
6062	1368	77695	82155	45.2 - 45.4	60.7	18.0	1.9	0.2	0.2	0.5	1.7	1.9	14.5	65	X	X	
6063	1369	77863	82055	42.5 - 43.5	51.8	18.5	1.0	0.3	0.3	0.7	1.5	3.8	22.3	164	X	X	
6064	1393	78027	81957	41.8 - 42.0	2.9	1.5	0.0	1.1	1.5	1.6	0.1	12.7	76.7	63	X	X	
6070	1310	77815	82584	43 - 45	80.8	2.0	1.2	0.1	0.1	0.6	1.0	1.3	11.8	1390	X	X	
6071	1404	77900	82531	39 - 41	52.7	4.4	1.3	0.3	0.4	1.5	1.8	3.0	33.8	1600	X	X	
6072	1370	77984	82483	41.5 - 42.3	64.9	10.5	1.6	0.2	0.3	0.6	2.9	1.8	16.3	709	X	X	
6074	1371	78154	82382	38.8 - 39.8	8.5	5.3	0.3	1.1	1.5	2.3	2.2	6.5	70.2	112	X	X	
"	"	"	"	39.6 - 39.8	nd	nd	nd	nd	nd	nd	nd	nd	nd	nd	X		X
6076	1372	78315	82286	46.5 - 47.5	3.9	3.3	0.5	1.3	1.8	2.2	0.6	1.7	78.7	1020	X	X	
6077	1407	78407	82228	46.5 - 47.0	9.6	1.9	0.4	1.0	1.3	2.1	0.3	10.5	71.4	233	X	X	
"	"	"	"	46.5 - 46.7	nd	nd	nd	nd	nd	nd	nd	nd	nd	nd	X		X
6079	1408	78580	82136	45.9 - 47.1	3.9	1.0	0.4	0.8	1.1	2.6	0.1	14.1	73.2	85	X	X	
"	"	"	"	46.9 - 47.1	nd	nd	nd	nd	nd	nd	nd	nd	nd	nd	X		X
6080	1215	78680	82025	42 - 44	88.2	3.1	1.2	0.1	0.1	0.2	0.4	0.7	5.6	127	X	X	
6081	1493	78922	81918	46.8 - 47.4	12.6	5.4	0.2	0.8	1.3	1.4	0.4	4.1	70.4	505	X	X	
6085	1395	78499	82659	42.2 - 42.3	34.3	17.0	0.6	0.6	0.9	1.6	1.8	1.9	39.1	2860	X	X	
6086	1374	78668	82558	42.8 - 43.8	24.4	7.5	0.6	0.7	1.1	1.3	3.3	8.3	50.3	1710	X	X	
6088	1415	78747	82503	43.6 - 44.5	13.0	7.2	0.3	0.8	1.1	1.9	2.1	8.6	63.1	2070	X	X	
"	"	"	"	43.8 - 44.0	nd	nd	nd	nd	nd	nd	nd	nd	nd	nd	X		X
"	"	"	"	44.4 - 44.5	nd	nd	nd	nd	nd	nd	nd	nd	nd	nd	X		X
6089	1375	78839	82456	46.2 - 47.2	22.5	6.2	0.3	0.6	0.9	1.2	2.0	9.7	56.7	1780	X	X	
"	"	"	"	47.0 - 47.2	nd	nd	nd	nd	nd	nd	nd	nd	nd	nd	X		X
6091	1396	79013	82352	45.6 - 45.7	15.8	4.1	6.4	0.9	1.1	2.5	0.4	12.6	54.0	564	X	X	
6093	1376	78847	82921	43.9 - 44.8	68.2	3.8	1.0	0.2	0.3	0.8	1.3	2.6	20.2	2130	X	X	
6095	1377	79015	82820	40.2 - 40.9	2.8	0.8	0.5	0.8	1.1	1.8	0.2	17.0	74.3	205	X	X	
6096	1378	79185	82719	38.1 - 39.0	10.9	2.8	0.3	0.7	1.1	1.1	1.6	12.2	69.0	1600	X	X	
6097	1397	79354	82619	39.1 - 39.9	38.0	12.9	1.5	0.4	0.6	1.1	0.7	4.9	38.9	1080	X	X	
6099	1416	79528	82518	37.3 - 37.8	29.5	17.5	0.8	0.3	0.5	1.0	1.6	3.7	40.9	3730	X	X	
6114	1232	79391	83002	38 - 40	65.4	14.8	2.6	0.2	0.2	1.4	1.8	1.1	12.1	58	X	X	
6116	1233	79701	82833	38 - 40	76.4	3.6	1.6	0.1	0.2	0.6	2.4	1.6	12.6	1770	X	X	
6117	1400	79837	82759	40.3 - 40.4	25.8	16.2	0.7	0.3	0.5	1.0	4.8	4.1	42.4	4540	X	X	
6165	1213	75279	81446	38 - 40	17.5	2.7	0.6	0.6	0.9	1.6	0.9	4.0	70.4	59	X	X	
6167	657	74656	79838	41 - 42	46.7	26.8	0.9	0.3	0.2	1.1	1.5	0.4	21.4	5	X	X	

CSIRO 00-	Hole No.	East (m)	North (m)	Depth (m)	SiO_2 (%)	Al_2O_3 (%)	Fe_2O_3 (%)	MgO (%)	CaO (%)	Na_2O (%)	TiO_2 (%)	S (%)	LOI (%)	U (ppm)	Analyses		
															CHNO	NMR	Pet
6172	1023	74143	80144	38 - 40	46.3	29.0	0.8	0.1	0.1	0.5	2.3	0.3	20.1	68	X	X	
6178	1492	77702	82408	43.2 - 44.2	40.8	4.0	0.7	0.5	0.9	1.0	1.8	0.7	47.1	3180	X	X	
6186	1409	78304	82526	?	47.8	3.0	1.1	0.5	0.7	1.1	2.5	0.7	37.3	1920	X	X	
6187	1256	78390	82483	41.4 - 42.4	5.9	2.8	0.3	0.9	1.3	1.5	1.0	1.0	80.7	253	X	X	
6197	1525	78622	82820	45.5 - 46.5	58.5	2.0	0.5	0.4	0.6	0.6	1.5	0.5	33.8	1510	X	X	2
6198	1257	78722	82767	44.9 - 45.3	41.7	5.7	1.3	0.3	0.4	0.9	1.6	0.4	44.7	5210	X	X	
6199	1514	78829	82707	44.2 - 45.2	29.1	6.6	0.5	0.7	0.8	1.5	2.0	1.3	53.8	2110	X	X	
6210	1379	79445	82792	37.0 - 37.5	15.5	5.1	0.3	0.8	1.2	1.2	2.6	2.0	68.8	1110	X	X	2
6211	1509	79526	82741	35.2 - 36.2	14.9	7.7	2.3	0.6	0.7	1.1	1.6	0.9	68.0	1340	X	X	
6212	1399	79614	82692	41.7 - 42.3	27.0	1.1	0.5	0.6	0.9	1.2	0.5	0.6	64.3	442	X	X	
6213	1510	79684	82644	38.8 - 39.8	30.3	17.9	1.7	0.3	0.5	1.2	2.6	7.2	33.8	779	X	X	

nd: not determined X: single analysis
Pet: petrographic analysis 2: duplicate analysis

(iii) assuming gross analytical errors of 0.1% plus relative errors of 2% of the measured value and up to 25% error in the kaolinite correction, final errors for the corrected % C,H,O,N were calculated as -

$$\Delta C = 0.1 + 0.02 \times \%C$$

$$\Delta H = 0.1 + 0.02 \times \%H + 0.01 \times \%Al_2O_3 + 0.0022 \times \%H_2O^-$$

$$\Delta O = 0.5 + 0.08 \times \%Al_2O_3 + 0.018 \times \%H_2O^-$$

$$\Delta N = 0.1 + 0.02 \times \%N$$

(iv) C, H, O and N were converted to molarity and H/C, O/C and N/C atomic ratios calculated;

(v) as errors for the different elements are related, the proportional errors for the ratios were not simply the addition of the proportional errors for the two elements, but instead calculated as -

$$\Delta H/C = H/C \times \sqrt{[(\Delta H/H)^2 + (\Delta C/C)^2]}$$

$$\Delta O/C = O/C \times \sqrt{[(\Delta O/O)^2 + (\Delta C/C)^2]}$$

$$\Delta N/C = N/C \times \sqrt{[(\Delta N/N)^2 + (\Delta C/C)^2]}$$

8.4.4 Petrographic analyses

Two samples (CD-1379 and CD-1525) from the Ambassador deposit were examined in 1992 by the CSIRO Minerals Research Laboratories in Sydney. In 1995, an additional 14 samples, plus repeats of the original two samples, were examined by the same analyst.

8.5 Results

8.5.1 ^{13}C NMR

The spectra, as obtained from the analysts, are enclosed in the Appendix (Figures A6.1 - A6.52). There are clear differences in spectral quality, which seem to be primarily dependant on LOI (Figure 8.4), with no apparent correlation with concentration of Fe or any other potential interfering element (Section 8.3.1).

Figure 8.4 Estimated %Noise vs. LOI for ^{13}C NMR

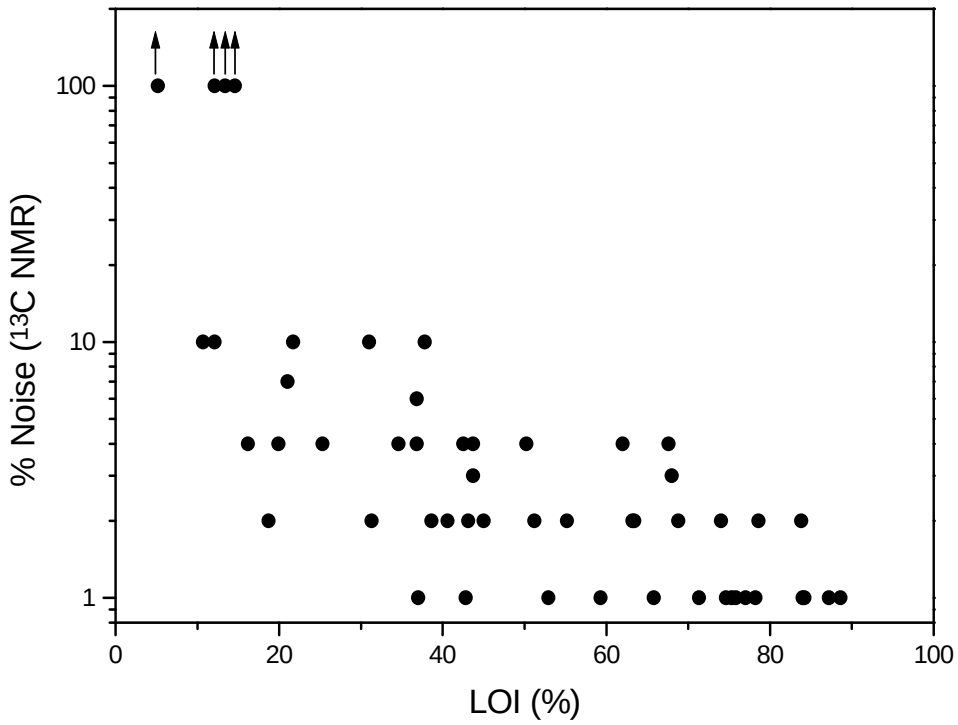

Comparisons of the spectra with recorded data (Figure 8.1) suggest that the material most closely matches alginite, both in terms of the high proportion of aliphatic C and the narrowness of the aliphatic peak. In some samples, the aromatic peak is relatively higher, although never to the amount observed for sporinite, vitrinite or fusinite (Figure 8.1). Other differences from samples shown in Figure 8.1 for the Ambassador samples were the observation of peaks due to O-containing groups such as carbohydrate, phenolic, carboxylic and carbonyl groups (Table 8.1). This is presumably a consequence of the low rank (*i.e.*, degree of maturation) of the lignites (see Section 8.3.2).

Under properly controlled conditions, the integrated area under a peak should be directly proportional to the fraction of C atoms in that environment. As a result of the complex multi-element composition of these samples, such conditions do not exist, though integrated peak areas (Table 8.3) should still give an approximate measure of the C fractions. Because of peak overlap and sensitivity problems, phenolic and carboxyl C data are only available for a more limited suite of the samples than for aromatic and carbonyl C.

Table 8.3: Calculated proportions of functional C groups, using ^{13}C NMR

CSIRO 00-	OM (%)	Error	Aliphatic position (ppm)	(%)	Aromatic position (ppm)	Phen.# pos.$	Aromatic + Phen. (%)	Carboxyl pos.	Carboxyl (%)	Carbonyl pos.	Carbonyl (%)
6028	45	1	34.32 ± 0.08	82	130.33 ± 0.06	155	14	175	2.2	211	2.2
6029	5	10	31.9 ± 1.5	75	nd	nd	19	nd	nd	nd	nd
6031	54	1	34.45 ± 0.08	72	130.68 ± 0.06	157	18	177	4.6	208	2.9
6035	55	1	34.32 ± 0.07	69	130.5 ± 1.5	155	24	177	3.3	214	2.7
6056	62	1	33.91 ± 0.06	80	130.07 ± 0.07	156	15	177	2.4	209	2.1
6062	7	100	nd	nd	nd	nd	nd	nd	nd	nd	nd
6070	9	10	33 ± 5	59	133 ± 8	nd	33	nd	nd	nd	nd
6076	66	1	31.51 ± 0.13	65	129.5 ± 0.3	155	27	175	3.3	208	3.6
6080	4	100	nd	nd	nd	nd	nd	nd	nd	nd	nd
6081	62	1	34.29 ± 0.07	81	131.67 ± 0.12	157	15	174	2.5	205	2.2
6114	5	100	nd	nd	nd	nd	nd	nd	nd	nd	nd
6116	11	100	nd	nd	nd	nd	nd	nd	nd	nd	nd
6117	31	4	32.18 ± 0.12	66	134.5 ± 5	nd	28	178	2.2	208	2.8
6178	39	2	31.63 ± 0.15	55	130.78 ± 0.29	nd	34	174	5.2	208	3.7
6030	64	1	32.93 ± 0.06	69	127.5 ± 1.5	155	22	173	4.5	205	1.6
6034	28	10	35.5 ± 2.5	54	nd	nd	nd	nd	nd	nd	nd
6037	32.9	4	31.34 ± 0.08	75	134.0 ± 2	nd	19	nd	1.7	209	4.0
6039	31.7	4	32.49 ± 0.06	69	131.0 ± 1	nd	21	nd	nd	nd	nd
6040	75.3	1	33.85 ± 0.07	72	130.0 ± 1	154	23	175	3.0	209	2.5
6054	33.4	1	33.79 ± 0.08	78	129.5 ± 1	155	18	175	2.6	205	2.1
6058	16.7	10	27.5 ± 2.0	nd	nd	nd	nd	nd	nd	nd	nd
6059	21.9	10	29.7 ± 0.7	55	134.49 ± 0.15	nd	nd	nd	nd	nd	nd
6061	24.9	6	31.24 ± 0.07	51	127.9 ± 0.5	152	38	178	6.6	210	3.0
6063	14.2	4	31.06 ± 0.09	68	127.92 ± 0.08	nd	25	175	4.2	208	3.2
6064	71.6	1	32.01 ± 0.08	55	127.02 ± 0.06	154	34	174	5.2	203	2.9
6071	28.8	4	29.19 ± 0.08	77	131.5 ± 1	nd	17	nd	nd	nd	nd
6074	58.8	1	32.28 ± 0.07	78	127 ± 2	155	17	178	2.6	204	1.6
6077	61.5	1	32.19 ± 0.05	58	126.5 ± 1.5	155	34	177	4.5	203	1.6
6079	66.2	2	31.98 ± 0.11	51	128.6 ± 2	145	41	174	3.7	201	2.8
6085	26.7	2	29.54 ± 0.1	73	130.04 ± 0.11	152	22	172	3.0	200	2.7
6086	41.5	2	29.46 ± 0.12	68	128.51 ± 0.09	nd	26	173	3.6	nd	1.9
6088	52.5	2	30.21 ± 0.1	86	129.2 ± 0.3	nd	12	nd	0.0	208	1.7
6089	50.1	2	30.19 ± 0.12	86	127.12 ± 0.12	nd	12	nd	0.4	200	1.4
6091	45.8	4	31.83 ± 0.12	83	128.7 ± 5	nd	13	nd	2.1	203	2.7
6093	16.4	7	29.57 ± 0.2	67	129.92 ± 0.2	nd	20	nd	nd	nd	nd
6095	73.1	1	32.43 ± 0.06	71	127.4 ± 1.5	155	24	175	2.8	207	2.0
6096	63.1	1	29.78 ± 0.09	70	128 ± 2	155	24	174	3.0	202	2.8
6097	30.4	4	29.41 ± 0.14	83	nd	nd	15	nd	0.5	208	1.5
6099	29.8	2	29.88 ± 0.1	76	132.8 ± 2.5	nd	21	nd	0.6	206	2.0
6072	9.9	4	32.4 ± 0.07	74	133.4 ± 0.3	159	18	179	4.5	212	3.1
6165	66.3	2	33.34 ± 0.07	61	130.4 ± 2	155	23	176	6.0	203	4.7
6167	8.7	4	34.48 ± 0.11	38	130.42 ± 0.08	159	42	177	13.1	209	4.3
6172	7.0	2	36.23 ± 0.1	62	133.9 ± 0.2	158	26	181	7.2	212	4.6
6186	30.2	1	31.93 ± 0.06	70	132.65 ± 0.11	159	20	176	2.9	212	5.3
6187	68.6	2	33.5 ± 0.1	62	132.2 ± 0.4	156	24	179	4.9	208	5.8
6197	26.0	2	31.9 ± 0.08	66	132.11 ± 0.07	nd	25	175	6.1	210	2.9
6198	36.0	3	31.9 ± 0.08	60	132.26 ± 0.08	nd	31	177	6.2	212	3.1
6199	40.7	2	32.73 ± 0.09	68	132.87 ± 0.13	nd	22	177	5.0	209	4.5
6210	57.7	3	33.74 ± 0.08	66	133.53 ± 0.2	158	24	179	5.3	210	3.5
6211	54.3	4	32.05 ± 0.12	72	131.82 ± 0.29	158	23	176	1.8	210	3.6
6212	55.1	2	33.16 ± 0.25	61	130.98 ± 0.29	156	26	179	5.4	205	5.2
6213	25.8	2	32.54 ± 0.13	78	131.65 ± 0.13	nd	12	nd	4.0	nd	6.3

nd - not determined due to inadequate spectral resolution # Phenolic C $ position (ppm)

The major phase is clearly aliphatic carbon (68 ± 10 %), with significant aromatic groups (aromatic + phenolic carbon = 23 ± 8 %). Thus, peak integration results are consistent with the above hypothesis that NMR results suggest primary exinite character, with some vitrinite present.

8.5.2 C,H,O,N Analyses

Analytical results for C, H, O and N are compiled in Table 8.4. Carbon content is, as expected, closely correlated with LOI (Figure 8.5), indicating that the major component of LOI is organic material. The minor amount of divergence from linearity is possibly due to other phases, such as sulphides and kaolinite, that lose weight during extreme heating. For most samples with low LOI (< 20%), the magnitude of the cumulative errors is such that the data are not usable. This is demonstrated for H/C in Figure 8.6; other ratios show similar trends. There is major variation in samples taken at differing depth from the same drill hole, indicating significant differences in the composition of the organic matter with depth. There are not enough samples to properly quantify this variation: this observation implies that any interpretation of spatial trends will be very difficult.

Figure 8.5 Organic matter content vs. LOI

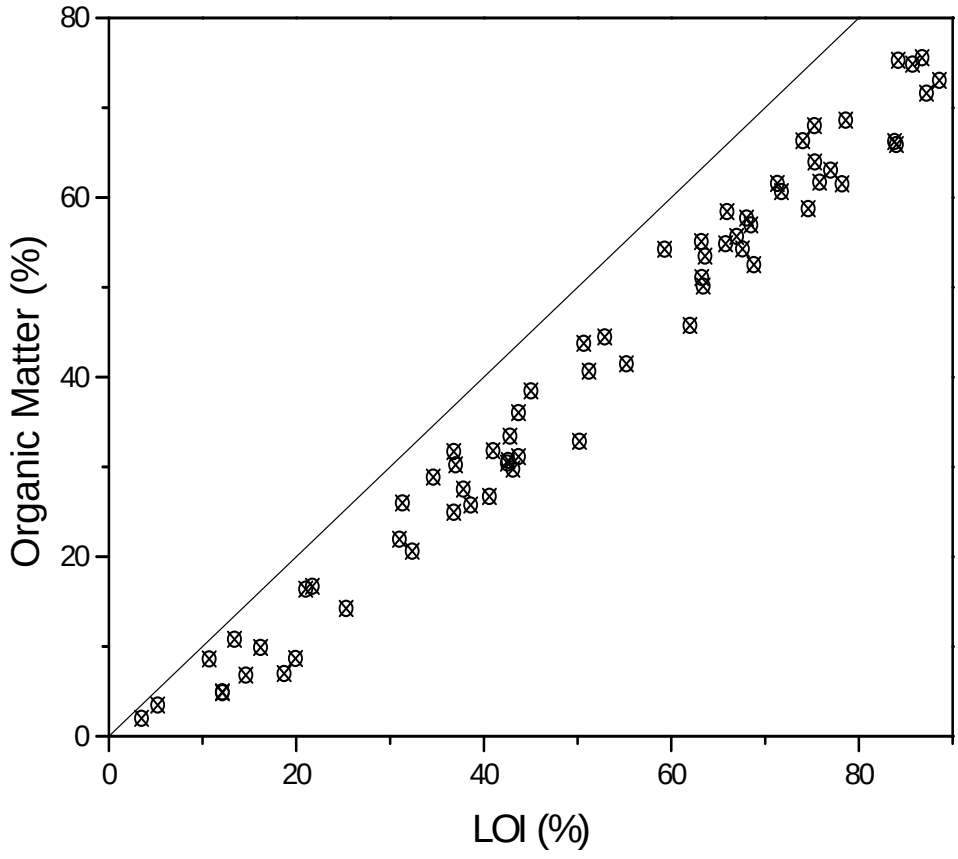

After disregarding those samples with potentially very high errors (although even these samples have atomic ratios within the range of the low-error samples), the H/C and O/C data have been plotted on the van Krevelan diagram (Figure 8.7). The samples exhibit wide variations in the degree of maturation, though most have similar compositions. They lie between exinite/liptinite and vitrinites, though some appear to have compositions similar to end-member exine or wood. Additionally, there are varying degrees of maturation (Section 8.3.2).

This interpretation resembles results for the NMR spectra, which suggests compositions between exinite and vitrinite, commonly with only minor maturation.

Table 8.4: Organic matter elemental analysis

CSIRO 00-	Hole No.	Depth (m)	H_2O- (%)	LOI (%)	OM (%)	Carbon in OM (%)	Atomic Ratios		
							H/C	O/C	N/C
6028	1489	39.4 - 39.8	6.3	52.9	44.5	72.2 ± 2.2	1.13 ± 0.05	0.209 ± 0.014	0.0107 ± 0.0014
6029	1488	39.8 - 40.4	0.8	12.1	4.9	72 ± 22	1.2 ± 0.9	0.2 ± 0.4	0.024 ± 0.012
6030	1387	38.5 - 38.7	9.0	75.3	63.9	64.9 ± 1.7	1.25 ± 0.05	0.317 ± 0.014	0.0116 ± 0.0012
6030	1387	38.5 - 38.7	4.6	75.3	68.0	53.7 ± 1.3	1.45 ± 0.06	0.540 ± 0.017	0.0188 ± 0.0014
6031	1360	37.8 - 38.7	4.1	59.3	54.3	62.1 ± 1.6	1.63 ± 0.05	0.349 ± 0.012	0.0074 ± 0.0013
6034	1388	39.2 - 39.3	3.7	37.8	27.5	75 ± 5	0.99 ± 0.15	0.17 ± 0.06	0.0153 ± 0.0022
6035	1487	49.5 - 50.5	7.2	65.8	54.9	80.7 ± 2.3	0.93 ± 0.04	0.111 ± 0.013	0.0108 ± 0.0011
"	"	49.8 - 50.0	3.5	50.7	43.7	72.0 ± 2.3	1.18 ± 0.06	0.207 ± 0.017	0.0128 ± 0.0015
"	"	50.2 - 50.4	4.3	65.9	58.4	72.9 ± 1.9	1.19 ± 0.04	0.197 ± 0.011	0.0091 ± 0.0011
6037	1490	41.3 - 41.4	7.6	50.2	32.9	59.0 ± 2.6	1.46 ± 0.11	0.42 ± 0.04	0.0088 ± 0.0023
"	"	"	2.7	41.0	31.8	71 ± 3	1.32 ± 0.09	0.21 ± 0.03	0.0113 ± 0.0020
6039	1412	39 - 41	2.5	36.8	31.7	70.3 ± 2.7	1.28 ± 0.07	0.227 ± 0.022	0.0111 ± 0.0020
6040	1362	41.0 - 41.8	6.6	84.2	75.3	66.8 ± 1.5	1.4 ± 0.04	0.279 ± 0.011	0.0072 ± 0.0009
6043	1298	25 - 27	0.3	3.5	2.0	nd	nd	nd	nd
6054	1365	41 - 42	5.2	42.8	33.4	69 ± 3	1.2 ± 0.1	0.25 ± 0.04	0.0078 ± 0.0019
"	"	41.0 - 41.2	3.4	42.6	30.7	75 ± 5	1.09 ± 0.17	0.17 ± 0.07	0.0148 ± 0.0020
6056	1366	41.9 - 42.9	9.2	75.8	61.7	73.6 ± 2.0	1.28 ± 0.05	0.183 ± 0.013	0.0077 ± 0.0010
"	"	41.9 - 42.1	4.4	67.0	55.7	70.3 ± 1.9	1.51 ± 0.05	0.196 ± 0.013	0.0303 ± 0.0012
6058	1367	37.3 - 38.0	1.1	21.7	16.7	74 ± 6	1.63 ± 0.17	0.15 ± 0.06	0.003 ± 0.003
6059	1305	33 - 35	3.0	31.0	21.9	66 ± 4	1.12 ± 0.17	0.31 ± 0.07	0.009 ± 0.003
6061	1306	39 - 41	3.4	36.8	24.9	64 ± 4	1.06 ± 0.21	0.34 ± 0.09	0.0086 ± 0.0028
"	"	"	3.5	32.4	20.6	71 ± 6	1.02 ± 0.23	0.22 ± 0.10	0.017 ± 0.003
6062	1368	45.2 - 45.4	1.0	14.6	6.8	52 ± 12	1.3 ± 0.9	0.6 ± 0.4	0.012 ± 0.012
6063	1369	42.5 - 43.5	3.3	25.3	14.2	65 ± 7	1.09 ± 0.36	0.32 ± 0.16	0.005 ± 0.005
6064	1393	41.8 - 42	11.0	87.2	71.6	72.5 ± 1.7	1.11 ± 0.04	0.209 ± 0.010	0.0073 ± 0.0009
6070	1310	43 - 45	0.9	10.7	8.6	67 ± 6	1.07 ± 0.20	0.30 ± 0.07	0.007 ± 0.008
6071	1404	39 - 41	2.2	34.6	28.8	72 ± 3	1.32 ± 0.08	0.201 ± 0.027	0.0021 ± 0.0021
6072	1370	41.5 - 42.3	1.9	16.2	9.9	63 ± 8	1.2 ± 0.4	0.28 ± 0.15	0.093 ± 0.008
6074	1371	38.8 - 39.8	10.9	74.6	58.8	72.5 ± 2.1	1.21 ± 0.06	0.204 ± 0.017	0.0052 ± 0.0011
"	"	39.6 - 39.8	5.3	68.5	57.0	71.1 ± 2.2	1.09 ± 0.07	0.226 ± 0.023	0.0125 ± 0.0012
6076	1372	46.5 - 47.5	11.6	84.0	65.9	70.4 ± 1.8	0.91 ± 0.05	0.250 ± 0.013	0.0102 ± 0.0010
6077	1407	46.5 - 47.0	12.1	78.2	61.5	73.8 ± 2.0	1.02 ± 0.04	0.194 ± 0.012	0.0098 ± 0.0010
"	"	46.5 - 46.7	6.5	85.7	74.8	72.0 ± 1.6	1.03 ± 0.03	0.218 ± 0.008	0.0108 ± 0.0009
6079	1408	45.9 - 47.1	12.5	83.8	66.2	62.4 ± 1.6	0.99 ± 0.05	0.386 ± 0.012	0.0048 ± 0.0011
"	"	46.9 - 47.1	6.1	86.8	75.6	67.9 ± 1.5	1.00 ± 0.03	0.288 ± 0.008	0.0050 ± 0.0009
6080	1215	42 - 44	0.4	5.2	3.5	60 ± 14	1.4 ± 0.6	0.39 ± 0.21	0.021 ± 0.021
6081	1493	46.8 - 47.4	6.9	71.3	61.6	59.3 ± 1.6	1.71 ± 0.07	0.400 ± 0.019	0.0094 ± 0.0013
6085	1395	42.2 - 42.3	6.5	40.6	26.7	64 ± 4	0.94 ± 0.19	0.34 ± 0.08	0.0189 ± 0.0027
6086	1374	42.8 - 43.8	6.6	55.2	41.5	71.8 ± 2.7	1.13 ± 0.08	0.221 ± 0.027	0.0029 ± 0.0015
6088	1415	43.6 - 44.5	9.3	68.8	52.5	72.7 ± 2.3	1.11 ± 0.07	0.209 ± 0.022	0.0038 ± 0.0012
"	"	43.8 - 44.0	4.6	63.2	51.1	72.2 ± 2.5	1.12 ± 0.08	0.208 ± 0.028	0.0118 ± 0.0013
"	"	44.4 - 44.5	4.3	63.6	53.5	76.3 ± 2.3	1.21 ± 0.06	0.149 ± 0.017	0.0099 ± 0.0012
6089	1375	46.2 - 47.2	6.2	63.4	50.1	73.4 ± 2.3	1.24 ± 0.06	0.189 ± 0.020	0.0063 ± 0.0012
"	"	47.0 - 47.2	3.5	71.8	60.7	68.7 ± 2.0	1.16 ± 0.06	0.260 ± 0.020	0.0101 ± 0.0011
6091	1396	45.6 - 45.7	8.2	62.0	45.8	69.5 ± 2.3	1.29 ± 0.07	0.241 ± 0.019	0.0086 ± 0.0014
6093	1376	43.9 - 44.8	1.8	21.0	16.4	69 ± 4	1.21 ± 0.13	0.25 ± 0.05	0.0114 ± 0.0039

CSIRO 00-	Hole No.	Depth (m)	H_2O- (%)	LOI (%)	OM (%)	Carbon in OM (%)	Atomic Ratios		
							H/C	O/C	N/C
6095	1377	40.2 - 40.9	9.9	88.6	73.1	69.0 ± 1.6	1.26 ± 0.04	0.254 ± 0.009	0.0054 ± 0.0009
6096	1378	38.1 - 39.0	7.3	77.0	63.1	72.9 ± 1.9	1.17 ± 0.04	0.199 ± 0.012	0.0069 ± 0.0010
6097	1397	39.1 - 39.9	4.5	42.5	30.4	66 ± 3	1.2 ± 0.14	0.31 ± 0.06	0.0086 ± 0.0022
6099	1416	37.3 - 37.8	4.6	43.1	29.8	67 ± 4	1.18 ± 0.17	0.29 ± 0.07	0.0108 ± 0.0023
6114	1232	38 - 40	1.3	12.1	4.8	41 ± 12	1.8 ± 1.4	0.9 ± 0.6	0.034 ± 0.022
6116	1233	38 - 40	0.8	13.4	10.8	47 ± 4	1.59 ± 0.27	0.74 ± 0.10	0.017 ± 0.009
6117	1400	40.3 - 40.4	3.4	43.7	31.2	73 ± 4	0.99 ± 0.14	0.20 ± 0.06	0.0157 ± 0.0020
6165	1213	38 - 40	5.6	74.0	66.3	69.3 ± 1.7	1.18 ± 0.04	0.255 ± 0.011	0.0043 ± 0.0010
6167	657	41 - 42	1.5	19.9	8.7	63 ± 13	0.91 ± 0.78	0.4 ± 0.4	0.047 ± 0.008
6172	1023	38 - 40	1.3	18.7	7.0	67 ± 18	1.4 ± 0.96	0.2 ± 0.4	0.070 ± 0.010
6178	1492	43.2 - 44.2	3.7	45.0	38.5	50.4 ± 1.8	1.22 ± 0.09	0.647 ± 0.029	0.0177 ± 0.0024
6186	1409	?	3.7	37.0	30.2	70.2 ± 2.8	1.06 ± 0.07	0.250 ± 0.023	0.0040 ± 0.0021
6187	1256	41.4 - 42.4	4.9	78.6	68.6	72.9 ± 1.8	1.29 ± 0.04	0.195 ± 0.010	0.0029 ± 0.0009
6197	1525	45.5 - 46.5	3.2	31.3	26.0	69.3 ± 2.9	1.08 ± 0.08	0.244 ± 0.023	0.0243 ± 0.0026
6198	1257	44.9 - 45.3	3.1	43.7	36.0	65.5 ± 2.5	1.02 ± 0.08	0.317 ± 0.028	0.0171 ± 0.0020
6199	1514	44.2 - 45.2	5.4	51.2	40.7	68.4 ± 2.5	1.21 ± 0.08	0.264 ± 0.026	0.0083 ± 0.0016
6210	1379	37.0 - 37.5	5.5	68.0	57.7	69.3 ± 1.9	1.22 ± 0.05	0.247 ± 0.016	0.0105 ± 0.0012
6211	1509	35.2 - 36.2	5.4	67.6	54.3	67.9 ± 2.1	1.29 ± 0.07	0.268 ± 0.022	0.0074 ± 0.0012
6212	1399	41.7 - 42.3	5.7	63.2	55.1	69.2 ± 1.8	1.19 ± 0.04	0.257 ± 0.011	0.0034 ± 0.0012
6213	1510	38.8 - 39.8	3.0	38.6	25.8	60 ± 4	1.48 ± 0.22	0.38 ± 0.09	0.0176 ± 0.0029

Figure 8.6 **Atomic H/C percentage error vs. LOI**

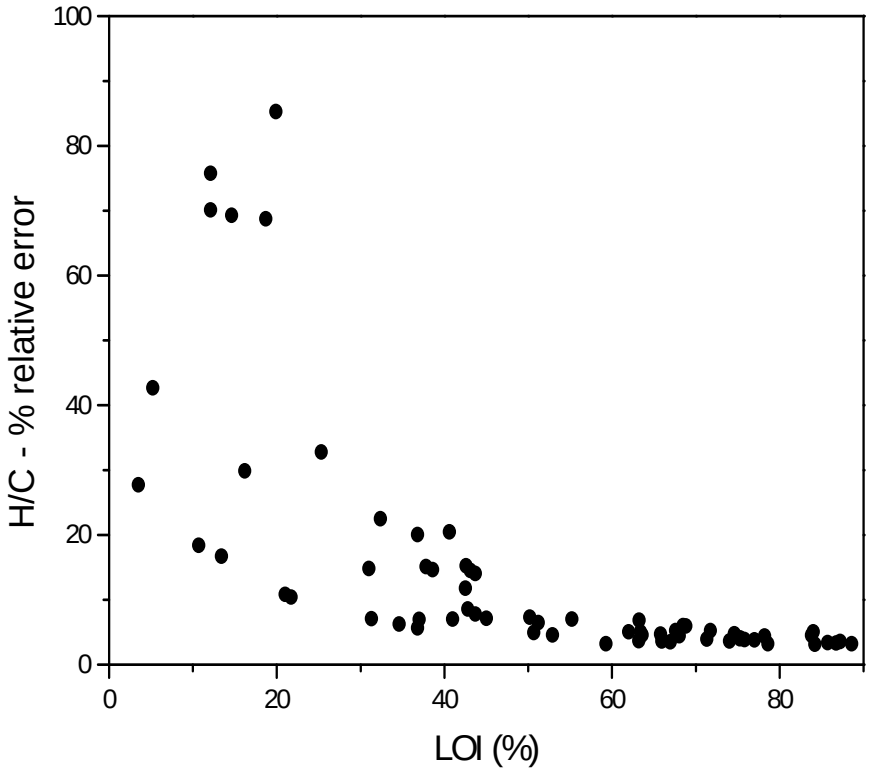

Figure 8.7 **H/C vs. O/C data for Ambassador superimposed on van Krevelen development lines of the macerals**
(see Figure 8.2)

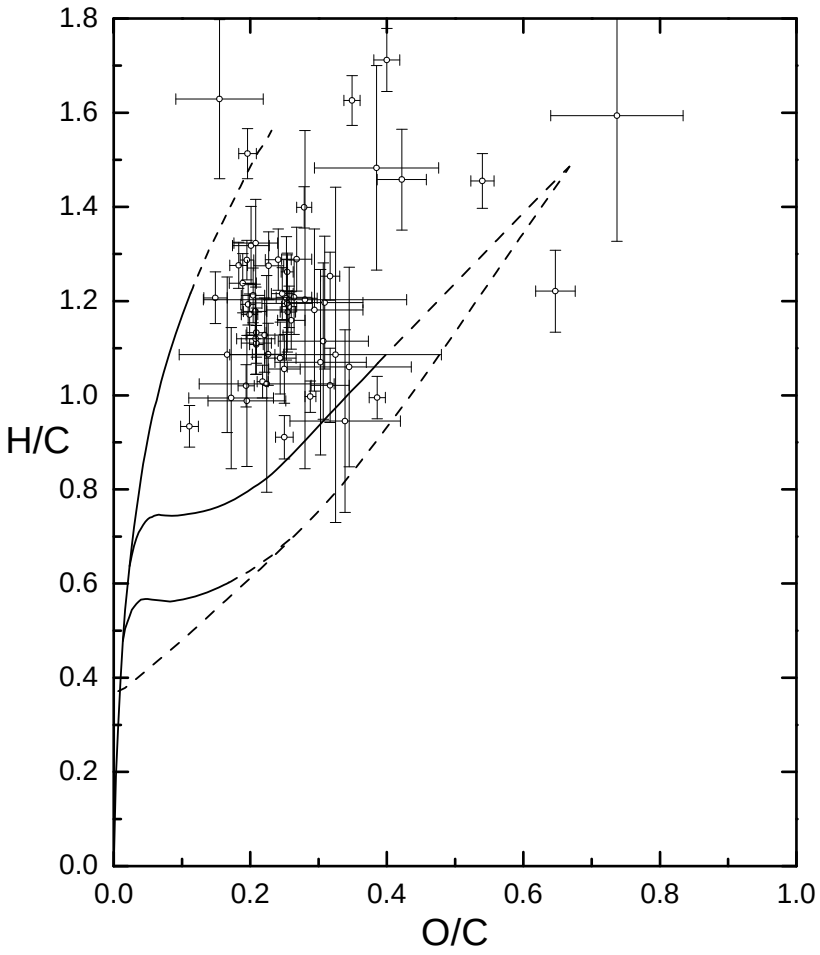

8.5.3 Petrographic Analysis

Comparative results for analysis of two samples over 3 years difference are shown in Table 8.5. The significant differences are presumably due to sample heterogeniety and/or changes in operator assessment of maceral types. In both cases, the second set of analyses had lower recorded liptinite and higher percentage of organic matrix. These results suggest that petrographic analysis, though very useful (see below), has significant operator dependence. The results shown in Table 8.6 are for the later series of analyses, which are considered to be self-consistent. Sample micrographs are shown in Plates 8.1 - 8.6, which show most of the various macerals. Vitrinite fragments can be clearly identified in a number of samples (*e.g.*, Plates 8.2A, 8.4B, 8.5), whereas other samples showed high levels of fine organic matter, often intermixed with mineral matter (*e.g.*, Plates 8.1A, 8.1B, 8.2B, 8.3). Fragments of liptinite macerals are sometimes observed (*e.g.*, Plates 8.3, 8.6).

Note that these results are for volume rather than mass percentage, and will give higher organic and lower mineral contents than for mass calculations, due to the lower density of OM. The dominant maceral is vitrinite, which runs contrary to the results from NMR and chemical analyses. This discrepancy may be due to the high levels of finely intermixed organic and mineral matter (petrographically identified as organic/mineral and mineral/organic matrix). Note that previous petrological analyses tended to give lower matrix and higher

liptinite content, suggesting that this matrix material is of liptinitic character. It is possibly primarily composed of degraded plant fragments, or coagulated humic matter.

Table 8.5: Petrographic results (% of organic and mineral groups) for duplicate analyses of samples from the Ambassador deposit

Constituent	CD-1379 (00-6210)		CD-1525 (00-6197)	
	1st Run	2nd Run	1st Run	2nd Run
LIPTINITE	**30**	**19**	**30**	**16**
Liptodetrinite	12	9	21	10.8
Sporinite	10	4.3	6	1
Cutinite	3	2		1
Resinite	2	2	2	3
Suberinite	2	1		
Fluorinite	1			
Alginite		0.1	1	0
Bituminite		0.4		0.2
VITRINITE	**32**	**45.6**	**5**	**5.5**
Detrovitrinite	20	38.6	4	5
Telovitrinite	12	7	1	0.5
GROUNDMASS (fine particles of vitrinite, micrinite and mineral matter dispersed in bituminite)	**28**		**25**	
MATRIX (mineral matter intermixed with organic matter)		**30.2**		**53.3**
INERTINITE		**0.2**		**0.2**
Sclerotinite		0.2		0.2
MINERAL MATTER (kaolinite, quartz, pyrite and gypsum)	**10**	**5**	**40**	**25**
CLASSIFICATION	Brown coal	Transition of shale to brown coal	Carbominerite	Not given

Table 8.6: Compiled petrographic results (% of organic and mineral groups) for Ambassador samples

CSIRO 00-	Depth (m)	Vitrinite	Liptinite	Inertinite	Organic/ mineral matrix	Mineral/ organic matrix	Mineral matter	Mineral Grains	Classification
6035	49.8 - 50.0	38	7	0.5	25	23	0	6	Carbonaceous shale
6035	50.2 - 50.44	48	11	0.5	9	28	0	5	Carbonaceous shale
6056	41.9 - 42.1	7	6	0	0	79	0	9	Shale
6030	38.5 - 38.7	54	7	0.7	21	11	0	6	Carbonaceous shale transitional to sub-bituminous coal
6037	41.3 - 41.4	0	0	0	2	31	47	20	Argillaceous shale
6054	41.0 - 41.2	15	1	0.2	0	83	0	1	Argillaceous shale
6059	33 - 35	13	5	0	0	51	0	31	Clastic deposit
6061	39 - 41	18	2	0	0	55	0	25	Clastic deposit
6074	39.6 - 39.8	66	3	0.2	0	0	27	3	Carbonaceous shale transitional to sub-bituminous coal
6077	46.5 - 46.7	81	11	0.8	0	0	8	0	Brown coal
6079	46.9 - 47.1	93	1	0	0	0	7	0	Jet
6088	43.8 - 44.0	47	3	0.2	8	38	0	5	Carbonaceous shale
6088	44.4 - 44.5	19	9	0	15	51	0	7	Carbonaceous shale
6089	47.0 - 47.2	33	24	0	0	44	0	0	Carbonaceous shale
6197	46.7 - 46.9	6	16	0.2	0	53		25	Not given
6210	?	46	19	0.2	0	30		5	Transition of shale to brown coal

The classifications of the materials all indicate a poorly matured coal material (with considerable mineral content in many cases), consistent with previous results.

8.5.4 Multiple linear regression analysis

(MLRA) was used to examine the inter-relationships between the data generated by these techniques, and to then correlate this information with U enrichment. Multiple linear regression analysis of the petrographic results (Section 8.5.3), regressed the clay and organic elemental variables (namely Al_2O_3, H_2O-, OM, % C in OM, H/C, O/C and N/C). Good regression co-efficients are achieved for vitrinite (Figure 8.8) and mineral/organic matter (Figure 8.9) - the two major organic containing phases (Table 8.6). This indicates consistency between elemental and petrographic analyses, and also enables the larger data-set of elemental analyses to be used to determine a calculated vitrinite and mineral/organic content for all samples tested (Section 8.5.5).

Plate 8.1A: Petrographic Analysis of Sample 00-6037
(Scale bar = 40 µm)

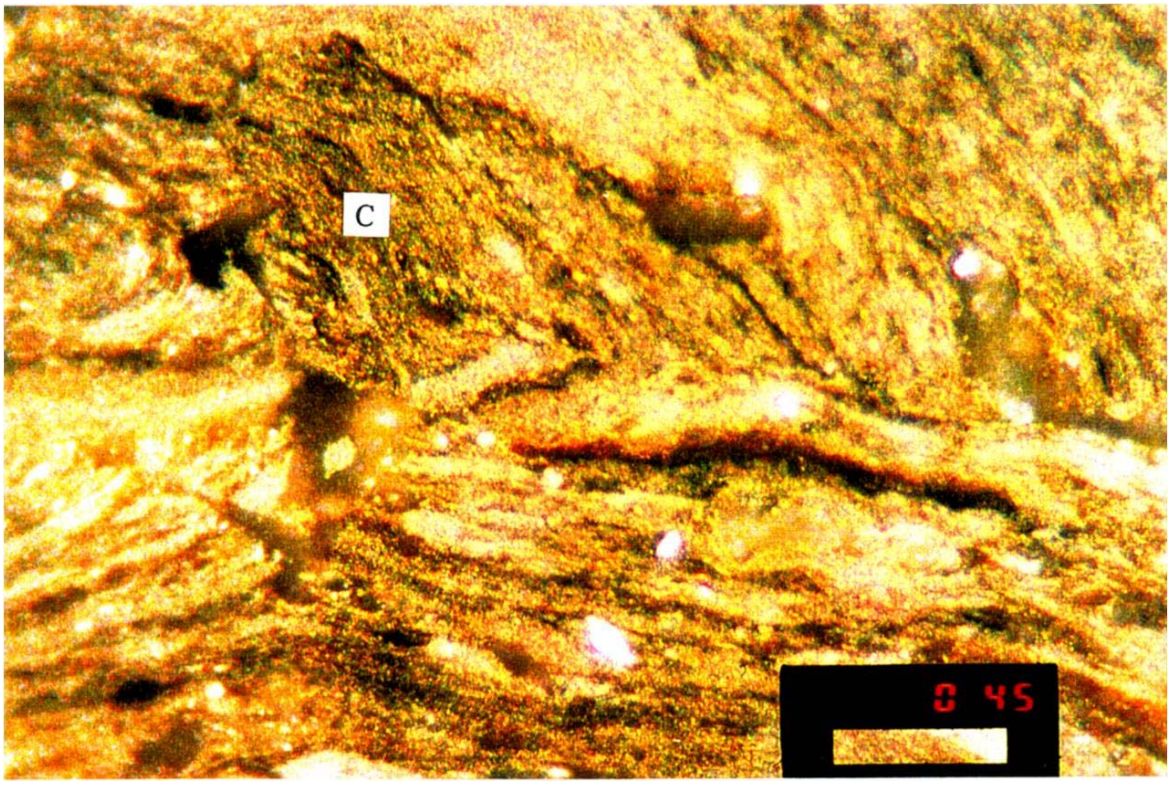

Photo 45: C – clay grain

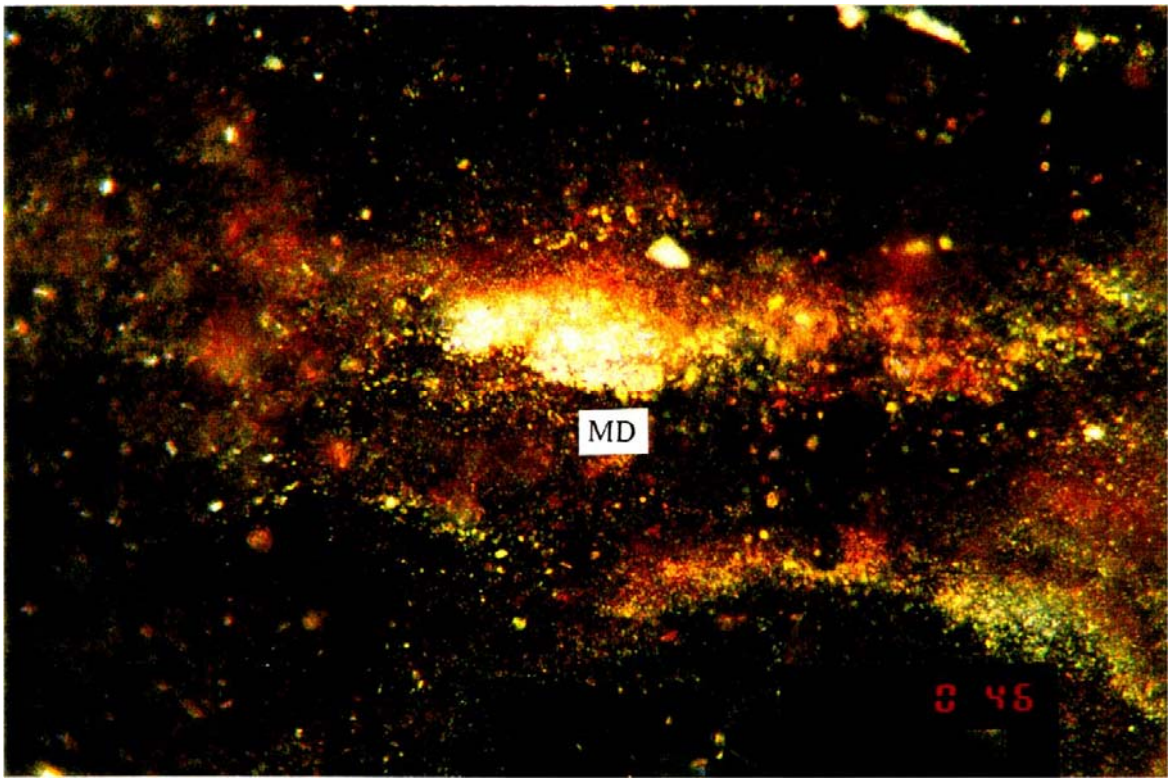

Photo 46: MD – Matrix of mineral matter with some organic matter

Plate 8.1B: Petrographic Analysis of Sample 00-6037 continued (Scale bar = 40 µm)

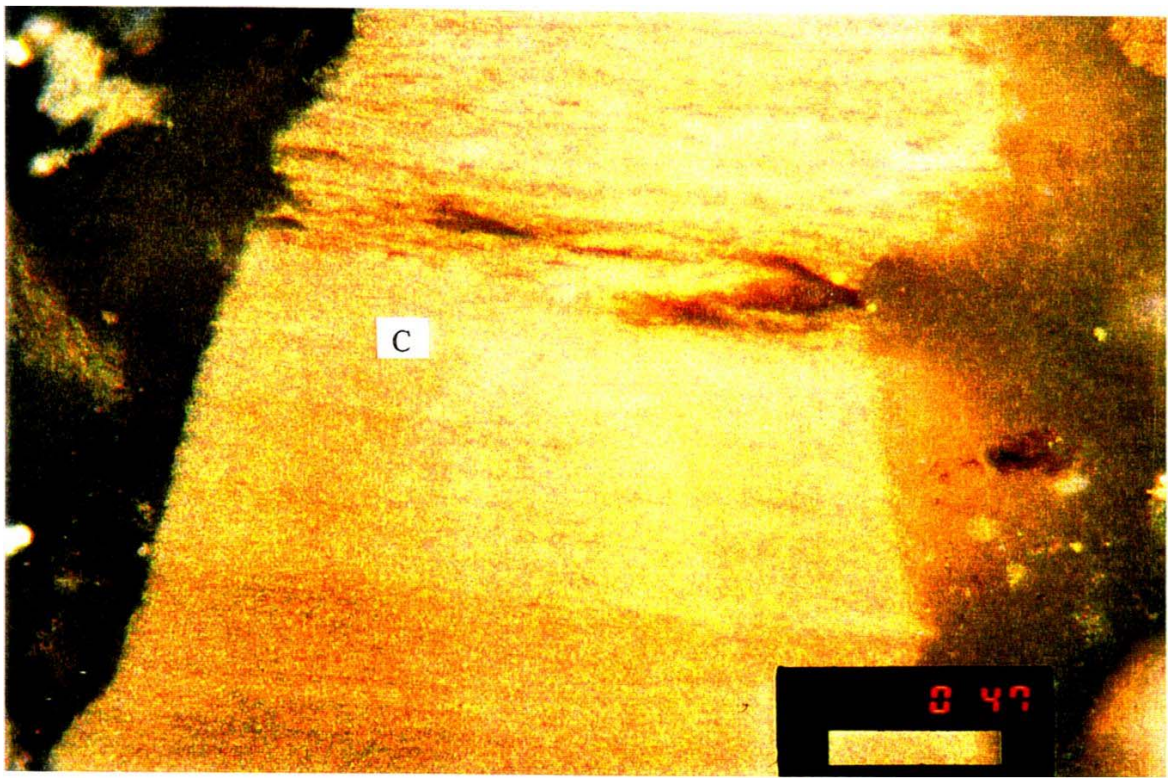

Photo 47: ***C – clay particle showing fine lamination***

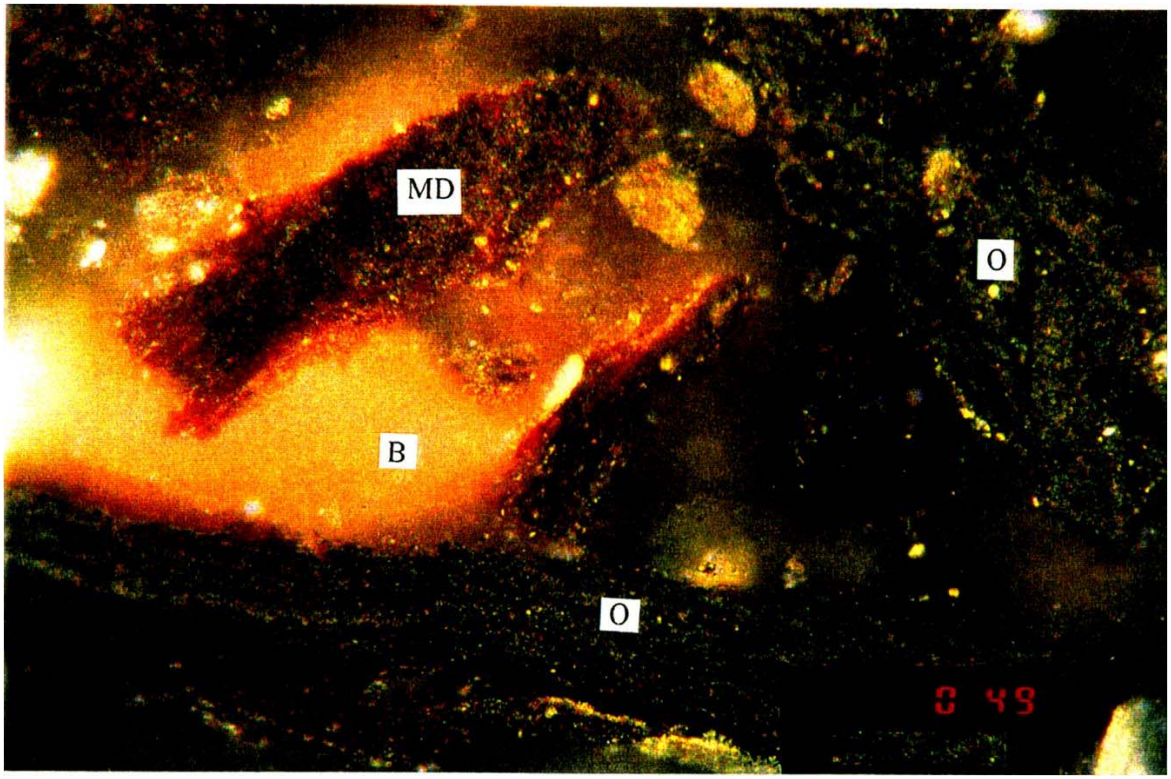

Photo 49: ***O – Fine organic matter in high concentration in the matrix***
MD – Matrix of mineral matter intermixed with submicron size of organic matter
B – binding agent (polyester resin)

Plate 8.2A: Petrographic Analysis of Sample 00-6054
(Scale bar = 40 µm)

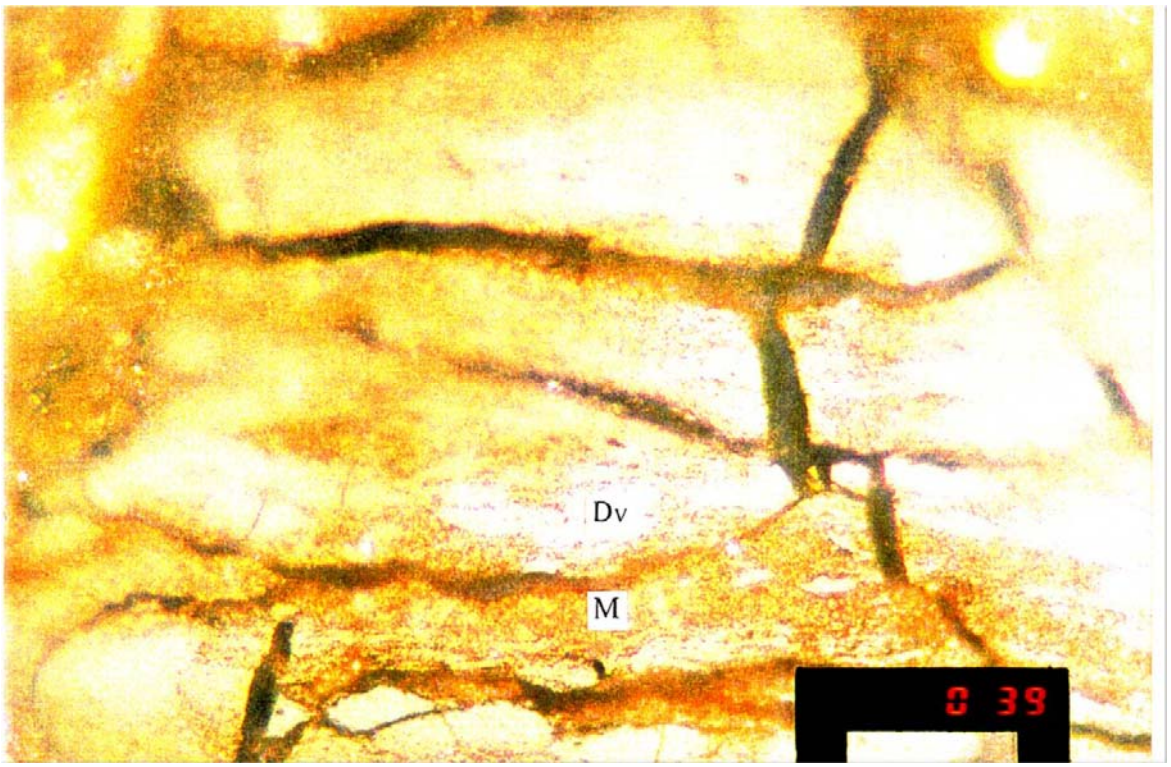

Photo 39: ***Dv – Detrovitrinite***
M – Matrix

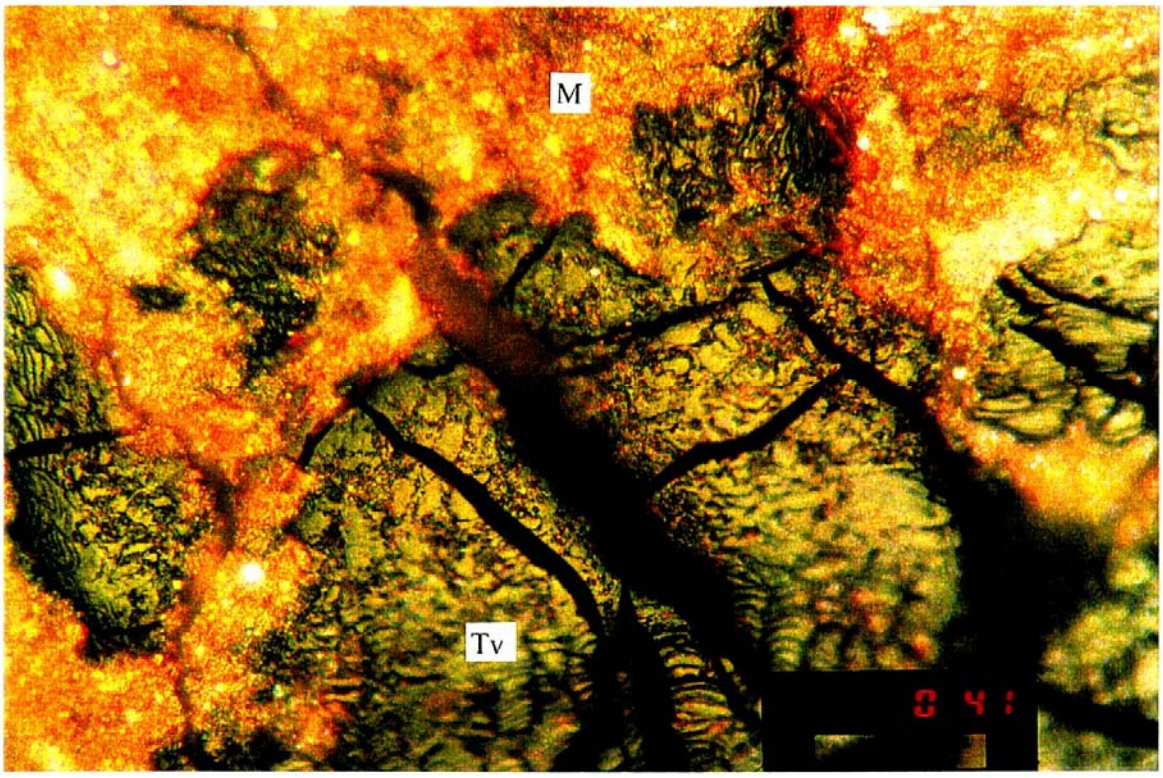

Photo 41: ***Tv – Telovitrinite (woody tissue with preserved cell structure) in mineral matrix***

Plate 8.2B: Petrographic Analysis of Sample 00-6054 continued (Scale bar = 40 µm)

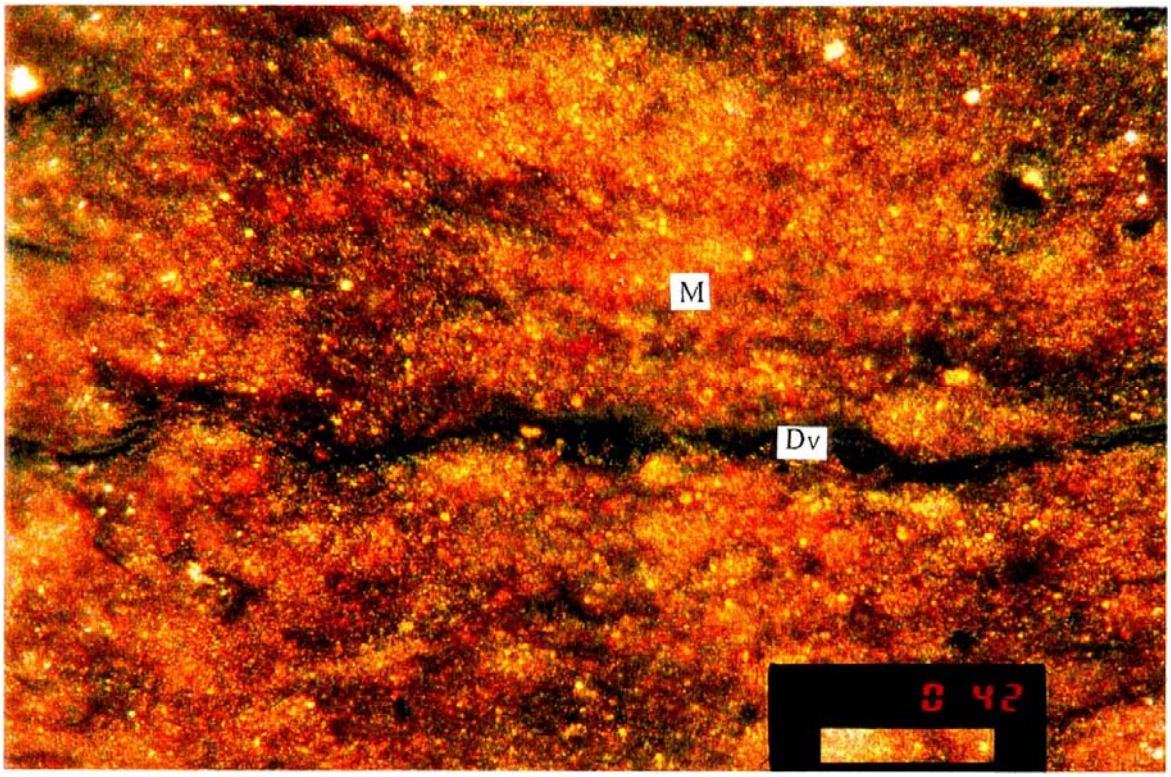

Photo 42: Dv – Detrovitrinite in mineral matrix intermixed with organic matter

Plate 8.3: **Petrographic Analysis of Sample 00-6056**
(Scale bar = 40 µm)

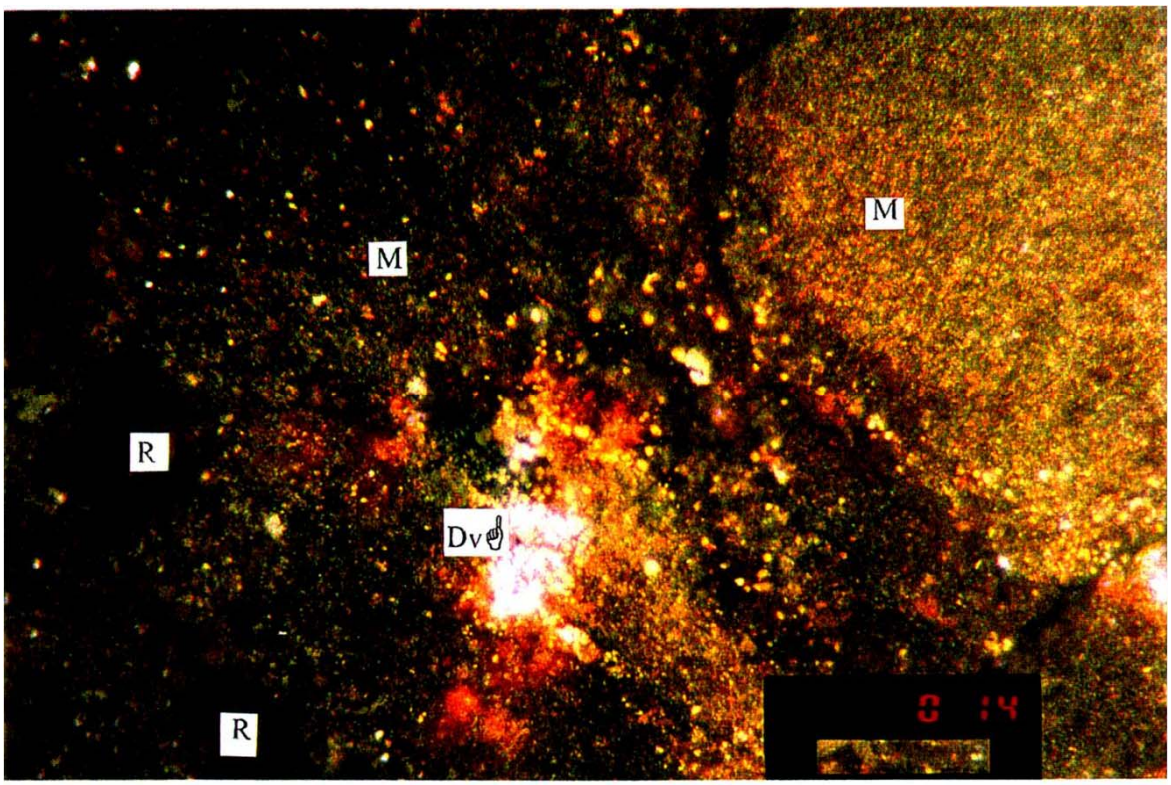

Photo 14: ***R – Resinite***
Dv – Detrovitrinite

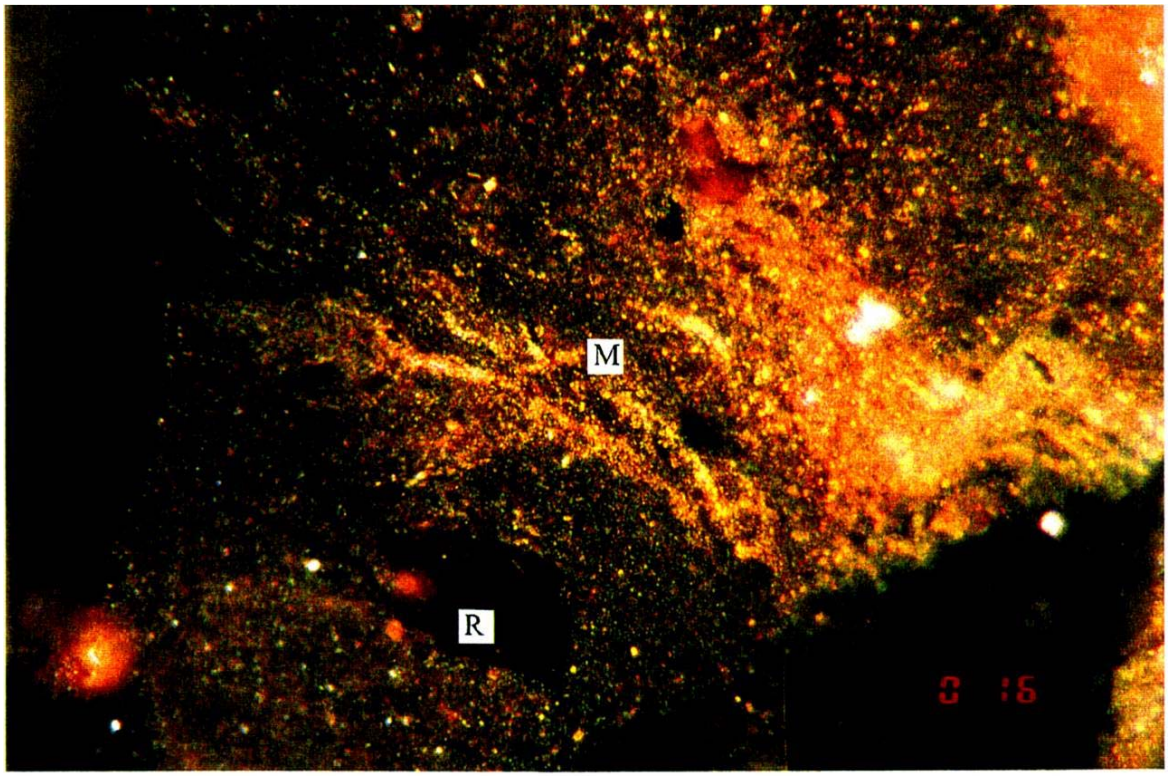

Photo 16: ***R – Resinite***
M - Matrix

Plate 8.4A: Petrographic Analysis of Sample 00-6061
(Scale bar = 40 µm)

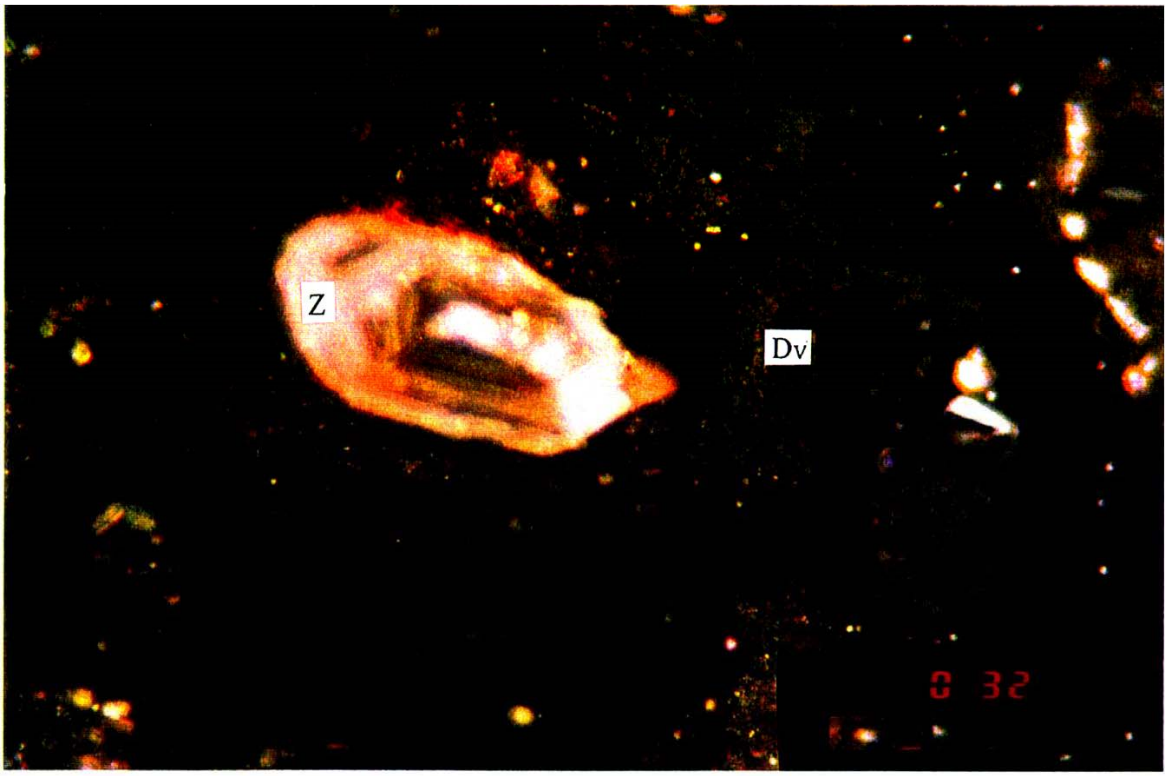

Photo 32: ***Dv – Detrovitrinite***
Z - Zircon

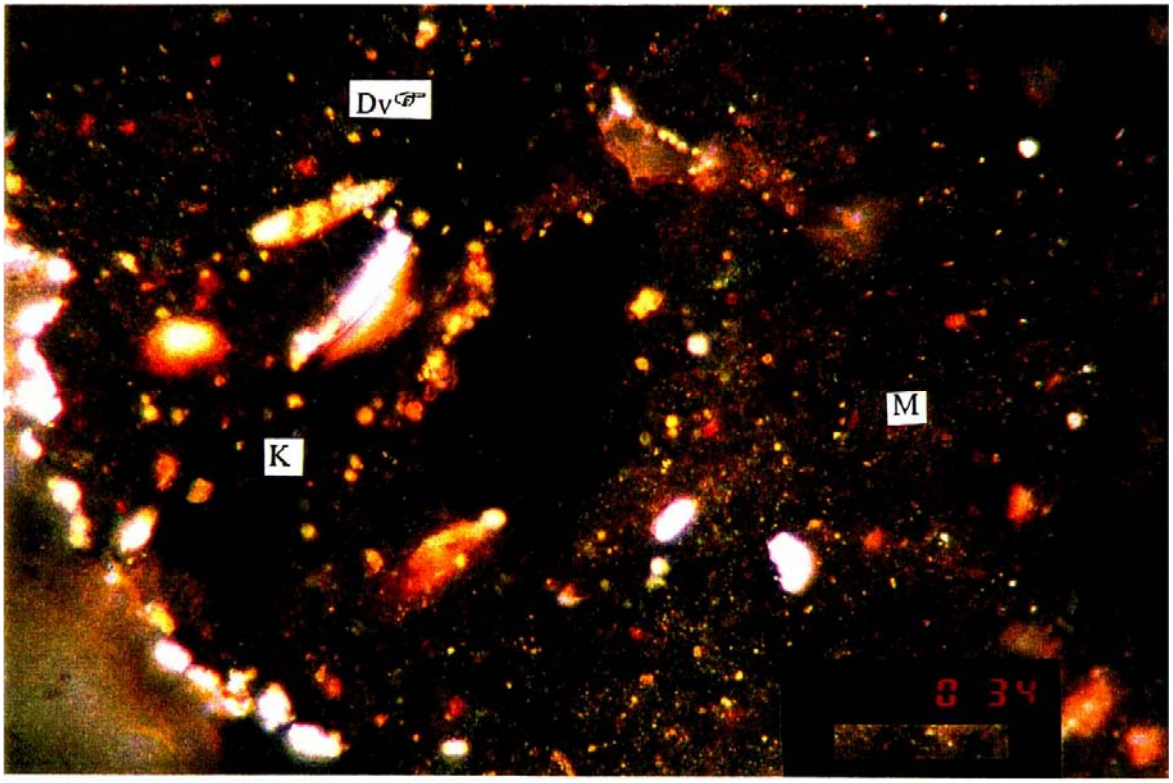

Photo 34: ***Dv – Detrovitrinite***
K – Kaolinite flake
M – Matrix

Plate 8.4B: Petrographic Analysis of Sample 00-6061 continued (Scale bar = 40 µm)

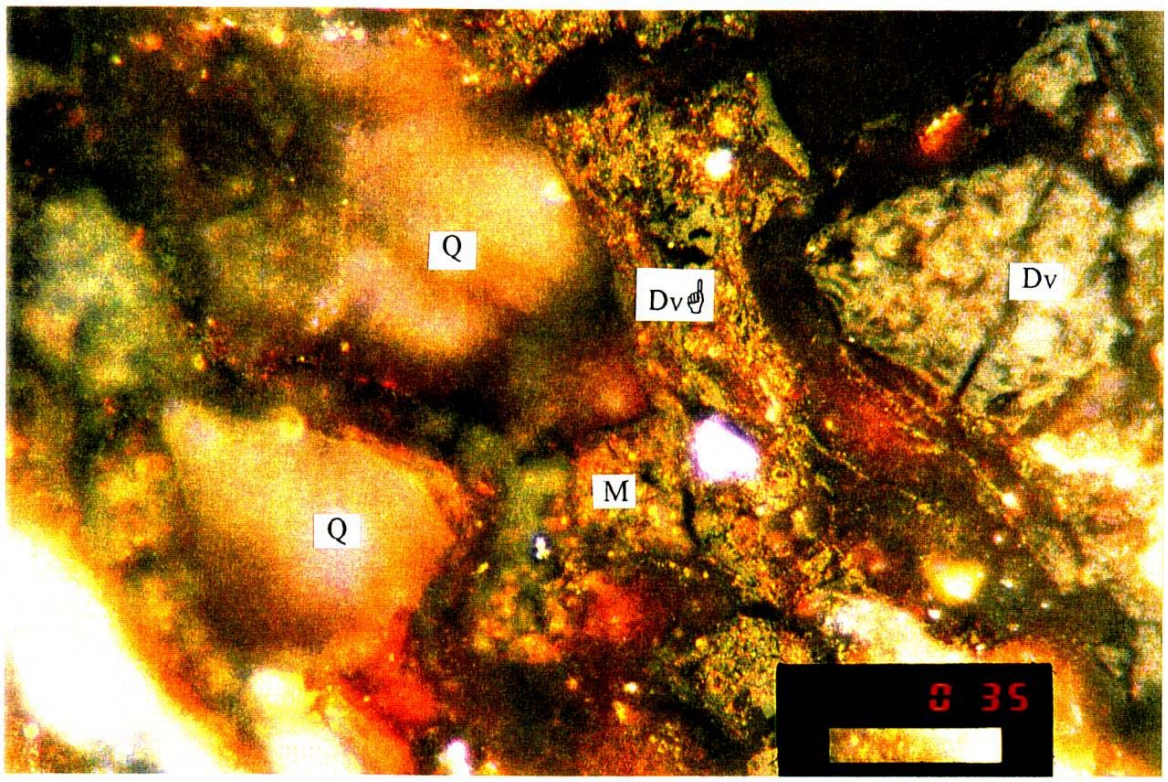

Photo 35: ***Dv – Detrovitrinite***
M – Matrix
Q - Quartz

Plate 8.5: **Petrographic Analysis of Sample 00-6074**
(Scale bar = 40 µm)

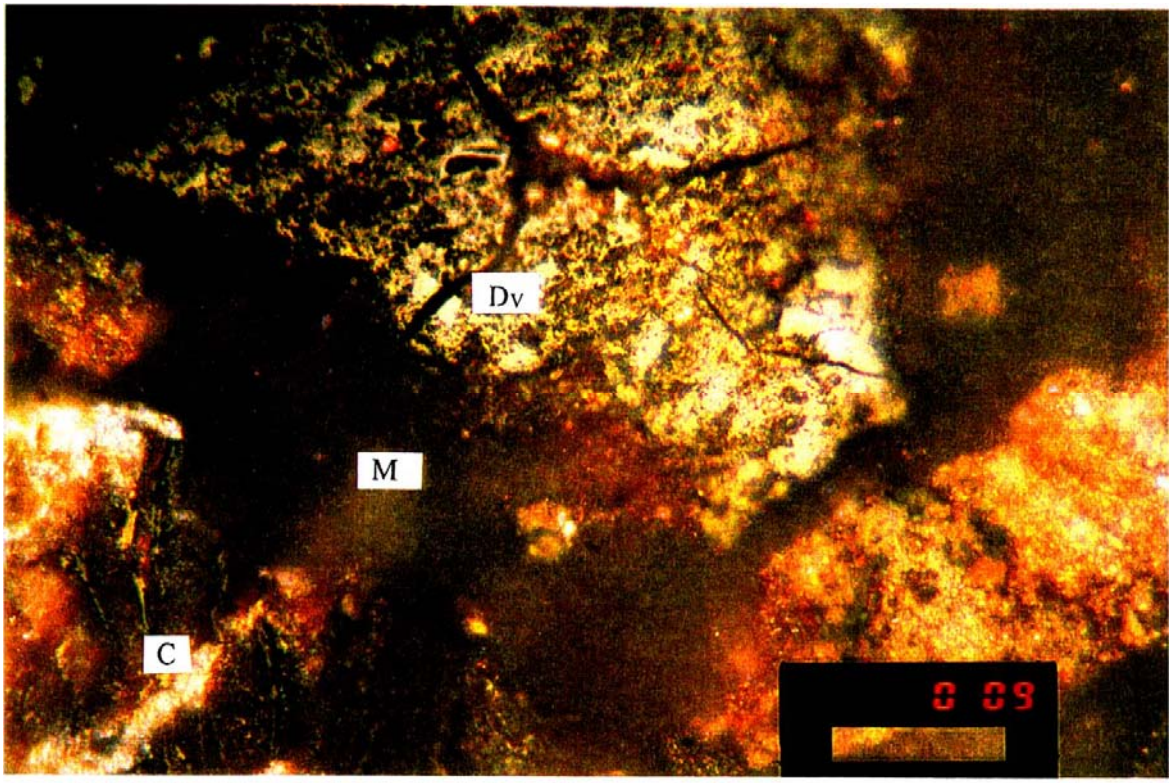

Photo 9: ***Dv – Detrovitrinite***
C – Clay
M – Mounting medium (binder)

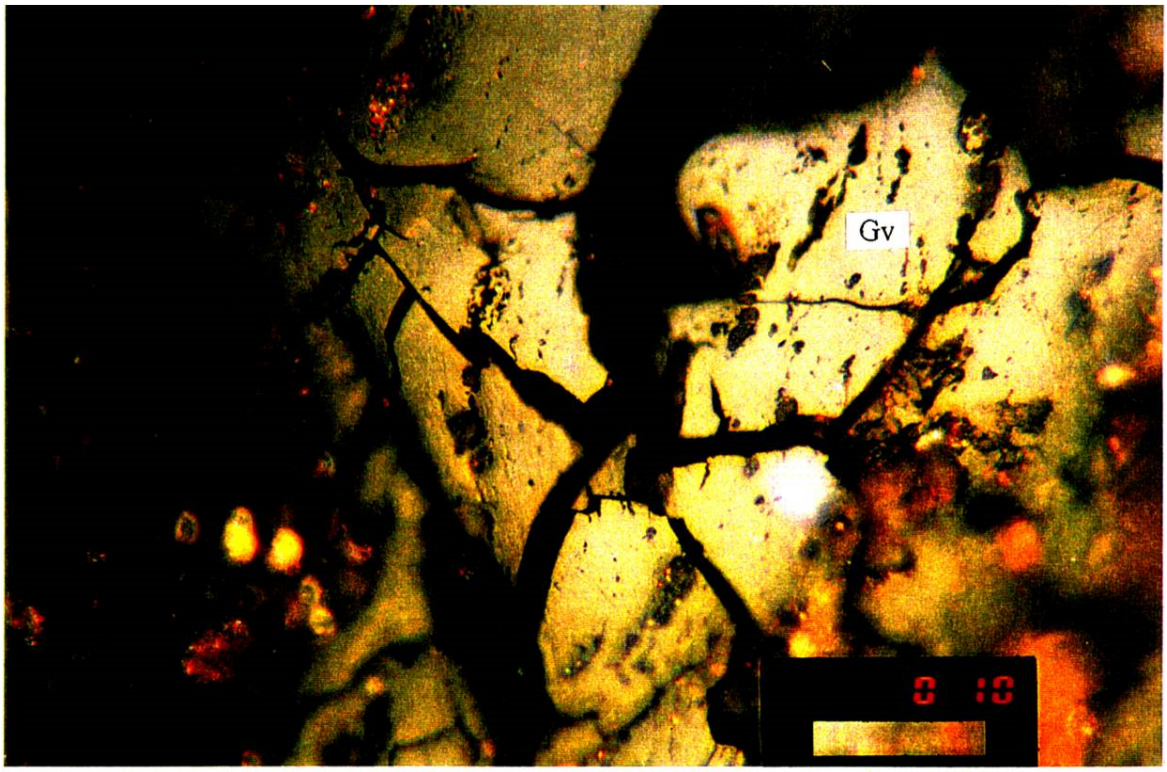

Photo 10: ***Gv – Gelovitrinite***

Plate 8.6: **Petrographic Analysis of Sample 00-6089**
(Scale bar = 40 µm)

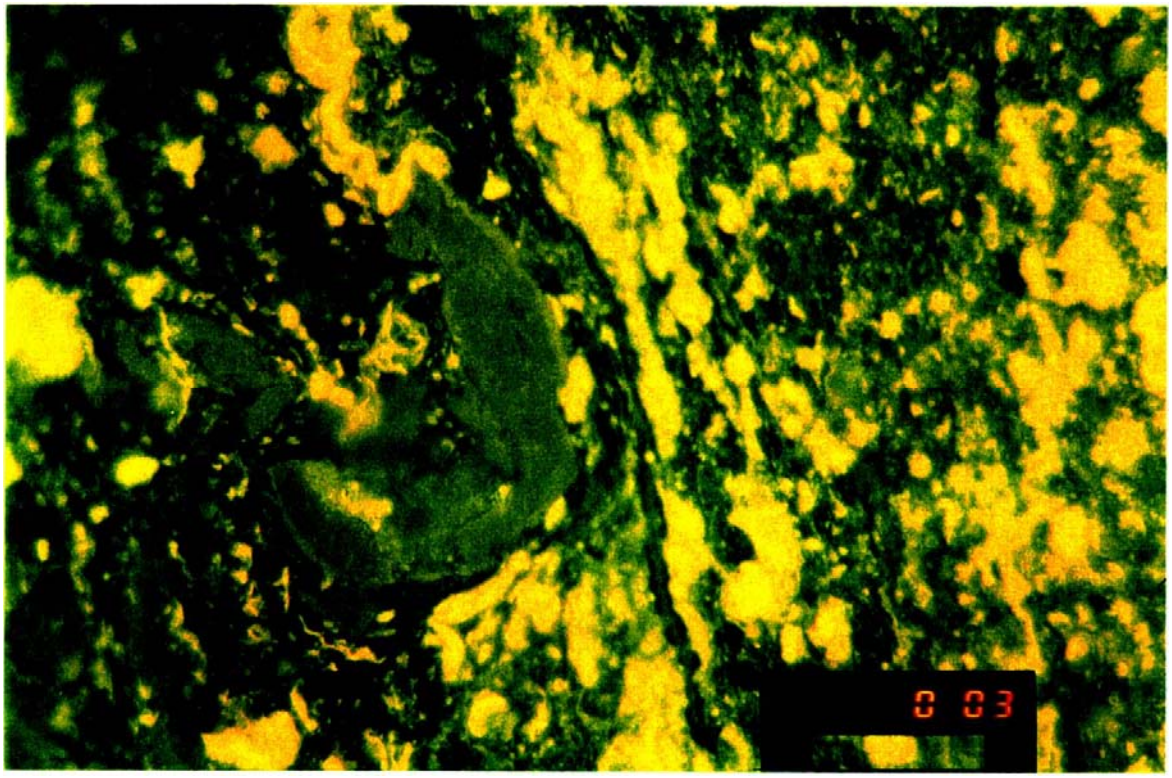

Photo 3: ***Under blue-light excitation. The yellow fluorescing parts are the macerals of the liptinite group (mainly liptodetrinite)***

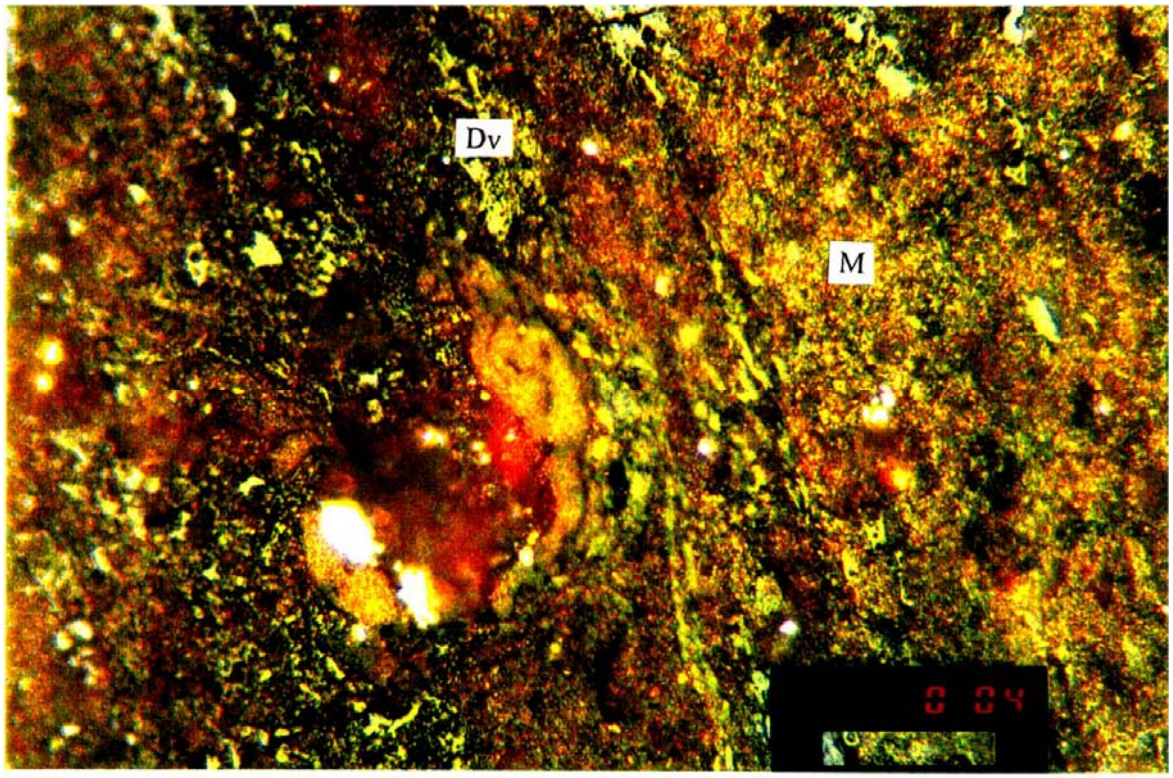

Photo 4: ***Same field as Photo 3***
M – Matrix rich in liptinite
Dv – Detrovitrinite

Figure 8.8 MLRA for vitrinite, for Ambassador samples

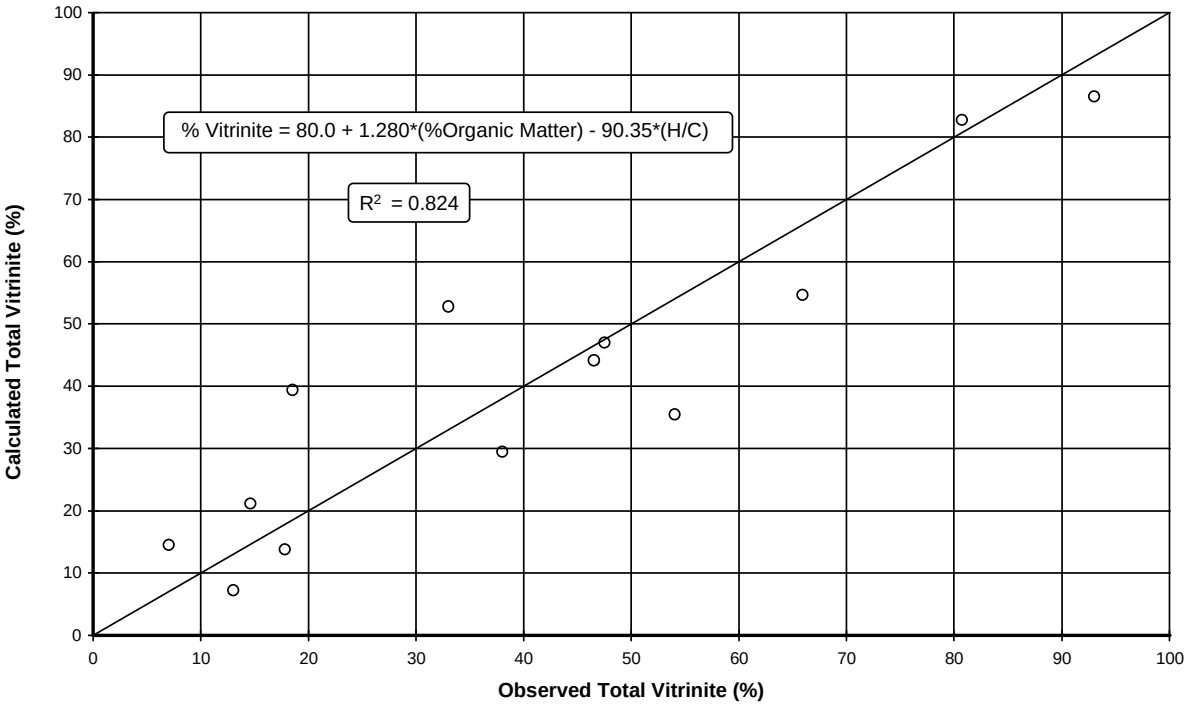

Figure 8.9 MLRA for mineral/organic matrix, for Ambassador samples

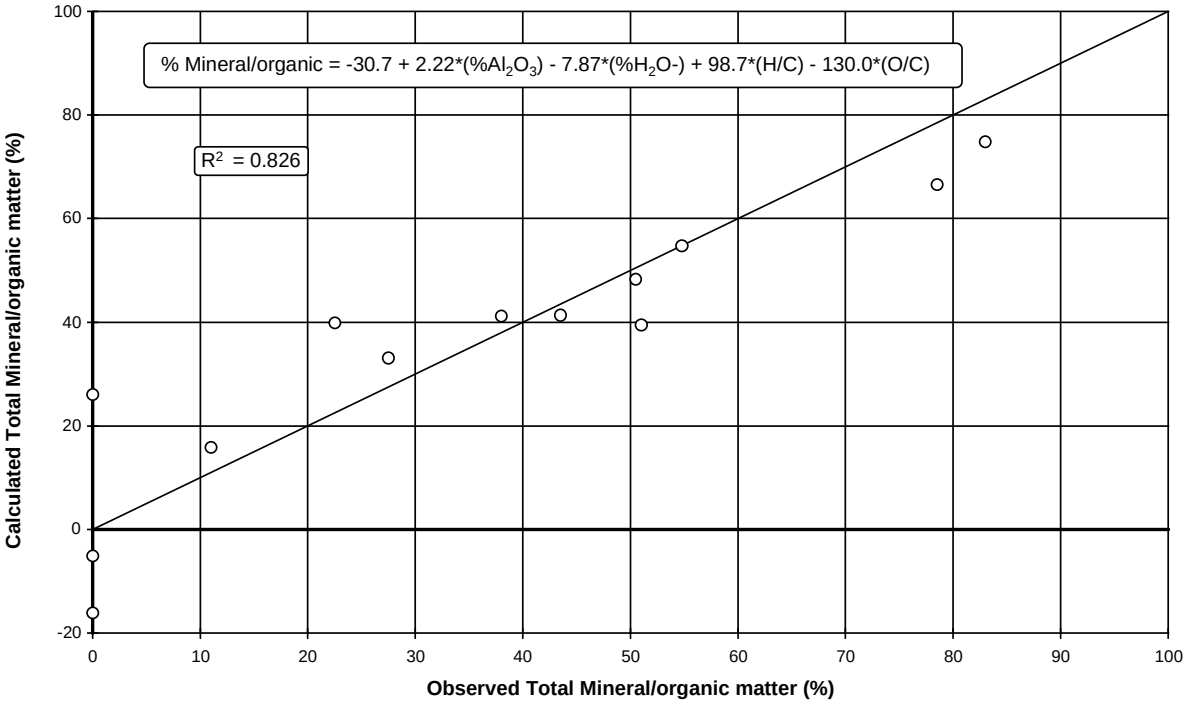

The MLRA method was also used to regress NMR and elemental results against each other, with a suite of other results (namely Al, Fe, Ce, Zn, U and S) also included. Results for each variable are discussed below.

Atomic H/C ratio

Atomic H/C gives a moderate correlation using MLRA (Figure 8.10), involving the amount of organic material (H_2O- and OM) and aromatic content:

H/C = 1.40 - 0.030*(H_2O-) + 0.0055*(OM %) - 0.012*(aromatic %) - R^2 = 0.434

A weaker, though still statistically significant, correlation is observed for aromatic content alone:

Atomic H/C = 1.48 - 0.0125*(aromatic %) - R^2 = 0.277

The negative correlation with aromatic content is probably due to the lower H/C for aromatic C (H/C approximately 1) relative to aliphatic C (H/C approximately 2).

Figure 8.10 MLRA for atomic H/C, for Ambassador samples

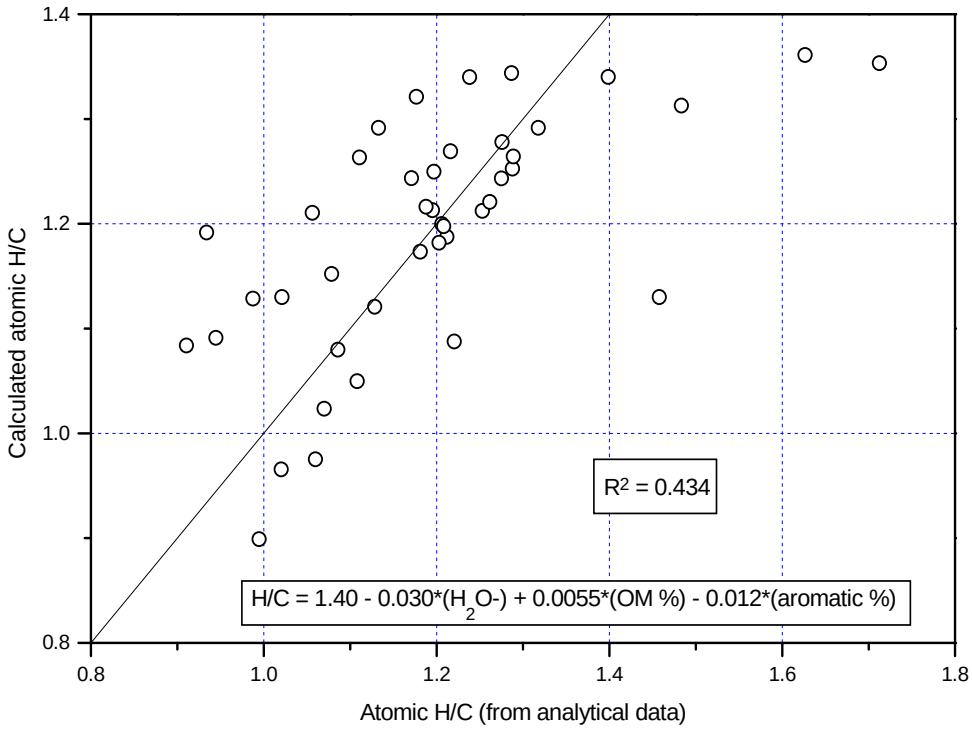

Atomic O/C ratio

No significant correlations are observed, for the variables tested.

% C in OM

No significant correlations are observed, for the variables tested.

Aliphatic content

Aliphatic content gives a moderate correlation using MLRA (Figure 8.11), involving the amount of organic material (H2O- and OM) and H/C and O/C ratios:

% aliphatic = 34.3 + 1.9*(H_2O-) - 0.34*(OM %) + 44.4*(H/C) - 51.1*(O/C) - R^2 = 0.475

Weaker, though still statistically significant, correlations are observed for H/C and O/C:

% aliphatic = 41.6 + 32.1*(H/C) - 40.0*(O/C) - R^2 = 0.332

and for H/C alone:

% aliphatic = 38.6 + 25.4*(H/C) - R^2 = 0.205

The correlation with the H/C atomic ratio is sensible, as aliphatic C is expected to have a relatively high H/C ratio (approximately 2).

Figure 8.11 MLRA for aliphatic content, for Ambassador samples

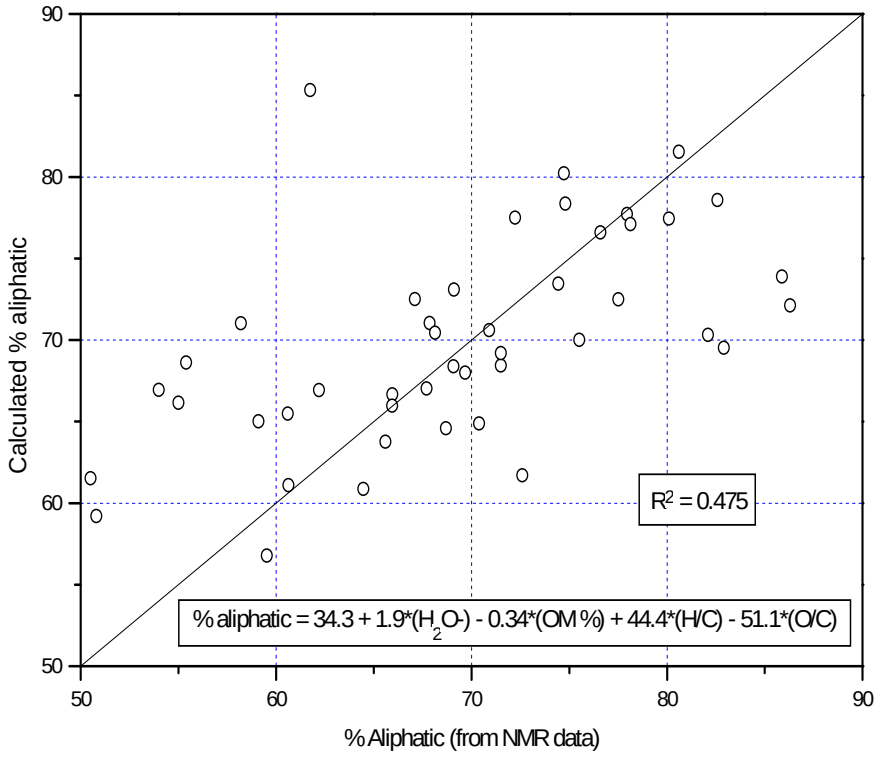

Aromatic content

Aromatic content gives a strong correlation (Figure 8.12), with OM and H/C and O/C ratios:

% aromatic = 42.8 + 0.12*(OM %) - 30.6*(H/C) + 41.2*(O/C) - R^2 = 0.516

A moderate correlation is observed with H/C and O/C:

% aromatic = 46.4 - 27.6*(H/C) + 34.1*(O/C) - R^2 = 0.443

and there is a weak, though still statistically significant, correlation for H/C alone:

% aliphatic = 49.3 - 22.2*(H/C) - R^2 = 0.277

As with the previous results, the negative correlation with H/C is probably due to the lower H/C of aromatic C. The correlation with O/C, implies that aromatic C has more O-groups than aliphatic C, which commonly occurs as long-chain fats.

Figure 8.12 MLRA for aliphatic content, for Ambassador samples

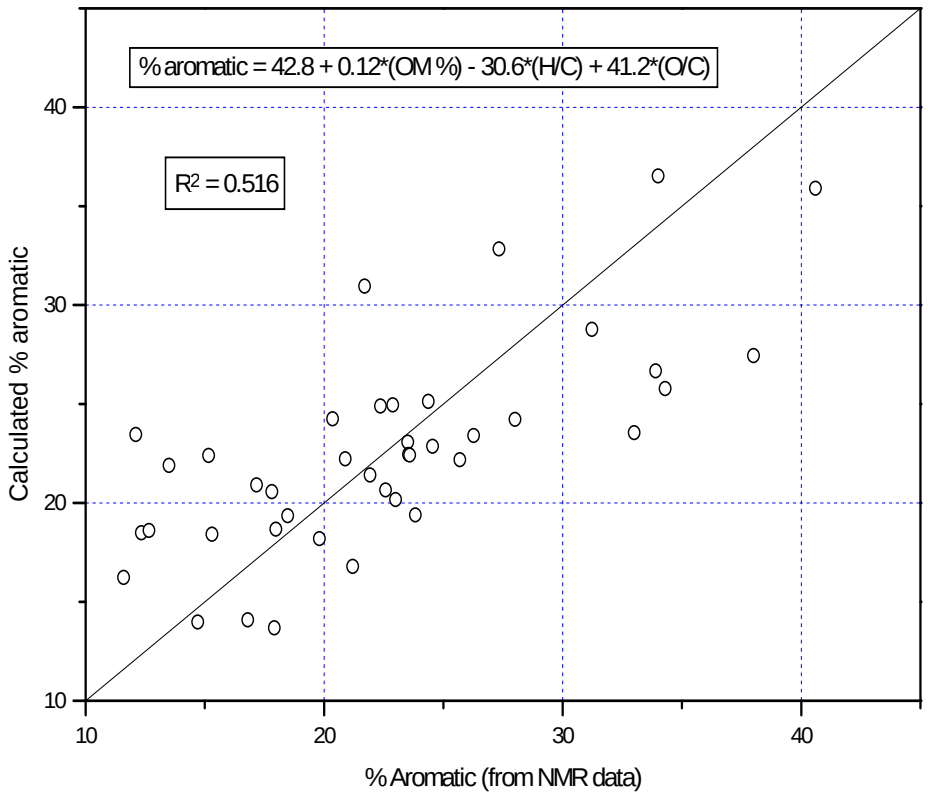

Carboxylic content

Carboxylic content gives a weak correlation using MLRA (Figure 8.13), involving the amount of organic material (H_2O- and OM) and H/C and O/C ratios:

% carboxylic = 6.3 - 0.43*(H_2O-) + 0.071*(OM %) - 4.7*(H/C) + 7.2*(O/C) - R^2 = 0.306

Clearly, a positive correlation with the O/C atomic ratio is sensible, as carboxylic C has a high O/C.

Figure 8.13 MLRA for carboxylic content, for Ambassador samples

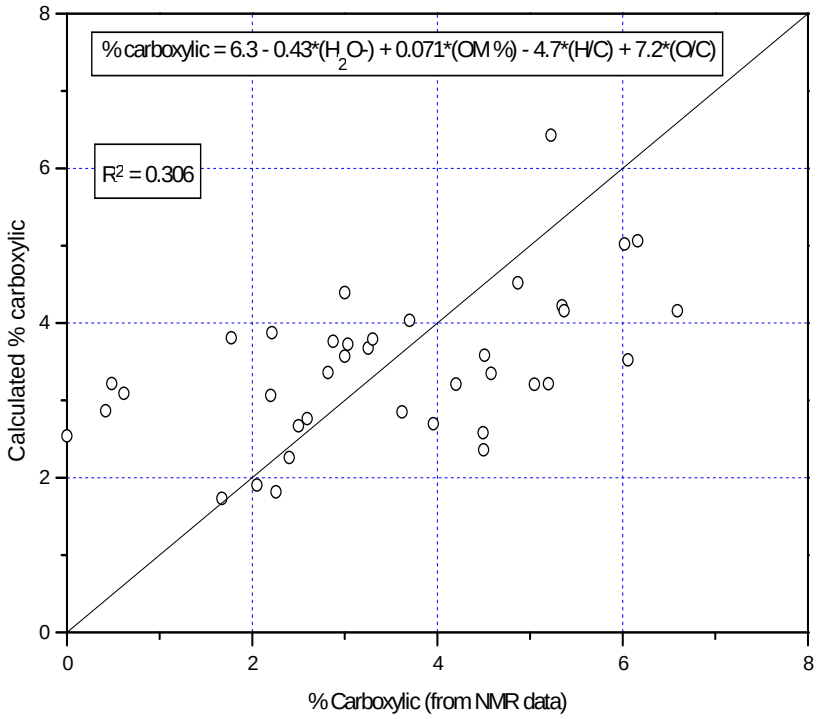

Aliphatic peak position

The high aliphatic content, the small aliphatic peak-width and separation from other phases, allows precise determination of the aliphatic peak position (commonly to approximately 0.1 ppm error). The position gives a very strong correlation (Figure 8.14), involving OM, H/C and N/C ratios and S and logU content:

Ali-pos = 29.03 + 0.047*(OM) + 2.73*(H/C) + 87.3*(N/C) - 0.121*(S) - 0.97*(logU) - R^2 = 0.656

Figure 8.14 MLRA for Aliphatic peak position, for Ambassador samples

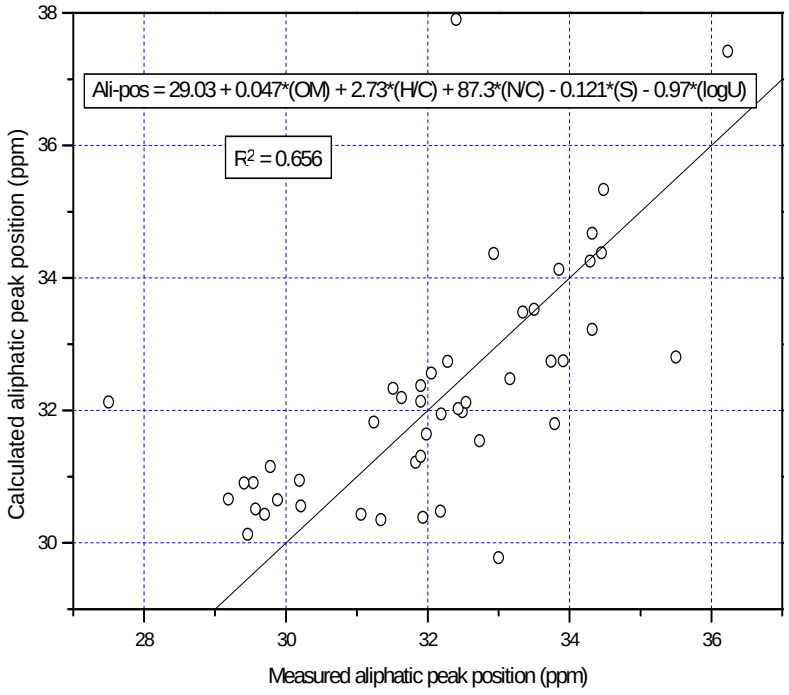

The primary variable controlling the peak position is U, and even logU alone (Figure 8.15) gives a moderate correlation:

Ali-pos = 35.6 - 1.30*(logU) - R^2 = 0.382

Figure 8.15 Linear regression for Aliphatic peak position vs. logU, for Ambassador samples

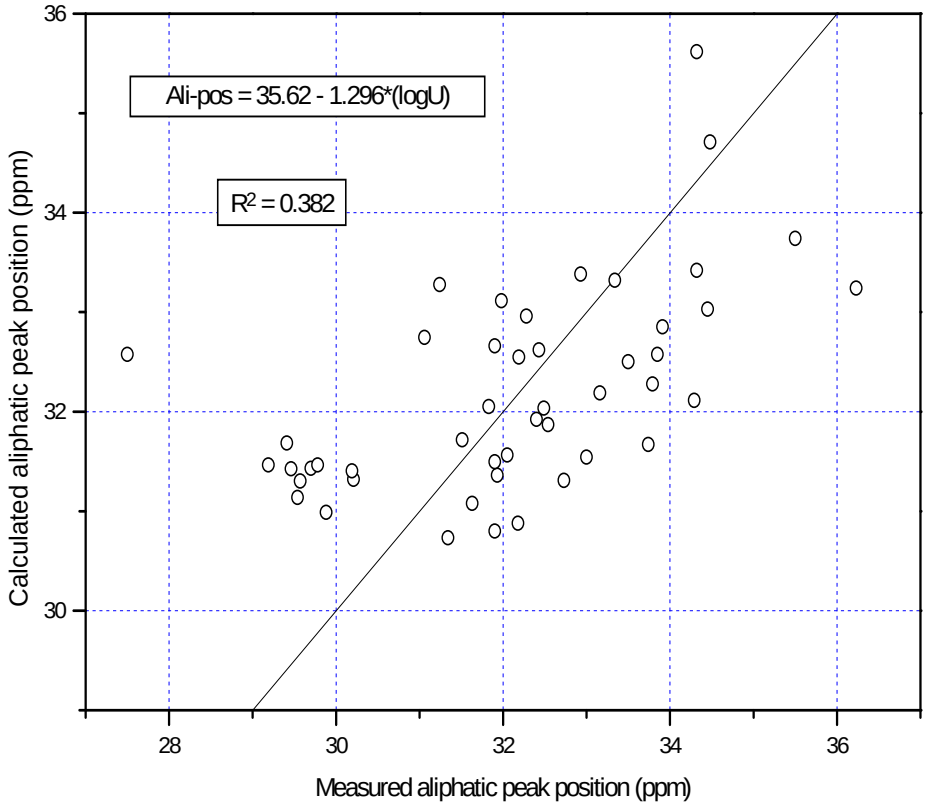

If U content is not included in the variable list, the best significant correlation achievable is 0.161. Thus, the aliphatic peak position appears to be dominantly correlated with U content.

Uranium content

The best MLRA correlation for U (expressed as the logarithm: the straight concentration gave very similar relationships, though with lower correlations), involves aliphatic and aromatic peak positions:

logU = -23.83 - 0.495*(ali-pos) + 0.325*(aro-pos) - R^2 = 0.693

This only involved 26 samples, due to difficulties in obtaining good peak position estimations for the aromatic NMR peak for many of the samples. When the aromatic peak position was not used (and the full sample set therefore used) the only significant MLRA result is obtained using the aliphatic position alone (Figure 8.16):

logU = 12.13 - 0.295*(ali-pos) - R^2 = 0.382

Figure 8.16 Linear regression for logU vs. Aliphatic peak position, for Ambassador samples

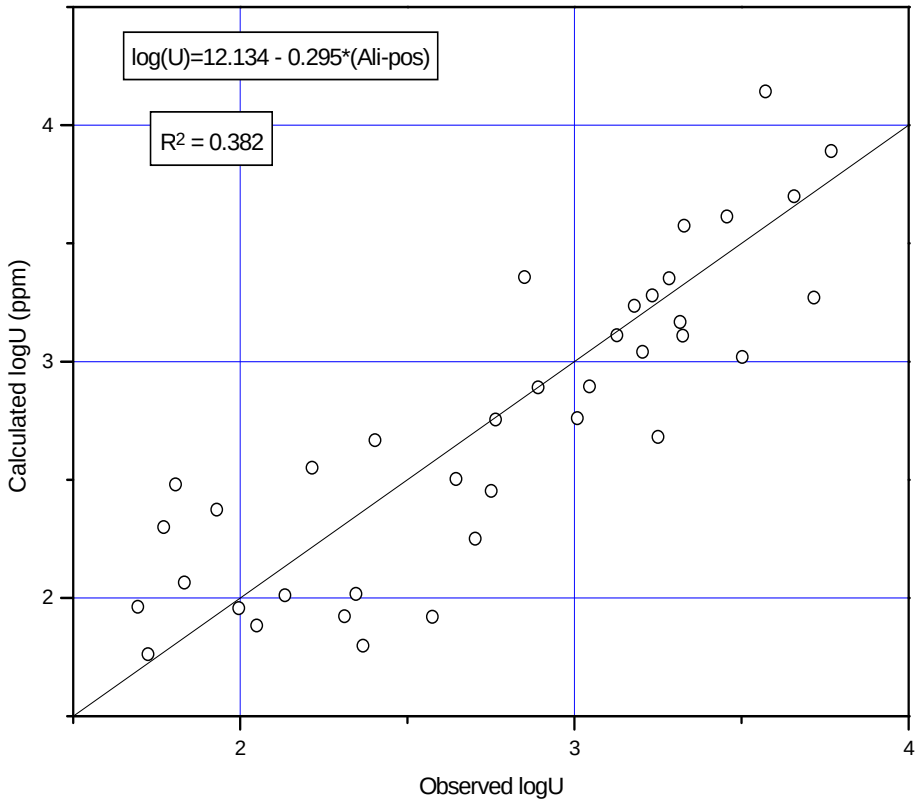

8.5.5 Mapping of the data

The data for each variable determined are mapped, as shown in Appendix 6; Figures A6.53 - A5.65, and with mapped data for calculated vitrinite, calculated mineral/organic matter, aliphatic peak position, aromatic peak position and U concentration duplicated in Figures 8.17 - 8.21. As observed, most of the data show no clear spatial patterns, possibly due to the lack of depth control (Section 8.5.2). Exceptions are the calculated vitrinite (Figure 8.17), which shows higher contents closer to the southern edge of the channel, and the calculated mineral/organic matrix (Figure 8.18), which is highest near the centre of the channel. This is as expected: vitrinite represents woody fragments, which will be higher closer to the shoreline, whereas the mineral/organic matter could have liptinite components, which are commonly wind-blown and could also contain coagulated humic matter, both of which might well be expected to be higher in the centre of the channel.

The other observation is the correlation of lower aliphatic peak position (Figure 8.19) and higher aromatic peak position (Figure 8.20) with U (Figure 8.21), which is consistent with the close relationship between these two variables (Section 8.5.4).

Figure 8.17 **Distribution of calculated vitrinite concentration for the Ambassador deposit, Mulga Rock**

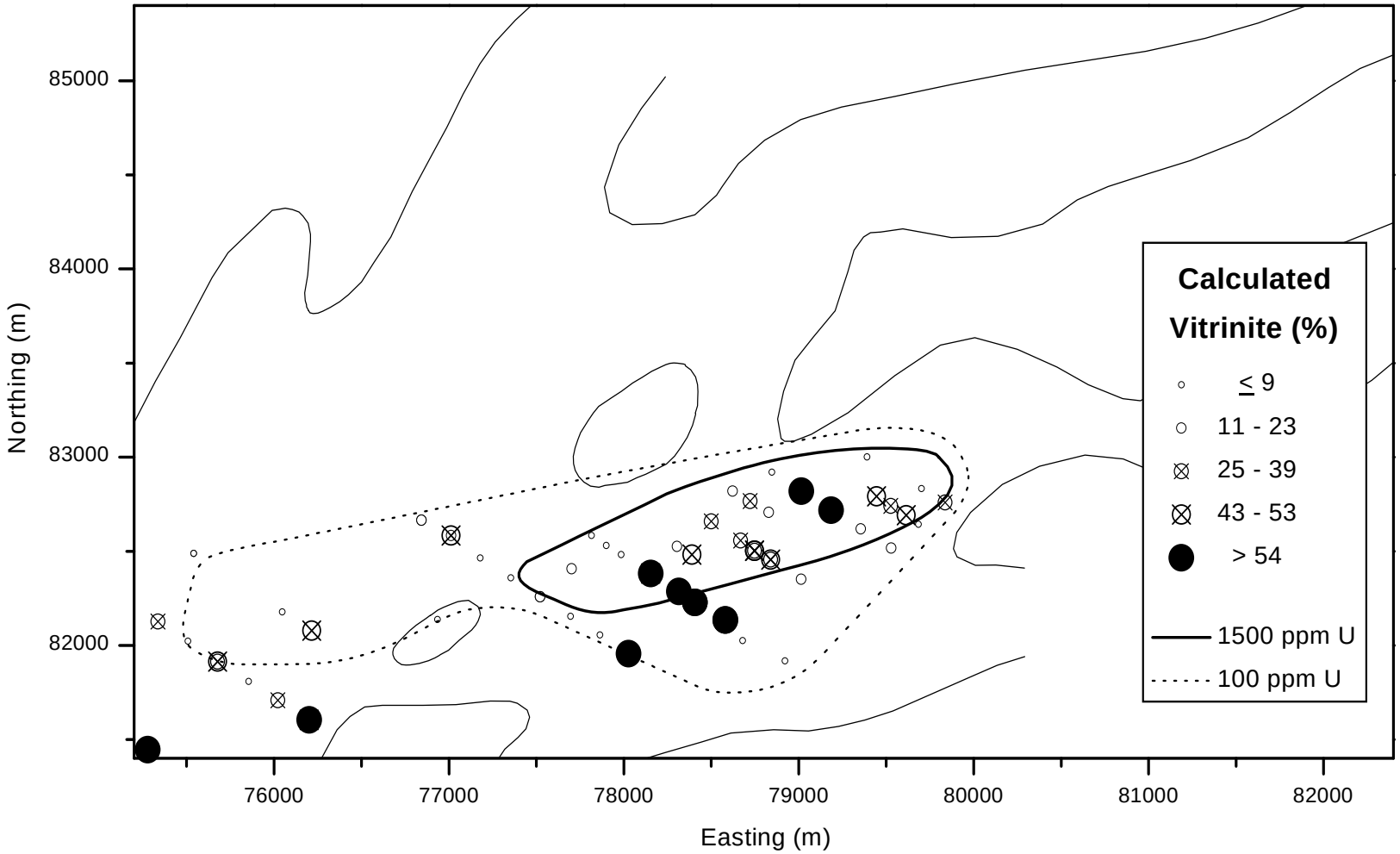

Figure 8.18 **Distribution of calculated mineral/organic matter concentration for the Ambassador deposit, Mulga Rock**

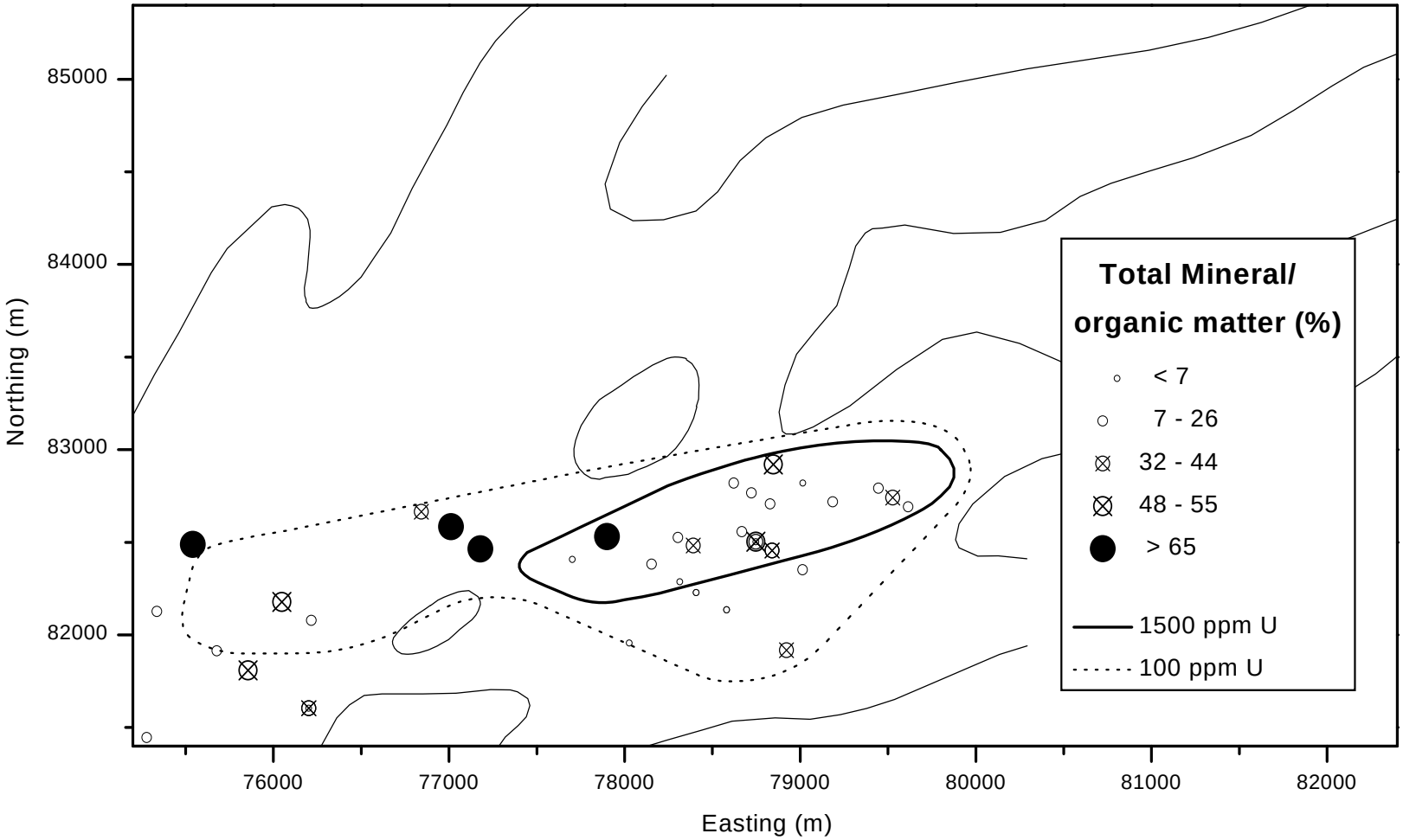

Figure 8.19 **Distribution of the Aliphatic Peak Position for the Ambassador deposit, Mulga Rock**

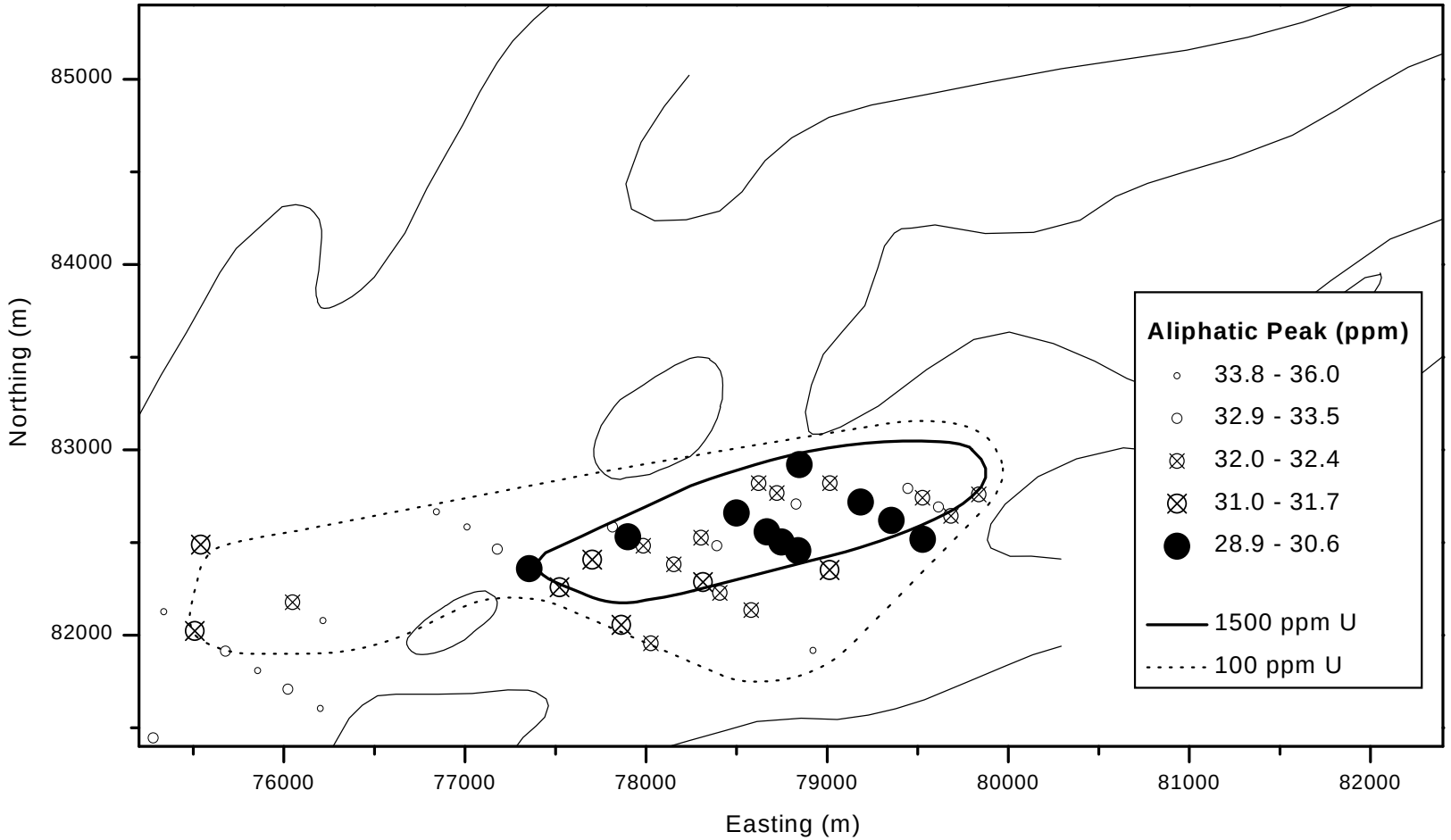

Figure 8.20 **Distribution of the Aromatic Peak Position for the Ambassador deposit, Mulga Rock**

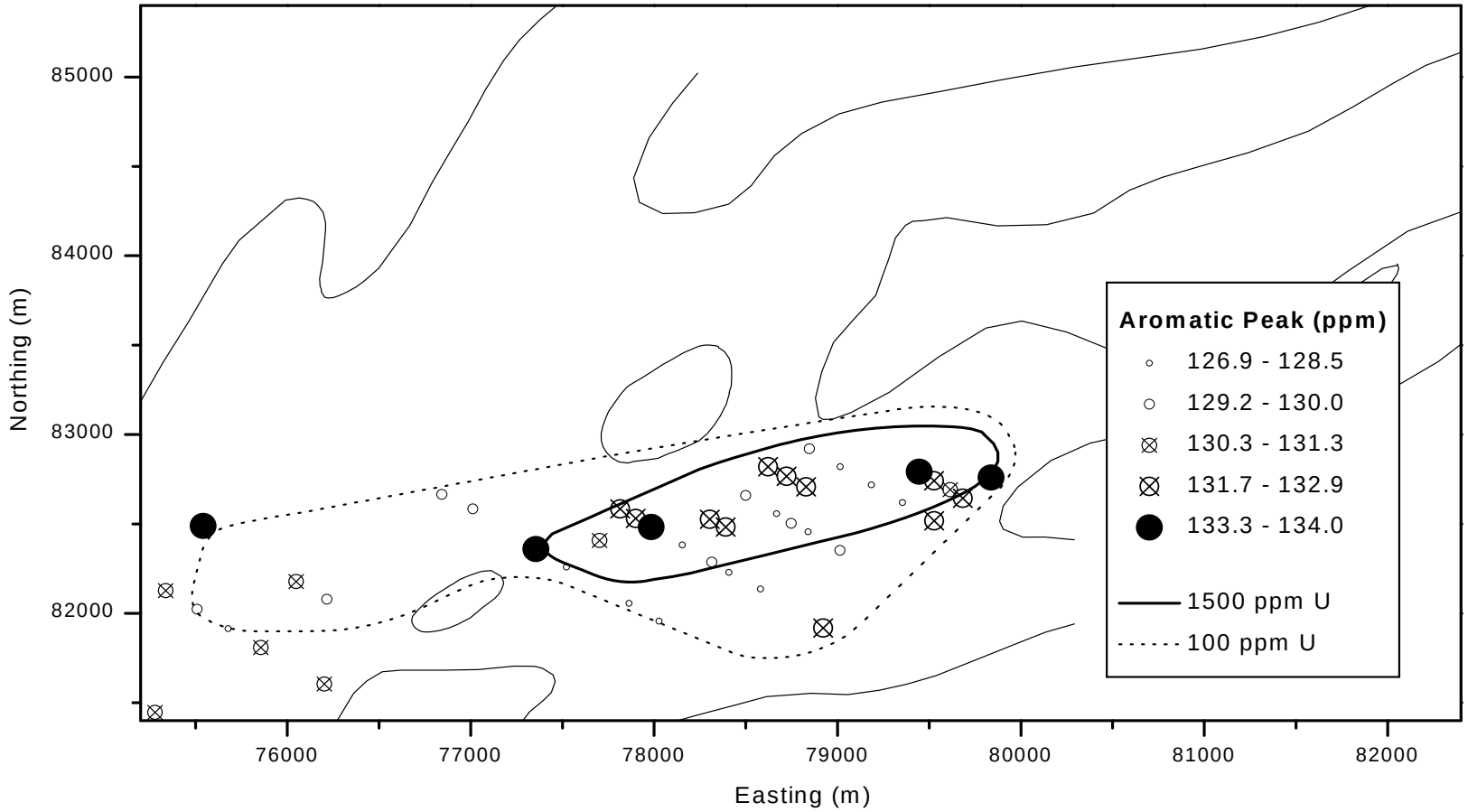

Figure 8.21 **Distribution of U for samples used for organic matter characterization at the Ambassador deposit, Mulga Rock**

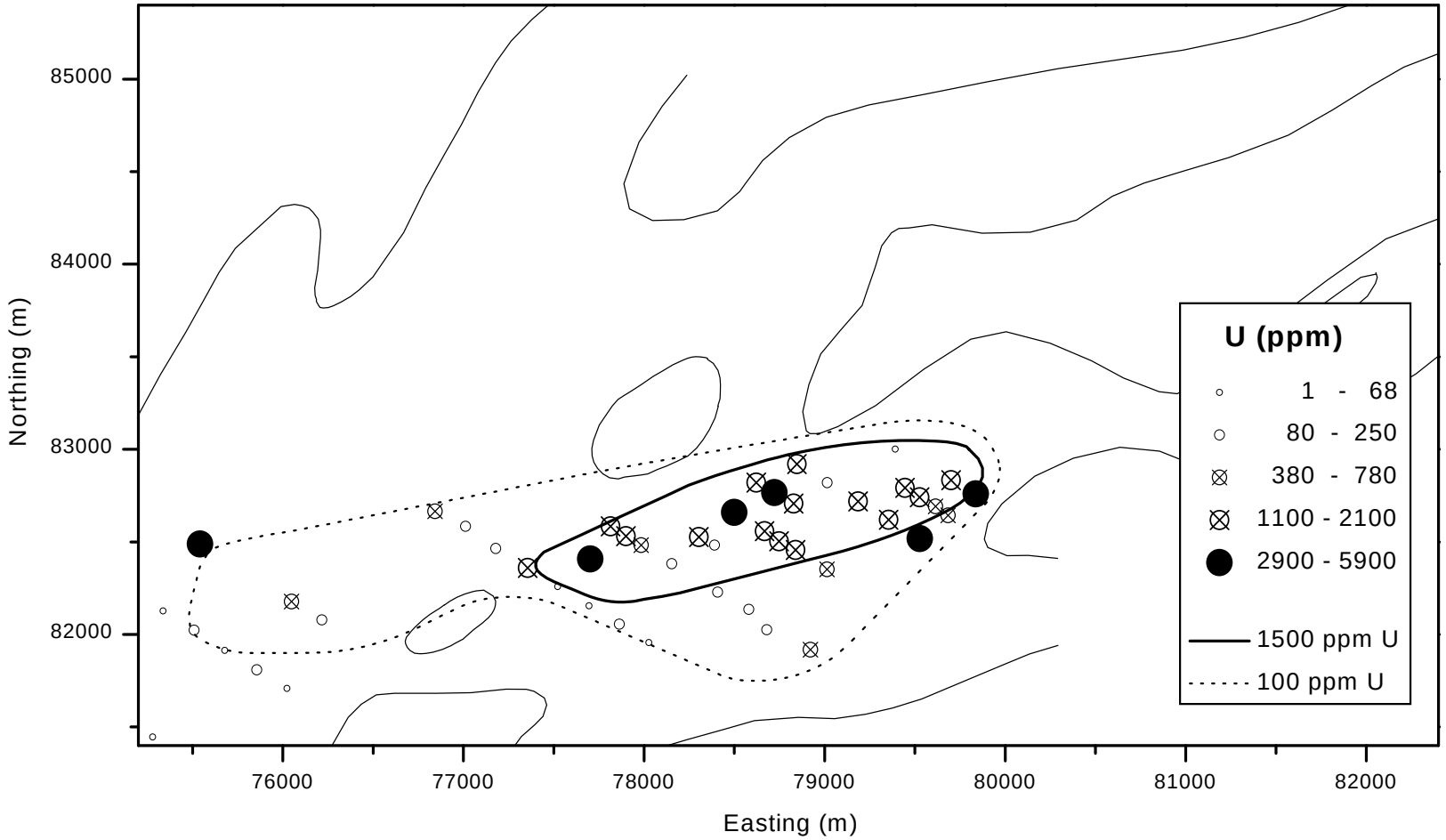

8.6 Discussion

Any conclusions based on the data presented in this Chapter are tentative, due primarily to the significant variation observed between samples at the same site at differing depth (Section 8.5.2). However, some interesting observations can still be made.

Of primary interest is the correlation of U with the aliphatic and aromatic peak positions. Other peak positions might also have similar correlations, but are not observable due to the poor peak resolution. There are two possible explanations for this effect:

(i) U precipitation is controlled by the form of the organic matter, as indicated by the NMR peak positions;

(ii) U is precipitated in intimate association with organic matter, causing shift in the peak positions with higher U concentrations.

Each of these hypotheses is feasible, and would have significant implications on the form of the U in the deposit. Further work might well demonstrate the cause of the NMR peak position - U correlation.

For the samples examined, between 0 and 90% of the identifiable organic matter is directly derived from plants, with the remainder comprising humic materials or other fine grained constituents. These humic materials may have been concentrated and deposited in an aquatic environment due to the complexing of organic functional groups by dissolved cations (Section 2.3.3). Alternatively, some of the humic material may have been derived from the humification (degradation) of precursor plant remains. Although the direct influence of seawaters is precluded by the absence of any identifiable marine macro-organisms or fossils and on palynological grounds (see later), the action of saline waters may have acted as a coagulant and concentrated the humic material. This is supported by the observations of higher levels of mineral/organic matrix in the centre of the channel (Section 8.5.5). Such a coagulation of humic material may have been syngenetic *i.e.,* in an estuarine or in a lagoonal setting, or epigenetic *i.e.,* due to the movement of saline groundwaters during diagenesis.

Preservation of the organic matter was probably accomplished via two main mechanisms. Firstly, it is possible that, given the low regional topographic gradients, subtle tectonic movements could have altered the course of existing palaeochannels, thus leaving the organic matter to consolidate and eventually be covered by younger sedimentary material. This process could also explain the absence of organic matter in other palaeochannel systems, which may have been scoured out following drainage capture. Secondly, a marine transgression may have drowned an entire palaeochannel system, depositing a prograde sedimentary sequence. There is no evidence for marine sediments in this region, although marine sediments have been identified in drainage systems south of Kalgoorlie. Nevertheless there is little definitive understanding of the origin of the sedimentary units that infill the Mulga Rock palaeochannels and hence this scenario cannot be discounted. Further maceral, palaenotological and sedimentological analysis is required, however, on a local and regional scale to definitively establish the environment that prevailed during the mid-Eocene.

8.7 Conclusions

Any conclusions based on the data presented in this Chapter are tentative, due to the significant but un-quantified depth effect. The most successful analyses were achieved for samples that had > 20% LOI, although results for some samples having between 10 and 20% LOI were adequate.

NMR data indicate that, on the basis of peak heights, the lignite material is dominantly aliphatic, and the spectra resemble those of liptinite, though with significant aromatic content, suggesting significant vitrinite material. The presence of carbohydrate and carboxylic groups suggests poor maturation.

C,H,O,N analyses are consistent with the NMR results, suggesting the samples to vary from virtually chemically unaltered wood and exine to more mature forms, with more than half of the samples showing significant or dominant exinite/liptinite character. There is no apparent spatial pattern for degree of maturation.

Maceral analysis suggests that the liptinite component indicated by the other methods is primarily in a finely divided form, suggesting that it may be at least partially due to coagulated humic matter. This is supported by the higher concentrations of this finely divided material in the centre of the channel.

Uranium concentration appears to be highly correlated with the NMR peak positions, indicating a strong chemical interaction between these two phases. This has implications for the origin of this deposit; with two possible explanations for this effect:

(i) U precipitation is controlled by the form of the organic matter;

(ii) U is precipitated in intimate association with organic matter.

Each of these hypotheses is feasible, and would have significant implications on the form of the U in the deposit. Further work might well demonstrate the cause of the NMR peak position - U correlation.

9.0 A U-Th DISEQUILIBRIUM STUDY OF THE AMBASSADOR DEPOSIT

9.1 Introduction

Disequilibrium in the relative concentrations of U and its daughter products is a common occurrence, especially in recently formed, secondary U deposits. Disequilibrium develops in decay chains when they are present in open systems, which permits the fractionation of daughter products due the relative differences in geochemistry compared to U. The ^{238}U decay series is particularly susceptible to the development of disequilibrium because it contains several distinct daughters with long half-lives that behave differently under variable Eh-pH conditions and in the presence of different substrates *e.g.*, organic matter or clays (Section 2.3.2, 2.3.3). Disequilibrium is usually expressed as the ratio of the ^{238}U concentration/daughter concentration. Three main types of disequilibrium can occur;

(a) ^{238}U/daughter = 1, secular equilibrium, where the concentration of U and its daughter are in approximate equilibrium,

(b) ^{238}U/daughter >1, positive disequilibrium, where U is in excess of its daughter, due to the preferential deposition of U or the leaching of daughters,

(c) ^{238}U/daughter <1, negative disequilibrium, where U has been preferentially leached, or daughters deposited.

Rosholt (1959) further subdivided the types of disequilibrium in U-deposits in terms of six categories, expressed in terms of the radionuclides ^{238}U, ^{231}Pa, ^{230}Th and ^{226}Ra. As the activity of ^{231}Pa was not measured in this study, this type of disequilibrium is expressed in terms of the three other radionuclides.

1.	$^{238}U>^{230}Th>^{226}Ra$	Indicates that leaching of daughter products has taken place or U may have migrated to its present location over less time than that required by its daughter products to reach approximate equilibrium, *i.e.,* is less than 300,000 y. The former explanation is more probable in carnotite deposits (*e.g.,* Yeelirrie) and other types of deposits where U is present as a discrete mineral phase.
2.	$^{238}U>>^{230}Th>^{226}Ra$	Deposits with this pattern show considerable daughter product deficiency and are probably the result of very recent accumulation of U. Disequilibrium patterns of this type have been reported in peat bogs in Canada.
3.	$^{238}U<^{230}Th<^{226}Ra$	Disequilibrium is believed to be the result of rather recent deposition of U contaminated with significant amounts of daughter products other than ^{230}Th, or the deposition of daughter products alone. Sections of roll front deposits may display this disequilibrium pattern.

4.	$^{238}U<^{230}Th>^{226}Ra$	Disequilibrium found in samples taken from an oxidized environment, and is the result of U leaching. Samples from the rear of a roll front could exhibit this disequilibrium pattern.
5.	$^{238}U<^{230}Th<<^{226}Ra$	This is a disequilibrium pattern that occurs in pyritic ores or ore dumps, and is the result of differential leaching of all radionuclides under acidic conditions. Some Australian deposits in acidic saline groundwaters could show this pattern.
6.	$^{238}U=0$, ^{226}Ra, ^{228} Ra present	This disequilibrium pattern is not applicable to U deposits, but is a pattern commonly found around springs, in swamps and on the margins of salt lakes throughout Australia, and also in oil and gas field brines.

The disequilibrium profiles, both down hole and laterally across the Ambassador deposit, have been examined in an attempt to gain an insight into the processes operative in the redistribution of U, Th and their daughters at the redox front (Tables 9.1-2, Figures 9.1-3). Furthermore, the distribution of the parent and daughter radionuclides may give an insight into how other elements with a similar geochemistry behave at the redox front.

9.2 Experimental

Approximately 20-50 g of ground sample were analysed by γ-spectroscopy, at CSIRO in Sydney, using the methods of Gulson and Mizon, (1980).

9.3 Results and discussion

Results of the γ-spectroscopy are given in Table 9.1 and interpretation of the disequilibrium profiles is given in Table 9.2. Down hole disequilibrium profiles of the isotopic ratios of $^{238}U/^{210}Pb$, $^{238}U/^{230}Th$ $^{238}U/^{226}Ra$ and $^{230}Th/^{232}Th$ of holes 6096, 6184 and 6221 are given in Figures 9.1-9.3. The three radionuclides ^{226}Ra, ^{210}Pb, and ^{230}Th have been chosen as they represent three elements with a widely differing geochemical behaviour and possess sufficiently long half lives such that they may be remobilized in a coherent manner over time. The relative depletion or excess of daughter products for the overall sample is expressed as a ratio of the actual U concentration to that estimated by γ-spectroscopy (*i.e.*, U-ave/U-γ), where equilibrium is 1 and daughter excess or depletion are <1 and >1 respectively. Note that γ-U is analogous to equivalent U (eU) and the latter will be used in the following discussion. *Apparent concentrations* (ppm eU) of radionuclide daughters given in Table 9.1 and in the text are expressed as gamma (γ) equivalent grades compared to U (and are thus designated eU), and are not actual concentrations.

Table 9.1: Results of γ-spectroscopy of Ambassador samples. All daughter product concentrations are expressed as equivalent U (eU) concentrations

Radionuclide (ppm) Energy (KeV) Sample	Hole	Depth Interval	210Pb -16.5	230Th 67.8	226Ra 186.0	232Th(2) 238.0	ave [U] grade	[U]est gamma	[U] ave/gamma	[Th]est gamma
6031	1360	37.76-38.86	52	75	102	50	164+/-8	52+/-4	3.2+/-0.3	52+/-4
DISEQUIL. RATIO (1)			3.42+/-0.90	1.96+/-1.64	1.76+/-0.21	1.5+/-13				
6059	1305	33.00-35.00	1774	1553	1434	38	1845+/-35	1263+/-25	1.5+/-0.0	38+/-9
DISEQUIL.RATIO			1.08+/-0.05	1.24+/-0.27	1.36+/-0.07	30.3+/-9.7				
6062	1368	45.20-45.40	81	30	56	28	68+/-3	62+/-2	1.1+/-0.1	28+/-1
DISEQUIL.RATIO			0.83+/-0.07	2.25+/-2.57	1.19+/-0.11	1.1+/-1.3				
6096a	1378	38.08-38.18	1668	2452	1335	269	2951+/-37	1463+/-21	2.0+/-0.0	269+/-11
DISEQUIL.RATIO			1.84+/-0.08	1.25+/-0.20	2.31+/-0.08	9.1+/-1.5				
6096b	1378	38.18-38.30	3250	3578	2640	30	3756+/-51	2280+/-33	1.6+/-0.0	30+/-11
DISEQUIL.RATIO			1.21+/-0.05	1.09+/-0.17	1.49+/-0.05	119.3+/-46.6				
6096c	1378	38.30-38.50	3650	2288	3070	25	2970+/-61	3167+/-55	0.9+/-0.0	25+/-18
DISEQUIL.RATIO			0.85+/-0.46	1.35+/-0.40	1.04+/-0.06	91.5+/-73.2				
6096d	1378	38.50-38.70	1125	1164	842	10	1236+/-19	933+/-14	1.3+/-0.0	10+/-5
DISEQUIL.RATIO			1.15+/-0.05	1.11+/-0.21	1.55+/-0.34	116.4+/-65.0				
6117	1400	40.35-40.41	5060	2963	4415	129	2744+/-65	4514+/-71	0.6+/-0.0	129+/-24
DISEQUIL.RATIO			0.56+/-0.04	0.95+/-0.29	0.65+/-0.04	23.0+/-8.1				
6184a	1394	45.70-45.90	74	100	54	38	89+/-4	65+/-2	1.4+/-0.1	38+/-1
DISEQUIL.RATIO			1.11+/-0.11	0.81+/-0.38	1.51+/-0.15	2.6+/-0.6				
6184b	1394	45.90-46.03	110	10	105	47	96+/-4	106+/-4	0.9+/-0.1	47+/-2
DISEQUIL.RATIO			0.97+/-0.11	11.07+/-55.11	0.98+/-0.10	0.2+/-1.0				
6184d	1394	46.20-46.35	54	55	36	40	53+/-3	39+/-2	1.4+/-0.1	40+/-1
DISEQUIL.RATIO			0.88+/-0.11	0.87+/-0.57	1.32+/-0.18	1.4+/-0.9				
6221a	1526	42.00-42.20	208	195	174	41	222+/-5	181+/-4	1.2+/-0.0	41+/-2
DISEQUIL.RATIO			1.09+/-0.08	1.16+/-0.37	1.35+/-0.09	4.8+/-1.5				
6221b	1526	42.20-42.40	70	70	52	25	72+/-3	61+/-2	1.2+/-0.1	24+/-1
DISEQUIL.RATIO			0.97+/-0.09	0.97+/-0.51	1.29+/-0.12	2.8+/-0.8				
6221c	1526	42.40-42.60	45	86	41	20	36+/-3	37+/-2	1.0+/-0.1	20+/-1
DISEQUIL.RATIO			0.63+/-0.10	0.34+/-0.13	0.70+/-0.11	4.3+/-0.6				
6221d	1526	42.60-42.80	68	84	49	17	66+/-3	59+/·2	1.1+/-0.1	17+/-1
DISEQUIL.RATIO			0.88+/-0.09	0.72+/-0.33	1.24+/-0.13	4.9+/-2.3				
6221e	1526	42.80-43.00	64	23	51	21	32+/-3	57+/-2	0.6+/-0.1	21+1-1
DISEQUIL.RATIO			0.44+/-0.07	1.21+/-1.68	0.55+/-0.09	1.1+/-2.1				

(1) DISEQUILIBRIUM RATIO =(AVERAGE 238U GRADE/DAUGHTER). ERROR IS +/-3 STD. DEV. (2) 230Th / 232Th RATIO

Table 9.2: Interpretation of U-Th disequilibrium of Ambassador samples

Sample	Hole	Depth Interval	Disequilibrium Pattern	Comments
6031	1360	37.76-38.86	Ra<U= ?Th	U-rich, migration of U within the last 300,000 years, and/or daughter deficiency
6059	1305	33.00-35.00	Ra<U>=Th	U-rich, migration of U within the last 300,000 years, and/or daughter deficiency
6062	1368	45.20-45.40	Ra<U ?Th	U-rich, migration of U within the last 300,000 years, and/or daughter deficiency, large 230Th counting error
6096a	1378	38.08-38.18	Ra<U>=Th	U-rich, migration of U within the last 300,000 years, and/or daughter deficiency
6096b	1378	38.18-38.30	Ra<U=Th	U-rich, migration of U within the last 300,000 years, and/or daughter deficiency
6096c	1378	38.30-38.50	Ra=U=Th	238U, 230Th and 226Ra near equilibrium
6096d	1378	38.50-38.70	Ra<U=Th	U-rich, migration of U within the last 300,000 years, and/or daughter deficiency
6117	1400	40.35-40.41	Ra>U=Th	226Ra-rich, indicates recent deposition of U and enriched daughters other than 230Th and/or leaching by acid saline groundwaters
6184a	1394	45.70-45.90	Ra<U<=Th	U-rich, migration of U within the last 300,000 years, and/or daughter deficiency
6184b	1394	45.90-46.03	Ra=U ?Th	238U, 226Ra near equilibrium very large 230Th counting error
6184d	1394	46.20-46.35	Ra<U=Th	U-rich, migration of U within the last 300,000 years, and/or daughter deficiency
6221a	1526	42.00-42.20	Ra<U=Th	U-rich, migration of U within the last 300,000 years, and/or daughter deficiency
6221b	1526	42.20-42.40	Ra<U=Th	U-rich, migration of U within the last 300,000 years, and/or daughter deficiency
6221c	1526	42.40-42.60	Ra>U<Th	226Ra-rich, indicates recent deposition of U and enriched daughters other than 230Th and/or leaching by acid saline groundwaters
6221d	1526	42.60-42.80	Ra<U=<Th	U-rich, migration of U within the last 300,000 years, and/or daughter deficiency
6221e	1526	42.80-43.00	Ra>U= ?Th	226Ra-rich, indicates recent deposition of U and enriched daughters other than 230Th and/or leaching by acid saline groundwaters

Figure 9.1 Down hole disequilibrium profile of hole 6096

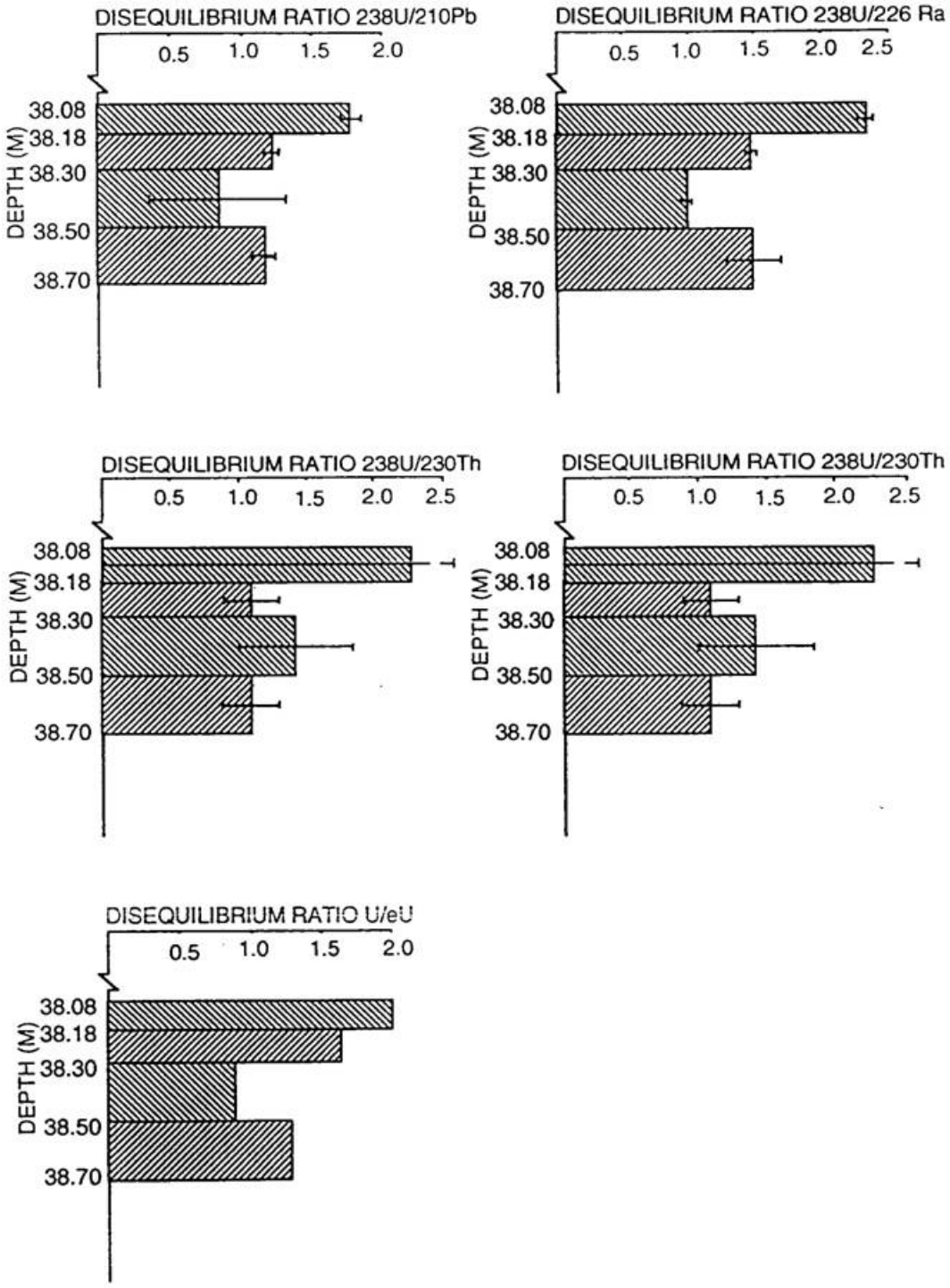

Figure 9.2 Down hole disequilibrium profile of hole 6184

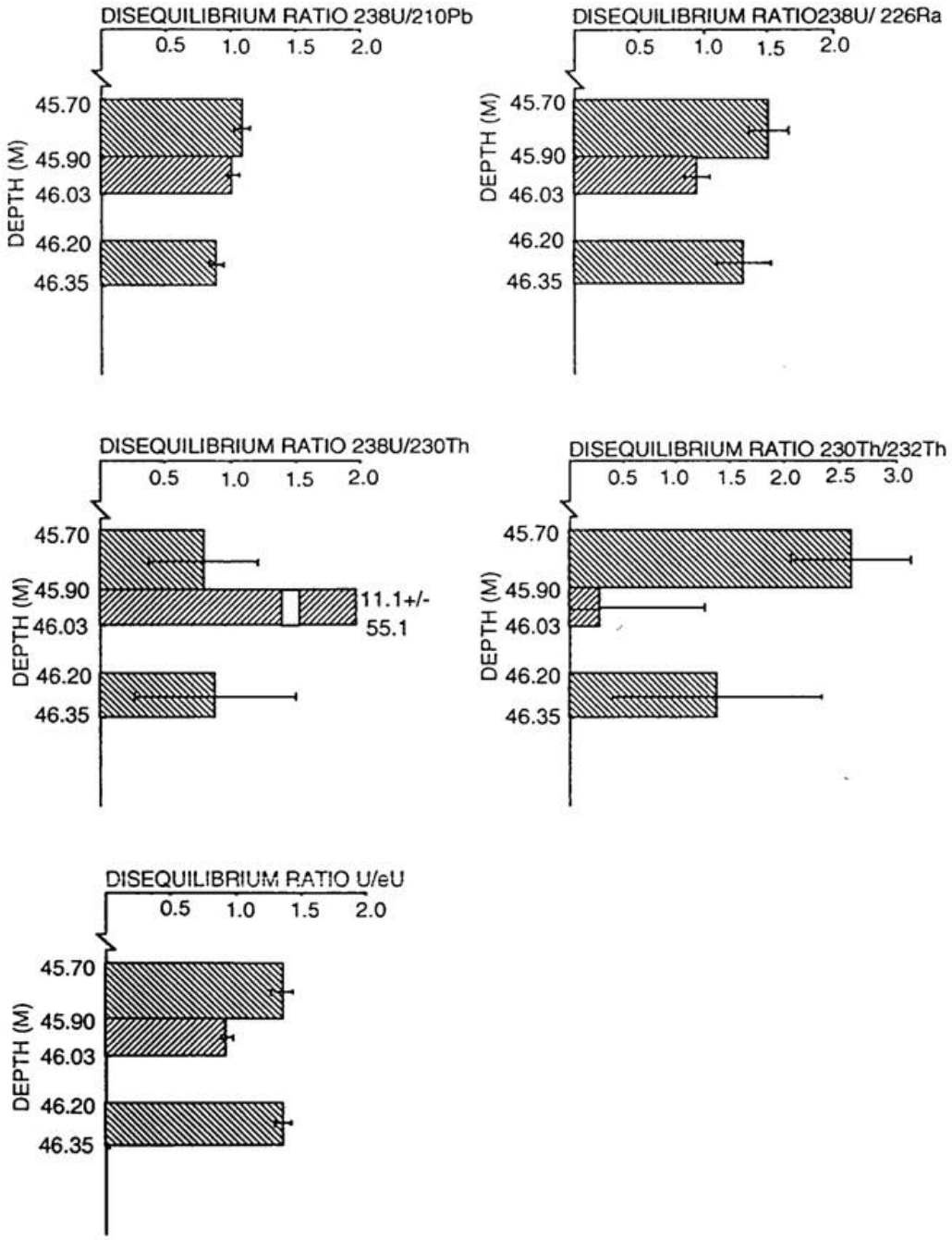

Figure 9.3 Down hole disequilibrium profile of hole 6221

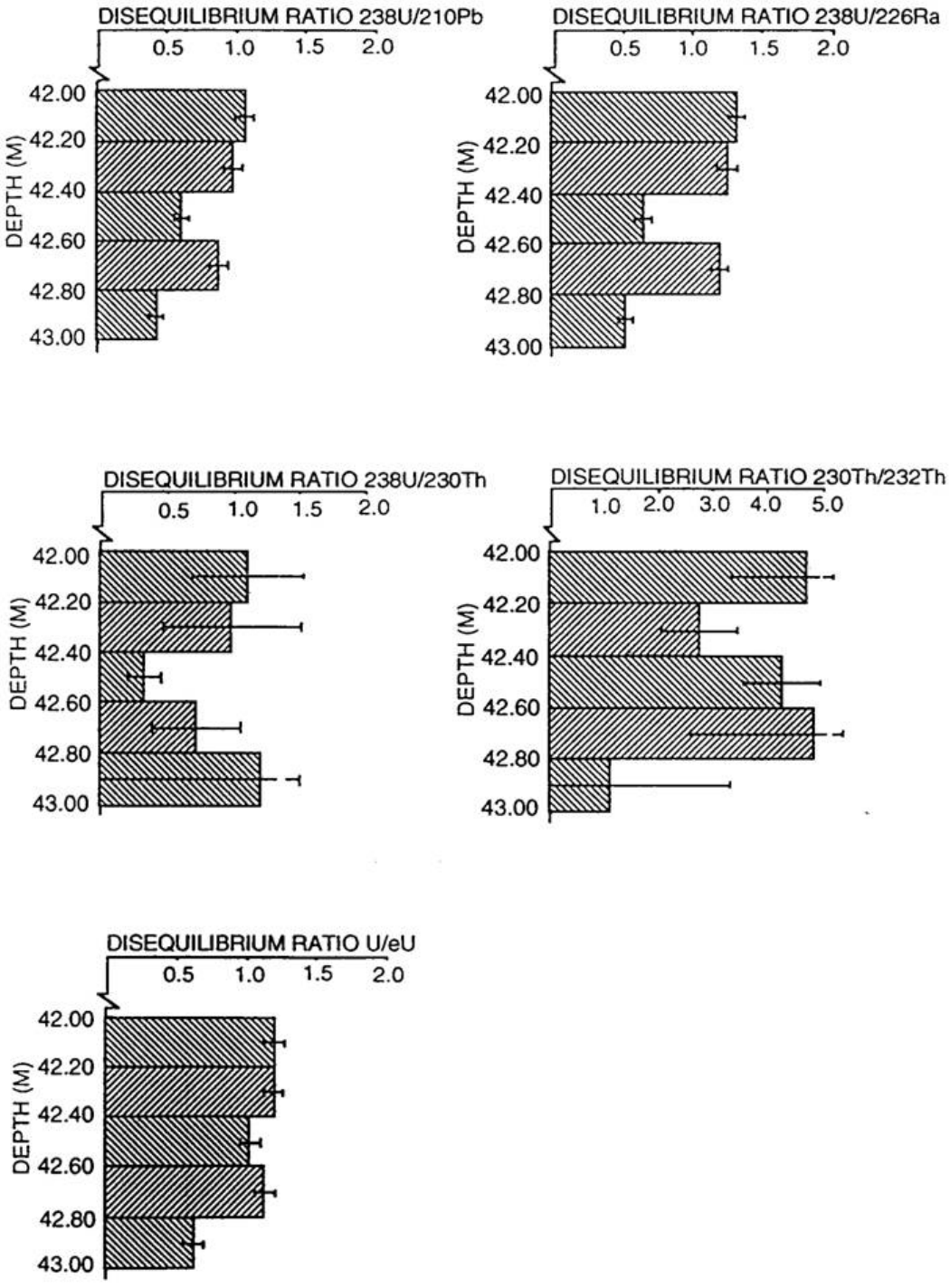

The $^{230}Th/^{232}Th$ disequilibrium ratio has also been calculated (Table 9.1), because this ratio has been used to indicate potential heavy mineral (specifically, detrital monazite) contributions to the Th present in sedimentary, organic hosted U-deposits *e.g.,* Ralston *et al.,* (1986). High $^{230}Th/^{232}Th$ ratios (>15) indicate that the environment in which U accumulated was essentially detrital monazite-free; ^{232}Th is the primordial Th isotope whereas ^{230}Th which is contributed to by the decay of ^{238}U. Samples that have low $^{230}Th/^{232}Th$ ratios suggest that monazite may have contributed significantly to the mineralization, at least for Th and possibly also the LREE. The use of $^{230}Th/^{232}Th$ disequilibrium ratios assumes, however, that all the Th is contained in monazite and little or no U has been derived from monazite.

Only two of the 16 samples from the Ambassador deposit (6096c, 6184b) are in equilibrium with respect to U, Th and Ra (Table 9.2). Two other samples (6221c, 6221e) are relatively enriched in ^{226}Ra, indicating recent deposition of U and enriched daughters other than those from ^{230}Th and/or leaching by saline groundwaters. The remainder of the samples display a wide range of disequilibrium patterns with the most predominant being U excess and/or daughter deficiency; this pattern developing in the last 300,000 years. These patterns of disequilibrium are consistent with U and other radionuclides being moved in response to geologically recent changes in the position of the redox front which will tend to separate elements with different chemical characteristics as described in Section 9.1. The three down hole disequilibrium profiles (Holes 6096, 6184 and 6221) will be discussed first, followed by a discussion of single samples from four other holes (6031, 6059, 6062, 6117).

PROFILE OF HOLE 6096

The down hole ^{238}U disequilibrium profile for the radionuclides ^{210}Pb, ^{226}Ra and ^{230}Th in hole 6096 show a remarkably uniform distribution, especially in the bottom three samples (Table 9.1, Figure 9.1). The disequilibrium ratio is generally in the range 1.0-1.5, indicating mild disequilibrium due to the depletion of daughter products relative to ^{238}U. The depletion of the daughter products is also confirmed by the U ave./U-γ ratio (0.9-2.0), which indicates that in general, there is relative depletion of the daughter products relative to ^{238}U. The only noteworthy exception is the 10 cm interval at the top of the hole, which is significantly depleted in ^{226}Ra, ^{210}Pb, and ^{230}Th, with disequilibrium ratios of 1.84, 2.31 and 2.25 respectively. The ^{230}Th concentration is doubtful due to the large associated counting error ($\pm$2.6). The equivalent U (eU) concentration of radionuclides is at its maximum in the middle two samples (38.18-38.30 and 38.30-38.50 m), and is lowest in the deepest sample (38.50-38.70 m).

The apparent depletion of daughter products in the uppermost sample (38.08-38.18 m) may be indicative of the presence of remnant redox fronts that have formed due to the preferential leaching of daughter products from this horizon. This is supported by the reduced radionuclide (eU) concentrations in this sample interval, which are generally depleted to at least or greater than that of ^{238}U.

The $^{230}Th/^{232}Th$ disequilibrium profile in hole 6096 varies by an order of magnitude, with the uppermost sample (38.08-38.18m) being significantly depleted in ^{230}Th. It is possible that monazite-derived Th may have contributed significantly to the uppermost samples, either from the dissolution of *in situ* monazite, or the preferential remobilization from other localities, with little or no monazite-Th contribution in the deeper samples. The possible contribution of monazite is also suggested by the elevated eU equivalent concentrations of ^{232}Th relative to other samples, particularly in the uppermost sample (269 ppm eU ^{232}Th).

PROFILE OF HOLE 6184

The down hole ^{238}U disequilibrium profile for the radionuclides ^{210}Pb, ^{226}Ra and ^{230}Th in hole 6096 show a variable distribution (Table 9.1, Figure 9.2). The disequilibrium ratio for ^{210}Pb is in the range 0.9-1.1 indicating mild disequilibrium due to marginal excess or depletion of daughter products relative to ^{238}U, with the deletion increasing towards the top of the hole. The ^{226}Ra disequilibrium ratio is depleted in two samples (1.51, 1.32) relative to ^{238}U, with the remaining sample near equilibrium (0.98). ^{230}Th displays a wide range of disequilibrium (0.8-11.1), but the large errors do not allow any further interpretation.

The highest equivalent U concentration of the radionuclides is generally in the interval from 45.90-46.03 m, although the highest eU concentration of ^{230}Th is in the upper interval from 45.70-45.90 m. In two of the three samples, a relative depletion of daughter products relative to ^{238}U is suggested by the U ave./U-γ ratio. The U ave. /U-γ ratio for the other sample indicates marginal daughter product excess.

The $^{230}Th/^{232}Th$ ratio is low (0.2-2.6) and suggests that there is probably a substantial monazite contribution to the Th present in the samples from this hole. The range of $^{230}Th/^{232}Th$ ratios in the hole is in excess of an order of magnitude, which is primarily due to the variable ^{230}Th concentration (10-100 ppm), as the ^{232}Th concentration is nearly constant (38-47).

PROFILE OF HOLE 6221

As with hole 6184, the down hole ^{238}U disequilibrium profile for the radionuclides ^{210}Pb, ^{226}Ra and ^{230}Th in hole 6096 have a variable distribution (Table 9.1, Figure 9.3). The disequilibrium ratio for ^{210}Pb is in the range 0.4-1.1, indicating mild to significant disequilibrium due to marginal excess of, or significant depletion of, daughter products relative to ^{238}U. The depletion of ^{210}Pb generally increases towards the top of the hole. The one exception is the interval from 42.60-42.80 m, which although having a relatively higher $^{238}U/^{210}Pb$ ratio, still has excessive ^{210}Pb. The ^{226}Ra disequilibrium ratio is similar to that of the ^{210}Pb although ^{226}Ra is, in general, more depleted relative to ^{238}U, with a range of disequilibrium ratios of 0.6-1.4. The ^{230}Th disequilibrium ratio is extremely variable.

The highest equivalent U (eU) concentration of the radionuclides occur in the upper sample intervals from 42.00-42.20 m. The U ave./U-γ ratio for hole 6221 indicates near equilibrium, or marginal daughter product depletion relative to ^{238}U for the samples from 42.00-42.80 m. The deepest sample from 42.80-43.00 m, however, due to an excess of daughter products, particularly ^{210}Pb and ^{226}Ra.

The $^{230}Th/^{232}Th$ ratio ranges from near equilibrium to a deficiency in ^{232}Th. The deepest sample from 42.80-43.00 m is near equilibrium due to the very low concentration of ^{230}Th relative to samples from the rest of the hole.

SINGLE ASSAYS: HOLES 6031, 6059, 6062 AND 6117

Hole 6031 is particularly depleted in ^{210}Pb, ^{230}Th and ^{226}Ra relative to ^{238}U (Table 9.1). This is also reflected in the U ave./U-γ ratio, which is the highest (3.2) for any of the samples in this study. Equivalent U concentrations of all elements in this sample are low compared to most other samples except those from hole 6221. The low ^{230}Th/^{232}Th ratio also suggests that monazite is a major contributor to the Th and perhaps LREE concentrations.

Hole 6059 has a near equilibrium concentration of ^{210}Pb, but is depleted in ^{230}Th and ^{226}Ra relative to ^{238}U, which contributes to a U ave./U-γ ratio of 1.5, indicating an overall depletion of daughter products (Table 9.1). The high ^{230}Th/^{232}Th ratio (41) suggests that monazite was not a major contributor of Th to this sample.

Hole 6062 is in near equilibrium (Table 9.1), with only slightly depleted ^{210}Pb, a marginal excess of ^{226}Ra, and hence has a U ave./U-γ ratio near unity (1.1). The low ^{230}Th/^{232}Th ratio (1.1) suggests that monazite-derived Th was a major contributor of Th to this sample.

Hole 6117 is in disequilibrium, with ^{210}Pb and ^{226}Ra in large excess relative to ^{238}U (Table 9.1). This disequilibrium pattern is reflected in the U ave./U-γ ratio of 0.6. The moderately high ^{230}Th/^{232}Th ratio (23) suggests that monazite-derived Th was not a major contributor to this sample.

9.4 Conclusion

A study of the natural U-Th series disequilibrium in the Ambassador deposit indicate that there is a wide range of disequilibrium patterns present, with daughter products both in excess and deficient compared to U. The most predominant disequilibrium pattern, however, is U-excess and/or daughter deficiency, with the pattern developing within the last 300,000 years. This disequilibrium pattern is consistent with geologically recent changes in the position of the redox front, probably induced by changes in the groundwater level. The variable ^{230}Th/^{232}Th ratio in a number of the locations suggests that the dissolution of detrital minerals such as monazite cannot explain the observed distribution of Th (and LREE) throughout the entire Ambassador deposit even though the dissolution of monazite may be a significant contributor of Th to some samples. Furthermore, a large amount of monazite (not observed in mineralogical studies) would be required to account for other elements enriched in the deposit. Three down hole profiles of radionuclide distribution indicate that there may be both daughter excess and depletion in the same hole, ranging from 0.6-3.2, with the variable down hole disequilibrium pattern due to the overprinting of successive redox fronts.

10.0 GENESIS OF THE AMBASSADOR DEPOSIT

10.1 Introduction

In proposing a genetic model for the formation of the Ambassador deposit mineralization, it is stressed that this is a preliminary (tentative) model only, with further research required to resolve a number of key points (Section 10.2). However, a number of broad conclusions may be reached. The various aspects critical to the formation of the Ambassador deposit include the environment of deposition, the source(s) of U and trace metals and the process of diagenesis and enrichment. These are discussed in the following sections.

10.1.1 Environment of deposition

The environment of deposition of the organic matter was likely to have been a lowland area, probably a swamp, floodplain or marsh, situated on a flat-lying stable platform. Petrographic analysis of the macerals (Section 8.2) has indicated that the dominant flora was low heathland or sub-aquatic plants, devoid of trees or large plants. The presence of abundant algae (species undetermined) suggests the presence of a huge biomass when alive and indicate that the waters were probably well oxygenated, clear and nutrient rich. The accumulation of algal material also suggests quiescent conditions that allowed the deposition and preservation of humic material and plant detritus. The presence of abundant organic matter in the palaeochannel sediments suggests that this has been introduced in colloidal or dissolved form and was deposited by coagulation (Section 2.3.3), a process that also requires quiescent conditions. The coagulation of colloidal or dissolved humic matter is known to occur in modern estuarine systems at the interface of fresh and saline waters due to the complexation of humic matter by divalent cations, particularly Ca, present in the latter. The proximity of the Ambassador deposit to possible mid to late-Eocene shorelines (sea levels in the Eocene were approximately 300m higher than the present day (Cockbain and Hocking, 1990); suggests that the interaction of fluvially transported organic matter with seawater or saline groundwaters is possible. Studies of the S concentration in peats from both marine and freshwater environments indicate that the elevated concentrations of S at Mulga Rock (commonly up to 10%) are consistent with a marine environment (Casagrande *et al*., 1977), since terrestrial organic matter rarely exceeds 1% S. However, S may have also been introduced later in groundwaters or marine-derived aerosols, with the locally high concentrations being due to remobilization. An alternative depositional environment of deposition may have involved a spatially extensive terrestrial marsh setting, situated on a stable basement with a low gradient, far removed from marine influences. This is exemplified by the Henkries deposit (Section 2.1.6), which formed in a barred, shallow aquatic environment . Other possible depositional environments of deposition for the Ambassador deposit include a fluvio-deltaic environment as exemplified by the Eocene Coutras deposit (Section 2.1.2) and a freshwater seasonal floodplain environment exemplified by the present day Magela Creek floodplain system (Section 2.1.5), which contains extensive accumulations of organic matter formed from the flocculation of dissolved organic matter and the *in situ* decay of sub-aquatic plant materials.

10.1.2 Sources of U and trace elements

There are two principal sources for the elemental suite that forms the mineralization of the organic matter at Mulga Rock.

(a) *Yilgarn Block and Albany-Fraser Province*. These Archaean and Proterozoic basement rocks represent a diffuse, non-point source via the extensive palaeochannel system that has existed since at least the Permian. Recent research (Douglas, unpubl. data) has demonstrated that the organic matter in major river systems may be significantly enriched in trace metals (*e.g.*, up to 1,000 ppm Cu and Zn). This organic matter accounts for only a small proportion of the total load but, if it is preferentially removed from a fluvial system at one location (*e.g.*, estuarine mixing), an accumulation of highly mineralized organic matter may develop. (This accumulation of organic matter may not, however, account for the mass balance of U required, see Section 10.1.3). If the enormous area of the Yilgarn Block with its diversity of lithologies, coupled with the extensive palaeochannel system and the deep weathering profile is considered, it is reasonable to assume that the multi-element suite observed at the Ambassador deposit could be produced.

(b) *Lamproites or carbonatites*. The Pb-Pb isotopic data suggest that a very distinctive lithology, Archaean or Proterozoic in age, with a high Th/U ratio is the likely source for the mineralization. In particular the isotopic composition corresponds to that of West Australian lamproites and carbonatites. Few carbonatites are known within the Yilgarn Block, but the Mt. Weld carbonatite occurs adjacent to a palaeochannel system (200 km NW) and several smaller carbonatites are known or are inferred to occur in the Mulga Rock area. Additional isotopic analysis using Rb-Sr and Sm-Nd isotopic systems also supports the theory that lamproites or carbonatites could be the source of the mineralization. However, the Sr and Nd isotopic data are also compatible with a number of lithologies in the Yilgarn block. Lamproites and carbonatites are also geochemically compatible source rocks because they are commonly enriched in a wide range of trace elements, in particular U, Th and REE. These rocks could thus represent a point source of mineralization located either within the basement proximal to the palaeochannel or directly linked via one of the branches of the Minigwal palaeochannel system.

The timing of mineralization of the organic matter by U and trace elements is difficult to quantify, due to the homogenization of the Rb-Sr, Sm-Nd and Pb-Pb isotopic systems. Information on the process of mineralization of other organic matter-rich deposits, especially those that do not have a readily identifiable point source, indicate that mineralization is probably a continuous cycle of accumulation, remobilization and precipitation. Additionally, the thick weathering profile and possible erosional events tend to obscure the relationship of the palaeochannel with confining lithologies, and movements of the redox front and groundwater, coupled with the degradation of organic matter and the growth of authigenic minerals, combine to obliterate much of the primary lithological and geochemical structure.

10.1.3 Diagenesis and enrichment

The diagenetic changes within the Ambassador deposit have resulted in a unique suite of minerals and organic-trace element associations. The mineralogy of the main mineralized area indicates that there has been appreciable movement of elements such as Si, Ti, U, Th and S, not only in response to the different Eh-pH conditions imposed by the vertical movement of the redox front, but also lateral movement as seen by the systematic change in the ratio of light rare earth element (LREE) to heavy rare earth element (HREE) along the main mineralized zone. Furthermore, the presence of elevated levels of Ca in the main mineralized zone may indicate the presence of a phase of mobile humic matter which has been influenced by groundwater movement and composition. This feature has been recognized in other organic deposits in which mineralization occurs at the interface between freshwater and brines, at which mobile organic matter in the former is coagulated and deposited (Sanford, 1990). The uneven distribution of the mineralization may be related to the different origins

of the groundwater as identified by ^{18}O and ^{2}H isotopic studies (Section 6.3.3) and their different compositions, particularly the Ca concentration (Section 2.3.3). Alternatively, it has been demonstrated that in deposits where organic matter is the agent of fixation, the spatial distribution of U may be due to factors such as the permeability of the palaeochannel (host) sediments (le Roux, 1991).

Enrichment of the mineralized zone within the Ambassador deposit probably occurred as a result of both syngenetic and epigenetic processes. Estimates of the amount of syngenetic U derived from the accumulation of organic matter in the main mineralized zone of the Ambassador deposit have been made assuming a non-point source. Data from the Murray-Darling River system which covers in excess of 14% of the Australian continent and thus provides a good average crustal estimate of U concentration in fluvial systems, indicates that organic matter contains approximately 150 ppb U. If the channel dimensions in the main Ambassador mineralized zone are assumed to be 4km in length, 1 km wide and 50 m deep and the density of the lignite is 1.0g/cm^3, a mass of approximately 30 tonnes U could accumulate by syngenetic processes. This mass is at least two orders of magnitude less than that contained within the Ambassador deposit. This calculation assumes, however, that the channel is a closed system (no lateral transport of U) following deposition of the peat and there is no enriched point source of U. However, if subsequent migration of water through the channels could supply the additional U and, with each additional bed (channel) volume of groundwater contributing similar tonnages, only a relatively short epigenetic enrichment period would be required. It is also interesting to note that if an average grade of 1,400 ppm U in the organic matter (Fulwood and Barwick, 1990) is assumed, a concentration factor of almost 10,000 is required for the U contained in the fluvial organic matter, similar to that estimated by Szalay (1958) as the maximum potential concentration factor for U by humic materials. It has also been shown in a number of studies (Read *et al*., 1992) that the limiting factor in the accumulation of U in organic-hosted deposits is the supply of U rather than the amount of organic material, with experiments having shown that up to 16% U is required to saturate peat. Assuming a closed system for the Ambassador deposit, concentration of U via redox processes also cannot account for the enrichment observed at the redox interface. Even if 50 m of the lignite is compressed to only 20 cm (*i.e*., a concentration factor of 250) the concentration of U would still only be approximately 40 ppm at the redox front. Thus, a point source and/or open system behaviour (epigenetic mineralization) are required to explain the concentrations of U found in the Ambassador deposit. However, for trace elements, and particularly, some of the transition metals, the average concentration (*e.g.* Cu, Zn, 1000 ppm) in fluvial organic material is sufficiently high to account for the concentrations observed in the redox front with little or no reconcentration (enrichment) by diagenetic processes. Variable $^{230}Th/^{232}Th$ ratios in a number of locations in the Ambassador deposit suggests that the dissolution of detrital minerals such as monazite cannot explain the observed distribution of Th and REE. Furthermore, unreasonably large amounts of monazite (that have not been observed in mineralogical studies) would be required to account for other elements, especially U, enriched in the deposit.

Diagenetic alteration of the organic matter in the Ambassador deposit is probably only minor as there are still abundant identifiable plant macerals within the samples. Nevertheless, the presence of abundant humic material in the groundmass may either represent primary accumulation of dissolved organic matter or may be indicative of a degree of humification (degradation) of the organic matter.

Evidence of diagenesis has been identified by U and Pb isotopic studies and includes the development of U-daughter disequilibria in the organic matter, and the homogenization of Pb isotopes over a large area of the

mineralization by the redox front. The predominant U disequilibria pattern is that of U excess and/or daughter product deficiency, this pattern developing within the last 300,000 years. Additionally, the presence of U-decay series daughter products in the oxidized sediments overlying the present redox front, which probably occur as radionuclides adsorbed to the surfaces of clays, co-precipitated with Fe-oxides or incorporated into secondary minerals, indicates the level of former redox horizons or possibly the upward diffusion of elements by capillarity. The remnant redox horizons may also be an indication of oxidative weathering that could have consumed the upper portions of the organic matter and released U for complexation by the organic matter. This weathering process has been noted in unconformity type U deposits, where lateritization releases U from overburden, it is pre-concentrated by adsorption to iron (hydroxy) oxides and is leached and transported to a reduced zone by acidic groundwater brines (Pagel, 1991). This process has also been observed in saprolites where U, Th and REE are concentrated at the interface between the weathered zone and a groundwater controlled redox front (Braun and Pagel, 1990). Thus, the cover sediments may also have contributed U and trace elements to the organic matter during lateritization.

10.2 Recommendations for future research

A number of areas have been identified as potential subjects for future research in the Mulga Rock area. It is envisaged that this additional research will further the understanding of the genesis and post-depositional behaviour of trace elements in organic deposits. Furthermore, identification of the source of the mineralization may prove to be an extremely useful exploration tool in the search for other organic hosted U-trace element deposits, whether they be in palaeochannels or other geological settings. There are four major areas for future research:-

10.2.1 Organic matter and element enrichment

i. Investigate variation in organic matter variation with depth. Further study the correlation of ^{13}C NMR peak positions with U, using laboratory investigations and NMR of samples away from the mineralized area.

ii. Characterize the colloids present in groundwaters at Mulga Rock with particular reference to the speciation of U and trace elements and U-Pb disequilibria. Use the information to compare the colloidal matter at Mulga Rock to that characterized in natural analogue studies elsewhere.

10.2.2 Origin of mineralization

i. Further characterize the geochemical (major, trace element and isotopic) and mineralogical characteristics of the mineralized sequence, within and peripheral to one or more of the principal deposits, and compare them with carbonaceous U-base metal mineralization elsewhere.

ii. Interpret the relationship between the redox front, the confines of the palaeochannel and the relationship of mineralization to the palaeochannel and surrounding lithologies on both an individual palaeochannel and regional scale from information supplied by PNC. This type of information could be potentially useful for defining zones of organic matter that may be potential exploration targets in other palaeochannel systems. CSIRO are currently developing a computer visualization programs suitable for the portrayal and detailed analysis of three-dimensional geological and geochemical data.

10.2.3 Element speciation

i. Use SEM/TEM to characterize the authigenic mineral suite in the Ambassador deposit. Use this information to gain an insight into the physiochemical processes operative at the redox front.

ii. Identify and document the occurrence of new minerals.

10.2.4 Regional studies

i. On the basis of existing isotopic and geochemical information obtained in recent research, interpret the nature and occurrence of the deposits in the contexts of the geological, weathering and climatic histories of the region, and to develop some preliminary chemical models for their formation.

ii. Attempt to establish the source(s) of the metals and their prospectivity, principally using isotopic tracing techniques and predict environments where further economic mineralization (of any of the elements) may occur.

10.2.5 Benefits

Benefits of the research into the areas of element enrichment, the origin of the mineralization, element speciation and regional studies will include:-

i. A detailed description of an unusual U-base metal deposit.

ii. A natural analogue study focusing on the mobility of U and daughter products in an organic-rich environment.

iii. A better understanding of the element mobility and deposition in the weathering environment and hence a greater ability to interpret exploration geochemical data.

iv. Assessments as to the potential for economic enrichments of U and other commodities.

v. Assessments as to the probable source(s) of the metals and hence the potential for concealed mineralization.

ACKNOWLEDGEMENTS

A number of present and former staff from CSIRO are thanked for their support in the preparation of the report. These include A.Z. Gedeon and M.J. Pascoe who undertook the initial data compilation of samples and performed SEM analyses, R. Bilz and J.F. Crabbe who were involved in sample preparation for geochemical and petrological analysis, and M.K.W. Hart and M. Cheeseman who performed XRF analyses. J.V. Turner is thanked for the groundwater isotopic analyses, and G.R. Carr and D.J. Whitford for the Sr, Nd and Pb isotopic analyses. G.D. Longman is thanked for his assistance in the laboratory. Finally, MERIWA are thanked for their partial financial support of the first part of this project.

REFERENCES

Ahmad, M. U. and Finlay, R. W., 1987. "Radioactivity in the Hocking River Basin". in "Radon, Radium and Other Radioactivity in Groundwater". Ed. Graves, B. *Lewis*, 153-170.

Aitken, G. G., Mc Night, D. M., Wershaw, R. L. and Mc Carthy, P., 1985. "Humic Substances in Soil, Sediment and Water". *Wiley*. 692 pp

Andrews, M.J., Bibby, J.M., Fuge, R. and Johnson, C.C., 1984. The distribution of iodine and chlorine in soils over lead-zinc mineralisation, east of Glogfawr, mid-Wales. *J. Geochem. Explor.*, **20**:19-32.

Avogadro, A. and De Marsily., 1984. "The role of colloids in nuclear waste disposal". *Mat. Res. Symp. Proc.*, **26**: 495-505.

Bates, J. J., Bradley, J. P., Teetsov, A., Bradley, C. R. and Buchholtz ten Brink, M., 1992. "Colloid Formation During Waste Form Reaction: Implications for Nuclear Waste Disposal". *Science*, **256**: 649-651.

Beckett, R. and Le, N. P., 1990. "The role of organic matter and ionic composition in determining the surface charge of suspended materials in natural waters". *Colloids and Surfaces,* **44**: 35-49.

Bennett, P. C. and Siegel, D. I., 1987. "Increased solubility of quartz in H2O due to complexing by organic compounds". *Nature*, **326**: 684-686.

Binks, P. J. and Hooper, G. J., 1984. "Uranium in Tertiary palaeochannels-West Coast Area, South Australia". *Proc. Australas. Inst. Min. Metall.*, **289**: 271-275.

Bouska, V., 1981. "Geochemistry of coal". Elsevier, 281pp.

Boyle, R. W., 1982. "Geochemical Prospecting for Thorium and Uranium Deposits". *Elsevier*, 498 pp.

Braun, J. J. and Pagel, M., 1990. "U. Th and REE in the Akongo lateritic profile (SW Cameroon)". In., Abstracts, Geochemistry of the earth's surface and of mineral formation. 2nd International Symposium. 357-359.

Breit, G. N. and Wanty, R. B., 1991. "Vanadium accumulation in carbonaceous rocks: A review of geochemical controls during deposition and diagenesis". *Chem. Geol.*, **91**: 83-97.

Brookins, D. G., 1988. "Eh-pH Diagrams for Geochemistry". *Springer-Verlag*, 176 pp.

Casagrande, D. J., Siefert, K, Berschinski, C. and Sutton, N., 1977. "Sulphur in peat-forming systems of the Okefenokee Swamp and Florida Everglades: origins of sulphur in coal". *Geochim. Cosmochim. Acta*, **41**: 161-167.

Choppin, G. R., 1988. "Humics and radionuclide formation". *Radiochim. Acta*, **44**/**45**: 23-28.

Cockbain, A. E. and Hocking, R. M., 1990. "Phanerozoic". In, Geology and Mineral Resources of Western Australia. Western Australian Geological Survey, Memoir 3: 750-755.

Cotton, F. A. and Wilkinson, G., 1980. "Advanced Inorganic Chemistry". *John Wiley and Sons*, 1396 pp.

Crowe, A.S. and Longstaffe, F.J., 1987. Extension of geochemical modelling techniques to brines: coupling of the Pitzer equations to PHREEQE, in: Proceedings of Solving Ground Water Problems with Models, NWWA Conference, Feb. 10-12, 1987, Denver, Colorado, pp 110-129.

Culbert, R. R. and Leighton. D. G., 1988. "Young Uranium". in Ed. Gabelman, J. W. *Ore Geology Reviews*, **3**: 313-330.

Dickson, B. L. and Herczeg, A. L., 1992. "Naturally-occurring radionuclides in acid-saline groundwaters around Lake Tyrrell, Victoria, Australia. In Eds. Lyons, W. B., Long, D. T., Herczeg, A. L. and Hines, M. E., "The Geochemistry of Acid Groundwater Systems". *Chem. Geol*., **96**: 95-114.

Dionex, 1985. Technical Note 16. (PO Box 3603 Sunnyvale, California, USA).

Disnar, J. R., 1981. "Etude experimental de la fixation de metaux par un materiau sedimentaire actuel d'origine algire-II. Fixation 'in vitro' de UO_2^{2+}, Cu^{2+}, Ni^{2+}, Pb^{2+}, Co^{2+}, Mn^{2+}, ainsi que de VO_3^-, Mo_4^{2-} et Ge_3^{2-}". Geochim. Cosmochim. Acta, 45: 363-379.

Doi, K, Hirono, S and Sakawaki, Y., 1975. "Uranium mineralization by groundwater in sedimentary rocks, Japan". *Econ. Geol*., **70**: 628-646.

Drever, J.I., 1982. "The Geochemistry of Natural Waters." (Prentice-Hall, Inc., Englewood Cliffs, N.J. U.S.A.). 388 p.

Eakin, P. and Gize, A. P., 1992. "Reflected-light microscopy of uraniferous bitumens". *Min. Mag*., **56**: 85-99.

Ellsworth, H. V., 1928. "Thucolite-A Remarkable Primary Carbon Mineral From the Vicinity of Parry Sound, Ontario". *Amer. Mineral*., **13**: 419-441.

Fee, J. A., Gaudette, H. E., Lyons, W. B. and Long, D. T., 1992. "Rare earth element distribution in Lake Tyrrell groundwaters, Victoria, Australia". In Eds. Lyons, W. B., Long, D. T., Herczeg, A. L. and Hines, M. E., "The Geochemistry of Acid Groundwater Systems". *Chem. Geol*., **96**: 67-94.

Ferguson, J. and Winer, P., 1980. "Pine Creek Geosyncline: Statistical treatment of whole rock data". In. Ferguson, J. and Goleby, A. B. (Eds). Uranium in the Pine Creek Geosyncline. IAEA, 760 pp.

Finkelman, R. B., 1982. "Modes of occurrence of trace elements and minerals in coal: an analytical approach". in Atomic and Nuclear Methods in Fossil Energy Research, Ed. Filby, R. H. *Plenum*. 141-149.

Finkelman, R. B., 1988. "The inorganic geochemistry of coal: a scanning electron microscopy view". *Scanning Microscopy*, **2(1)**: 97-105.

Fraser, K. J., Hawksesworth, C. J., Erlack, A. J., Mitchell, R. H. and Scott-Smith, B. H., 1985. "Sr, Nd and Pb isotope and minor element geochemistry of lamproites and kimberlites". *Earth Planet. Sci. Lett*., **76**: 57-70.

Fuge, R. and Johnson, C.C., 1984. Evidence for the chalcophile nature of iodine. *Chem. Geol.*, **43**:347-52.

Fuge, R. and Johnson, C.C., 1986. The geochemistry of iodine - a review. *Environ. geochem. Hlth.*, **8**:31-54.

Fuge, R., Andrews, M.J., Clevenger, T.E., Davies, B.E., Gale, N.L., Pavely, C.F. and Wixson, B.G., 1988. The distribution of chlorine and iodine in soil in the vicinity of lead mining and smelting operations, Bixby area, S.E. Missouri, U.S.A. *Appl. Geochem.*, **3**:517-21.

Fulwood, K. E. and Barwick, R. E., 1990. "Mulga Rock Uranium Deposits, Officer Basin". In, Hughes, F. E. (Ed). Geology of the Mineral Deposits of Australia and Papua New Guinea. pp 1621-1623. The Australian Institute of Mining and Metallurgy, Melbourne.

Gaffney, J. S., Marley, N. A. and Orlandini, K. A., 1992. "Evidence for Thorium Isotopic Disequilibria due to Organic Complexation in Natural Waters". *Environ. Sci. Technol*., **26**: 1248-1250.

Goldhaber, M. B., Hemingway, B. S., Monahageghi, A., Reynolds, R. L. and Northrop, H. R., 1987. "Origin of coffinite in sedimentary rocks by a sequential adsorption-reduction mechanism". *Bull. Mineral*., **110**: 131-144.

Gat, J.R. and Gonfiantini, R., 1981. "Stable Isotope Hydrology. Deuterium and Oxygen-18 in the Water Cycle." (Technical Reports Series No. 210, IAEA, Vienna 1981, ISBN 92-0-145281-0).

Giblin, A. M. and Dickson, B. L., 1992. "Source, distribution and economic significance of trace metals in groundwaters from Lake Tyrrell, Victoria, Australia". In Eds. Lyons, W. B., Long, D. T., Herczeg, A. L. and Hines, M. E., "The Geochemistry of Acid Groundwater Systems". *Chem. Geol*., **96**: 67-94.

Giesy, J. P., Geiger, R. A. and Kevern, N. R., 1986. "UO_2^{2+}-Humate Interactions in Soft, Acid, Humate-Rich waters". *J. Environ. Radioactivity*, **4**: 39-64.

Gray, D.J., 1990. Hydrogeochemistry of the Panglo Gold Deposit. (AMIRA P241: Weathering Processes). CSIRO Division of Exploration Geoscience Restricted Report 125R. 74 p.

Gray, D.J., 1991. Hydrogeochemistry in the Mount Gibson Gold District. (AMIRA P240: Laterite Geochemistry). CSIRO Division of Exploration Geoscience Restricted Report 120R. 80 p.

Griffin, T. J., 1990. "Eastern Goldfields Province". In, Geology and Mineral Resources of Western Australia. Western Australian Geological Survey, Memoir 3: 77-117.

Gulson, B. L. and Mizon, K. J., 1980. Lead isotope studies at Jabiluka. In "Uranium in the Pine Creek Geosyncline". (Eds. Ferguson and Goleby). IAEA, Austria. pp 439-455.

Hansley, P. L. and Spirakas, C. S., 1992. "Organic Matter Diagenesis as the Key to a Unifying Theory for the Genesis of Tabular Uranium-Vanadium Deposits in the Morrison Formation, Colorado Plateau". *Econ. Geol*. **87**: 352-365.

Hart, B. T., Douglas, G. B., Beckett, R., Van Put, A and Van Grieken, R. E., 1992. "Characterisation of colloidal and particulate matter transported by the Magela Creek system, northern Australia". Hydrol. Processes., (submitted).

Hart, M. K. W., 1989. "Analysis for total iron, chromium, vanadium and titanium in varying matrix geological samples by XRF, using pressed powder samples". Standards in x-ray analysis. Australian X-ray Analytical Association (W.A. Branch). Fifth State Conference. 117-129.

Ho, C. H. and Miller, N. H., 1985. "Effect of Humic Acid on Uranium Uptake by Hematite Particles". *J. Coll. Int. Sci.* **106**: 281-288.

Hooker, P. J., 1990. "The geology, hydrogeology and geochemistry of the Needle's Eye natural analogue site". *Tech. Report, WE/90/5, British Geological Survey*. 30 pp.

Idiz, E. F., Carlisle, D. and Kaplan, I. R., 1986. "Interaction between organic matter and trace metals in a uranium rich bog, Kern County, California, U. S. A. ". *Appl. Geochem*., **1**: 573-590.

Ikramuddin, M., Yemane, A, Nordstrom, P. L., Kinart, K. P., Martin, W. M., Digby, S. J. M., Elder, D. D., Nijak, W. F. and Afemari, A. A., 1983. "Thallium: A potential guide to mineral deposits". *J. Geochem. Expl*., **19**: 465-490.

Iler, R. K., 1979. "The chemistry of silica". *Wiley*, 866 pp.

Ilger, J. D., Ilger, W. A., Zingaro, R. A. and Mohan, M. S., 1988. "Modes of occurrence of uranium in Carbonaceous uranium deposits: characterization of uranium in a south Texas (U. S. A.) lignite. *Chem. Geol*., **63**: 197-216.

Islam, M. A., 1983. "Palynological report on samples from the western Eucla Basin". Report No. R12/83/1. ECL Australia Pty. Ltd.

Johnson, S. Y., Otton, J. K. and Macke, D. L., 1987. "Geology of the Holocene surficial uranium deposit of the north fork of Flodelle Creek, northeastern Washington". *Geol. Soc. Am. Bull.*, **98**: 77-85.

Korsch, M. J. and Gulson, B. L., 1986. "Nd and Pb isotopic studies of an Archaean layered mafic-ultramafic complex, Western Australia, and implications for mantle heterogeneity". *Geochim. Cosmochim. Acta*, **50**: 1-11.

Kwak, T. A. P. and Abeysinghe, P. B., 1987. "Rare earth and uranium minerals present as fluid inclusions, Mary Kathleen U-REE skarn, Queensland, Australia". *Min. Mag*. **51**: 665-670.

Just, J., 1988. "Report on mineralogical investigation of samples from drill holes CD-795, CD-1101 and CD-1406, prepared for PNC Exploration (Australia) Pty. Ltd". (unpublished).

Landais, P., 1986. "Analyse des matieres organiques associees aux minerlisations uraniferes: implications genetiques". *Geol. Geochem. Uranium Mem*., **10**: 1-257.

Landais, P., 1991. "Analysis of bitumens associated with uranium ores". in Eds. Pagel and Leroy, "Source, Transport and Deposition of Metals", 549-552.

Langmuir, D., 1978. "Uranium solution-mineral equilibria at low temperatures with applications to sedimentary ore deposits". *Geochim. Cosmochim. Acta*., **42**: 547-569.

le Roux, J. P., 1991. "Flume experiments on permeability and organic matter as related to the genesis of uranium deposits in the Beaufort Group". *S. Afr. J. Geol*., **94**, 212-219.

Leventhal, J. S., Daws, E. A. and Frye, J. S., 1986. "Organic geochemical analysis of sedimentary organic matter associated with uranium". *Appl. Geochem.*, **1**: 241-247.

Li, W. C., Victor, D. M. and Chakrabarti, C. L., 1980. "Effect of pH and Uranium Concentration on the Interaction of Uranium (VI) and Uranium (IV) with Organic Ligands in Aqueous Solutions". *Anal. Chem*., **52**: 520-523.

Lieser, K. H. and Hill, R., 1992. "Hydrolysis and Colloid Formation of Thorium in Water and Consequences for its Migration Behaviour-Comparison with Uranium". *Radiochim. Acta*, **56**: 37-45.

Macaskie, L. E., Empson, R. M., Cheetham, A. K., Grey, C. P. and Skarnulis, J., 1992. "Uranium Bioaccumulation by a *Citrobacter sp*. as a Result of Enzymically Mediated Growth of Polycystalline HUO_2PO_4". *Science*, **257**: 782-784.

Mc. Culloch, M. T., Jaques, A. L., Nelson, D. R. and J. R. Lewis., 1983. "Nd and Sr isotopes in kimberlites and lamproites from Western Australia: an enriched mantle origin". *Nature*, **302**: 400-403.

Mc Carthy, J. F. and Zachara, J. M., 1989. "Subsurface transport of contaminants". *Environ. Sci. Tech*., **23**: 496-502.

Mc. Intyre, N. S., Martin, R. B., Chauvin, W. J., Winder, C. G., Brown, J. R. and Mac. Phee, J. A., 1985. "Studies of elemental distributions within discrete coal macerals. Use of secondary ion mass spectrometry and X-ray photoelectron spectroscopy". *Fuel*, **64**: 1705-1712.

Mc Mahon, P. B. and Chapelle, F. H., 1991. "Microbial production of organic acids in aquitard sediments and its role in aquifer geochemistry". *Nature*, **349**: 233-235.

Macumber, P. G., 1992)Hydrological processes in the Tyrrell Basin, southeastern Australia". In Eds. Lyons, W. B., Long, D. T., Herczeg, A. L. and Hines, M. E., "The Geochemistry of Acid Groundwater Systems". *Chem. Geol*., **96**: 1-18.

Maiti, T. C., Smith, M. R. and Laul, J. C., 1989. "Colloid formation study of U, Th, Ra, Pb, Po, Sr, Rb and Cs in briny (high ionic strength) groundwaters: analog study for waste disposal". *Nucl. Technol*. **84**: 82-87.

Mann, A. W. and Deutscher, R, L., 1978. "Genesis principles for the formation of carnotite in calcrete drainages in Western Australia". *Econ. Geol*. **73**: 1724-1737.

Meunier, J. D., Landais, P. and Pagel, M., 1990. "Experimental evidence of uraninite formation from the diagenesis of uranium-rich organic matter". *Geochim. Cosmochim. Acta*, **54**: 809-817.

Meunier, J. D., 1991. "Diagenesis and mechanisms of uranium accumulation by detrital organic matter". in Eds. Pagel and Leroy, "Source, Transport and Deposition of Metals", 565-568.

Meunier, J. D., Trouiller, A., Bruhlet, J. and Pagel, M., 1991. "Uranium and organic matter in a palaeodeltaic environment: the Coutras deposit (Gironde, France)". *Econ. Geol*., **84**: 1541-1556.

Mitchell, R. H., 1989. "Aspects of the petrology of kimberlites and lamproites: some definitions and distinctions". In: Kimberlites 1. Kimberlites and related rocks. *Geol. Soc. Aust. Sp. Publ*. pp7-45.

Monagheghi, A., Updegraff, D. M. and Goldhaber, M. B., 1985. "The role of sulphate-reducing bacteria in the deposition of sedimentary uranium ores". *Geomicrobiol*., **4**: 153-173.

Moulin, V. and Ouzounian, G., 1992. "Role of colloids and humic substances in the transport of radioelements through the geosphere". *Appl. Geochem., Suppl. Issue No*. **1**: 179-186.

Murphy, J. and Riley, J.P., 1962. A modified single solution method for the determination of phosphate in natural waters. Analytica Chimica Acta, 27: 31-36.

Nakashima, S., Disnar, J. R., Perruchot, A. and Trichet, J., 1984. "Experimental study of mechanisms of fixation and reduction of uranium by sedimentary organic matter under diagenetic or hydrothermal conditions". *Geochim. Cosmochim. Acta*, **48**: 2321-2329.

Nash, K., Fried, S., Friedman, A. M. and Sullivan, J. C., 1981. "Redox Behaviour, Complexing, and Adsorption of Hexavalent Actinides by Humic Acid and Selected Clays". *Environ. Sci. Technol*., **15**: 834-837.

Nelson, D. R., Chivas, A. R., Chappell, B. W. and McCulloch, M. T., 1988. "Geochemical and isotopic systematics in carbonatites and implications for the evolution of ocean-island sources". *Geochim. Cosmochim. Acta*, 52: 1-17.

Nelson, D. R. and Mc. Culloch, M. T., 1989. "Enriched mantle components and mantle recycling of sediments". In. Kimberlites and Related Rocks. Volume 1. Geol. Soc. Aust. Sp. Publ. 14. Blackwell. 646 pp.

Nelson, D. R., 1992. "Isotopic characteristics of potassic rocks: evidence for the involvement of subducted sediments in magma genesis". *Lithos*, **28**: 403-420.

Nissenbaum, A. and Kaplan, I. R., 1972. "Chemical and isotopic evidence for the in situ origin of marine humic substances". *Limnol. Oceanog*., **17**: 570-582.

Noller, B. N. and Hart, B. T., 1992. "Uranium in sediments from the Magela Creek catchment, Northern Territory, Australia". Environ. Technol. Letts., (submitted).

Norrish, K. and Chappell, B. W., 1977. "X-ray fluorescence spectrometry". In J. Zussman (Ed). *Physical methods in determinative mineralogy*. Academic Press, London. 201-272.

Nutall, H. E. Jr., Rao, S., Jain, R., Long, R. and Triay, R. I., 1992. "Colloid remediation in groundwater by polyelectrolyte capture". *ACS Symp. Ser*. **491** *(Transp. Rem. Subsurf. Contam.)*: 71-82.

Nguyen-Trung, C., 1985. "Geochemie theorique et experimentale des 122xides d'uranium dans les solutions aqueses". Unpubl Ph D thesis, 462 pp.

Pagel, M., 1991. "Lateritization and paleogeomorphology: Their roles in the genesis of unconformity-type uranium deposits in Saskatchewan, Canada". in Eds. Pagel and Leroy, "Source, Transport and Deposition of Metals", 331-332.

Parkhurst, D.L., Thorstenson, D.C. and Plummer, L.N., 1980. PHREEQE, a computer program for geochemical calculations. U.S. Geol. Surv. Water Resources Investigations 80-96, 210p.

Parnell, J., 1988. "Mineralogy of Uraniferous Hydrocarbons in Carboniferous-hosted Mineral Deposits, Great Britain". *Uranium*, **4**: 197-218.

Pascoe, M. J., 1991. "SEM investigation of Mulga Rock lignites". Unpublished. CSIRO

Petrova, L. S. and Chistilin, P. Ye., 1987. "Electron-microscope data on the mechanism of epigenetic uranium mineralization". *Int. Geol. Rev*. **29(2)**: 185-192.

Peuraniemi, V and Aario, R., 1991. "Hydromorphic dispersion of uranium in a surficial environment in northern Finland". *J. Geochem. Explor*., **41**: 197-212.

Pointer, C. M., Ashworth, J. R. and Simpson, P. R., 1989. "Genesis of coffinite and the U-Ti association in Lower Old Red Sandstone sediments, Ousdale, Caithness, Scotland". *Mineral Deposita*, **24**: 117-123.

Ralston, I. T., Levinson, A. A. and Harmon, R. S., 1986. "Uranium series disequilibrium in young lacustrine sediments from an arid environment at Henkries, Republic of South Africa". *Appl. Geochem*., **1**: 535-548.

Raymond, Jr. R., Gladney, E. S., Bish, D. L., Cohen, A. D. and Maestas, L. M., 1990. "Variation of inorganic content of peat with depositional and ecological setting". *Geol. Soc. Am. Sp. Paper*, **248**: 1-12.

Read, D., Bennett, D., Hooker, P. J., Ivanovich, M, Longworth, G., Milodowski, A. E. and Noy, D. J., 1992. "The migration of uranium into peat rich soils at Broubster, Caithness, Scotland". J. Contam. Hydrol. (submitted).

Reynolds, R. L. and Goldhaber, M. E., 1978. "Origin of a South Texas roll-type uranium deposit: 1. Alteration of iron-titanium oxide minerals". *Econ. Geol*., **73**: 1677-1689.

Sahama, T. G., 1974. "Potassium-rich alkaline rocks". In: Sorensen, H., The alkaline rocks. *Wiley*, London, pp. 96-109.

Sanford, R. F., 1990. "Hydrogeology of an ancient arid closed basin: Implications for tabular sandstone-hosted uranium deposits". *Geology*., **18**: 1099-1102.

Shanbhag, P, M. and Choppin, G, R., 1981a. "Binding of calcium by humic acid". *J. inorg. nucl. Chem*., **43**: 921-922.

Shanbhag, P, M. and Choppin, G, R., 1981b. "Binding of uranyl by humic acid". *J. inorg. nucl. Chem*., **43**: 3369-3372.

Short, S. A., Lowson, R. T. and Ellis, J., 1988. "$^{234}U/^{238}U$ and $^{230}Th/^{234}U$ activity ratios in the colloidal phases of aquifers in lateritic weathered zones". *Geochim. Cosmochim. Acta*, **28**: 1605-1614.

Sikora, L. J. and Keeney, D. R., 1983. "Further aspects of soil chemistry under anaerobic conditions". In Gore, A. J. P. (Ed). Ecosystems of the world. pp 247-256.

Smith, C. B., 1983. "Pb, Sr and Nd isotopic evidence for sources of southern African Cretaceous kimberlites". *Nature*, **304**: 51-54.

Stach, E, Machowsky, M.-Th., Teichmüller, M., Taylor, G.H., Chandra, D. and Teichmüller, R., 1982. "Coal Petrology". (Gebrüder Borntraeger, Berlin.)

Stevenson, F. J., 1985. "Geochemistry of Soil Humic Substances". in Eds. Aitken, G, R., Mc. Knight, D. M. and Wershaw, R. L. "Humic Substances in Soil , Sediment and Water". *Wiley*, 692 pp.

Swaine, D. J., 1990. "Trace Elements in Coal". *Butterworths*, 278 pp.

Szalay, A.,(1964. "Cation exchange properties of humic acids and their importance in the geochemical enrichment of UO_2^{2+} and other cations". *Geochim. Cosmochim. Acta*, **52**: 2555-2563.

Theng, B. K. G., 1974. "The chemistry of clay-organic reactions". *Hilger*, 343 pp.

Thurman, E. R., 1985. "Organic Geochemistry of Natural Waters". *Dordrecht*. 497 pp

Tissot, B. P. and Welte, D. H., 1984. "Petroleum formation and occurrence". 2nd. ed. Springer-Verlag, 699 pp.

Toens, P. D., 1981. "Uranium provinces and their time-bound characteristics". *Trans. geol. Soc. S. Afr.*, **84**: 293-312.

Tsezos, M. and Volesky, B., 1982. "The mechanism of uranium biosorption by *Rhizopus arrhizus*". *Biotech. Bioengin*., **24**: 385-401.

Turner, J.V., Townley, L.R., Rosen, M.R. and Sklash, M.K., 1992. Coupling the spatial distribution of solute concentration and stable isotope enrichments to hydrological processes in hypersaline paleochannel aquifers. In "Water-Rock Interaction". (Eds. Kharaka and Maest). Balkema, Rotterdam. pp 217-221.

Van der Weijden, C. H. and Van Leeuwin, M., 1985. "The effect of pH on the adsorption of uranyl onto peat". *Uranium*, **2**: 59-66.

Van Krevelen, D.W., 1963. Geochemistry of coal. *In* "Organic Geochemistry" (Ed. E. Ingerson). (Pergamon Press). pp 183-247.

Vassiliou, A. H., 1986. "The form of occurrence of uranium in deposits associated with organic matter". *Econ. Geol.*, **75**: 605-617.

Ward, C. R., 1985. "Coal Geology and Coal Technology". *Blackwell*, 352 pp.

Weast, R.C., Astle, M.J. and Beyer, W.H., 1984. "CRC Handbook of Chemistry and Physics." F-154 Elements in Sea Water. (64th Edition; CRC Press Inc., Florida, USA).

Weis, D and Demaiffe, D., 1985. "A depleted mantle source for kimberlites from Zaire: Nd, Sr and Pb isotopic evidence". *Earth Planet. Sci. Lett*., **73**: 269-277.

Wellin, E., 1966. "The occurrence of asphaltite and thucloite in Precambrian rock of Sweden". *Geol. Forens. Stockholm Forhandl*., **87**: 509-526.

Wilson, M.A., 1987. "NMR Techniques and Applications in Geochemistry and Soil Chemistry." (Pergamon Press).

Xie Xuejing, Sun Huanzhen and Li Shanfang, 1981. Geochemical exploration in China. J. Geochem. Explor., 15:489-506.

Zielinski, R. A., Otton, J. J., Wanty, R. B. and Pierson, C. T., 1987. "The geochemistry of water near a surficial organic-rich uranium deposit, northeastern Washington State, U.S.A.". *Chem. Geol*., **62**: 263-289.

Zielinski, R. A., Otton, J. J., Wanty, R. B. and Pierson, C. T., 1988. "The Aqueous Geochemistry of Uranium in a Drainage Containing Uraniferous Organic-rich Sediments, Lake Tahoe area, Nevada, U. S. A. ". *Uranium*, **4**: 281-305.

Zielinski, R. A.and Meier, A. L., 1988. "The association of uranium with organic matter in peat: an experimental leaching study". *Appl. Geochem*., **3**: 631-643.



GEOCHEMISTRY, MINERALOGY AND HYDROGEOCHEMISTRY

OF THE AMBASSADOR MULTI-ELEMENT LIGNITE DEPOSIT, WESTERN AUSTRALIA

G. B. DOUGLAS, D. J. GRAY AND C. R. M. BUTT, MARCH, 1993

WITH ADDITIONAL INVESTIGATIONS ON THE CHARACTERIZATION OF ORGANIC MATTER

D. J. GRAY, APRIL, 1996

FINAL REPORT FOR PNC (EXPLORATION) PTY LTD

VOLUME 2 – APPENDICES

CRC LEME is an unincorporated joint venture between the Australian National University, University of Canberra, Australian Geological Survey Organisation and CSIRO Exploration and Mining

This report was reformatted by Energy and Minerals Australia Limited in 2013 from a scan of the original report

APPENDIX 1

MAJOR AND TRACE ELEMENT PLOTS

AMBASSADOR DEPOSIT

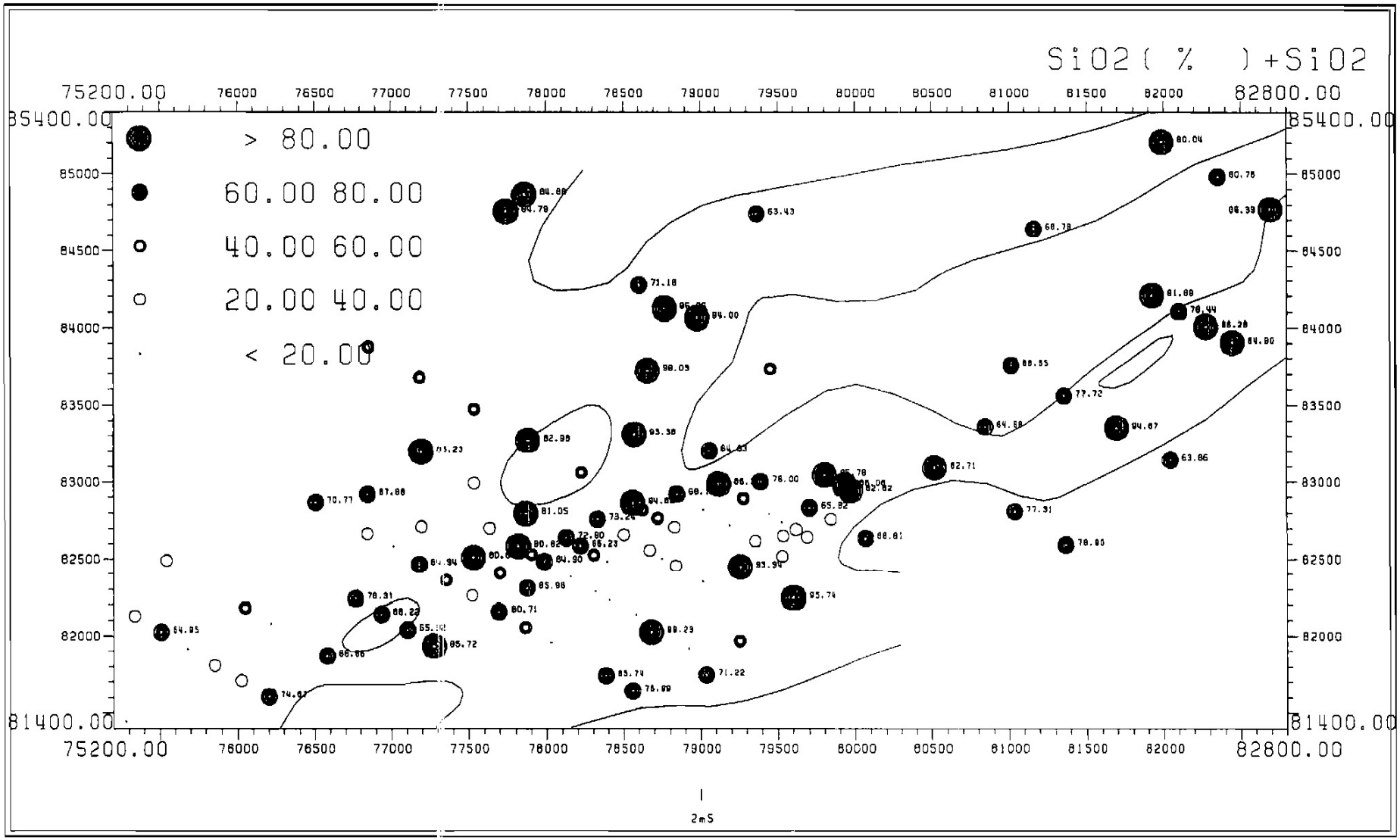
SiO2(%)+SiO2
> 80.00
60.00 80.00
40.00 60.00
20.00 40.00
< 20.00
75200.00
76000
76500
77000
77500
78000
78500
79000
79500
80000
80500
81000
81500
82000
82800.00
85400.00
85000
84500
84000
83500
83000
82500
82000
81400.00
2mS

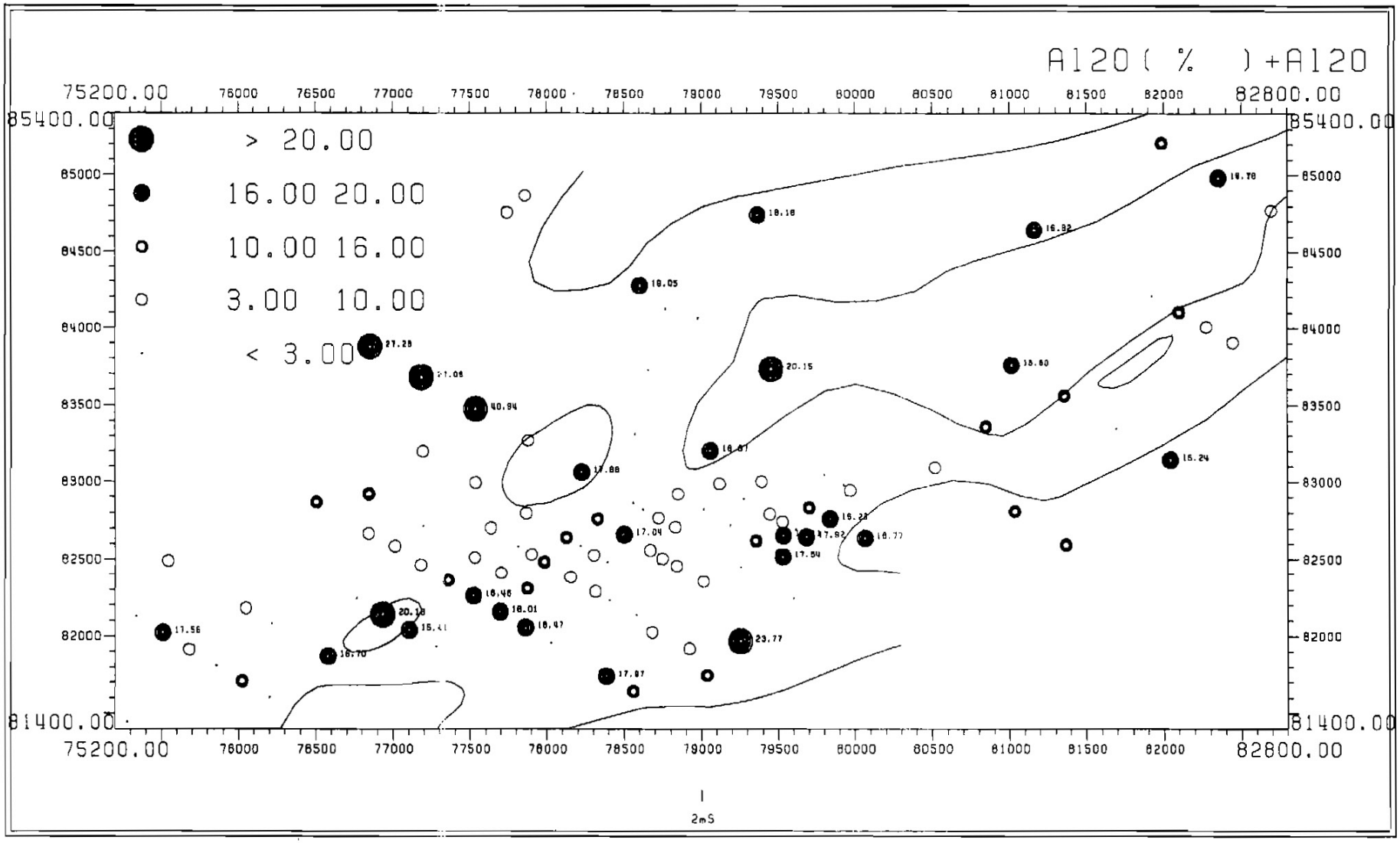
A120 (%) +A120
> 20.00
16.00 20.00
10.00 16.00
3.00 10.00
< 3.00
75200.00
76000
76500
77000
77500
78000
78500
79000
79500
80000
80500
81000
81500
82000
82800.00
85400.00
85000
84500
84000
83500
83000
82500
82000
81400.00
2mS

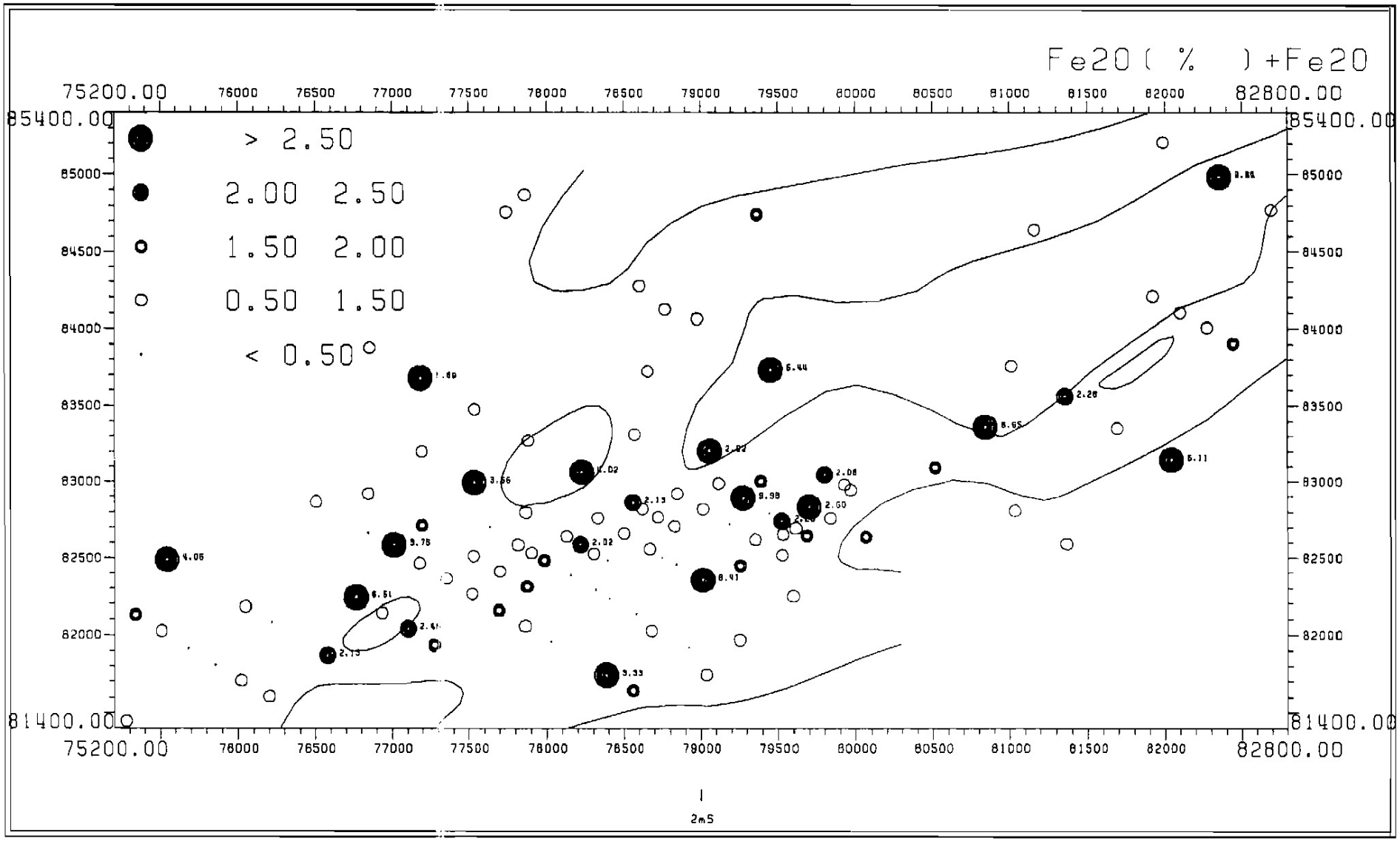
Fe2O (%) +Fe2O
> 2.50
2.00 2.50
1.50 2.00
0.50 1.50
< 0.50
75200.00
76000
76500
77000
77500
78000
78500
79000
79500
80000
80500
81000
81500
82000
82800.00
85400.00
85000
84500
84000
83500
83000
82500
82000
81400.00
2mS

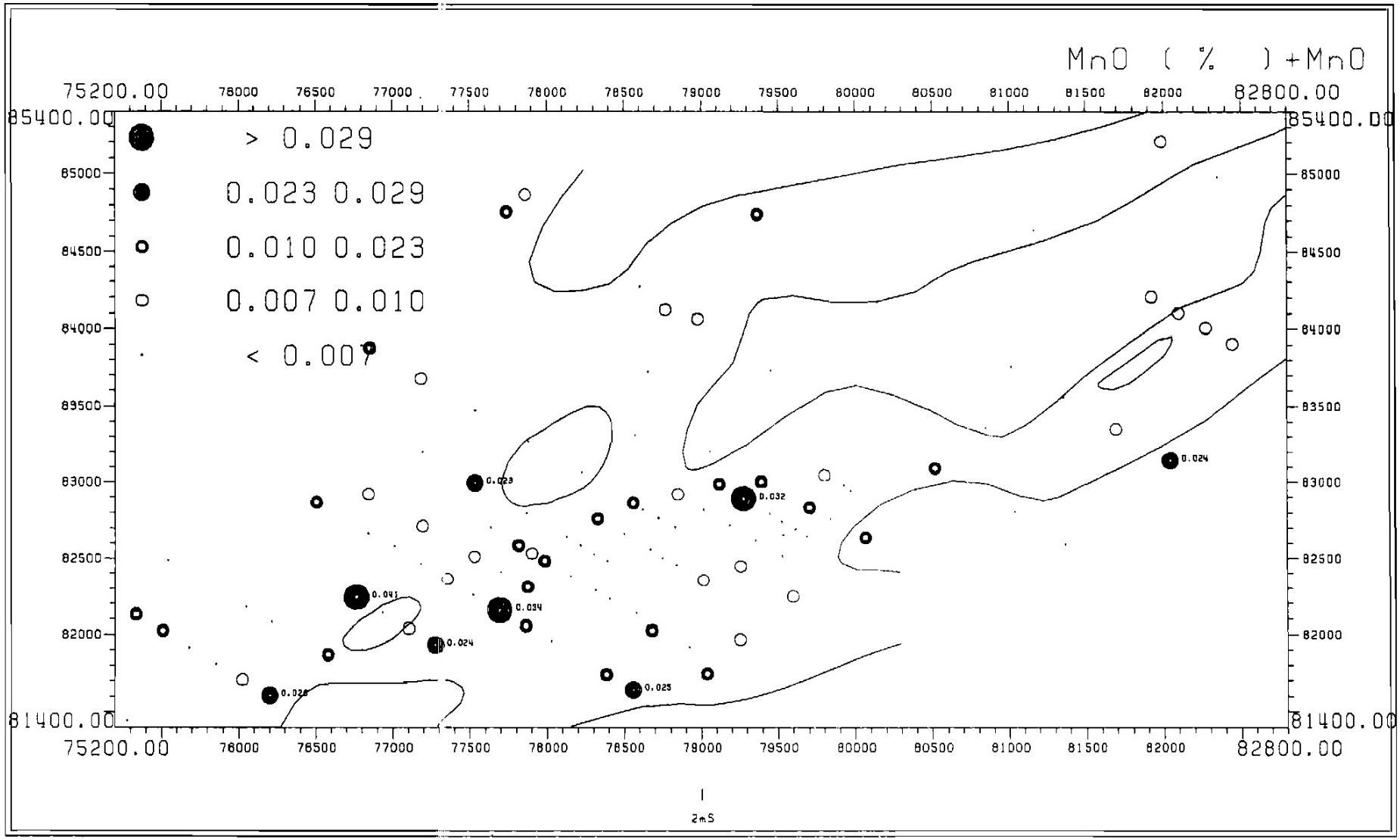
MnO (%) +MnO
> 0.029
0.023 0.029
0.010 0.023
0.007 0.010
< 0.007
75200.00
78000
76500
77000
77500
78000
78500
79000
79500
80000
80500
81000
81500
82000
82800.00
85400.00
85000
84500
84000
83500
83000
82500
82000
81400.00
0.023
0.032
0.024
0.041
0.034
0.024
0.026
0.025
2mS

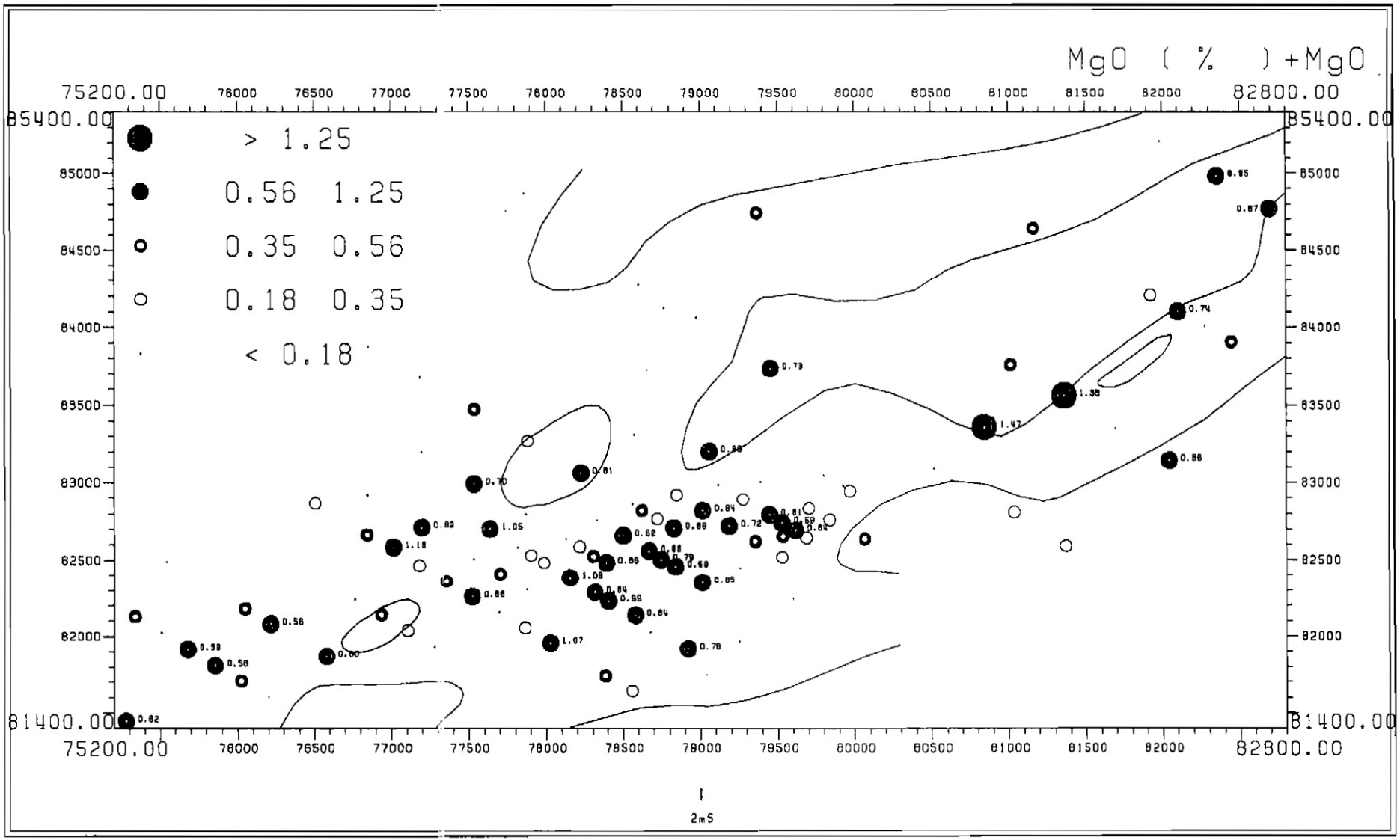
MgO (%) +MgO
> 1.25
0.56 1.25
0.35 0.56
0.18 0.35
< 0.18
75200.00
76000
76500
77000
77500
78000
78500
79000
79500
80000
80500
81000
81500
82000
82800.00
85400.00
85000
84500
84000
83500
83000
82500
82000
81400.00
2mS

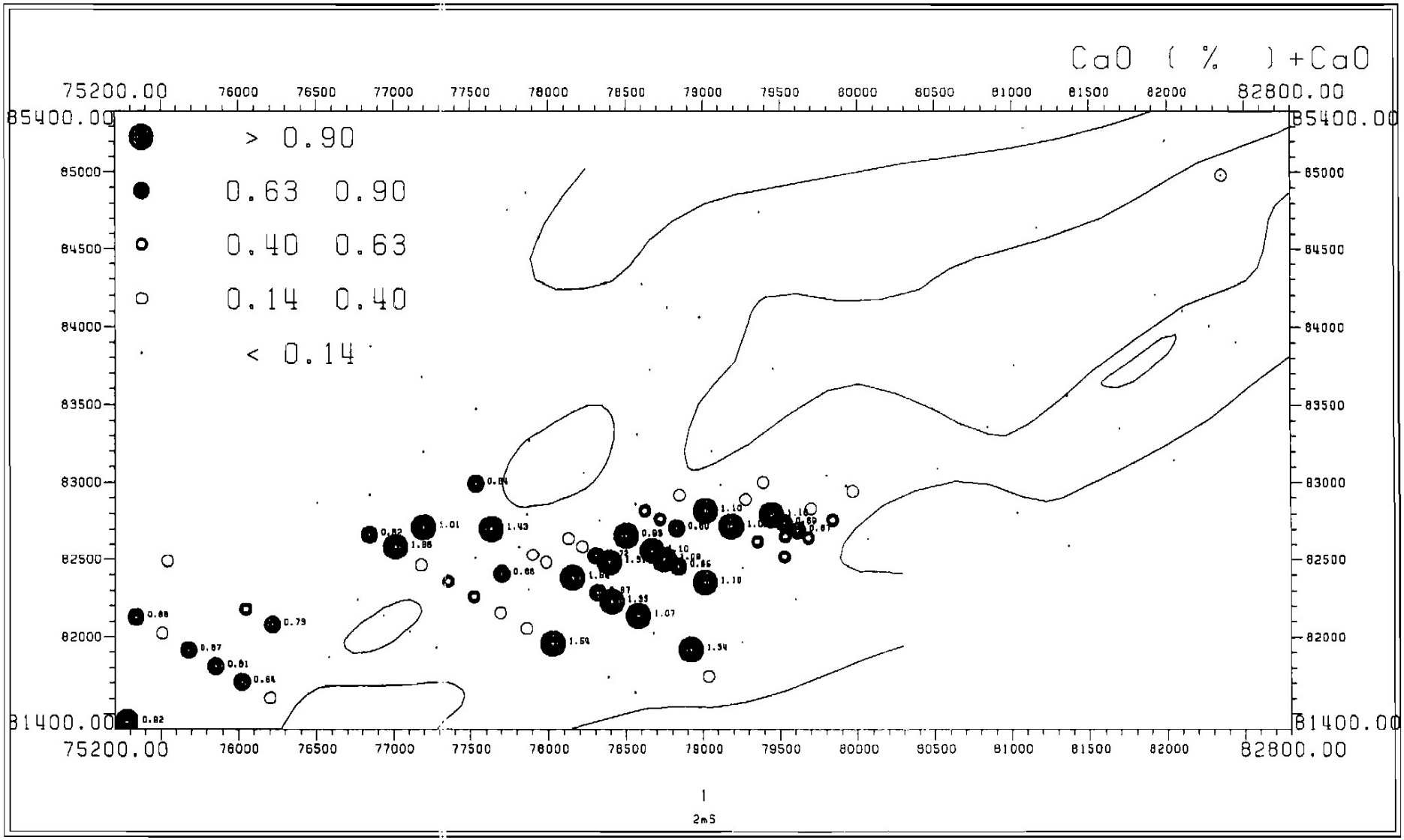
CaO (%) +CaO
> 0.90
0.63 0.90
0.40 0.63
0.14 0.40
< 0.14
75200.00
76000
76500
77000
77500
78000
78500
79000
79500
80000
80500
81000
81500
82000
82800.00
85400.00
85000
84500
84000
83500
83000
82500
82000
81400.00
1
2mS

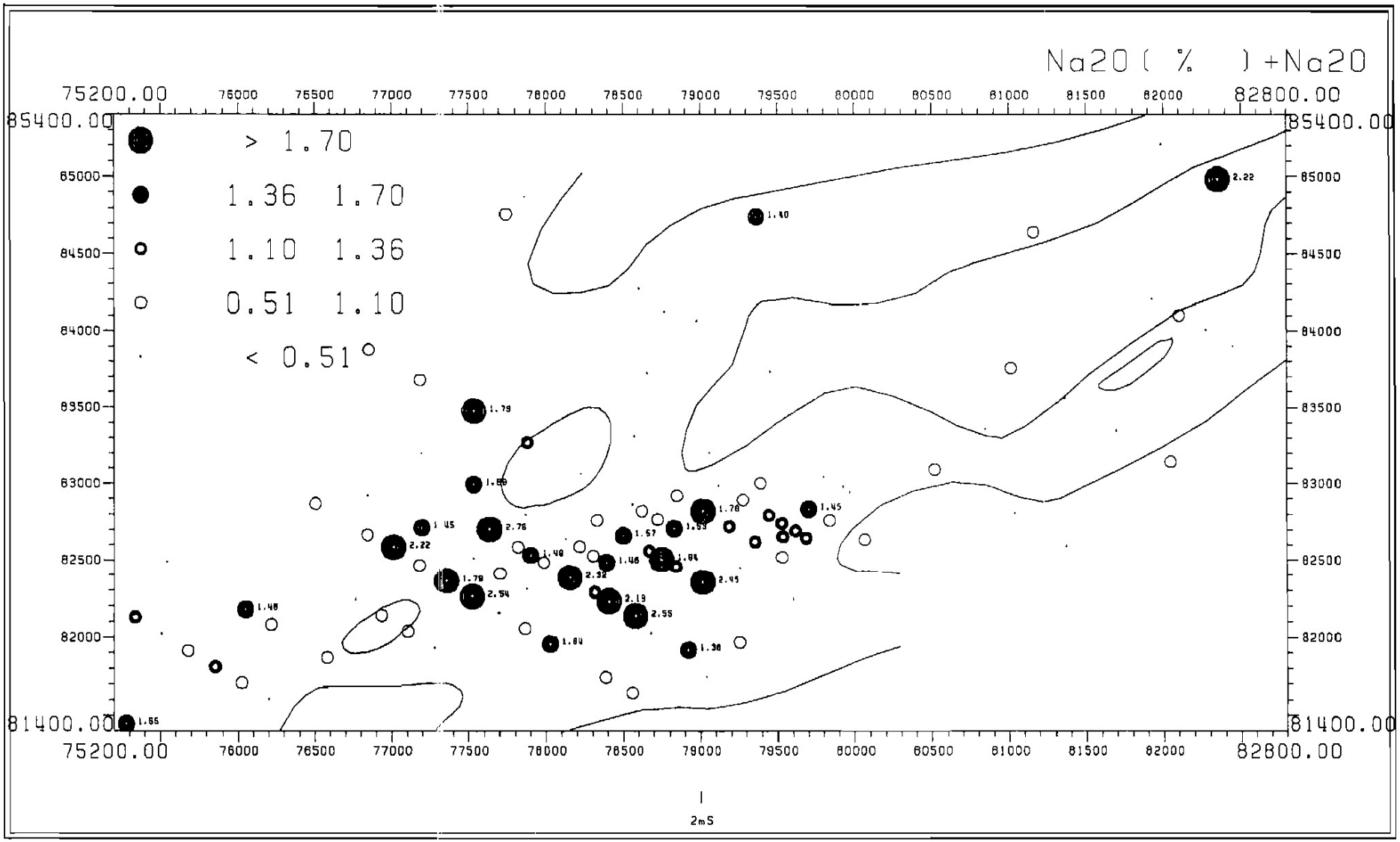
Na2O (%) +Na2O
> 1.70
1.36 1.70
1.10 1.36
0.51 1.10
< 0.51
75200.00
76000
76500
77000
77500
78000
78500
79000
79500
80000
80500
81000
81500
82000
82800.00
85400.00
85000
84500
84000
83500
83000
82500
82000
81400.00
2mS

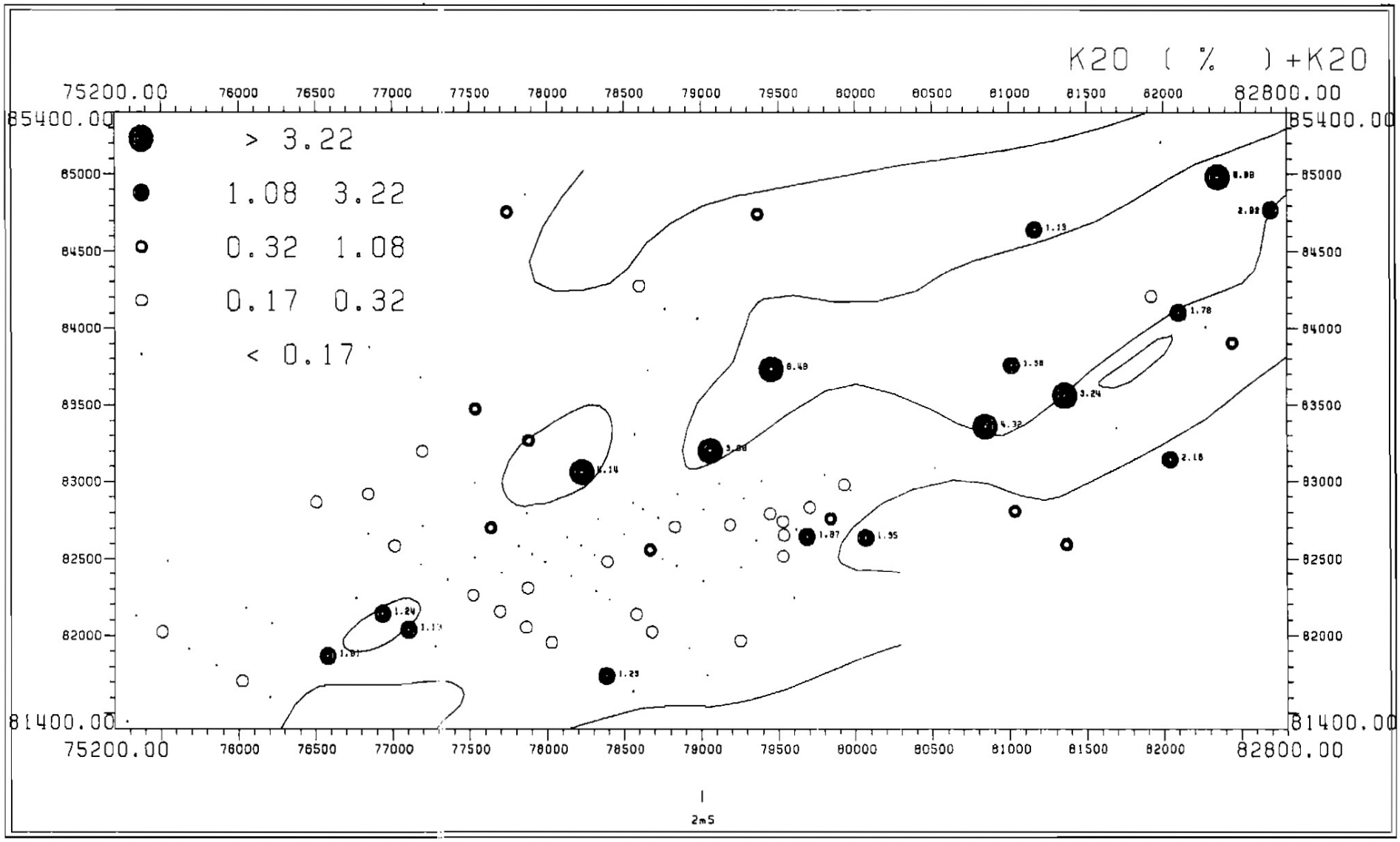
K20 (%) +K20
> 3.22
1.08 3.22
0.32 1.08
0.17 0.32
< 0.17
75200.00
76000
76500
77000
77500
78000
78500
79000
79500
80000
80500
81000
81500
82000
82800.00
85400.00
85000
84500
84000
83500
83000
82500
82000
81400.00
2mS

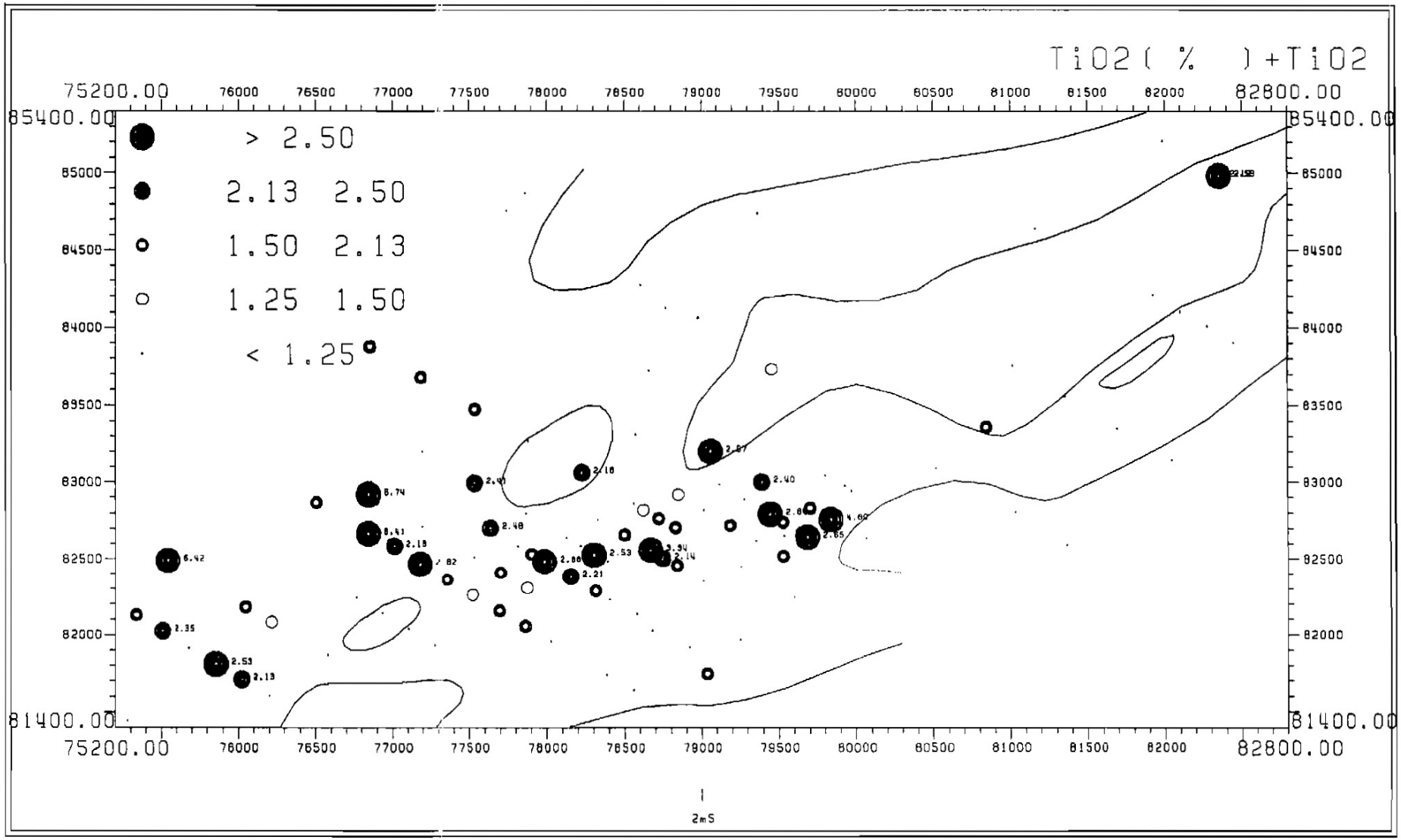
TiO2(%)+TiO2
> 2.50
2.13 2.50
1.50 2.13
1.25 1.50
< 1.25
75200.00
76000
76500
77000
77500
78000
78500
79000
79500
80000
80500
81000
81500
82000
82800.00
85400.00
85000
84500
84000
83500
83000
82500
82000
81400.00
2mS

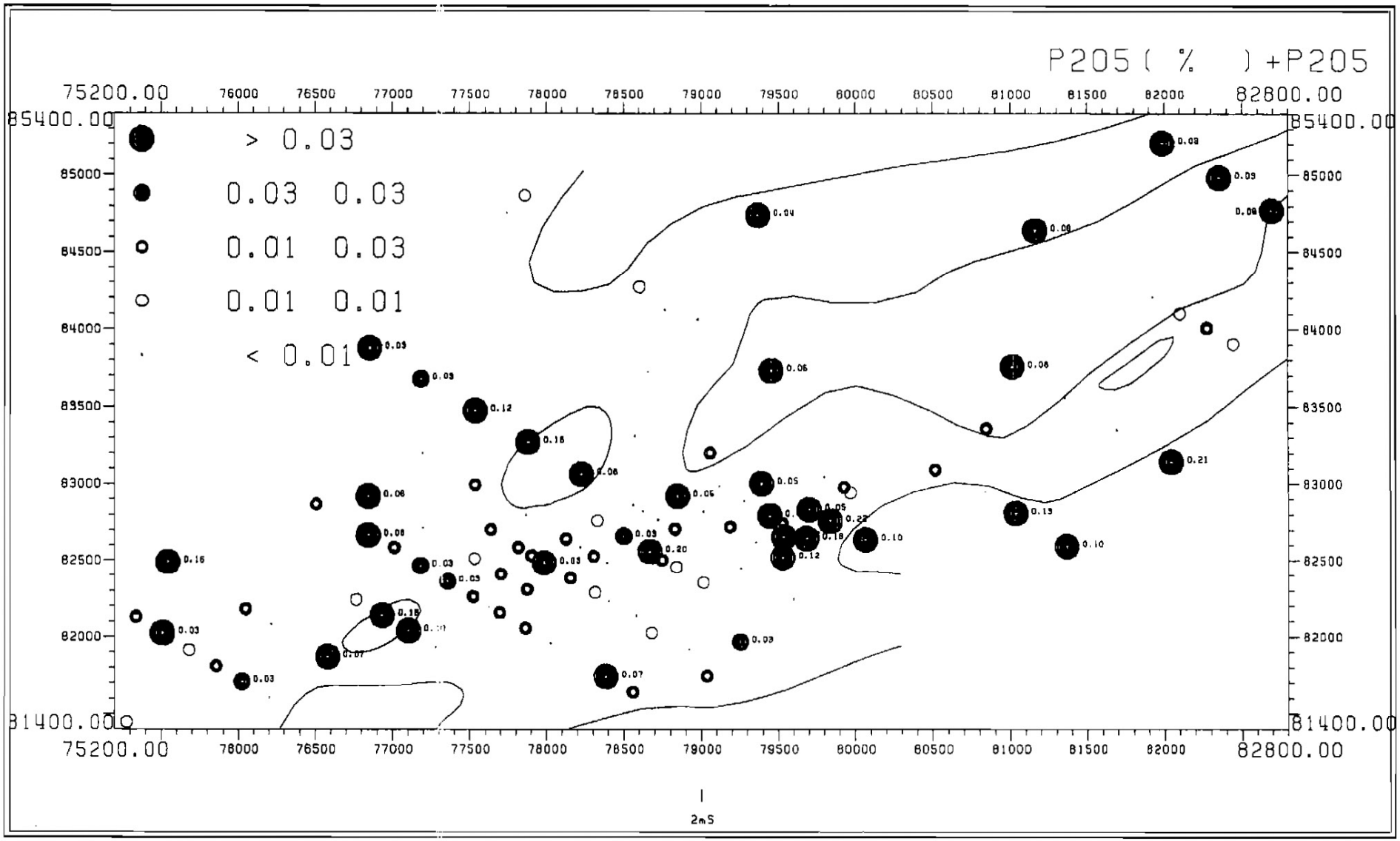
P205 (%) +P205
> 0.03
0.03 0.03
0.01 0.03
0.01 0.01
< 0.01
75200.00
76000
76500
77000
77500
78000
78500
79000
79500
80000
80500
81000
81500
82000
82800.00
85400.00
85000
84500
84000
83500
83000
82500
82000
81400.00
2mS

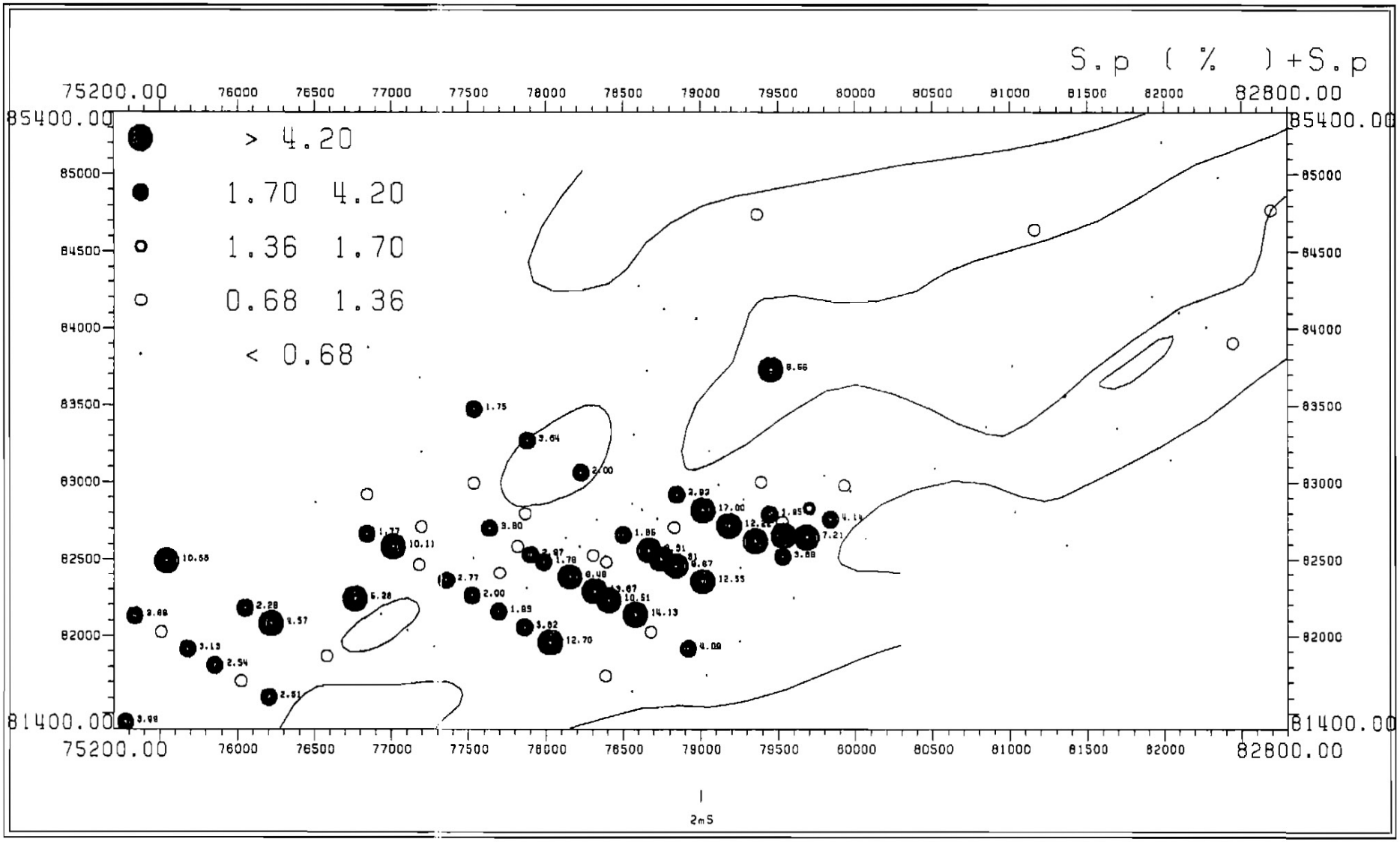
S.p (%) +S.p
> 4.20
1.70 4.20
1.36 1.70
0.68 1.36
< 0.68
75200.00
76000
76500
77000
77500
78000
78500
79000
79500
80000
80500
81000
81500
82000
82800.00
85400.00
85000
84500
84000
83500
83000
82500
82000
81400.00
2mS

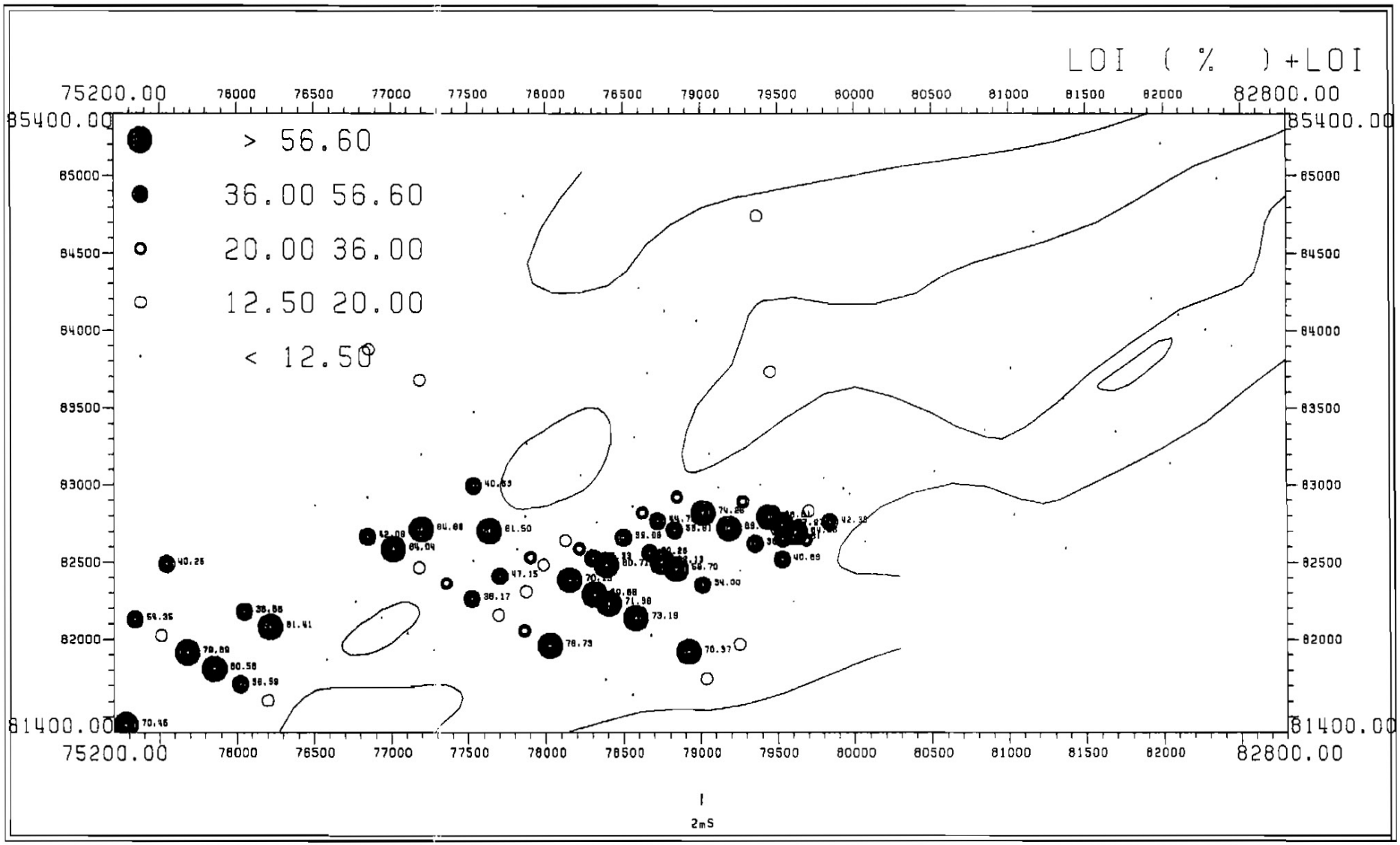
LOI (%)+LOI
> 56.60
36.00 56.60
20.00 36.00
12.50 20.00
< 12.50
75200.00
76000
76500
77000
77500
78000
78500
79000
79500
80000
80500
81000
81500
82000
82800.00
85400.00
85000
84500
84000
83500
83000
82500
82000
81400.00
2mS

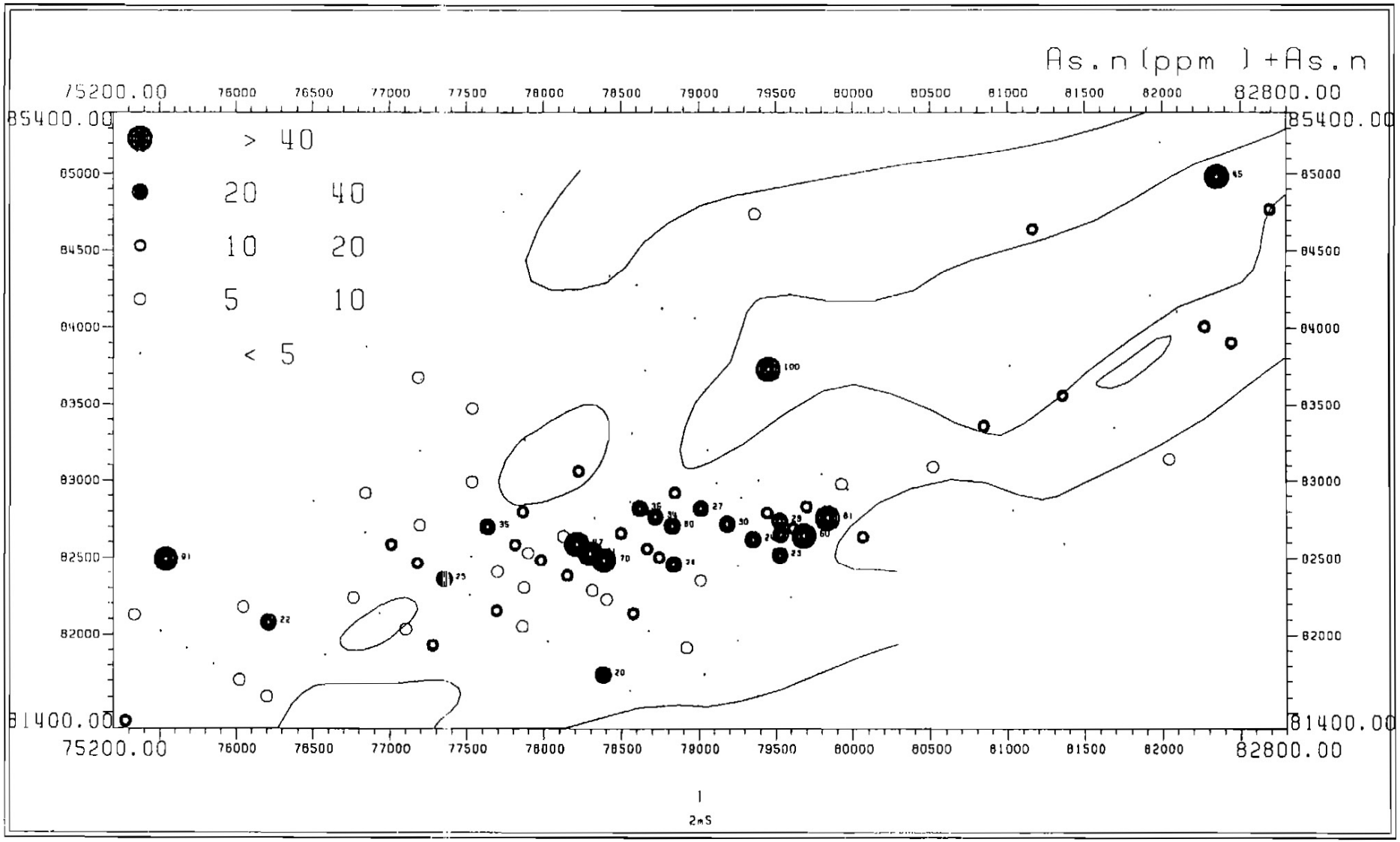
As.n(ppm)+As.n
> 40
20 40
10 20
5 10
< 5
75200.00
76000
76500
77000
77500
78000
78500
79000
79500
80000
80500
81000
81500
82000
82800.00
85400.00
85000
84500
84000
83500
83000
82500
82000
81400.00
2mS

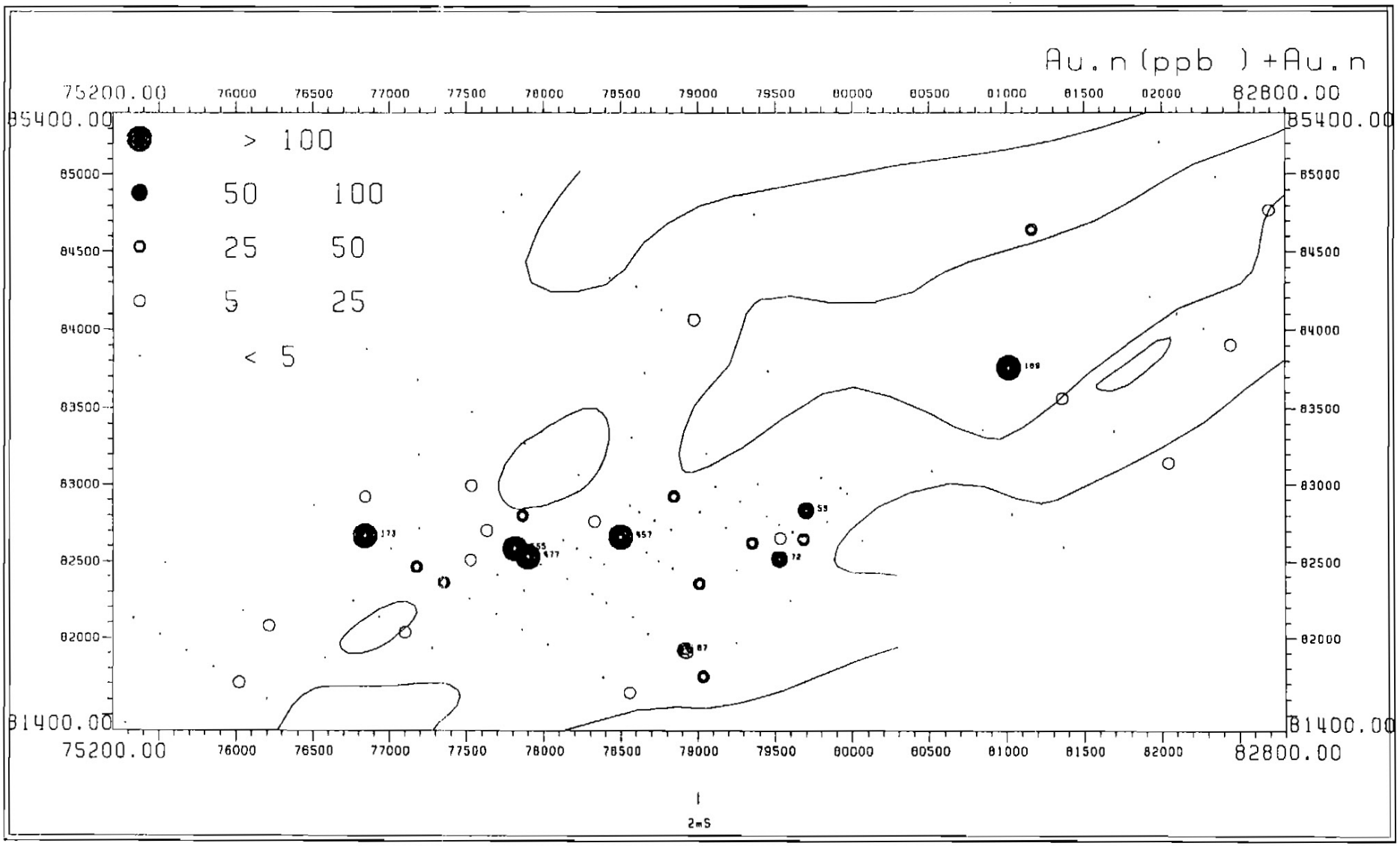
Au.n(ppb) +Au.n
> 100
50 100
25 50
5 25
< 5
75200.00
76000
76500
77000
77500
78000
78500
79000
79500
80000
80500
81000
81500
82000
82800.00
85400.00
85000
84500
84000
83500
83000
82500
82000
81400.00
2mS

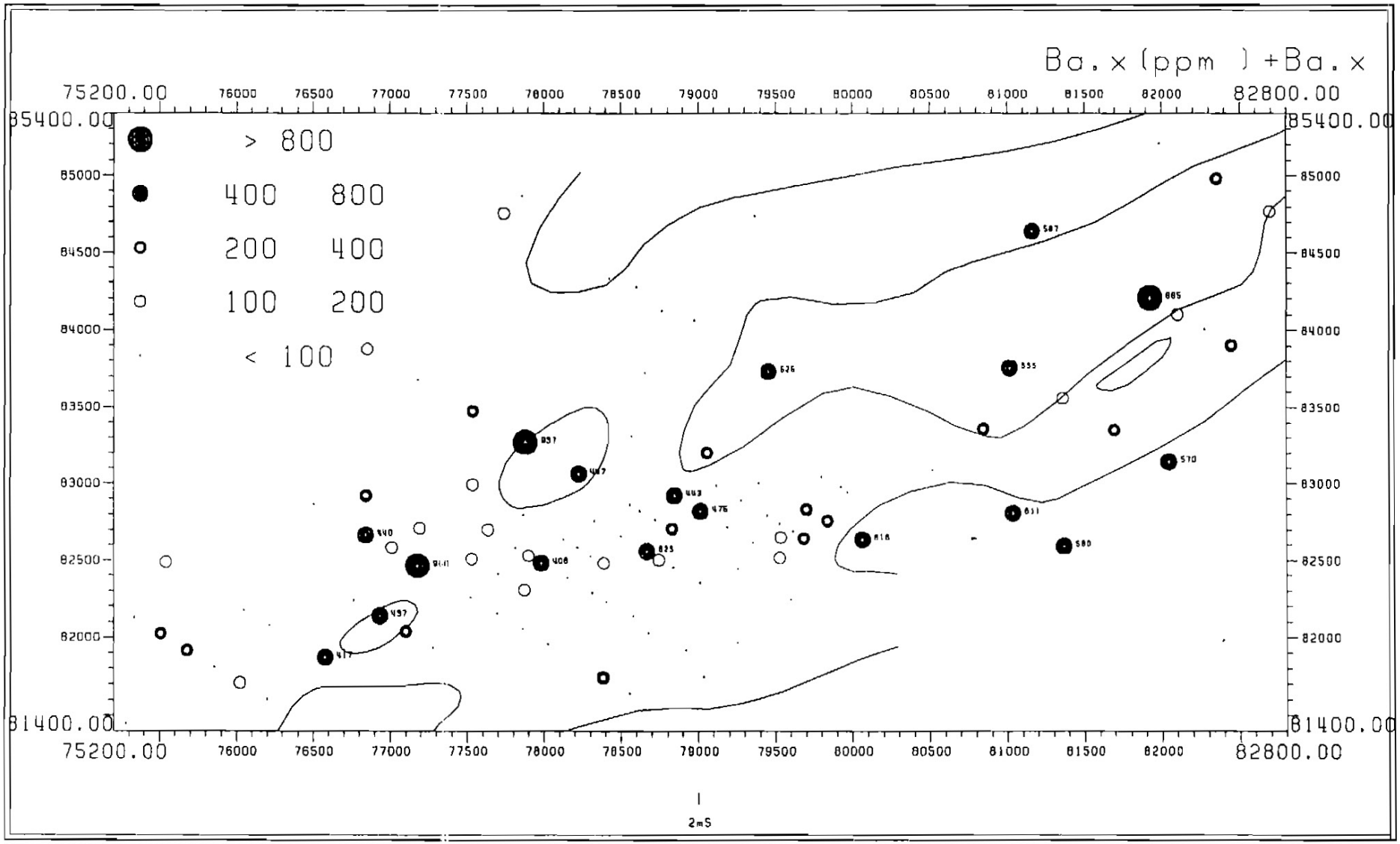
Ba.x (ppm) +Ba.x
> 800
400 800
200 400
100 200
< 100
75200.00
76000
76500
77000
77500
78000
78500
79000
79500
80000
80500
81000
81500
82000
82800.00
85400.00
85000
84500
84000
83500
83000
82500
82000
81400.00
2mS

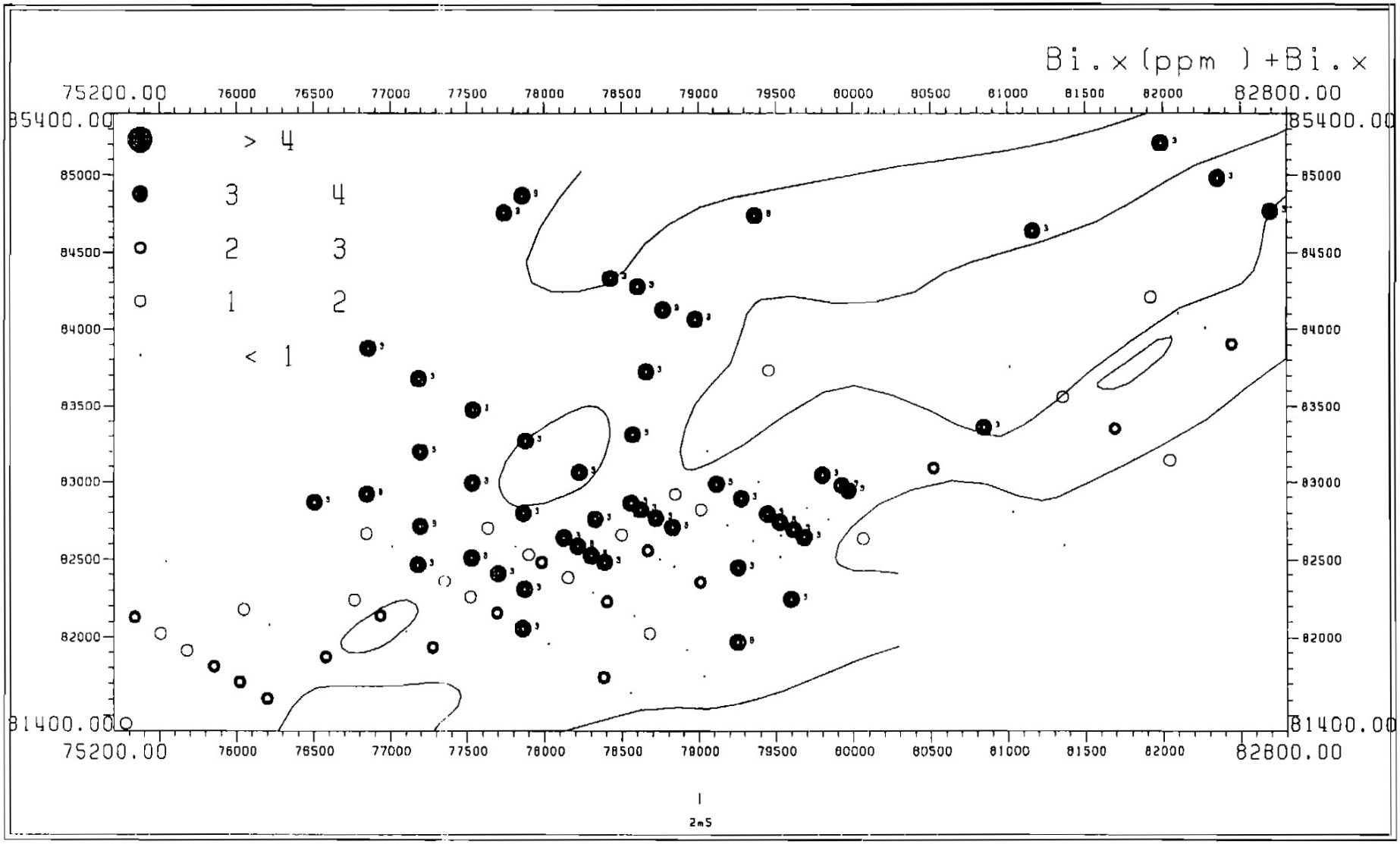
Bi.x(ppm)+Bi.x
> 4
3 4
2 3
1 2
< 1
75200.00
76000
76500
77000
77500
78000
78500
79000
79500
80000
80500
81000
81500
82000
82800.00
85400.00
85000
84500
84000
83500
83000
82500
82000
81400.00
2m5

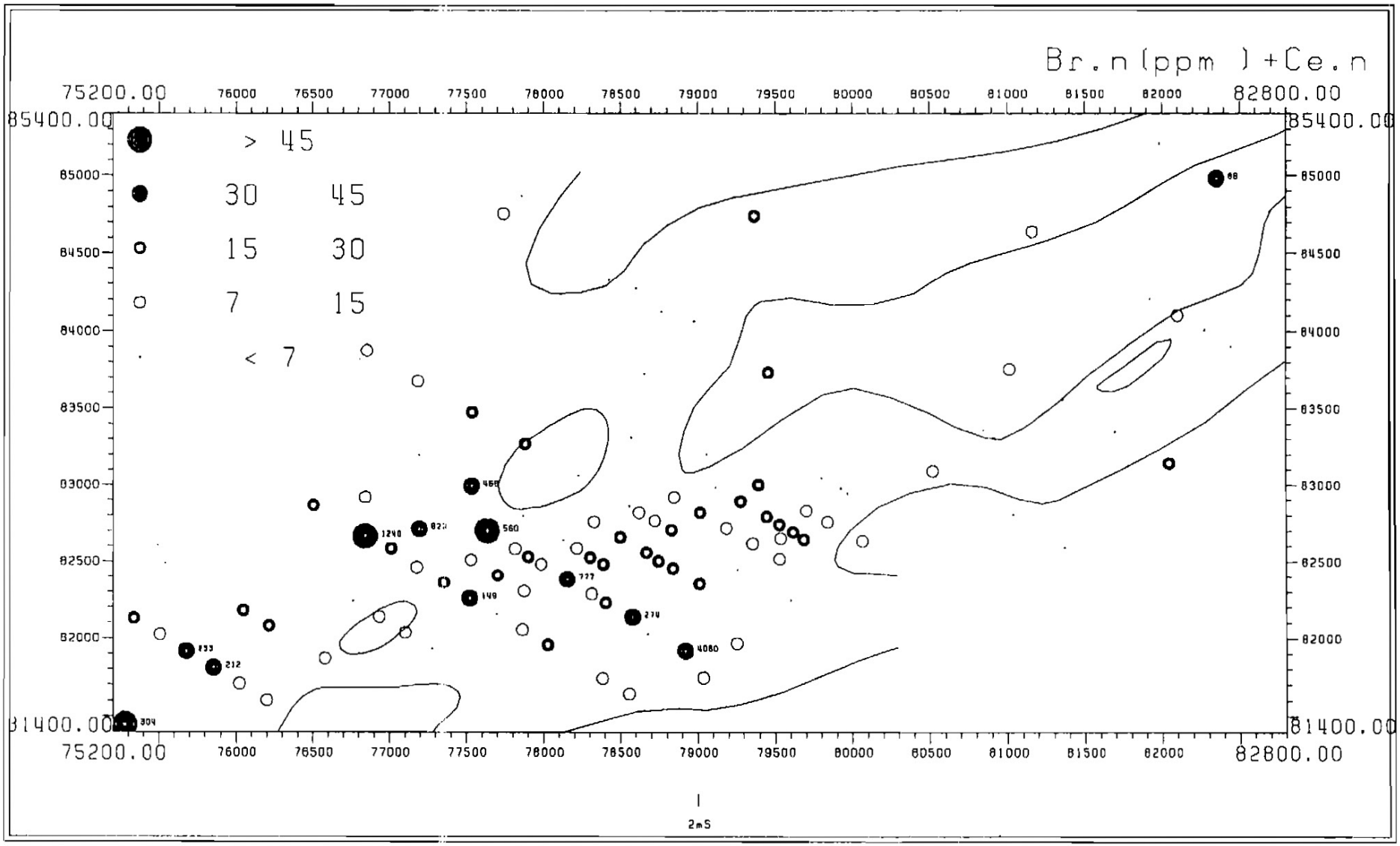
Br.n(ppm)+Ce.n
75200.00
76000
76500
77000
77500
78000
78500
79000
79500
80000
80500
81000
81500
82000
82800.00
85400.00
85000
84500
84000
83500
83000
82500
82000
81400.00
> 45
30 45
15 30
7 15
< 7
2mS

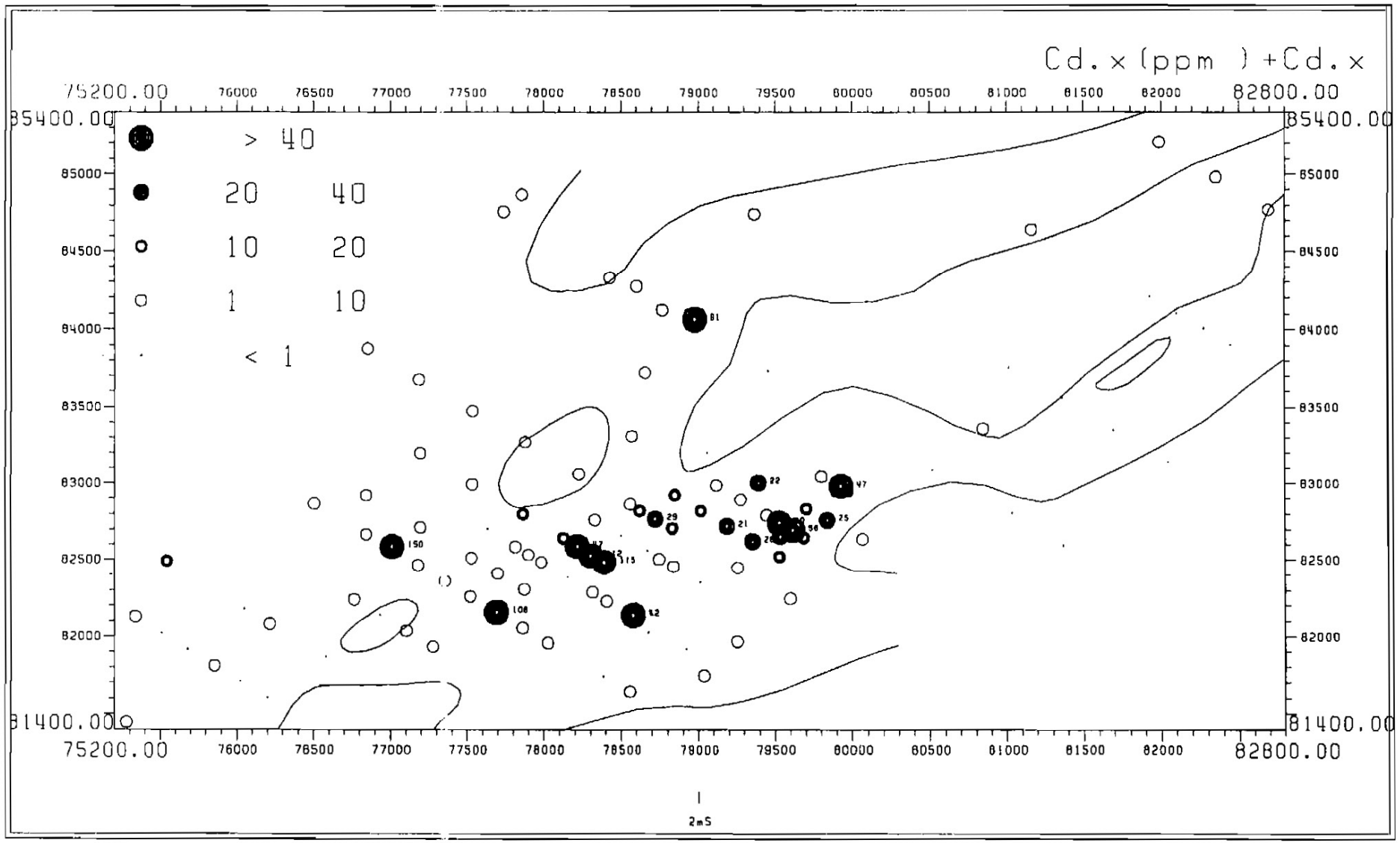
Cd.x(ppm)+Cd.x
> 40
20 40
10 20
1 10
< 1
75200.00
76000
76500
77000
77500
78000
78500
79000
79500
80000
80500
81000
81500
82000
82800.00
85400.00
85000
84500
84000
83500
83000
82500
82000
81400.00
2mS

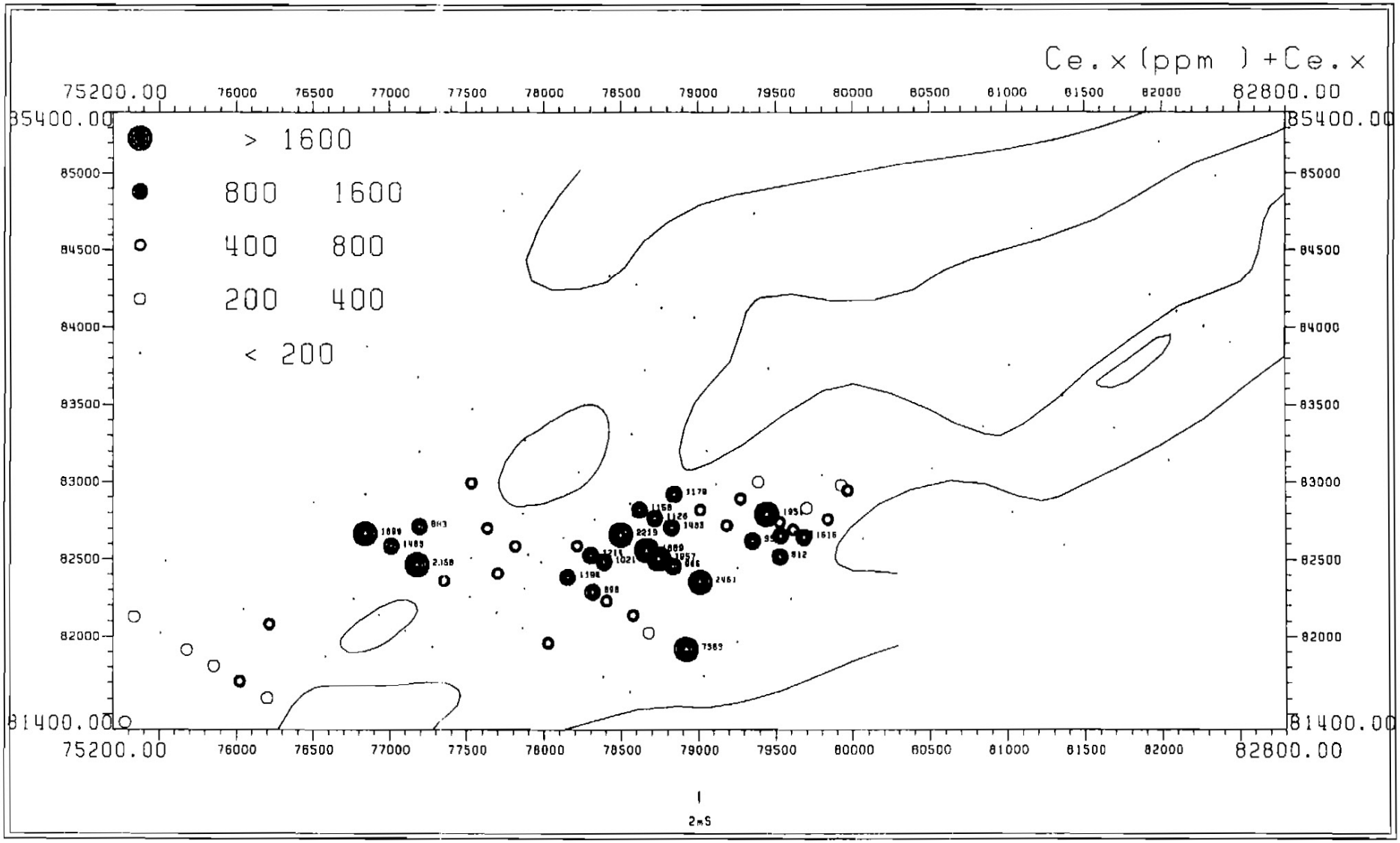
Ce.x(ppm)+Ce.x
> 1600
800 1600
400 800
200 400
< 200
75200.00
76000
76500
77000
77500
78000
78500
79000
79500
80000
80500
81000
81500
82000
82800.00
85400.00
85000
84500
84000
83500
83000
82500
82000
81400.00
2mS

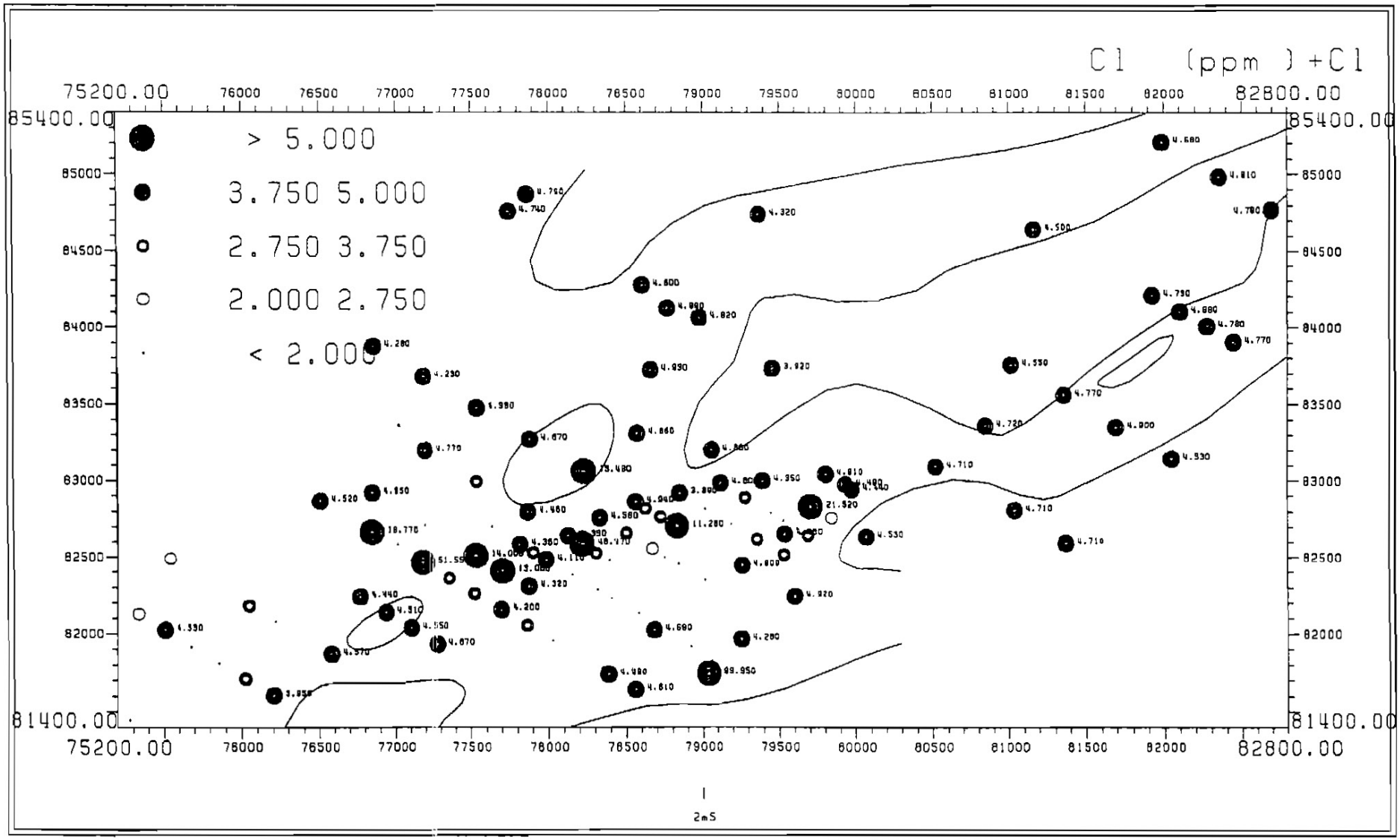
Cl (ppm) +Cl
> 5.000
3.750 5.000
2.750 3.750
2.000 2.750
< 2.000
75200.00
76000
76500
77000
77500
78000
78500
79000
79500
80000
80500
81000
81500
82000
82800.00
85400.00
85000
84500
84000
83500
83000
82500
82000
81400.00
2mS

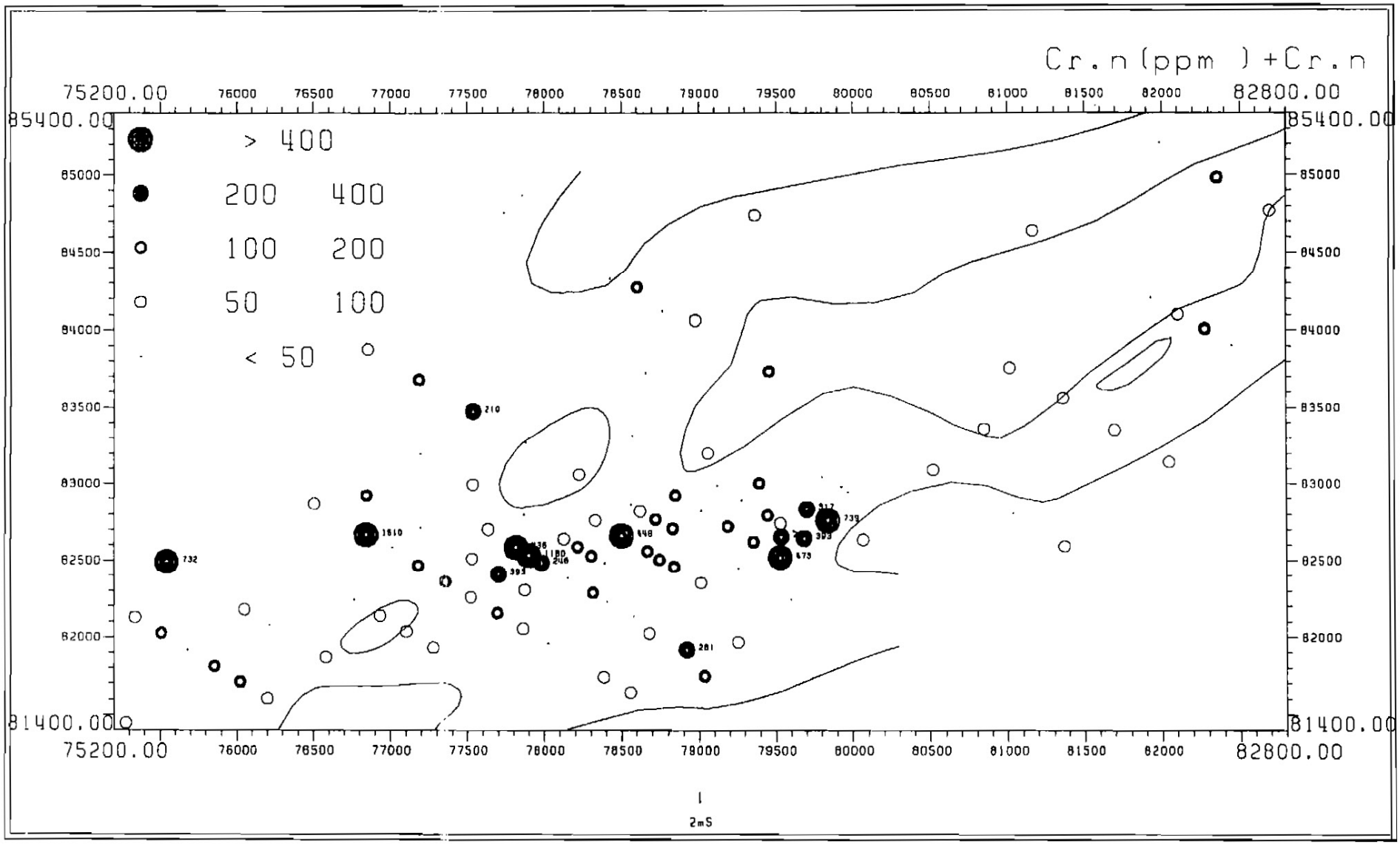
Cr.n(ppm)+Cr.n
> 400
200 400
100 200
50 100
< 50
75200.00
76000
76500
77000
77500
78000
78500
79000
79500
80000
80500
81000
81500
82000
82800.00
85400.00
85000
84500
84000
83500
83000
82500
82000
81400.00
2mS

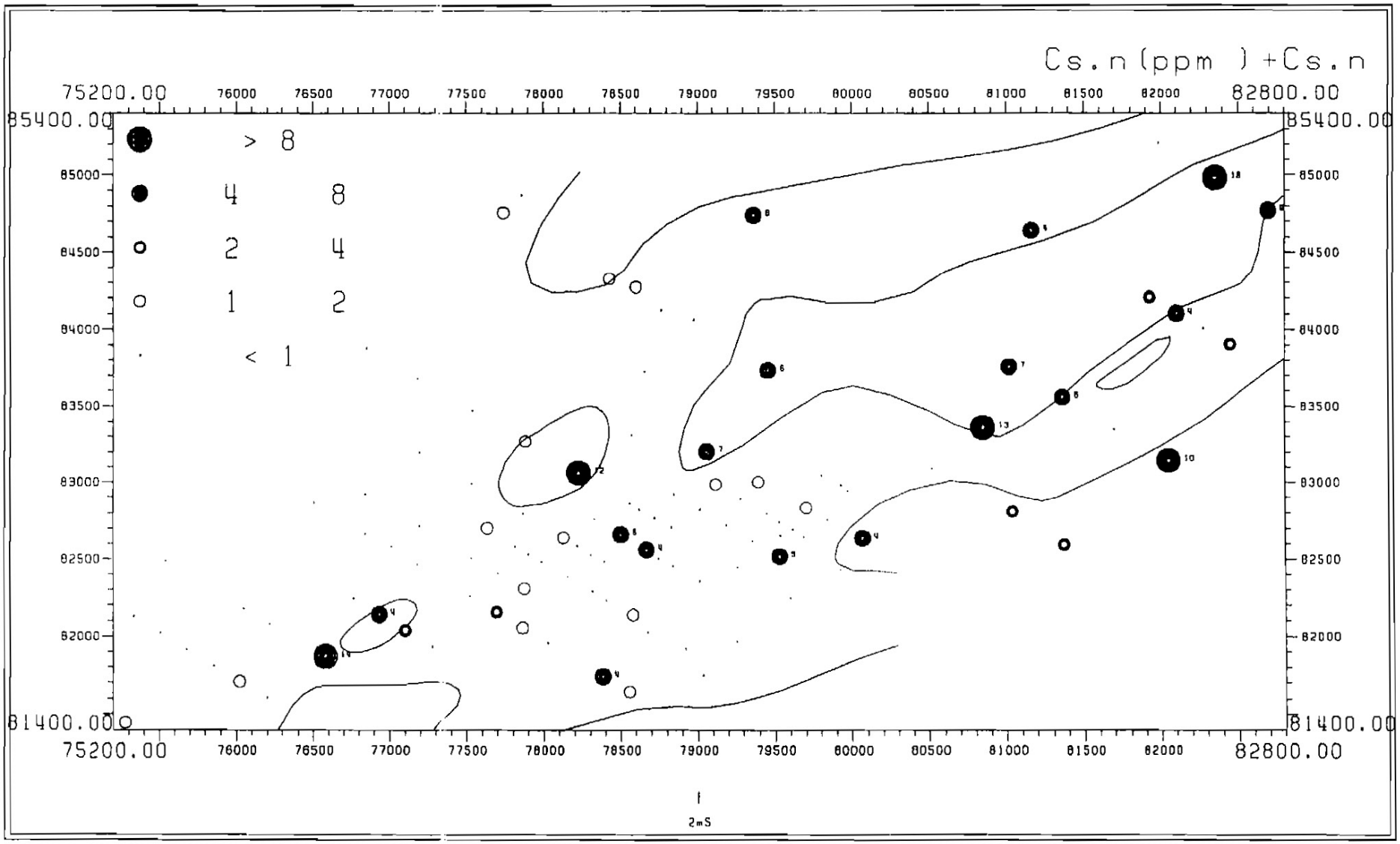
Cs.n(ppm)+Cs.n
> 8
4 8
2 4
1 2
< 1
75200.00
76000
76500
77000
77500
78000
78500
79000
79500
80000
80500
81000
81500
82000
82800.00
85400.00
85000
84500
84000
83500
83000
82500
82000
81400.00
2mS

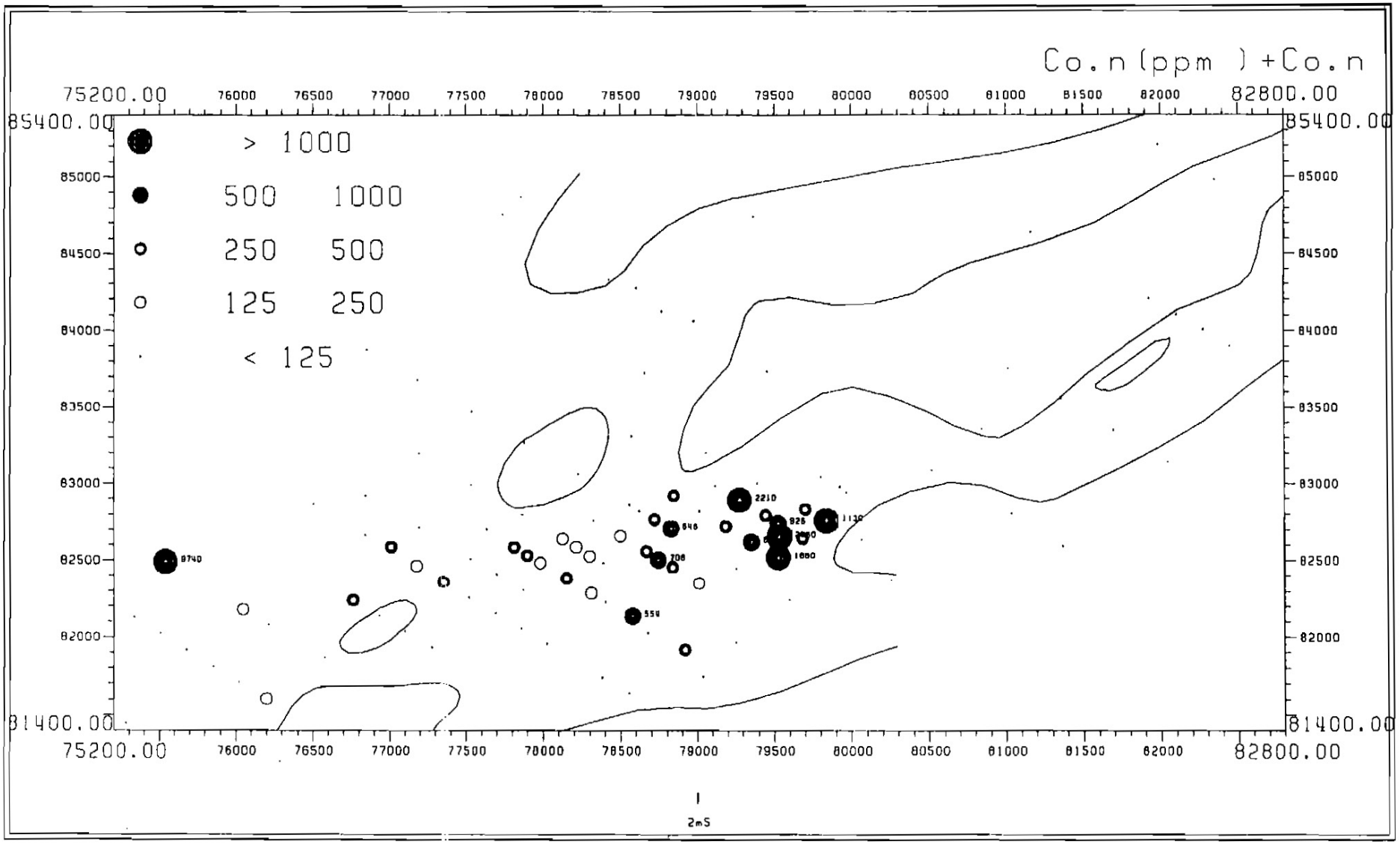
Co.n (ppm) +Co.n
> 1000
500 1000
250 500
125 250
< 125
75200.00
76000
76500
77000
77500
78000
78500
79000
79500
80000
80500
81000
81500
82000
82800.00
85400.00
85000
84500
84000
83500
83000
82500
82000
81400.00
2210
1130
1660
2mS

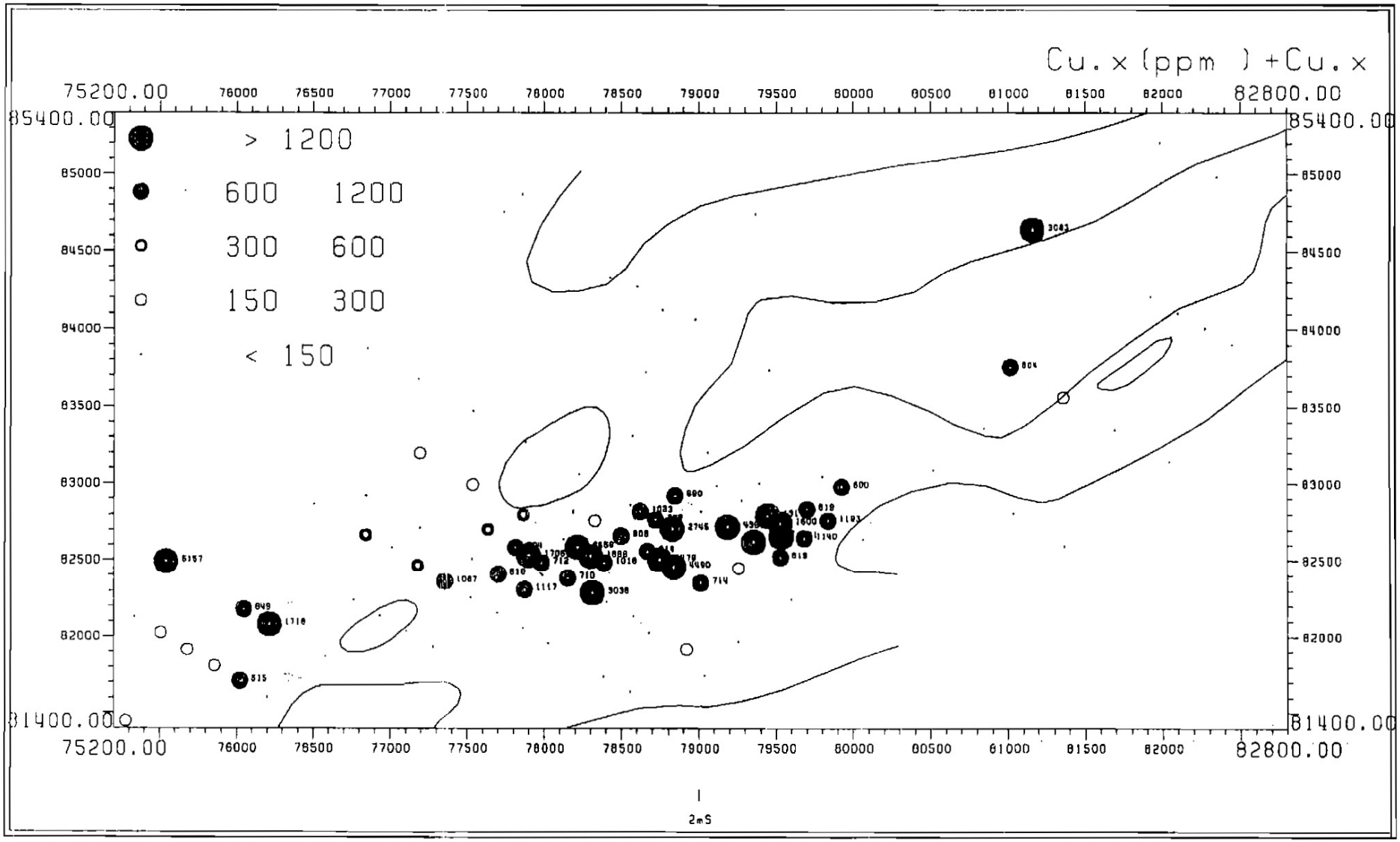
Cu.x (ppm) +Cu.x
> 1200
600 1200
300 600
150 300
< 150
75200.00
76000
76500
77000
77500
78000
78500
79000
79500
80000
80500
81000
81500
82000
82800.00
85400.00
85000
84500
84000
83500
83000
82500
82000
81400.00
2mS

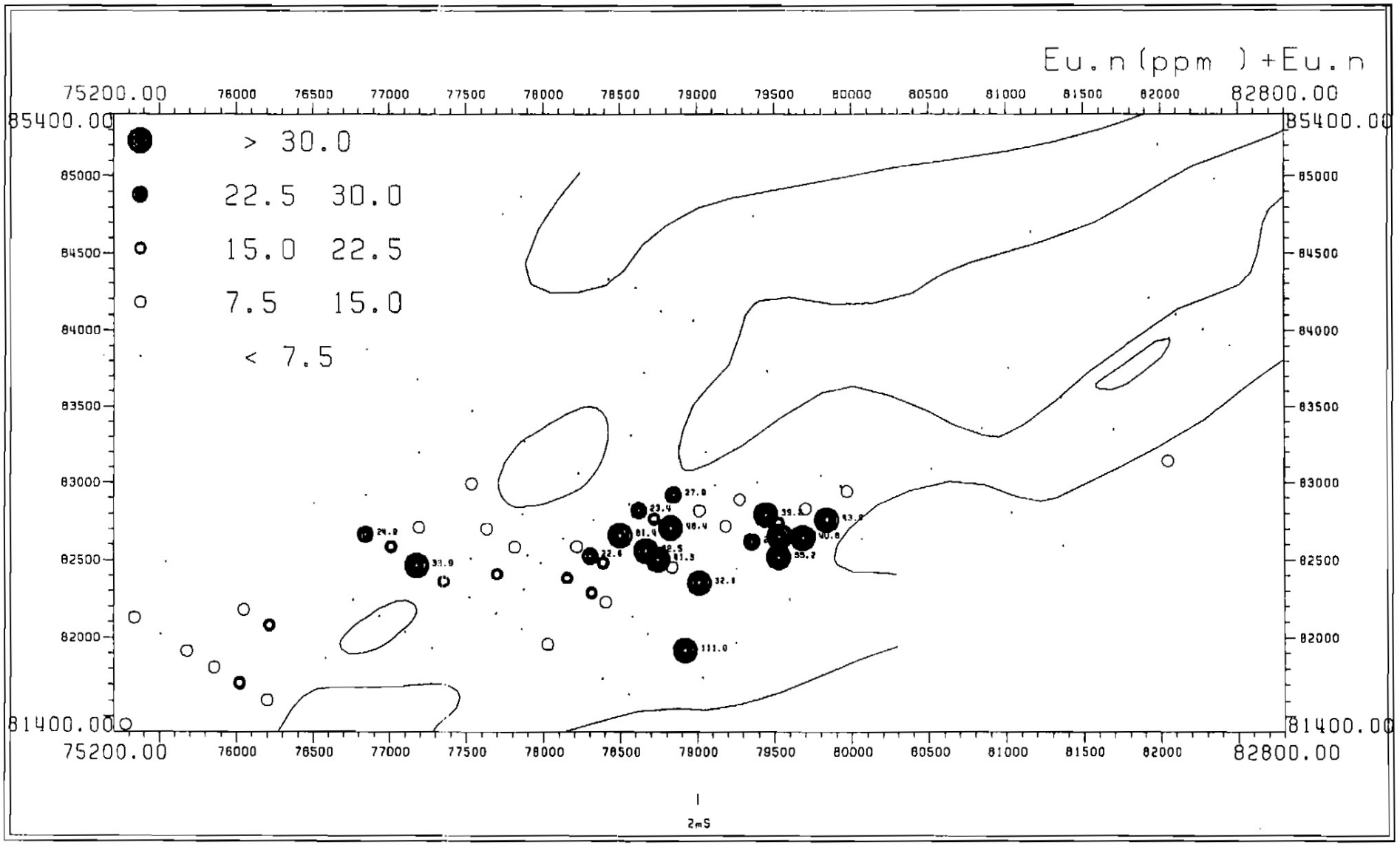
Eu.n(ppm)+Eu.n
> 30.0
22.5 30.0
15.0 22.5
7.5 15.0
< 7.5
75200.00
76000
76500
77000
77500
78000
78500
79000
79500
80000
80500
81000
81500
82000
82800.00
85400.00
85000
84500
84000
83500
83000
82500
82000
81400.00
2mS

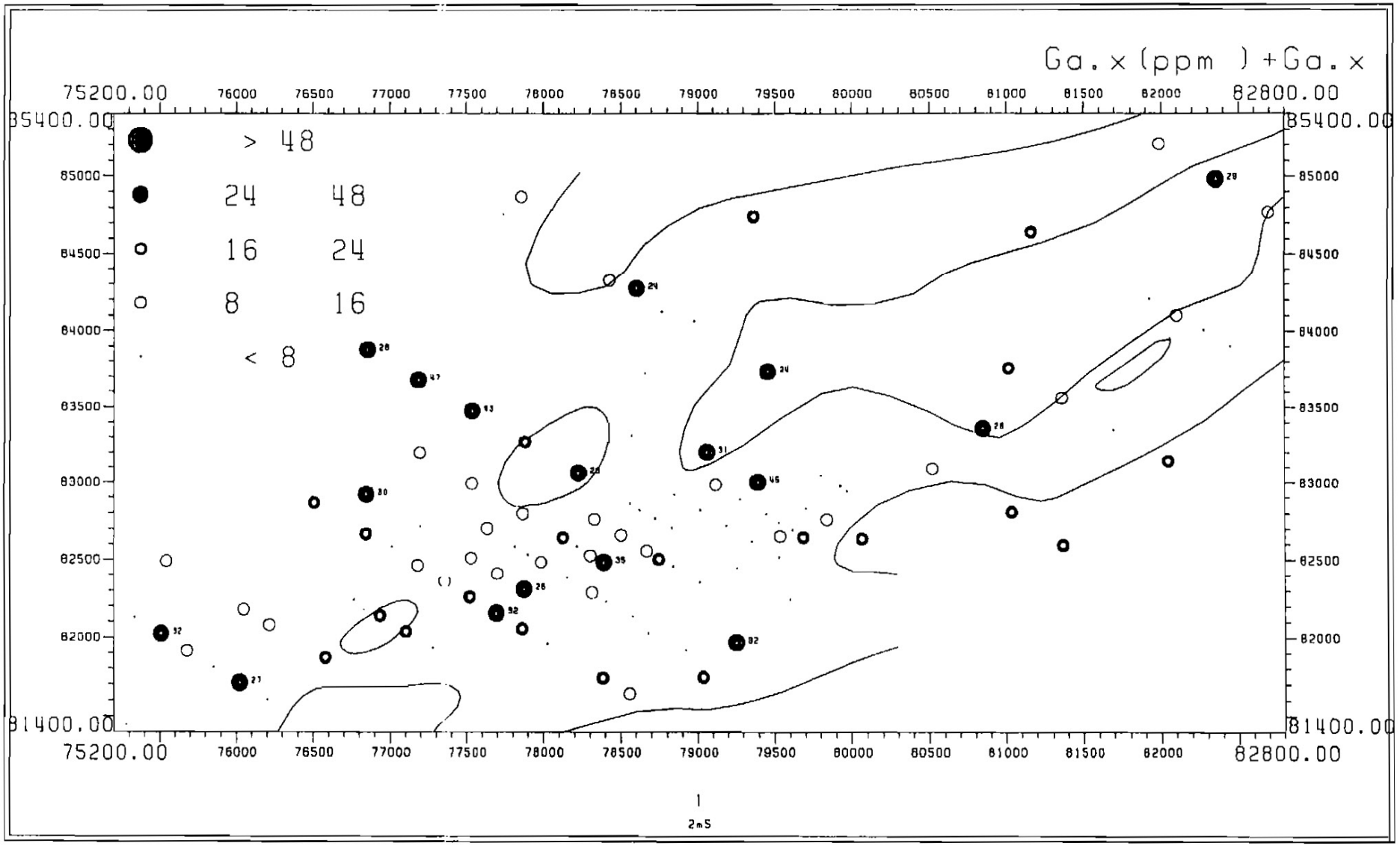
Ga.x(ppm)+Ga.x
> 48
24 48
16 24
8 16
< 8
75200.00
76000
76500
77000
77500
78000
78500
79000
79500
80000
80500
81000
81500
82000
82800.00
85400.00
85000
84500
84000
83500
83000
82500
82000
81400.00
2mS

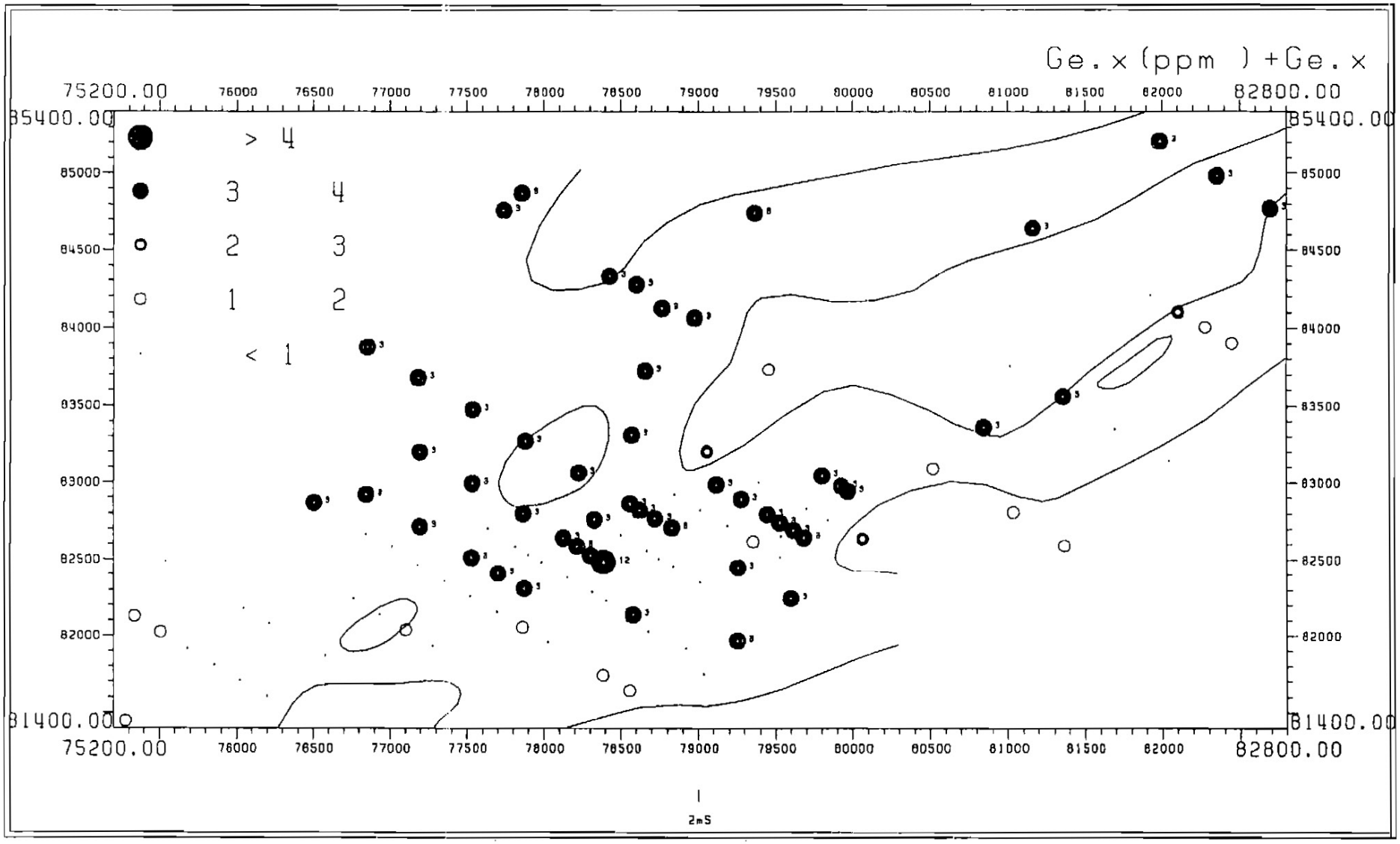
Ge.x (ppm) +Ge.x
> 4
3 4
2 3
1 2
< 1
75200.00
76000
76500
77000
77500
78000
78500
79000
79500
80000
80500
81000
81500
82000
82800.00
85400.00
85000
84500
84000
83500
83000
82500
82000
81400.00
2mS

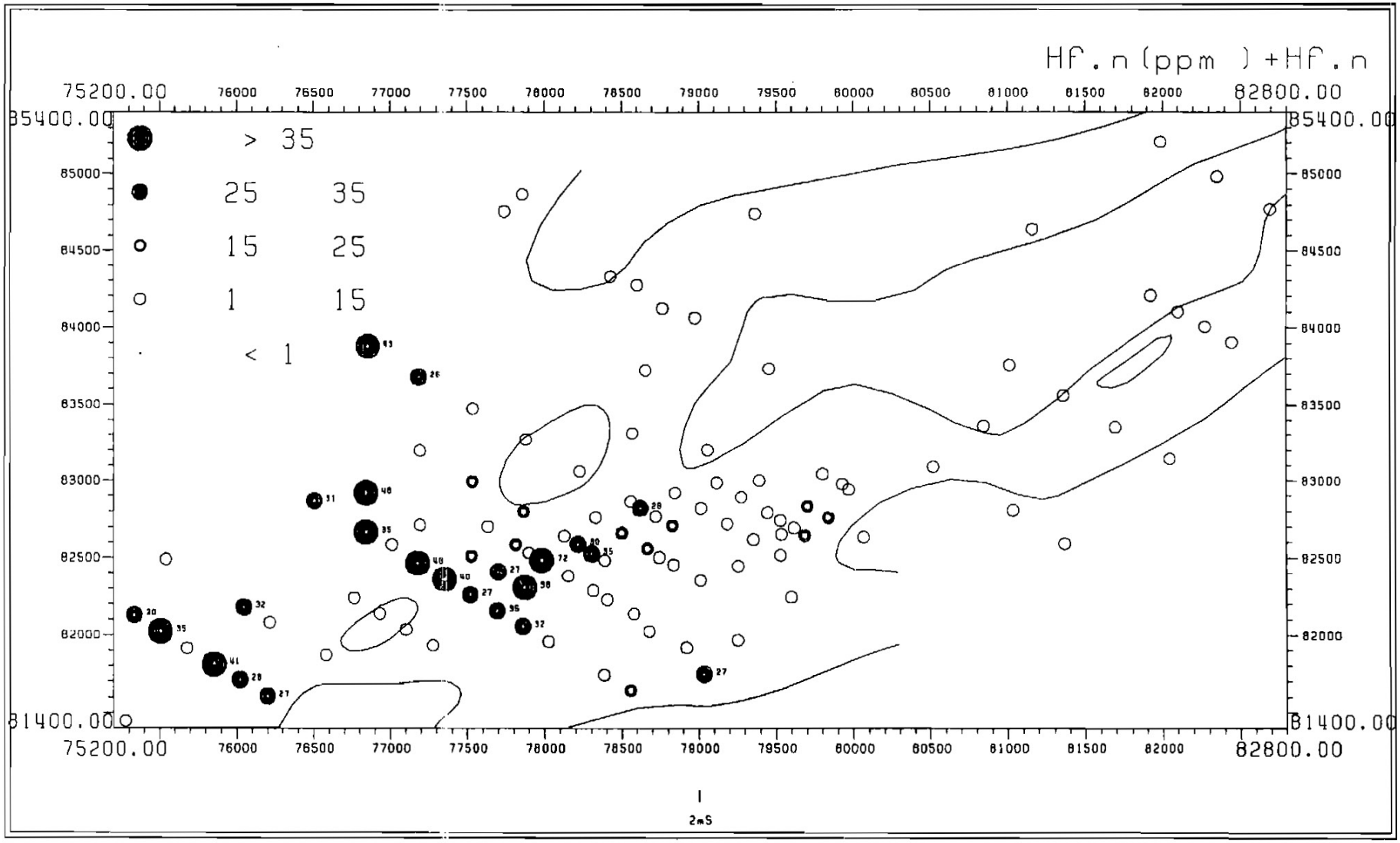
Hf.n (ppm) +Hf.n
> 35
25 35
15 25
1 15
< 1
75200.00
76000
76500
77000
77500
78000
78500
79000
79500
80000
80500
81000
81500
82000
82800.00
85400.00
85000
84500
84000
83500
83000
82500
82000
81400.00
2mS

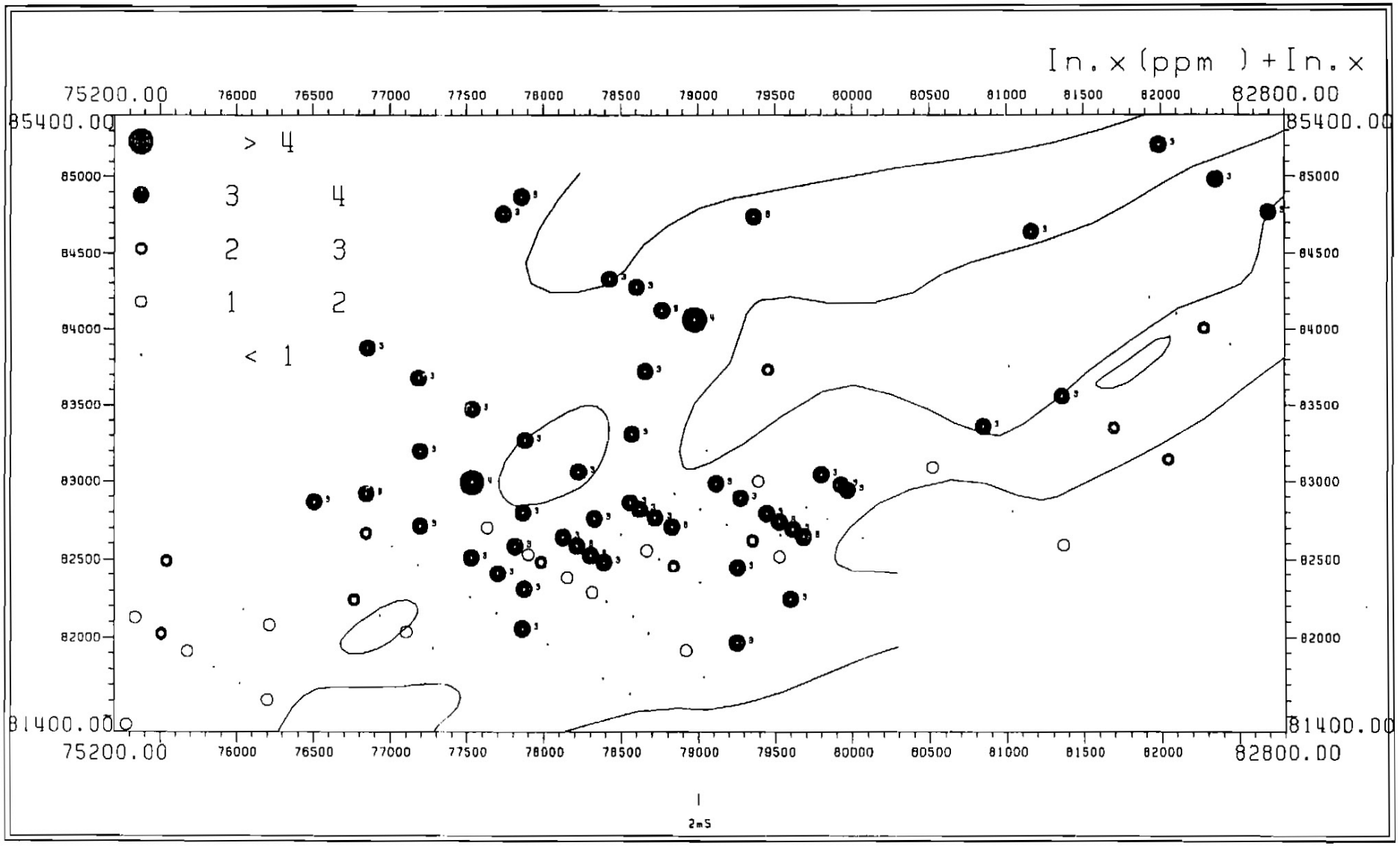
In.x(ppm)+In.x
> 4
3 4
2 3
1 2
< 1
75200.00
76000
76500
77000
77500
78000
78500
79000
79500
80000
80500
81000
81500
82000
82800.00
85400.00
85000
84500
84000
83500
83000
82500
82000
81400.00
2mS

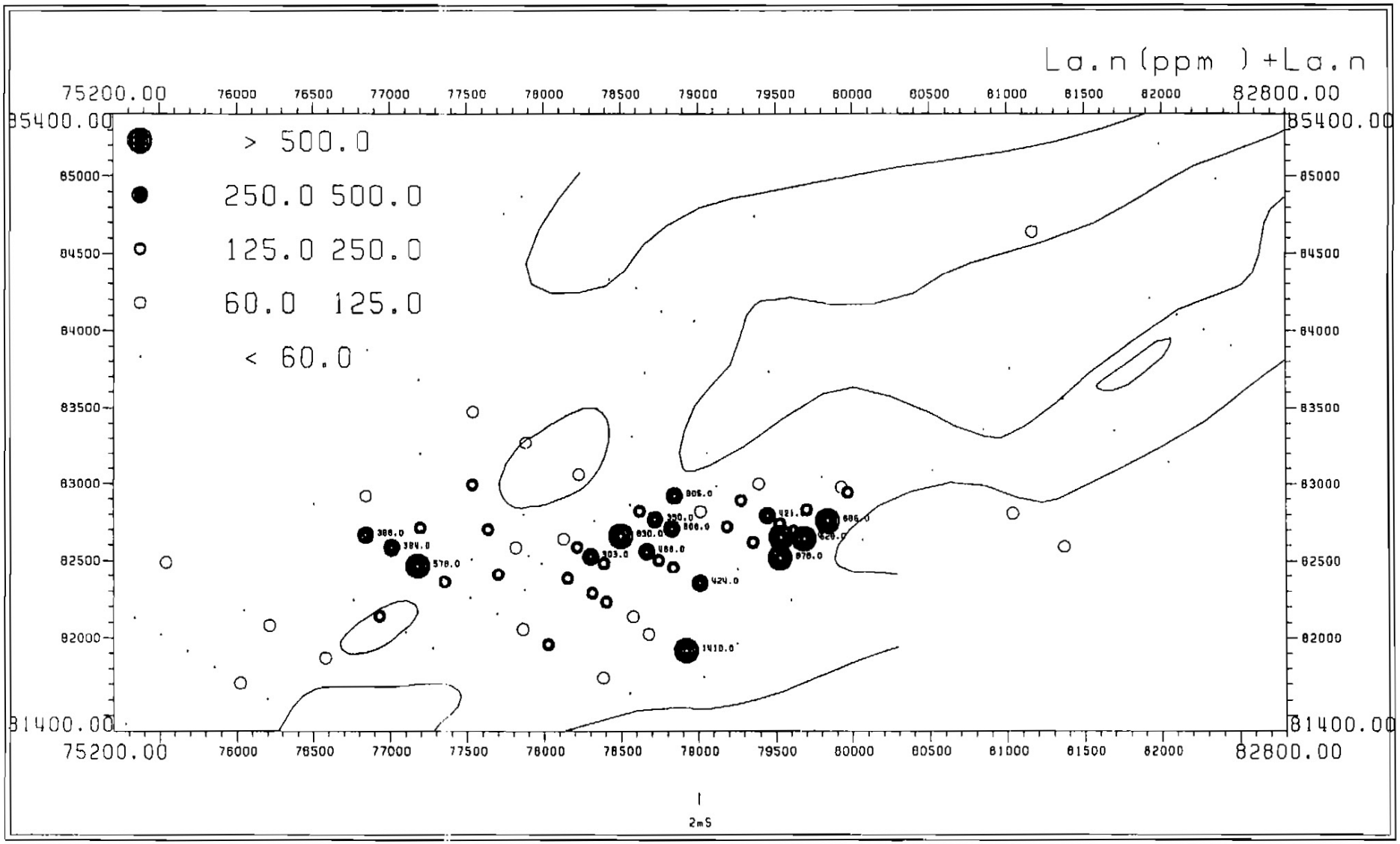
La.n(ppm)+La.n
> 500.0
250.0 500.0
125.0 250.0
60.0 125.0
< 60.0
75200.00
76000
76500
77000
77500
78000
78500
79000
79500
80000
80500
81000
81500
82000
82800.00
85400.00
85000
84500
84000
83500
83000
82500
82000
81400.00
386.0
384.0
578.0
424.0
1410.0
2mS

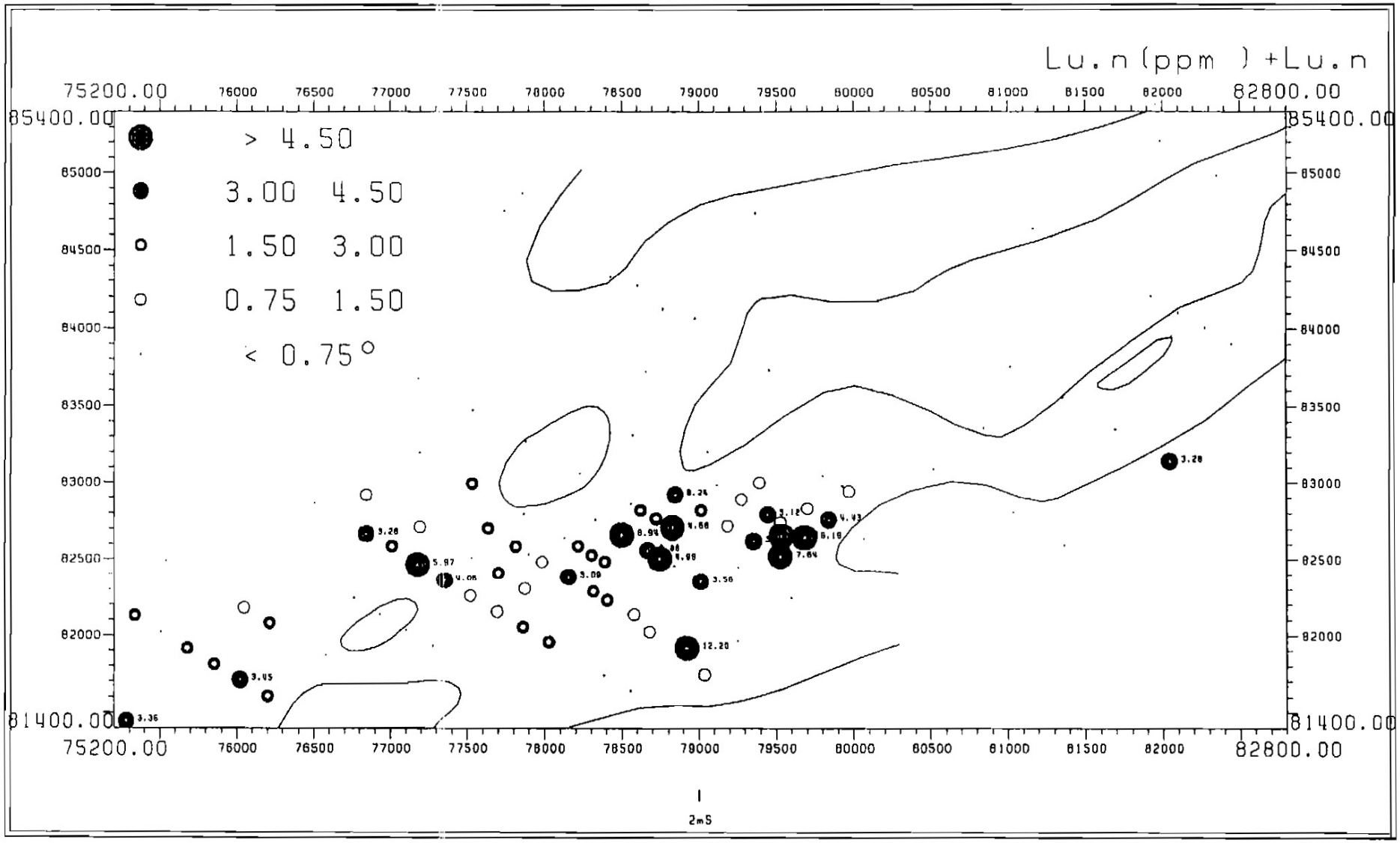
Lu.n (ppm) +Lu.n
> 4.50
3.00 4.50
1.50 3.00
0.75 1.50
< 0.75
75200.00
76000
76500
77000
77500
78000
78500
79000
79500
80000
80500
81000
81500
82000
82800.00
85400.00
85000
84500
84000
83500
83000
82500
82000
81400.00
2mS

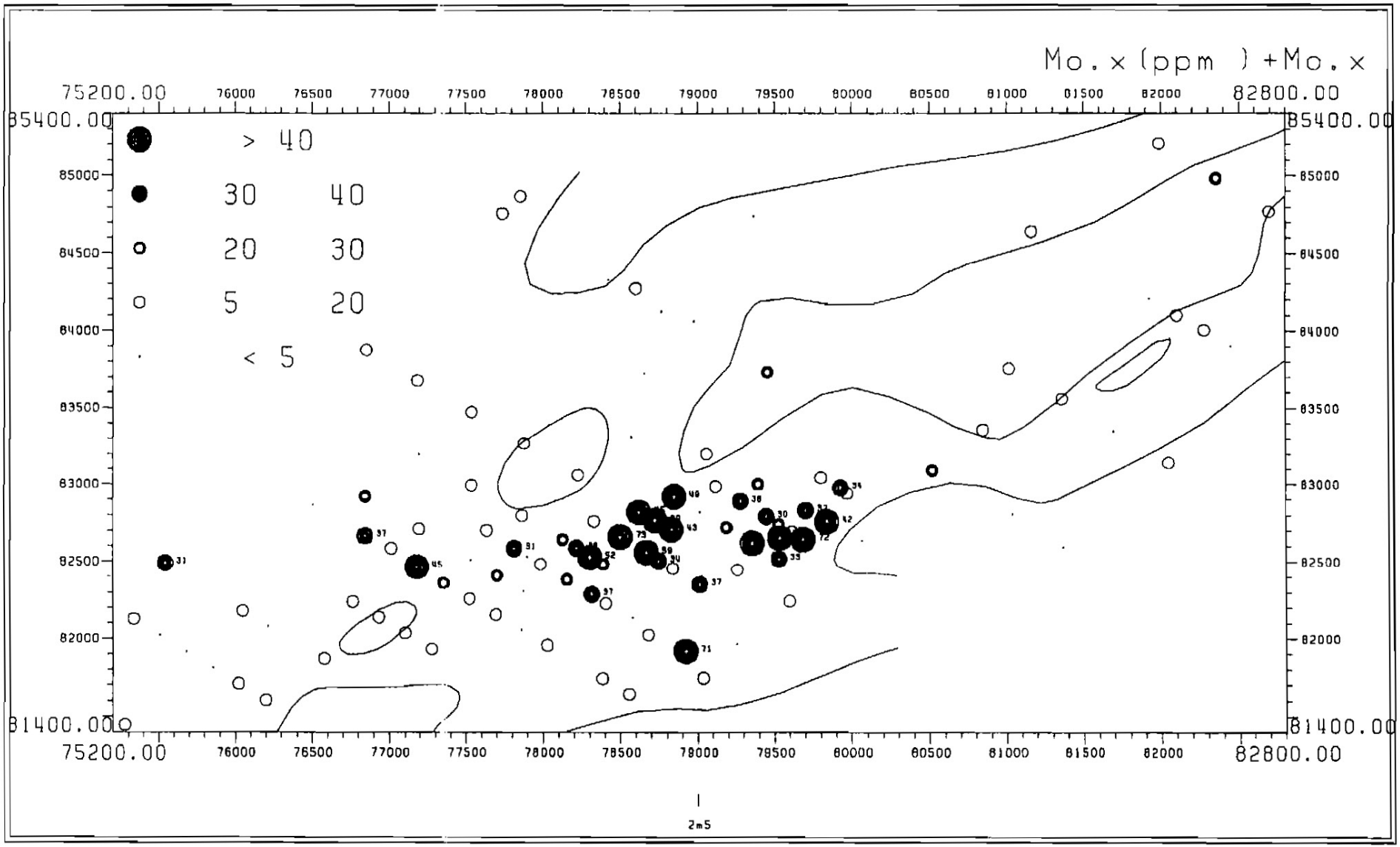
Mo.x(ppm)+Mo.x
> 40
30 40
20 30
5 20
< 5
75200.00
76000
76500
77000
77500
78000
78500
79000
79500
80000
80500
81000
81500
82000
82800.00
85400.00
85000
84500
84000
83500
83000
82500
82000
81400.00
2m5

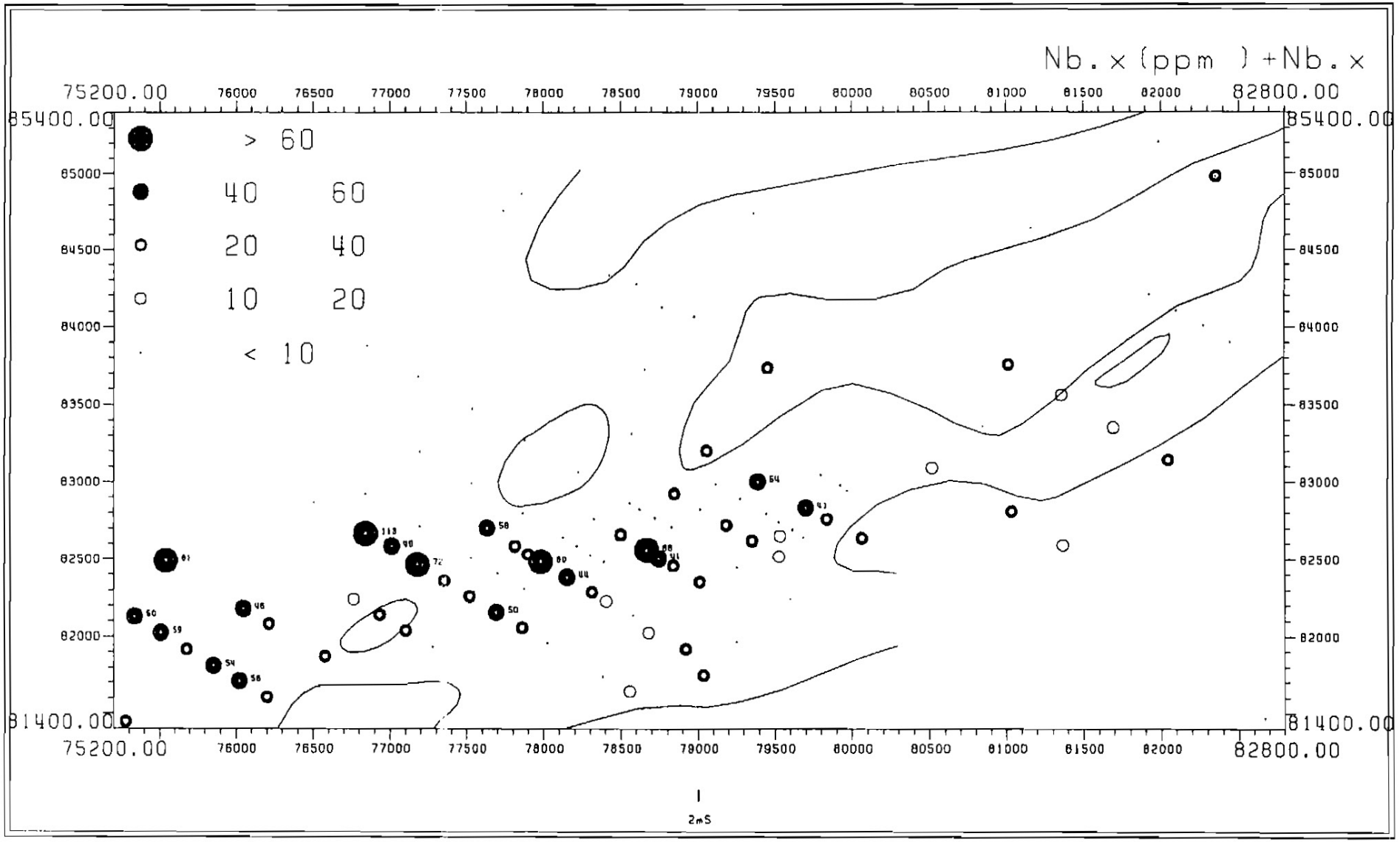
Nb.x(ppm)+Nb.x
> 60
40 60
20 40
10 20
< 10
75200.00
76000
76500
77000
77500
78000
78500
79000
79500
80000
80500
81000
81500
82000
82800.00
85400.00
85000
84500
84000
83500
83000
82500
82000
81400.00
2mS

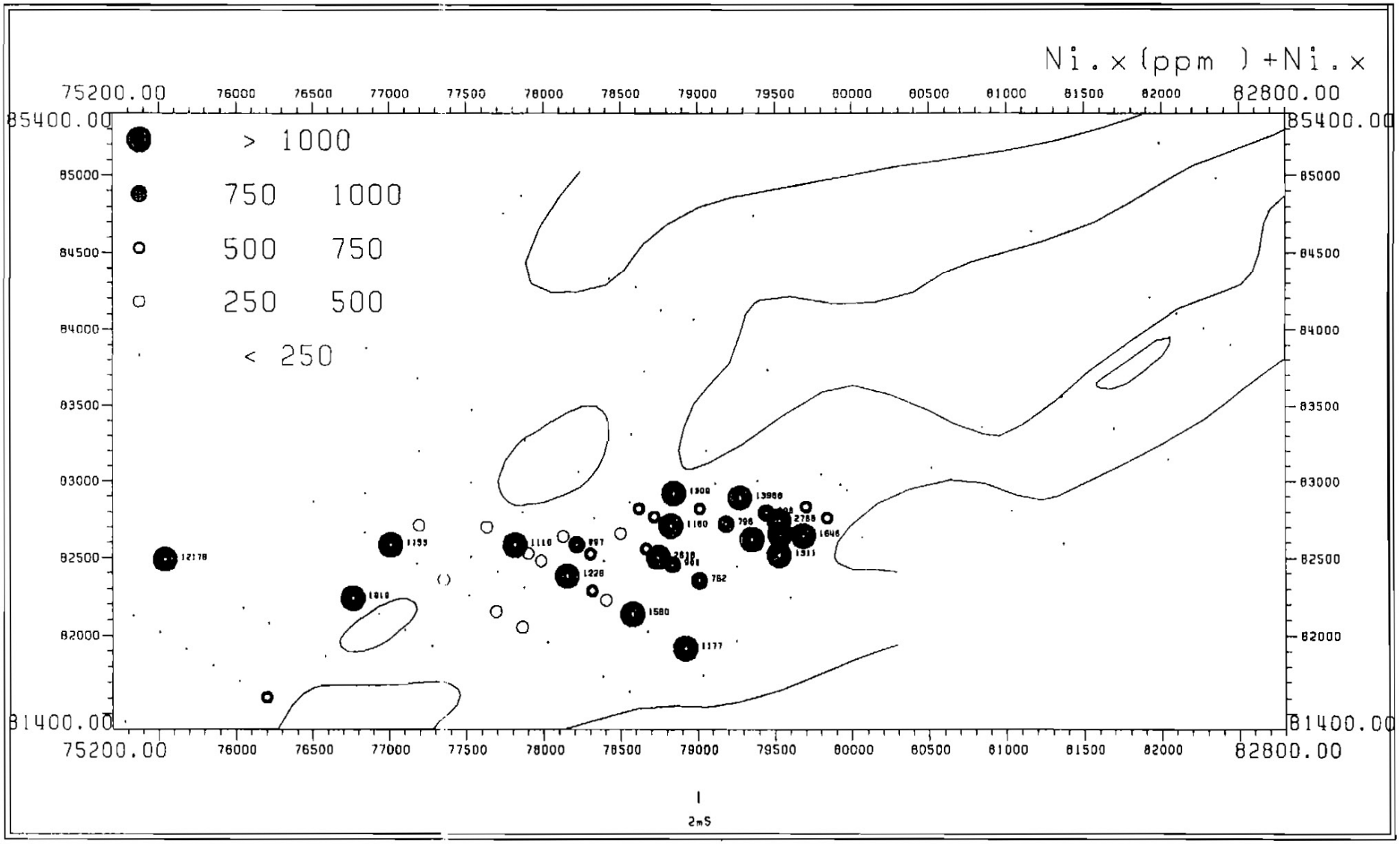
Ni.x(ppm)+Ni.x
> 1000
750 1000
500 750
250 500
< 250
75200.00
76000
76500
77000
77500
78000
78500
79000
79500
80000
80500
81000
81500
82000
82800.00
85400.00
85000
84500
84000
83500
83000
82500
82000
81400.00
2mS

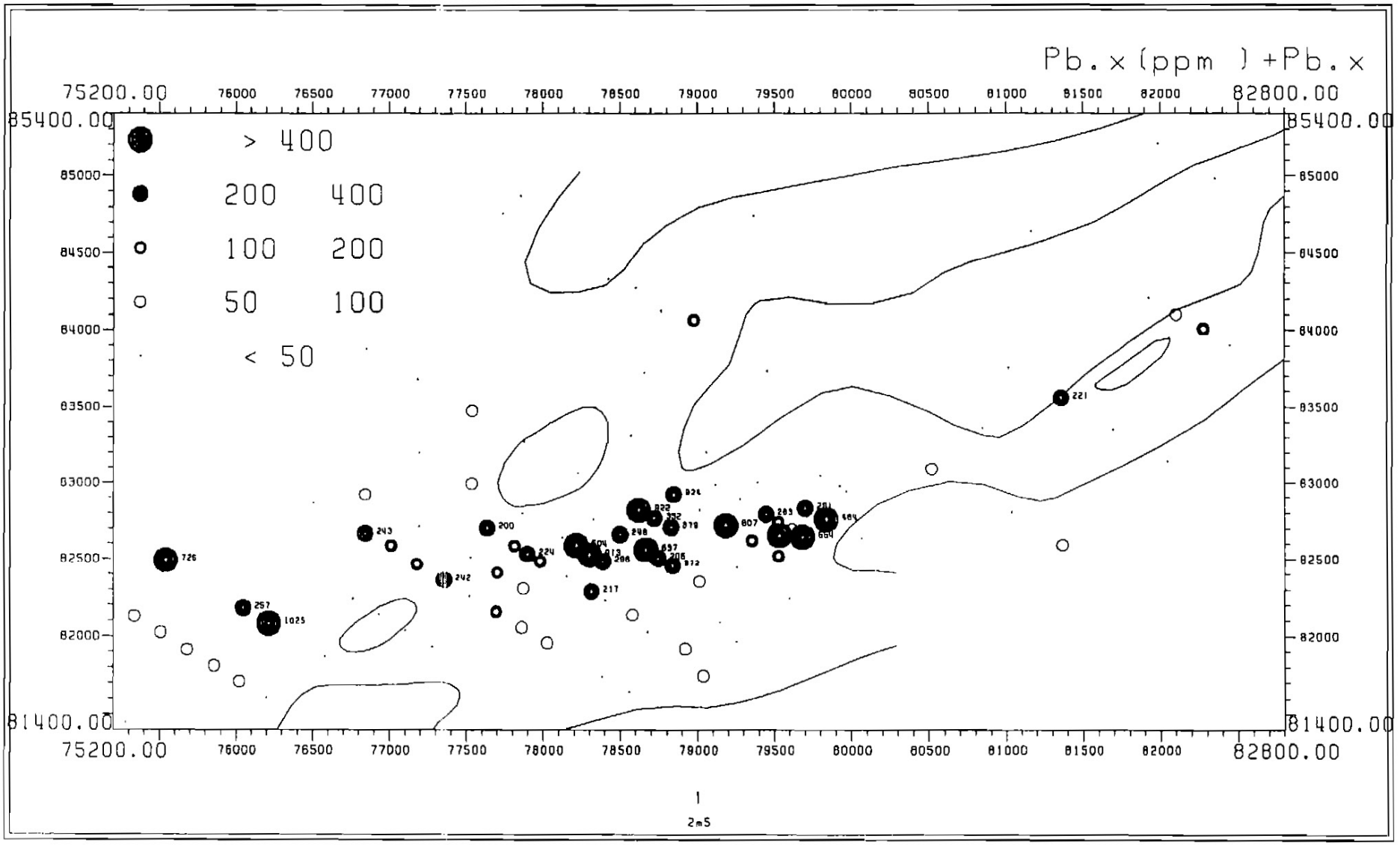
Pb.x (ppm) +Pb.x
> 400
200 400
100 200
50 100
< 50
75200.00
82800.00
85400.00
81400.00
2mS

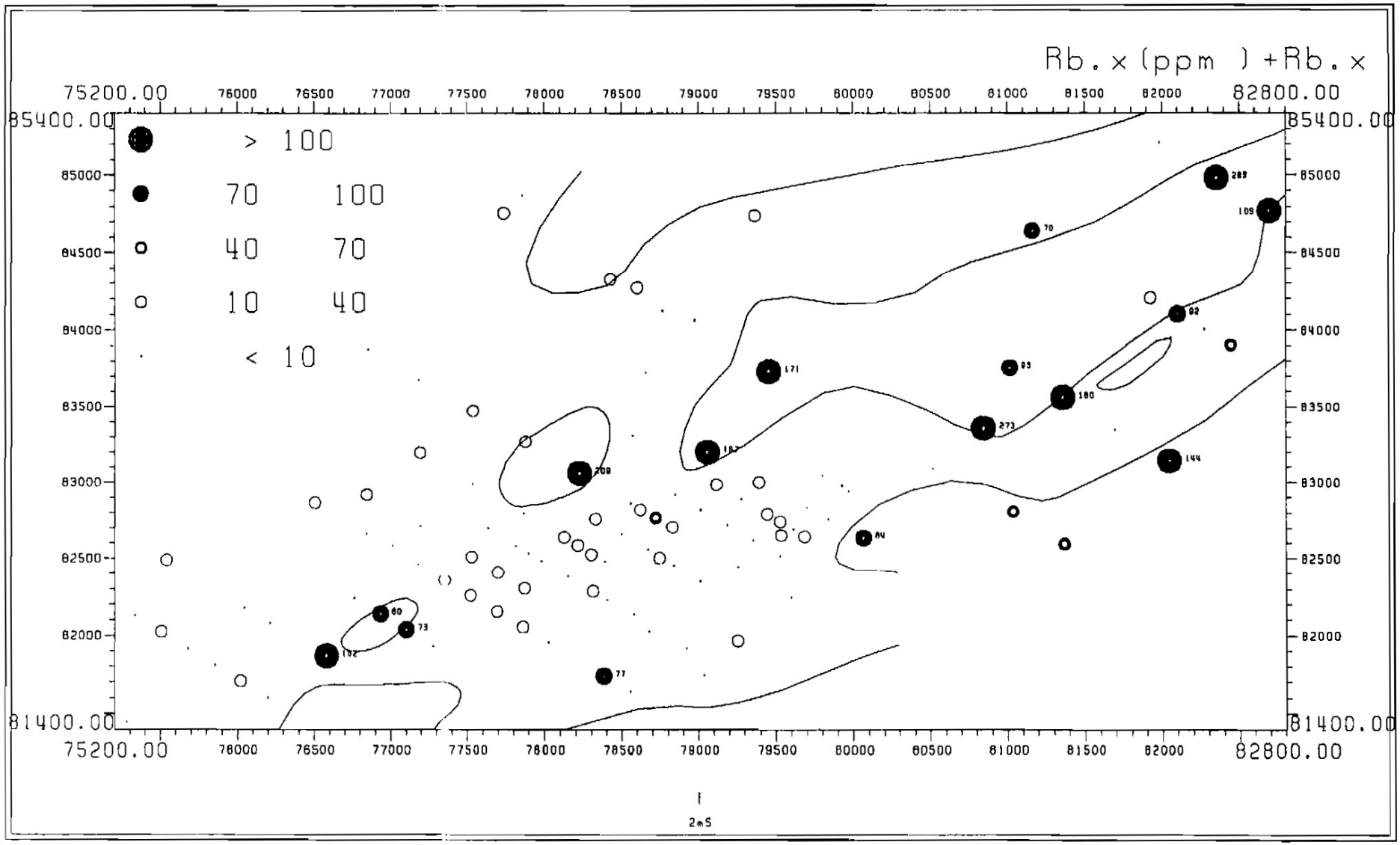
Rb.x(ppm)+Rb.x
> 100
70 100
40 70
10 40
< 10
75200.00
76000
76500
77000
77500
78000
78500
79000
79500
80000
80500
81000
81500
82000
82800.00
85400.00
85000
84500
84000
83500
83000
82500
82000
81400.00
2mS

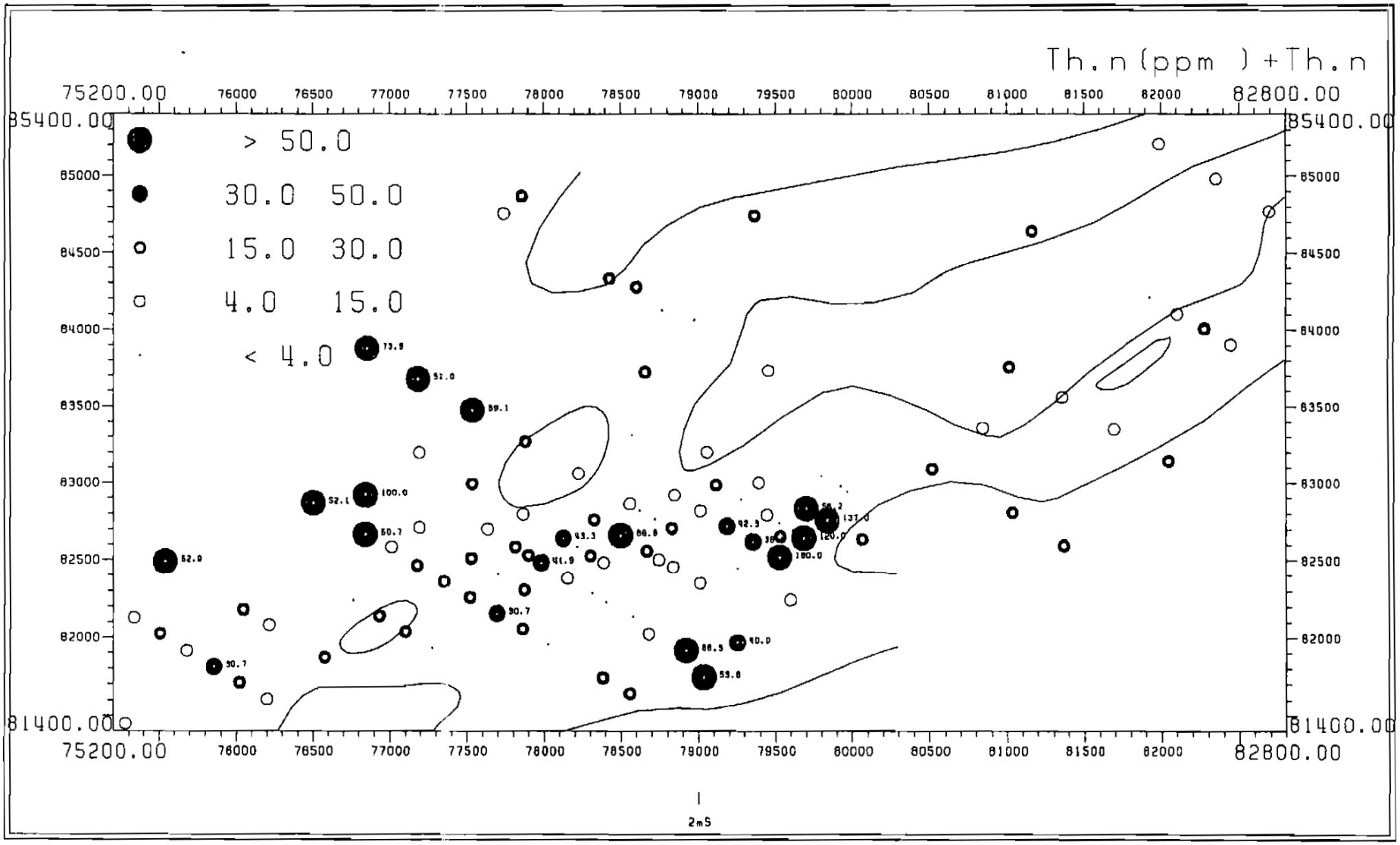
Th.n (ppm) + Th.n
> 50.0
30.0 50.0
15.0 30.0
4.0 15.0
< 4.0
75200.00
76000
76500
77000
77500
78000
78500
79000
79500
80000
80500
81000
81500
82000
82800.00
85400.00
85000
84500
84000
83500
83000
82500
82000
81400.00
2mS

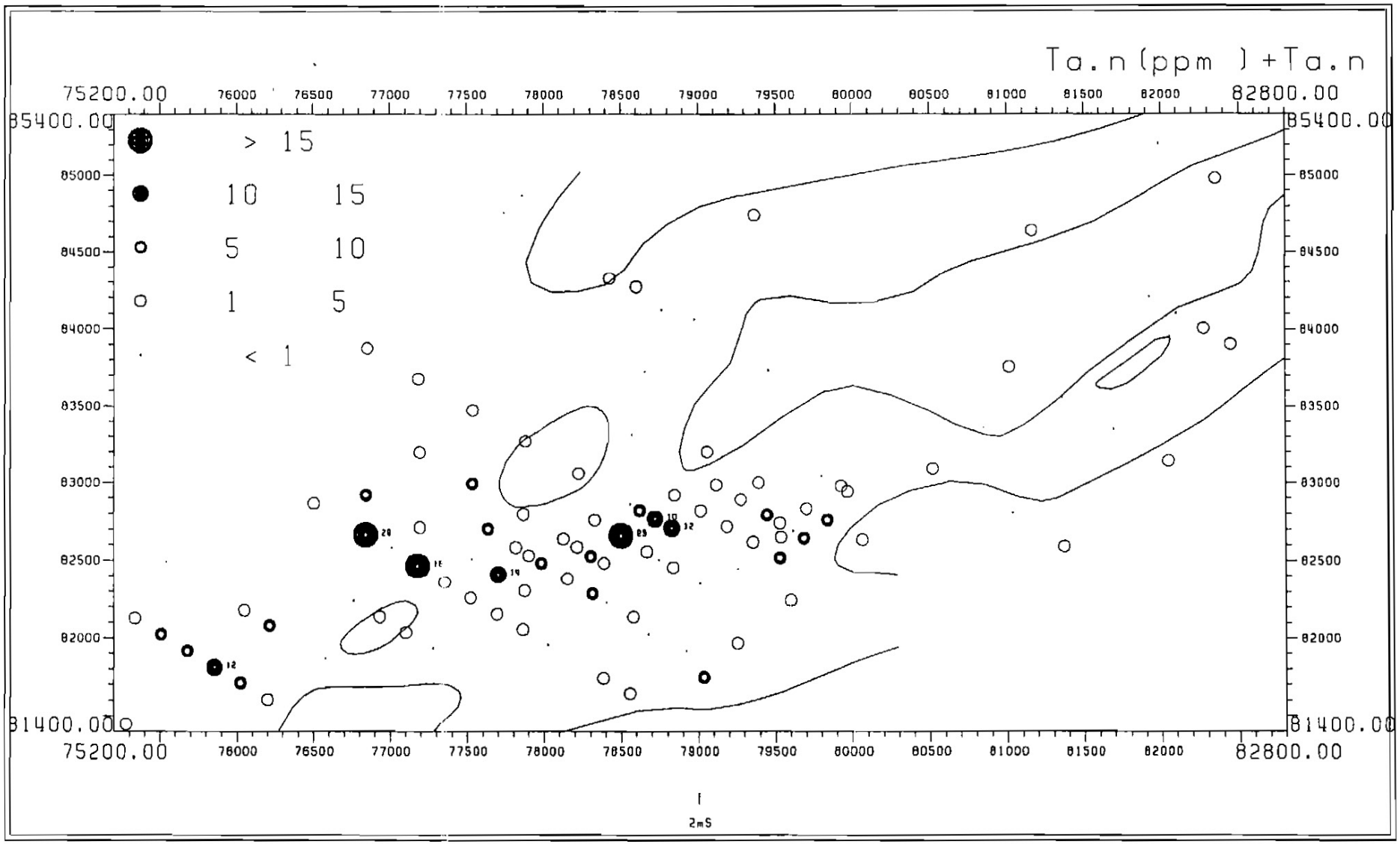
Ta.n(ppm)+Ta.n
> 15
10 15
5 10
1 5
< 1
75200.00
76000
76500
77000
77500
78000
78500
79000
79500
80000
80500
81000
81500
82000
82800.00
85400.00
85000
84500
84000
83500
83000
82500
82000
81400.00
2mS

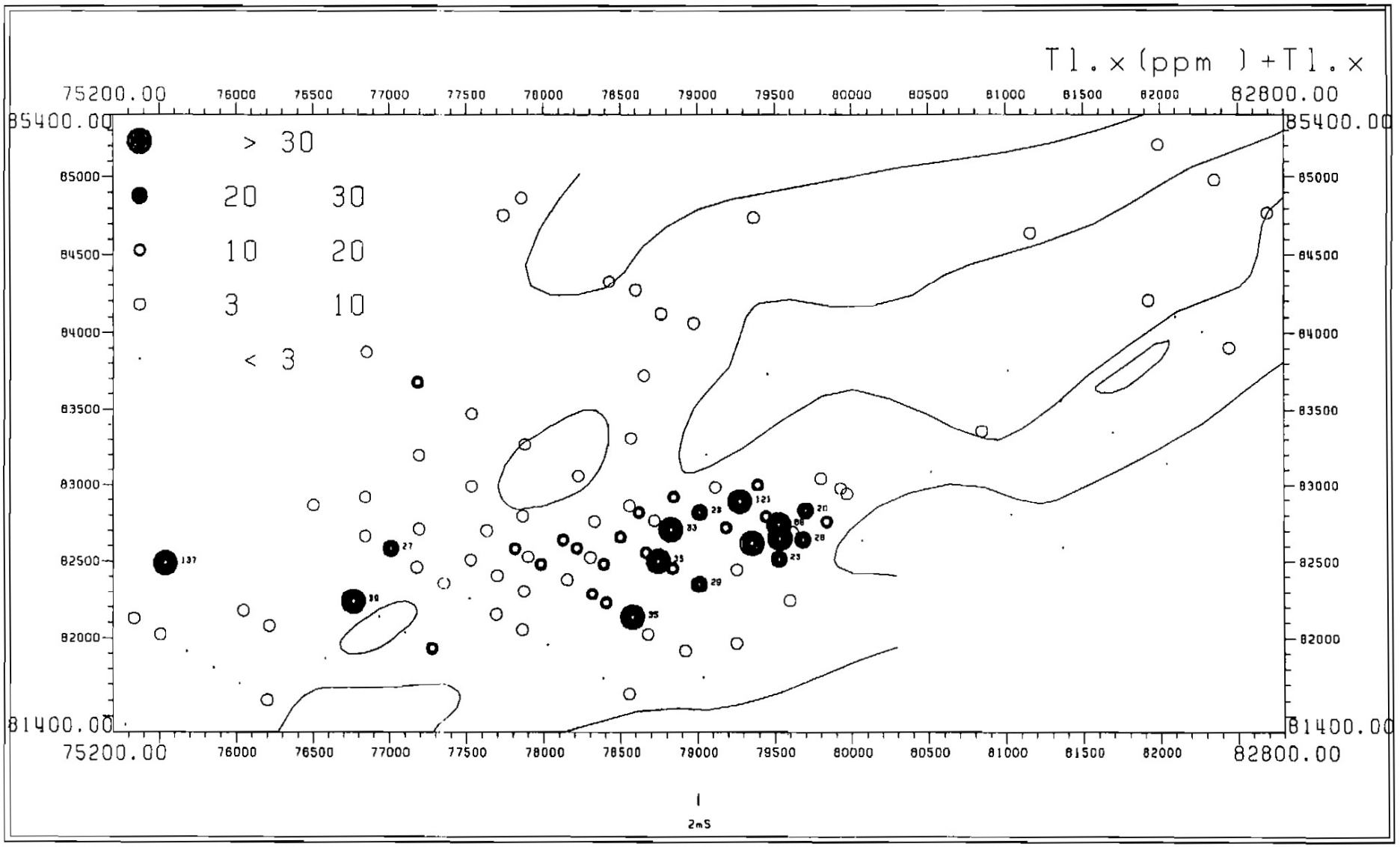
Tl.x(ppm)+Tl.x
> 30
20 30
10 20
3 10
< 3
75200.00
76000
76500
77000
77500
78000
78500
79000
79500
80000
80500
81000
81500
82000
82800.00
85400.00
85000
84500
84000
83500
83000
82500
82000
81400.00
2mS

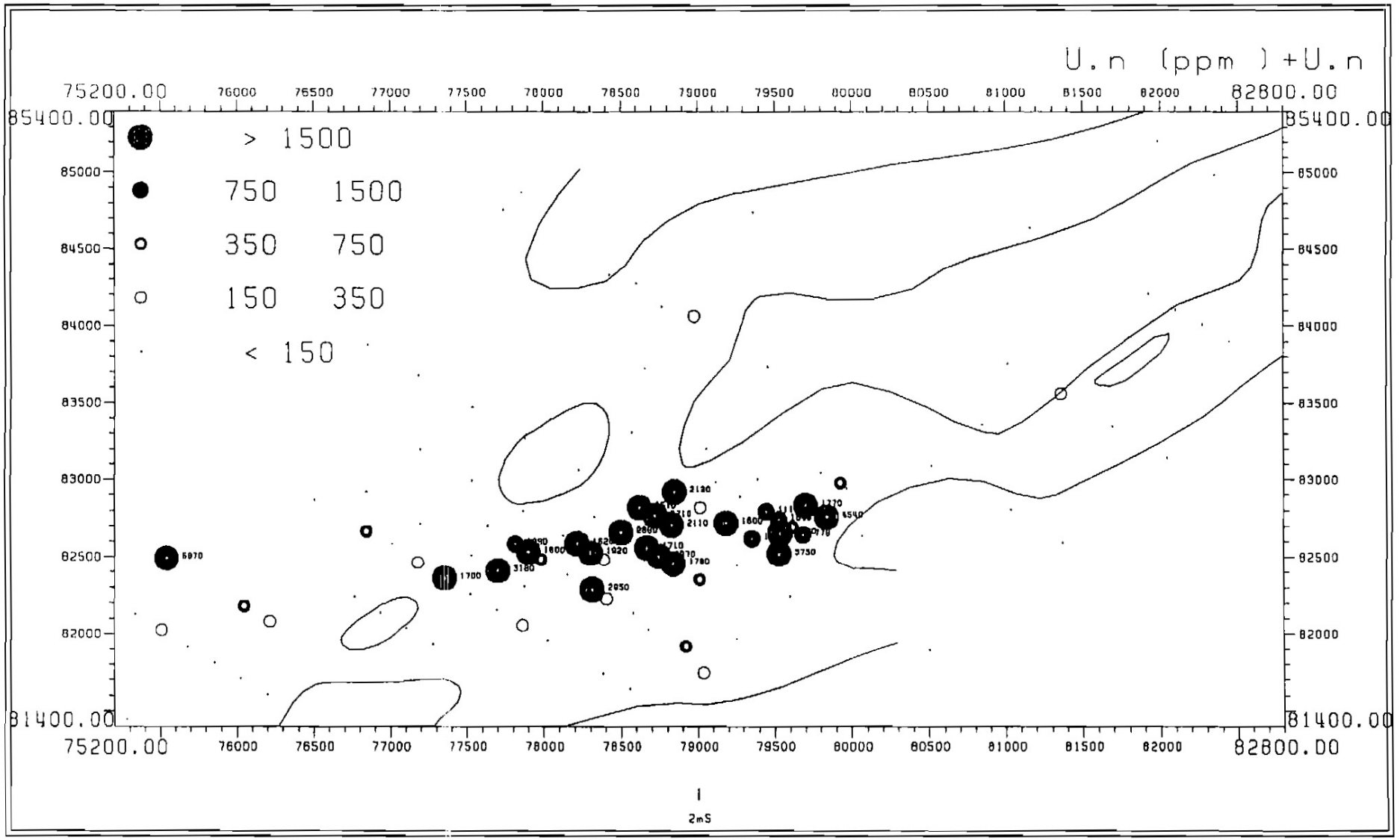
U.n (ppm) +U.n
> 1500
750 1500
350 750
150 350
< 150
75200.00
76000
76500
77000
77500
78000
78500
79000
79500
80000
80500
81000
81500
82000
82800.00
85400.00
85000
84500
84000
83500
83000
82500
82000
81400.00
2mS

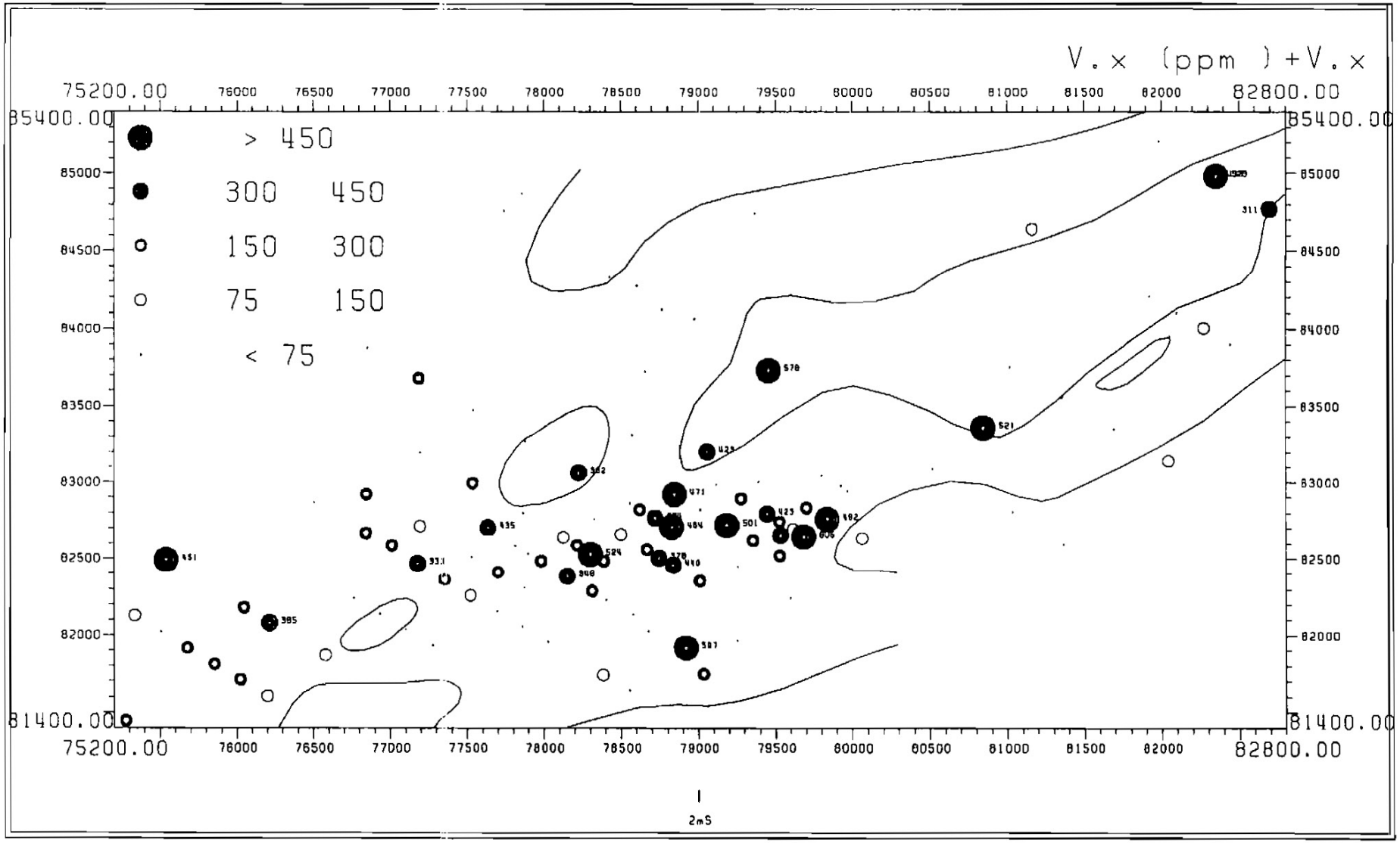
V.x (ppm) +V.x
> 450
300 450
150 300
75 150
< 75
75200.00
78000
76500
77000
77500
78000
78500
79000
79500
80000
80500
81000
81500
82000
82800.00
85400.00
85000
84500
84000
83500
83000
82500
82000
81400.00
2mS

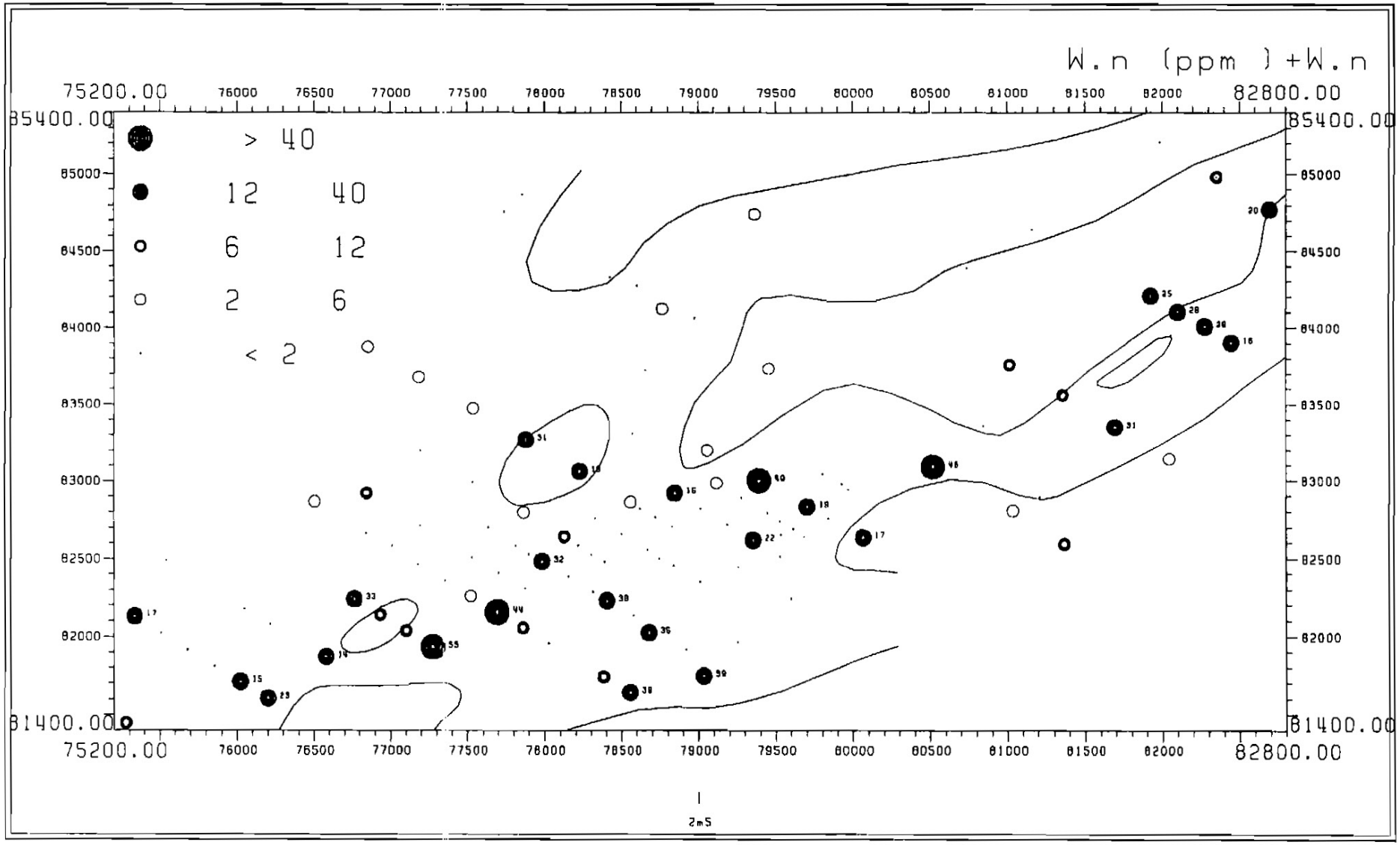
W.n (ppm) +W.n
> 40
12 40
6 12
2 6
< 2
75200.00
76000
76500
77000
77500
78000
78500
79000
79500
80000
80500
81000
81500
82000
82800.00
85400.00
85000
84500
84000
83500
83000
82500
82000
81400.00
2mS

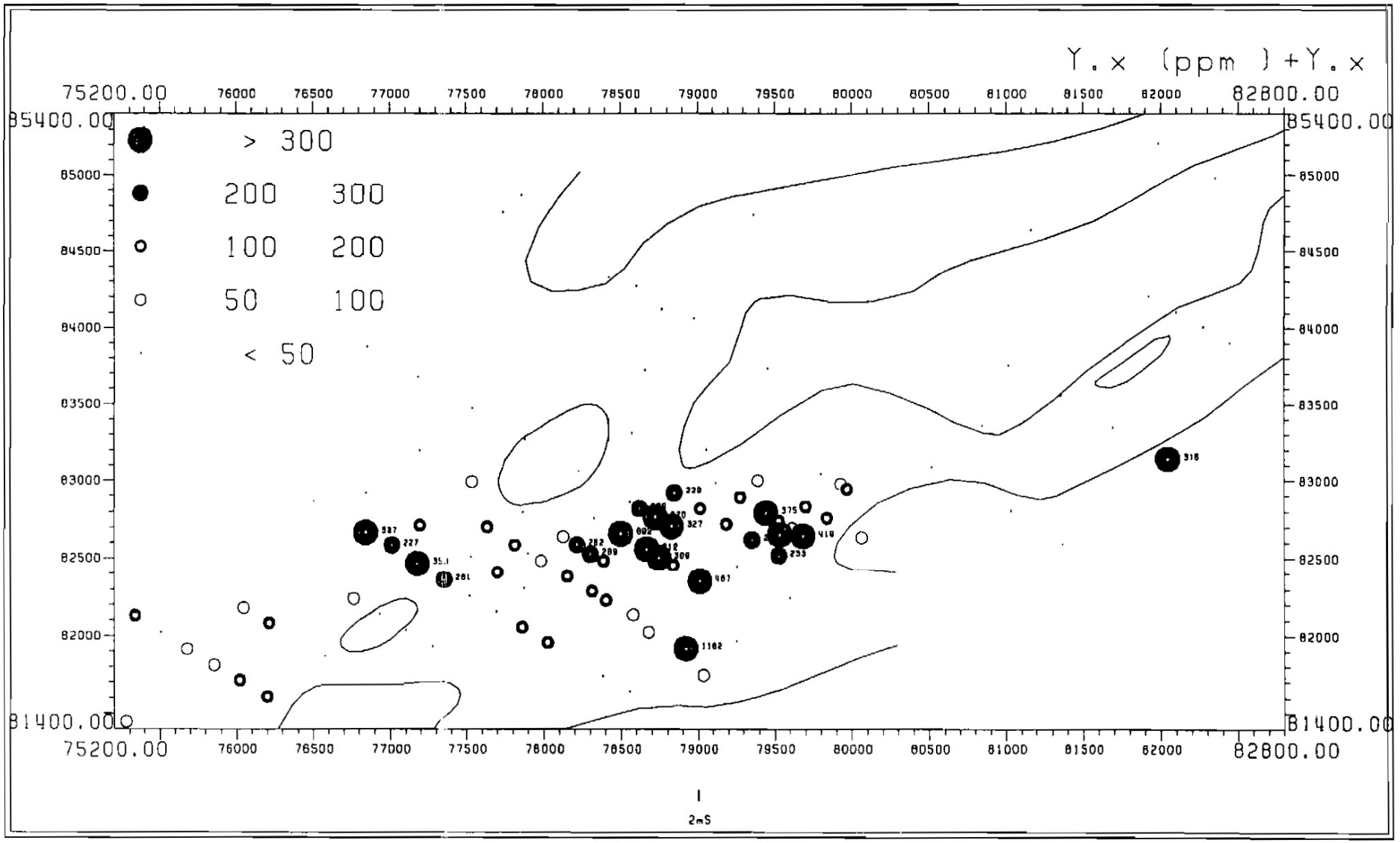
Y.x (ppm) +Y.x
> 300
200 300
100 200
50 100
< 50
75200.00
76000
76500
77000
77500
78000
78500
79000
79500
80000
80500
81000
81500
82000
82800.00
85400.00
85000
84500
84000
83500
83000
82500
82000
81400.00
2mS

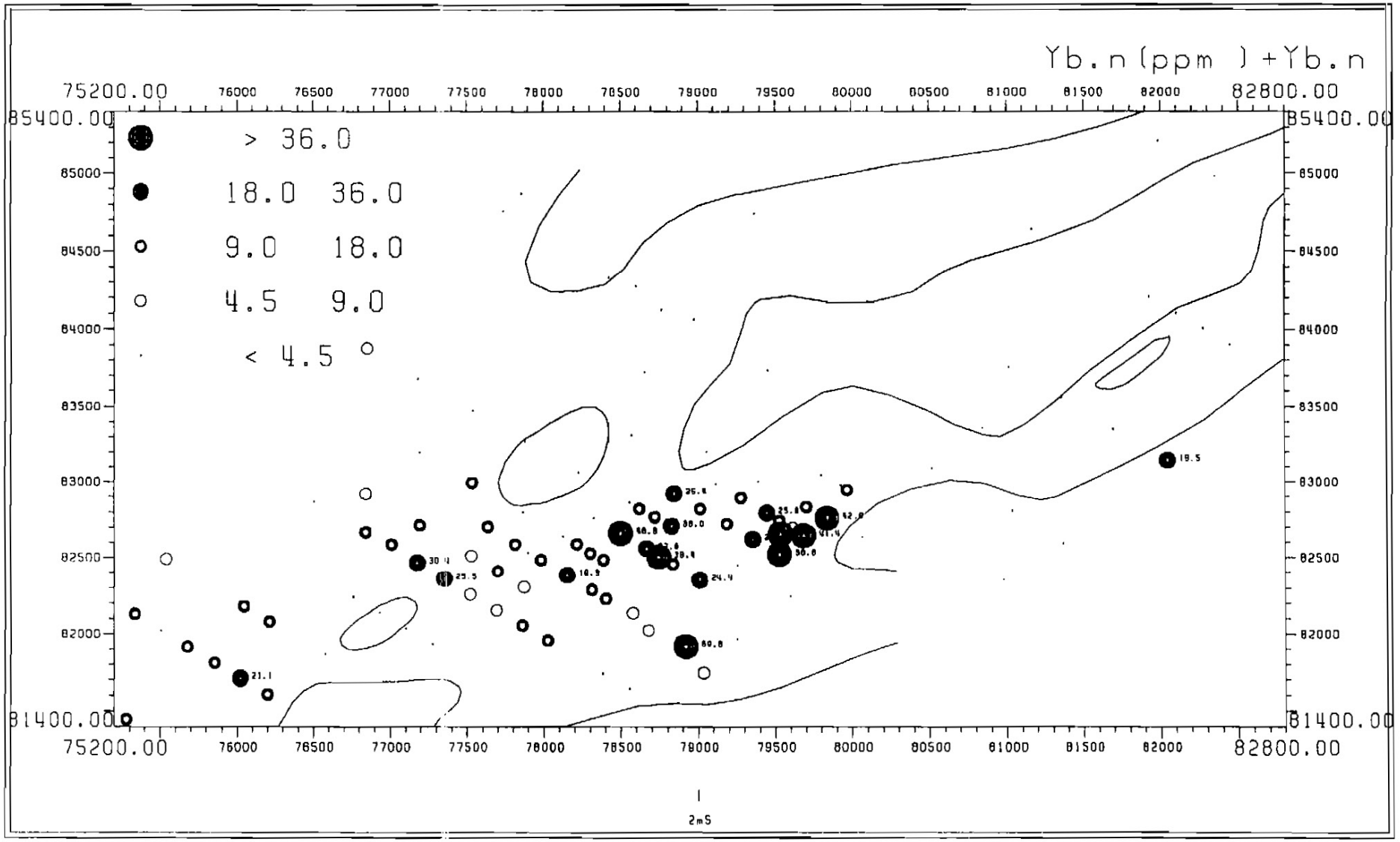
Yb.n(ppm)+Yb.n
> 36.0
18.0 36.0
9.0 18.0
4.5 9.0
< 4.5
75200.00
76000
76500
77000
77500
78000
78500
79000
79500
80000
80500
81000
81500
82000
82800.00
85400.00
85000
84500
84000
83500
83000
82500
82000
81400.00
2mS

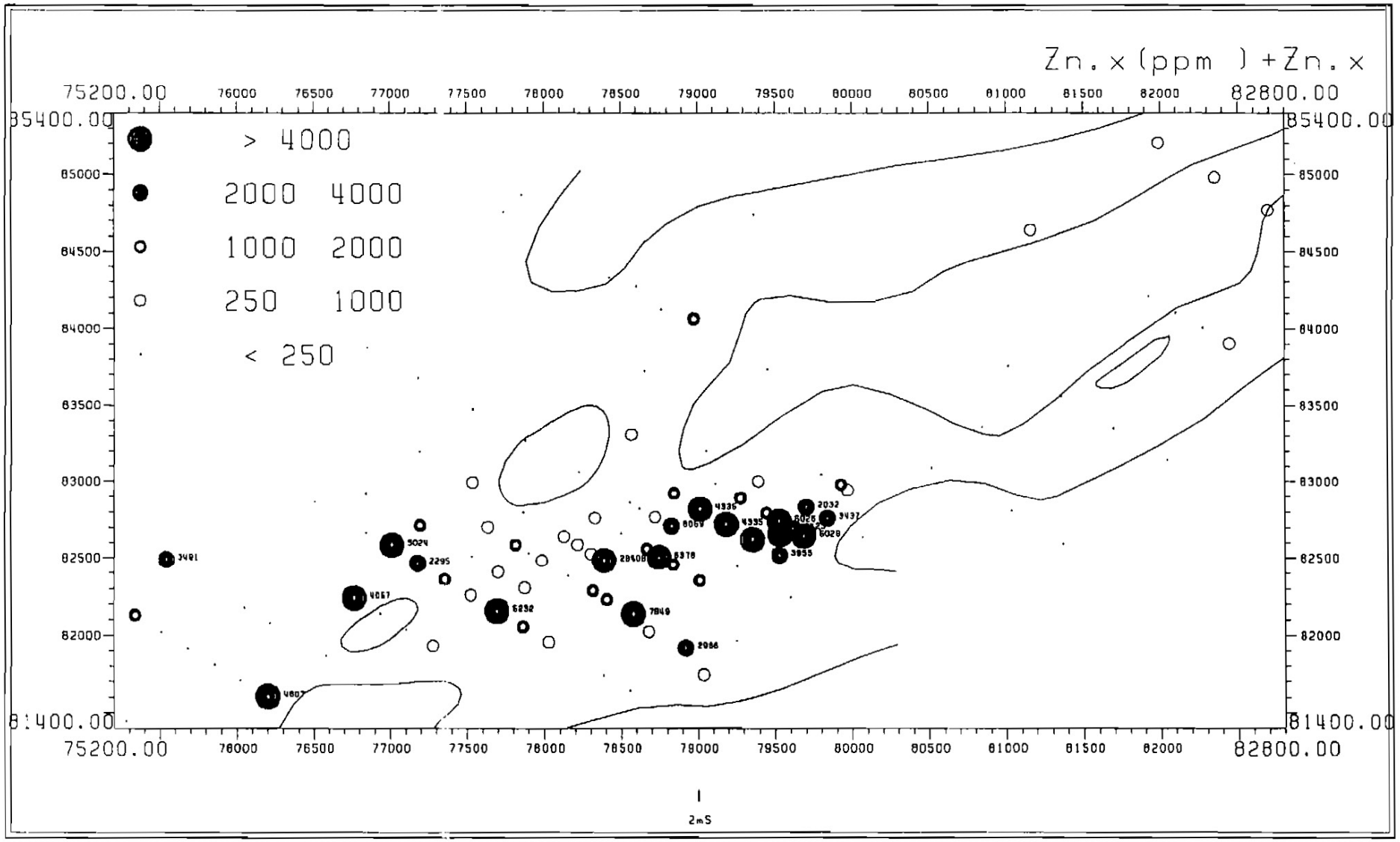
Zn.x (ppm) +Zn.x
> 4000
2000 4000
1000 2000
250 1000
< 250
75200.00
76000
76500
77000
77500
78000
78500
79000
79500
80000
80500
81000
81500
82000
82800.00
85400.00
85000
84500
84000
83500
83000
82500
82000
81400.00
2mS

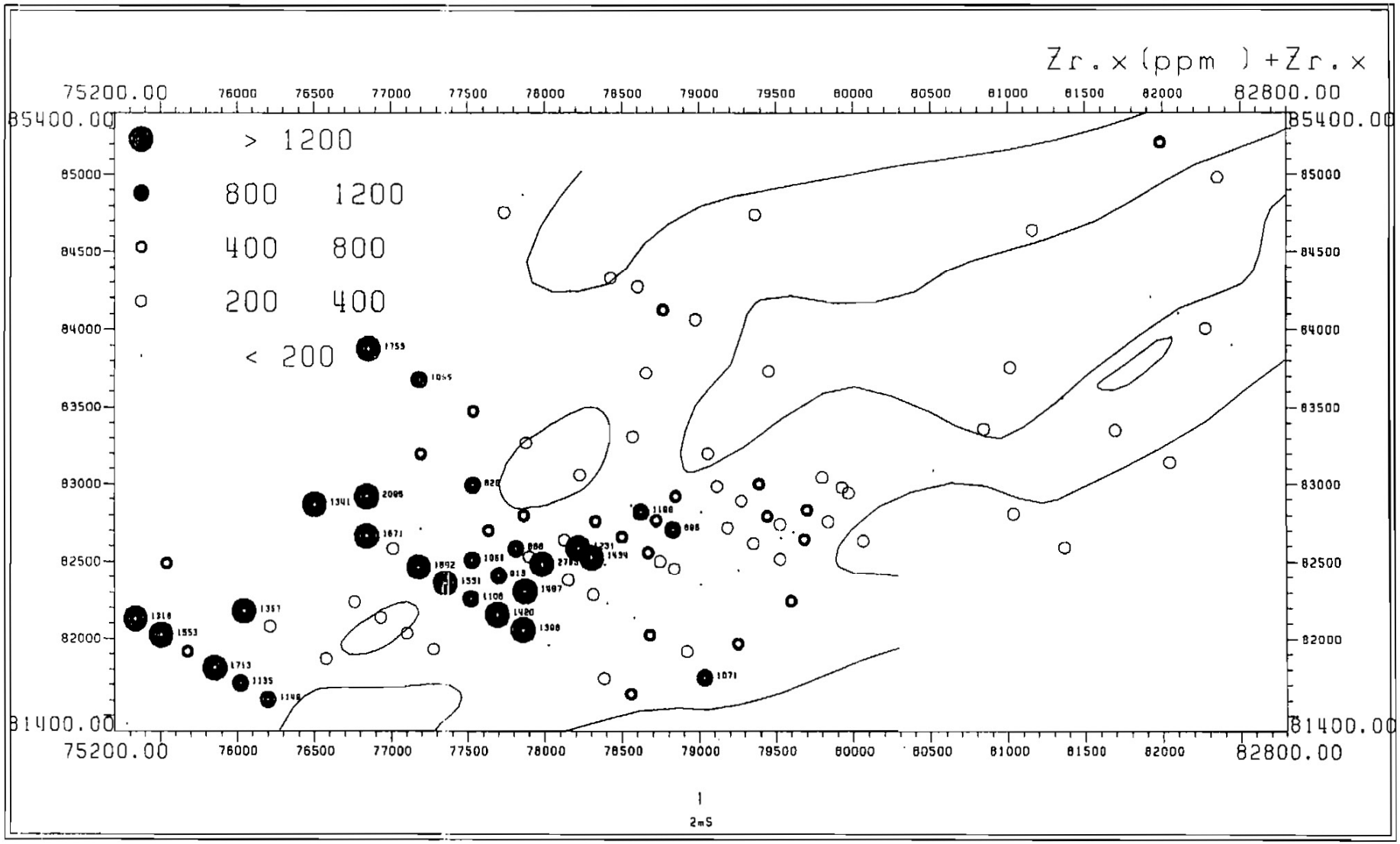
Zr.x(ppm)+Zr.x
> 1200
800 1200
400 800
200 400
< 200
75200.00
76000
76500
77000
77500
78000
78500
79000
79500
80000
80500
81000
81500
82000
82800.00
85400.00
85000
84500
84000
83500
83000
82500
82000
81400.00
1
2mS

APPENDIX 2

GEOCHEMISTRY OF THE AMBASSADOR PALAEOCHANNEL SAMPLES

Table A.2.1: Sample numbers and positions

CSIRO 00-	PNC Hole	Easting (m)	Northing (m)	Upper Depth (m)	Lower Depth (m)
6001	666	74571	76789	50	51
6004	358	75072	76507	51	52
6006	667	75672	76279	49	50
6010	65	76894	76049	33	35
6011	41	77135	76004	40	41
6014	1209	76297	78861	44	46
6015	1020	76811	78555	24	26
6016	1019	77671	78043	36	37
6018	993	78102	77508	28	30
6020	1018	78569	77508	46	48
6028	1489	75337	82127	39.4	39.8
6029	1488	75508	82023	39.75	40.35
6030	1387	75678	81914	38.51	38.71
6031	1360	75855	81809	37.76	38.66
6034	1388	76022	81709	39.23	39.33
6035	1487	76201	81604	49.8	50.44
6036	1487	76201	81604	51.04	51.8
6037	1490	75541	82489	41.29	41.39
6039	1412	76048	82178	39	41
6040	1362	76216	82079	41	41.8
6041	1338	76580	81870	39	41
6042	1391	76765	82239	44.8	45.2
6045	1298	76935	82138	37	39
6046	1299	77104	82037	27	29
6049	1300	77277	81933	49	51
6054	1365	76843	82665	41	42
6056	1366	77012	82584	41.9	42.9
6058	1367	77179	82464	37.25	37.95
6059	1305	77355	82359	33	35
6061	1306	77522	82259	39	41
6062	1368	77695	82155	45.2	45.4
6063	1369	77863	82055	42.5	43.5
6064	1393	78027	81957	41.8	42
6065	1303	78384	81741	49	51
6067	1307	78558	81642	45	47
6068	1337	77636	82701	41	43
6070	1310	77815	82584	43	45
6071	1404	77900	82531	39	41
6072	1370	77984	82483	41.5	42.3
6074	1371	78154	82382	38.84	39.8
6075	1372	78315	82286	45.38	46.3
6077	1407	78407	82228	46.51	47
6079	1408	78580	82136	45.9	47.1

Table A.2.1: Sample numbers and positions (continued)

CSIRO 00-	PNC Hole	Easting (m)	Northing (m)	Upper Depth (m)	Lower Depth (m)
6080	1215	78680	82025	42	44
6081	1493	78922	81918	46.8	47.35
6082	1224	79036	81746	40	42
6085	1395	78499	82659	42.22	42.3
6086	1374	78668	82558	42.8	43.8
6088	1415	78747	82503	43.6	44.5
6089	1375	78839	82456	46.17	47.2
6091	1396	79013	82352	45.6	45.7
6093	1376	78847	82921	43.9	44.8
6095	1377	79015	82820	40.15	40.9
6096	1378	79185	82719	38.08	39.01
6097	1397	79354	82619	39.08	39.9
6099	1416	79528	82518	37.3	37.8
6113	1236	79058	83201	30	32
6114	1232	79391	83002	38	40
6116	1233	79701	82833	38	40
6117	1400	79837	82759	40.35	40.41
6120	1234	80063	82635	40	42
6121	994	79455	83733	27	29
6122	1322	80517	83092	41	43
6126	1469	81035	82807	8	10
6127	1470	81367	82592	6	8
6128	1355	81013	83757	23	25
6129	1356	81357	83560	37	39
6131	1357	81693	83350	33	35
6132	1450	82044	83143	28	29
6133	1353	81923	84206	19	21
6134	1446	82100	84101	34	36
6135	1354	82275	84006	33	35
6137	1445	82446	83904	36	38
6138	1323	82352	84981	41	43
6139	1324	82692	84769	43	45
6140	1325	83040	84580	39	41
6142	1436	83255	84550	40	42
6143	1326	83373	84370	27	29
6144	1045	85431	83169	10	12
6145	1049	83710	84160	38	40
6146	1431	83732	85273	44	46
6147	1351	84085	85072	45	47
6148	1352	84432	84855	33	35
6150	1440	85125	84425	26	28
6151	1430	85298	84920	34	36
6152	1346	84783	85712	47	49

Table A.2.1: Sample numbers and positions (continued)

CSIRO 00-	PNC Hole	Easting (m)	Northing (m)	Upper Depth (m)	Lower Depth (m)
6154	1330	85135	85494	23	25
6155	1347	85479	85295	37	39
6156	1577	79533	82653	37.2	38.2
6157	324	74771	80764	34	35
6159	1026	75198	80510	40	42
6161	1148	75596	80272	38	40
6162	1151	75960	81036	54	56
6164	1212	76306	80827	38	40
6165	1213	75279	81446	38	40
6166	1226	74935	81653	34	36
6167	657	74656	79838	41	42
6170	1021	75952	79066	38	40
6171	1022	75006	79629	34	36
6172	1023	74143	80144	38	40
6174	1023	74143	80144	40	42
6175	1171	76845	82920	36	38
6176	1172	77195	82711	40	42
6177	1173	77530	82511	36	38
6178	1492	77702	82408	43.2	44.2
6180	1174	77873	82306	46	48
6181	1179	77194	83197	46	48
6182	1178	77535	82993	46	48
6183	1177	77866	82796	36	38
6184	1394	78127	82640	45.7	46.65
6185	1176	78216	82587	36	38
6186	1409	78304	82526	38.4	32
6187	1256	78390	82483	41.4	42.4
6188	1207	79253	81968	50	52
6189	1293	76853	83876	35	37
6190	1291	77186	83677	29	31
6191	1315	77537	83474	41	43
6192	1316	77880	83269	17	19
6194	1216	78226	83062	34	36
6196	1217	78560	82863	50	52
6197	1525	78622	82820	45.5	46.5
6198	1257	78722	82767	44.9	45.3
6199	1514	78829	82707	44.2	45.2
6200	1219	79256	82448	40	42
6201	1220	79598	82244	24	26
6207	1479	78570	83310	50	52
6208	1501	79117	82987	46.8	47.8
6209	1398	79276	82893	37.4	37.6
6210	1379	79445	82792	36.95	37.47

Table A.2.1: Sample numbers and positions (continued)

CSIRO 00-	PNC Hole	Easting (m)	Northing (m)	Upper Depth (m)	Lower Depth (m)
6211	1509	79526	82741	35.2	36.2
6212	1399	79614	82692	41.7	42.3
6213	1510	79684	82644	38.76	39.76
6214	1472	78656	83723	40	42
6215	1317	79798	83045	37	39
6216	1506	79925	82979	41.14	41.34
6217	1401	79967	82945	42.3	42.5
6218	1443	77859	84867	60	62
6219	1319	77741	84755	49	51
6221	1526	78602	84273	42	43
6222	1320	78767	84122	53	55
6223	1468	78977	84062	52	54
6224	1451	80845	83359	50	52
6225	1478	79366	84740	40	42
6226	1447	81160	84640	44	46
6227	1048	81988	85206	42	44
6228	1323	82352	84981	39	41
6231	1324	82692	84768	45	47
6232	1304	76505	82867	33	35
6234	1314	78330	82760	45	47

Table A.2.2: Geochemistry of the Ambassador palaeochannel samples

Concentrations are expressed in % for major elements and in ppm for all trace elements except Au (ppb).
All major elements were analysed by fusion-XRF, and trace elements were analysed by either neutron activation analysis (n), XRF pressed powder (x) or XRF fusion (f).

Sample	SiO2	Al2O3	Fe203	MnO	MgO	CaO	Na2O	K2O	TiO2	P2O5	S	LOI
6001	26.06	22.07	0.63	0.0022	0.40	0.36	1.71	0.45	3.34	0.072	0.77	44.21
6004	57.60	17.73	1.86	0.0116	0.30	0.27	1.12	0.24	0.89	0.020	0.42	19.80
6006	43.14	34.01	0.94	0.0026	0.30	0.16	1.54	0.44	2.38	0.045	0.59	17.35
6010	57.14	28.53	0.97	0.0052	0.20	0.32	0.38	0.40	1.61	0.029	0.52	11.98
6011	46.25	33.16	1.00	0.0039	0.28	0.10	1.20	0.55	1.18	0.029	0.22	16.21
6014	72.70	11.04	1.31	0.0164	0.12	0.16	0.36	0.10	0.99	0.017	0.6	12.66
6015	49.22	4.84	0.69	0.0119	0.01	0.00	0.05	0.73	0.23	0.013	2.27	42.26
6016	88.00	4.14	1.89	0.0096	0.32	0.02	0.03	1.41	0.19	0.038	0.46	3.44
6018	59.02	17.97	2.51	0.0071	0.34	0.01	0.18	2.09	2.52	0.018	1.3	13.61
6020	62.60	18.59	3.03	0.0021	0.94	0.01	0.14	4.33	2.54	0.024	0.73	7.12
6028	34.51	1.73	1.51	0.0124	0.52	0.88	1.11	0.09	1.86	0.023	3.66	54.35
6029	64.95	17.56	1.09	0.0145	0.13	0.15	0.47	0.31	2.35	0.031	0.78	12.76
6030	10.22	3.06	0.10	0.001	0.59	0.87	0.90	0.11	1.09	0.011	3.13	79.89
6031	29.95	1.31	0.13	0.0002	0.58	0.81	1.16	0.16	2.53	0.019	2.54	60.56
6034	39.18	15.79	0.93	0.0085	0.48	0.64	0.74	0.28	2.13	0.028	1.15	38.59
6036	74.87	0.81	0.84	0.0262	0.13	0.16	0.43	0.02	1.07	0.009	2.51	19.00
6037	27.18	5.41	4.05	0.0053	0.10	0.17	0.41	0.03	6.42	0.155	10.58	40.25
6039	52.86	3.27	0.54	0.0053	0.39	0.46	1.48	0.09	2.03	0.017	2.29	36.56
6040	7.11	2.75	0.09	0.001	0.56	0.73	1.07	0.07	1.49	0.009	4.57	81.41
6041	65.66	16.70	2.13	0.0148	0.60	0.07	0.72	1.91	0.70	0.070	0.79	8.02
6042	78.31	2.87	6.51	0.0409	0.09	0.10	0.33	0.03	0.20	0.011	5.28	6.92
6045	66.22	20.16	1.01	0.0069	0.42	0.08	0.84	1.24	0.73	0.157	0.31	9.53
6046	65.32	16.41	2.46	0.0098	0.31	0.07	0.65	1.13	0.71	0.097	0.51	8.59
6049	95.72	0.46	1.75	0.0245	0.03	0.04	0.15	0.01	0.10	0.006	0.48	2.31
6054	38.16	8.71	0.27	0.001	0.53	0.82	0.82	0.16	5.41	0.056	1.77	42.09
6056	9.11	3.37	3.76	0.0021	1.18	1.96	2.22	0.17	2.18	0.016	10.11	64.04
6058	64.94	8.44	1.02	0.005	0.18	0.30	0.63	0.06	2.82	0.025	1.14	19.77
6059	50.27	10.66	1.30	0.0085	0.47	0.46	1.79	0.16	1.63	0.029	2.77	29.65
6061	37.88	18.48	0.60	0.0047	0.68	0.62	2.54	0.23	1.42	0.022	2	36.17
6062	60.71	18.01	1.95	0.0337	0.17	0.16	0.47	0.26	1.66	0.021	1.93	14.50
6063	51.78	18.47	0.96	0.0188	0.29	0.30	0.72	0.19	1.51	0.019	3.82	22.33
6064	2.91	1.52	0.05	0.0014	1.07	1.54	1.64	0.21	0.06	0.000	12.7	76.73
6065	65.74	17.97	3.33	0.011	0.40	0.06	0.52	1.25	0.69	0.074	1.25	9.19
6067	76.99	11.83	1.84	0.0249	0.18	0.06	0.77	0.09	0.77	0.017	0.5	7.43
6068	22.49	3.53	0.34	0.004	1.05	1.43	2.76	0.32	2.48	0.017	3.6	61.50
6070	80.82	1.95	1.19	0.0117	0.14	0.13	0.57	0.10	0.97	0.017	1.31	11.77
6071	52.73	4.43	1.27	0.0077	0.34	0.36	1.49	0.09	1.82	0.018	2.97	33.80
6072	64.90	10.55	1.58	0.0175	0.25	0.32	0.61	0.16	2.88	0.030	1.79	16.34
6074	8.54	5.27	0.28	0.001	1.06	1.54	2.32	0.14	2.21	0.024	6.48	70.15

Table A.2.2: Geochemistry of the Ambassador palaeochannel samples (continued)

Sample	SiO2	Al2O3	Fe203	MnO	MgO	CaO	Na2O	K2O	TiO2	P2O5	S	LOI
6075	7.59	3.80	0.09	0.0007	0.64	0.87	1.26	0.11	1.96	0.012	13.87	69.85
6077	9.57	1.94	0.42	0.0025	0.99	1.33	2.13	0.15	0.28	0.003	10.51	71.36
6079	3.92	0.96	0.41	0.0024	0.84	1.07	2.55	0.18	0.14	0.000	14.13	73.19
6080	88.23	3.10	1.25	0.0155	0.07	0.08	0.22	0.20	0.41	0.010	0.69	5.55
6081	12.62	5.41	0.16	0.001	0.76	1.34	1.36	0.11	0.42	0.005	4.09	70.37
6082	71.22	11.70	1.46	0.021	0.16	0.23	0.43	0.06	1.52	0.022	0.43	12.74
6085	34.26	17.04	0.61	0.001	0.62	0.93	1.57	0.09	1.84	0.026	1.85	39.08
6086	24.40	7.54	0.59	0.001	0.68	1.10	1.29	0.99	3.34	0.202	8.31	50.28
6088	13.02	7.23	0.30	0.001	0.79	1.09	1.94	0.13	2.14	0.015	8.61	63.13
6089	22.48	6.20	0.30	0.0035	0.59	0.85	1.23	0.07	1.95	0.011	9.67	56.70
6091	15.82	4.08	6.41	0.0076	0.85	1.10	2.45	0.11	0.42	0.010	12.55	54.00
6093	68.19	3.82	0.99	0.0083	0.23	0.32	0.82	0.05	1.29	0.054	2.62	20.17
6095	2.80	0.82	0.51	0.0019	0.84	1.10	1.78	0.11	0.17	0.001	17	74.26
6096	10.91	2.78	0.32	0.0018	0.72	1.06	1.15	0.19	1.56	0.018	12.22	69.03
6097	38.05	12.91	1.45	0.0067	0.39	0.58	1.14	0.12	0.65	0.006	4.91	38.91
6099	29.55	17.54	0.82	0.001	0.28	0.53	1.02	0.24	1.59	0.122	3.69	40.89
6113	64.33	18.97	2.52	0.0028	0.93	0.04	0.28	3.86	2.57	0.022	0.07	6.78
6114	76.00	3.58	1.57	0.0185	0.13	0.20	0.61	0.14	2.40	0.050	1.11	12.10
6116	65.82	14.84	2.60	0.0113	0.25	0.19	1.45	0.28	1.86	0.053	1.6	12.61
6117	25.83	16.23	0.72	0.001	0.31	0.53	0.97	0.50	4.80	0.218	4.14	42.36
6120	68.61	16.77	1.68	0.0125	0.43	0.06	0.61	1.35	0.73	0.103	0.48	9.05
6121	42.01	20.15	5.44	0.0017	0.73	0.02	0.27	6.43	1.42	0.049	6.56	16.34
6122	82.71	8.47	1.84	0.0213	0.12	0.09	0.74	0.12	0.58	0.016	0.31	5.57
6126	77.31	14.41	0.50	0.0035	0.19	0.04	0.07	0.84	0.63	0.127	0.03	5.81
6127	78.90	13.01	0.60	0.0047	0.29	0.04	0.12	0.79	0.56	0.102	0.02	5.88
6128	68.55	16.80	1.49	0.0068	0.51	0.09	0.92	1.56	0.75	0.064	0.27	8.88
6129	77.72	10.12	2.28	0.0053	1.35	0.03	0.38	3.24	0.46	0.009	0.52	4.21
6131	94.67	2.07	1.13	0.0104	0.02	0.01	0.10	0.08	0.36	0.004	0.11	1.84
6132	63.66	16.24	6.11	0.0239	0.86	0.07	0.79	2.16	0.69	0.212	0.12	9.24
6133	91.89	0.88	0.96	0.0089	0.18	0.01	0.19	0.17	0.10	0.001	0.11	5.35
6134	76.44	13.22	1.13	0.0086	0.74	0.05	0.65	1.78	0.36	0.014	0.09	6.13
6135	86.28	7.43	1.12	0.0103	0.05	0.03	0.28	0.05	0.56	0.017	0.1	4.39
6137	84.90	6.21	1.87	0.0081	0.45	0.06	0.49	0.95	0.29	0.013	0.86	4.00
6138	60.78	17.10	2.61	0.0036	1.15	0.13	2.22	3.80	2.19	0.032	0.47	9.49
6139	85.35	6.35	1.30	0.0071	0.41	0.06	0.48	1.21	0.18	0.084	0.38	4.13
6140	81.46	6.54	2.38	0.0104	0.09	0.01	0.40	0.11	0.73	0.016	0.69	7.46
6142	78.90	11.95	1.61	0.015	0.11	0.06	0.67	0.15	0.40	0.017	0.14	6.72
6143	78.36	10.07	1.49	0.0141	0.20	0.13	0.27	0.16	0.86	0.018	0.37	8.15
6144	86.07	7.00	1.14	0.0136	0.38	0.07	0.07	1.62	0.38	0.007	0.01	3.12
6145	66.14	18.34	1.40	0.0108	0.35	0.10	0.17	0.49	1.33	0.051	0.33	10.62
6146	51.38	25.30	1.97	0.0086	0.49	0.21	2.69	0.32	0.98	0.047	0.39	16.03
6147	94.48	1.82	1.23	0.0138	0.01	0.01	0.08	0.02	0.11	0.005	0.1	1.76
6148	92.84	3.81	0.89	0.0103	0.02	0.01	0.08	0.03	0.16	0.002	0.02	2.28
6150	67.05	14.50	4.54	0.011	0.91	0.08	0.86	3.82	0.55	0.081	1.01	6.28

Table A.2.2: Geochemistry of the Ambassador palaeochannel samples (continued)

Sample	SiO2	Al2O3	Fe203	MnO	MgO	CaO	Na2O	K2O	TiO2	P2O5	S	LOI
6151	74.59	12.40	2.37	0.0152	0.40	0.05	0.37	1.20	1.23	0.068	0.61	6.33
6152	48.37	15.90	0.95	0.0141	0.10	0.05	0.50	0.16	0.84	0.015	0.13	32.87
6154	46.07	30.41	3.50	0.0099	0.08	0.03	0.30	0.05	2.76	0.015	1.18	15.01
6155	89.90	4.09	1.77	0.0097	0.01	0.01	0.12	0.10	0.10	0.018	0.8	3.28
6156	20.47	16.11	1.42	0.00	0.39	0.59	1.28	0.24	0.55	0.07	7.41	47
6157	39.54	13.50	1.08	0.0062	0.60	0.82	1.76	0.28	2.34	0.034	0.6	39.39
6159	10.12	4.22	0.56	0.001	0.71	1.02	1.34	0.10	0.74	0.006	4.76	75.68
6161	31.22	8.43	0.87	0.006	0.66	0.92	1.29	0.20	0.81	0.010	2.98	52.63
6162	74.81	11.73	2.29	0.0272	0.88	0.21	0.36	3.35	0.54	0.113	0.54	5.05
6164	62.23	13.72	7.47	0.1128	1.89	0.34	0.49	3.98	0.64	0.165	1.2	7.76
6165	17.47	2.73	0.64	0.0047	0.62	0.92	1.55	0.14	0.86	0.011	3.99	70.45
6166	78.57	13.71	0.99	0.0072	0.02	0.01	0.12	0.08	0.62	0.024	0.18	5.76
6167	46.74	26.78	0.94	0.006	0.30	0.21	1.10	0.52	1.47	0.032	0.35	21.45
6170	19.05	12.98	0.54	0.0003	0.62	0.87	1.17	0.24	1.59	0.022	2.83	59.93
6171	59.22	26.31	0.97	0.006	0.11	0.04	0.34	0.42	1.03	0.020	0.39	11.33
6172	46.34	28.99	0.84	0.0027	0.14	0.08	0.52	0.36	2.29	0.045	0.32	20.11
6174	41.54	22.76	0.78	0.0039	0.29	0.33	0.68	0.34	1.28	0.029	1.18	30.23
6175	67.89	15.11	1.00	0.0097	0.09	0.05	0.45	0.25	5.74	0.059	0.85	8.33
6176	25.00	2.22	1.57	0.0093	0.62	1.01	1.45	0.14	0.85	0.005	0.74	64.68
6177	80.60	9.83	1.41	0.0095	0.08	0.06	0.26	0.14	1.06	0.014	0.23	6.50
6178	40.78	3.97	0.65	0.0013	0.54	0.86	1.00	0.09	1.82	0.019	0.68	47.15
6180	65.96	15.70	1.69	0.0178	0.15	0.13	0.49	0.27	1.45	0.021	0.26	13.36
6181	85.23	8.93	0.65	0.0041	0.07	0.02	0.18	0.23	0.38	0.006	0.13	4.54
6182	39.86	8.98	3.56	0.0229	0.70	0.84	1.69	0.16	2.41	0.017	0.96	40.63
6183	81.05	5.38	1.36	0.0055	0.04	0.03	0.18	0.04	0.91	0.007	0.7	10.25
6184	72.90	10.70	1.06	0.0064	0.16	0.16	0.31	0.16	0.84	0.024	0.37	12.71
6185	65.23	1.54	2.02	0.0056	0.19	0.30	0.51	0.05	1.16	0.008	0.37	25.13
6186	47.79	3.03	1.11	0.0017	0.48	0.72	1.06	0.09	2.53	0.017	0.68	37.33
6187	5.90	2.77	0.28	0.0016	0.88	1.31	1.48	0.25	1.04	0.007	0.95	80.71
6188	58.05	23.77	1.41	0.0092	0.15	0.06	0.67	0.29	0.98	0.027	0.26	14.27
6189	54.10	27.26	1.17	0.021	0.12	0.04	0.60	0.14	1.84	0.032	0.42	13.99
6190	48.68	27.06	5.69	0.0097	0.13	0.04	0.72	0.07	1.73	0.029	0.38	15.07
6191	53.15	40.94	1.18	0.0065	0.36	0.11	1.79	0.47	1.57	0.123	1.75	-1.21
6192	82.98	5.33	1.45	0.0073	0.28	0.07	1.32	0.74	0.90	0.162	3.64	3.65
6194	59.50	17.88	4.02	0.0036	0.81	0.04	0.32	4.14	2.18	0.057	2	8.47
6196	94.68	1.98	2.13	0.0111	0.01	0.00	0.06	0.08	0.13	0.001	0.5	0.81
6197	58.52	1.98	0.50	0.0002	0.38	0.60	0.60	0.12	1.49	0.007	0.53	33.82
6198	41.71	5.68	1.33	0.0047	0.32	0.43	0.94	0.08	1.64	0.009	0.42	44.75
6199	29.11	6.56	0.50	0.001	0.69	0.80	1.53	0.23	2.02	0.024	1.31	53.81
6200	93.94	1.81	1.95	0.0089	0.02	0.02	0.07	0.05	0.20	0.007	0.11	1.90
6201	95.74	0.31	1.37	0.0088	0.03	0.02	0.07	0.02	0.91	0.003	0.1	1.53
6207	93.38	2.26	1.35	0.0066	0.02	0.00	0.08	0.05	0.13	0.000	0.07	2.41
6208	86.30	7.72	0.80	0.0111	0.05	0.02	0.17	0.14	0.65	0.008	0.07	4.03
6209	59.42	1.42	9.98	0.0316	0.26	0.24	0.73	0.10	0.56	0.002	0.13	26.15

Table A.2.2: Geochemistry of the Ambassador palaeochannel samples (continued)

Sample	SiO2	Al2O3	Fe203	MnO	MgO	CaO	Na2O	K2O	TiO2	P2O5	S	LOI
6210	15.49	5.06	0.35	0.0004	0.81	1.18	1.21	0.30	2.64	0.031	1.95	68.81
6211	14.88	7.68	2.29	0.0043	0.59	0.69	1.13	0.18	1.57	0.015	0.9	67.97
6212	27.03	1.09	0.51	0.0044	0.64	0.87	1.24	0.12	0.54	0.003	0.57	64.30
6213	30.33	17.92	1.65	0.0029	0.31	0.49	1.21	1.37	2.65	0.191	7.21	33.85
6214	96.03	1.72	0.76	0.0042	0.02	0.02	0.15	0.01	0.43	0.001	0.05	1.27
6215	95.78	0.31	2.08	0.0102	0.01	0.01	0.06	0.02	0.17	0.001	0.07	1.82
6216	86.06	2.15	0.53	0.0054	0.10	0.12	0.19	0.20	0.06	0.015	1.32	9.21
6217	82.82	4.04	0.75	0.0044	0.21	0.25	0.33	0.08	0.75	0.010	0.63	10.68
6218	84.88	8.49	0.77	0.0088	0.07	0.03	0.32	0.08	0.28	0.010	0.15	5.13
6219	84.79	6.88	1.07	0.0171	0.15	0.07	0.57	0.79	0.30	0.009	0.3	4.90
6221	71.18	19.05	0.60	0.0059	0.06	0.01	0.15	0.20	0.60	0.014	0.14	7.90
6222	95.36	0.79	1.43	0.0079	0.02	0.02	0.06	0.04	0.36	0.003	0.1	2.12
6223	94.00	1.26	1.37	0.008	0.05	0.03	0.20	0.03	0.13	0.002	0.05	3.65
6224	64.68	14.71	6.65	0.0033	1.47	0.02	0.16	4.32	1.93	0.015	0.17	5.47
6225	63.43	18.18	1.57	0.0188	0.35	0.10	1.40	0.55	0.76	0.038	0.76	12.91
6226	68.78	16.82	1.29	0.0065	0.38	0.07	0.65	1.13	0.64	0.084	1.09	9.10
6227	80.04	12.12	1.08	0.0091	0.06	0.03	0.15	0.06	0.45	0.030	0.36	6.20
6228	56.90	16.78	4.44	0.0061	0.95	0.20	0.76	4.12	2.53	0.024	0.32	11.57
6231	84.37	6.96	1.12	0.0028	0.67	0.02	0.13	2.32	0.39	0.037	0.68	4.03
6232	70.77	15.66	1.18	0.0181	0.19	0.08	0.93	0.24	1.53	0.020	0.34	9.32
6234	73.24	15.82	0.94	0.013	0.12	0.05	0.58	0.15	0.61	0.014	0.18	8.57

Sample	As.n	Au.n	Ba.x	Bi.x	Br.n	Cd.x	Ce.n	Cl.f	Co.n	Cr.n	Cs.n	Cu.x	Eu.n	Ga.x	Ge.x
6001	3	3	184	3	60	3	140	3	1	196	1	95	4.3	62	5
6004	2	23	178	3	16	3	46	4	5	178	1	193	2.4	29	2
6006	1	73	1164	3	22	3	46	4	2	166	2	45	1.4	81	2
6010	1	6	612	3	8	3	37	4	2	90	2	40	0.8	69	2
6011	1	3	134	3	21	3	34	4	3	66	2	10	0.5	66	2
6014	2	17	310	3	12	3	100	4	92	99	1	45	3.5	17	2
6015	9	3	70	3	10	3	23	3	1	73	1	45	0.5	12	2
6016	54	3	178	3	4	3	24	5	2	80	1	92	0.6	7	2
6018	27	3	165	3	11	3	51	4	2	104	3	13	0.9	29	2
6020	9	3	287	3	4	3	59	5	20	99	9	103	1.3	31	2
6028	9	3	55	3	26	4	244	2	28	76	1	4	10.9	5	2
6029	3	3	224	3	12	3	48	4	50	154	1	247	1.2	32	2
6030	1	3	389	3	37	3	233	1	11	49	1	166	13.5	13	2
6031	3	3	57	3	44	3	212	2	2	114	1	206	13.6	5	2
6034	9	19	119	3	13	3	529	3	32	103	1	615	20.9	27	2
6036	7	3	93	3	7	3	212	4	201	56	1	3	11.2	3	2
6037	91	3	127	3	1	16	1	3	9740	732	1	5157	4.4	12	2
6039	7	3	85	3	20	3	130	3	200	93	1	849	8.3	8	2
6040	22	13	46	3	23	3	433	1	53	45	1	1718	18.2	9	2

Table A.2.2: Geochemistry of the Ambassador palaeochannel samples (continued)

Sample	As.n	Au.n	Ba.x	Bi.x	Br.n	Cd.x	Ce.n	Cl.f	Co.n	Cr.n	Cs.n	Cu.x	Eu.n	Ga.x	Ge.x
6041	2	3	417	3	12	3	196	5	3	77	14	30	2.1	21	2
6042	9	3	12	3	5	3	122	4	485	50	1	3	2.6	3	2
6045	3	3	437	3	14	3	337	5	2	59	4	37	2.5	20	2
6046	6	21	399	3	14	3	84	5	11	76	3	86	0.9	22	2
6049	11	3	5	3	1	7	37	5	23.2	64.6	1	39	0.9	3	2
6054	1	173	440	3	54	9	1240	20	37	1610	1	548	24.9	20	2
6056	10	3	154	3	29	150	980	1	256	47	1	13	16.5	7	2
6058	11	35	960	3	13	3	2080	52	195	156	1	473	33.9	13	2
6059	25	37	51	3	28	6	876	3	310	184	1	1087	21.9	14	2
6061	3	3	91	3	42	3	149	3	8	77	1	5	3.3	23	2
6062	19	3	93	3	5	108	89	4	38	129	3	84	1.9	32	2
6063	6	3	53	3	11	5	240	4	63	86	2	3	6.7	22	2
6064	5	3	10	3	24	3	641	1	33	21	1	2	11.1	3	2
6065	20	3	343	3	8	3	128	4	16	90	4	17	1.6	21	2
6067	3	18	22	3	12	3	90	5	55	91	2	26	1.7	10	2
6068	35	22	138	3	50	3	560	2	63	64	1	584	13.8	8	2
6070	11	555	57	3	10	7	453	4	481	436	1	704	12.5	3	2
6071	8	477	129	3	28	3	1	3	254	1180	1	1705	3.2	4	2
6072	18	3	408	3	10	7	174	4	208	246	1	712	6	14	2
6074	13	3	62	3	34	3	777	1	262	44	1	710	22.2	5	2
6075	10	3	58	3	14	3	613	1	242	128	1	3038	16	12	2
6077	6	3	26	3	28	9	449	1	78	30	1	69	8.4	3	2
6079	11	3	6	3	37	42	274	1	554	14	2	5	4.7	5	3
6080	3	3	45	3	5	3	271	5	73	81	1	128	6.2	3	2
6081	9	67	0	3	36	3	4060	1	398	281	1	290	111	5	2
6082	4	27	46	3	7	3	132	100	78	152	1	81	7.2	18	2
6085	11	457	0	3	19	3	1950	3	138	446	6	608	81.4	11	2
6086	17	3	625	3	23	3	1400	2	251	175	4	914	32.5	14	2
6088	17	3	124	3	21	6	965	1	708	100	1	1479	41.3	16	2
6089	26	3	55	3	19	3	583	2	361	137	1	4490	13.9	7	2
6091	5	26	0	3	30	3	1570	2	168	86	1	714	32.8	4	2
6093	11	32	443	3	11	17	1030	4	448	162	1	690	27.9	3	2
6095	27	3	475	3	26	10	358	1	94	20	1	3	10.1	4	2
6096	30	3	88	3	9	21	447	1	416	180	1	4391	13.6	5	2
6097	24	34	0	3	14	28	947	3	843	160	1	1801	27	5	2
6099	23	72	129	3	13	17	1630	3	1680	473	5	819	55.2	6	2
6113	4	3	277	3	4	3	31.6	5	2.68	99.3	6.72	44	1.33	31	2
6114	2	3	98	3	23	22	255	4	70	126	1	67	4.8	45	2
6116	17	53	337	3	9	14	334	22	321	317	1	619	10.2	5	2
6117	61	3	241	3	8	25	1040	3	1130	739	1	1193	43.9	12	2
6120	18	3	616	3	9	3	116	5	39	88	4	27	2.2	21	2
6121	100	3	525	3	21	3	56	4	2	113	6	16	1	24	2
6122	5	3	48	3	11	3	84	5	12	96	1	33	0.5	11	2

Table A.2.2: Geochemistry of the Ambassador palaeochannel samples (continued)

Sample	As.n	Au.n	Ba.x	Bi.x	Br.n	Cd.x	Ce.n	Cl.f	Co.n	Cr.n	Cs.n	Cu.x	Eu.n	Ga.x	Ge.x
6126	3	3	611	3	1	3	134	5	1	46	2	2	0.9	21	2
6127	3	3	580	3	4	3	123	5	2	53	2	1	1.7	20	2
6128	1	189	555	3	13	3	80	5	11	74	7	804	0.9	22	2
6129	13	22	153	3	5	3	42	5	20	77	6	198	0.7	14	3
6131	3	3	284	3	3	3	9	5	2	54	1	8	0.5	5	2
6132	6	12	570	3	15	3	120	5	10	82	10	28	9.4	21	2
6133	1	3	885	3	4	3	37	5	20	45	2	27	1	3	2
6134	1	3	171	3	8	3	26	5	2	81	4	8	0.5	12	2
6135	14	3	66	3	6	3	35	5	2	175	1	84	1.3	4	2
6137	11	16	223	3	5	3	38	5	46	46	4	19	0.5	6	2
6138	11	3	311	3	33	7	66	5	23	109	12	85	1.7	29	2
6139	15	11	196	3	6	4	106	5	48	70	4	74	1.3	7	3
6140	8	39	251	3	10	5	121	5	70	226	1	54	3.7	6	2
6142	2	23	75	3	8	3	88	5	10	98	1	282	0.6	12	2
6143	7	3	64	3	4	3	97	5	36	109	2	25	3.5	20	2
6144	1	3	262	3	1	3	11	5	3	56	5	5	0.5	11	3
6145	7	3	2155	3	2	3	173	4	32	115	9	287	2.8	31	2
6146	17	3	202	3	40	9	142	4	27	148	1	49	2.9	36	2
6147	4	3	33	3	1	3	16	5	54	52	1	112	0.5	3	2
6148	2	3	28	3	1	3	4	5	3	51	1	5	0.5	4	2
6150	13	9	626	3	9	3	243	5	46	94	11	147	2.8	19	4
6151	12	3	264	3	4	3	149	5	51	91	11	34	2.4	19	2
6152	3	3	62	3	11	3	22	3	30	161	1	11	0.5	30	2
6154	28	33	105	3	3	3	22	4	58	230	1	225	0.7	62	4
6155	12	3	29	3	1	4	65	5	110	47	1	96	0.5	3	2
6156	30	13	111	3	8	40	1432	2	2564	235	1	1771	40	12	2
6157	5	3	107	3	34	3	251	3	12	141	1	122	16.4	34	2
6159	7	6	141	3	23	4	530	1	321	82	1	15	30.3	10	2
6161	8	3	83	3	17	4	607	2	116	84	1	78	19.8	19	2
6162	5	3	572	3	4	3	96	5	15	75	5	19	2	15	2
6164	4	3	596	3	5	3	116	5	16	72	7	32	1.7	21	2
6165	10	3	86	3	47	3	304	1	19	74	1	163	14.8	6	2
6166	2	8	32	3	1	3	30	5	2	105	1	7	0.5	19	2
6167	1	3	143	3	16	3	62	4	2	112	2	13	1.9	58	2
6170	11	49	439	3	26	3	582	55	483	201	1	411	24	37	2
6171	1	31	189	3	4	3	46	4	43	106	2	419	1.1	34	2
6172	1	21	538	3	9	3	74	4	3	130	1	75	2.1	76	3
6215	1	3	11	3	1	3	32	5	97	11	1	69	1	3	3
6216	5	3	46	3	3	47	196	4	124	13	1	600	6	3	3
6217	1	3	3	3	6	3	454	4	60	19	1	10	12.8	3	3
6218	1	3	18	3	5	3	50	5	7	25	1	18	0.5	8	3
6219	2	3	134	3	9	3	43	5	6	25	1	40	0.8	7	3
6221	1	3	66	3	3	4	22	5	13	110	1	77	0.5	24	3

Table A.2.2: Geochemistry of the Ambassador palaeochannel samples (continued)

Sample	As.n	Au.n	Ba.x	Bi.x	Br.n	Cd.x	Ce.n	Cl.f	Co.n	Cr.n	Cs.n	Cu.x	Eu.n	Ga.x	Ge.x
6222	1	3	43	3	1	3	9	5	28	20	1	6	0.5	3	3
6223	1	5	14	3	4	61	22	5	32	75	1	42	2.2	3	3
6224	11	3	228	3	2	3	97	5	23	87	13	31	2.5	26	3
6225	5	3	88	3	24	3	67	4	11	74	6	3	0.8	18	3
6226	10	37	587	3	9	3	137	5	30	60	4	3083	2.4	21	3
6227	2	3	59	3	3	3	123	5	23	39	1	19	2.1	11	3
6228	45	3	237	3	10	8	72	4	55	93	13	21	1.8	25	3
6231	7	3	181	3	2	3	67	5	7	54	6	13	1.3	13	3
6232	3	3	82	3	18	3	35	5	2	77	1	7	0.5	19	3
6234	3	21	30	3	8	5	60	5	68	84	1	299	1.2	14	3

Sample	Hf.n	In.x	la.n	lu.n	Mo.x	Nb.x	Ni.x	Pb.x	Rb.x	Sb.n	Sc.n	Se.n	Sm.n	Sr.x	Ta.n
6001	12	3	115	0.98	13	87	27	125	24	0.7	41	5	22	115	8.0
6004	7	3	35.8	0.32	8	21	34	26	11	0.7	38.6	143	11.3	50	2.0
6006	10	3	65.9	0.2	13	67	23	51	17	0.3	39.6	35	5.03	106	5.0
6010	12	3	51	0.33	3	44	20	30	28	0.4	9.9	9	3.69	53	3.0
6011	7	3	50.4	0.24	10	27	25	40	37	0.3	9.9	5	3.56	50	4.0
6014	18	3	38.9	0.83	11	37	169	24	8	0.4	11.2	9	17.9	36	3.0
6015	7	3	23.1	0.1	18	19	8	26	4	1.3	4.2	5	1.26	80	0.5
6016	1	3	14.2	0.1	23	3	42	21	55	16.1	4.09	5	3.39	66	0.5
6018	7	3	33.7	0.32	9	37	11	18	98	2.7	18.7	5	3.68	30	2.0
6020	7	3	34.9	0.35	10	40	35	66	258	1.8	26.2	5	5.82	15	2.0
6028	30	3	55.8	2.48	7	50	110	75	3	0.6	9.3	5	53.1	80	5.0
6029	35	3	38.6	0.64	4	59	161	58	19	0.3	143	5	7.79	46	6.0
6030	11	3	41.7	1.9	4	25	38	51	4	0.3	208	21	73.6	128	8.0
6031	41	3	36.8	2.18	3	54	10	73	3	0.3	189	10	72.9	93	0.5
6034	28	3	105	3.45	8	56	136	56	18	0.9	20.4	13	107	96	6.0
6036	27	3	31.2	2.64	12	39	688	4	3	0.6	7.7	5	56.9	19	2.0
6037	13	3	121	0.1	31	81	12178	726	14	0.3	1090	208	21.4	38	0.5
6039	32	3	25.2	1.37	8	46	224	257	5	0.3	89.8	5	40	62	4.0
6040	4	3	75.2	2.48	3	31	192	1025	3	0.3	76.5	5	92.7	73	6.0
6041	6	3	80.2	0.62	13	23	15	19	152	0.5	14.7	5	12.8	136	0.5
6042	5	3	43.4	0.58	9	19	1819	3	3	0.3	8.2	5	11.4	10	0.5
6045	6	3	177	0.49	17	30	5	47	80	0.3	14	5	18.3	240	2.0
6046	6	3	46.4	0.44	10	25	16	28	73	0.6	10.1	5	6.42	176	0.5
6049	7	3	11.5	0.26	5	5	77	24	3	0.4	1.6	5	4.4	4	1.0
6054	35	3	356	3.26	37	113	178	243	8	0.3	273	29	140	118	29.0
6056	6	3	394	2.09	14	40	1153	139	3	0.7	10.2	5	87.8	110	0.5
6058	48	3	578	5.97	45	72	215	128	3	0.3	76	59	190	52	0.6
6059	40	3	194	4.06	27	33	441	242	11	0.3	44.4	127	104	48	5.0
6061	27	3	54.1	1.05	15	26	36	21	12	0.3	10	5	18.1	67	3.0
6062	35	3	43.6	0.93	19	50	451	101	22	0.6	11.1	5	10	25	4.0

Table A.2.2: Geochemistry of the Ambassador palaeochannel samples (continued)

Sample	Hf.n	In.x	la.n	Iu.n	Mo.x	Nb.x	Ni.x	Pb.x	Rb.x	Sb.n	Sc.n	Se.n	Sm.n	Sr.x	Ta.n
6063	32	3	76.2	1.6	4	32	290	56	12	1.3	14.1	5	32.5	37	4.0
6064	1	3	223	2.09	9	8	224	75	3	0.3	1.68	7	62.3	102	0.5
6065	6	3	62.2	0.37	11	9	23	48	77	0.5	11.5	5	10	200	0.5
6067	17	3	29.1	0.62	11	19	93	23	7	0.4	9.4	9	9.82	15	2.0
6068	12	3	165	1.97	5	58	293	200	4	0.3	119	5	74.5	122	7.0
6070	25	3	114	1.66	31	23	1110	132	5	2.2	97.4	97	69	65	4.0
6071	15	3	15.5	0.1	4	26	302	224	4	0.3	373	479	8.95	35	3.0
6072	72	3	55.3	1.26	19	60	360	141	9	0.3	127	98	27.8	44	7.0
6074	5	3	195	3.09	21	44	1226	44	3	0.8	36.1	5	120	164	5.0
6075	5	3	168	1.67	37	34	643	217	10	1.2	90.6	5	78.3	64	6.0
6077	2	3	132	1.6	7	10	251	41	4	0.3	3.4	5	43.6	85	0.5
6079	1	3	103	0.91	3	3	1580	93	3	0.3	1.0	5	27.2	68	3.0
6080	11	3	79.5	1.23	12	19	173	38	4	0.4	8.0	20	33.2	74	0.5
6081	10	3	1410	12.2	71	28	1177	91	3	0.3	68.7	5	482	101	0.5
6082	27	3	45.6	1.35	19	28	231	92	3	0.4	33.8	42	33.2	54	5.0
6085	18	3	630	6.94	73	33	372	246	8	0.3	377	328	338	73	23.0
6086	19	3	466	3.88	59	66	695	637	8	1.2	97.7	96	166	846	5.0
6088	5	3	205	4.98	34	41	2618	206	11	0.3	44.3	5	202	86	0.5
6089	6	3	173	0.58	17	39	903	372	8	1.3	59.7	5	65.3	60	5.0
6091	2	3	424	3.56	37	21	762	80	6	0.3	10.8	27	175	83	0.5
6093	13	3	305	3.24	46	23	1309	324	9	1.5	75.9	75	137	152	4.0
6095	1	3	113	1.73	3	3	623	39	3	0.3	5.0	5	50.4	86	2.0
6096	10	3	140	0.93	21	21	796	607	8	3	50.7	96	57.5	125	4.0
6097	9	3	219	3.49	40	30	1850	115	7	0.3	61.7	144	138	41	3.0
6099	15	3	978	7.64	33	10	1311	187	6	2	93.9	1410	223	207	9.0
6113	6.5	3	18.7	0.33	9	27	18	12	187	3.3	19.9	6	4.14	27	1.3
6114	14	3	110	0.77	21	54	139	23	17	1.2	9.3	5	24.4	44	4.0
6116	22	3	144	1.19	32	41	721	291	7	0.3	74	141	40.6	222	4.0
6117	24	3	686	4.43	42	30	708	484	7	2.5	93.2	1350	169	459	6.0
6120	7	3	54.9	0.64	3	26	200	22	84	0.4	12.5	5	11.8	164	0.5
6121	5	3	32.5	0.26	22	29	14	33	171	10.1	20.9	5	4.54	95	0.5
6122	5	3	48.9	0.24	21	11	40	67	9	1	5.4	6	5.59	16	0.5
6126	7	3	78	0.31	4	26	5	38	49	0.5	7.2	5	5.37	438	0.5
6127	6	3	70.7	0.47	3	14	8	50	48	0.3	7.1	5	9.14	288	0.5
6128	6	3	45.9	0.43	5	22	17	23	95	0.3	12.3	18	5	95	2.0
6129	4	3	26.5	0.25	6	11	36	221	160	0.9	7.2	18	2.45	11	0.5
6131	7	3	7.3	0.1	3	11	10	16	3	0.5	4.8	5	0.75	14	0.5
6132	5	3	54.3	3.28	5	21	31	25	144	0.3	15.5	5	33.9	408	0.5
6133	2	3	29.3	0.25	3	5	54	47	24	0.6	1.4	5	4.36	50	0.5
6134	4	3	20	0.23	15	4	18	52	92	1.8	8.4	5	1.61	31	0.5
6135	7	3	31.2	0.34	16	3	19	111	3	0.6	36.3	5	6.43	66	2.0
6137	3	3	21.3	0.22	3	3	79	48	52	0.7	5.1	5	2.99	22	2.0
6138	6	3	35.4	0.34	20	27	48	25	233	2.5	23.9	5	6.67	41	0.5
6139	1	3	56.2	0.35	10	3	139	26	61	8.8	6.6	5	7.64	328	0.5

Table A.2.2: Geochemistry of the Ambassador palaeochannel samples (continued)

Sample	Hf.n	In.x	la.n	Iu.n	Mo.x	Nb.x	Ni.x	Pb.x	Rb.x	Sb.n	Sc.n	Se.n	Sm.n	Sr.x	Ta.n
6140	14	3	38.9	0.82	13	13	208	62	4	0.5	34.6	5	19.9	52	2.0
6142	5	3	53	0.27	3	18	30	67	11	0.6	6.7	12	5.16	21	2.0
6143	15	3	32.8	0.75	18	25	138	29	13	0.7	18	5	18	28	2.0
6144	5	3	5.1	0.3	3	13	22	23	92	1.1	6.9	5	1.36	20	0.5
6145	14	3	80.4	0.81	9	58	72	33	37	0.9	20.4	20	14.5	77	3.0
6146	12	3	65.9	0.7	17	23	89	117	20	0.3	12.2	19	16.9	46	2.0
6147	3	3	4.8	0.1	9	8	102	149	3	0.3	3.5	5	0.89	6	0.5
6148	3	3	4.1	0.1	3	4	14	10	3	0.3	2.8	5	0.51	6	0.5
6150	4	3	125	0.51	6	11	131	59	214	2.7	17.3	5	16	200	2.0
6151	12	3	99	0.84	17	30	101	36	98	1.9	10.7	5	12.4	119	3.0
6152	23	3	17.3	0.42	8	23	68	17	16	1.5	18.8	5	2.83	23	2.0
6154	51	3	12.6	1.01	19	50	34	55	4	0.5	33	16	3.9	14	4.0
6155	2	3	33.7	0.1	3	11	146	48	3	0.3	3.3	8	2.5	79	0.5
6156	4	3	536	6	51	15	4324	486	14	4.7	177	180	192	243.2	0.5
6157	14	3	109	1.96	9	60	28	94	13	0.7	39.4	5	68.9	110	4.0
6159	5	3	192	4.53	3	27	526	72	3	0.3	9.3	5	120	87	0.5
6161	7	3	258	1.93	5	27	242	20	10	0.3	5.8	5	92.3	84	2.0
6162	9	3	75.7	0.53	3	36	29	24	153	0.4	11	5	9.35	82	0.5
6164	6	3	63.5	0.51	10	28	37	29	195	0.4	15.5	5	8.63	79	0.5
6165	3	3	53.4	3.36	6	24	39	31	3	0.3	16.8	5	53.3	89	0.5
6166	12	3	20.5	0.22	3	29	17	14	5	0.3	9.1	5	1.13	21	0.5
6167	13	3	77.3	0.62	3	46	18	45	33	0.4	28.6	5	7.85	58	3.0
6170	5	3	155	0.7	11	41	1300	131	13	0.5	80.6	5	63.7	97	3.0
6171	14	4	44.4	0.77	6	30	122	75	25	0.3	20.9	6	0.1	26	2.0
6172	11	3	92.1	0.99	3	61	20	56	21	0.5	37.8	6	4.1	74	4.0
6174	10	3	97.2	0.82	7	44	481	87	19.7	0.4	46.4	6	22.6	66	3.0
6175	48	3	79.8	0.96	24	80	12	16	0.08	0.7	22	5	5.39	85	9.0
6176	5	3	234	1.39	6	24	313	3	5.79	0.3	5.2	5	56.9	23	2.0
6177	25	3	26.3	0.66	3	19	18	10	0.13	0.4	16.4	5	8.9	68	0.5
6178	27	3	169	1.83	29	109	77	37	5.27	0.3	504	232	76.4	26	0.5
6180	36	3	48.2	0.83	3	80	245	21	0.52	0.4	11.3	18	9.18	13	4.0
6181	10	3	8.6	0.1	3	11	5	18	0.09	0.3	4.2	9	1.17	96	0.5
6182	20	4	138	1.67	16	80	209	9	1.31	1.2	46.4	18	62.5	7	8.0
6183	16	3	8.6	0.38	17	15	35	4	0.59	2.1	5.9	46	3.75	37	0.5
6184	9	3	62.3	0.61	24	21	437	14	1.47	0.5	9.1	5	18	37	0.5
6185	30	3	183	1.64	38	504	897	18	3.52	2.2	105	5	36.8	68	3.0
6186	35	3	303	1.79	52	913	675	23	4.46	0.3	264	5	82.7	95	9.0
6187	4	3	149	2.08	23	296	44	4	10.4	0.3	15.2	5	79.4	95	3.0
6188	11	3	50.9	0.34	3	40	41	19	0.23	0.3	11.6	5	4.43	26	0.5
6189	43	3	33.4	0.77	5	33	24	6	0.09	1.3	14.3	5	3	42	3.0
6190	26	3	24.8	0.42	9	25	14	3	0.16	0.3	11.1	6	1.81	38	3.0
6191	10	3	119	0.25	19	74	27	25	0.22	0.3	16.7	5	5.65	175	0.5
6192	8	3	70.8	0.34	12	28	4	36	0.23	0.4	6.9	5	5.82	364	2.0
6194	5	3	70.8	0.2	14	21	65	209	1.87	2.7	25.3	5	3.8	200	2.0

Table A.2.2: Geochemistry of the Ambassador palaeochannel samples (continued)

Sample	Hf.n	In.x	la.n	lu.n	Mo.x	Nb.x	Ni.x	Pb.x	Rb.x	Sb.n	Sc.n	Se.n	Sm.n	Sr.x	Ta.n
6196	2	3	8.4	0.1	3	7	12	5	0.06	0.4	2.2	5	1.32	5	0.5
6197	28	3	239	1.96	45	922	517	18	3.99	0.3	194	5	87.4	53	8.0
6198	15	3	350	1.59	50	352	718	63	4.91	0.3	718	5	46.4	42	0.5
6199	25	3	308	4.56	43	379	1160	25	5.91	0.3	162	118	168	131	0.5
6200	4	3	23.7	0.1	10	19	39	3	0.33	0.3	2.9	7	6.23	11	0.5
6201	12	3	13.5	0.3	5	15	33	3	0.09	0.3	7.9	5	5.52	10	2.0
6207	10	3	7.7	0.1	3	6	171	3	0.51	0.3	2.6	5	2.54	7	0.5
6208	7	3	37	0.27	7	13	16	13	0.27	0.4	4.7	5	4.25	7	0.5
6209	6	3	135	1.13	38	18	13968	3	15	0.3	23.2	5	48.5	133	3.0
6210	13	3	421	3.12	30	263	826	12	7.53	0.3	40.3	5	145	195	7.0
6211	5	3	208	1.01	22	116	2758	14	10.7	0.3	14	105	58.2	90	2.0
6212	4	3	150	0.73	12	67	179	5	8.31	1.8	1.96	5	27.8	57	0.5
6213	18	3	528	6.19	72	554	1646	13	5	0.3	99.1	41	152	21	9.0
6214	5	3	4.4	0.1	3	9	4	3	0.04	0.3	5.9	5	0.68	5	0.5
6215	6	3	9.2	0.22	8	10	187	3	0.49	0.3	4.6	26	4.3	7	0.5
6216	7	3	86.2	0.57	34	35	217	7	1.97	0.3	4.9	56	21.2	132	0.5
6217	9	3	133	1.33	17	5	202	3	0.78	0.4	4.9	5	48.6	63	3.0
6218	4	3	29.9	0.1	15	24	16	6	0.2	0.4	5.5	5	2.45	15	0.5
6219	9	3	18.7	0.26	10	29	11	33	0.52	0.3	6.1	5	3.94	30	0.5
6221	9	3	17.7	0.2	8	19	32	18	0.18	0.3	12.3	8	1.56	14	2.0
6222	12	3	5.3	0.2	3	6	55	3	0.2	0.3	8.1	5	1.37	10	0.5
6223	8	4	4.8	0.56	4	169	71	4	0.22	0.3	11.5	5	8.84	3	0.5
6224	5	3	49.1	0.35	8	10	48	273	0.51	2.1	19.4	5	8.94	17	0.5
6225	7	3	39.7	0.25	4	32	11	38	0.19	0.6	12.7	5	4.22	76	2.0
6226	6	3	65.4	0.48	8	30	54	70	0.28	0.3	12.9	21	11.1	108	3.0
6227	11	3	49.9	0.4	7	24	41	5	0.37	0.3	6.6	5	8.96	32	0.5
6228	6	3	38.6	0.32	12	31	170	227	2.27	2.4	23.9	5	6.33	35	3.0
6231	3	3	35.3	0.52	12	22	52	109	0.07	3	7.9	5	5.83	66	0.5
6232	31	3	28.7	0.56	3	22	7	14	0.24	0.3	13.9	5	2.67	29	3.0
6234	10	3	27.6	0.43	13	20	74	11	0.34	0.5	8.5	6	6.16	15	0.5

Sample	Th.n	Tl.x	U.n	V.x	W.n	Y.x	Yb.n	Zn.x	Zr.x	traces	MAJORS	MAJORS+trace
6001	67	3	43	165	5	37	5.2	21	523	2228	100.07	100.29
6004	23.8	3	121	36	35	20	2.4	14	242	1551	100.26	100.42
6006	70.9	3	26	77	6	16	1.7	27	451	2662	100.91	101.17
6010	22.6	3	8	54	7	14	1.9	25	500	1780	102.10	102.27
6011	13.9	3	38	47	3	13	1.2	29	314	1084	100.18	100.29
6014	17.6	3	46	41	36	43	5	124	803	2200	100.08	100.30
6015	12.3	3	1	80	22	7	1	9	288	879	100.33	100.42
6016	4.6	3	4	259	32	10	0.6	76	33	1135	99.94	100.06
6018	25.3	3	6	261	11	23	1.9	31	336	1395	99.57	99.71
6020	7.3	3	49	454	5	28	2	30	309	2032	100.04	100.25

Table A.2.2: Geochemistry of the Ambassador palaeochannel samples (continued)

Sample	Th.n	Tl.x	U.n	V.x	W.n	Y.x	Yb.n	Zn.x	Zr.x	traces	MAJORS	MAJORS+trace
6028	11.5	7	1	107	17	126	14.4	1385	1318	3946	100.25	100.64
6029	28.6	3	191	64	1	42	4.5	35	1553	3293	100.59	100.92
6030	13.6	3	53	188	1	83	12.3	9	572	2476	99.97	100.22
6031	30.7	3	99	278	1	93	13.2	49	1713	3539	99.76	100.12
6034	23.1	3	28	155	15	144	21.1	48	1135	3709	99.93	100.30
6036	6.9	9	55	91	23	105	15	4607	1149	7568	99.86	100.62
6037	52.9	137	5870	451	1	39	6.3	3491	629	41092	94.75	98.86
6039	16.3	4	581	158	1	60	9.9	119	1357	4521	99.98	100.43
6040	5.7	5	222	385	1	133	15.6	158	211	5105	99.87	100.39
6041	21	3	6	81	14	39	3.3	30	275	1740	97.39	97.57
6042	1.8	39	61	45	33	65	3.6	4057	208	7159	100.68	101.40
6045	20.1	3	7	27	8	48	3	11	262	1962	100.70	100.90
6046	26.3	3	7	58	10	32	2.5	8	252	1520	96.25	96.41
6049	2.8	13	1	26	54.7	14	1.4	749	286	1503	101.08	101.23
6054	50.7	6	376	231	1	337	17.9	55	1671	8321	98.80	99.63
6056	7.6	27	136	159	1	227	12.8	5024	245	9478	98.12	99.07
6058	26.8	8	222	333	1	353	30.4	2295	1892	10632	99.31	100.37
6059	26.2	8	1700	162	1	261	25.5	1627	1531	9278	99.20	100.12
6061	26.1	3	64	81	5	49	5.5	660	1108	2714	100.65	100.92
6062	30.7	7	65	54	44	45	5.1	5232	1420	8295	99.88	100.71
6063	26.6	9	164	70	9	110	9.4	1748	1398	4651	100.41	100.88
6064	1.3	3	63	41	1	171	11.9	979	19	2772	98.44	98.71
6065	29	3	9	87	6	21	2.1	26	258	1569	100.48	100.64
6067	25.4	9	30	47	39	24	3.8	67	726	1545	100.51	100.66
6068	9.8	7	113	435	1	125	11.3	520	559	4377	99.54	99.98
6070	19.2	12	1390	69	1	133	13.5	1101	968	7671	98.97	99.74
6071	29.1	5	1600	52	1	23	3.1	240	378	7148	99.33	100.05
6072	41.9	10	709	153	32	71	10	658	2765	7288	99.43	100.15
6074	9.6	5	112	346	1	171	18.3	165	267	4909	98.02	98.51
6075	3.1	15	2950	281	1	137	12.2	1161	239	10304	100.03	101.06
6077	2.9	12	233	43	36	158	10.2	1308	80	3186	98.68	99.00
6079	1.5	35	85	47	1	76	5.8	7949	40	11096	97.40	98.51
6080	13.1	5	127	42	35	67	7.6	515	463	2380	99.82	100.06
6081	86.5	6	505	597	1	1162	69.6	2966	253	14309	96.66	98.09
6082	53.6	3	207	211	39	53	7.9	428	1071	3326	99.99	100.33
6085	88.8	15	2860	146	1	692	48.6	161	470	10293	97.92	98.95
6086	21.3	18	1710	265	1	312	27.8	1523	699	11212	98.74	99.86
6088	8.3	35	2070	378	1	309	38.4	6378	302	16471	98.40	100.05
6089	6.6	15	1780	440	1	143	11.1	1795	275	11887	100.06	101.25
6091	5.7	29	564	269	1	487	24.4	1423	105	7164	97.83	98.54
6093	10.6	17	2130	471	15	229	25.4	1887	484	10602	98.57	99.63
6095	4.8	23	205	53	1	186	10.2	4335	41	6831	99.40	100.08
6096	42.3	19	1600	501	1	123	11.2	4335	372	14555	99.95	101.41
6097	36.4	46	1080	205	22	234	26.3	4323	349	12844	99.12	100.41
6099	190	23	3730	165	1	233	58.6	3955	200	17909	96.27	98.06
6113	7.56	3	27.2	423	3.62	26	2.13	83	271	1704	100.37	100.54

Table A.2.2: Geochemistry of the Ambassador palaeochannel samples (continued)

Sample	Th.n	Tl.x	U.n	V.x	W.n	Y.x	Yb.n	Zn.x	Zr.x	traces	MAJORS	MAJORS+trace
6114	9.4	14	58	68	49	56	4.3	635	592	2678	97.92	98.19
6116	56.2	20	1770	199	19	107	12.3	2032	785	8755	101.57	102.44
6117	137	15	4540	492	1	110	42.8	3437	301	17646	96.61	98.37
6120	22.1	3	1	85	17	50	3.7	17	271	2017	99.88	100.08
6121	7.2	3	10	578	4	18	1.6	61	200	2205	99.41	99.63
6122	29.7	3	5	46	46	12	1.2	125	158	980	100.60	100.69
6126	21.9	3	1	55	3	18	1.7	4	293	1902	99.95	100.14
6127	19.4	3	1	49	7	30	2.7	6	226	1660	100.34	100.50
6128	23	3	86	65	7	25	2.6	21	242	2405	99.89	100.13
6129	10.1	3	255	61	12	18	1.5	88	156	1655	100.32	100.49
6131	9.7	3	1	30	31	5	0.7	4	288	841	100.40	100.48
6132	18.5	3	27	100	5	316	19.5	81	233	2442	100.18	100.42
6133	1.9	3	97	17	25	15	1.4	136	73	1636	99.85	100.01
6134	9.3	3	1	55	26	13	1.4	15	165	871	100.60	100.69
6135	22.7	3	111	86	26	11	1.8	16	312	1300	100.31	100.44
6137	8.1	5	55	34	16	11	1.2	294	148	1234	100.10	100.22
6138	6.9	3	40	523	7	28	2.1	293	279	2357	99.98	100.22
6139	5.9	4	18	234	20	23	1.9	561	53	2119	99.94	100.16
6140	29.4	4	64	93	24	45	4.7	1263	592	3355	99.95	100.29
6142	22.3	3	123	34	42	15	1.4	59	206	1333	100.74	100.87
6143	16.4	3	59	92	37	36	4.4	41	632	1647	100.08	100.25
6144	6.8	3	1	42	15	18	1.7	25	211	894	99.82	99.91
6145	18.2	3	61	136	24	48	4.5	25	629	4218	99.32	99.74
6146	37	3	32	170	359	34	3.9	621	451	2838	99.81	100.10
6147	3	3	103	8	43	5	0.5	432	103	1288	99.63	99.75
6148	6.1	3	4	10	26	3	0.3	9	124	357	100.15	100.19
6150	14.9	3	16	105	15	37	3	75	138	2429	99.70	99.94
6151	17	3	6	145	22	66	4.6	351	518	2331	99.63	99.86
6152	42.7	3	27	82	29	21	2.5	24	937	1740	99.91	100.08
6154	103	3	37	170	1	37	5.6	24	1875	3306	99.42	99.75
6155	8.7	8	36	17	25	6	0.5	66	76	965	100.20	100.30
6156	15.5	70	4316	398	1	385	38	18081	125	35918	95.34	98.93
6157	23.3	1.47	56	63	19	132	11.9	75	26	1702	99.96	100.13
6159	6	0.93	17	24	5	80	37.2	177	1828	4403	99.26	99.70
6161	6.5	0.98	4	5	13	37	17.6	201	826	2918	100.04	100.33
6162	12.7	0.6	1	5	11	69	4.7	56	55	1477	99.89	100.04
6164	18.3	0.68	2	5	4	90	3.2	33	100	1620	99.99	100.15
6165	4.6	1.03	59	91	7	159	16.7	54	31	1488	99.38	99.53
6166	28.1	0.72	2	5	8	68	0.6	11	11	487	100.09	100.14
6167	23.2	1.11	5	6	6	74	2.5	21	26	929	99.90	99.99
6170	24.2	1.74	14	501	1	196	15.2	116	236	5292	99.85	100.38
6171	18.3	0.88	56	82	6	37	1	15	51	1501	100.20	100.35
6172	24.3	2.31	68	105	3	78	1	17	25	1640	100.02	100.18
6174	22.3	1.64	29	229	3	104	5.7	49	104	2811	100.16	100.35
6175	100	5	12	229	6	44	6.4	13	2095	3370	99.83	100.17
6176	4.4	5	1	83	1	176	9.7	1171	179	3272	98.28	98.61
6177	23.6	4	35	43	1	30	4.7	28	1058	1768	100.20	100.37

Table A.2.2: Geochemistry of the Ambassador palaeochannel samples (continued)

Sample	Th.n	Tl.x	U.n	V.x	W.n	Y.x	Yb.n	Zn.x	Zr.x	traces	MAJORS	MAJORS+trace
6178	2.7	7	3180	220	1	135	12.1	317	913	7915	97.57	98.36
6180	27	9	117	59	1	48	5.8	347	1487	4154	99.49	99.91
6181	10.8	3	43	29	1	9	1.3	4	432	953	100.38	100.47
6182	21	6	73	200	1	94	12	329	825	3265	99.84	100.17
6183	12.6	3	126	61	6	20	2.9	218	621	1696	99.94	100.11
6184	43.3	11	54	105	8	50	4.4	723	359	2508	99.40	99.65
6185	3.2	15	1620	210	1	262	12.6	838	1231	15338	96.53	98.06
6186	15.5	8	1920	524	1	289	15.6	466	1434	9998	94.84	95.84
6187	8.1	16	253	212	1	110	16.8	29408	146	32810	95.56	98.84
6188	40	6	17	72	1	16	2.3	77	517	1285	99.95	100.08
6189	73.9	5	5	74	2	35	5	59	1753	2527	99.73	99.98
6190	52	11	5	193	3	17	2.8	17	1055	1849	99.61	99.80
6191	59.1	8	9	66	3	14	1.7	25	425	1745	101.54	100.41
6192	15.5	6	1	66	31	21	2.4	4	354	1863	100.52	100.71
6194	7.4	6	13	382	19	16	1.6	18	235	1909	99.42	99.62
6196	7.8	3	12	11	2	6	0.7	32	86	293	100.38	100.41
6197	3.5	10	1510	215	1	288	15.2	224	1198	7510	98.56	99.31
6198	0.3	5	5210	304	1	620	11.2	556	708	11457	97.32	98.47
6199	23.4	33	2110	464	1	327	33	3069	895	14216	96.58	98.00
6200	3.5	3	32	22	1	12	1.3	64	158	757	100.09	100.16
6201	13.9	3	59	43	1	14	2.1	94	531	1093	100.10	100.21
6207	1.5	4	8	6	1	9	1.2	471	379	1297	99.75	99.88
6208	24.4	3	11	41	5	14	1.7	191	259	856	99.97	100.06
6209	3.1	121	105	298	1	112	9.5	1552	213	19483	99.03	100.97
6210	10.9	11	1110	423	1	375	25.9	1769	487	9132	97.83	98.75
6211	1.4	88	1340	253	1	173	12.4	5025	218	13601	97.90	99.26
6212	1.8	4	442	91	1	89	5.6	3425	134	5259	96.90	97.42
6213	120	26	779	805	1	419	41.4	5029	700	14692	97.19	98.66
6214	18.3	3	4	15	1	5	0.8	10	201	370	100.46	100.50
6215	2.9	6	59	13	1	13	1.6	150	222	975	100.35	100.45
6216	0.3	6	634	41	1	74	4.3	1062	294	3649	99.96	100.32
6217	2.4	4	80	38	1	125	9.5	375	368	2025	100.55	100.75
6218	16.3	3	36	31	1	8	0.8	54	154	566	100.21	100.27
6219	7.2	3	13	22	1	14	1.5	9	394	880	99.84	99.92
6221	25.7	4	96	71	1	10	1.2	175	354	1204	99.90	100.02
6222	2.8	3	22	18	2	8	1.4	124	516	930	100.30	100.40
6223	1	3	282	14	1	22	3.4	1325	357	2571	100.78	101.04
6224	5.1	6	17	521	1	41	2.5	117	225	1906	99.61	99.80
6225	23.6	3	15	26	3	13	1.7	14	295	867	100.07	100.16
6226	18.1	6	25	76	1	38	3.3	636	238	5287	100.03	100.56
6227	12.3	3	10	49	1	23	2.7	668	472	1703	100.58	100.75
6228	6.3	9	21	433	1	22	2.4	835	259	2714	98.60	98.87
6231	10.9	3	12	311	1	30	3.6	58	99	1156	100.72	100.84
6232	52.1	4	4	28	2	24	3.5	8	1341	1862	100.28	100.47
6234	19.9	3	69	31	1	18	2.8	254	431	1598	100.29	100.45

APPENDIX 3

DENDOGRAMS AND INTERPRETATION OF HOLE BASED CLUSTER ANALYSIS

CLUSTER GROUP A

Cluster 1

This cluster comprises only 1 hole that is differentiated from all the others by its high Ni (approx. 1.4%) content

Cluster 2

This cluster comprises 21 holes, mainly from within the high grade zone of mineralisation and is characterized by its high organic content, high Zr content, and high U/Th ratio. Moderate levels of transition metals and rare earth elements are also present. The moderate level of Al_20_3 and low levels of Th and K_2O indicate that there is an absence of any significant heavy mineral component. This also implies that the high Zr concentration is derived from the remobilization of Zr rather than the presence of primary detrital zircon.

Cluster 3

This cluster accounts for only 2 holes and is characterized by high Cr, Nb, Zr concentrations and a high (La/Yb)n ratio which indicates that these holes are likely to contain significant heavy mineral accumulations.

Cluster 4

This cluster comprises 47 holes and is characterized by high Al_20_3 concentrations (low Al_2O_3/LOI ratio), moderate concentrations of K_20, Cr, Th, Nb and Zn and low concentrations of transition metals. These geochemical characteristics combined with the close spatial association of these holes with the margins and shallow regions of the palaeochannel indicates these holes are predominantly unmineralized clay-rich sediments.

Cluster 5

This cluster of 20 holes is characterized by high S, CaO and LOI concentrations and low to moderate transition metal and rare earth element concentrations. The close association of these holes both within the highest mineralized areas and immediately to the west imply that these are areas rich in organic matter that have not been significantly mineralized possibly due to factors such as the extent and direction of groundwater flow and the level of the redox horizon. This group of holes is closely related to the single hole of cluster 1 which is only differentiated by its unusually high Ni concentration.

Cluster 6

This cluster of 2 holes is characterized by their high total rare earth element and LOI concentrations, high U/Th ratio and low (La/Yb)n ratio. This heavy rare earth element enrichment and high U/Th ratio is indicative of an organic complexation mechanism due to remobilization of elements rather than a detrital accumulation. Note the similarity of this cluster to cluster 2, with which it is directly linked but is differentiated from cluster 2 by its higher U, Ni, Zn, Al_20_3, CaO, K_20 and LOI concentrations and its higher U/Th ratio.

Cluster 7

This single hole is linked to cluster 3 as a result of its high concentration of elements associated with heavy mineral phases, however is clearly differentiated by its significantly higher TiO_2, Sc, Ni, Cu, U, Th, Ni and S concentrations and higher U/Th ratio

Cluster 8

This group of 12 holes is closely linked to cluster 4, however is differentiated by its higher K_20 concentration and higher (La/Yb)n ratio. These geochemical characteristics, coupled with the exclusive association of this cluster and cluster 4 to the channel margins and highs indicates that these holes intersect predominantly unmineralised clay rich zones.

Cluster 9

This cluster of 36 holes is closely associated spatially and geochemically to clusters 4 and 8 however is differentiated by its generally lower concentration of major and trace elements. This is due to the more SiO_2 rich nature of the sediments in these holes (*i.e.* these holes are sand rather than silt rich).

Cluster 10

This cluster of 5 holes is closely associated with clusters 3 and 7, however is differentiated in that its has the highest concentrations of La, Sm, Yb, Th and Mo. Interestingly however the holes of this cluster are in the main on the margin of the main mineralized zone, while the holes of clusters 3 and 7 may be located well to the west of the main mineralized zone.

CLUSTER GROUP A

Cluster 1
6209

Cluster 2
6186 6197 6040 6185 6178 6198 6116 6070 6059 6093 6097 6058 6086 6089 6096 6075 6199 6210 6088 6211 6091

Cluster 3
6071 6054

Cluster 4
6067 6143 6014 6152 6082 6114 6036 6061 6063 6029 6062 6190 6189 6177 6232 6180 6154 6072 6175 6127 6142 6166 6221 6225 6234 6188 6128 6041 6065 6046 6126 6120 6151 6045 6132 6226 6004 6146 6011 6171 6145 6010 6167 6172 6191 6006 6001

Cluster 5
6182 6034 6157 6028 6031 6039 6165 6161 6170 6030 6159 6068 6074 6056 6176 6212 6064 6077 6079 6095

Cluster 6
6156 6187

Cluster 7
6037

Cluster 8
6018 6020 6113 6138 6194 6228 6224 6121 6150 6129 6162 6164

Cluster9
6137 6139 6144 6134 6231 6016 6201 6183 6080 6217 6219 6192 6181 6227 6208 6218 6122 6135 6140 6184 6216 6015 6042 6049 6207 6222 6200 6215 6148 6196 6133 6155 6131 6214 6147 6223

Cluster 10
6213 6085 6099 6117 6081

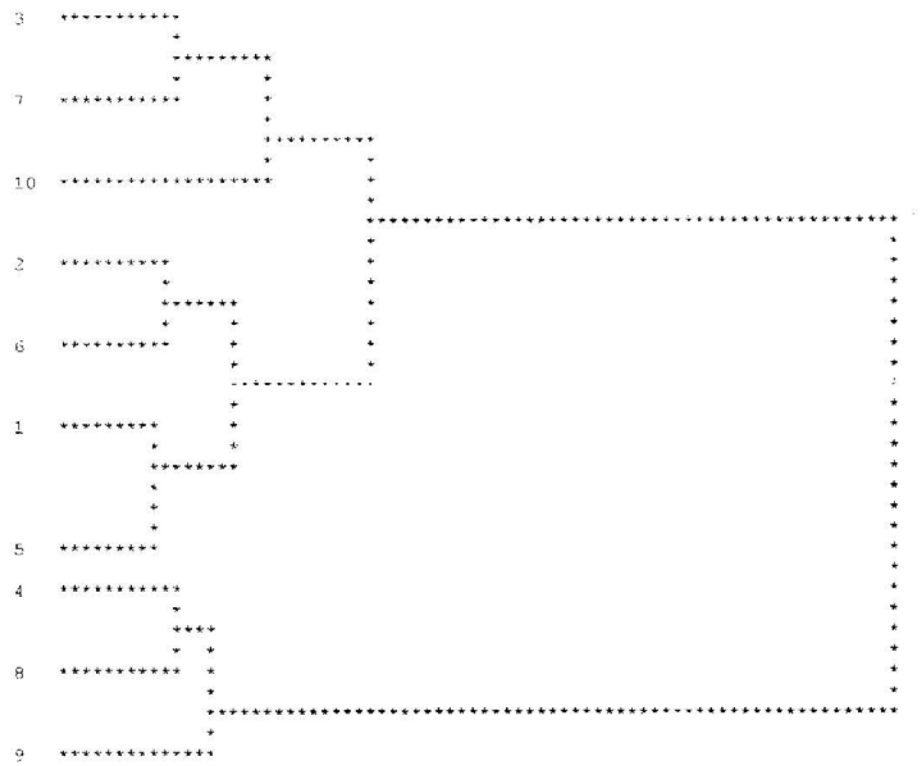

Cluster	No. obs	Cr.n	La.n	Sc.n	Sm.n	Th.n	U.n	Yb.n	Cu.x	Mo.x	Nb.x	Ni.x	Pb.x	S.p	Zn.x	Zr.x	Al203	CaO	K20	Ti02	LOI	U/Th	(La/Yb)n	Al203/LOI
1	1	26	135	23.2	48.5	3.1	105	9.5	82	38	8	13968	18	1300	1552	213	14200	2400	1000	5600	261500	34	9.6	0.05
2	21	166	256.5	136.2	105.5	15.7	1771	19.6	1929	35	25	947	378	43329	2014	728	58333	6838	1705	17595	455262	113	8.8	0.13
3	2	1395	185.8	323	74.47	39.9	988	10.5	1127	21	70	240	234	23700	148	1025	65700	5900	1250	36150	379450	25	12.0	0.17
4	47	110	56.7	21.3	11.66	32.6	61	4.2	187	9	27	92	45	6983	371	744	185396	1260	5038	13719	132396	2	9.1	1.40
5	20	70	143.9	44.9	67.89	11.2	119	13.9	217	8	29	435	83	52365	1488	485	48360	10450	1695	13650	614435	11	7.0	0.08
6	2	139	342.5	96.0	135.7	11.8	2287	27.6	1393	37	11	2184	391	41800	23744	136	94400	9500	2450	7950	637600	194	8.4	0.15
7	1	732	121	1090	21.4	52.9	5870	6.3	5157	31	81	12178	726	105800	3491	629	54100	1700	300	64200	402500	111	13.0	0.13
8	12	92	50.4	19.1	6.7	10.8	38	2.4	60	11	22	54	46	12408	149	245	160183	942	39567	16725	85125	4	14.2	1.88
9	36	54	30.3	7.16	7.3	10.7	61	2.2	69	10	7	127	34	6156	389	273	47900	444	3822	3725	55731	6	9.3	0.86
10	5	466	846.4	146.4	272.8	125	2483	52.2	810	58	21	1043	312	41960	3110	385	148280	7640	4620	22600	453100	20	11.0	0.33

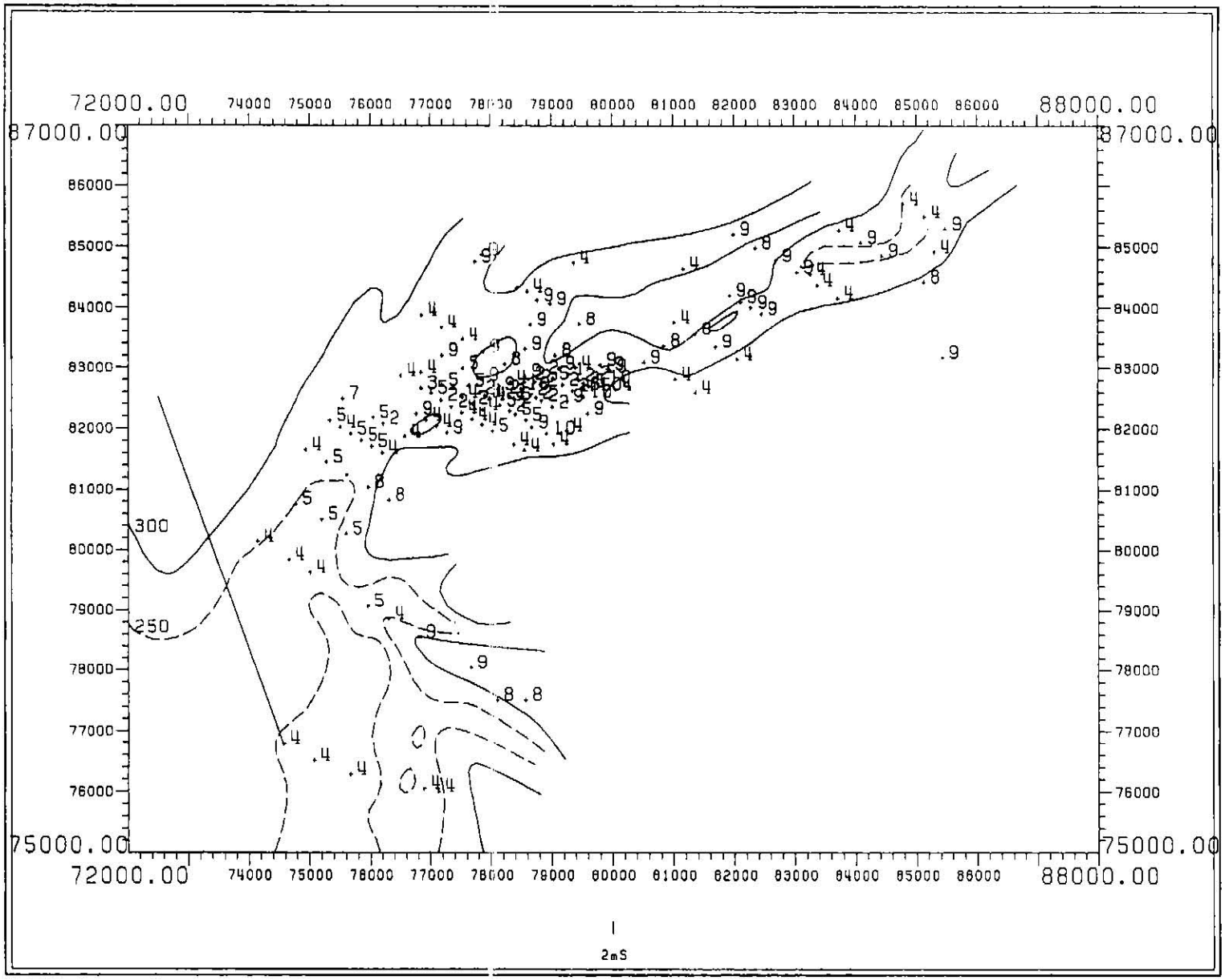
72000.00
74000
75000
76000
77000
78000
79000
80000
81000
82000
83000
84000
85000
86000
88000.00
87000.00
86000
85000
84000
83000
82000
81000
80000
79000
78000
77000
76000
75000.00
300
250
2mS

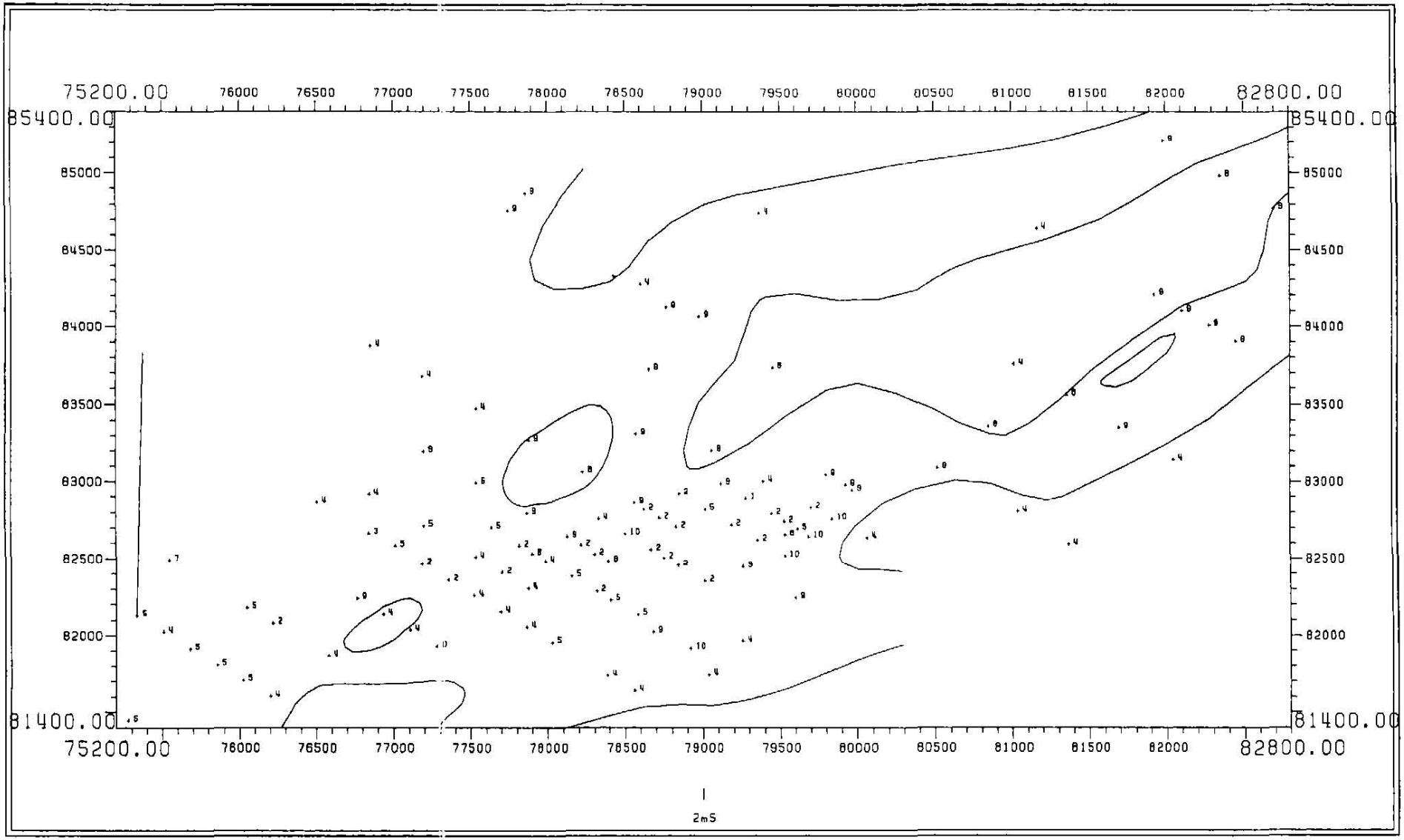
75200.00
76000
76500
77000
77500
78000
78500
79000
79500
80000
80500
81000
81500
82000
82800.00
85400.00
85000
84500
84000
83500
83000
82500
82000
81400.00
2mS

CLUSTER GROUP B

Cluster 1

This cluster contains 4 holes which are characterized by high rare earth element (La, Sm and Yb) U and base metal (Cu and Zn) concentrations and moderate levels of other metals. The holes of this cluster are located on the margins of the main mineralized zone and interestingly correspond to the locations of cluster 10 of the previous cluster group.

Cluster 2

This group of 5 holes is characterized by a high concentration of elements associated with heavy mineral phases (*i.e.* Nb, Zr, TiO_2) and are mostly located to the west of the main mineralized zone.

Cluster 3

This cluster of 18 holes is characterized by high LOI, Zn and S concentrations with moderate levels of trace metals and rare earth elements and a low U/Th and high Al_20_3/L0I ratio. These holes are distributed throughout the western half of the palaeochannel system and can be classified as organic rich sediments selectively enriched in Zn by groundwaters.

Cluster 4

This large cluster of 41 holes is characterized by high concentrations of Eu, Al_20_3 and high Al_20_3/LOI and (La/Yb)n ratios, moderate concentrations of Nb, Zr and TiO_2 and low levels of trace metals and rare earth elements. These geochemical characteristics and the preferential association of these holes within the channel margins indicate that they are predominantly unmineralized sediments. Note that the elevated levels of Eu are not probably not due to rare earth element mineralization but reflect a possible feldspathic component in these sediments. The presence of high Eu concentrations in what are ostensibly unmineralized areas of channel sediments, with concentrations often exceeding those of mineralized areas are probably due to the substitution of the reduced Eu^{2+} ion for Ca^{2+} in clay rich and/or feldspathic sediments.

Cluster 5

This cluster comprising 16 holes is characterized by high concentrations of Th, U and Pb, moderate levels of trace metals and rare earth elements. Low (La/Yb)n and Al_20_3/LOI ratios indicate that this cluster of holes is heavy rare earth element (HREE) enriched and has a high organic content, that interestingly have been enriched in both U and Th, the majority of these holes located in the main mineralized zone. Note however the low mobility of Th suggests that there may be a heavy mineral component present in these holes

Cluster 6

This single hole is distinguished by its high rare earth element, LOI, Cu and V concentrations and hence is related to cluster 1, the only major difference being the more inorganic nature (higher Al_20_3 concentration) of the holes of cluster 1.

Cluster 7

This cluster of 21 holes is characterized by having a high concentration of Zr and a high U/Th ratio with moderate concentrations of trace and rare earth elements and a low (La/Yb)n ratio indicating heavy rare earth element

enrichment. This cluster is closely related to cluster 2, however cluster 2 does not have the same level of HREE or U enrichment. Interestingly the majority of the holes contained within cluster 7 occur within the western half or clearly to the west of the main mineralized zone indicating a region of HREE and U enrichment, and hence indicate significant, broad elemental speciation within the palaeochannel. Note that this enrichment is likely to have resulted from enrichment via groundwater remobilization as the low levels of Th and light rare earth elements (LREE), hence the high (La/Yb)n ratio and the elevated U concentrations preclude heavy mineral accumulation (*e.g.* monazite) as being a primary source of mineralization.

Cluster 8

This single hole is distinguished from all others by its high Ni content, however is associated with cluster 3 due to similar concentrations of other elements.

Cluster 9

This cluster of 39 holes is clearly differentiated from all others by its high Eu concentration and its close spatial association to the margins and outside of the palaeochannel. This cluster is closely related to cluster 4 which displays similar geochemical and spatial characteristics.

Cluster 10

This single hole is clearly defined by its very high $Ti0_2$ concentration (approx. 6.4%), high S concentration (approx. 10.6%) and elevated levels of Sc, Th, U, Nb, Ni, Pb and (La/Yb)n ratio however it displays geochemical similarities with cluster 5 (which has a higher total rare earth element concentration and a greater degree of heavy rare earth enrichment) with which it is associated. The high (La/Yb)n ratio implies there may be a significant heavy mineral component to this hole, however the high LOI and trace metal concentrations indicate mineralization via groundwater flow has also probably occurred.

CLUSTER GROUP B

Cluster 1
6117 6213 6099 6085

Cluster 2
6154 6175 6072 6058 6054

Cluster 3
6170 6157 6068 6074 6056 6159 6091 6176 6212 6161 6165 6030 6187 6211 6064 6077 6079 6095

Cluster 4
6126 6164 6041 6120 6046 6004 6128 6045 6221 6225 6234 6065 6188 6146 6132 6226 6067 6143 6140 6014 6162 6166 6151 6114 6145 6172 6010 6167 6171 6011 6191 6006 6001 6018 6020 6113 6138 6224 6194 6228 6121

Cluster 5
6040 6186 6197 6178 6198 6088 6097 6093 6199 6210 6086 6156 6089 6096 6075 6185

Cluster 6
6081

Cluster 7
6182 6070 6116 6071 6028 6036 6039 6031 6034 6059 6152 6082 6061 6063 6177 6232 6180 6190 6189 6062 6029

Cluster 8
6209

Cluster 9
6122 6208 6135 6184 6192 6127 6142 6150 6134 6129 6016 6139 6231 6207 6222 6201 6183 6227 6181 6219 6216 6080 6217 6015 6042 6049 6215 6131 6214 6200 6133 6148 6196 6137 6155 6144 6218 6147 6223

Cluster 10
6037

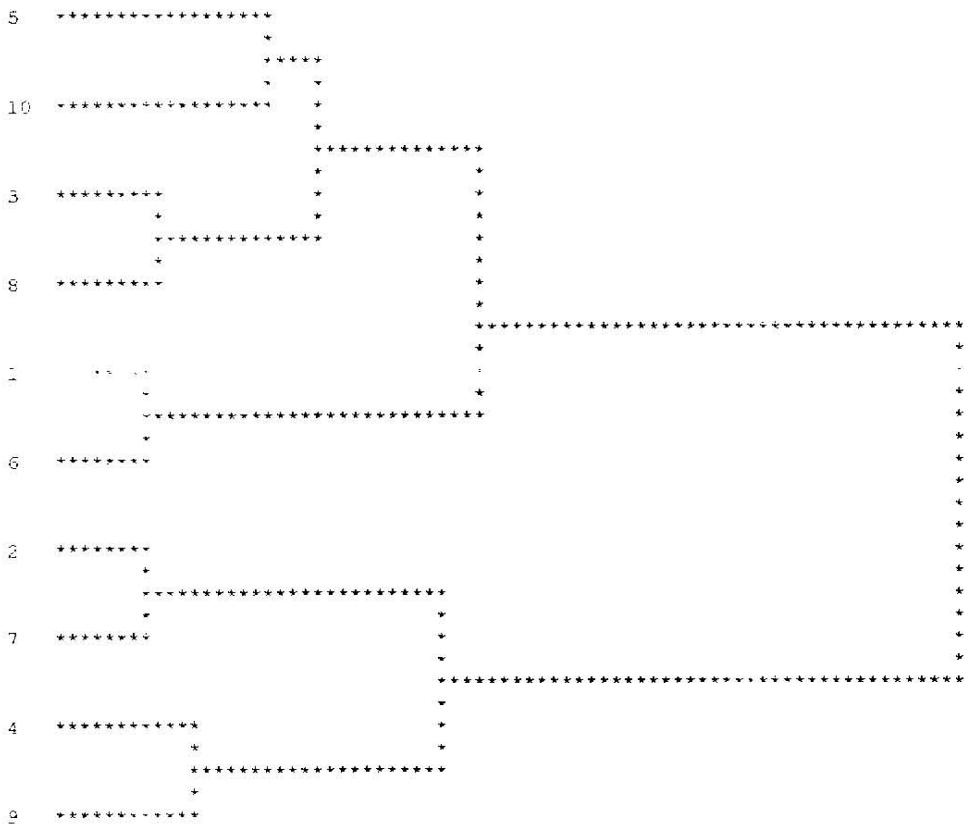

Cluster	No. obs	Lu.n	La.n	Sc.n	Sm.n	Th.n	U.n	Yb.n	Cu.x	Eu.n	Nb.x	Ni.x	Pb.x	S.p	Zn.x	Zr.x	V.x	Al2O3	TIO2	LOI	U/Th	(La/Yb)n	Al203/LOI
1	4	6.3	705.5	165.8	220.5	64.5	2977	55.3	47.8	393	19	1009	368	42225	3146	418	402	171825	27200	390450	46	8.6	0.4
2	5	2.49	216.3	106.2	73.4	7.6	271	13.3	14	320	59	160	129	13460	609	2060	223	146440	39220	203080	36	11.0	0.7
3	18	2.04	183.3	32.4	74.2	22.8	208	16.6	14.5	155	23	643	90	60294	3538	212	157	44539	10761	667144	9	7.5	0.1
4	41	0.56	59	18.0	9.6	13.1	31	2	3.1	2318	27	57	38	7234	155	383	148	187324	13159	112315	2	19.9	1.7
5	16	2.71	266.3	170.1	110.7	86.5	2158	25.7	20.8	290	21	1138	464	48831	2930	620	355	56850	17644	504431	25	7.0	0.1
6	1	12.2	1410	68.7	482.0	32.2	505	111	69.6	363	28	1177	91	40900	2966	253	597	54100	4200	703700	16	8.6	0.1
7	21	1.43	61.7	59.5	35.5	3.1	390	7.2	9.4	82	29	262	93	15467	958	1207	116	123524	16771	251014	126	5.8	0.5
8	1	1.13	135	23.2	48.5	10.8	105	12.8	9.5	78	8	13968	18	1300	1552	213	298	14200	5600	261500	10	7.1	0.1
9	39	0.32	34	6.7	7.1	52.9	65	1.5	2.1	5157	7	117	40	5938	332	256	57	55251	3756	55451	1	15.3	1.0
10	1	0.1	121	1090	21.4	134	5870	4.4	6.3	940	81	12178	726	105800	3491	629	451	54100	64200	402500	44	18.6	0.1

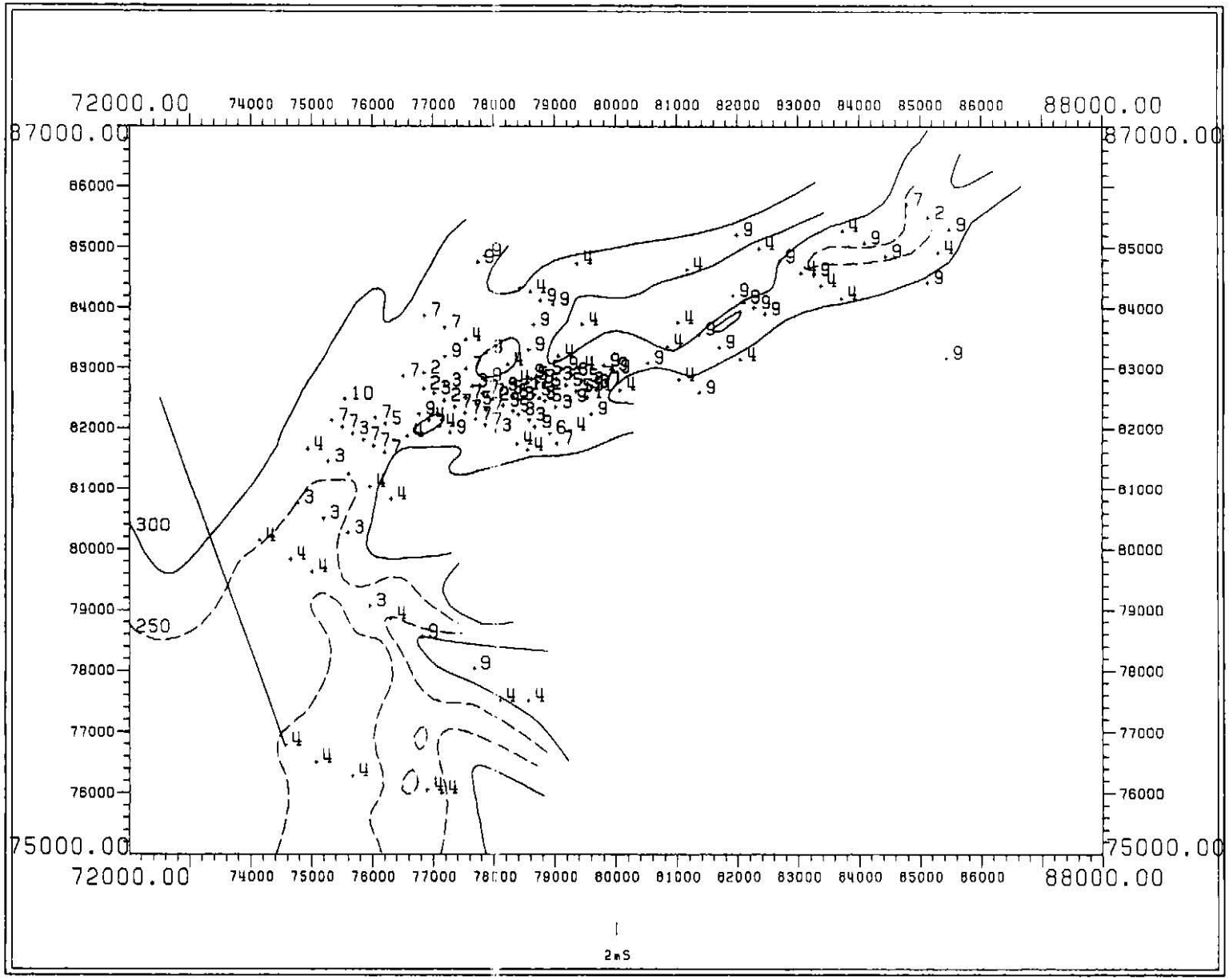
72000.00
74000
75000
76000
77000
78000
79000
80000
81000
82000
83000
84000
85000
86000
88000.00
87000.00
86000
85000
84000
83000
82000
81000
80000
79000
78000
77000
76000
75000.00
300
250
2mS

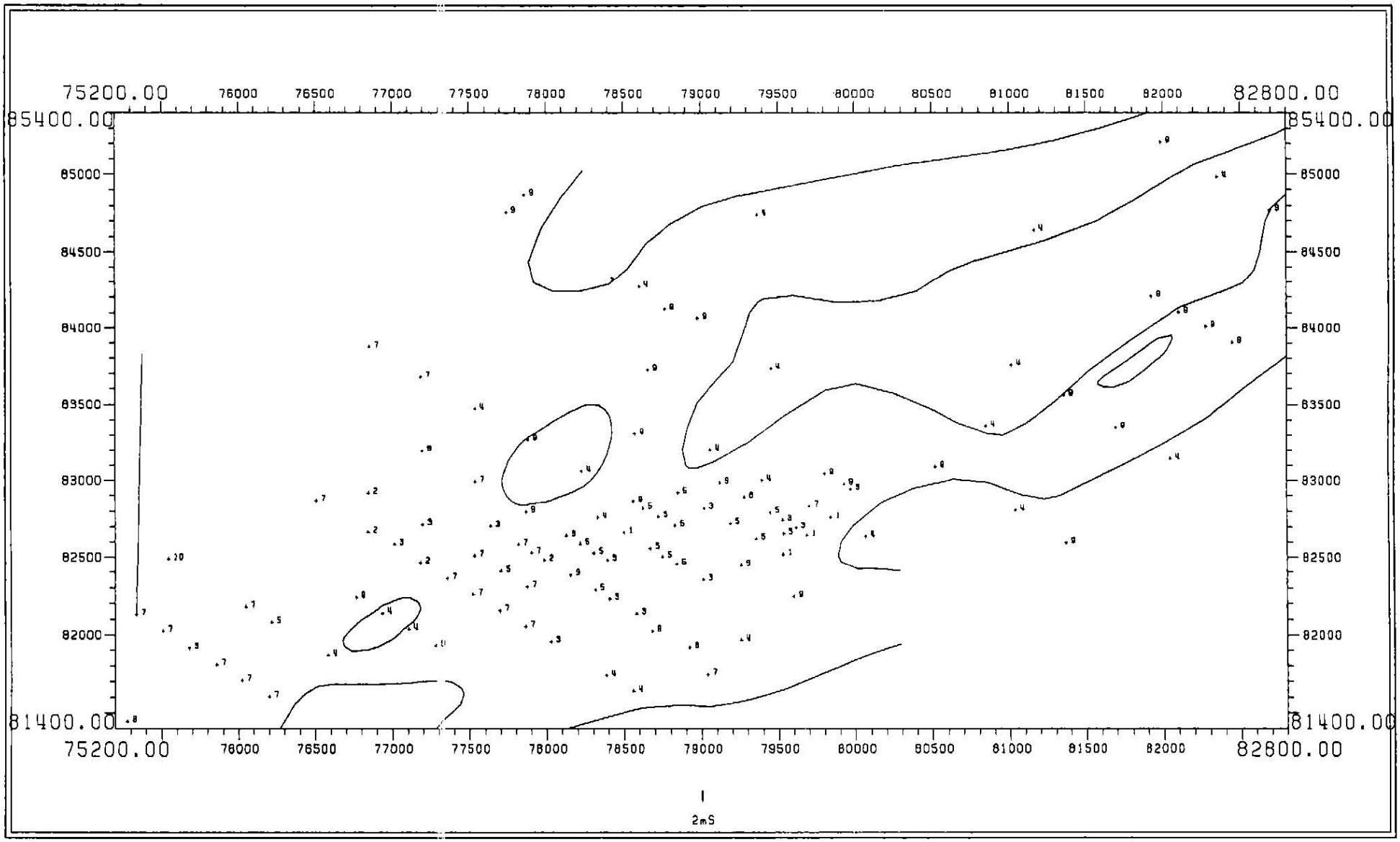
75200.00
76000
76500
77000
77500
78000
78500
79000
79500
80000
80500
81000
81500
82000
82800.00
85400.00
85000
84500
84000
83500
83000
82500
82000
81400.00
2mS

CLUSTER GROUP C

Cluster 1

This cluster comprising 34 holes is characterized by a high (La/Yb)n ratio, moderate Th and low rare earth element concentrations. These holes are located predominantly near the margins or within the palaeochannels and represent unmineralised channel sediments, with the high (La/Yb)n ratio due to a low abundance of LREE enriched heavy minerals such as monazite.

Cluster 2

This group of 6 holes is characterized by a high U/Th ratio and U concentration, a moderate concentration of rare earth elements and a low (La/Yb)n ratio (indicating HREE enrichment). These geochemical characteristics suggest that these holes, which are located in the northern portion of the main mineralized zone have probably formed by organic complexation of U and HREE's derived from groundwaters. Presumably the presence of carboxylic functional groups in the organic matter are analogous to those of free carbonate species and hence a similar style of U and HREE fixation occurs.

Cluster 3

This cluster of 23 holes is similar in its geochemical characteristics and spatial distribution to cluster 1, however is differentiated on the basis of its slightly higher levels of rare earth and U, lower Th and lower (La/Yb)n ratio. These geochemical signature *i.e.* higher U/Th ratio and relatively higher HREE enrichment imply that these holes have been enriched by complexation and redox processes.

Cluster 4

This group of 4 holes are characterized by high REE, Th and U concentrations and are located in the main zone of mineralization. These holes have also been identified in previous clustering exercises and have been shown to have elevated concentrations of Mo, Cu and Zn.

Cluster 5

This large cluster of 47 holes which has been classified on the basis of low rare earth element, U and Th concentrations also has a high (La/Yb)n ratio are predominantly located on the margins and to the east of the main mineralized zone are indicative of unmineralised channel sedimentary material.

Cluster 6

This cluster of 8 holes is distinctive in that it has a high U/Th ratio, moderate concentrations of rare earth elements, low Th and a low (La/Yb)n ratio. These holes are primarily located within the main area of mineralization, with the elemental enrichment resulting from groundwater flow, organic complexation and redox processes. These holes are associated with cluster 2, however have far higher Eu and lower Sc concentrations.

Cluster 7

This cluster of two holes located to the west of the main mineralized zone are characterized by having relatively low U and Th concentrations, moderate abundances of rare earth elements and a relatively high level of Sc.

This cluster is associated with clusters 2 and 6 however is distinguished from them by its low U/Th ratio and higher degree of LREE enrichment.

Cluster 8

This single hole is closely geochemically and spatially associated to cluster 4 however it has a distinctly lower U/Th ratio and a Eu concentration almost 3 times that of cluster 4.

Cluster 9

This cluster which comprises 8 holes is associated with clusters 2, 6 and 7 and characterized by high U and Sc and moderate rare earth element concentrations and a very high U/Th ratio.

Cluster 10

This cluster of 19 holes has relatively low concentrations of all elements and is generally distributed in a similar area to related clusters 1, 3 and 5, however is generally closer to the main mineralized zone. This cluster has the lowest (La/Yb)n ratio, indicating that even though rare earth element concentrations are low there is still a significant degree of HREE enrichment.

CLUSTER GROUP C

Cluster 1
6010 6167 6172 6114 6145 6001 6006 6151 6080 6140 6146 6067 6143 6014 6018 6020 6162 6166 6171 6126 6046 6128 6041 6120 6164 6004 6142 6045 6042 6011 6015 6113 6138 6121

Cluster 2
6059 6199 6185 6070 6186 6197

Cluster 3
6096 6116 6075 6089 6170 6068 6157 6074 6161 6056 6040 6165 6132 6182 6030 6209 6217 6064 6176 6077 6095 6187 6211

Cluster 4
6213 6099 6117 6085

Cluster 5
6194 6192 6221 6234 6208 6225 6135 6065 6122 6127 6226 6150 6223 6222 6207 6181 6219 6220 6201 6227 6183 6184 6188 6191 6214 6218 6147 6155 6129 6231 6016 6133 6139 6134 6137 6200 6148 6196 6144 6131 6049 6215 6224 6228 6216 6079 6212

Cluster 6
6159 6093 6097 6088 6086 6091 6210 6156

Cluster 7
6054 6058

Cluster 8
6081

Cluster 9
6071 6178 6198 6037

Cluster 10
6063 6039 6028 6036 6034 6029 6062 6031 6152 6061 6177 6082 6190 6232 6180 6072 6175 6189 6154

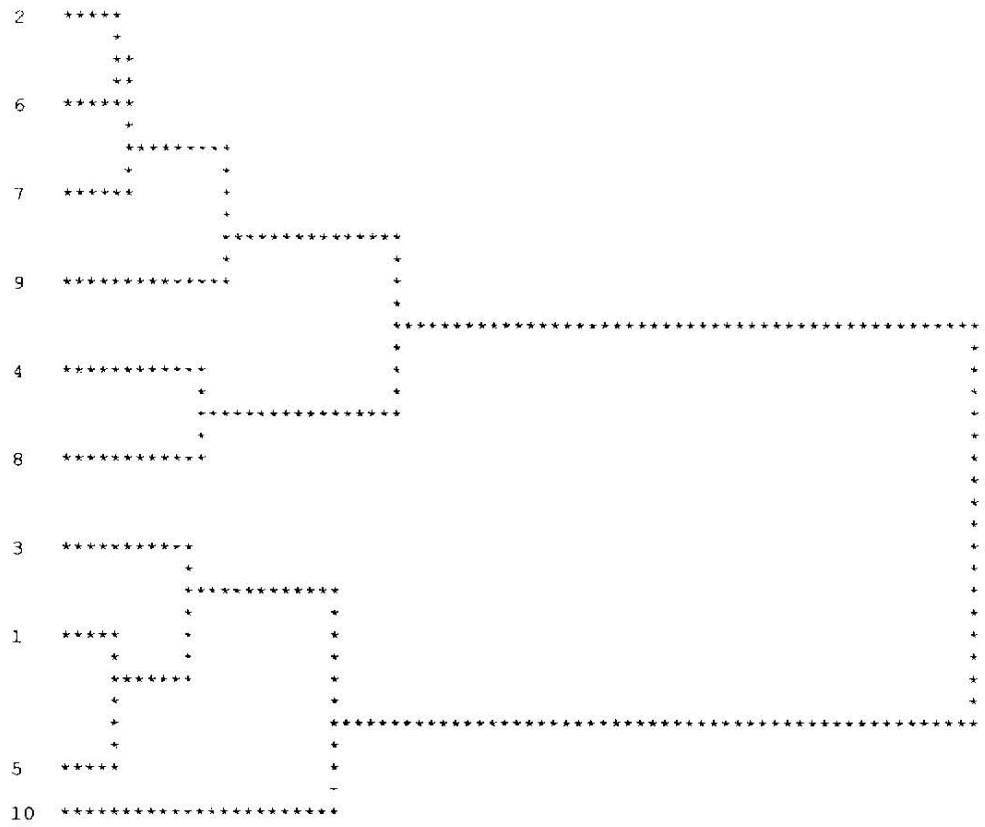

Cluster	No. obs	Lu.n	La.n	Sc.n	Sm.n	Th.n	U.n	Yb.n	Ce.n	Eu.n	U/Th	(La/Yb)n
1	34	0.55	59.5	17.49	10.19	21.5	38	2	3	105	2	20.1
2	6	2.61	223.5	144.5	91.32	15.2	1708	23.4	19.2	622	112	6.5
3	23	1.79	156.1	43.56	65.77	12.2	489	14.9	13.1	490	40	7.1
4	4	6.3	705.5	165.8	220.5	134	2977	55.3	47.8	1445	22	8.6
5	47	0.3	38.4	8.4	6.29	13.2	63	1.3	2	77	5	20.0
6	8	4.06	346	64.6	159.4	14.3	1625	33.9	30.5	1143	114	6.9
7	2	4.61	467	174.5	165	38.8	299	29.4	24.1	1660	8	10.7
8	1	12.2	1410	68.7	482	86.5	505	111	69.6	4060	6	8.6
9	4	0.91	163.9	671.3	38.29	21.2	3965	10.6	8.2	211	187	10.4
10	19	1.29	44.1	41.89	26.16	40.5	127	5.1	8	137	3	5.8

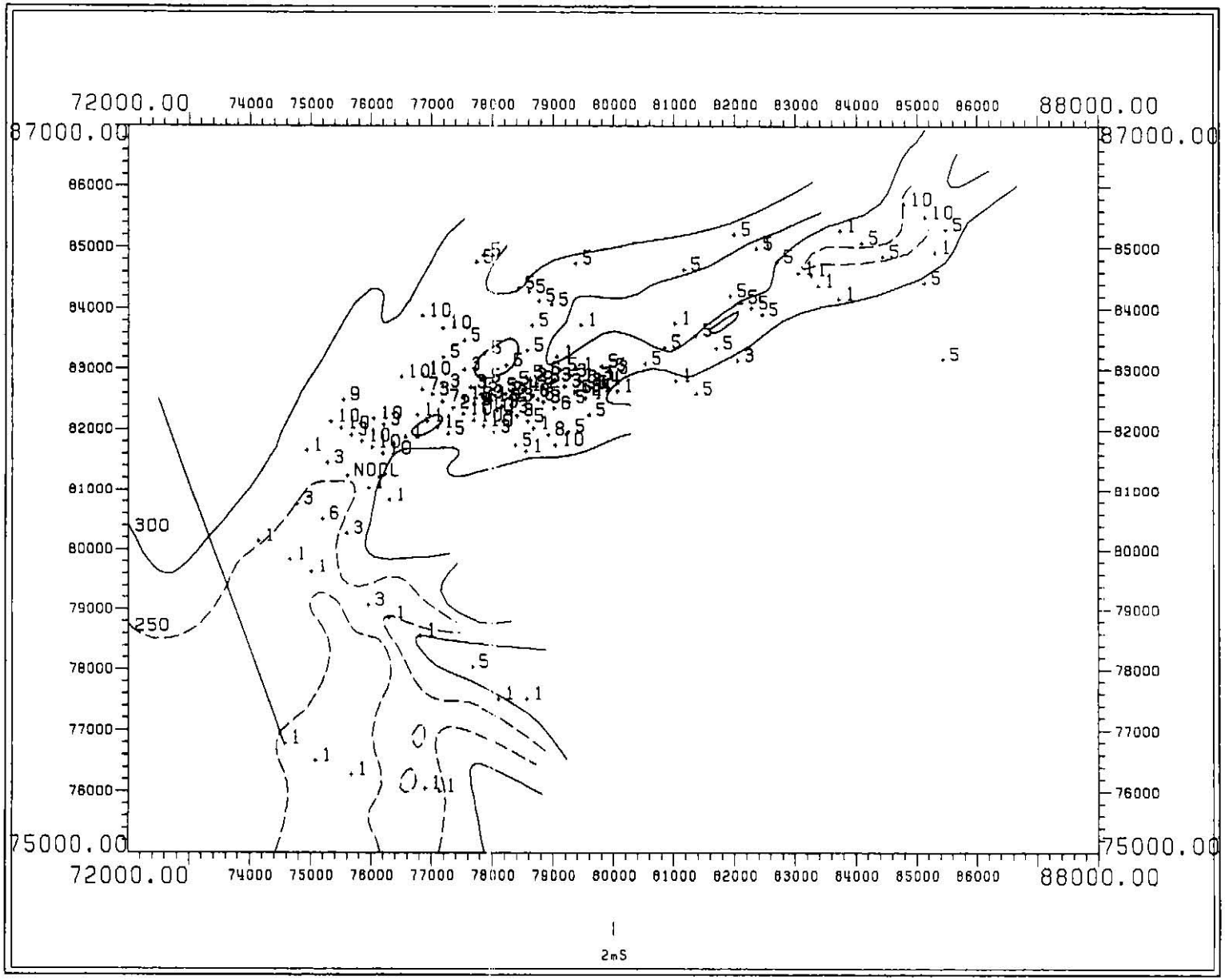
72000.00
74000
75000
76000
77000
78000
79000
80000
81000
82000
83000
84000
85000
86000
88000.00
87000.00
86000
85000
84000
83000
82000
81000
80000
79000
78000
77000
76000
75000.00
NOCL
300
250
2mS

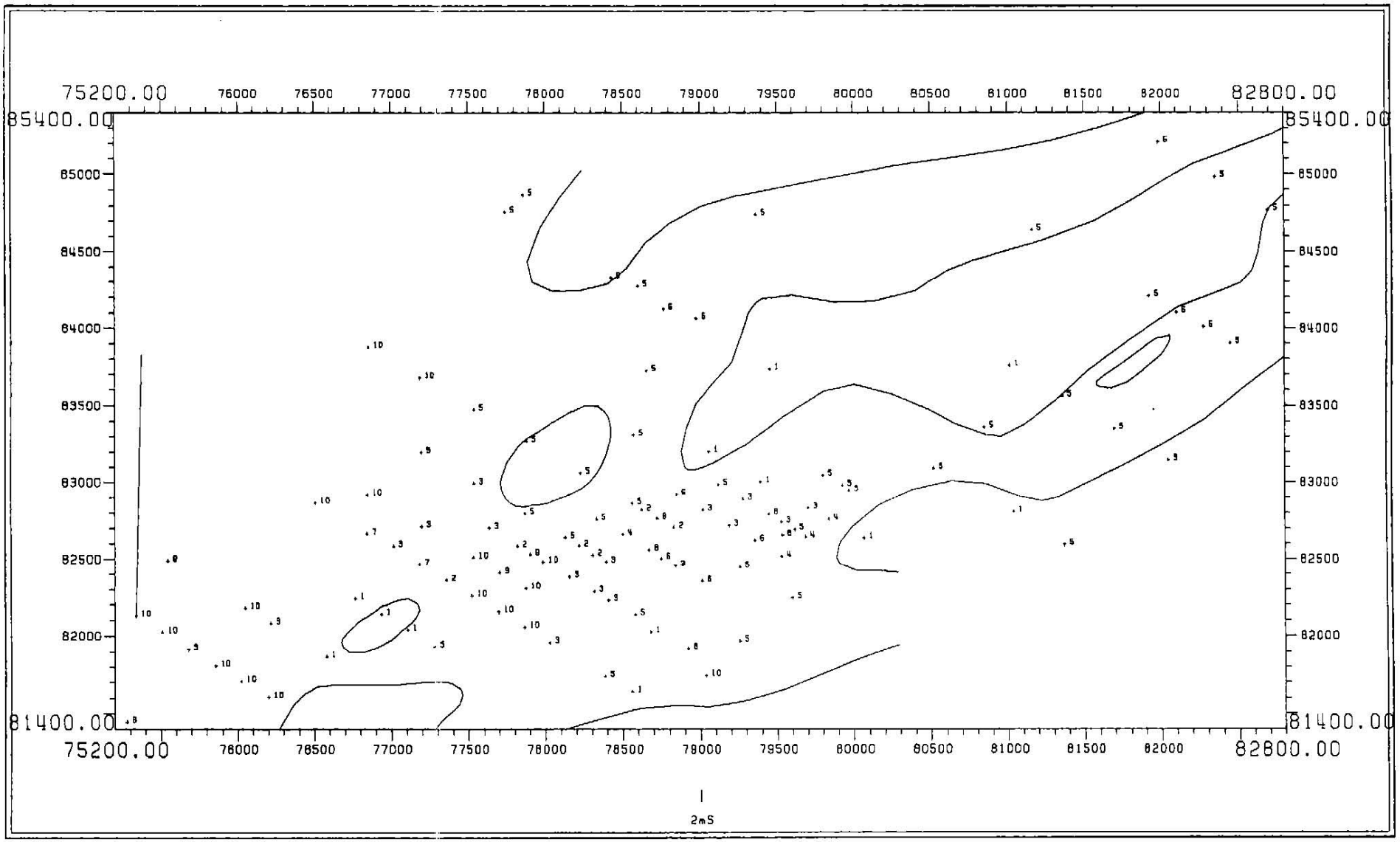
75200.00
76000
76500
77000
77500
78000
78500
79000
79500
80000
80500
81000
81500
82000
82800.00
85400.00
85000
84500
84000
83500
83000
82500
82000
81400.00
2mS

CLUSTER GROUP D

Cluster I

This cluster consists of 2 holes which with elevated concentrations of Ni, Mn and Rb, intermediate concentrations of Br, Co, Ba, Ga, Mo, Zn and V and a low U/Th ratio. The presence of elevated Mn and low S concentrations suggest that these holes may possibly contain (?partially) oxidized material which may have scavenged some of the trace metals.

Cluster 2

This cluster again consists of only 2 holes and contains elevated concentrations of As, Mo and Zn and has a high U/Th ratio. This geochemical assemblage implies organic scavenging may have been the dominant process leading to the trace metal and As enrichment.

Cluster 3

This group of 19 holes is characterized by high Ga and Nb concentrations moderate enrichments of Cr, Br, Co, Ba, Cu, Pb, S, Mn, Sr, Th and U and a low U/Th ratio. The holes associated with this cluster are mainly located outside the main ore zone within the palaeochannel. Previous cluster exercises have shown that the holes are mainly associated with clay-rich sedimentary material with a minor heavy mineral component. This is also confirmed by the high Ga (c.f. Al_2O_3) and Nb (in heavy minerals) content.

Cluster 4

This cluster of 31 holes is delineated by its high Ba and Rb concentrations (indicative of clays). The spatial distribution of these holes is similar to that of non-mineralized clay-rich channel and non channel sediments identified in previous clustering exercises. Note that these holes are associated with cluster 1, which is only separated by its high Ni concentration.

Cluster 5

This is the largest cluster containing some 51 holes and is characterized by having moderate to high Ga, Mn and Th concentrations and a low U/Th ratio. This cluster is related to clusters 1 (2 holes) and 4 (31 holes), however is differentiated from cluster 4 (the second largest cluster) by having higher Cr, Co, Ni, Zn, Th and U and having lower As, Ba, Cu, Nb, S, Rb, Sr and V concentrations. The spatial distribution of this cluster is mainly within the palaeodrainage (channel) system, as opposed to cluster 4 which is generally distributed on the margins or outside the palaeochannels.

Cluster 6

This cluster of only 4 holes has been identified in previous clusters as a group of three holes occurring on the eastern edge and 1 on the northern edge of the main mineralized zone and is distinguished by having high S and trace metal (Cr, Cu, Mo, Ni, Pb, Zn, Th, U, Sr and V) concentrations and a intermediate U/Th ratio. This cluster of 4 holes is related to the two holes of cluster 2, the major differences being however, the far lower Zn and higher Th and Sr concentrations and a similar U concentration and hence the lower U/Th ratio.

Cluster 7

This single hole although related to the 14 holes of cluster 3, however is differentiated from all other holes by having a very high W concentration, while all other elements are generally present in low to intermediate concentrations.

Cluster 8

This cluster of 22 holes is generally restricted to the main mineralized zone and is characterized by having a high concentration of Cu and a high U/Th ratio, with intermediate concentrations of Cr, As, Br, Co, Ba, Mo, Nb, Ni, Pb, S, Zn, Mn, Rb, Th, U, Sr and V. This cluster is related to clusters 2 (2 holes) and 6 (4 holes) however is differentiated on the basis of generally lower trace metal concentrations (except for Cu).

Cluster 9

This cluster of 19 holes is characterized by having intermediate Br, Co, Cu, Nb, Ni, S, Zn and Zr and low U and Th concentrations and a low U/Th ratio. The majority of these holes occur within or on the western margin of the main mineralized zone. This cluster is related to clusters 3 and 7, however may be distinguished on the basis of higher Cr, Co, Ni, S and Zn and lower Ba, Mn, Rb and Th concentrations and a lower U/Th ratio.

Cluster 10

This single hole is clearly separated from all others by its elevated concentrations of As, Cr, Co, Cu, Nb, Ni, Pb, S, U and V and its high U/Th ratio. This hole which is located well to the west of the main mineralized zone has been clearly recognized in other clustering exercise due to its elevated trace element concentrations. Because of the unusually enriched nature of this hole its is only weakly related to clusters 2, 6 and 8 which represent others holes with significant mineralization.

CLUSTER GROUP D

Cluster 1
6209 6164

Cluster 2
6156 6187

Cluster 3
6071 6054 6029 6034 6157 6114 6170 6001 6154 6011 6167 6010 6172 6006

Cluster 4
6133 6226 6018 6041 6151 6162 6128 6045 6046 6065 6120 6129 6231 6137 6144 6134 6016 6139 6132 6126 6127 6192 6145 6150 6194 6228 6138 6020 6113 6224 6121

Cluster 5
6015 6080 6143 6142 6067 6122 6082 6135 6140 6184 6014 6004 6152 6063 6166 6171 6062 6036 6042 6189 6190 6188 6232 6225 6180 6175 6191 6216 6208 6227 6218 6234 6219 6177 6221 6183 6217 6181 6201 6214 6207 6222 6196 6200 6215 6223 6147 6049 6148 6155 6131

Cluster 6
6099 6117 6086 6213

Cluster 7
6146

Cluster 8
6186 6197 6040 6088 6075 6089 6096 6185 6072 6116 6058 6085 6081 6059 6097 6210 6211 6093 6199 6070 6178 6198

Cluster 9
6176 6212 6182 6159 6161 6028 6039 6030 6165 6061 6031 6068 6074 6056 6091 6064 6077 6079 6095

Cluster 10
6037

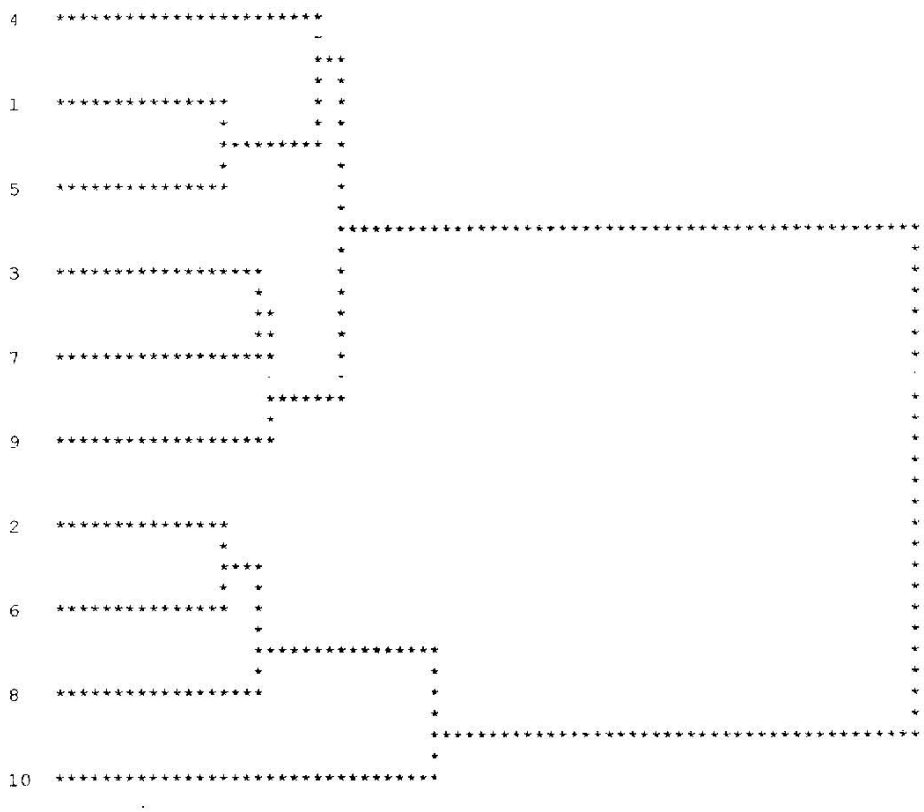

Cluster	No. obs	Cr.n	As.n	Br.n	Co.n	W.n	Ba.x	Ga.x	Cu.x	Mo.x	Nb.x	Ni.x	Pb.x	S.p	Zn.x	Mn.x	Rb.x	Th.n	U.n	Sr.x	V.x	U/Th
1	2	49	4	10	1113	3	308	12	57	24	18	7003	24	6650	826	722	99	10.7	54	46	194	5
2	2	139	50	16	1287	1	120	23	1393	37	11	2184	391	41800	23744	8	9	11.8	2287	169	305	194
3	14	322	5	23	72	8	317	48	301	11	57	172	88	10829	104	63	18	36.7	182	73	112	5
4	31	78	14	8	19	12	464	20	173	9	18	50	38	8300	131	86	120	13.8	28	134	187	2
5	51	79	4	7	47	15	81	14	98	10	12	137	38	6455	515	130	9	22.2	65	34	55	3
6	4	445	40	17	884	1	321	12	1017	52	28	1090	466	58375	3486	7	9	117.1	2690	558	432	23
7	1	148	17	40	27	359	202	36	49	17	23	89	117	3900	621	86	20	37	32	46	170	1
8	22	191	22	17	350	5	151	8	1840	36	25	924	350	35391	1961	43	14	23.6	1772	86	315	75
9	19	59	10	32	131	5	111	8	206	9	25	423	78	60368	1660	49	4	9.8	153	91	150	16
10	1	732	91	1	9740	1	127	12	5157	31	81	12178	726	105800	3491	53	14	52.9	5870	38	451	111

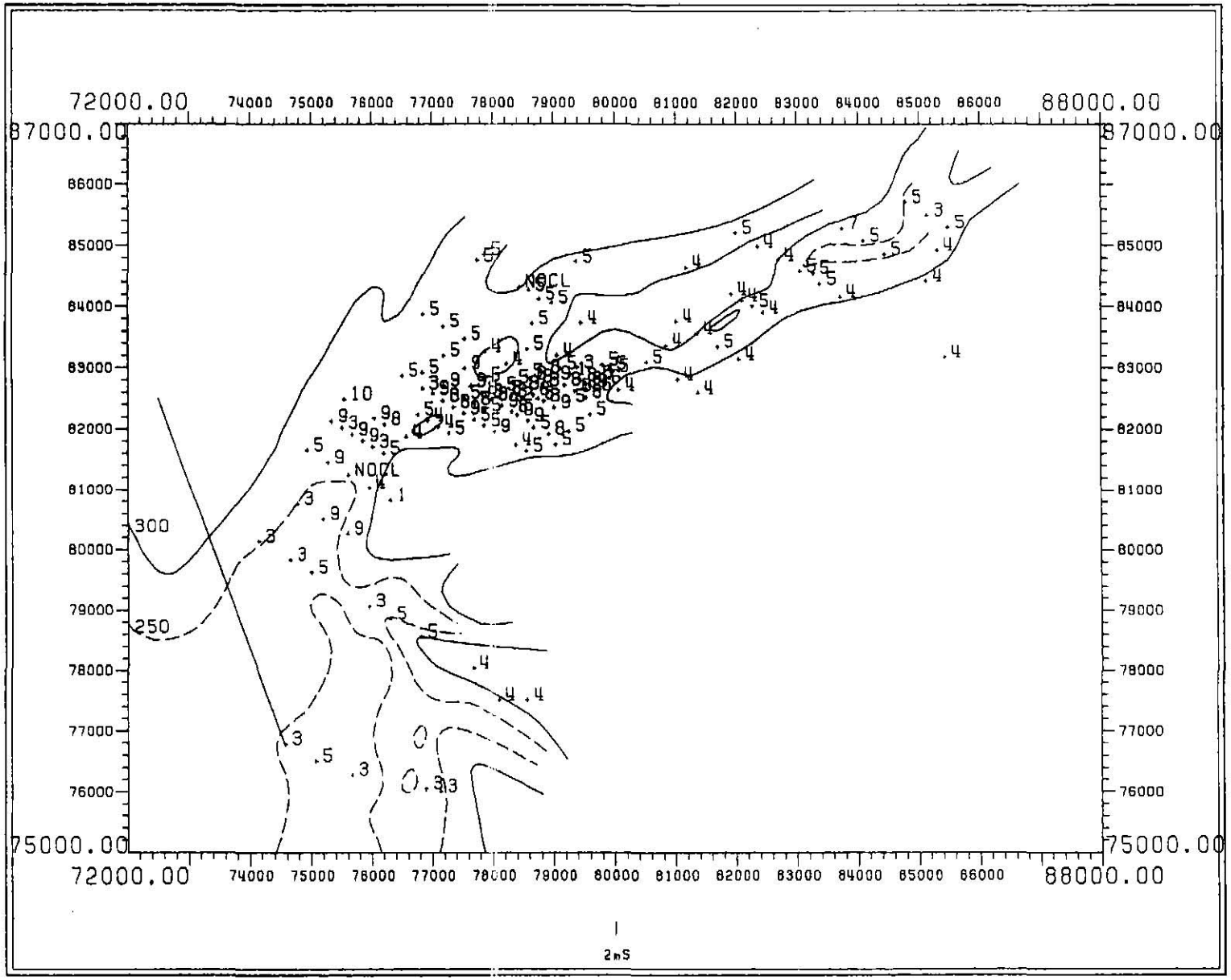
72000.00
74000
75000
76000
77000
78000
79000
80000
81000
82000
83000
84000
85000
86000
88000.00
87000.00
86000
85000
84000
83000
82000
81000
80000
79000
78000
77000
76000
75000.00
NOCL
300
250
2mS

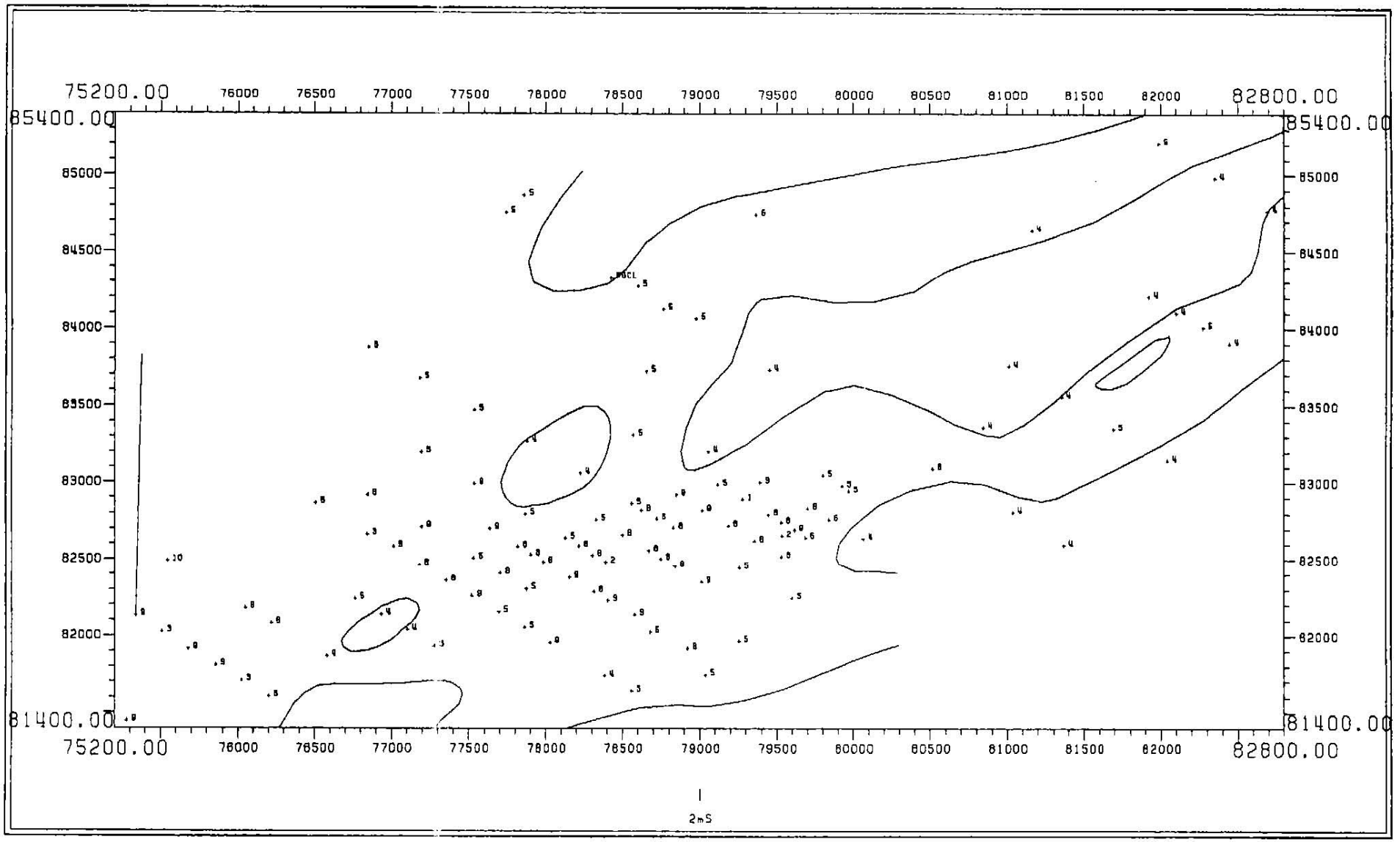
75200.00
76000
76500
77000
77500
78000
78500
79000
79500
80000
80500
81000
81500
82000
82800.00
85400.00
85000
84500
84000
83500
83000
82500
82000
81400.00
2mS

CLUSTER GROUP E

Cluster 1

This cluster of only 2 holes, 1 located outside (west) and 1 within the main mineralized zone are characterized by high Tl, Co, Mo and Ni concentrations and a low U/Th ratio.

Cluster 2

This cluster again of only 2 holes is distinguished by having high Au, Co and Zn and low W, Cl, Nb and Th concentrations and a high U/Th ratio. Both of the holes are located within the main mineralized zone. The spatial distribution of low solid Cl concentrations within the main mineralized zone suggests that distribution of some elements may be potentially influenced by the ionic strength of groundwaters. High ionic strength groundwaters may inhibit the effective complexation of dissolved metal ions, or possibly remobilize them after deposition.

Cluster 3

This cluster of 14 holes is characterized by having moderate enrichments of Nb, Cl, Au, Br, Cr, Cu, Pb, S, Sc, U, Th and Ta and a low U/Th ratio. The majority of these holes are located to the south of the main mineralized zone within the confines of the palaeochannel. Previous clustering exercises have shown these holes to be mainly associated with clay-rich sediments containing some organic matter and a small degree of heavy mineral enrichment relative to other areas in the palaeochannel.

Cluster4

This cluster of 31 holes are predominantly located on the margins or outside the palaeochannel and are distinguished by their absence of any significant enrichment of any elements. These holes represent areas of unmineralised palaeochannel and surrounding sediments.

Cluster 5

This large cluster of 51 holes contains a relatively moderate enrichment of Au and generally low abundances of all other trace elements. These holes are throughout the entire palaeochannel system and are related to clusters 1 and 4 in that they represent areas of unmineralised sedimentary material. Note however that cluster 4 holes occur predominantly outside and cluster 5 holes predominantly within the palaeochannel system and are differentiated geochemically by cluster 5 holes having higher Au, Co, Ni, Zn, Th and U and lower As, Cu, Nb, S and V.

Cluster 6

These 4 holes occur within the main mineralized zone and are characterized by enrichments of Cr, Mo, Cu, Ni, Zn, Pb, Sc, Th, U, Ta and V. These holes have been recognized in previous clustering exercises *e.g.* cluster 6 Cluster Group D as being enriched in a wide range of trace elements. This cluster is associated with cluster 2 and is differentiated by having higher Cr, Mo, Nb, Pb, S, Sc, Th, U, Ta and V and lower Au, As, Co, Cu, Ni, Zn and Tl concentrations and a lower U/Th ratio.

Cluster 7

This single hole is distinguished from all others by a its very high W concentration and due to this feature has been delineated in a number of previous clustering exercises. Also elevated are levels of Au and Br. Note that this hole is related to the 14 holes associated with cluster 3.

Cluster 8

This cluster of 22 holes occur almost exclusively within the main mineralized zone and are characterized by a moderately high concentration of Cu, Zn, Ta and Cl. This cluster is associated with clusters 2 and 6 and represents an area of enrichment of a wide range of trace elements, presumably by complexation with organic matter and incorporation into sulfide phases.

Cluster 9

This cluster of 19 holes occurs mainly in the western half and further to the west of the main mineralized zone. These holes are distinguished by their relatively high S concentrations and intermediate levels of a wide range of trace elements and a low U/Th ratio. This cluster is associated with clusters 3 and 7 by virtue of its similar low to intermediate levels of trace elements.

Cluster 10

This single hole has been delineated in a number of previous clustering exercises and in this case is differentiated from all other holes by its elevated concentrations of As, Co, Cr, Cu, Nb, Ni, Pb, S, Zn, Tl, U and V and its high U/Th ratio.

CLUSTER GROUP E

Cluster 1
6209 6164

Cluster 2
6156 6187

Cluster 3
6071 6054 6029 6034 6157 6114 6170 6001 6154 6011 6167 6010 6172 6006

Cluster 4
6133 6226 6018 6041 6151 6162 6128 6045 6046 6065 6120 6129 6231 6137 6144 6134 6016 6139 6132 6126 6127 6192 6145 6150 6194 6228 6138 6020 6113 6224 6121

Cluster 5
6015 6080 6143 6142 6067 6122 6082 6135 6140 6184 6014 6004 6152 6063 6166 6171 6062 6036 6042 6189 6190 6188 6232 6225 6180 6175 6191 6216 6208 6227 6218 6234 6219 6177 6221 6183 6217 6181 6201 6214 6207 6222 6196 6200 6215 6223 6147 6049 6148 6155 6131

Cluster 6
6099 6117 6086 6213

Cluster 7
6146

Cluster 8
6186 6197 6040 6088 6075 6089 6096 6185 6072 6116 6058 6085 6081 6059 6097 6210 6211 6093 6199 6070 6178 6198

Cluster 9
6176 6212 6182 6159 6161 6028 6039 6030 6165 6061 6031 6068 6074 6056 6091 6064 6077 6079 6095

Cluster 10
6037

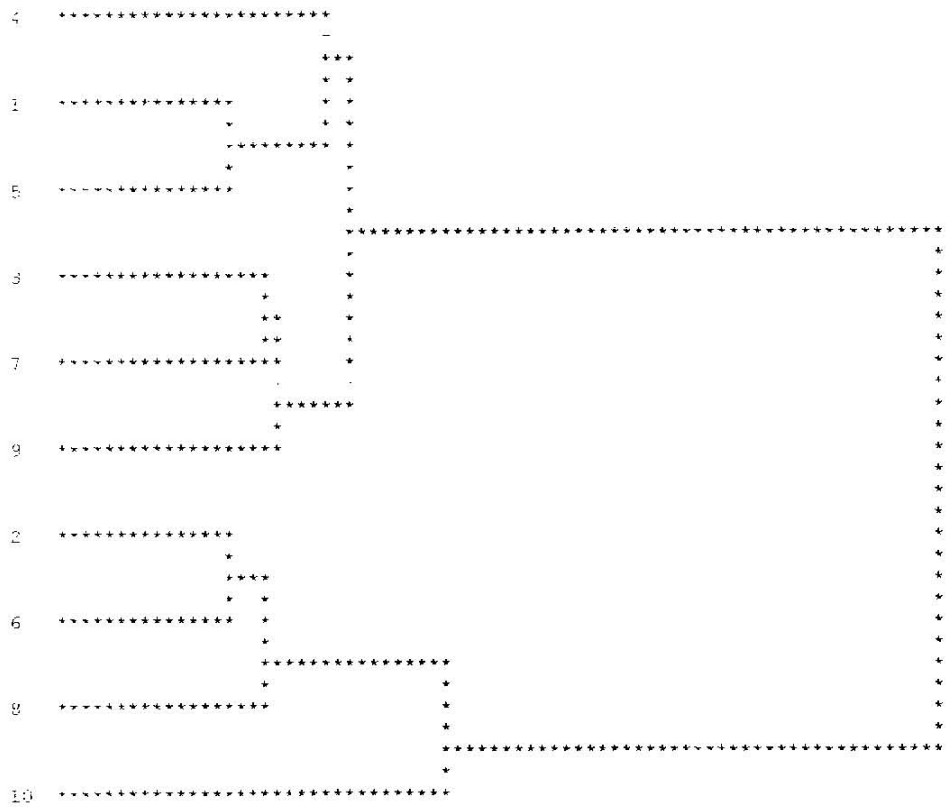

Cluster	No. obs	Au.n	As.n	Br.n	Co.n	W.n	Cr.n	Cl	Cu.x	Mo.x	Nb.x	Ni.x	Pb.x	S.p	Zn.x	Tl.x	Se.n	Th.n	U.n	Ta.n	V.x	U/Th
1	2	3	4	10	1113	3	49	4.1	57	24	18	7003	24	6650	826	61	3	10.7	54	2	194	5
2	2	62	50	16	1287	1	139	2.6	1393	37	11	2184	391	41800	23744	43	91	11.8	2287	4	305	194
3	14	12	5	23	72	8	322	8.6	301	11	57	172	88	10829	104	4	43	36.7	182	6	112	5
4	31	7	14	8	19	12	78	4.9	173	9	18	50	38	8300	131	3	5	13.8	28	1	187	2
5	51	26	4	7	47	15	79	6.6	98	10	12	137	38	6455	515	5	10	22.2	65	2	55	3
6	4	3	40	17	884	1	445	2.7	1017	52	28	1090	466	58375	3486	21	724	117.1	2690	8	432	23
7	1	60	17	40	27	359	148	4.2	49	17	23	89	117	3900	621	0	19	37	32	2	170	1
8	22	6	22	17	350	5	191	8.5	1840	36	25	924	350	35391	1961	19	75	23.6	1772	7	315	75
9	19	3	10	32	131	5	59	1.6	206	9	25	423	78	60368	1660	10	6	9.8	153	3	150	16
10	1	3	91	1	9740	1	732	2.6	5157	31	81	12178	726	105800	3491	137	208	52.9	5870	1	451	111

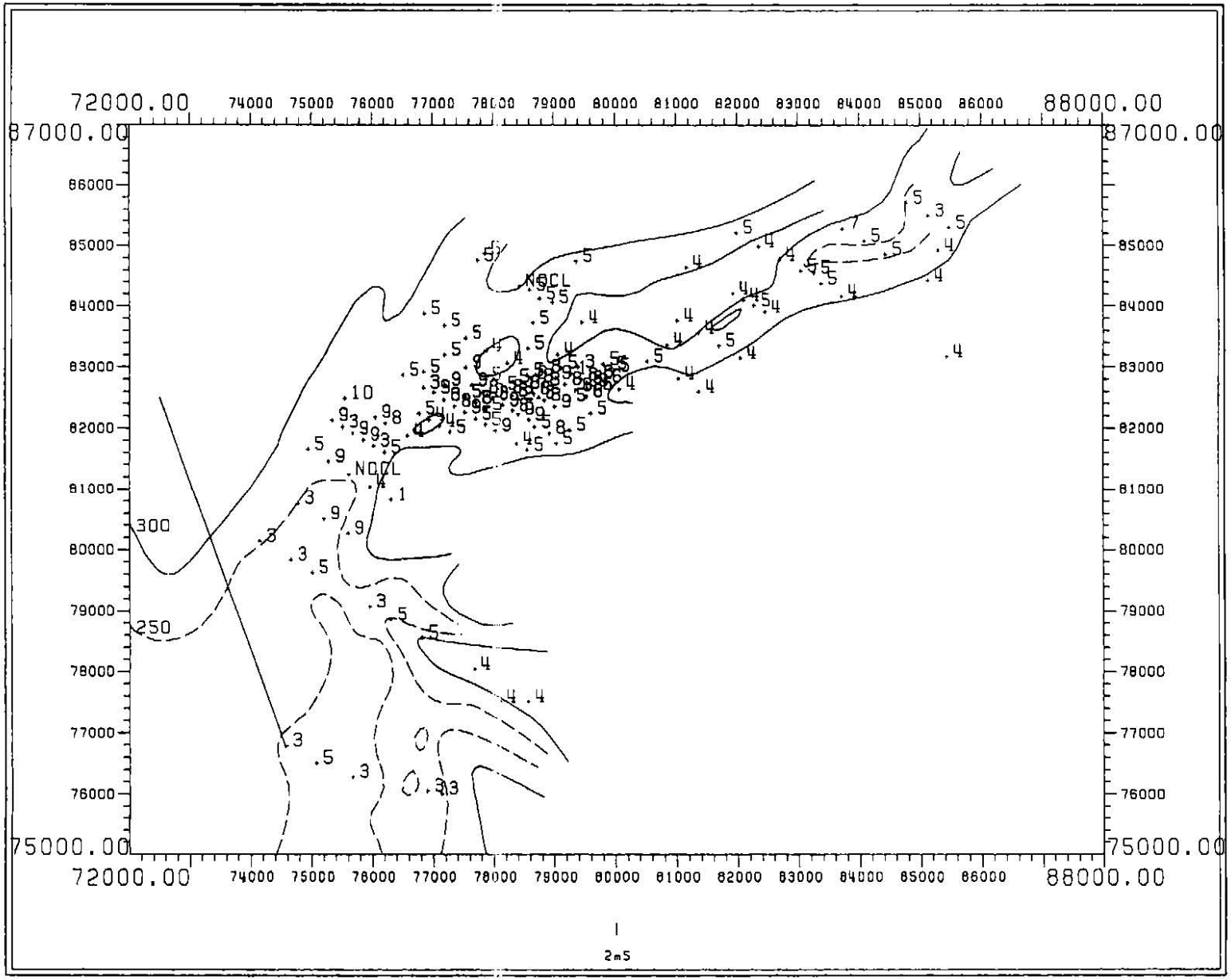
72000.00
74000
75000
76000
77000
78000
79000
80000
81000
82000
83000
84000
85000
86000
88000.00
87000.00
86000
85000
84000
83000
82000
81000
80000
79000
78000
77000
76000
75000.00
NDCL
300
250
2mS

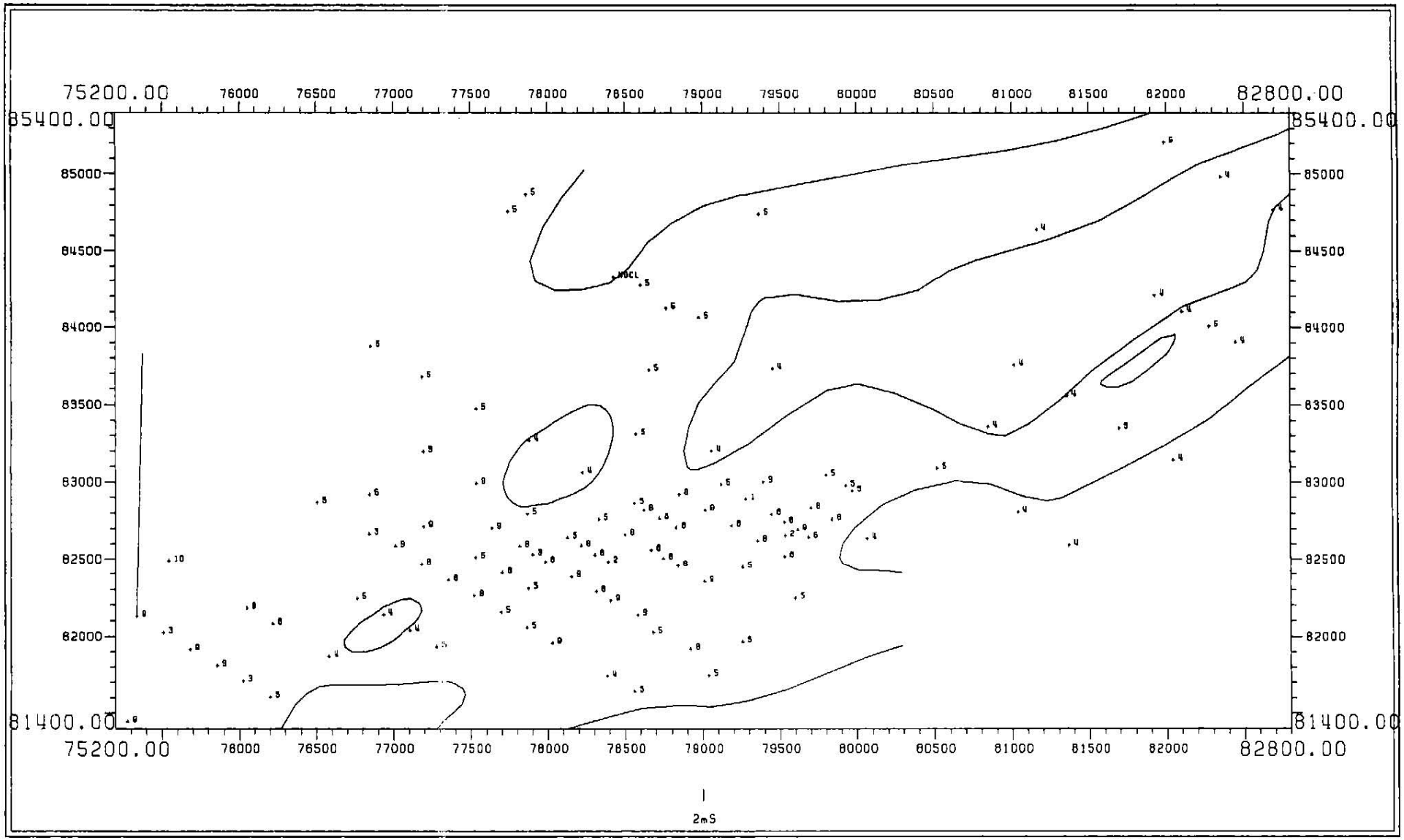
75200.00
76000
76500
77000
77500
78000
78500
79000
79500
80000
80500
81000
81500
82000
82800.00
85400.00
85000
84500
84000
83500
83000
82500
82000
81400.00
2mS

APPENDIX 4

GEOCHEMISTRY OF THE BASEMENT LITHOLOGIES:

HOLES CD-1594, CD-1595 AND CD-1596

Appendix 4: Geochemistry of the basement lithologies: holes CD-1594, CD-1595 and CD-1596.

Concentrations are expressed in % for the major elements and in ppm (except Au, ppb) for the trace elements. All major elements were analysed by XRF-fusion, and trace elements by either neutron activation analysis (n), XRF pressed powder (x) or XRF fusion (f).

Sample	SiO2	Al2O3	Fe203	MnO	MgO	CaO	Na20	K2O	TiO2	P205	S	LOI%	Total
CD1594-1	96.17	0.73	0.54	0.003	0.05	0.03	0.06	0.06	1.88	0.003	0.01	0.47	100.00
CD1594-2	75.20	14.00	2.19	0.003	0.86	0.02	0.09	3.48	0.63	0.010	0.29	3.24	100.01
CD1594-3	74.69	12.62	3.07	0.003	0.98	0.02	0.18	3.80	1.42	0.021	0.43	2.79	100.01
CD1594-4	68.22	17.45	2.43	0.002	0.99	0.02	0.10	4.33	1.48	0.019	0.55	4.44	100.02
CD1594-5	63.48	14.38	5.43	0.002	0.87	0.03	0.15	3.44	1.37	0.037	3.05	8.01	100.24
CD1594-6	63.95	16.27	4.12	0.002	1.41	0.02	0.18	5.06	1.95	0.016	1.36	5.74	100.08
CD1594-7	58.59	18.80	4.22	0.002	1.17	0.02	0.20	4.96	2.74	0.024	1.71	7.69	100.13
CD1594-8	70.89	11.62	3.59	0.006	0.90	0.02	0.17	3.87	0.44	0.040	1.83	6.76	100.12
CD1594-9	71.29	11.29	3.31	0.006	0.86	0.02	0.17	3.81	0.41	0.040	1.66	7.27	100.12
CD1594-10	72.13	10.76	3.72	0.005	0.87	0.01	0.11	3.77	0.44	0.021	1.7	6.58	100.11
CD1594-11	72.43	11.12	3.31	0.005	0.93	0.06	0.11	3.99	0.50	0.043	1.36	6.24	100.08
CD1595-1	97.39	0.63	0.50	0.005	0.25	0.21	0.10	0.20	0.02	0.003	0.08	0.61	100.00
CD1595-2	96.85	0.60	0.91	0.007	0.18	0.16	0.04	0.12	0.01	0.003	0.3	0.83	100.00
CD1595-3	93.65	0.97	1.94	0.006	0.25	0.26	0.08	0.11	0.01	0.002	0.95	1.79	100.02
CD1595-4	60.20	6.21	12.74	0.011	0.50	0.09	0.22	1.03	0.14	0.008	9.07	10.76	100.98
CD1595-5	15.48	1.63	30.69	0.002	0.18	0.04	0.23	0.28	0.03	0.003	33.15	27.35	109.07
CD1595-6	3.83	0.12	0.42	0.059	21.0	29.83	0.01	0.02	0.00	0.002	0.49	44.42	100.22
CD1595-7	6.06	0.20	0.56	0.047	20.3	28.77	0.01	0.04	0.00	0.002	0.29	43.81	100.13
CD1595-8	3.63	0.32	0.55	0.054	21.0	29.54	0.01	0.08	0.01	0.002	0.3	44.65	100.13
CD1595-9	4.10	0.44	0.91	0.056	20.8	29.39	0.01	0.08	0.01	0.002	0.43	43.95	100.19
CD1595-10	5.80	0.44	0.64	0.058	20.3	28.74	0.01	0.10	0.01	0.005	0.26	43.74	100.11
CD1595-11	5.83	0.50	1.84	0.086	20.9	29.57	0.01	0.08	0.01	0.007	0.63	40.78	100.26
CD1595-12	4.83	1.36	2.42	0.115	20.4	28.82	0.07	0.13	0.03	0.014	1.45	40.96	100.59
CD1595-13	1.41	0.15	1.99	0.069	21.9	30.96	0.01	0.02	0.00	0.002	0.42	43.22	100.18
CD1596-1	99.06	0.27	0.37	0.003	0.01	0.00	0.06	0.02	0.01	0.003	0.01	0.19	100.00
CD1596-2	56.35	26.07	2.17	0.003	1.62	0.07	0.44	5.27	0.81	0.047	0.15	7.01	100.01
CD1596-3	98.07	0.80	0.48	0.003	0.05	0.02	0.05	0.09	0.02	0.002	0.02	0.40	100.00
CD1596-4	62.30	20.71	3.01	0.003	1.97	0.03	0.28	5.64	0.60	0.029	0.14	5.30	100.01
CD1596-5	84.09	7.02	3.10	0.009	0.65	0.05	0.18	1.33	0.29	0.023	0.12	3.13	100.00
CD1596-6	98.37	0.37	0.93	0.004	0.02	0.00	0.03	0.04	0.02	0.001	0.01	0.21	100.00
CD1596-7	93.65	0.76	0.78	0.004	0.10	0.07	0.43	0.13	0.14	0.003	0.04	3.91	100.00
CD1596-8	71.02	15.71	2.86	0.008	1.16	0.05	0.28	3.19	0.53	0.014	0.19	5.00	100.00
CD1596-9	96.79	0.34	1.81	0.008	0.08	0.07	0.04	0.03	0.01	0.003	0.01	0.81	100.00
CD1596-10	65.24	15.70	5.46	0.014	2.36	0.11	0.24	4.95	0.51	0.033	0.07	5.31	100.00

Sample	As.n	Au.n	Ba.x	Bi.x	Br.n	Cd.x	Ce.n	Cl.x	Co.n	Cr.n	Cs.n	Cu.x	Eu.n	Ga.x	Ge.x
CD1594-1	2.1	2.5	266	1	1	2	10.1	5	0.5	25.4	0.5	6	0.50	13	1
CD1594-2	11.1	2.5	207	1	2	1	15.3	5	0.5	248	6.7	31	0.50	19	3
CD1594-3	5.2	2.5	317	1	3	1	22	5	0.5	70.9	8.5	21	0.93	26	3
CD1594-4	2.9	2.5	315	1	1	1	20	5	0.5	65.6	7.7	40	1.21	27	2
CD1594-5	32.6	2.5	279	1	2	1	86.8	5	17.4	49.7	6.9	98	1.69	23	2
CD1594-6	22.5	2.5	311	2	3	1	58.6	5	21.0	102	13.2	23	1.29	27	2
CD1594-7	23.5	2.5	318	1	3	6	70.6	5	41.4	90.4	11.7	27	1.78	31	3
CD1594-8	157	14.2	342	1	2	41	57.8	5	14.1	144	7.4	245	1.24	19	2
CD1594-9	134	17.2	347	1	2	61	56	5	8.8	170	6.6	451	1.22	15	4
CD1594-10	110	10.4	261	1	1	13	47.7	5	9.2	121	7.4	130	0.97	18	2
CD1594-11	121	20.5	249	1	1	43	42.6	5	7.6	200	9.8	433	0.78	18	1
CD1595-1	2.5	2.5	34	1	1	1	12.8	5	4.3	5.4	0.5	8	0.50	3	1
CD1595-2	5.4	2.5	54	1	1	1	12.6	20	16.1	2.5	0.5	7	0.50	3	1
CD1595-3	7.6	2.5	14	1	3	1	9.8	151	20.1	5.2	0.5	7	0.50	3	1
CD1595-4	43.7	2.5	274	2	4	2	61.4	5	54.0	20.4	2.5	13	0.98	8	1
CD1595-5	168	2.5	30	3	5	1	66.8	5	171	6.7	2.3	25	1.14	7	5
CD1595-6	1.6	2.5	19	1	2	1	21	5	5.4	2.5	0.5	1	0.50	1	1
CD1595-7	1.6	2.5	21	1	1	1	12.1	5	8.9	2.5	0.5	1	0.50	3	1
CD1595-8	3.8	2.5	19	1	1	1	4.69	5	4.7	2.5	0.5	2	0.50	2	1
CD1595-9	2.7	2.5	29	1	1	1	19.6	5	8.6	2.5	0.5	1	0.52	3	1
CD1595-10	1.7	2.5	36	1	1	1	15.2	377	12.9	2.5	0.5	2	0.50	3	1
CD1595-11	2.3	2.5	28	2	2	1	29.4	5	39.1	2.5	0.5	1	0.63	1	1
CD1595-12	8.0	2.5	34	1	4	1	48.7	44	24.1	9.2	1.3	3	0.96	3	1
CD1595-13	1.4	2.5	24	1	1	1	15.3	6	19.5	2.5	0.5	1	0.50	1	1
CD1596-1	1.0	2.5	12	1	1	1	7.03	5	0.5	2.5	0.5	5	0.50	2	1
CD1596-2	3.3	2.5	272	1	8	1	223	5	18.4	121	16.4	29	3.51	28	6
CD1596-3	1.0	2.5	25	1	1	1	5.04	5	0.5	5.4	0.5	6	0.50	1	1
CD1596-4	2.2	2.5	266	1	4	1	51.6	5	3.3	119	14.8	17	0.73	28	7
CD1596-5	1.9	2.5	102	1	3	1	40.8	5	3.1	45.1	3.1	11	0.50	11	3
CD1596-6	2.5	2.5	10	1	1	2	9.63	5	1.9	10.9	0.5	10	0.50	1	2
CD1596-7	2.0	2.5	181	1	3	1	90.6	5	5.0	53.1	5.4	10	0.58	14	5
CD1596-8	5.9	2.5	176	1	5	1	114	5	5.3	72.1	9.3	13	0.67	21	3
CD1596-9	1.3	2.5	25	1	3	1	3.47	5	3.1	8.6	0.5	10	0.50	3	1
CD1596-10	6.5	2.5	219	1	2	2	104	5	10.4	90.6	13.9	22	0.75	22	4

Sample	Hf.n	La.n	Lu.n	Mo.x	Nb.x	Ni.x	Pb.x	Rb.x	Sb.n	Sc.n	Se.n	Sm.n	Sr.x	Ta.n	Tb.n
CD1594-1	4.1	5.01	0.31	5	33	4	9	2	17.2	5.1	5	0.87	14	2.4	0.25
CD1594-2	2.1	8.92	0.1	44	9	48	25	132	30.0	10.8	5	1.88	16	0.5	0.25
CD1594-3	4.6	11.1	0.26	14	15	11	28	146	9.8	14.4	5	3.47	26	1.2	0.72
CD1594-4	6.5	8.31	0.44	11	21	25	12	165	8.1	18.0	5	4.29	23	1.7	0.9
CD1594-5	5.4	54	0.34	9	18	46	49	140	5.0	16.6	5	7.75	35	1.8	0.94
CD1594-6	4.8	31	0.22	9	18	63	9	226	5.2	17.2	5	5.21	15	1.1	0.87
CD1594-7	5.8	33.2	0.31	9	26	100	11	234	5.0	22.8	5	6.73	18	2.2	0.91
CD1594-8	1.6	33.4	0.34	84	6	280	33	143	28.5	9.4	8.5	6.28	46	0.5	0.88
CD1594-9	1.6	31.9	0.29	72	8	211	39	141	30.8	8.8	11.9	6.34	43	0.5	0.92
CD1594-10	1.4	30	0.33	69	6	213	24	140	24.8	9.0	6.6	4.57	28	0.5	0.63
CD1594-11	1.9	28.4	0.38	98	9	174	42	149	37.0	9.5	10.9	3.65	35	0.5	0.66
CD1595-1	0.5	5.61	0.1	1	1	13	1	10	1.1	0.5	5	0.97	4	0.5	0.25
CD1595-2	0.5	5.71	0.1	2	1	66	4	6	6.2	0.2	5	0.8	7	0.5	0.25
CD1595-3	0.5	4.4	0.1	2	1	48	4	6	2.0	0.3	5	0.85	4	0.5	0.25
CD1595-4	1.0	25.1	0.1	7	3	550	55	47	3.0	2.0	5	5.27	16	0.5	0.51
CD1595-5	0.5	23.1	0.1	6	1	1037	36	20	5.4	1.1	5	6.05	8	0.5	0.53
CD1595-6	0.5	9.28	0.1	3	1	16	2	2	0.3	0.6	5	2.02	67	0.5	0.25
CD1595-7	0.5	6.59	0.1	2	1	15	1	2	0.3	0.3	5	1.1	58	0.5	0.25
CD1595-8	0.5	2.47	0.1	2	1	12	2	5	0.3	0.5	5	0.48	48	0.5	0.25
CD1595-9	0.5	7.97	0.1	2	1	15	3	8	0.3	1.0	5	2.19	53	0.5	0.25
CD1595-10	0.5	6.84	0.1	1	1	17	1	7	0.3	1.4	5	1.78	50	0.5	0.25
CD1595-11	0.5	13.3	0.1	2	1	42	3	7	0.3	1.1	5	3.08	59	0.5	0.56
CD1595-12	0.7	22.1	0.25	2	1	43	11	21	0.4	2.1	5	4.41	55	0.5	0.74
CD1595-13	0.5	6.89	0.1	2	1	24	2	1	0.3	0.8	5	1.82	47	0.5	0.25
CD1596-1	0.5	2.91	0.1	2	1	4	1	1	0.3	0.4	5	0.56	4	0.5	0.25
CD1596-2	5.8	92.6	0.64	2	18	51	11	286	0.7	22.2	5	18.6	57	1.7	2.2
CD1596-3	0.7	2.33	0.1	2	1	5	1	5	0.3	0.5	5	0.38	3	0.5	0.25
CD1596-4	5.0	22.5	0.38	3	12	19	6	299	0.7	17.5	5	3.82	14	1.4	0.81
CD1596-5	5.5	18.7	0.24	3	8	16	3	71	0.4	5.5	5	2.85	8	0.5	0.54
CD1596-6	0.7	1.77	0.1	2	1	5	3	2	0.3	0.8	5	0.43	1	0.5	0.25
CD1596-7	6.0	29	0.29	1	12	13	11	105	0.7	8.4	5	3.65	10	1.0	0.25
CD1596-8	5.5	32.2	0.31	1	14	11	7	177	0.6	11.0	5	4.2	12	1.1	0.57
CD1596-9	0.6	1.41	0.1	1	1	7	2	1	0.3	0.7	5	0.55	3	0.5	0.25
CD1596-10	3.7	15.1	0.37	4	11	18	26	264	0.7	14.1	5	4.1	14	0.5	0.67

Sample	Te.x	Th.n	Tl.x	U.n	V.x	W.n	Y.x	Yb.n	Zn.x	Zr.x	Traces	Majors	Majors+trace
CD1594-1	0.5	9.3	1	6.9	89	3.8	13	1.59	4	211	790	100.00	100.08
CD1594-2	0.5	6.1	1	8.8	947	1	10	1.31	41	82	1992	100.01	100.21
CD1594-3	0.5	8.2	1	17.3	565	1	18	1.92	59	185	1641	100.01	100.18
CD1594-4	1	9.1	1	31.1	418	1	36	3.3	266	261	1838	100.02	100.21
CD1594-5	4	7.9	1	20.9	242	1	30	2.49	916	215	2449	100.24	100.49
CD1594-6	0.5	8.1	1	21.9	377	1	24	1.71	368	211	2026	100.08	100.28
CD1594-7	0.5	7.7	3	17.6	649	1	35	2.34	728	263	2829	100.13	100.41
CD1594-8	0.5	9.3	5	14.4	811	1	29	2.5	3726	61	6400	100.12	100.76
CD1594-9	0.5	9.2	5	10.4	768	1	22	2.12	4533	62	7306	100.12	100.85
CD1594-10	0.5	9.3	3	12.9	624	1	24	2.27	1194	57	3232	100.11	100.44
CD1594-11	0.5	10.3	2	14.6	932	1	25	2.63	3219	68	6034	100.08	100.69
CD1595-1	0.5	0.3	1	1	4	1	2	0.25	168	4	315	100.00	100.03
CD1595-2	1	0.3	1	1	2	1	1	0.25	165	1	398	100.00	100.04
CD1595-3	0.5	0.3	1	1	2	1	2	0.25	373	1	548	100.02	100.07
CD1595-4	0.5	3.6	2	3.2	27	1	13	1.46	3063	42	4377	100.98	101.41
CD1595-5	0.5	1.5	2	1	9	1	6	0.84	3822	7	5506	109.07	109.62
CD1595-6	1	0.3	1	1	1	1	10	0.79	50	1	247	100.22	100.25
CD1595-7	1	0.3	1	1	1	1	4	0.25	58	1	231	100.13	100.15
CD1595-8	0.5	0.6	1	1	6	1	4	0.25	28	3	183	100.13	100.15
CD1595-9	0.5	0.5	1	1	3	1	12	0.85	50	3	258	100.19	100.21
CD1595-10	0.5	0.3	1	1	5	1	23	1.28	235	1	454	100.11	100.16
CD1595-11	2	0.3	1	1	2	1	23	1.48	573	5	872	100.26	100.34
CD1595-12	3	1.7	1	1	11	1	29	1.94	277	19	668	100.59	100.66
CD1595-13	0.5	0.3	1	1	2	1	17	1.05	378	1	579	100.18	100.24
CD1596-1	0.5	0.9	1	1	1	1	3	0.25	16	14	113	100.00	100.02
CD1596-2	1	22.2	2	1	135	1	51	4.92	95	242	1875	100.01	100.20
CD1596-3	0.5	1.4	1	1	5	1	1	0.25	27	23	152	100.00	100.02
CD1596-4	0.5	18.8	3	1	118	1	24	2.78	37	224	1370	100.01	100.14
CD1596-5	1	9.8	1	2.34	34	1	12	1.88	308	212	971	100.00	100.10
CD1596-6	2	1.3	1	1	4	1	3	0.25	67	23	194	100.00	100.02
CD1596-7	1	13.5	1	2.48	53	1	19	2.12	231	245	1163	100.00	100.12
CD1596-8	0.5	15.7	1	1	84	1	18	2.18	72	211	1129	100.01	100.12
CD1596-9	0.5	1.6	1	1	3	1	3	0.25	64	22	199	100.00	100.02
CD1596-10	0.5	16.2	1	1	90	1	20	2.66	63	154	1243	100.00	100.13

APPENDIX 5

GROUNDWATER GEOCHEMISTRY

Table A5.1: Groundwater data for Minigwal

(All concentrations in mg/L unless otherwise noted).

No.	Sample	East	North	pH	Eh (mV)	TDS	Na	Mg	Ca	K	Cl	SO4	HCO3
MR1	Bore #1	76894	76049	7.71	78	25324	7938	850	316	177	13800	2180	89
MR3	Bore #3	62911	87292	5.28	167	81839	25594	2871	582	506	43200	9000	12
MR4	Bore #4	57157	91735	5.11	108	60854	19066	1930	511	444	32900	5920	24
MR5	Bore #5	62962	87565	5.47	152	51725	15653	1640	697	338	27900	5410	15
MR6	Bore #6	56572	91446	5.82	108	95423	30342	3269	457	685	50900	9570	155
MR7	Bore #7	75070	79915	6.30	125	31510	9422	1007	554	213	16900	3310	149
MR8	"	"	"	6.22	125	38144	11202	1248	704	231	20800	3880	71

No.	Br	1	Cat-An/ Total	Zn	Cu	Pb	Au (µg/L)	V	SB	Co	Al	Fe	Mn
MR1	16.3	0.53	0.00	<0.005	0.004	0.013	<0.001	<0.002	<0.005	<0.005	<0.1	0	3.10
MR3	46.4	0.52	0.00	0.035	0.013	0.004	0.009	<0.002	<0.005	0.011	2	30	1.45
MR4	30.9	0.63	-0.01	0.155	0.004	0.017	0.002	<0.002	<0.005	<0.005	0.7	39	0.95
MR5	22.5	0.30	-0.02	0.180	0.007	0.022	<0.001	<0.002	<0.005	<0.005	0.1	55	1.64
MR6	71.4	0.94	0.00	0.015	0.012	0.008	0.004	<0.002	<0.005	<0.005	0.8	50	1.80
MR7	18.0	0.36	-0.02	0.010	<0.004	0.002	0.009	<0.002	0.005	<0.005	<0.1	12	1.20
MR8	20.0	0.52	-0.03	0.010	0.005	0.004	<0.001	<0.002	0.010	<0.005	<0.1	23	1.36

No.	Ba	Cr	Ni	Sr	Si	W	U
MR1	0.016	0.003	<0.01	5.8	0.3	<0.0015	<0.002
MR3	0.026	0.077	0.07	10.1	4.4	<0.0015	<0.002
MR4	0.026	0.012	0.07	7.7	10.7	<0.0015	<0.002
MR5	0.032	0.002	0.01	9.7	14.7	<0.0015	<0.002
MR6	0.025	<0.002	0.02	8.8	3.3	<0.0015	<0.002
MR7	0.024	<0.002	0.01	8.7	12.5	<0.0015	<0.002
MR8	0.025	0.002	0.01	11.8	7.9	<0.0015	<0.002

Table A5.2: Groundwater data for Ambassador

(All concentrations in mg/L unless otherwise noted).

No.	Sample	East	North	pH	Eh (mV)	d180 (SMOW)	d2H (SMOW)	TDS	Na	Mg	Ca
MR2	1148	75596	80272	5.98	129	nd	nd	22678	6800	742	532
MR9	1213	75279	81446	5.46	148	-3.18	-26.4	12506	3769	350	246
MR10	1152	75614	81244	5.91	143	nd	nd	19522	5645	700	450
MR11	1151	75960	81036	6.36	144	nd	nd	14784	4392	467	319
MR12	1419	85380	86347	6.85	173	nd	nd	14535	4185	522	300
MR13	1500	82711	84258	6.01	293	-4.32	-32.1	18459	5276	651	415
MR14	1498	79628	83151	6.58	335	-4.24	-31.2	32875	9646	1176	858
MR15	1247	79548	82917	7.01	213	-3.57	-32.1	26887	7939	856	626
MR16	1515	78991	82602	4.27	147	-2.75	-24.0	35984	11278	1212	708
MR17	1216	78226	83063	6.45	9	-3.59	-32.2	25376	7717	681	515
MR18	1177	77866	82796	6.58	171	-3.47	-32.6	27343	8236	754	683
MR19	1409	78304	82526	6.58	-167	-3.50	-24.0	7519	2285	262	174
MR20	1366	77012	82584	6.46	80	-2.08	-14.0	8461	2271	290	461

No.	K	Cl	SO4	HCO3	Br	PO4	I	Cat-An/ Total	Zn	Cu	Pb
MR2	248	11800	2490	86	23.1	nd	0.64	0.00	0.005	0.001	0.003
MR9	138	6730	1250	24	10.6	nd	0.32	-0.02	0.055	0.027	0.011
MR10	231	10400	2060	30	20.7	nd	0.01	-0.01	0.030	0.001	0.048
MR11	169	7810	1560	104	15.0	nd	0.36	-0.01	0.005	nd	0.001
MR12	204	7430	1730	283	20.3	0.10	0.35	-0.01	0.087	0.006	0.016
MR13	207	9820	2020	107	16.6	0.02	0.32	-0.02	0.190	0.008	0.020
MR14	383	16600	4040	303	23.3	0.01	0.03	0.01	0.056	<0.001	0.009
MR15	308	14000	2950	382	20.4	0.00	0.04	-0.01	0.079	0.011	0.056
MR16	250	19000	3520	0	14.7	0.49	0.45	0.02	0.280	<0.001	0.014
MR17	249	13400	2630	339	13.0	0.19	0.77	-0.02	<0.005	<0.001	0.006
MR18	263	14200	3090	191	15.1	0.00	0.19	-0.01	<0.100	0.377	0.015
MR19	66	4070	55.7	1231	3.3	4.89	0.32	-0.02	<0.005	<0.001	0.005
MR20	84	4210	1140	nd	4.9	1.80	0.15	0.02	0.045	<0.001	0.014

No.	Au (µg/L)	V	Sb	Co	Al	Fe	Mu	Ba	Cr	Ni	Sr
MR2	<0.001	<0.002	<0.005	<0.005	<0.1	0.4	0.20	0.031	<0.002	0.01	6.9
MR9	0.005	<0.002	<0.005	<0.005	<0.1	0.46	0.22	0.027	0.002	0.01	3.3
MR10	<0.001	0.002	<0.005	0.005	<0.1	0.15	0.13	0.034	<0.002	0.02	6.3
MR11	<0.001	0.004	0.005	0.005	<0.1	0.88	0.24	0.021	<0.002	0.02	4.0
MR12	0.005	<0.002	0.020	0.005	<0.1	6.3	0.05	0.043	<0.002	0.02	3.4
MR13	0.014	<0.002	0.010	0.020	<0.1	1.02	0.27	0.023	<0.002	0.08	4.1
MR14	0.021	<0.002	0.015	0.015	<0.1	0	0.06	0.053	<0.002	0.04	11.6
MR15	<0.001	<0.002	0.010	0.008	<0.1	0.19	0.05	0.027	0.002	0.02	5.1
MR16	nd	nd	nd	<0.005	<0.1	0.18	1.34	0.048	0.004	0.04	7.9
MR17	<0.001	<0.002	<0.005	<0.005	<0.1	5.1	0.17	0.020	0.002	<0.01	4.1
MR18	0.005	<0.002	0.005	0.054	<0.1	7.8	0.28	0.052	0.004	0.04	5.9
MR19	<0.001	<0.002	0.015	<0.005	<0.1	0.22	0.60	0.138	0.003	0.01	1.7
MR20	nd	nd	nd	0.007	<0.1	0.34	0.32	0.155	<0.002	0.02	2.2

nd: not determined.

Table A5.2 (continued)

No.	Y	Cs	La	Ce	Pr	Nd	Sm	Eu	Gd	Tb	Dy
MR2	nd	nd	nd	nd	nd	nd	nd	nd	nd	nd	nd
MR9	nd	nd	nd	nd	nd	nd	nd	nd	nd	nd	nd
MR10	0.0032	0.014	0.0022	0.0038	0.0006	0.0029	0.0008	0.0002	0.0008	0.0001	0.0005
MR11	nd	nd	nd	nd	nd	nd	nd	nd	nd	nd	nd
MR12	0.0039	0.008	0.0015	0.0033	0.0008	0.0028	0.0013	0.0013	0.0015	0.0003	0.0008
MR13	0.0075	0.010	0.0012	0.0090	0.0007	0.0030	0.0010	0.0003	0.0011	0.0002	0.0008
MR14	nd	nd	nd	nd	nd	nd	nd	nd	nd	nd	nd
MR15	0.004	0.022	0.0006	0.0019	0.0004	0.0020	0.0013	0.0004	0.0010	0.0002	0.0006
MR16	nd	nd	nd	nd	nd	nd	nd	nd	nd	nd	nd
MR17	nd	nd	nd	nd	nd	nd	nd	nd	nd	nd	nd
MR18	nd	nd	nd	nd	nd	nd	nd	nd	nd	nd	nd
MR19	0.0018	0.001	0.0011	0.0009	0.0002	0.0008	0.0008	0.0003	0.0007	0.0001	0.0004
MR20	nd	nd	nd	nd	nd	nd	nd	nd	nd	nd	nd

No.	Ho	Si	W	U	Er	Tm	Yb	Lu	REE (total)	Tl	Th
MR2	nd	21	<0.0015	<0.002	nd	nd	nd	nd	nd	nd	nd
MR9	nd	21	<0.0015	<0.002	nd	nd	nd	nd	nd	nd	nd
MR10	0.0003	22	<0.0015	<0.002	0.0005	0.0001	0.0005	0.0001	0.0134	0.0005	0.0004
MR11	nd	15.4	<0.0015	<0.002	nd	nd	nd	nd	nd	nd	nd
MR12	0.0003	6.3	0.0039	<0.002	0.0006	0.0003	0.0005	0.0004	0.0157	0.0005	0.0008
MR13	0.0002	4	0.0035	<0.002	0.0005	0.0002	0.0005	0.0001	0.0188	0.0005	0.0002
MR14	nd	7.6	0.0026	0.038	nd	nd	nd	nd	nd	nd	nd
MR15	0.0003	4.6	0.0040	0.026	0.0006	0.0002	0.0005	0.0002	0.0102	0.0004	0.0004
MR16	nd	2.8	nd	nd	nd	nd	nd	nd	nd	nd	nd
MR17	nd	1.6	<0.0011	<0.002	nd	nd	nd	nd	nd	nd	nd
MR18	nd	3.2	<0.0011	0.020	nd	nd	nd	nd	nd	nd	nd
MR19	0.0001	2.9	0.0052	<0.002	0.0004	0.0001	0.0006	0.0001	0.0066	<0.0001	<0.0001
MR20	nd	4.6	nd	nd	nd	nd	nd	nd	nd	nd	nd

nd: not determined

Figure A5.1a: δ^2H vs. $\delta^{18}O$ for Ambassador and Mt. Gibson groundwaters

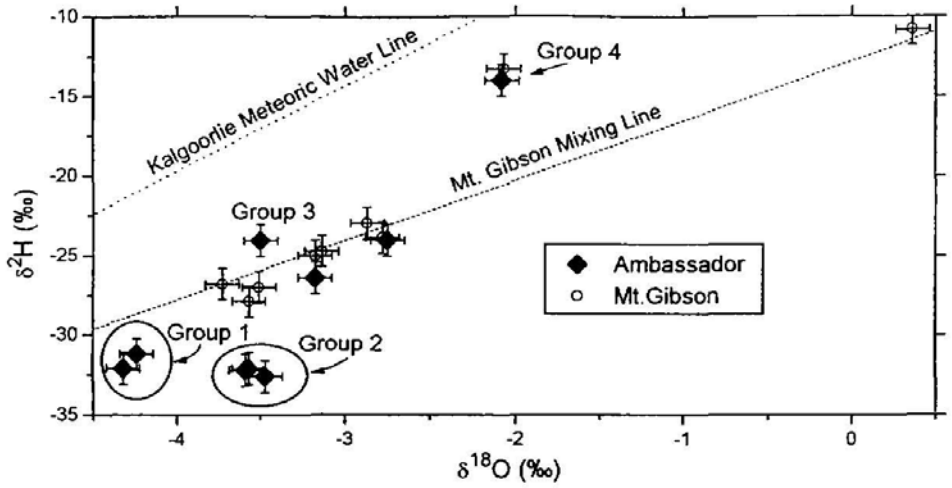

Figure A5.1b: δ^2H vs. TDS for Ambassador and Mt. Gibson groundwaters

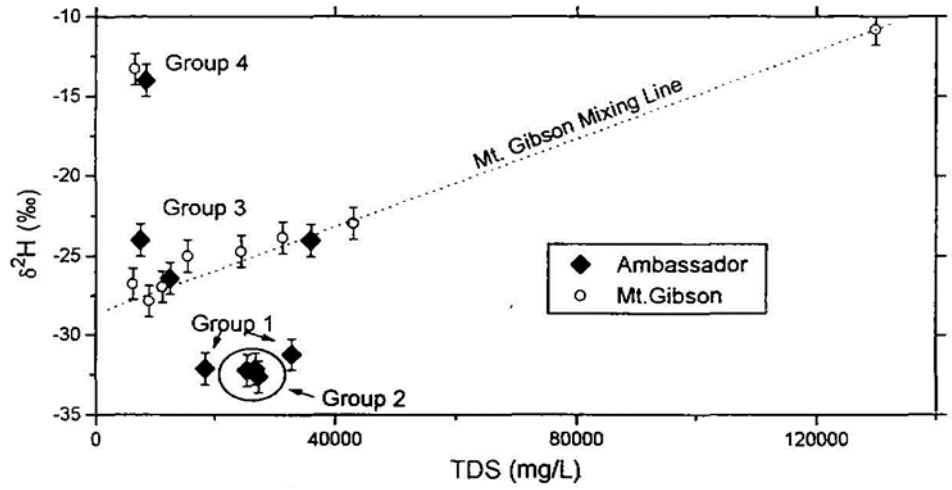

Figure A5.1c: $\delta^{18}O$ vs. TDS for Ambassador and Mt. Gibson groundwaters

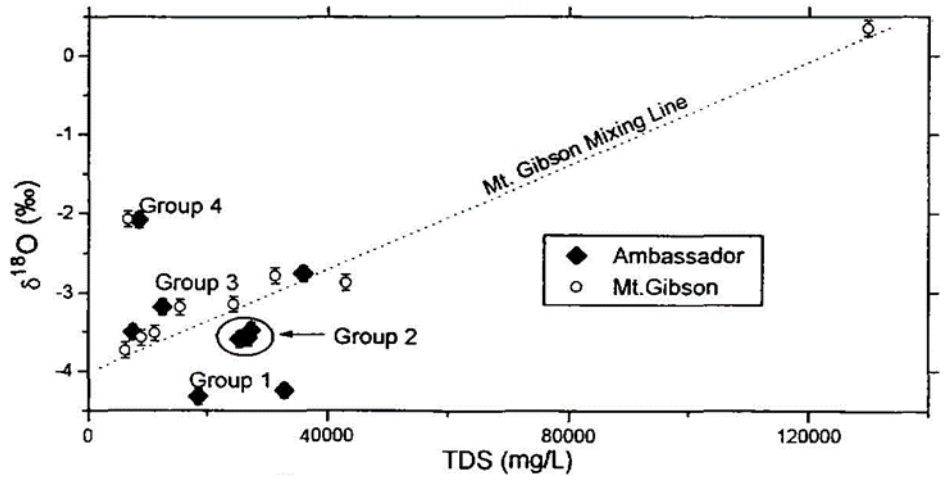

Figure A5.2: Sodium vs. TDS for groundwaters from Mulga Rock and other sites

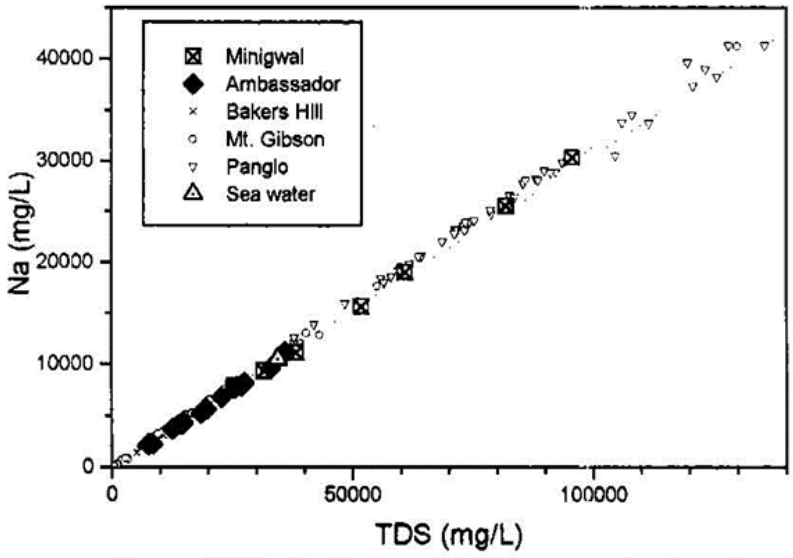

Figure A5.3: Magnesium vs. TDS for groundwaters from Mulga Rock and other sites

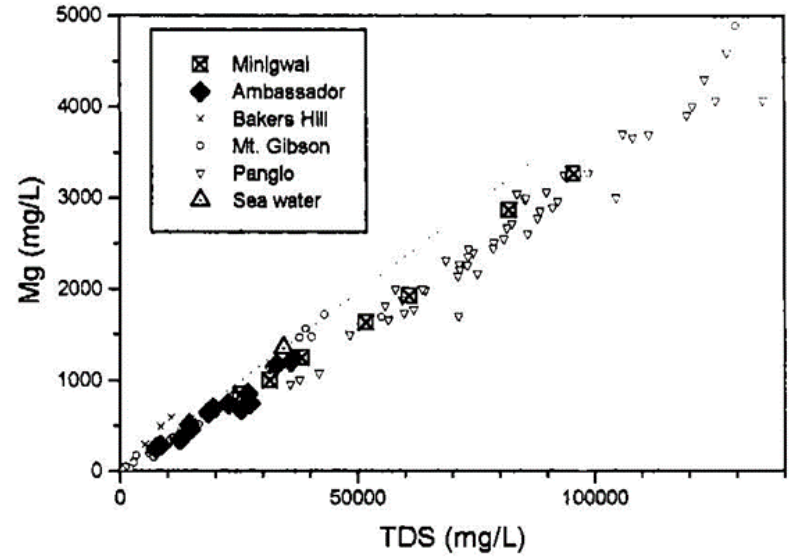

Figure A5.4: Potassium vs. TDS for groundwaters from Mulga Rock and other sites

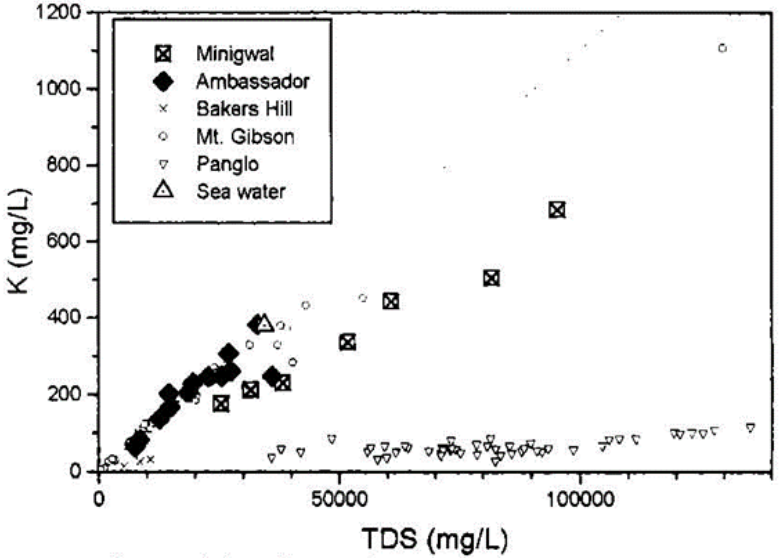

Figure A5.5: Sulphate vs. TDS for groundwaters from Mulga Rock and other sites

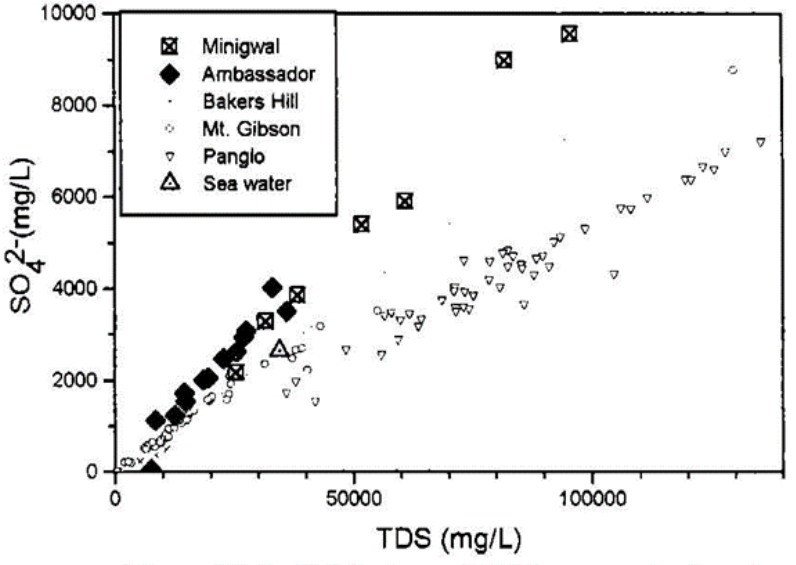

Figure A5.6: Bromine vs. TDS for groundwaters from Mulga Rock and other sites

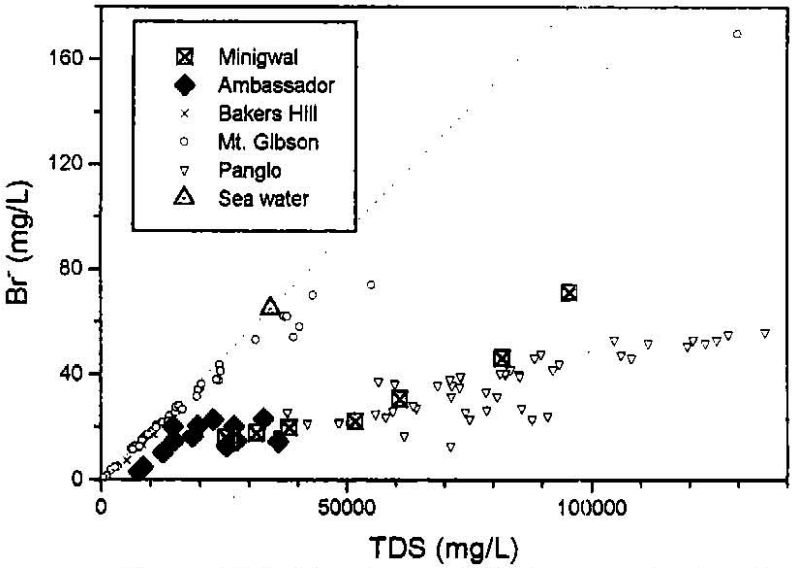

Figure A5.7: Calcium vs. TDS for groundwaters from Mulga Rock and other sites

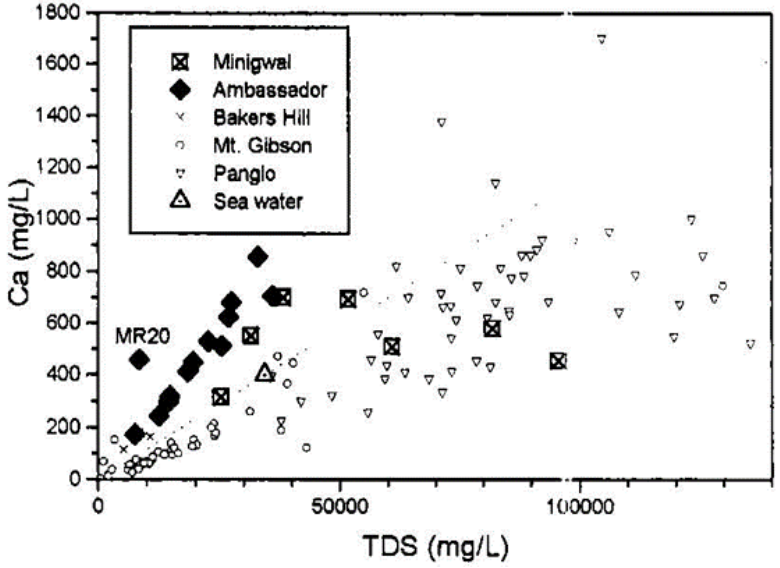

Figure A5.8: Strontium vs. TDS for groundwaters from Mulga Rock and other sites

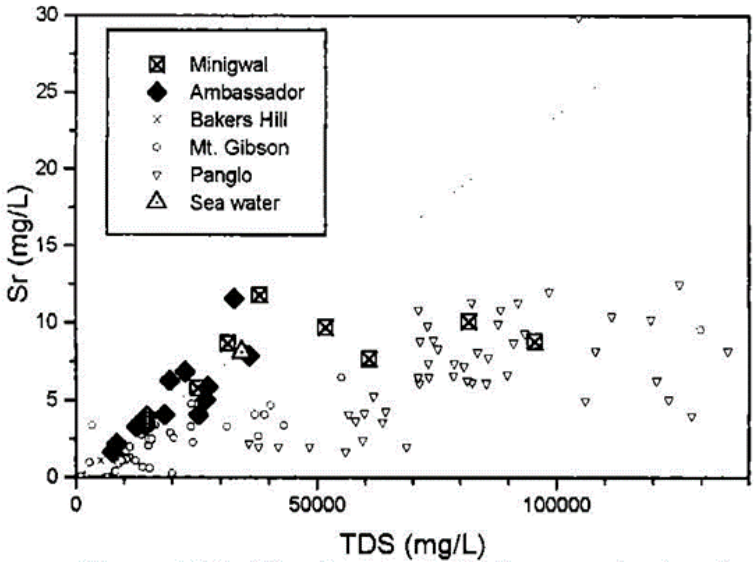

Figure A5.9: Barium vs. TDS for groundwaters from Mulga Rock and other sites

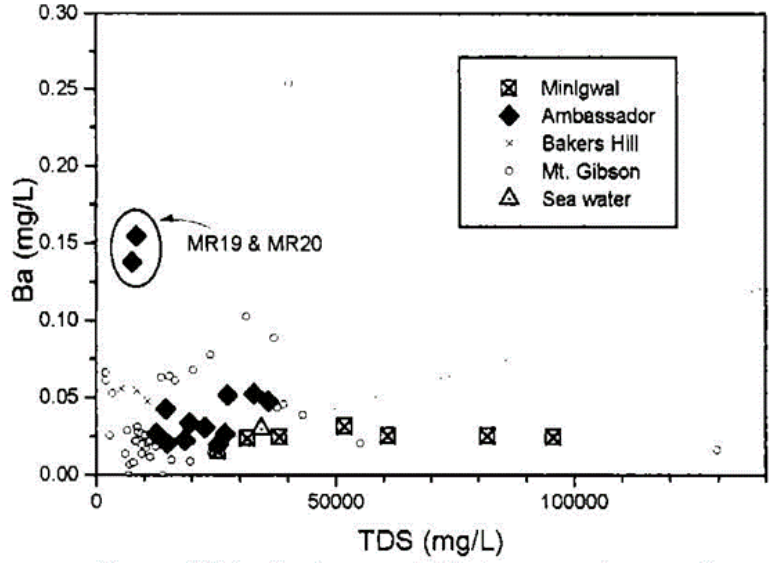

Figure A5.10: Bicarbonate vs. pH for groundwaters from Mulga Rock and other sites

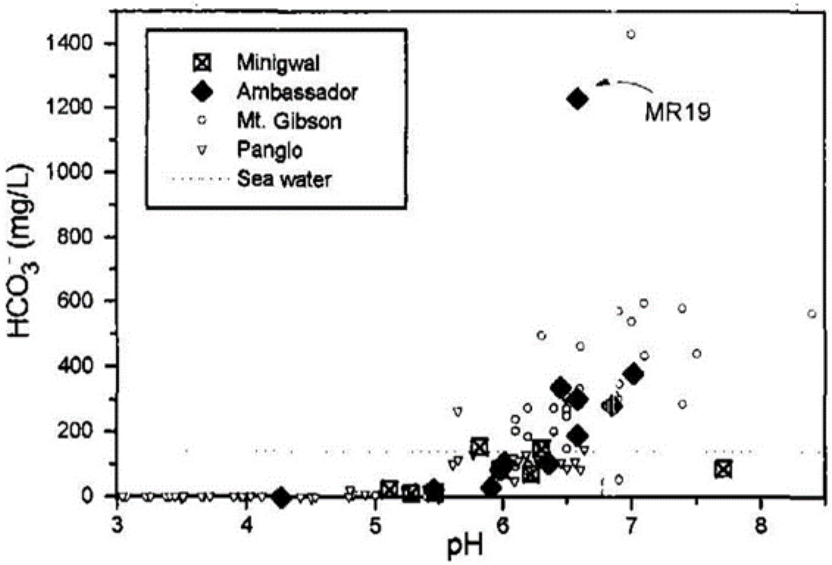

Figure A5.11: Phosphate vs. pH for groundwaters from Ambassador

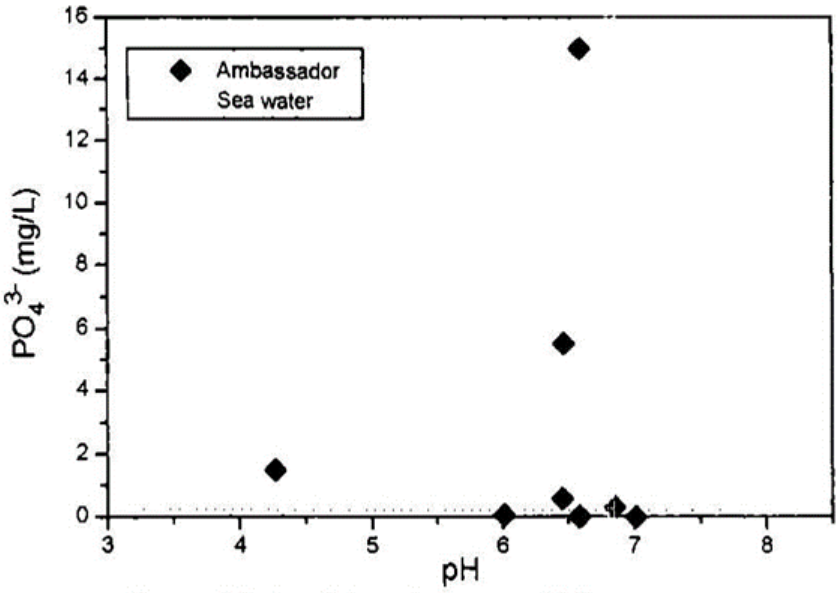

Figure A5.12: Silicon vs. pH for groundwaters from Mulga Rock and other sites

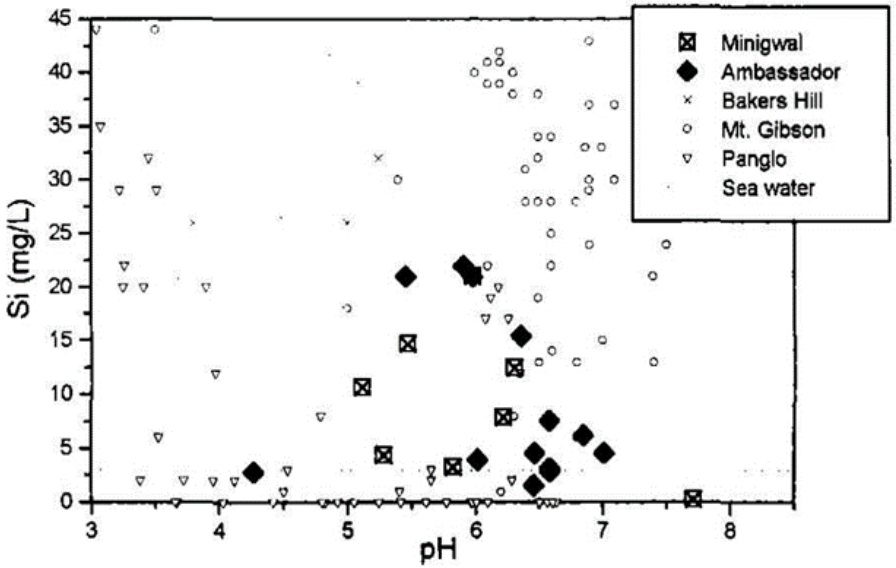

Figure A5.13: Aluminium vs. pH for groundwaters from Mulga Rock and other sites

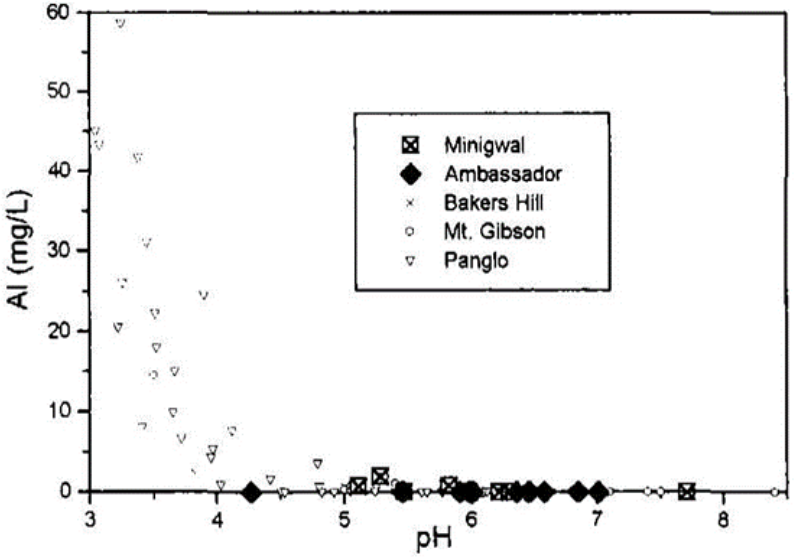

Figure A5.14: Chromium vs. pH for groundwaters from Mulga Rock and other sites

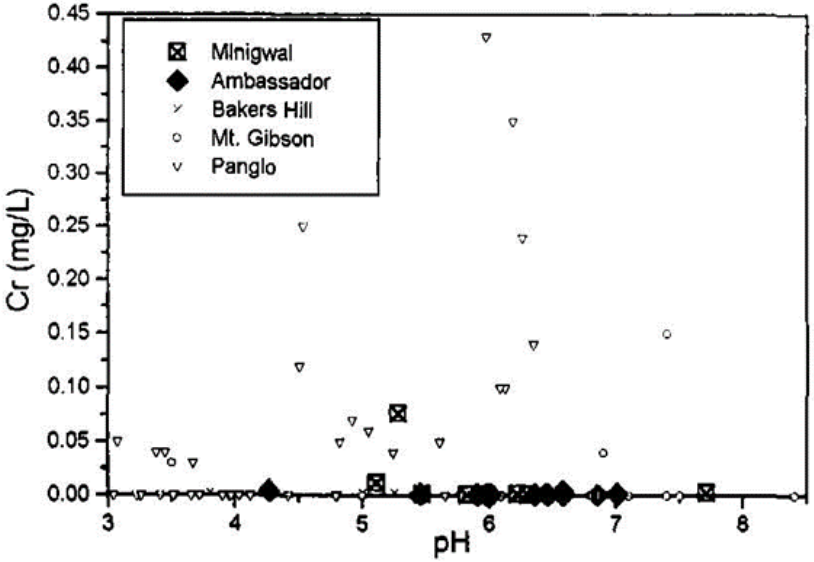

Figure A5.15: Manganese vs. pH for groundwaters from Mulga Rock and other sites

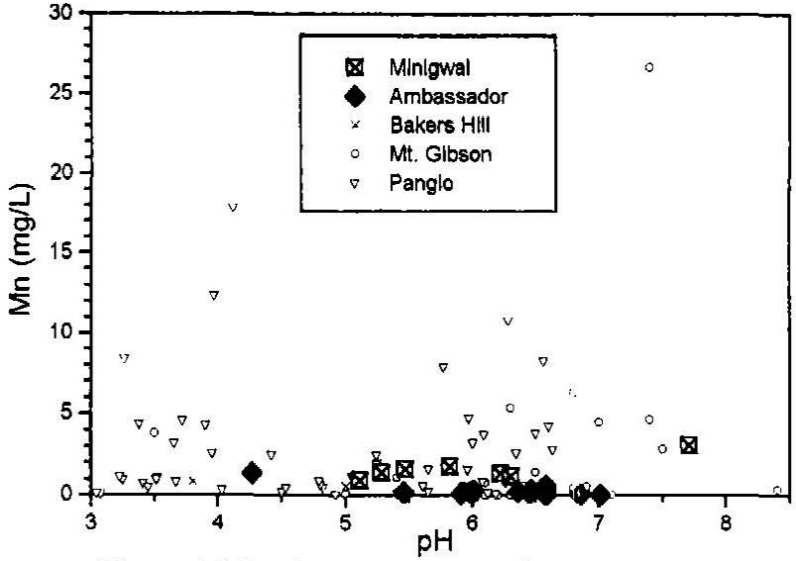

Figure A5.16: Iron vs. pH for groundwaters from Mulga Rock and other sites

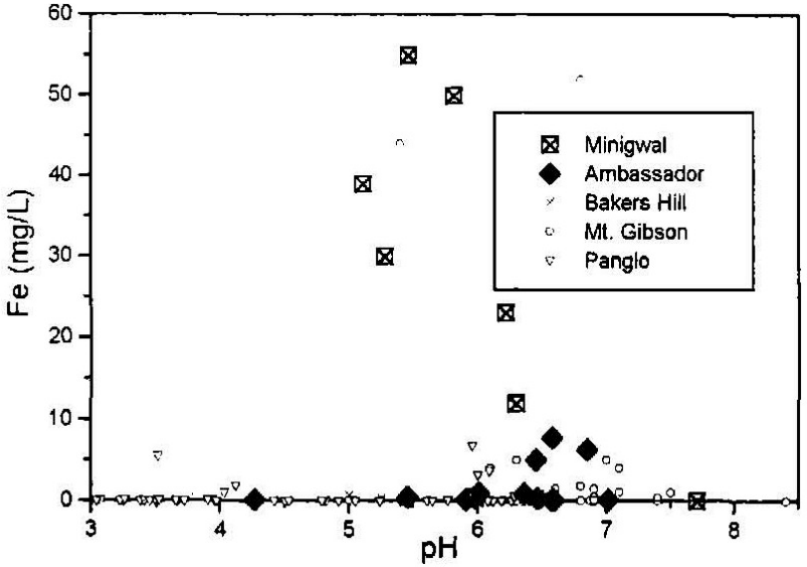

Figure A5.17: Cobalt vs. pH for groundwaters from Mulga Rock and other sites

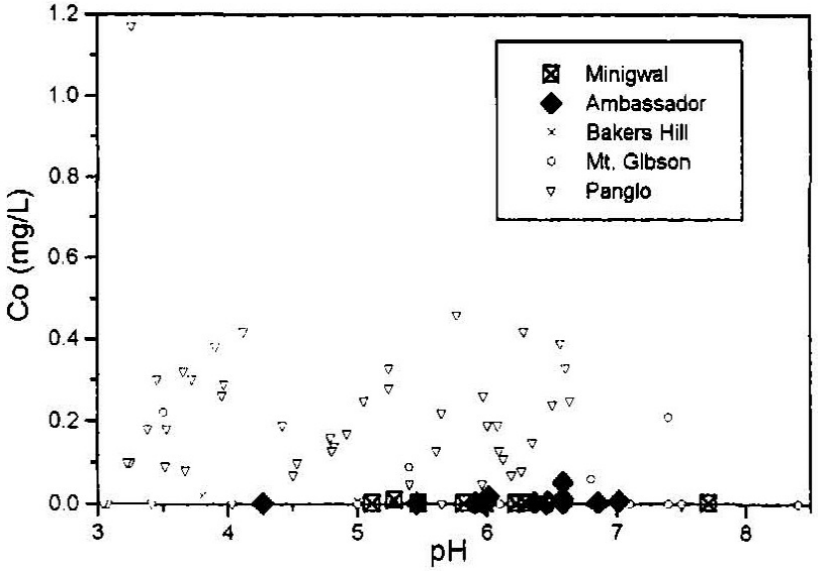

Figure A5.18: Nickel vs. pH for groundwaters from Mulga Rock and other sites

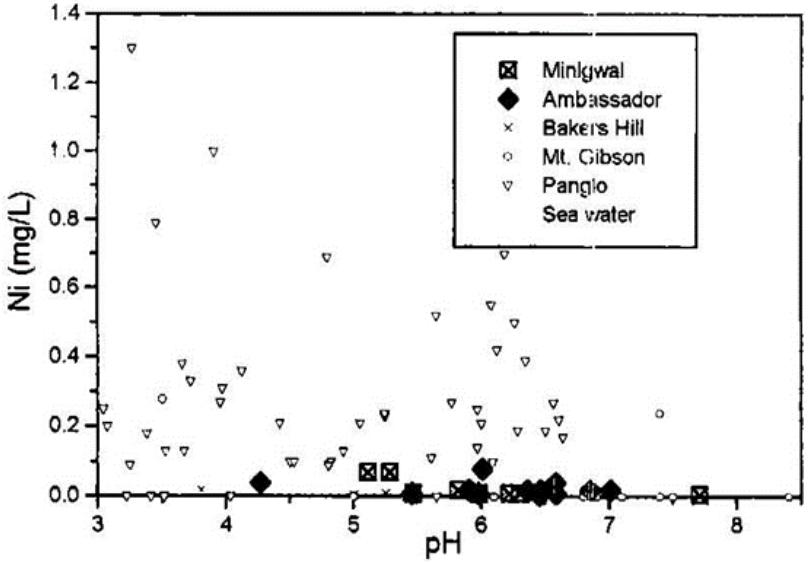

Figure A5.19: Copper vs. pH for groundwaters from Mulga Rock and other sites

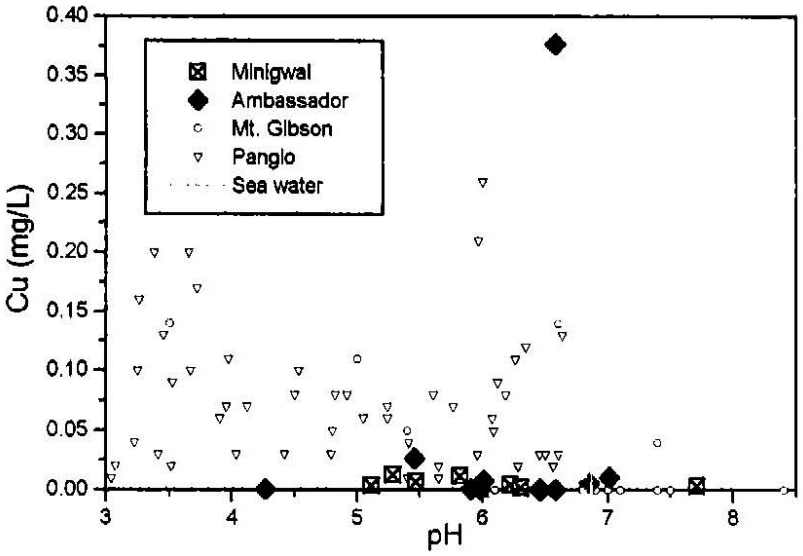

Figure A5.20: Zinc vs. pH for groundwaters from Mulga Rock and other sites

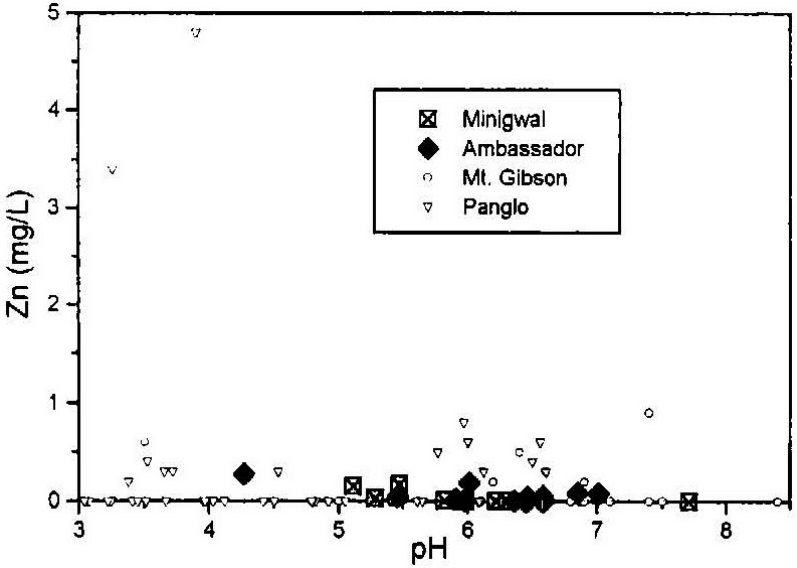

Figure A5.21: Yttrium vs. pH for groundwaters from Ambassador

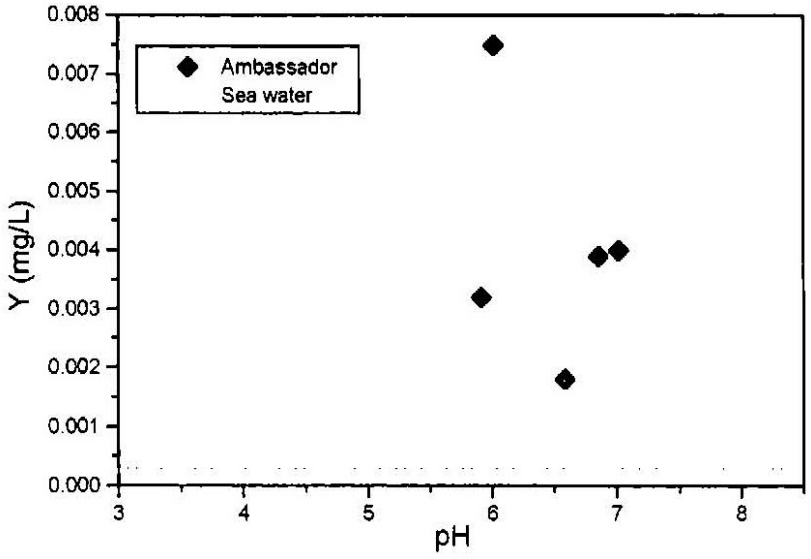

Figure A5.22: Iodide vs. pH for groundwaters from Mulga Rock and other sites

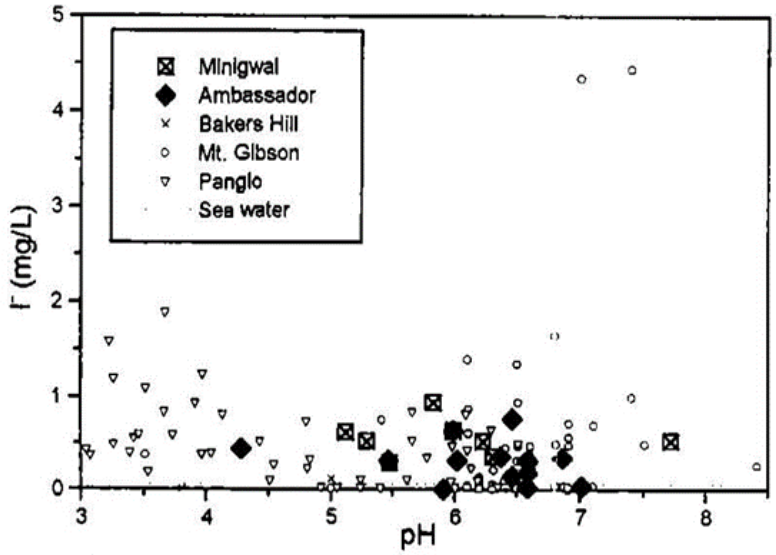

Figure A5.23: Lanthanum vs. pH for groundwaters from Ambassador

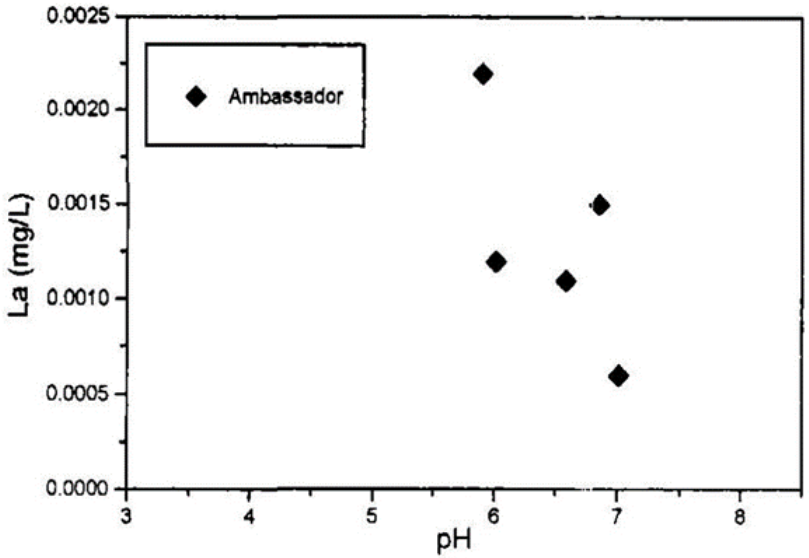

Figure A5.24: Gold vs. pH for groundwaters from Mulga Rock and other sites

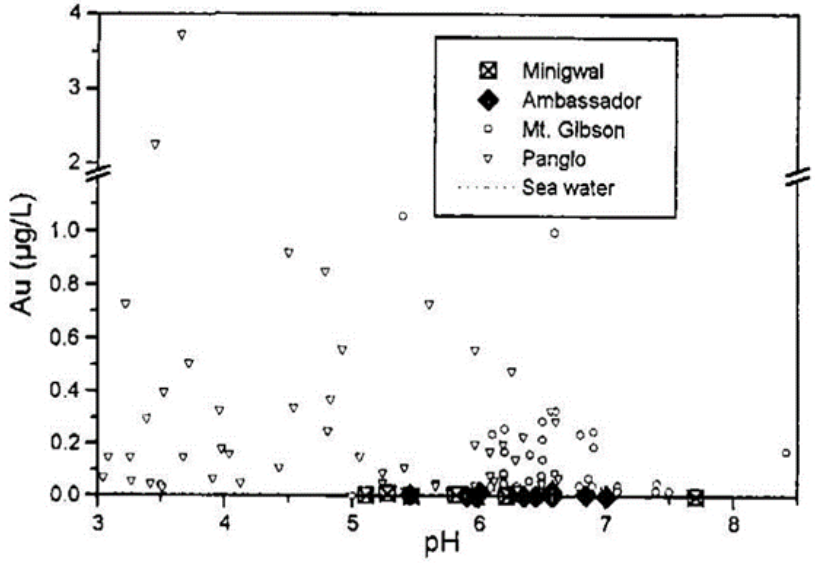

Figure A5.25: Lead vs. pH for groundwaters from Mulga Rock and other sites

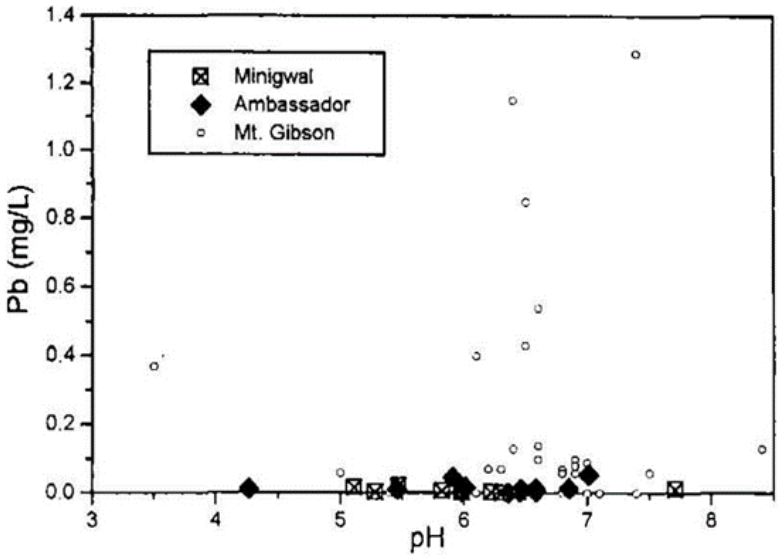

Figure A5.26: Thorium vs. pH for groundwaters from Ambassador

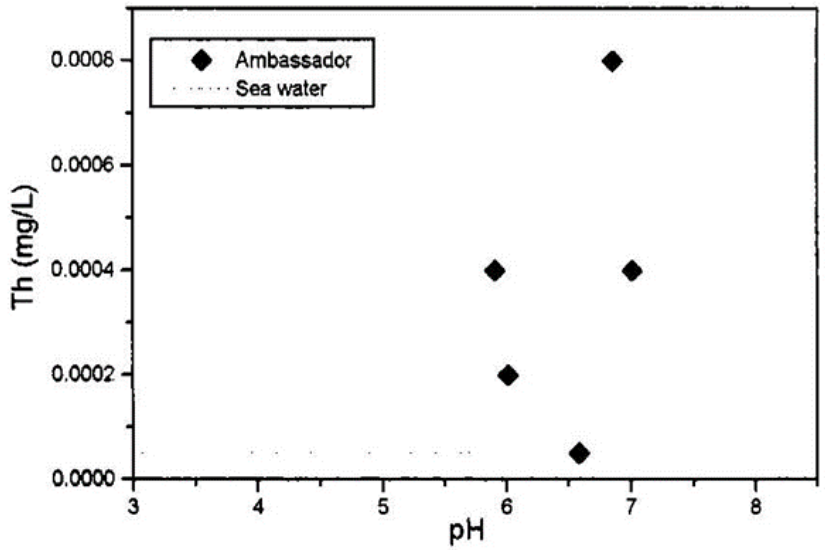

Figure A5.27: Uranium vs. pH for groundwaters from Mulga Rock

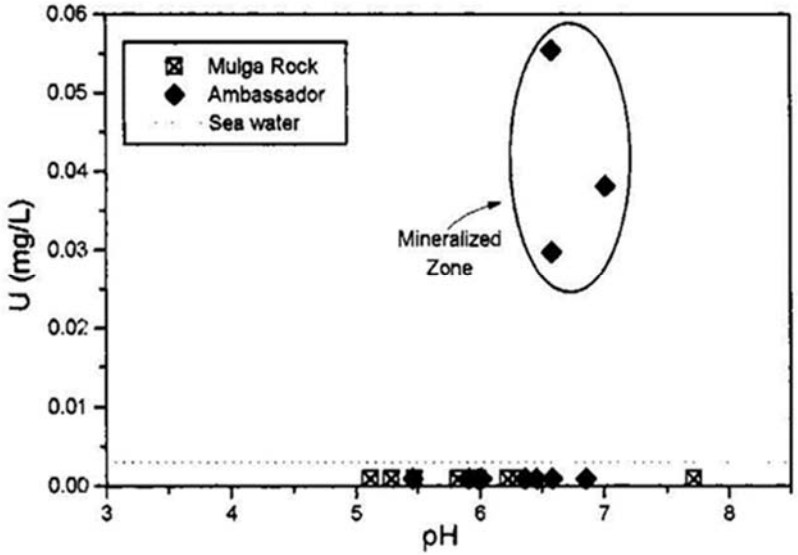

Table A5.3: SI values for Minigwal and Ambassador groundwaters

No.	pH	Eh (mV)	TDS (mg/L)	Calcite CaCO3	Gypsum CaSO4.2H2O	Dolomite CaMg(C03)2	Magnesite MgCO3	Epsomite MgSO4.7H20	Celestine SrSO4	Barite BaSO4
MR1	7.71	78	25324	-0.08	-0.74	0.80	0.03	-2.79	-0.92	-0.50
MR3	5.28	167	81839	-3.22	-0.30	-5.18	-2.81	-2.11	-0.51	-0.17
MR4	5.11	108	60854	-3.12	-0.42	-5.12	-2.84	-2.34	-0.69	-0.22
MR5	5.47	152	51725	-2.82	-0.28	-4.72	-2.74	-2.39	-0.58	-0.11
MR6	5.82	108	95423	-1.66	-0.41	-1.90	-1.08	-2.07	-0.57	-0.20
MR7	6.3	125	31510	-1.03	-0.41	-1.28	-1.09	-2.63	-0.66	-0.25
MR8	6.22	125	38144	-1.35	-0.30	-1.92	-1.41	-2.54	-0.53	-0.24
MR2	5.98	129	22678	-1.57	-0.43	-2.47	-1.74	-2.77	-0.77	-0.14
MR9	5.46	148	12506	-2.85	-0.83	-5.04	-3.03	-3.15	-1.14	-0.24
MR10	5.91	143	19522	-2.13	-0.53	-3.56	-2.27	-2.82	-0.83	-0.12
MR11	6.36	144	14784	-1.24	-0.69	-1.80	-1.41	-3.00	-1.04	-0.33
MR12	6.85	173	14535	-0.35	-0.67	0.06	-0.44	-2.91	-1.07	0.02
MR13	6.01	293	18459	-1.50	-0.55	-2.30	-1.64	-2.83	-1.01	-0.28
MR14	6.58	335	32875	-0.28	-0.17	0.10	-0.46	-2.52	-0.49	0.14
MR15	7.01	213	26887	0.16	-0.35	0.97	-0.03	-2.69	-0.89	-0.19
MR16	4.27	147	35984	nd	-0.34	nd	nd	-2.58	-0.74	0.02
MR17	6.45	9	25376	-0.52	-0.45	-0.40	-0.72	-2.81	-0.99	-0.33
MR18	6.58	171	27343	-0.54	-0.30	-0.51	-0.81	-2.73	-0.81	0.11
MR19	6.58	-167	7519	-0.03	-2.11	0.59	-0.22	-4.44	-2.55	-0.65
MR20	6.46	80	8461	nd	-0.51	nd	nd	-3.18	-1.28	0.56

No.	pH	Eh (mV)	TDS (mg/L)	Halite NaCl	Quartz SiO2	Gibbsite Al(OH)3	Jurbanite AlOHSO4	Pyrite FeS2	Siderite FeCO3	Goethite FeOOH
MR1	7.71	78	25324	-2.77	-1.00	nd	nd	nd	nd	nd
MR3	5.28	167	81839	-1.79	0.27	1.64	1.36	-48.7	-3.37	2.59
MR4	5.11	108	60854	-2.04	0.62	0.84	0.62	-32.1	-3.27	1.24
MR5	5.47	152	51725	-2.20	0.74	0.82	-0.07	-48.2	-2.66	3.24
MR6	5.82	108	95423	-1.64	0.17	2.14	0.92	-43.2	-1.09	3.41
MR7	6.3	125	31510	-2.62	0.63	nd	nd	-55.9	-0.98	4.68
MR8	6.22	125	38144	-2.46	0.44	nd	nd	-54.3	-1.14	4.70
MR2	5.98	129	22678	-2.90	0.84	nd	nd	-53.2	-3.12	2.36
MR9	5.46	148	12506	-3.36	0.82	nd	nd	-49.6	-4.41	1.26
MR10	5.91	143	19522	-3.03	0.85	nd	nd	-55.9	-4.09	1.98
MR11	6.36	144	14784	-3.24	0.69	nd	nd	-62.7	-2.09	4.15
MR12	6.85	173	14535	-3.28	0.30	nd	nd	-76.6	-0.27	6.97
MR13	6.01	293	18459	-3.08	0.11	nd	nd	-92.2	-2.54	5.65
MR14	6.58	335	32875	-2.62	0.42	nd	nd	nd	nd	nd
MR15	7.01	213	26887	-2.77	0.19	nd	nd	-90.0	-1.61	6.50
MR16	4.27	147	35984	-2.50	-0.01	nd	nd	-30.4	nd	-2.88
MR17	6.45	9	25376	-2.80	-0.27	nd	nd	-31.3	-0.78	2.83
MR18	6.58	171	27343	-2.75	0.03	nd	nd	-71.5	-0.71	6.13
MR19	6.58	-167	7519	-3.76	-0.05	nd	nd	4.2	-1.23	-0.96
MR20	6.46	80	8461	-3.76	0.15	nd	nd	-49.6	nd	3.03

nd: not determined

Table A5.3 (continued)

No.	pH	Eh (mV)	TDS (mg/L)	Rhodo-crosite MnCO3	Tenorite Cu(OH)2.H2O	Smithsonite ZnCO3	Otavite CdCO3	Cerrusite PbCO3	Ni(OH)2	Iodyrite AgI
MR1	7.71	78	25324	0.41	-5.51	nd	-1.83	-1.19	nd	nd
MR3	5.28	167	81839	-3.32	-9.27	-6.21	-5.54	-5.51	-7.06	-2.43
MR4	5.11	108	60854	-3.34	-10.94	-5.36	-4.82	-4.59	-7.36	nd
MR5	5.47	152	51725	-2.93	-9.11	-5.11	-4.95	-4.24	-7.46	-2.76
MR6	5.82	108	95423	-1.60	-9.32	-4.98	nd	-3.66	-6.57	-2.52
MR7	6.3	125	31510	-1.20	nd	-4.46	nd	-3.24	-5.74	nd
MR8	6.22	125	38144	-1.57	-7.97	-4.89	-3.34	-3.42	-5.92	nd
MR2	5.98	129	22678	-2.48	-8.56	-5.27	-3.46	-3.46	-6.34	nd
MR9	5.46	148	12506	-3.38	-7.33	-5.18	nd	-3.72	-7.29	nd
MR10	5.91	143	19522	-3.16	-8.35	-4.99	nd	-2.72	-6.15	nd
MR11	6.36	144	14784	-1.86	nd	-4.73	nd	-3.32	-5.22	-1.36
MR12	6.85	173	14535	-1.64	-4.87	-2.58	nd	-1.24	-4.25	nd
MR13	6.01	293	18459	-2.19	-4.67	-3.53	nd	-2.44	-5.35	nd
MR14	6.58	335	32875	-1.93	nd	-3.15	nd	-2.02	-4.58	nd
MR15	7.01	213	26887	-1.47	-4.20	-2.45	nd	-0.64	-4.01	nd
MR16	4.27	147	35984	nd	nd	nd	nd	nd	-9.20	nd
MR17	6.45	9	25376	-1.52	nd	nd	nd	-2.19	nd	nd
MR18	6.58	171	27343	-1.42	-4.24	nd	nd	-1.91	-4.56	nd
MR19	6.58	-167	7519	-0.17	nd	nd	nd	-1.44	-5.02	nd
MR20	6.46	80	8461	-1.27	nd	-3.30	-2.09	-1.64	-4.95	nd

No.	pH	Eh (mV)	TDS (mg/L)	CoCo3	Cr2O3	Au Metal Au	Uraninite UO2	Rutherfordine UO2CO3	Partial log (atm.)
MR1	7.71	78	25324	nd	6.99	nd	nd	nd	-2.99
MR3	5.28	167	81839	-6.45	1.86	6.63	nd	nd	-1.47
MR4	5.11	108	60854	nd	-0.77	7.06	nd	nd	-0.98
MR5	5.47	152	51725	nd	-0.90	nd	nd	nd	-1.53
MR6	5.82	108	95423	nd	nd	7.04	nd	nd	-0.91
MR7	6.3	125	31510	nd	nd	7.90	nd	nd	-1.34
MR8	6.22	125	38144	nd	1.99	nd	nd	nd	-1.59
MR2	5.98	129	22678	nd	nd	nd	nd	nd	-1.24
MR9	5.46	148	12506	nd	-1.07	7.65	nd	nd	-1.23
MR10	5.91	143	19522	-5.71	nd	nd	nd	nd	-1.62
MR11	6.36	144	14784	-4.68	nd	nd	nd	nd	-1.51
MR12	6.85	173	14535	-3.76	nd	6.95	nd	nd	-1.57
MR13	6.01	293	18459	-4.45	nd	5.54	nd	nd	-1.16
MR14	6.58	335	32875	-3.63	nd	4.87	-9.71	-4.17	-1.32
MR15	7.01	213	26887	-3.36	4.75	nd	-7.10	-5.13	-1.64
MR16	4.27	147	35984	nd	-6.13	nd	nd	nd	nd
MR17	6.45	9	25376	nd	2.80	nd	nd	nd	-1.11
MR18	6.58	171	27343	-3.25	3.88	7.05	-4.04	-4.22	-1.50
MR19	6.58	-167	7519	nd	3.34	nd	nd	nd	-0.62
MR20	6.46	80	8461	-4.07	nd	nd	nd	nd	-1.30

nd: not determined

Figure A5.28: SI for halite vs. TDS

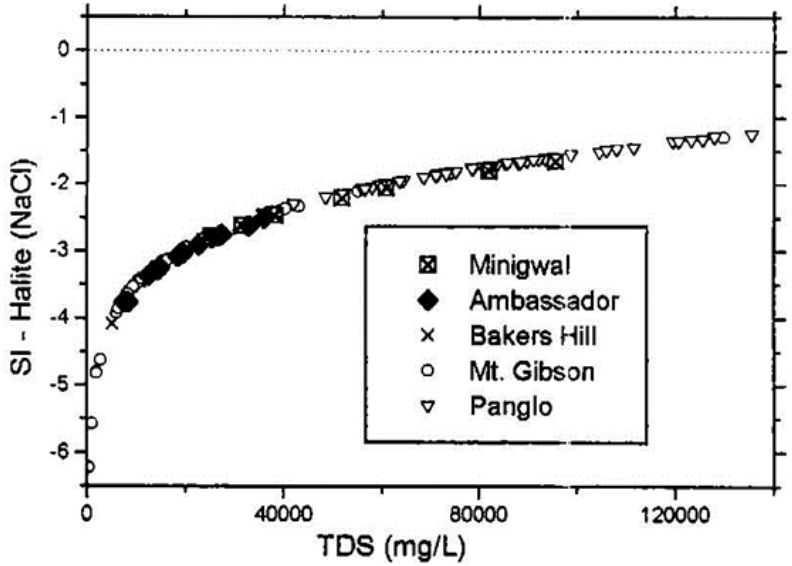

Figure A5.29: SI for gypsum vs. TDS

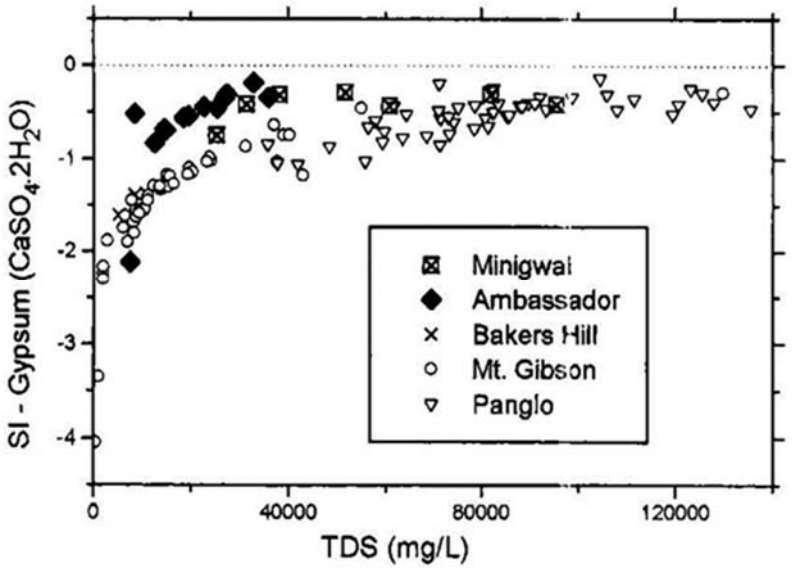

Figure A5.30: SI for celestine vs. TDS

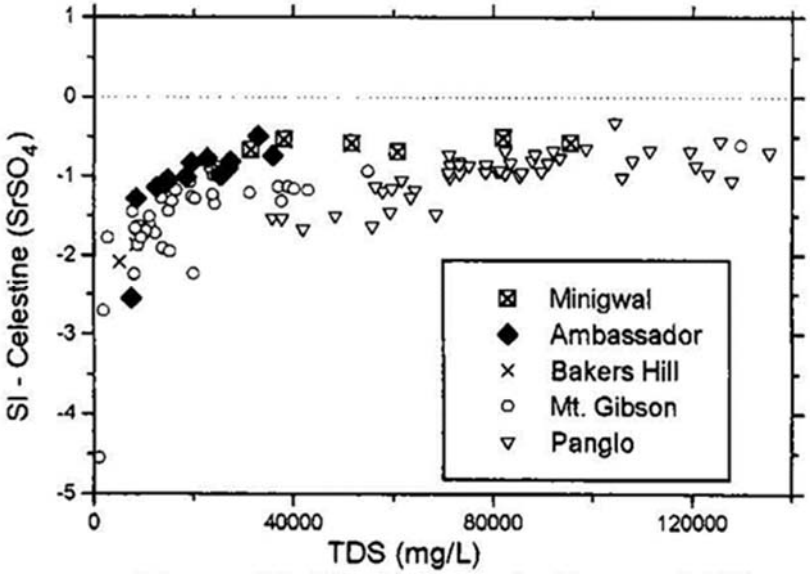

Figure A.5.30: SI for barite vs. TDS

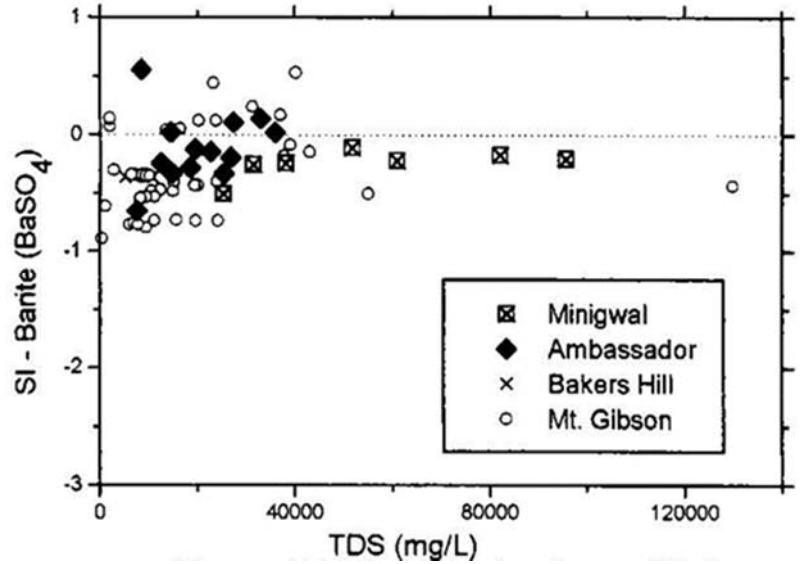

Figure A5.32: SI for calcite vs. pH

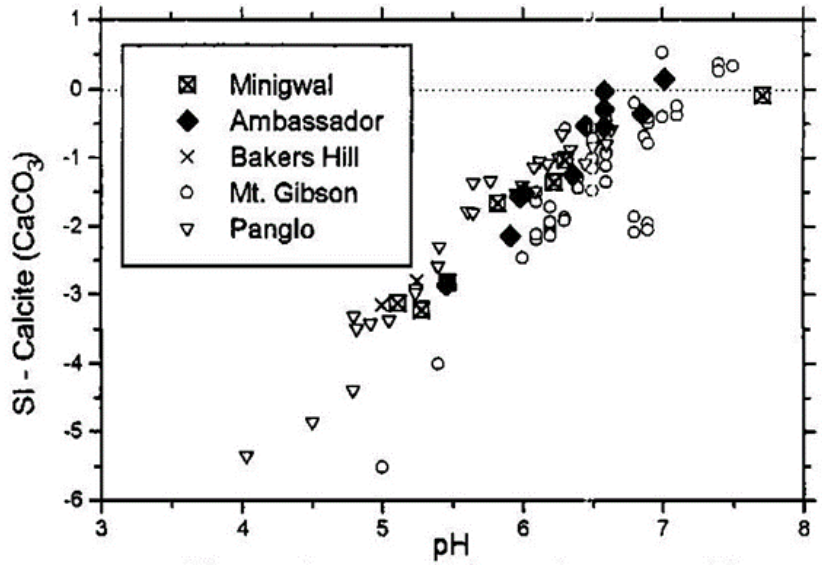

Figure A5.33: SI for dolomite vs. pH

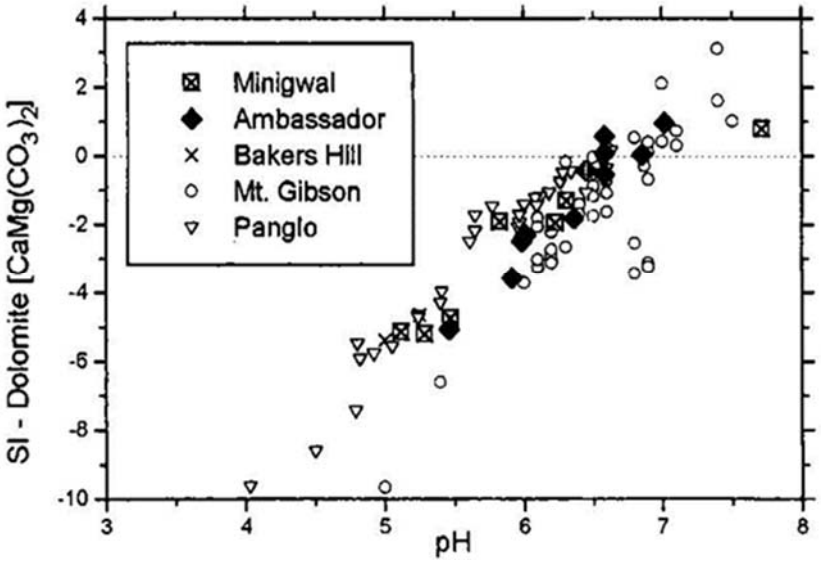

Figure A5.34: SI for magnesite vs. pH

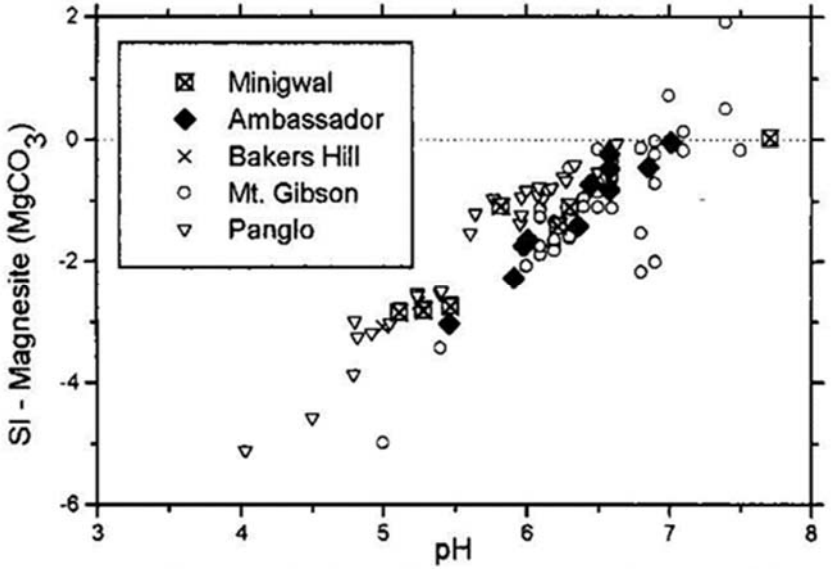

Figure A5.35: SI for silica vs. pH

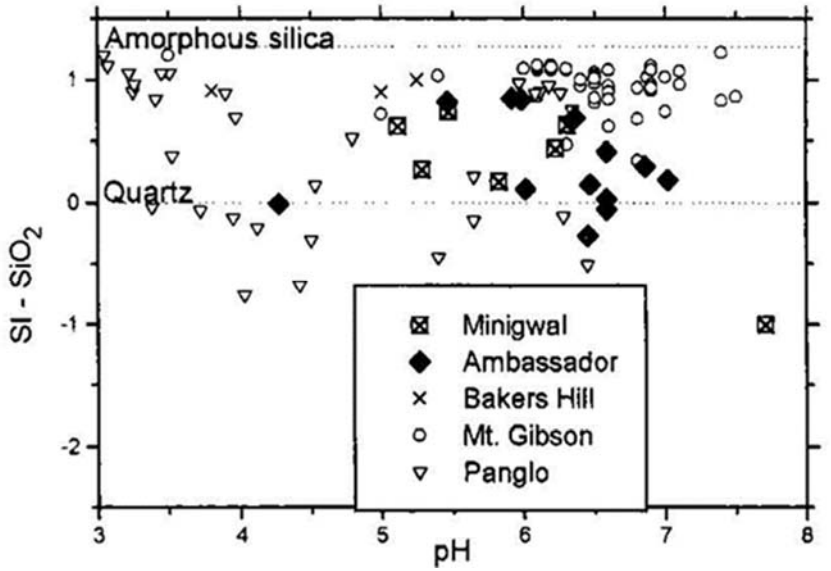

Figure A5.36: SI for alumina vs. pH

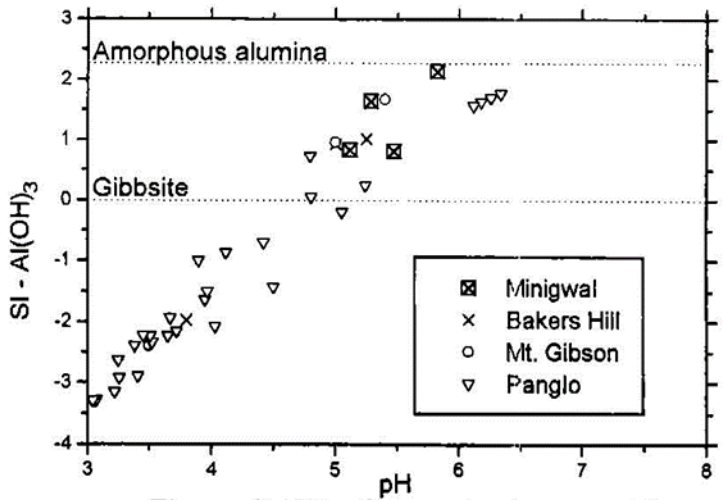

Figure A5.37: SI for jurbanite vs. pH

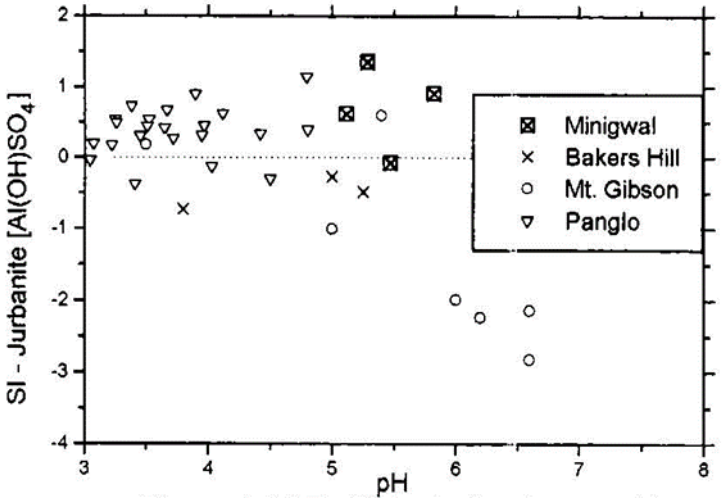

Figure A5.38: SI for pyrite vs. pH

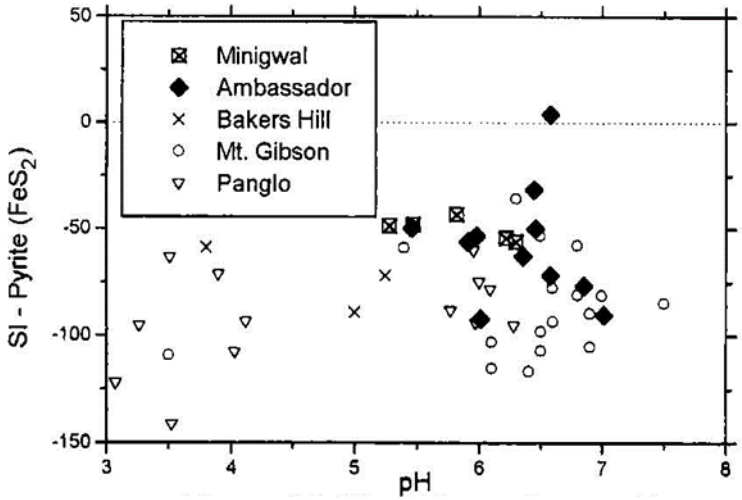

Figure A5.39: SI for siderite vs. pH

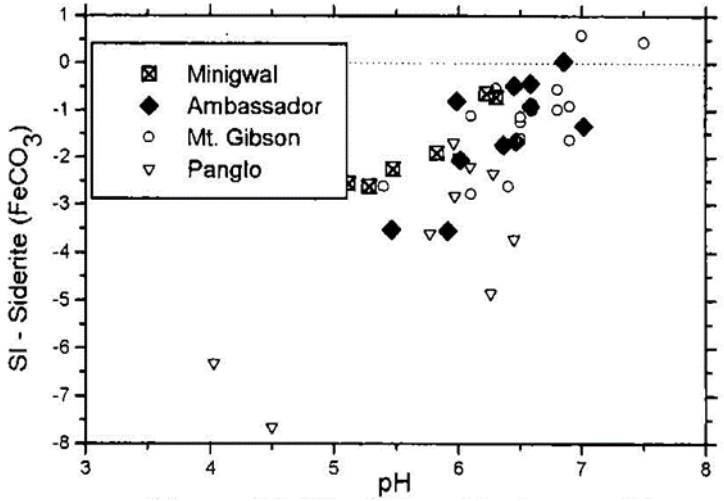

Figure A5.40: SI for $Fe(OH)_3$ vs. pH

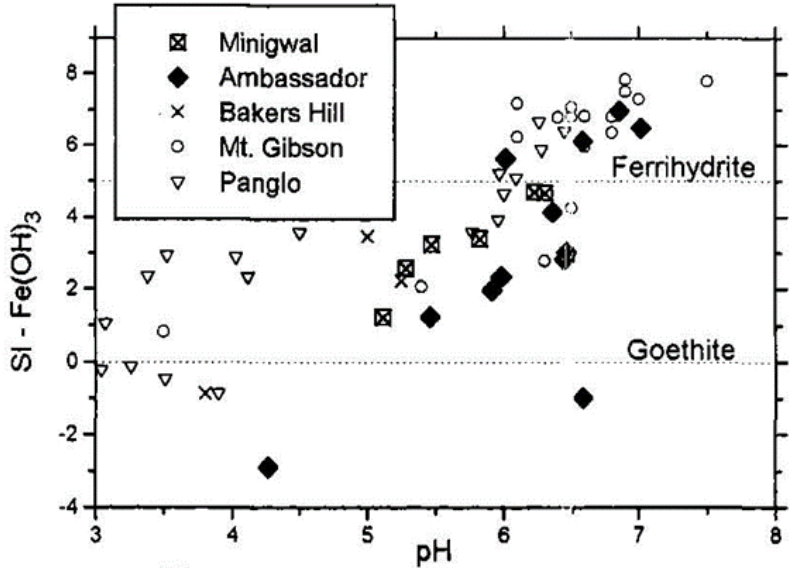

Figure A5.41: SI for rhodocrosite vs. pH

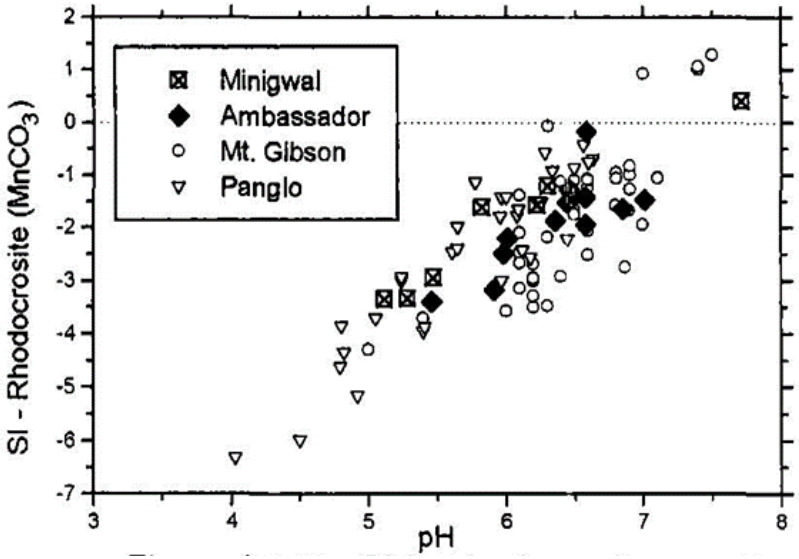

Figure A5.42: SI for tenorite vs. pH

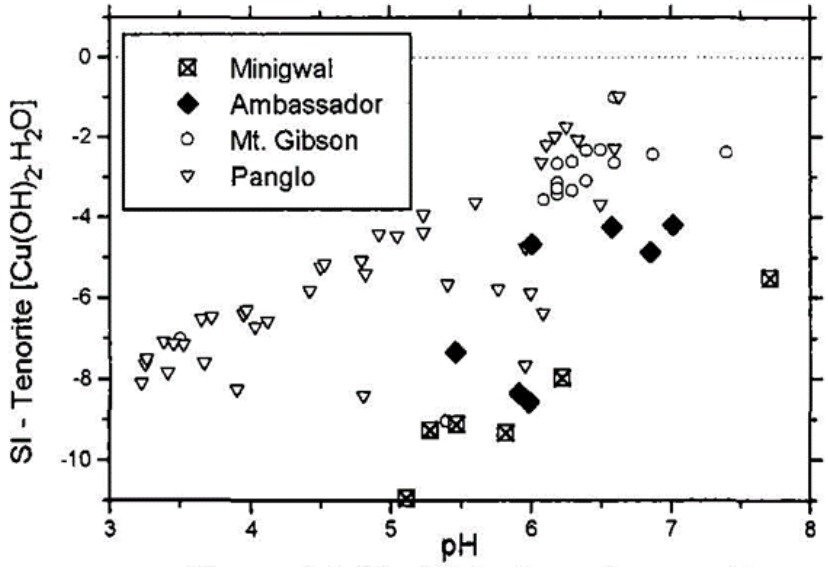

Figure A5.43: SI for smithsonite vs. pH

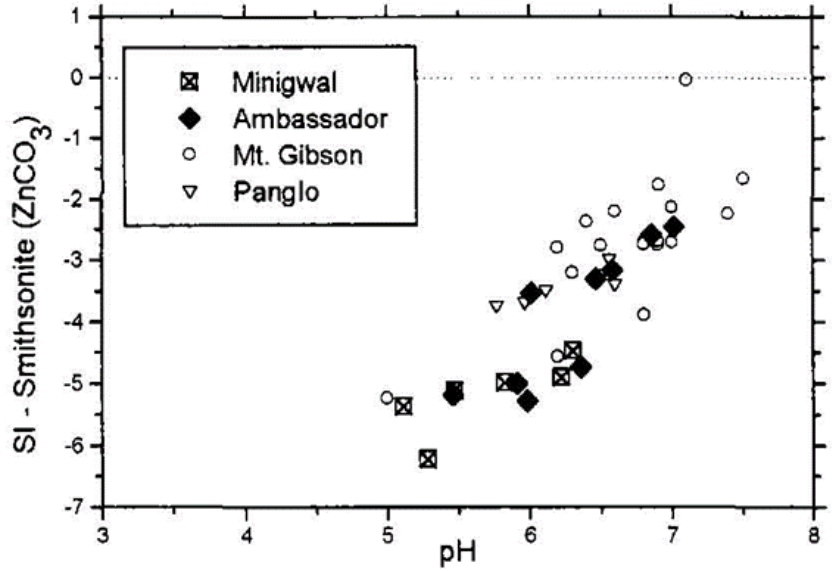

Figure A5.44: SI for otavite vs. pH

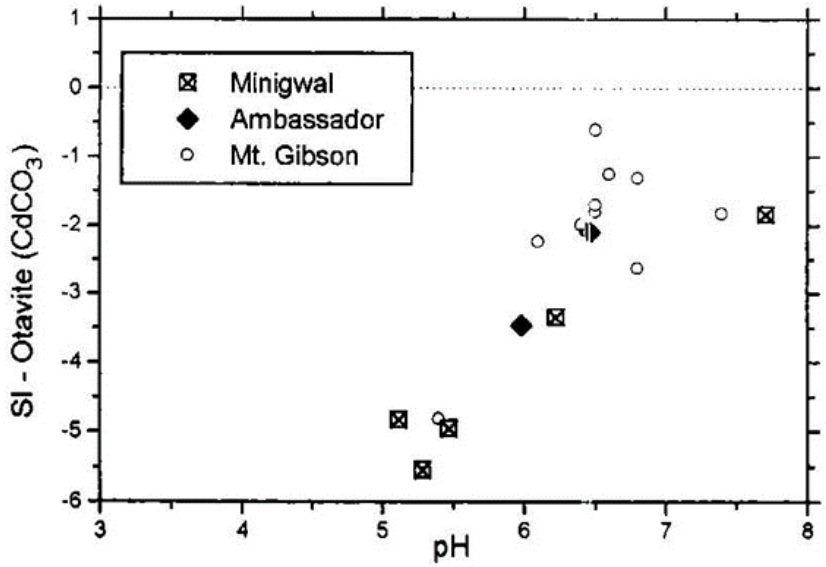

Figure A5.46: SI for $Ni(OH)_2$ vs. pH

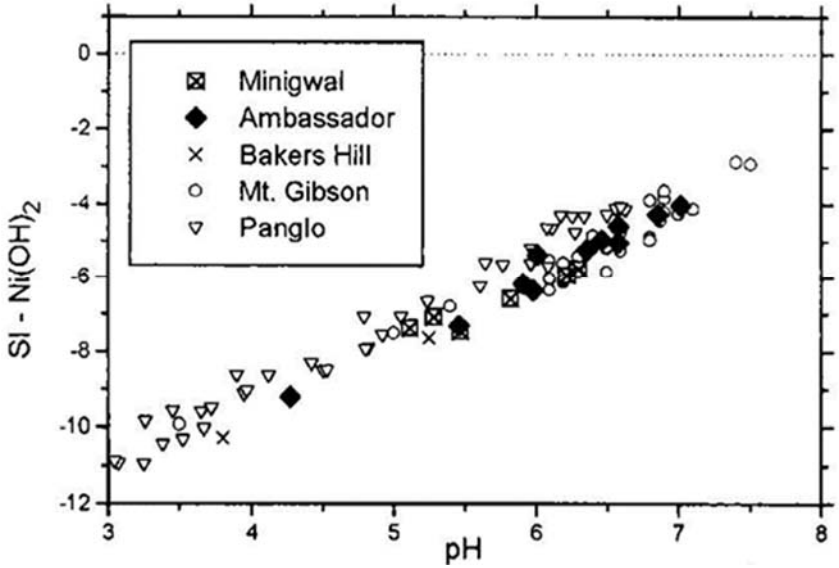

Figure A5.47: SI for cerrusite vs. pH

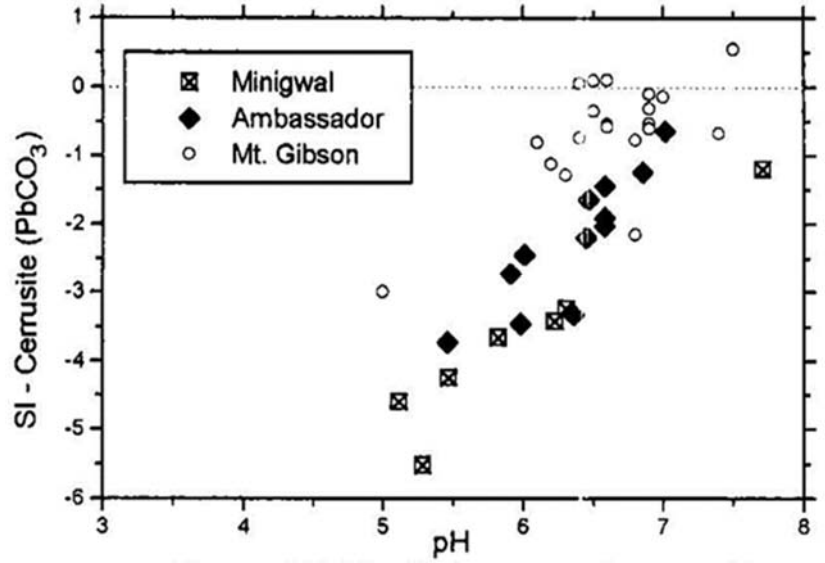

Figure A5.48: SI for iodyrite vs. pH

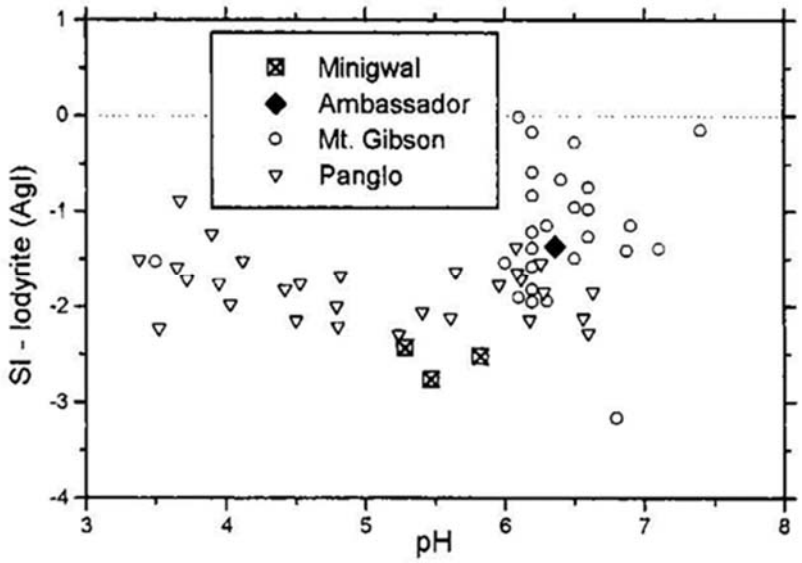

Figure A5.48: SI for $CoCo_3$ vs. PH

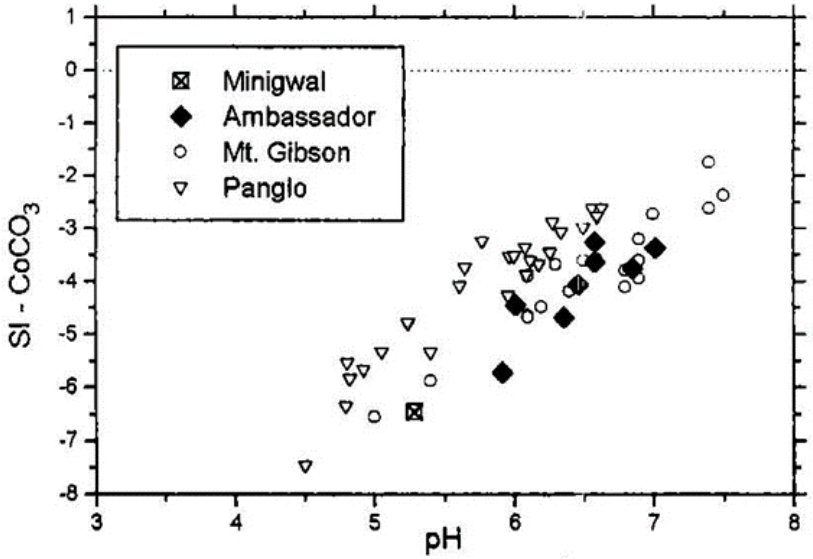

Figure A5.49: SI for Cr_2O_3 vs. pH

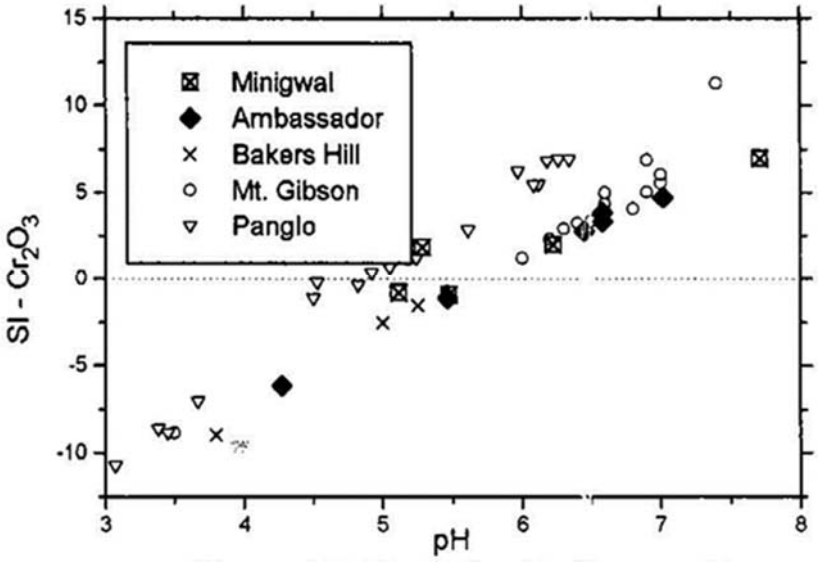

Figure A5.50: SI for uraninite vs. pH

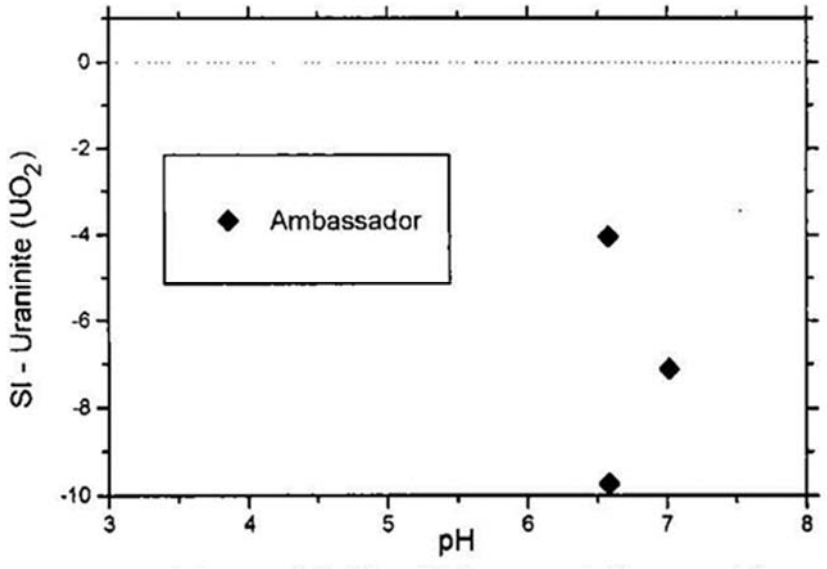

Figure A5.51: SI for rutherfordine vs. pH

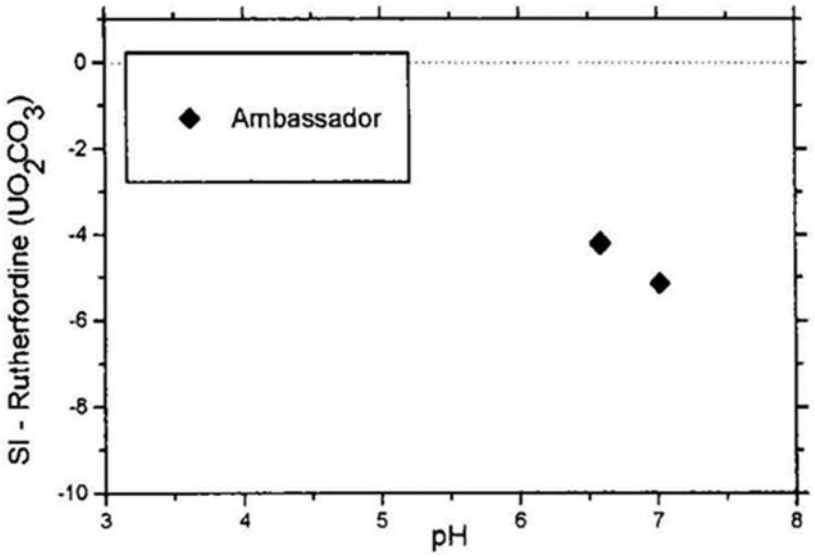

Figure A5.52: Mulga Rock – TDS Distribution

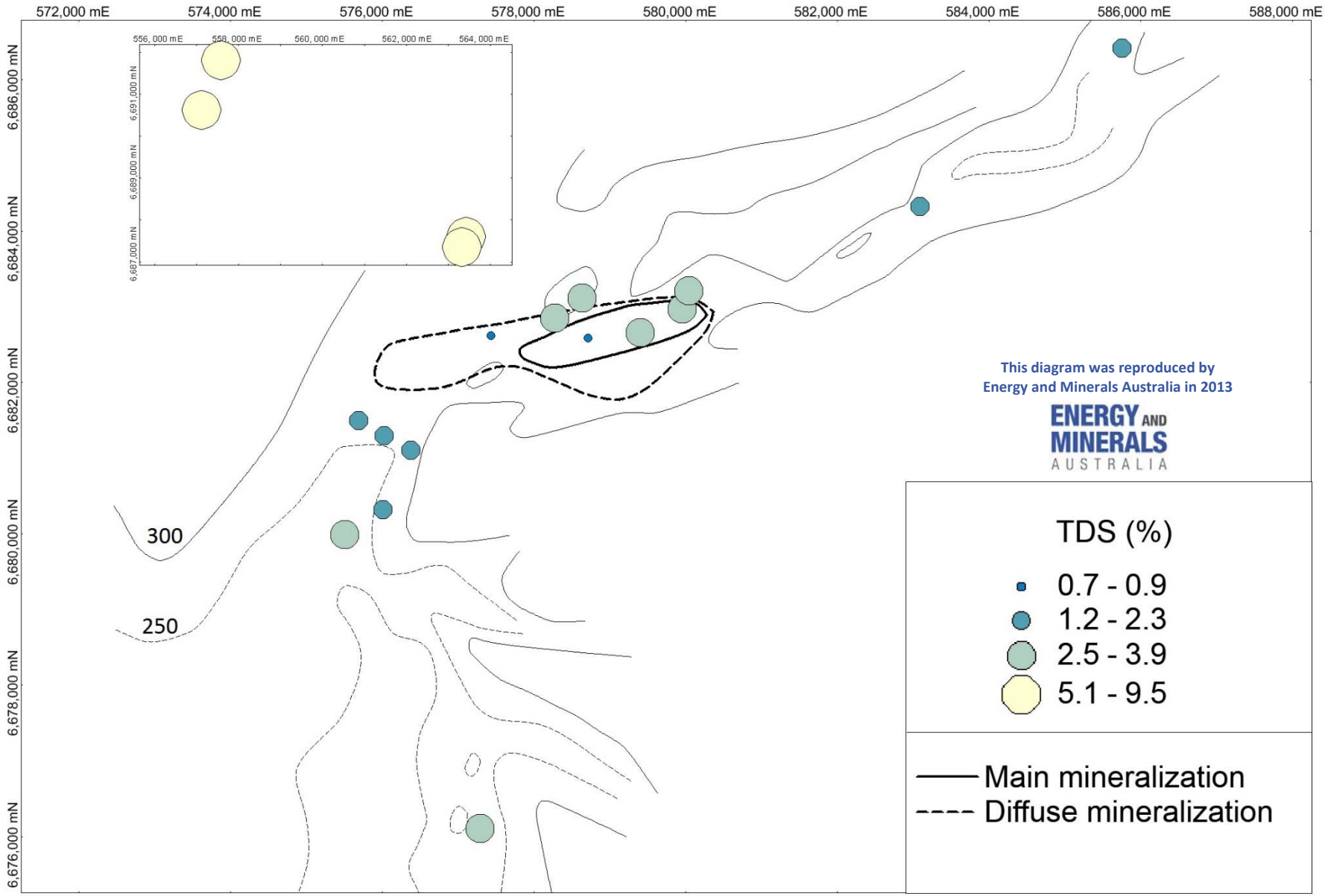

Figure A5.53: Mulga Rock – Water Isotope Groups

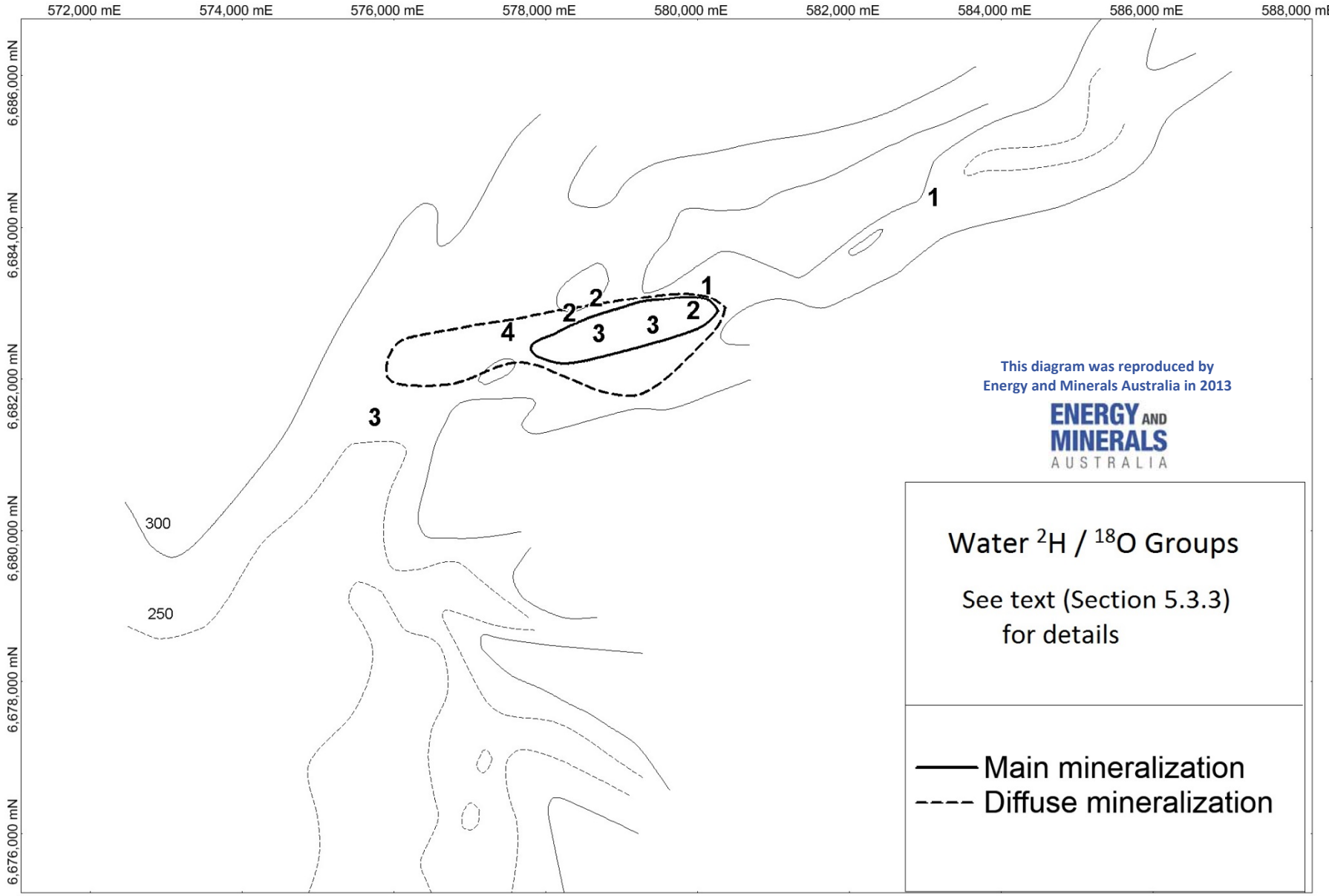

Figure A5.54: Mulga Rock – pH Distribution

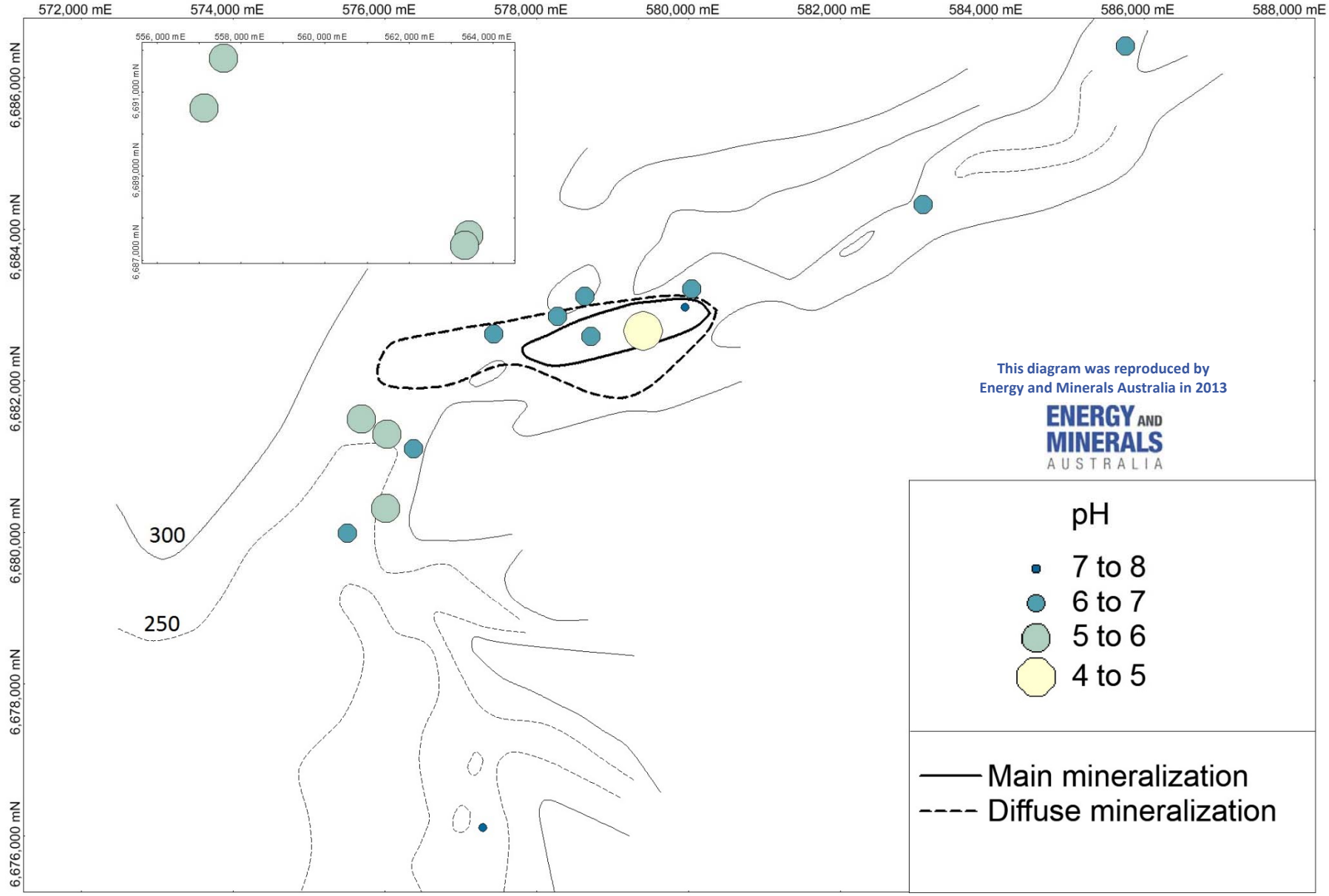

Figure A5.55: Mulga Rock – Eh Distribution

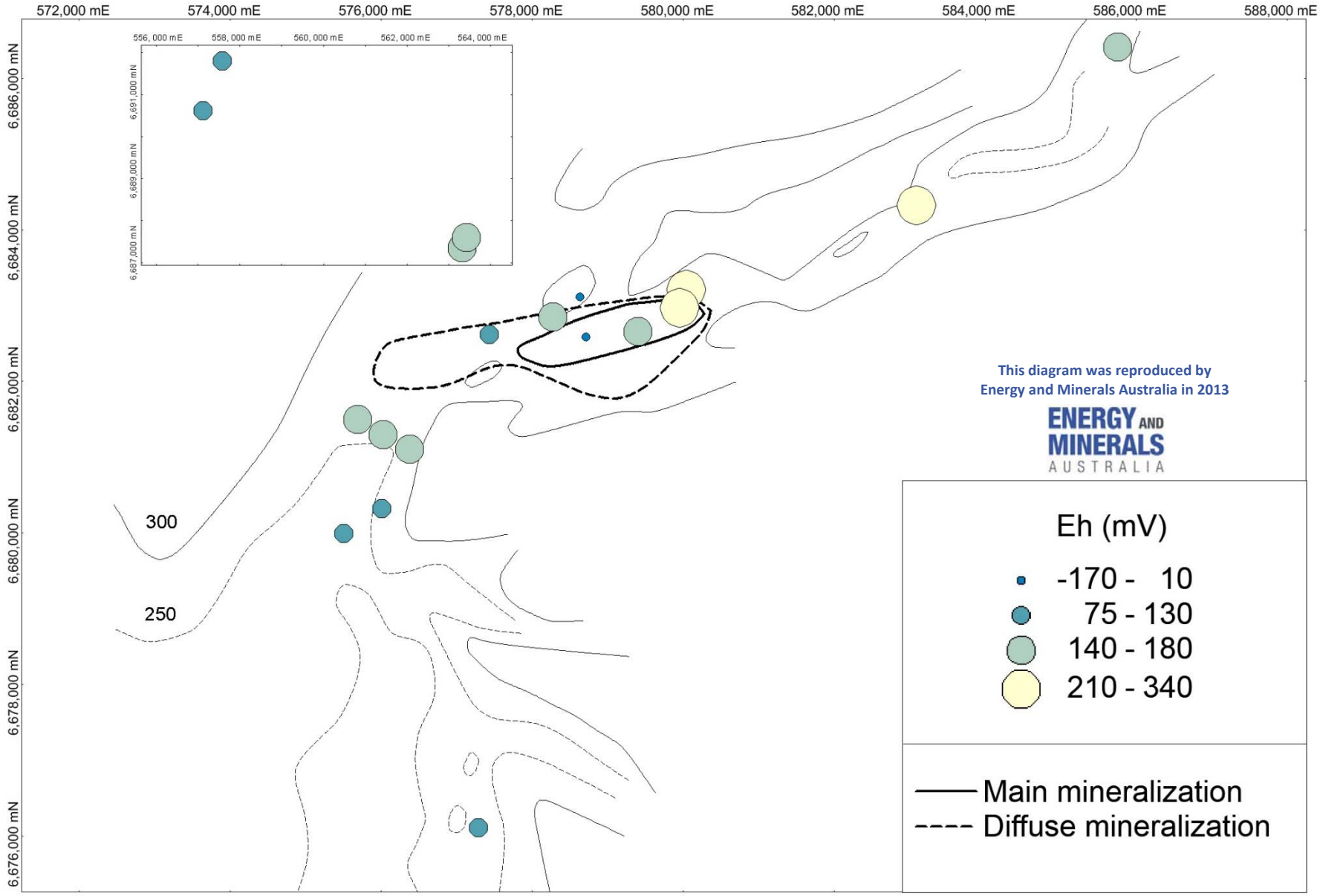

Figure A5.56: Mulga Rock – HCO^-_3 Distribution

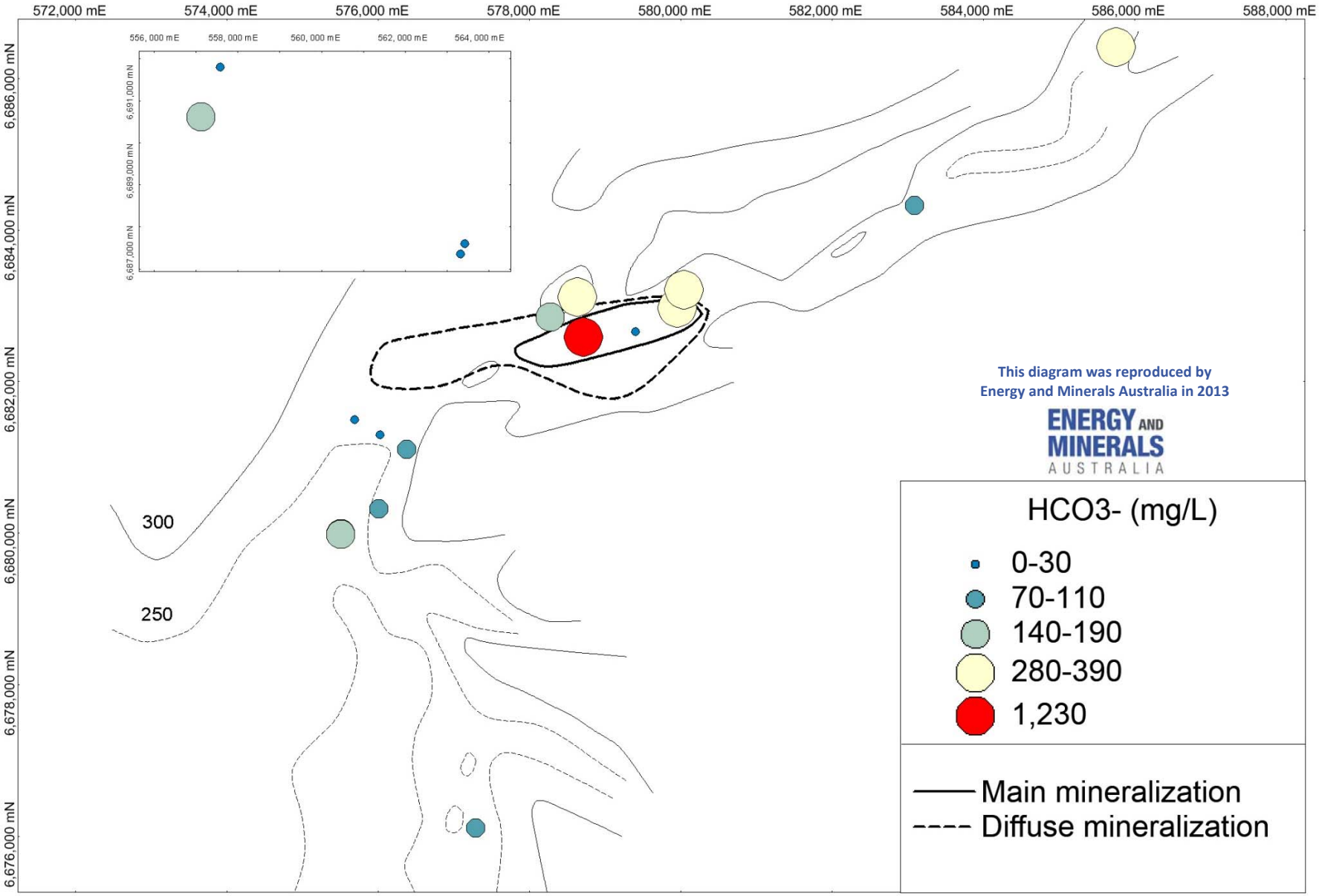

Figure A5.57: Mulga Rock – PO_4 Distribution

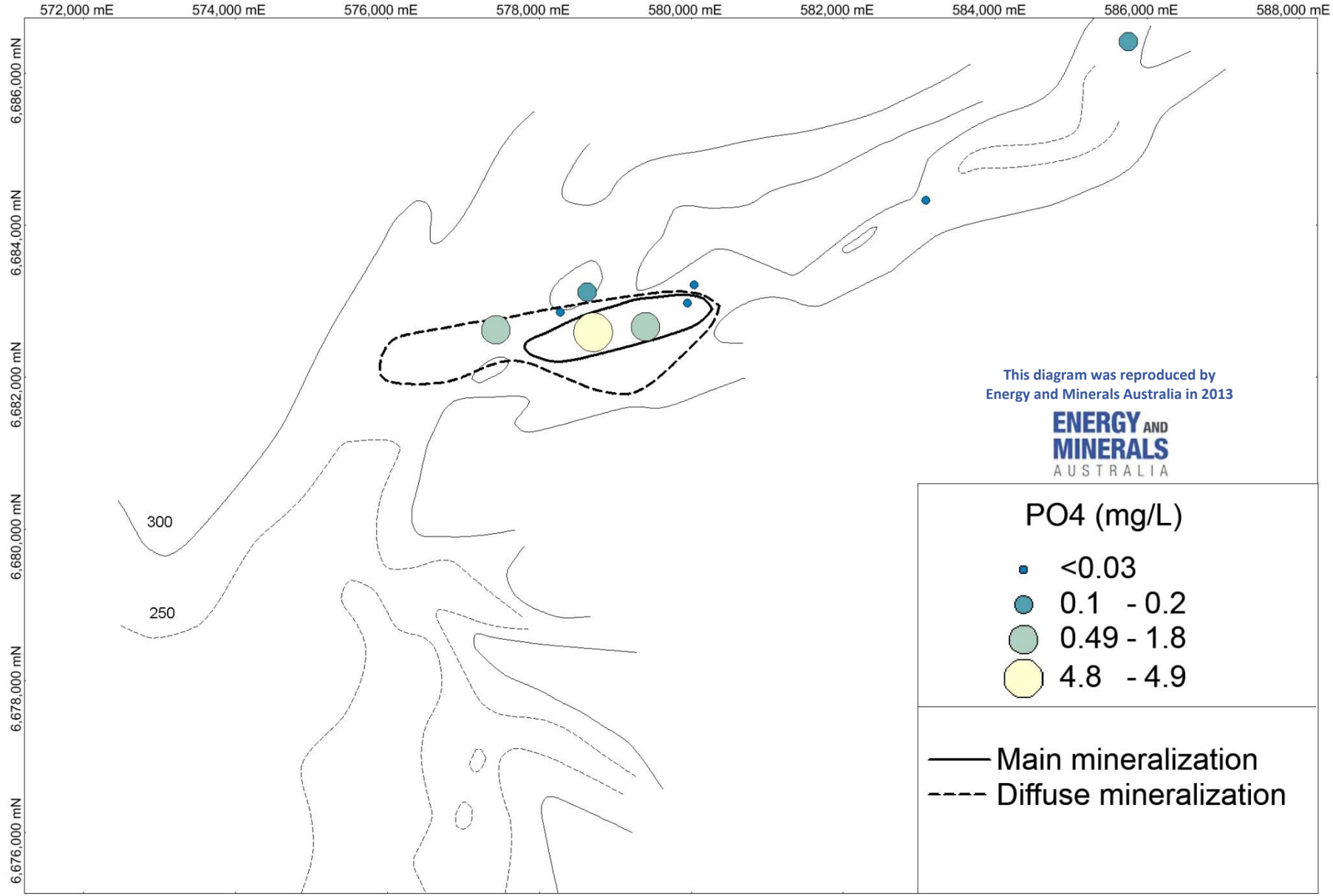

Figure A5.58: Mulga Rock – Ba Distribution

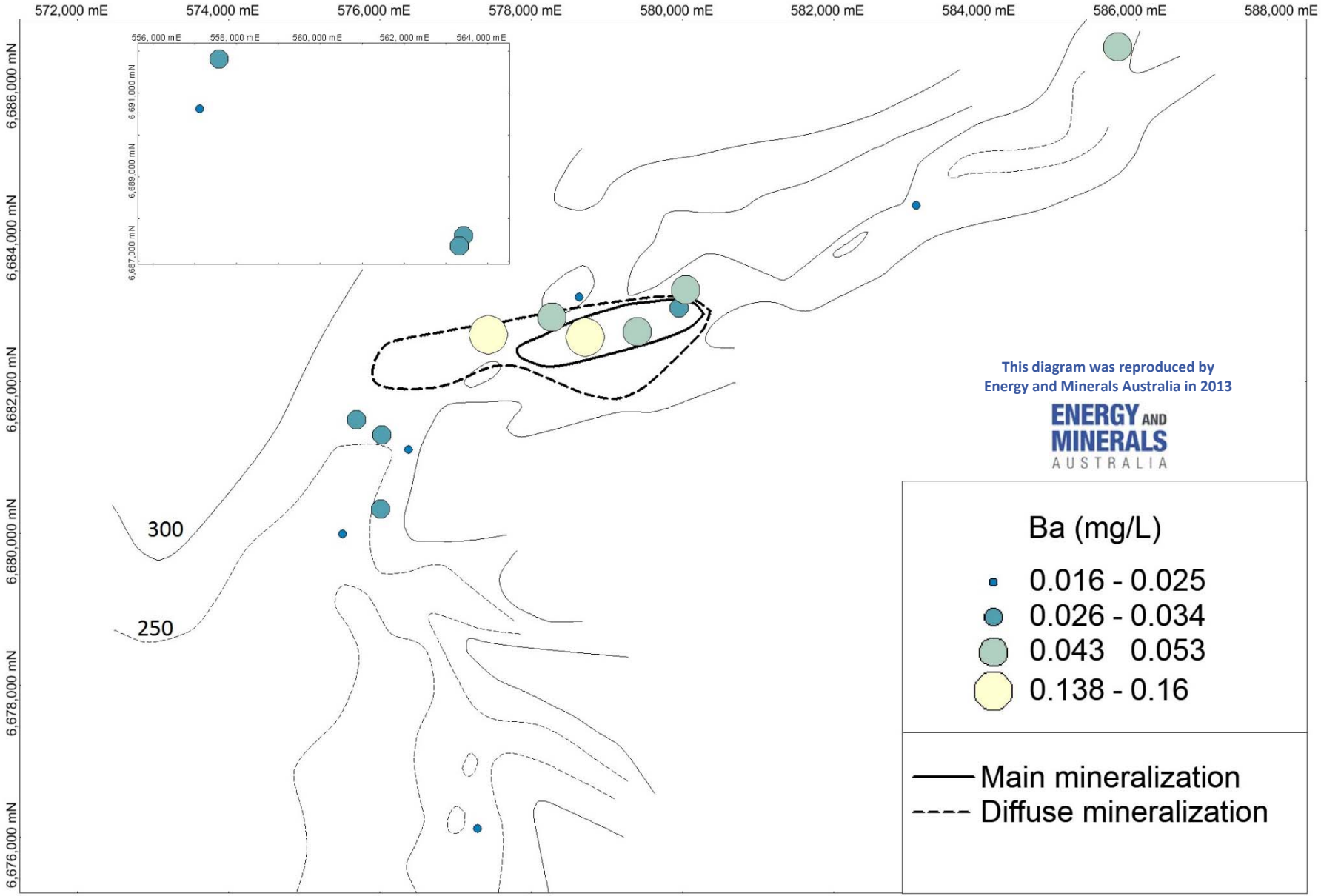

Figure A5.59: Mulga Rock – Al Distribution

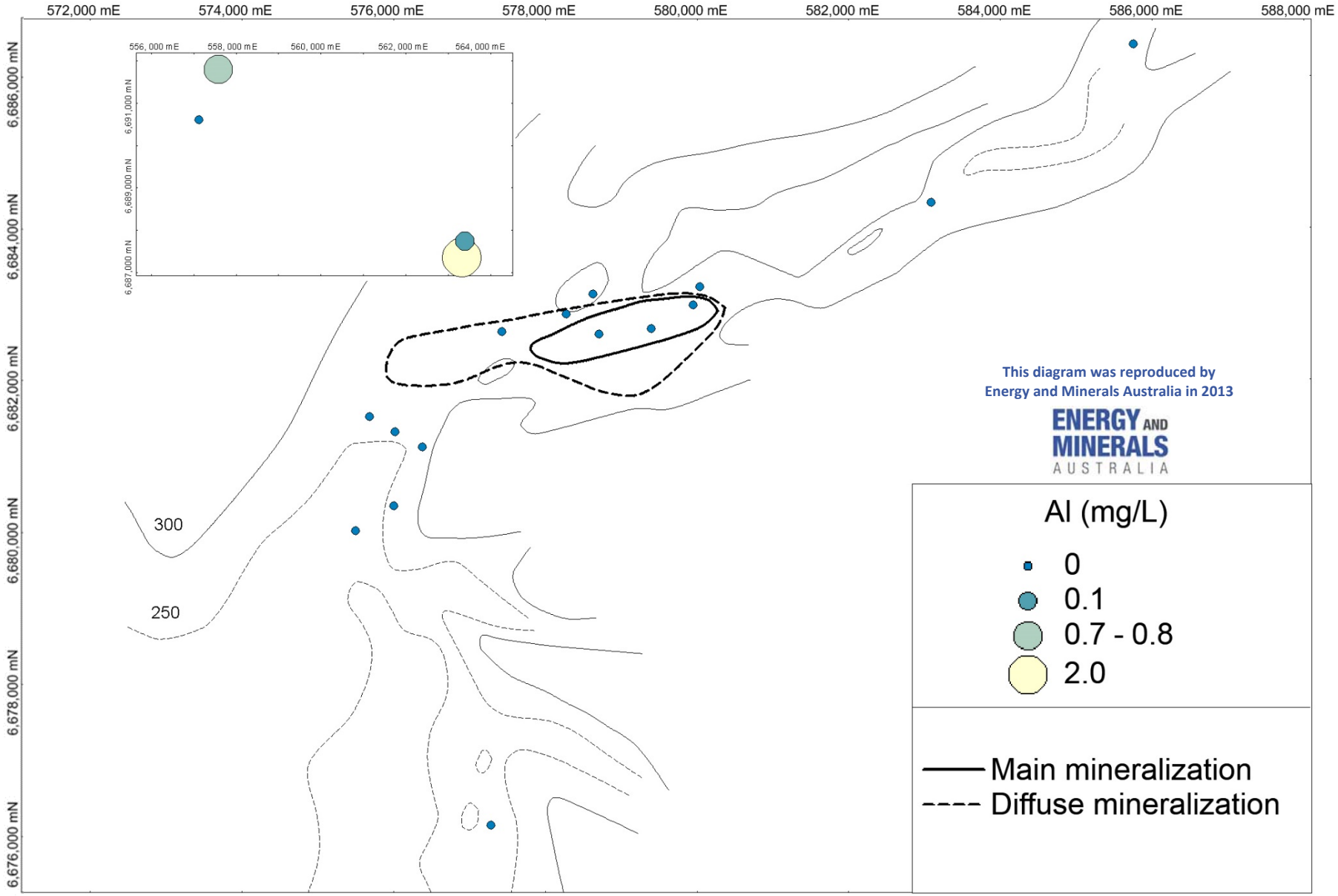

Figure A5.60: Mulga Rock – Si Distribution

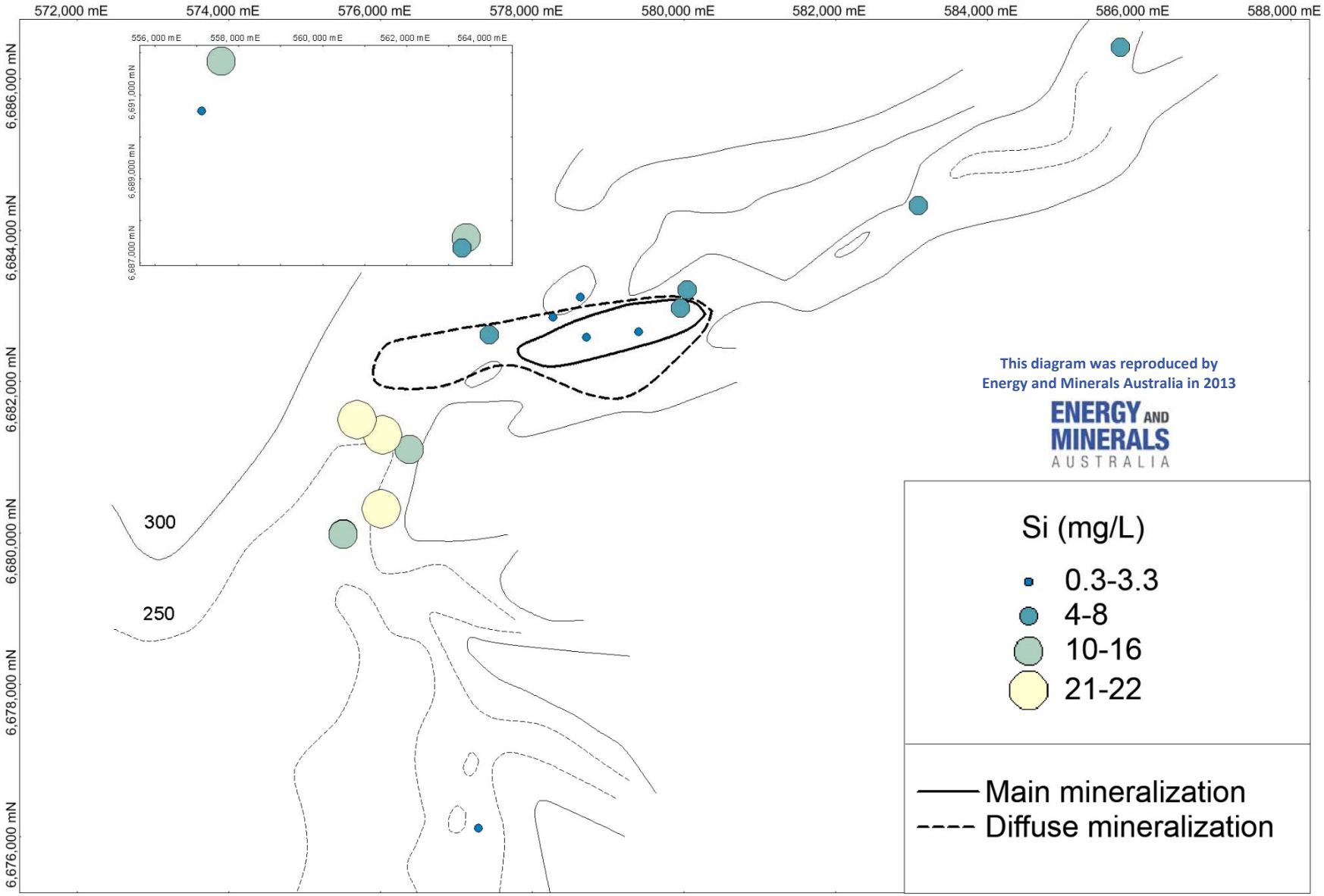

Figure A5.61: Mulga Rock – Fe Distribution

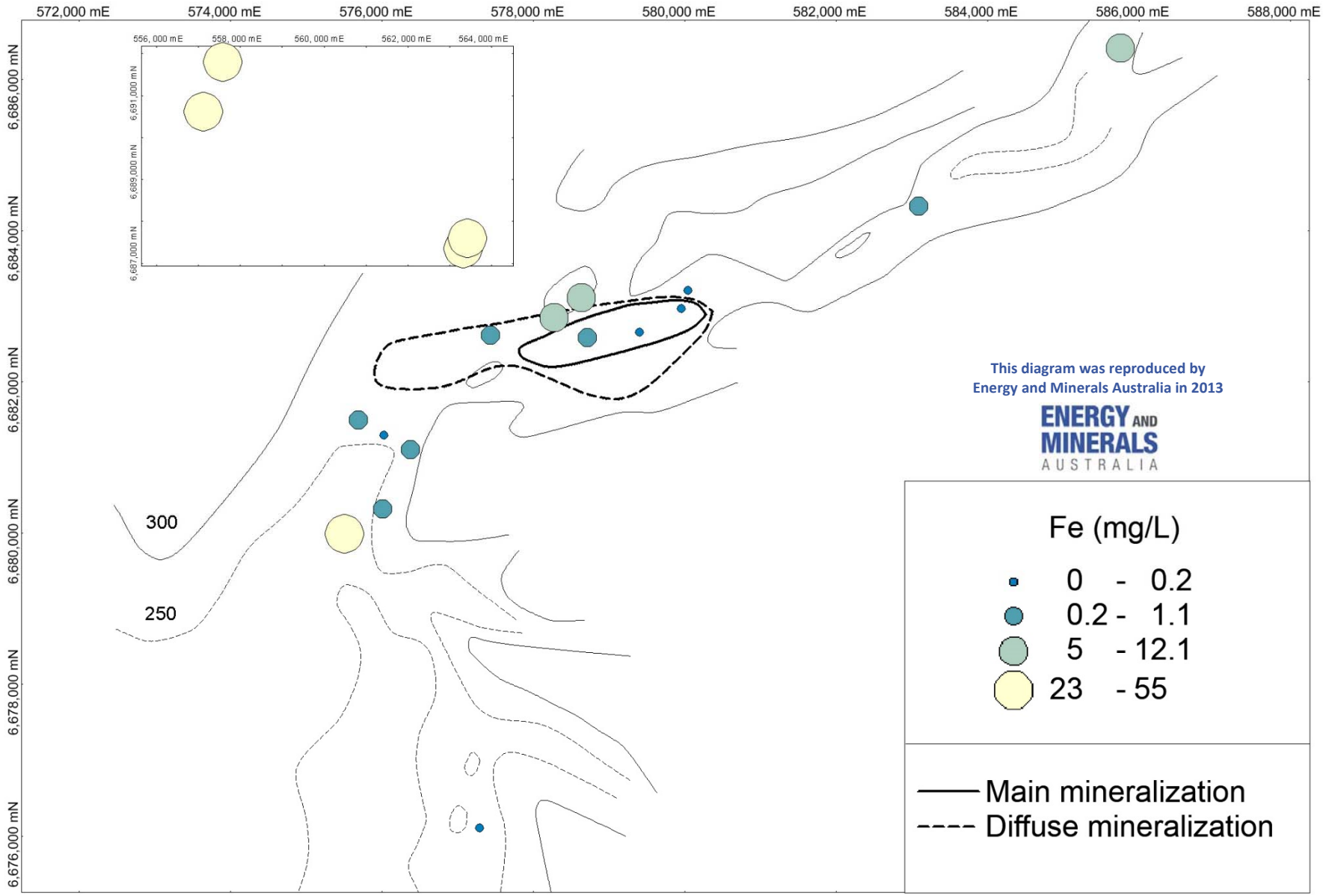

Figure A5.62: Mulga Rock – Mn Distribution

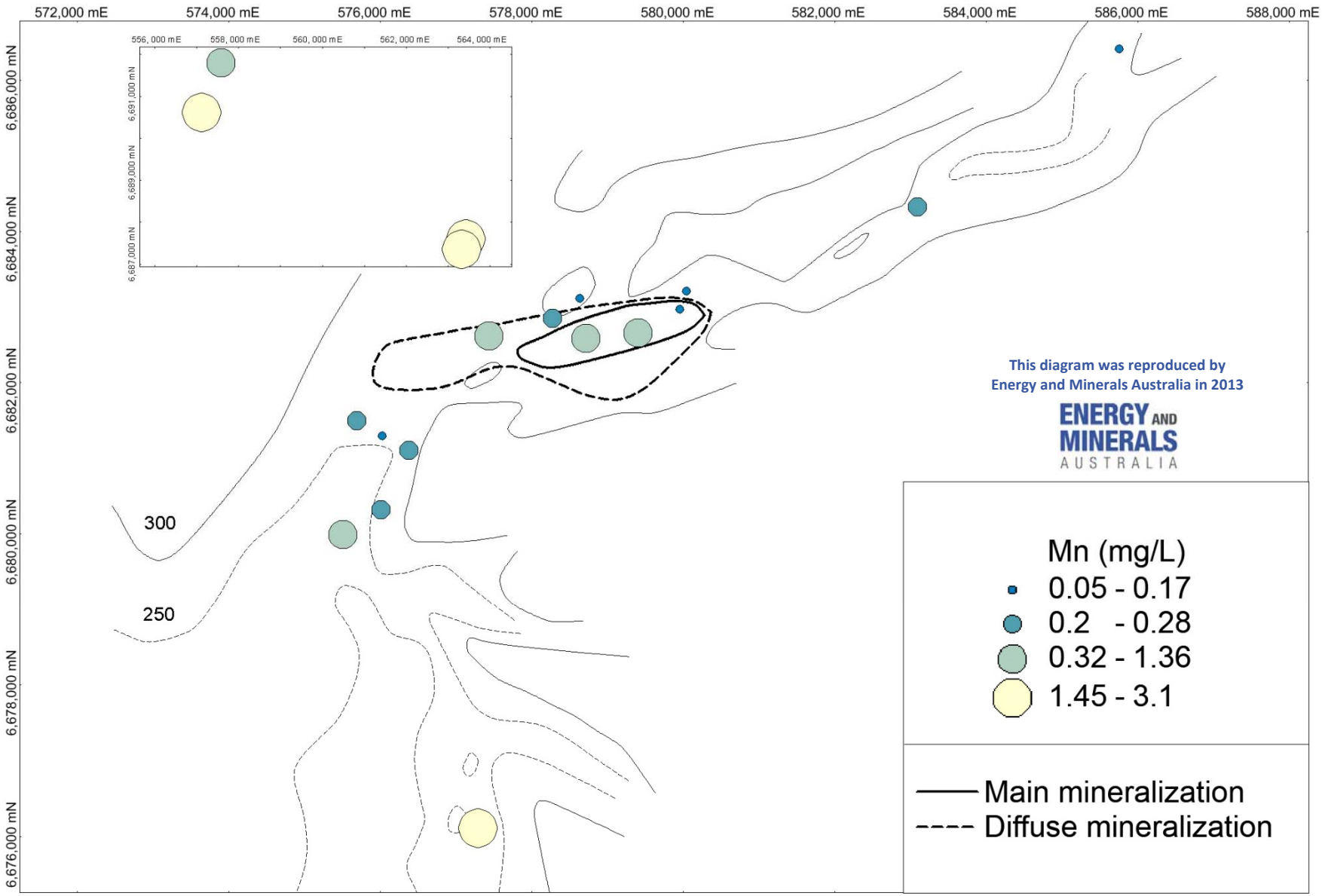

Figure A5.63: Mulga Rock – Cr Distribution

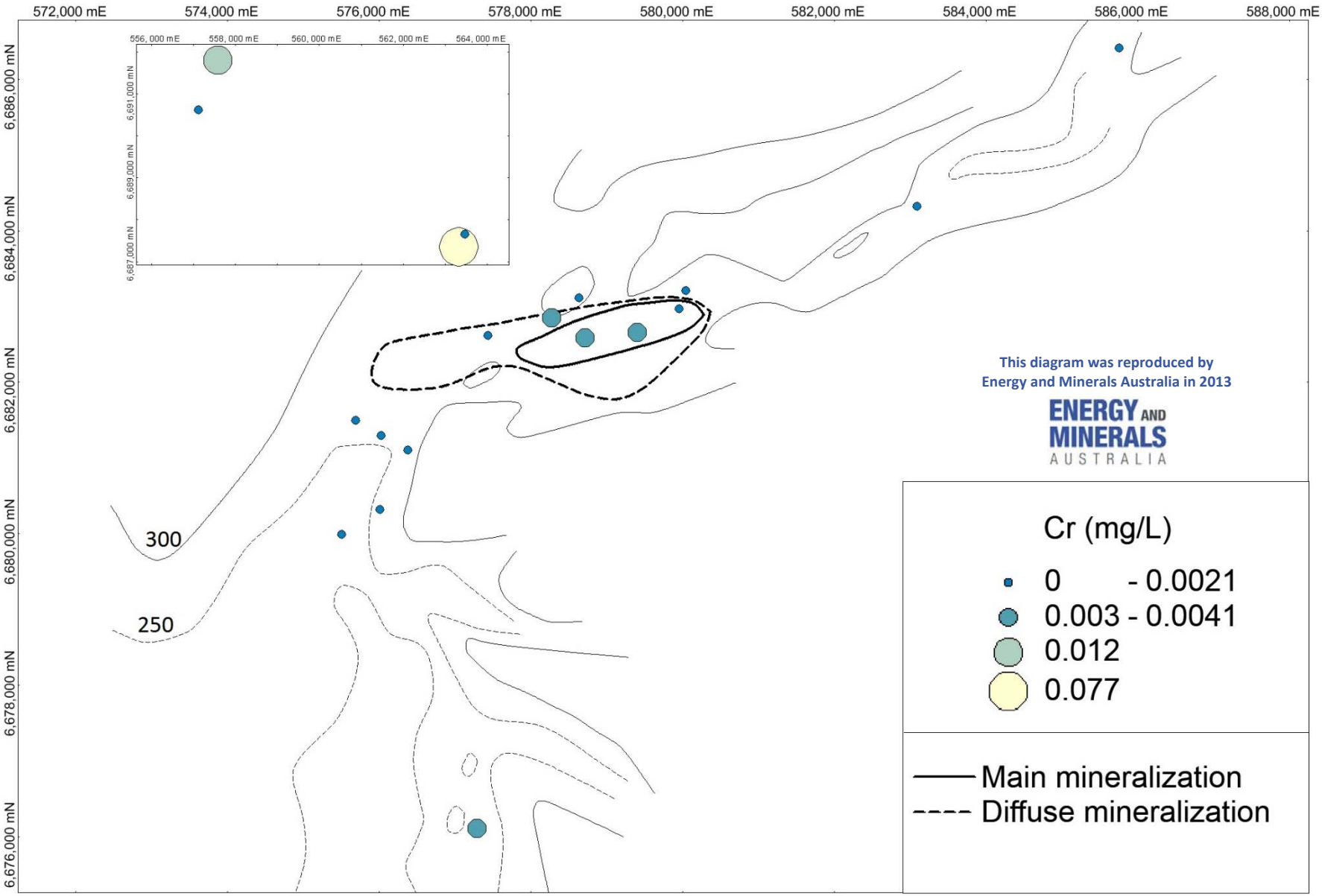

Figure A5.64: Mulga Rock – Co Distribution

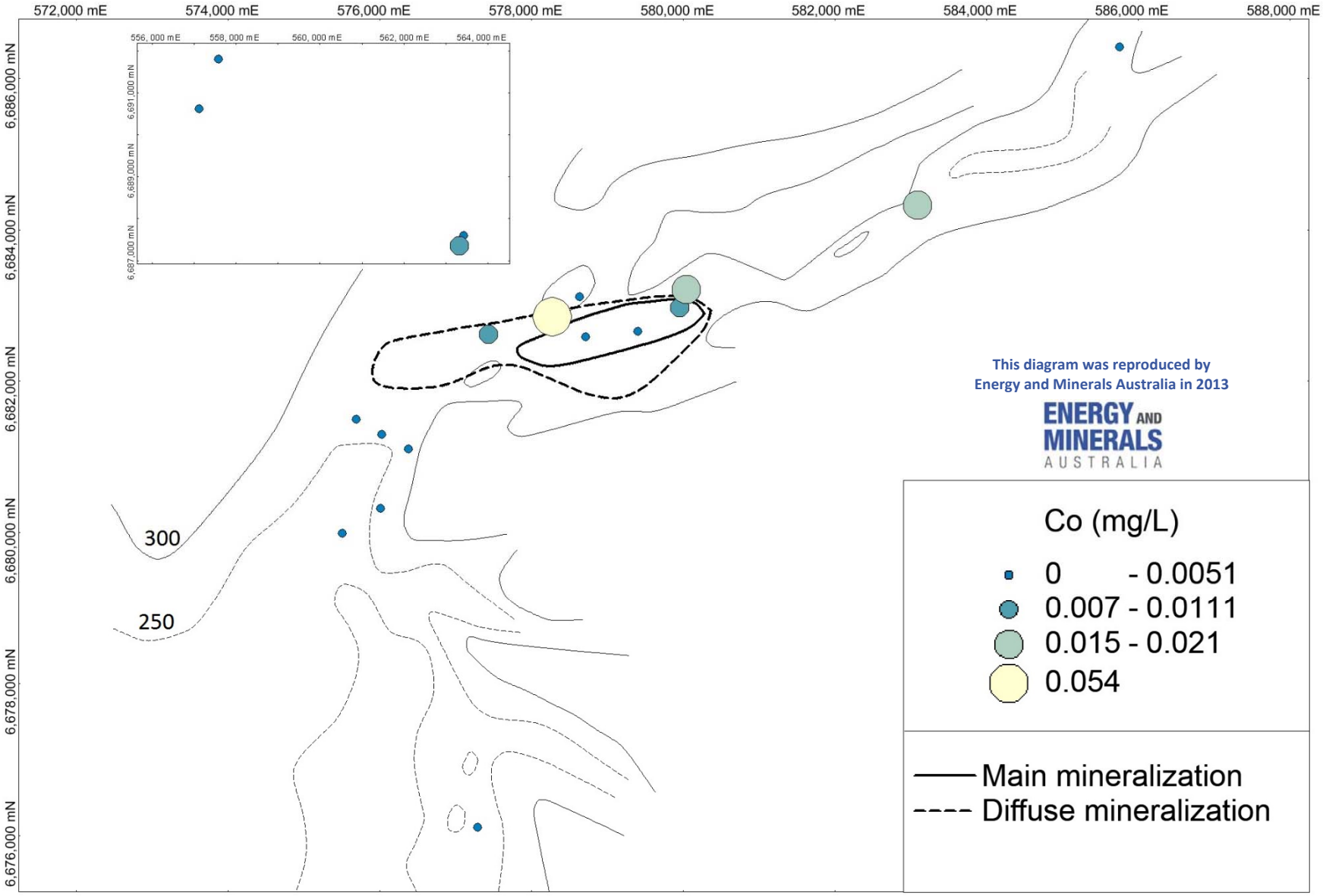

Figure A5.65: Mulga Rock – Ni Distribution

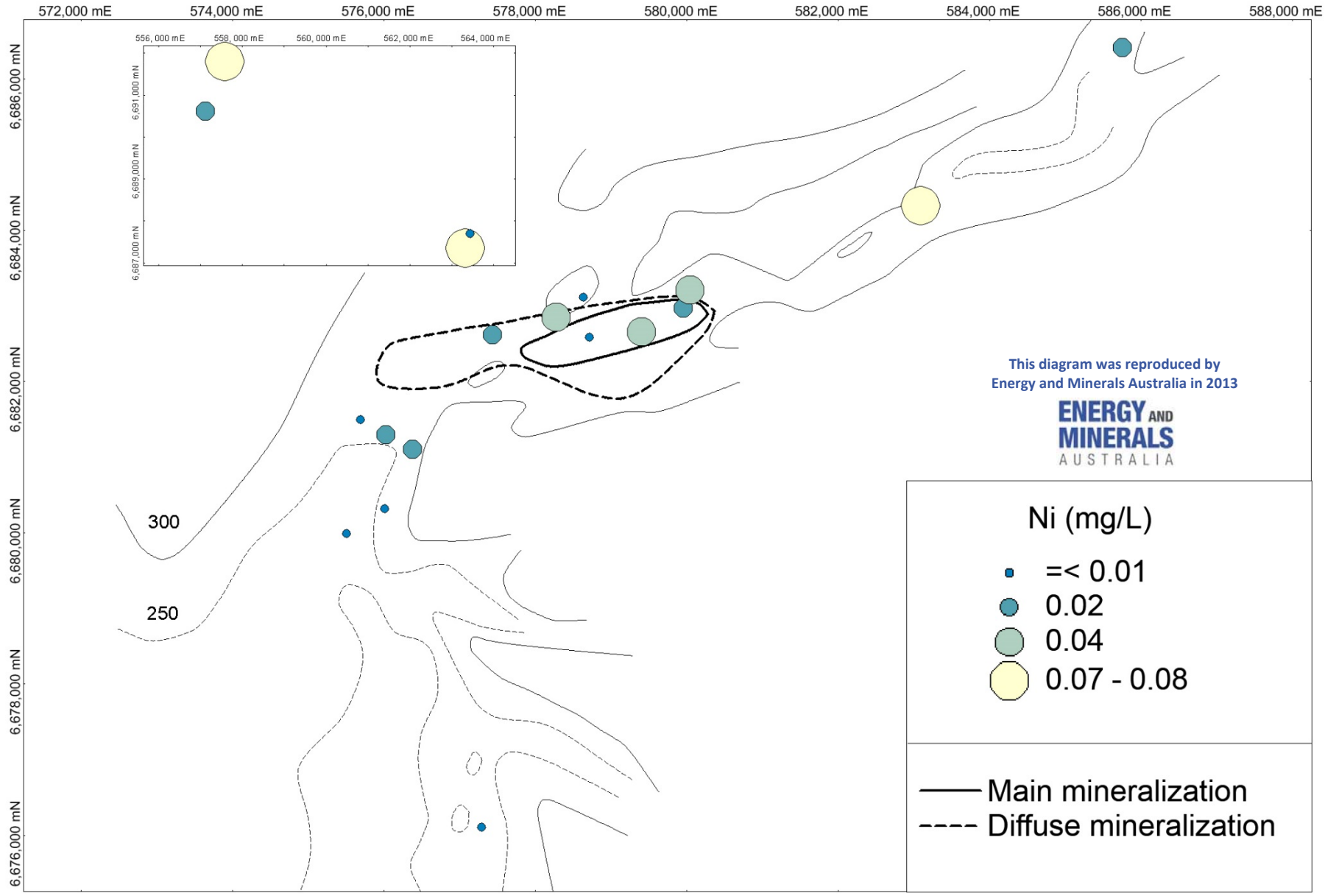

Figure A5.66: Mulga Rock – Cu Distribution

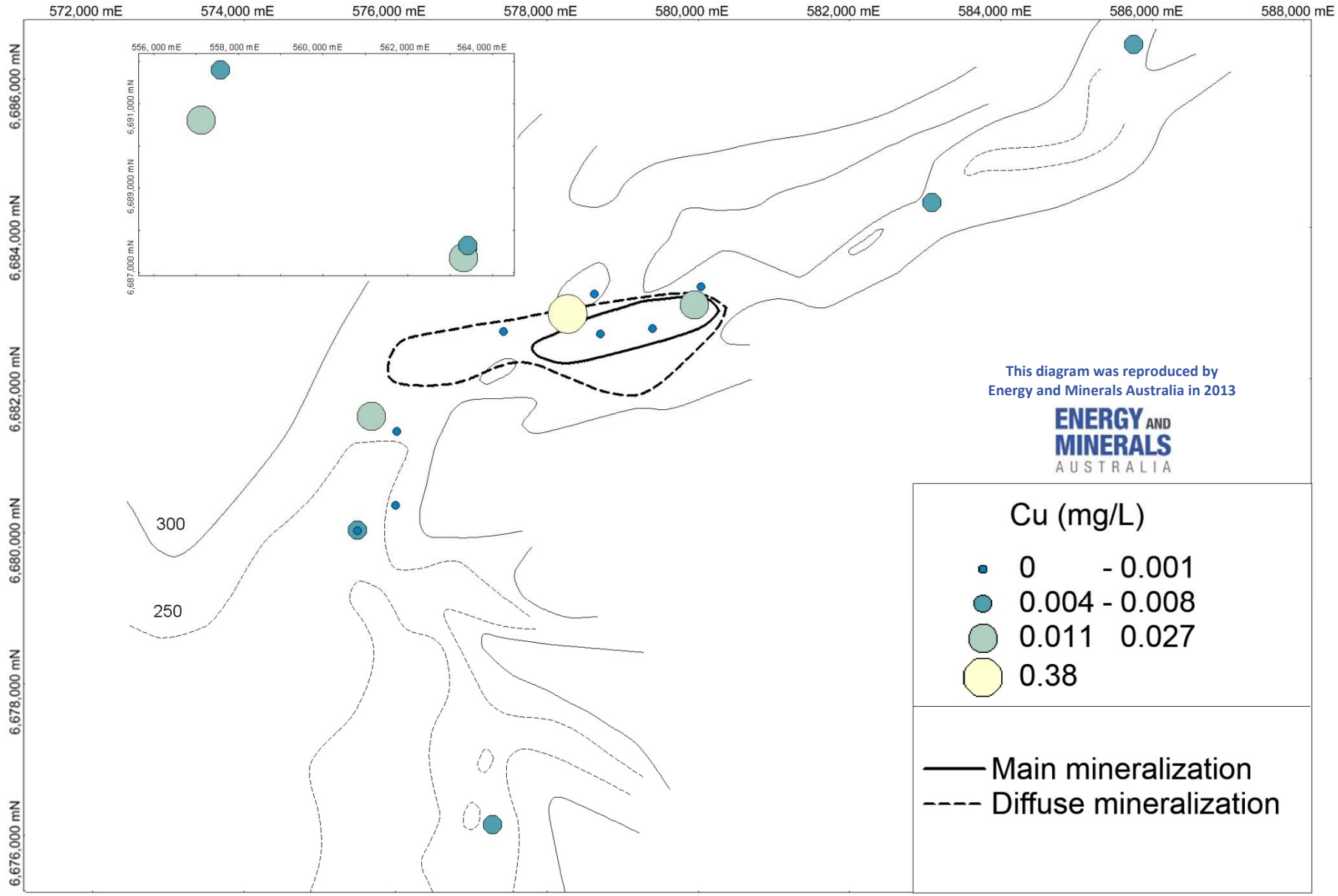

Figure A5.67: Mulga Rock – Zn Distribution

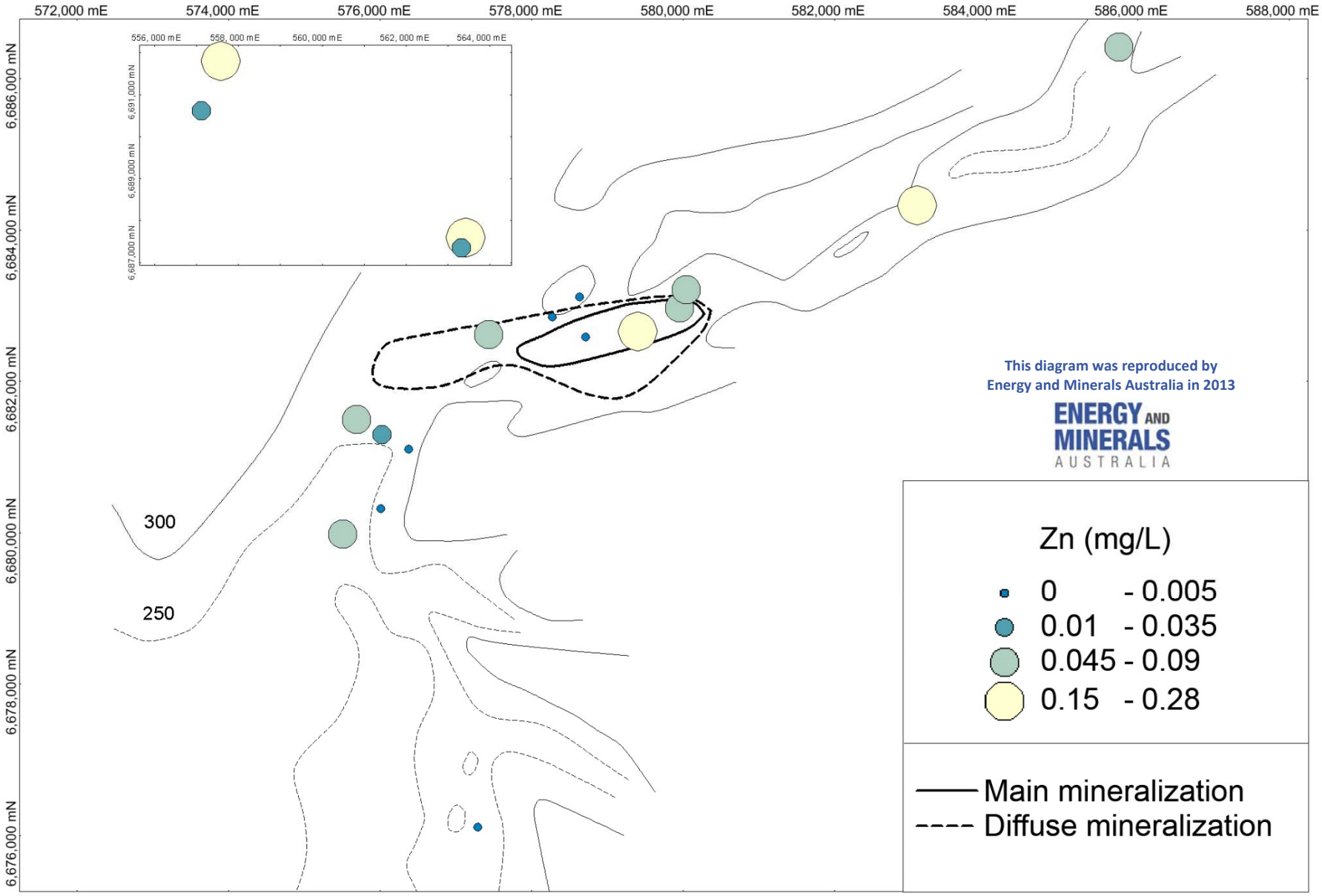

Figure A5.68: Mulga Rock – Pb Distribution

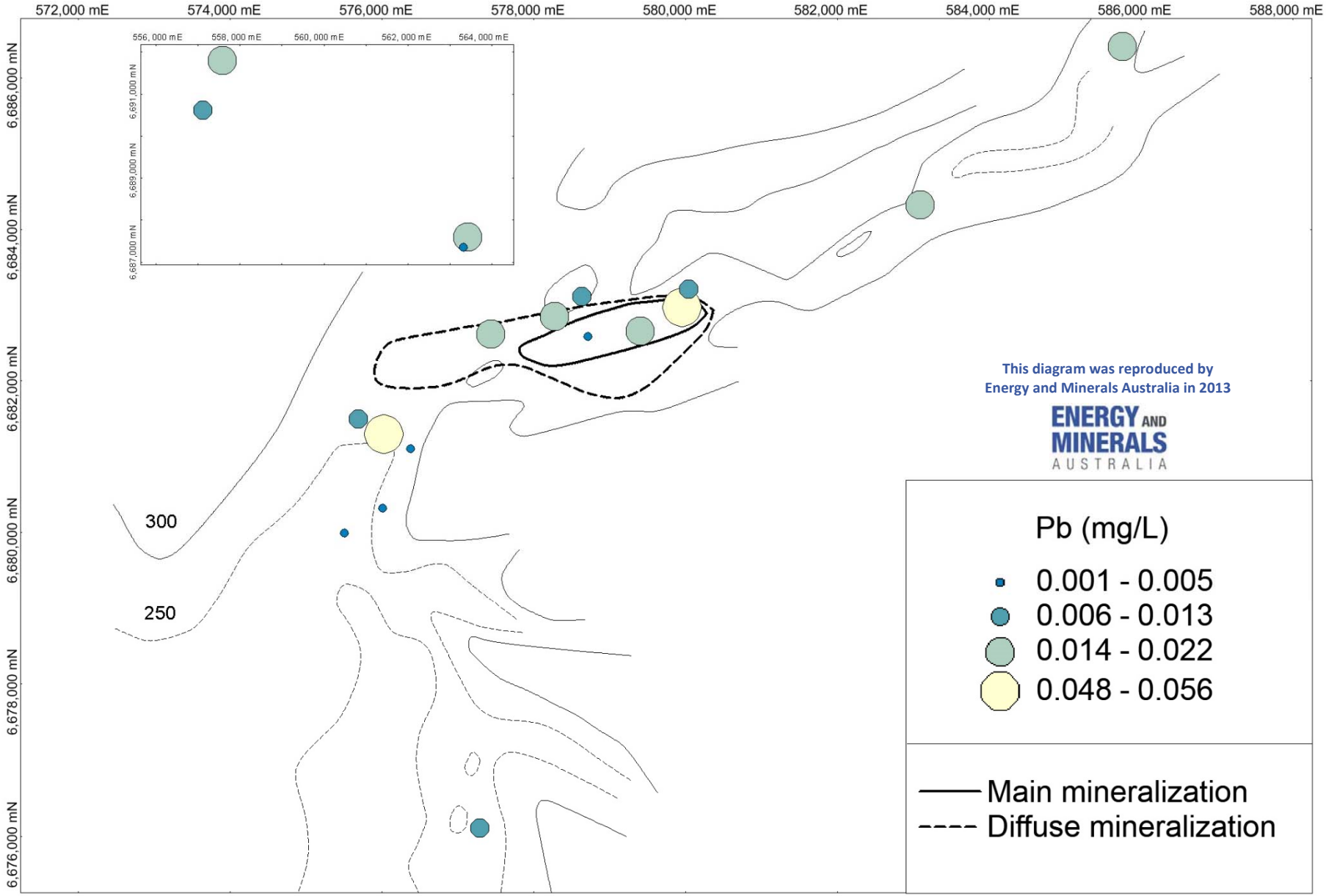

Figure A5.69: Mulga Rock – Y Distribution

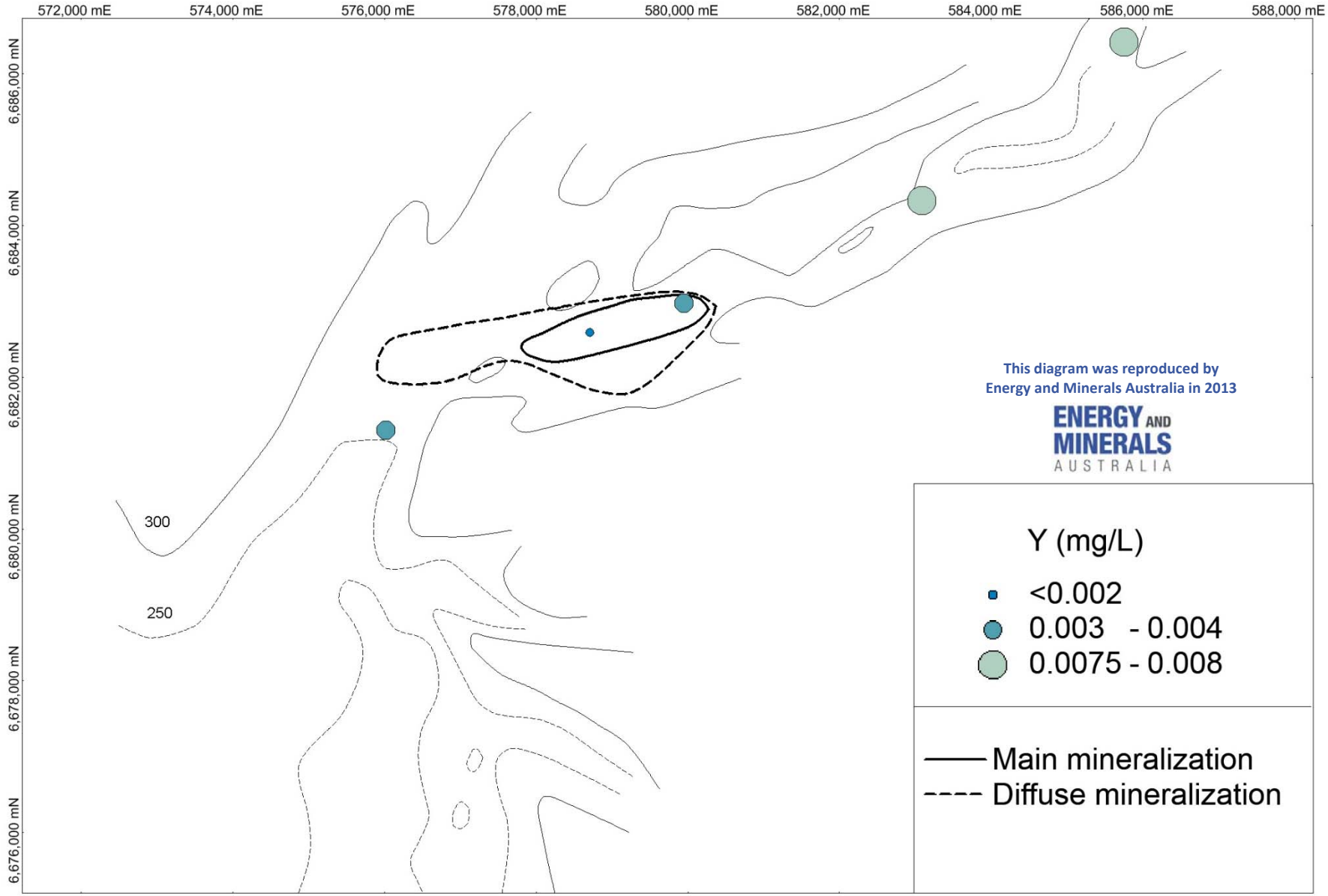

Figure A5.70: Mulga Rock – La Distribution

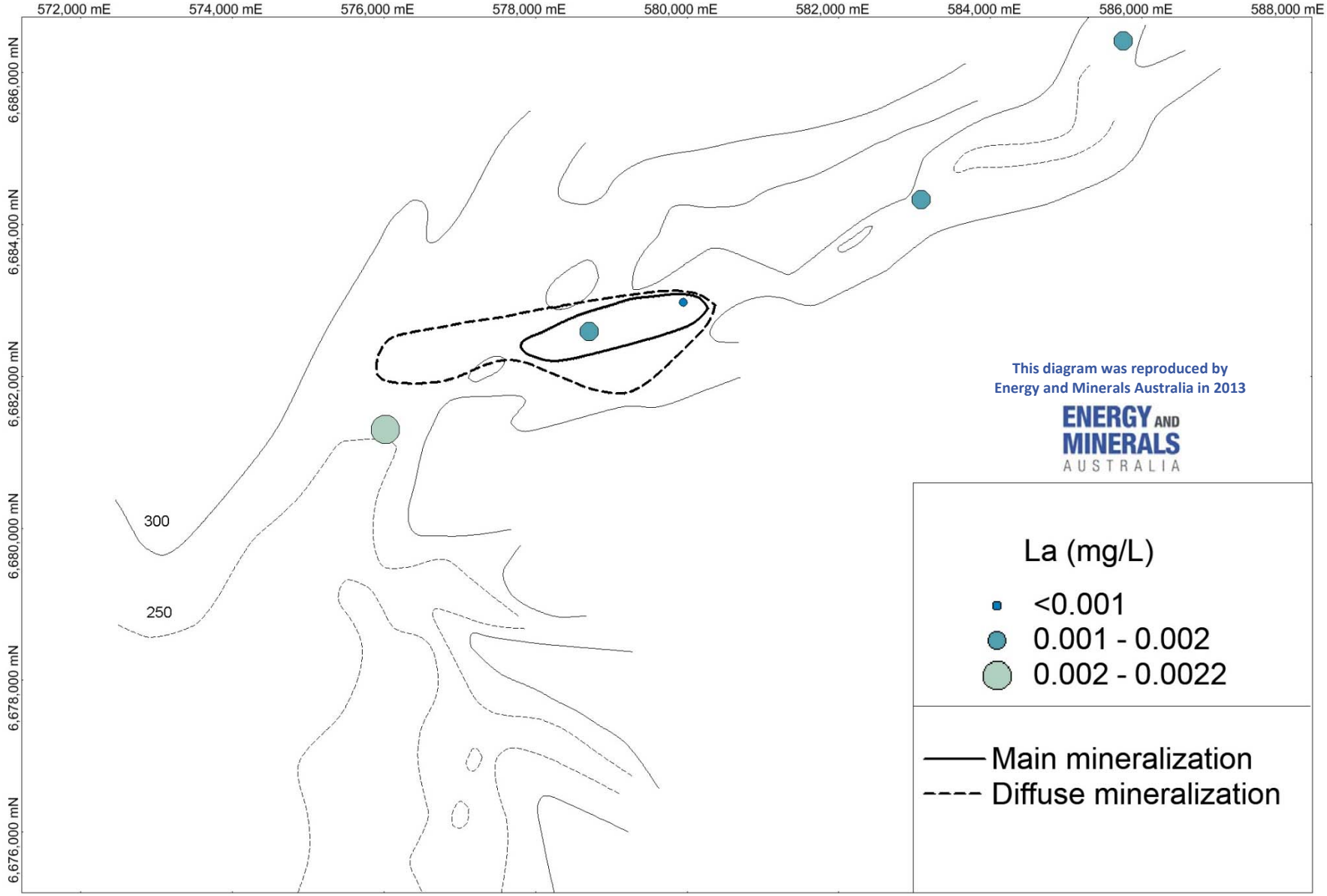

Figure A5.71: Mulga Rock – Ce Distribution

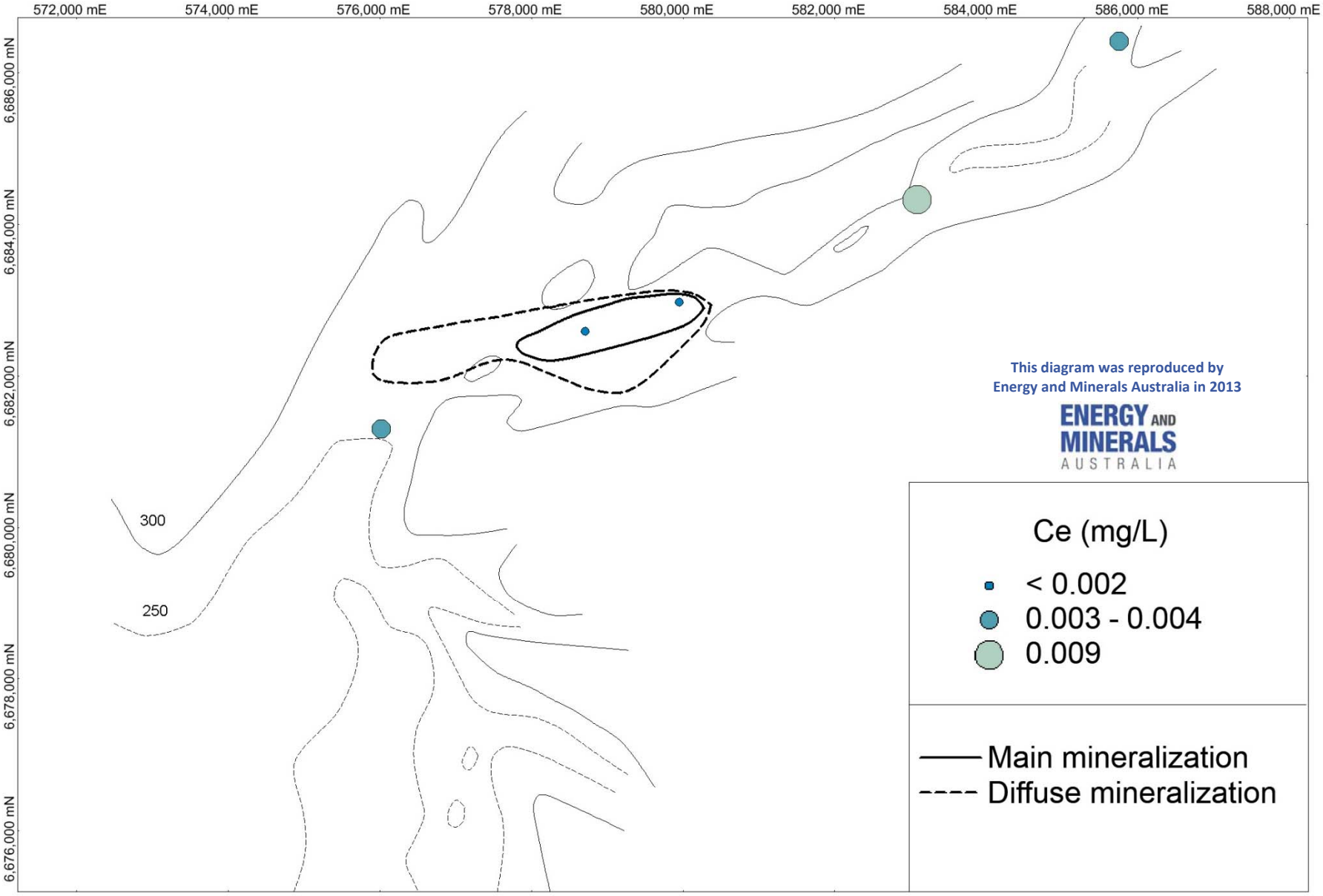

Figure A5.72: Mulga Rock – Total REE Distribution

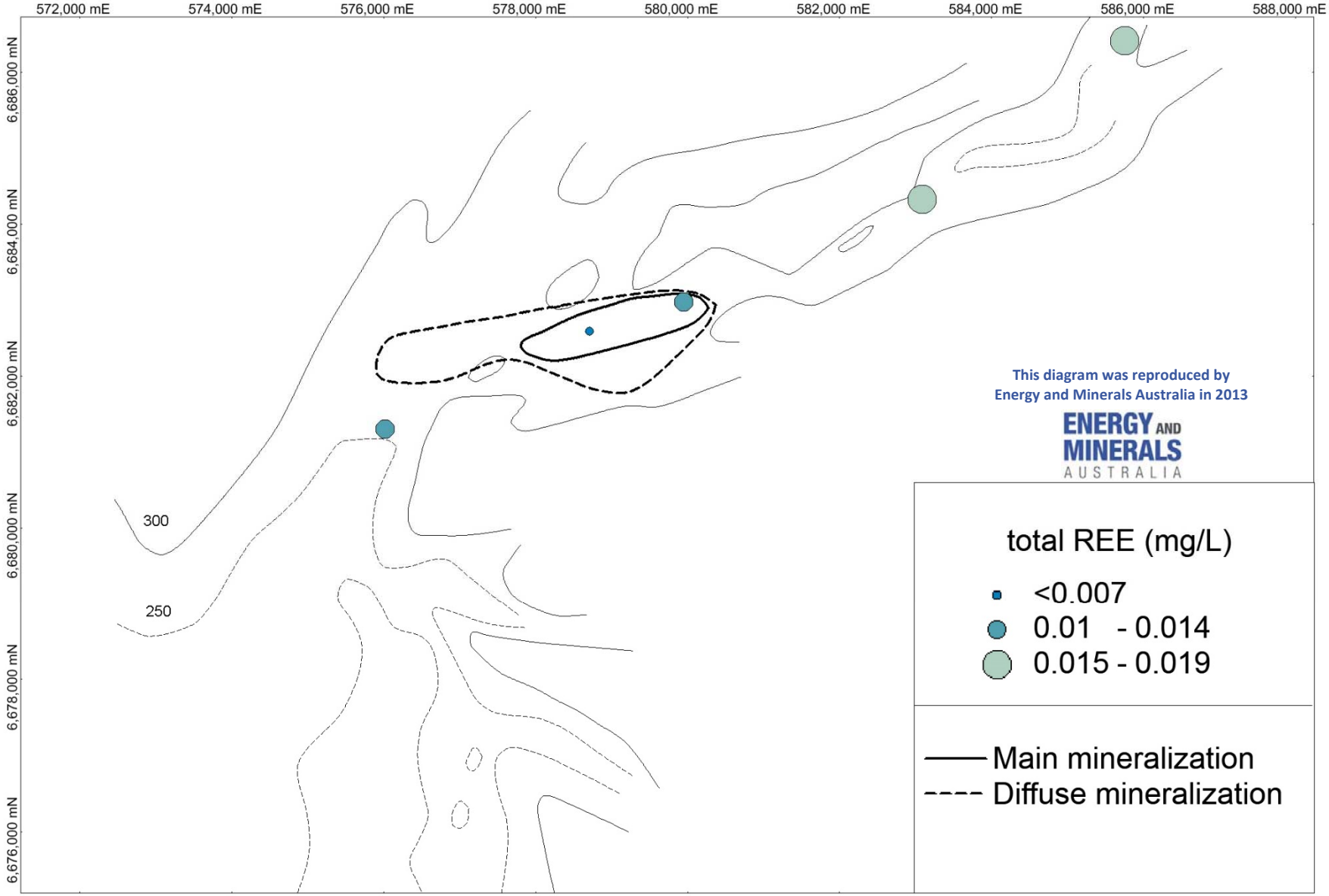

Figure A5.73: Mulga Rock – I^- Distribution

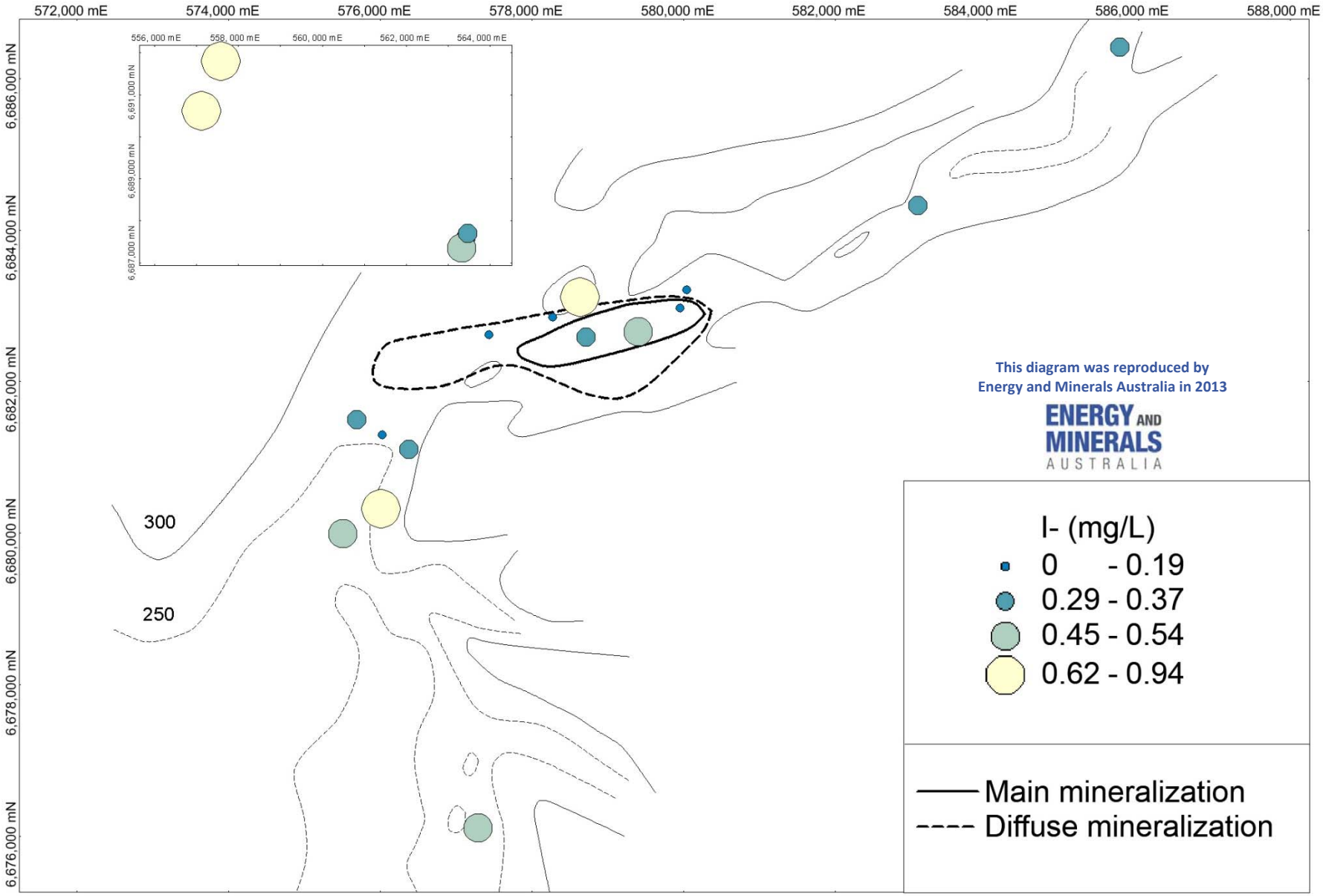

Figure A5.74: Mulga Rock – Au Distribution

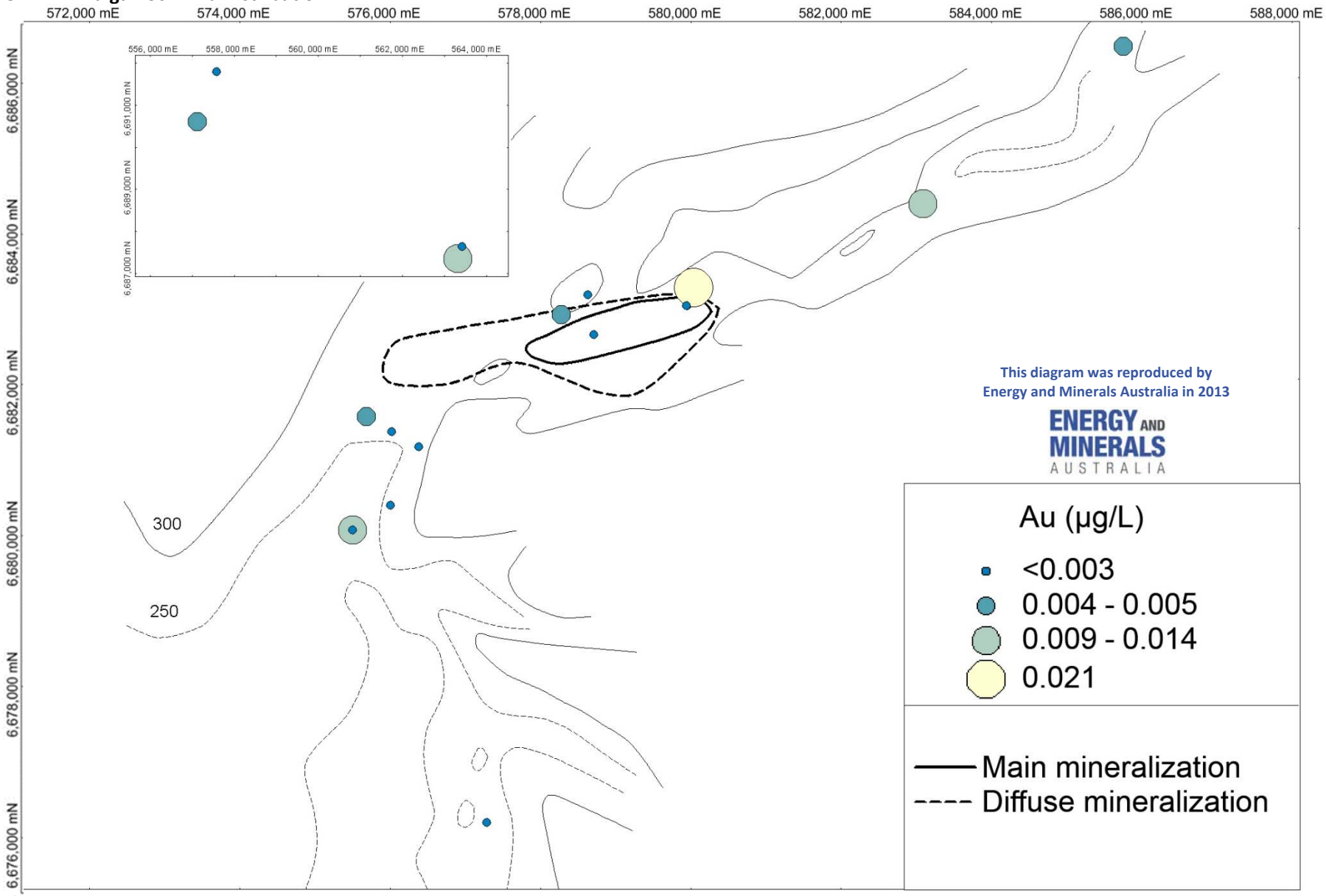

Figure A5.75: Mulga Rock – Cs Distribution

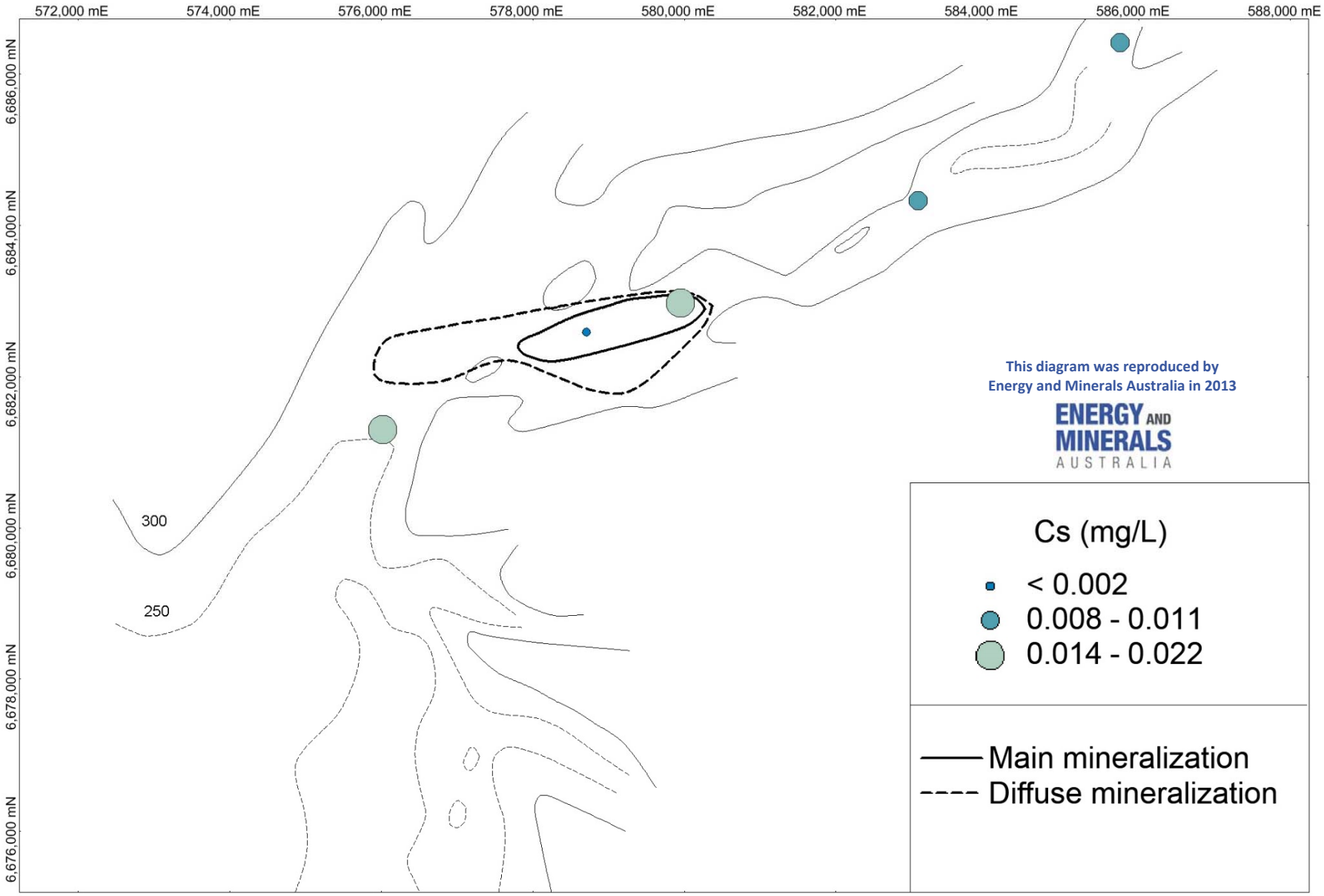

Figure A5.76: Mulga Rock – Th Distribution

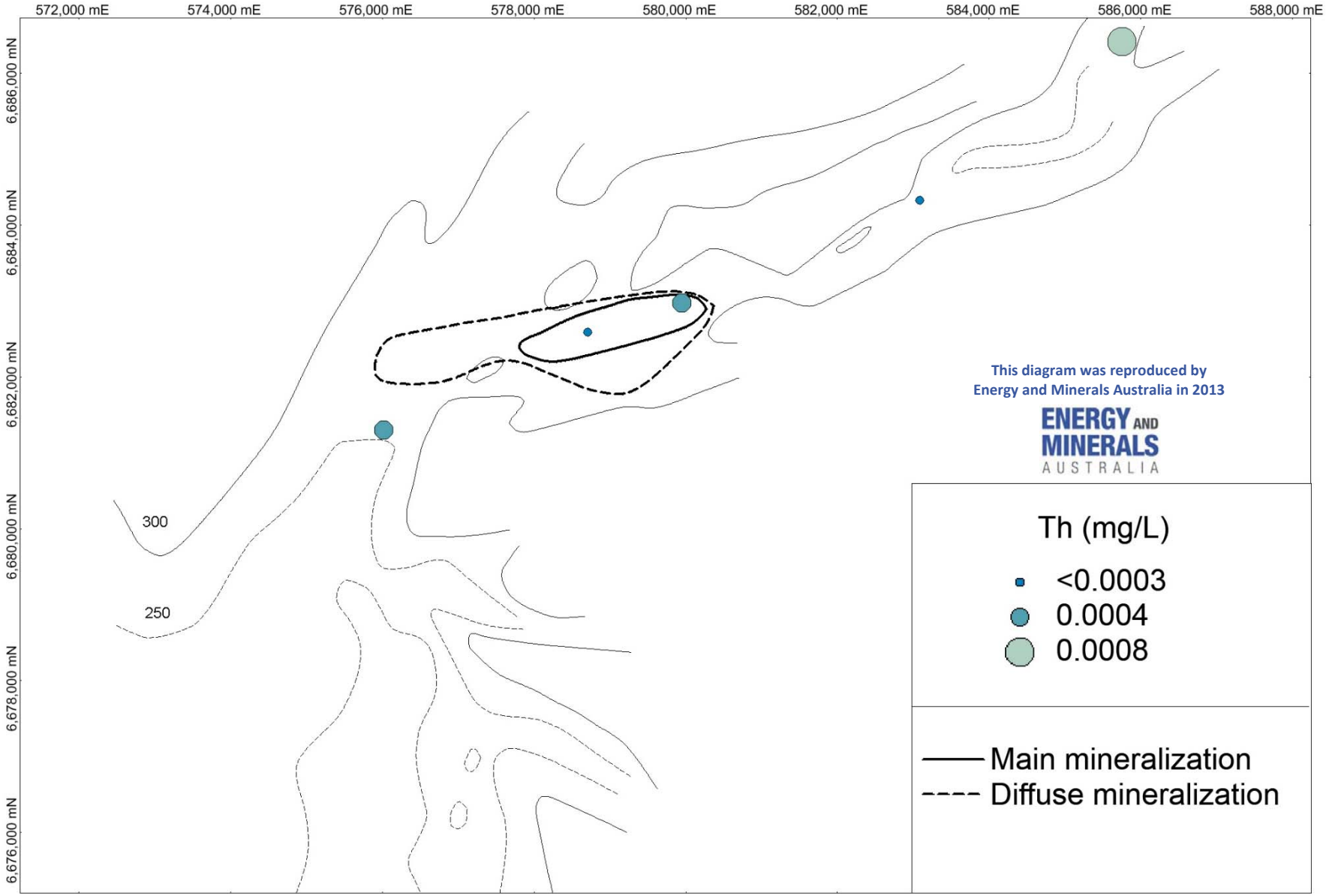

Figure A5.77: Mulga Rock – U Distribution

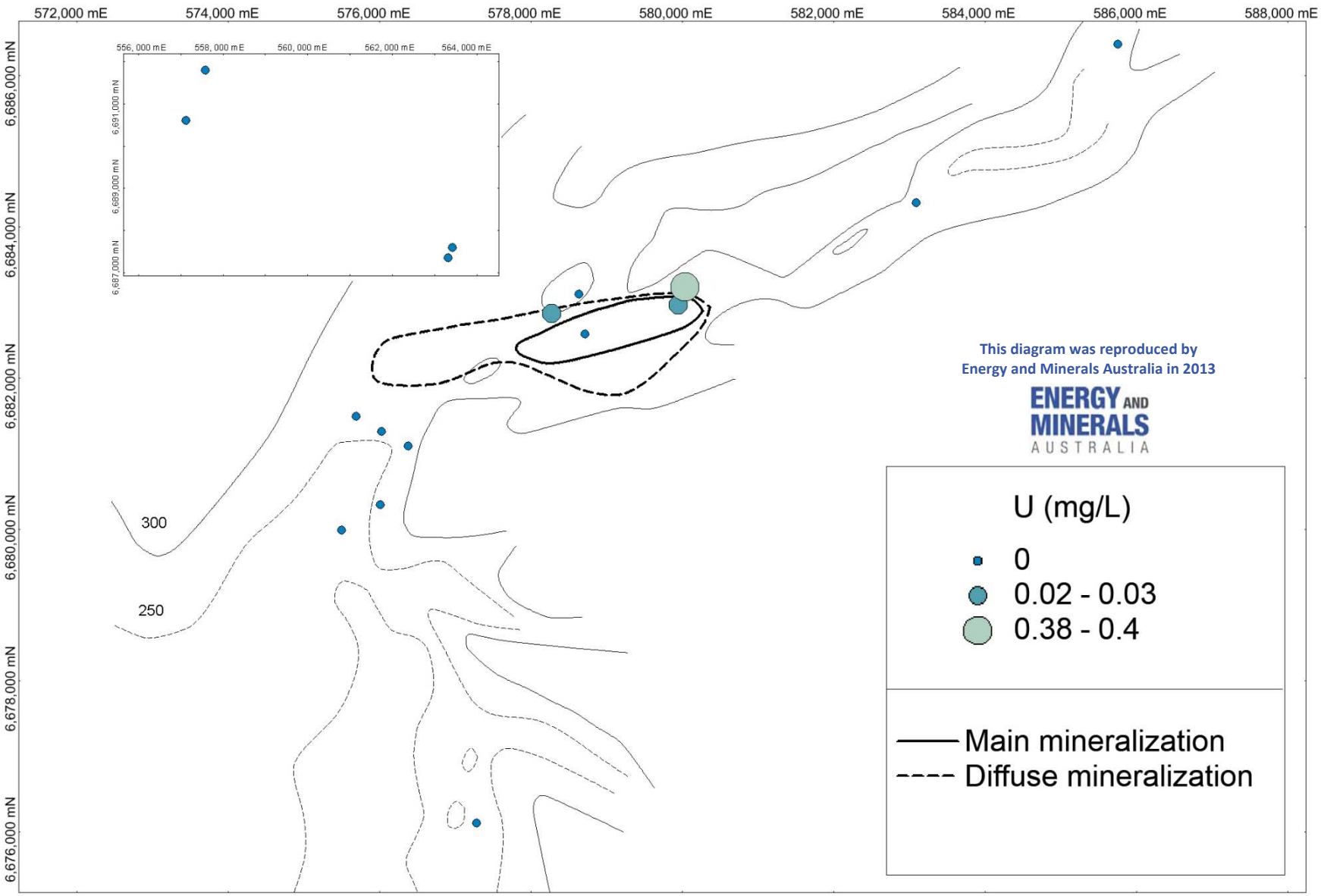

Figure A5.78: Mulga Rock – W Distribution

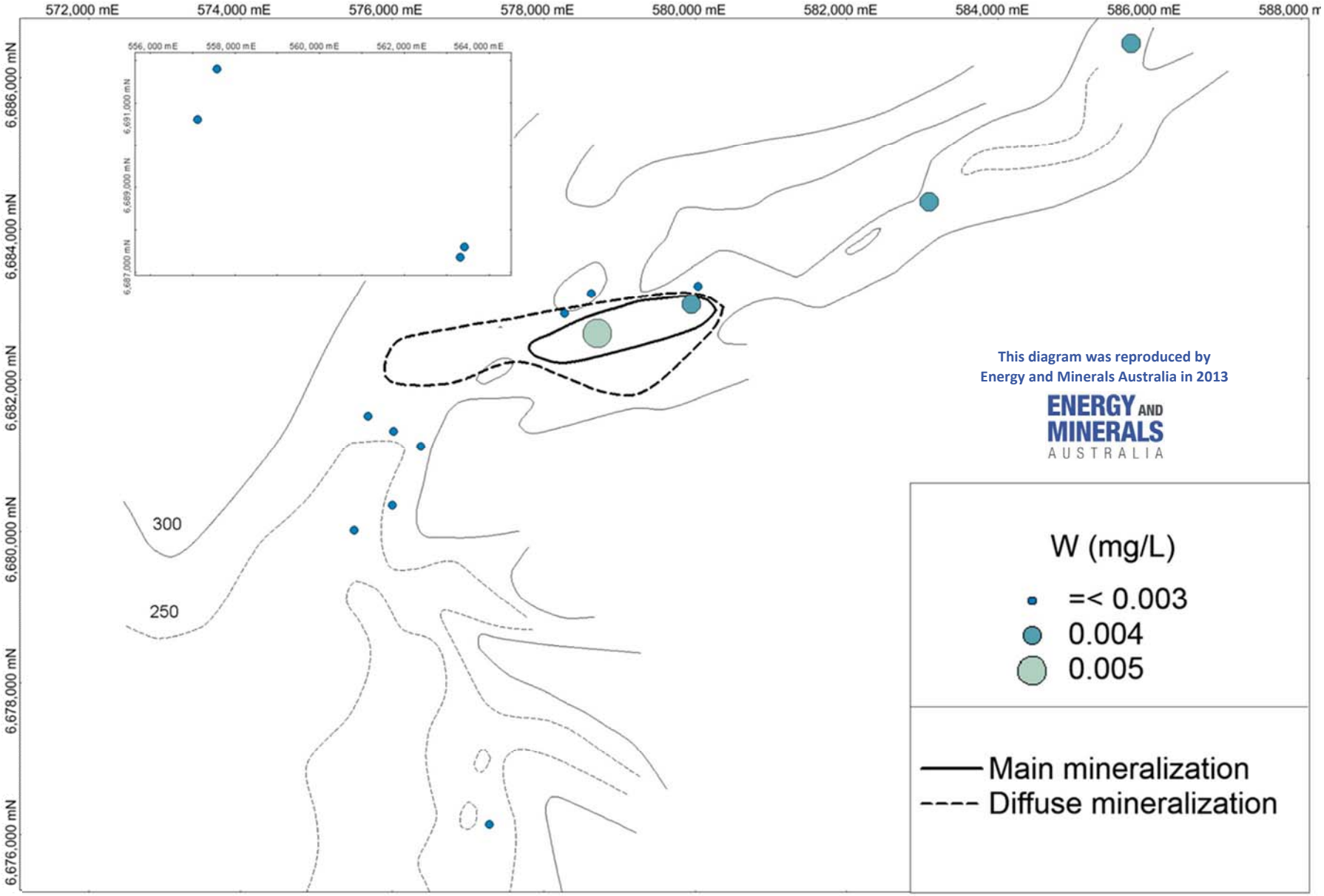

APPENDIX 6

ORGANIC MATTER CHARACTERIZATION

Figure A6.1 **^{13}C NMR spectrum and integrated intensities for sample 00-6028**

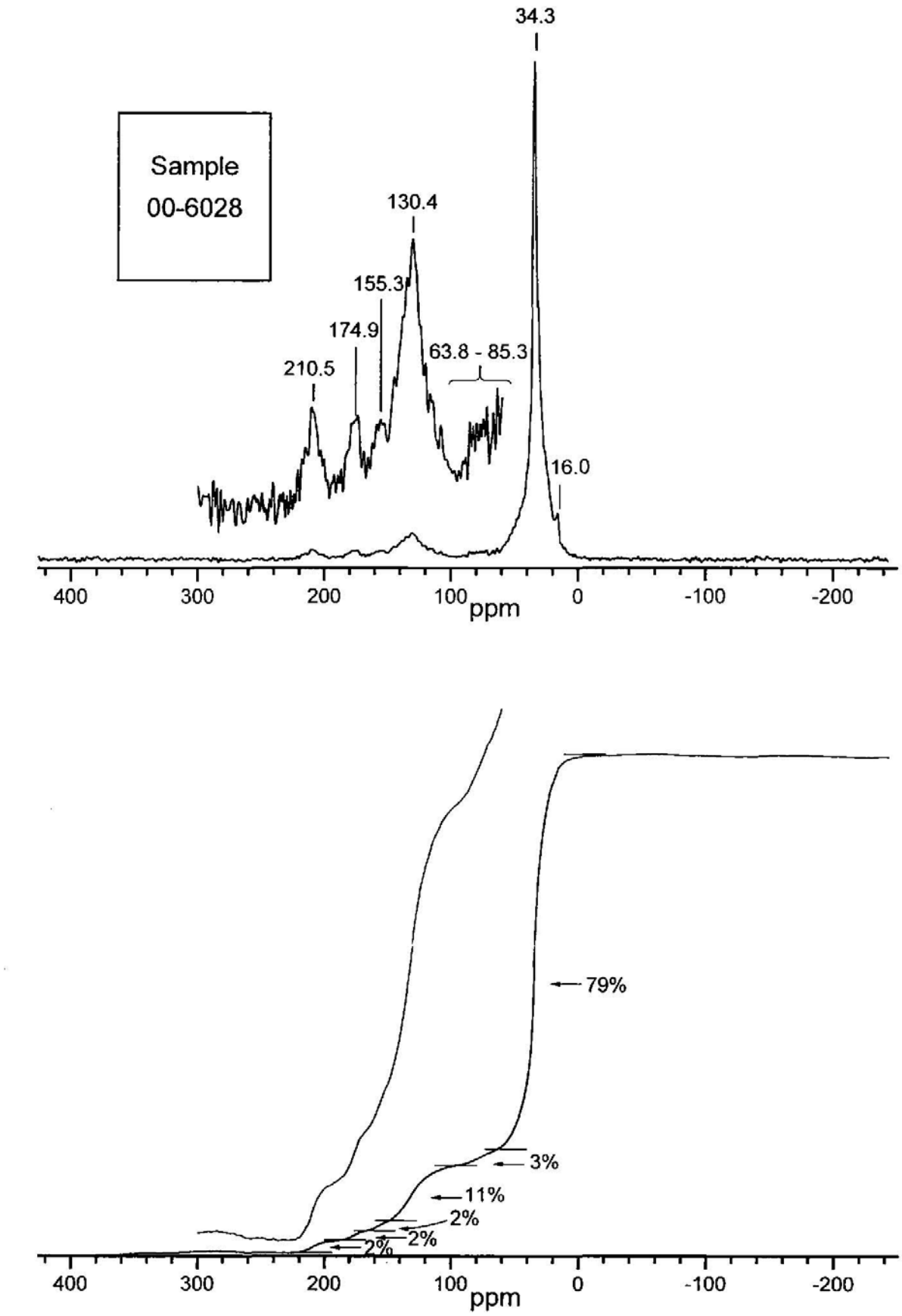

Figure A6.2 **^{13}C NMR spectrum and integrated intensities for sample 00-6029**

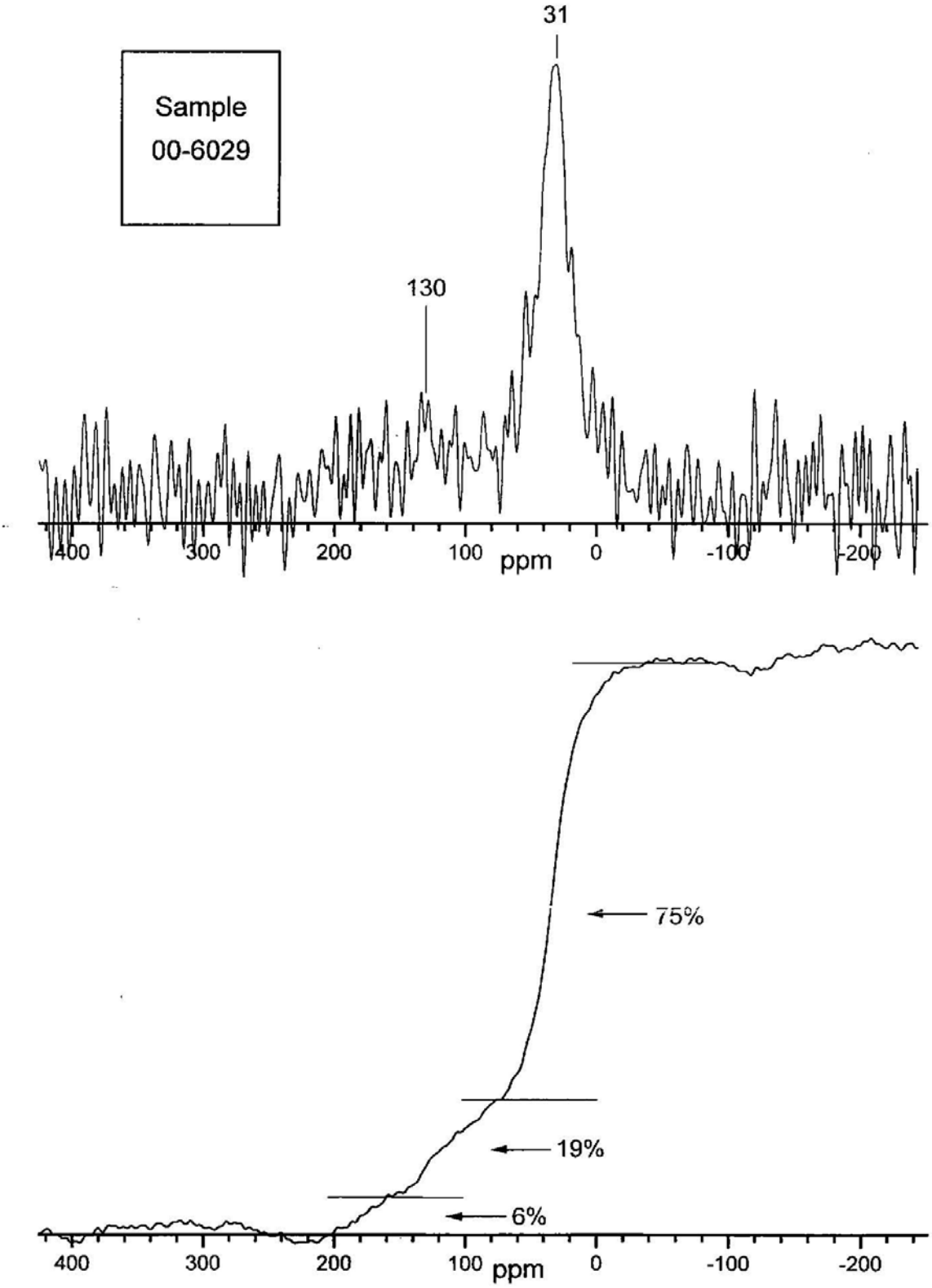

Figure A6.3 ^{13}C NMR spectrum and integrated intensities for sample 00-6030

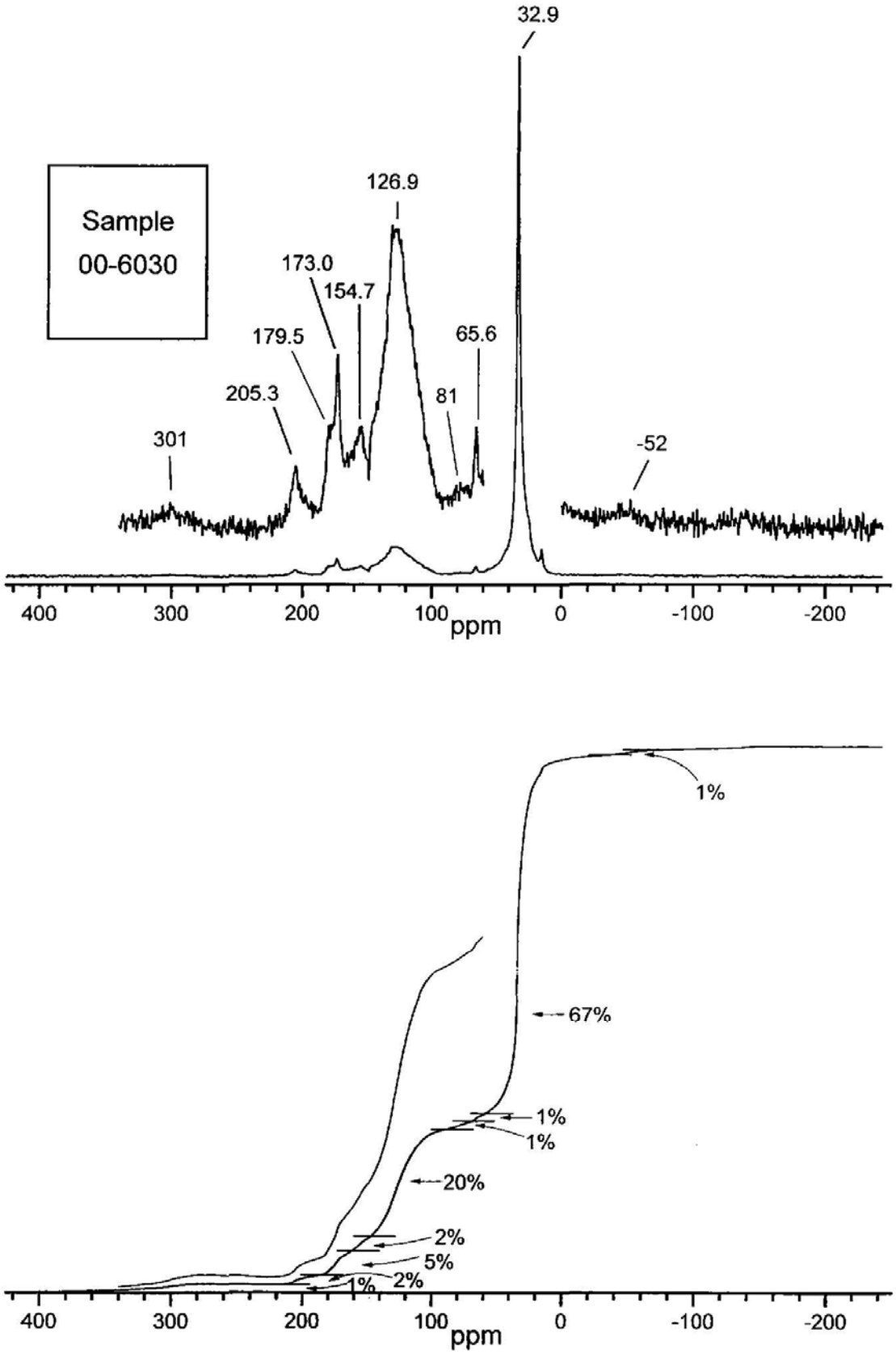

Figure A6.4 ^{13}C NMR spectrum and integrated intensities for sample 00-6031

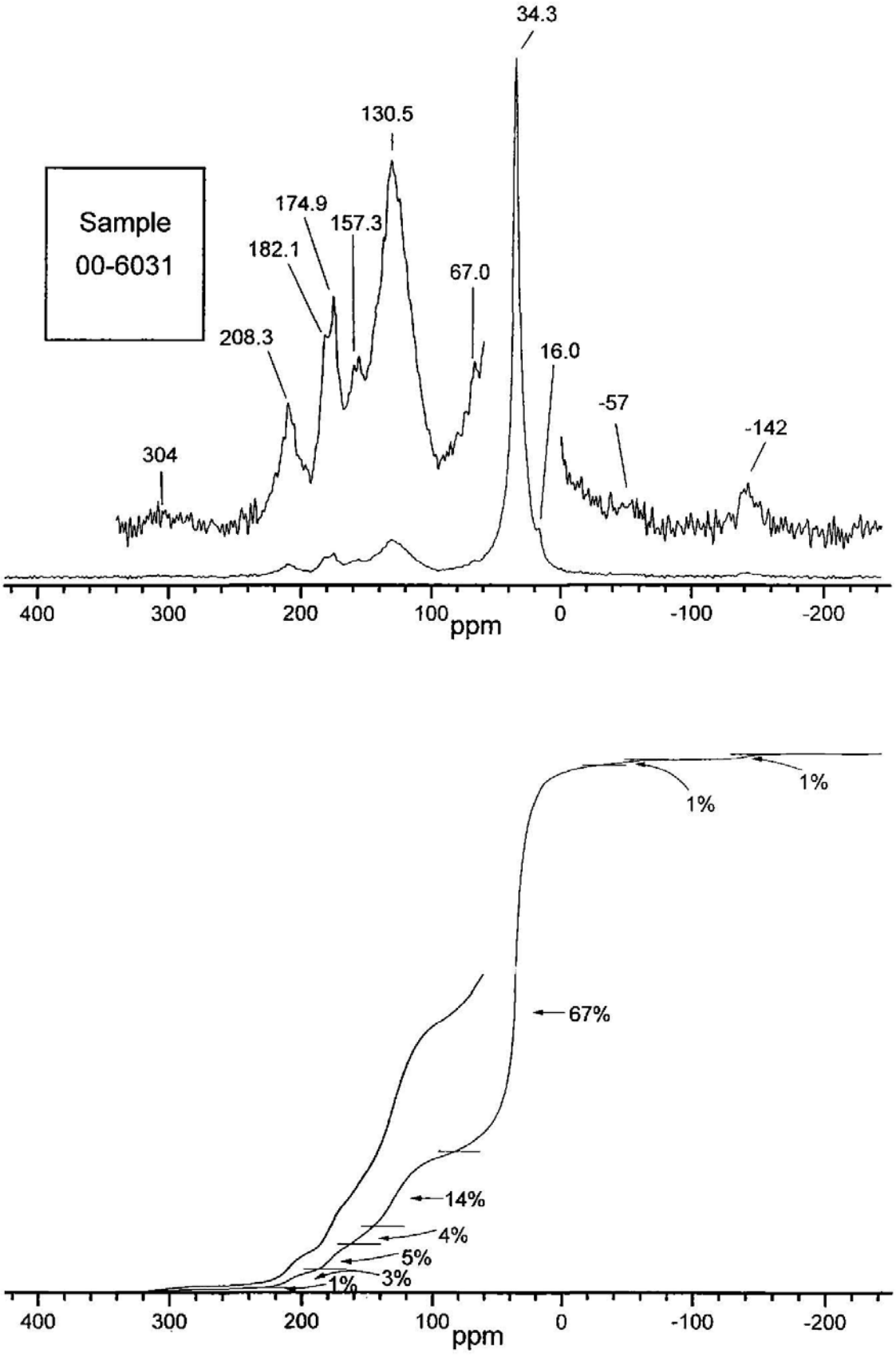

Figure A6.5 **^{13}C NMR spectrum and integrated intensities for sample 00-6034**

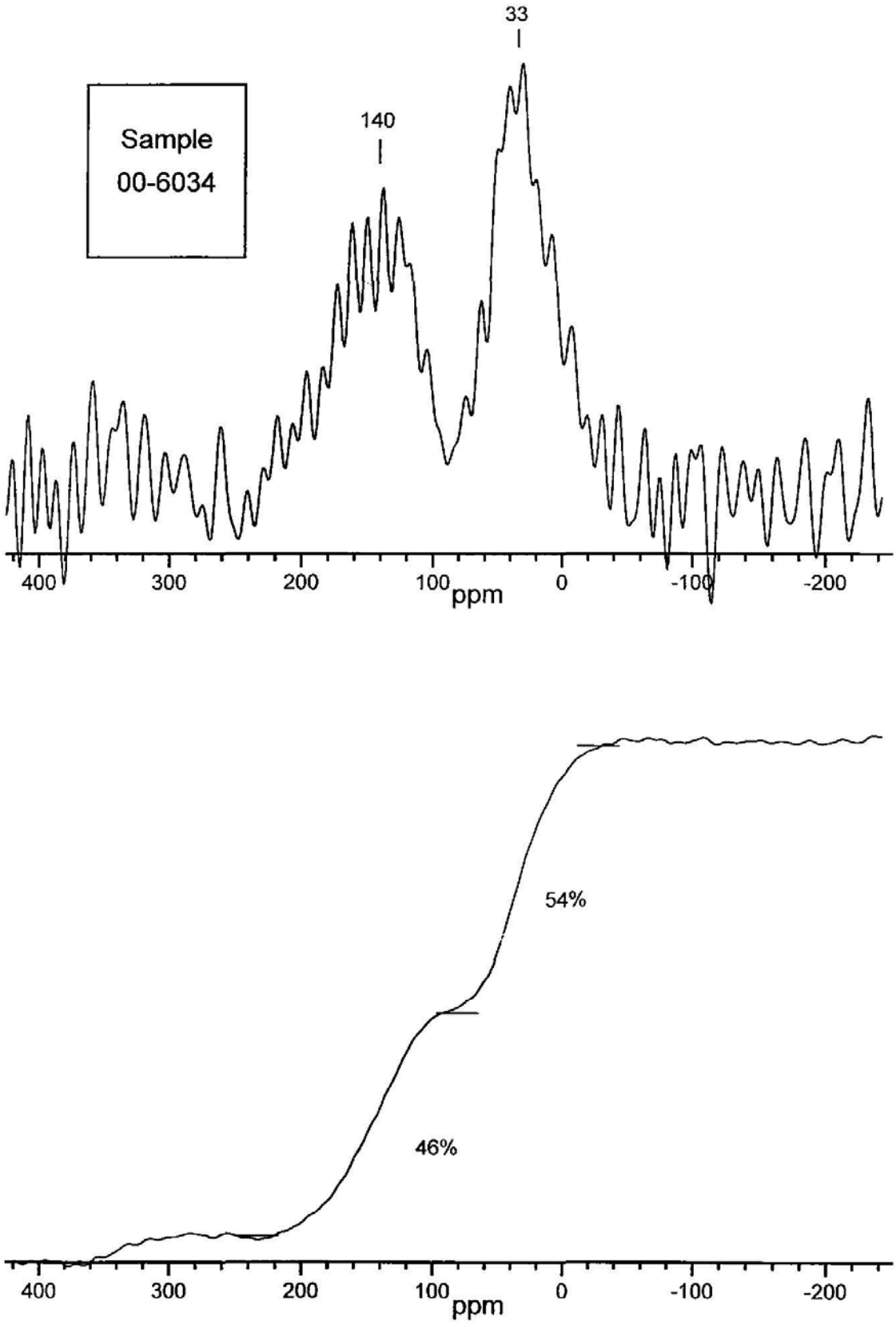

Figure A6.6 **^{13}C NMR spectrum and integrated intensities for sample 00-6035**

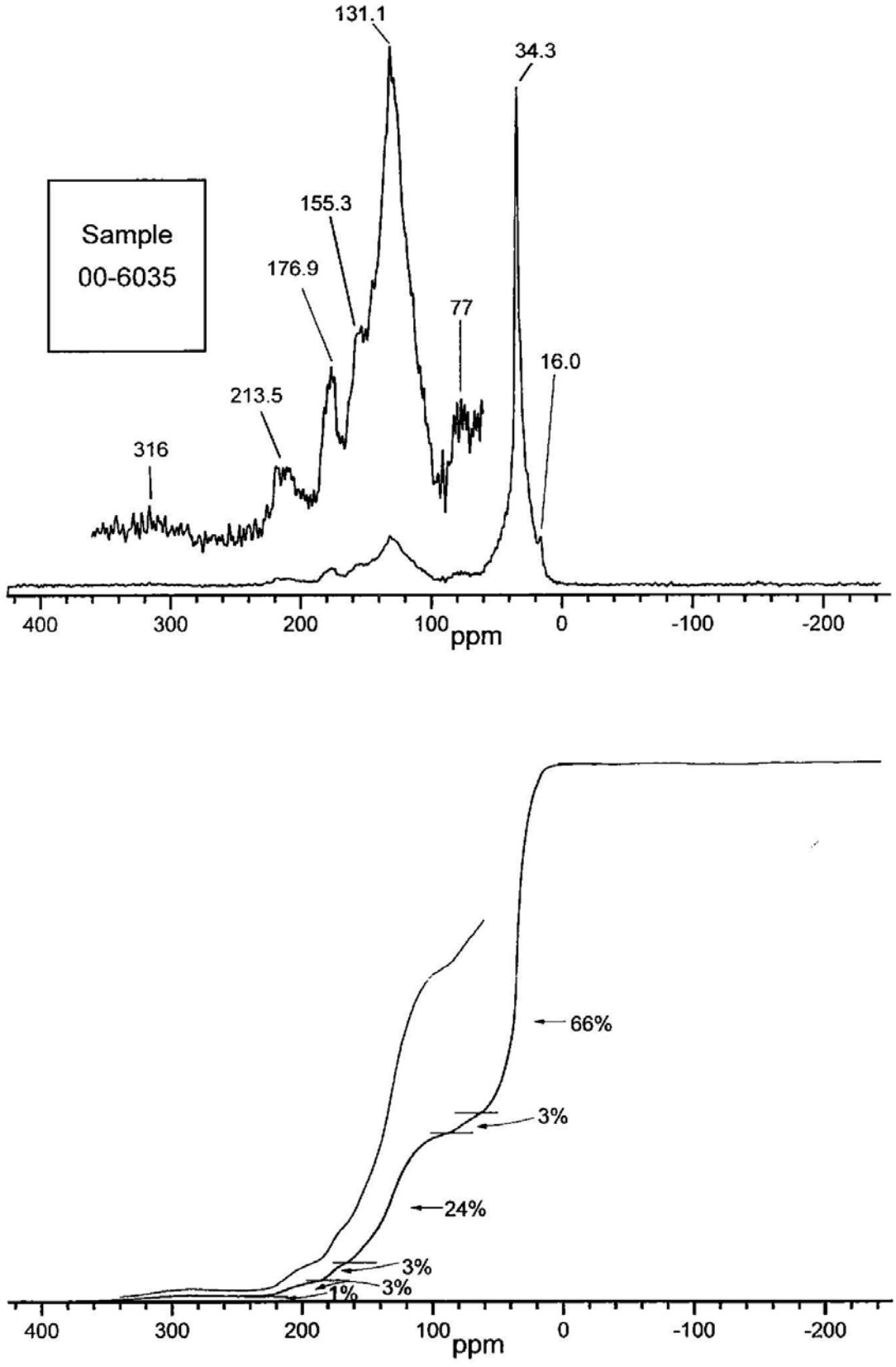

Figure A6.7 **^{13}C NMR spectrum and integrated intensities for sample 00-6037**

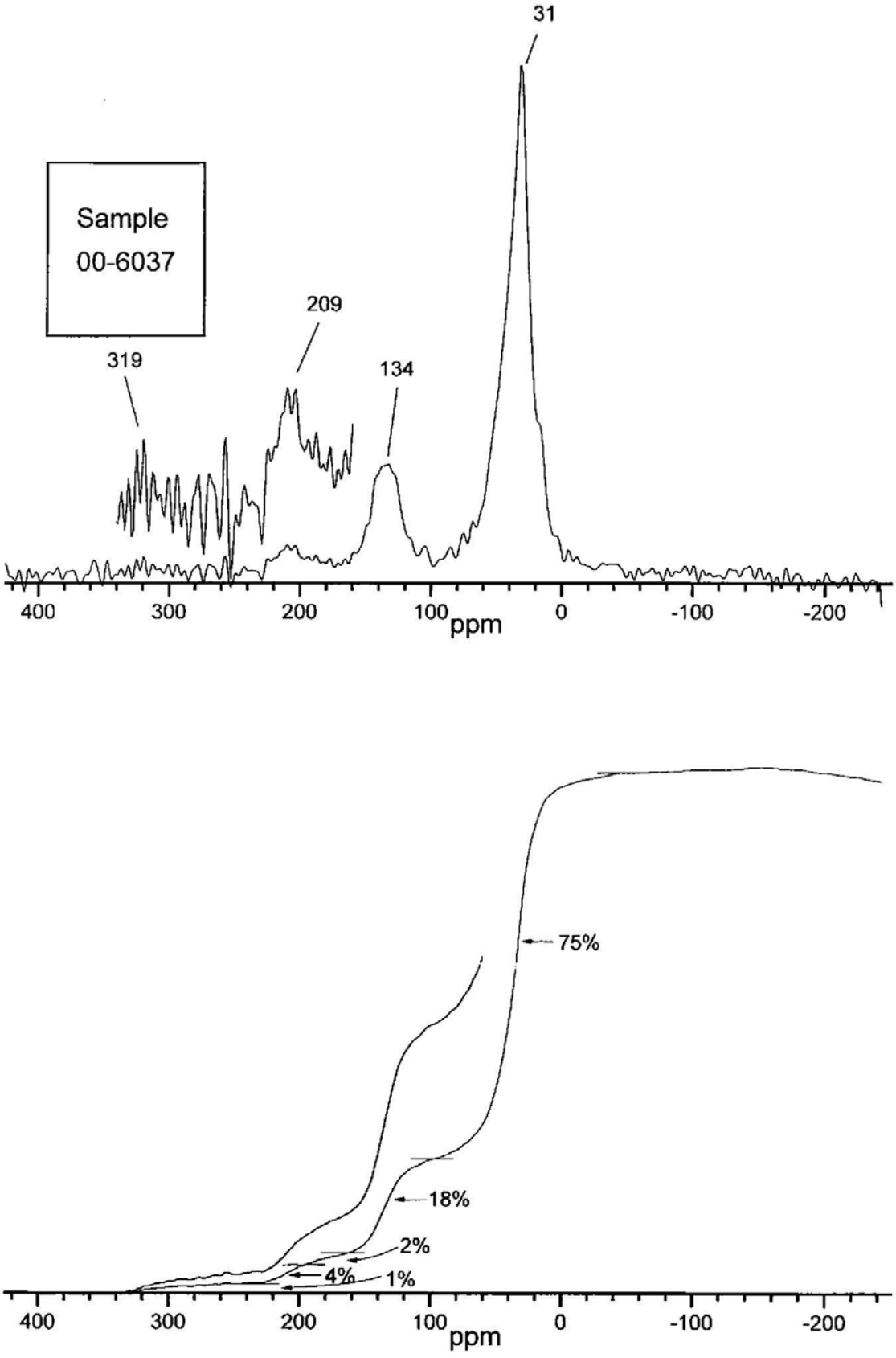

Figure A6.8 **^{13}C NMR spectrum and integrated intensities for sample 00-6039**

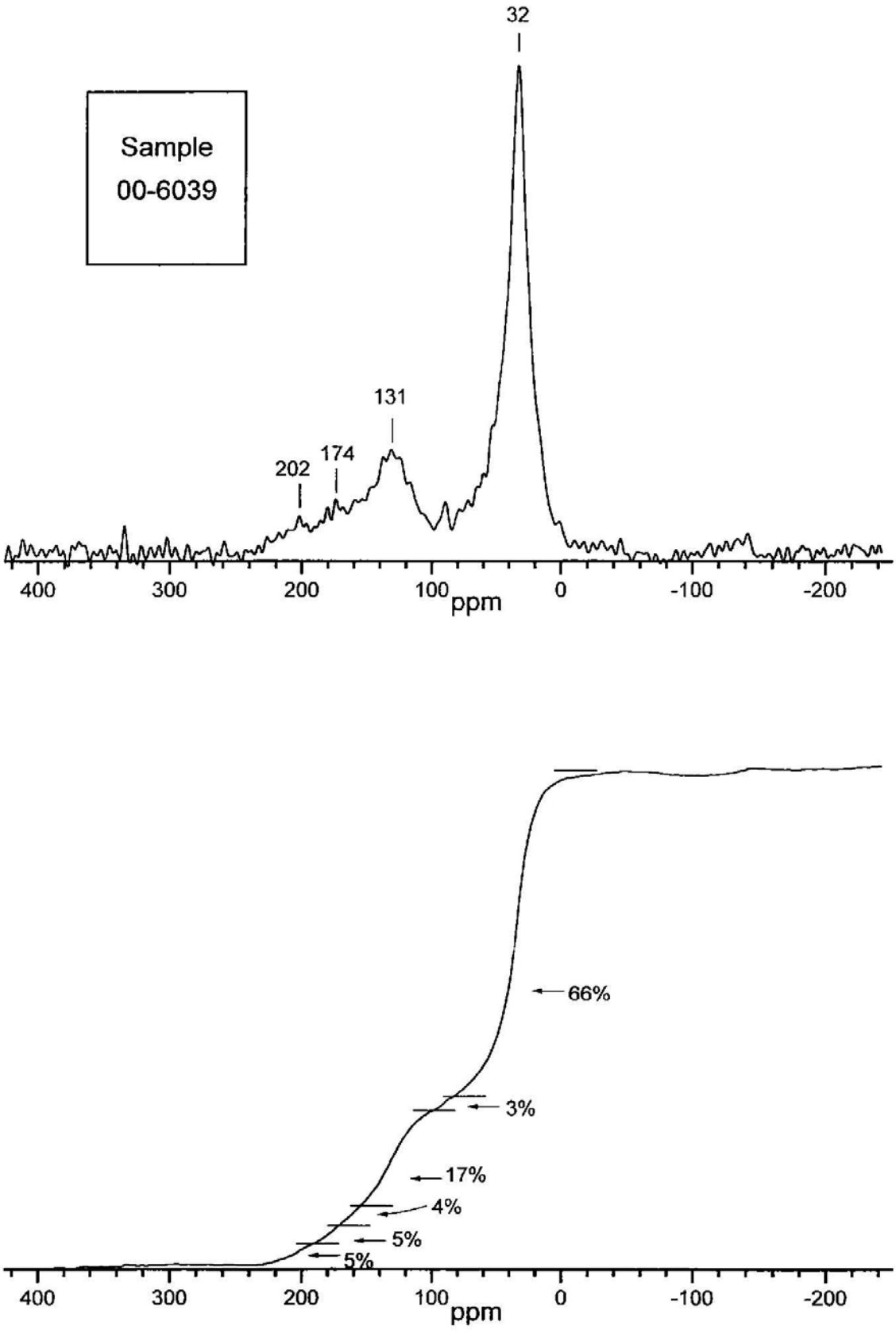

Figure A6.9 **^{13}C NMR spectrum and integrated intensities for sample 00-6040**

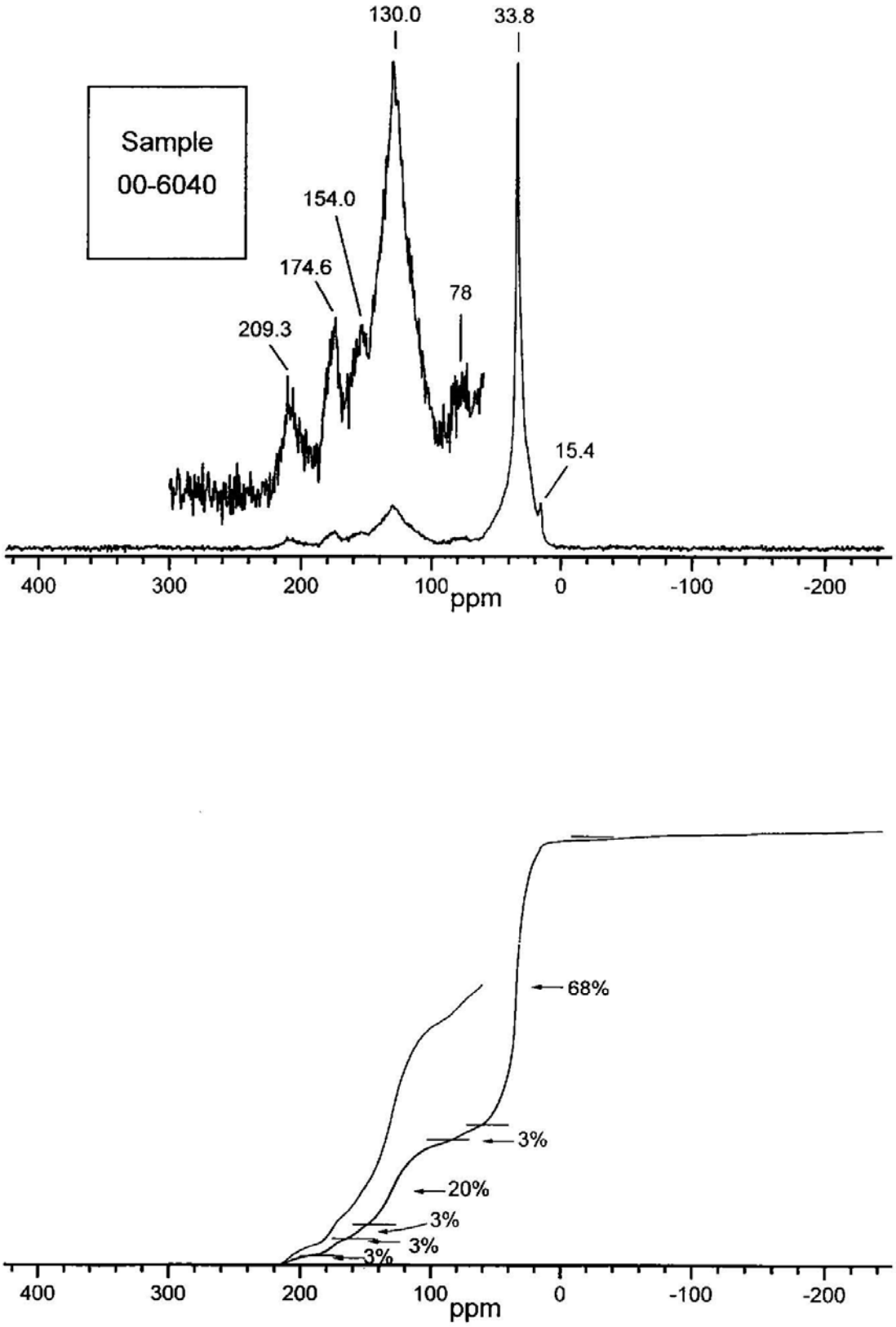

Figure A6.10 ^{13}C NMR spectrum and integrated intensities for sample 00-6054

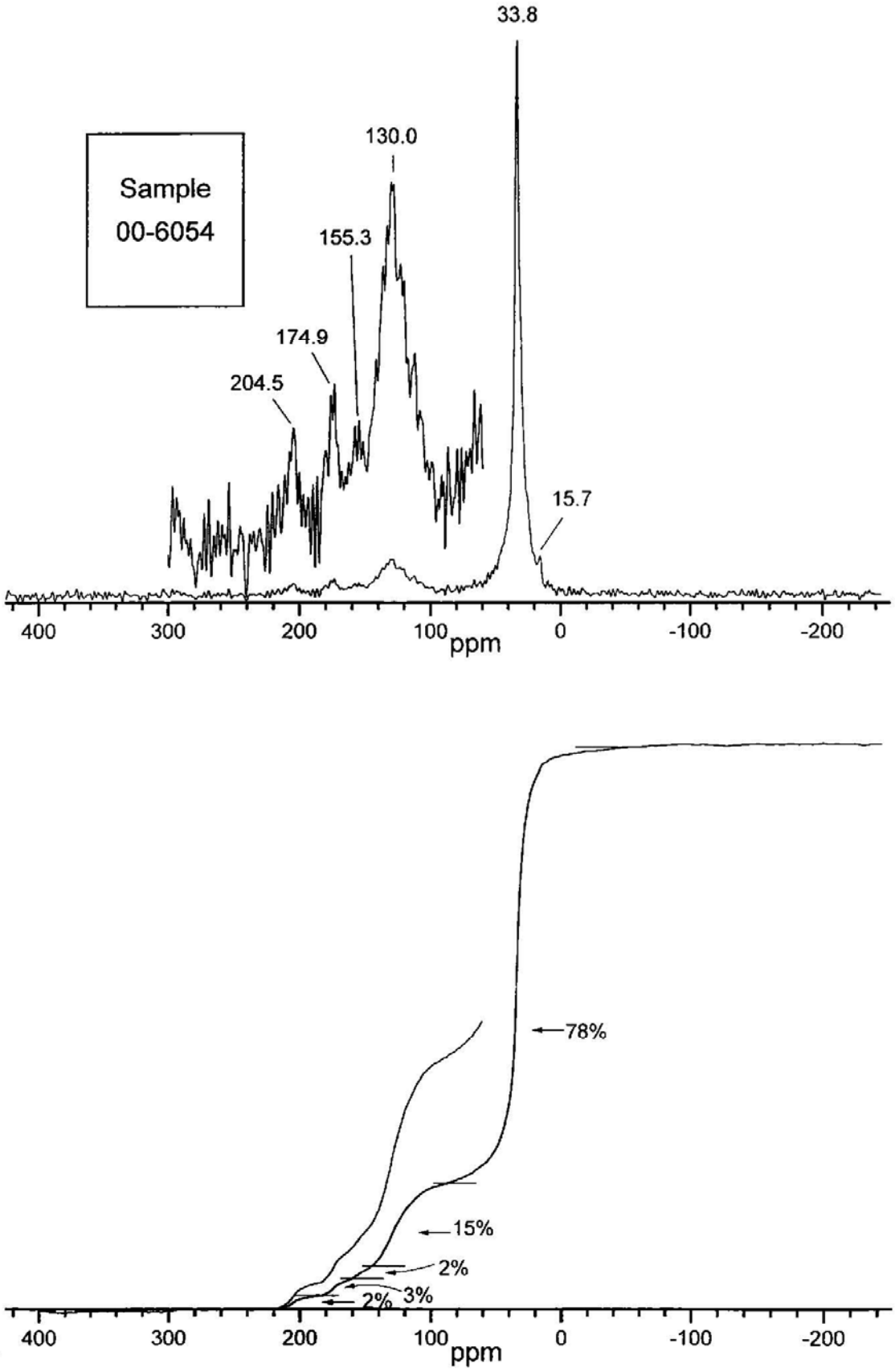

Figure A6.11 ^{13}C NMR spectrum and integrated intensities for sample 00-6056

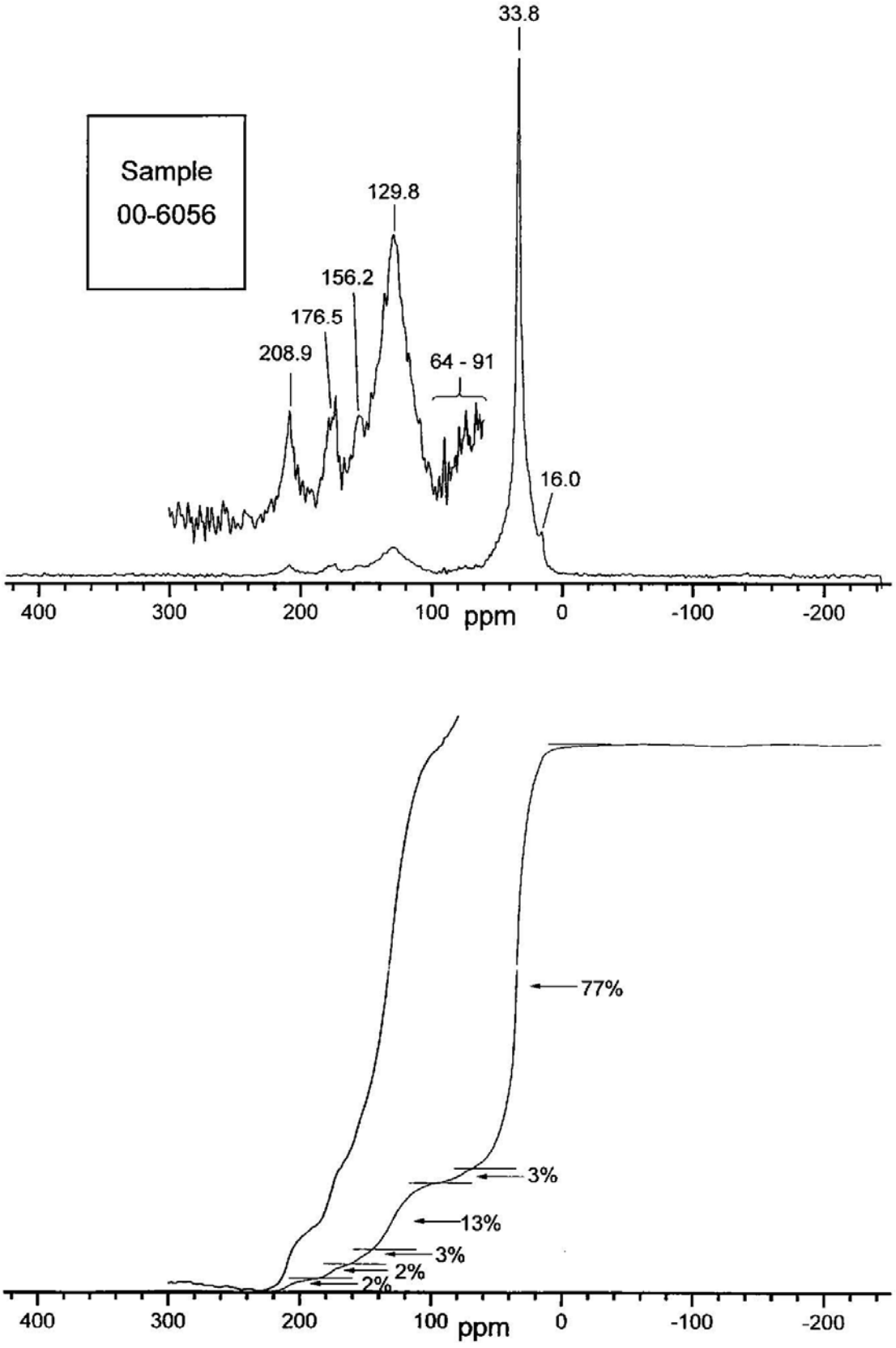

Figure A6.12 **^{13}C NMR spectrum and integrated intensities for sample 00-6058**

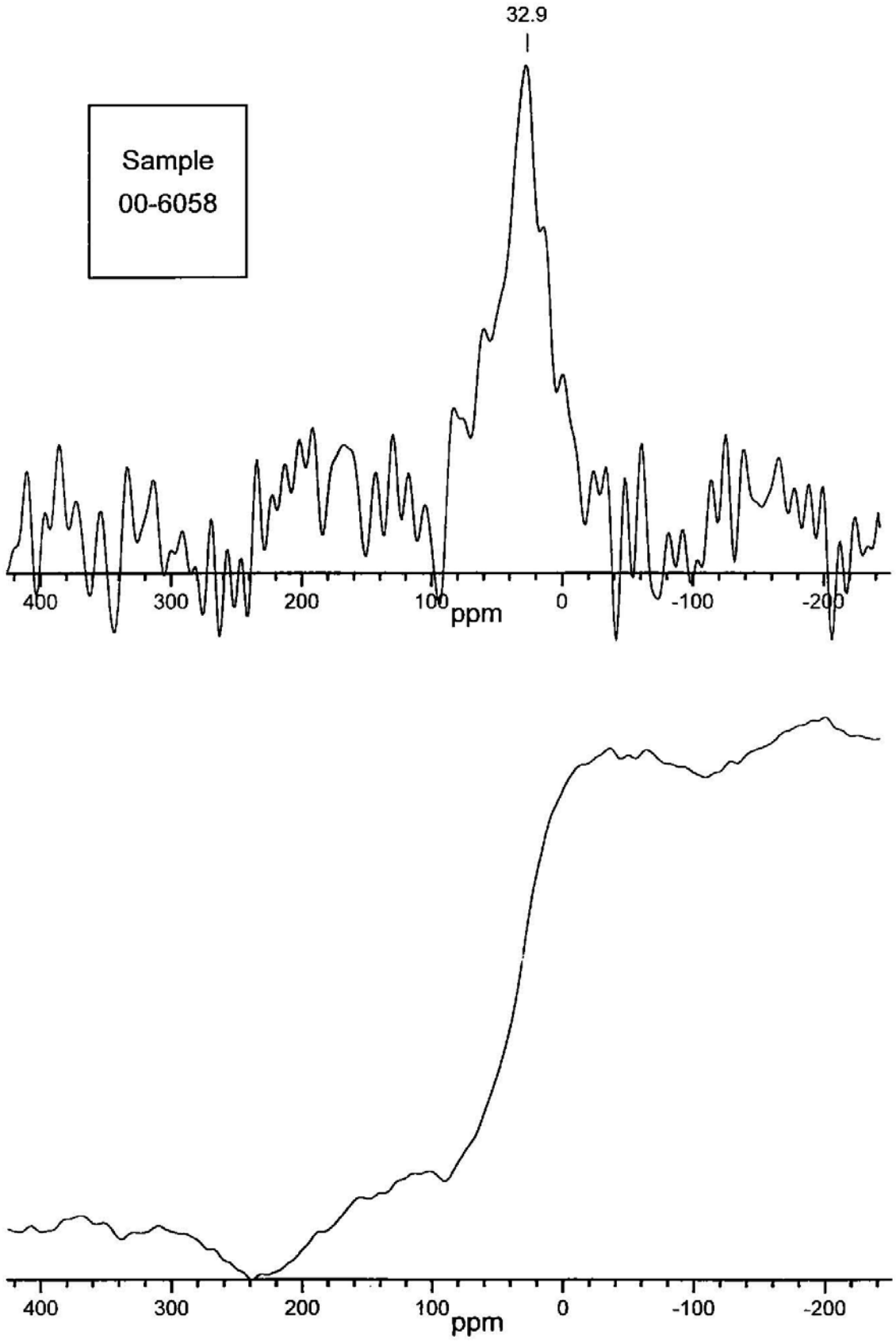

Figure A6.13 ^{13}C NMR spectrum and integrated intensities for sample 00-6059

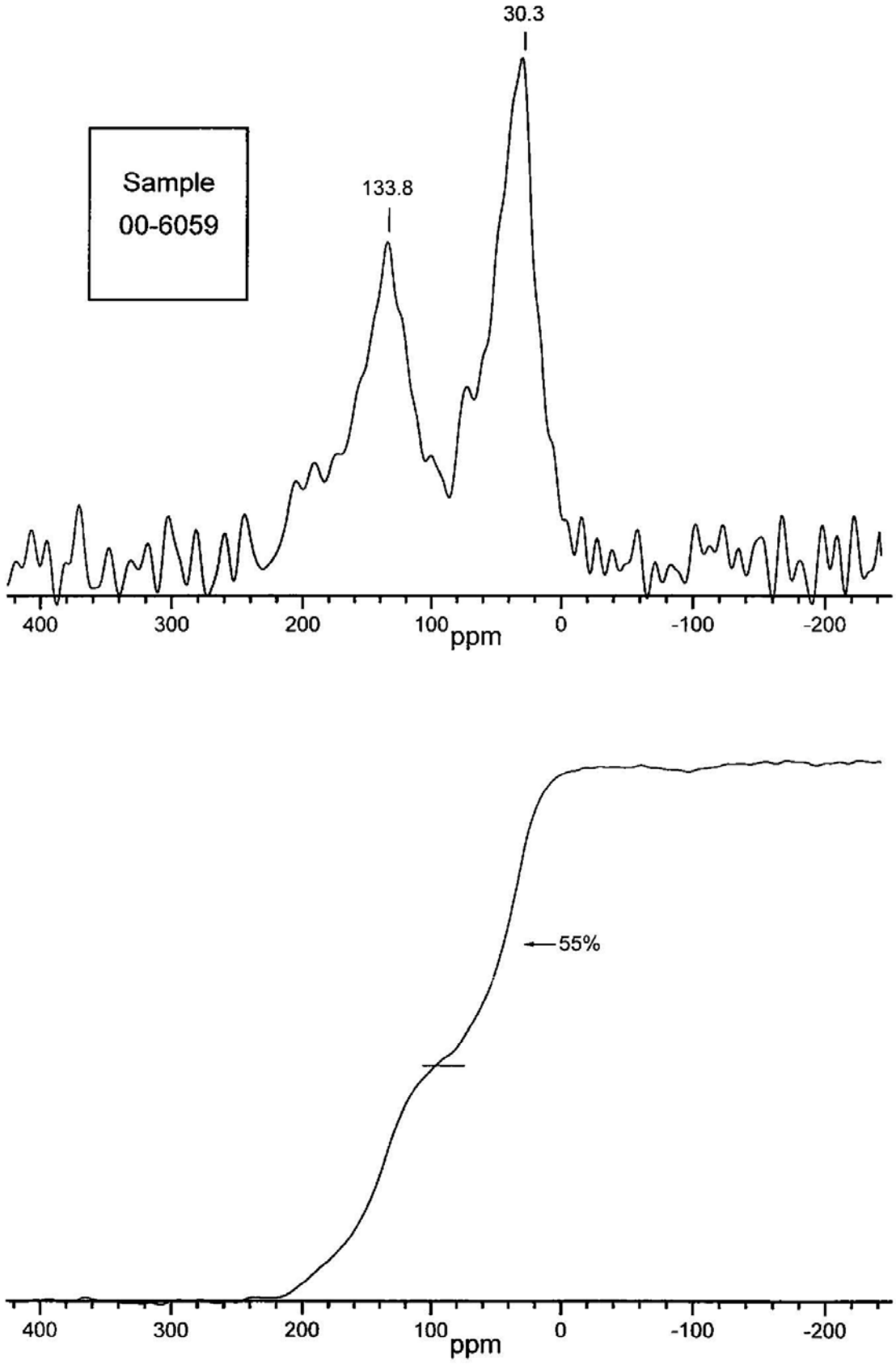

Figure A6.14 ^{13}C NMR spectrum and integrated intensities for sample 00-6061

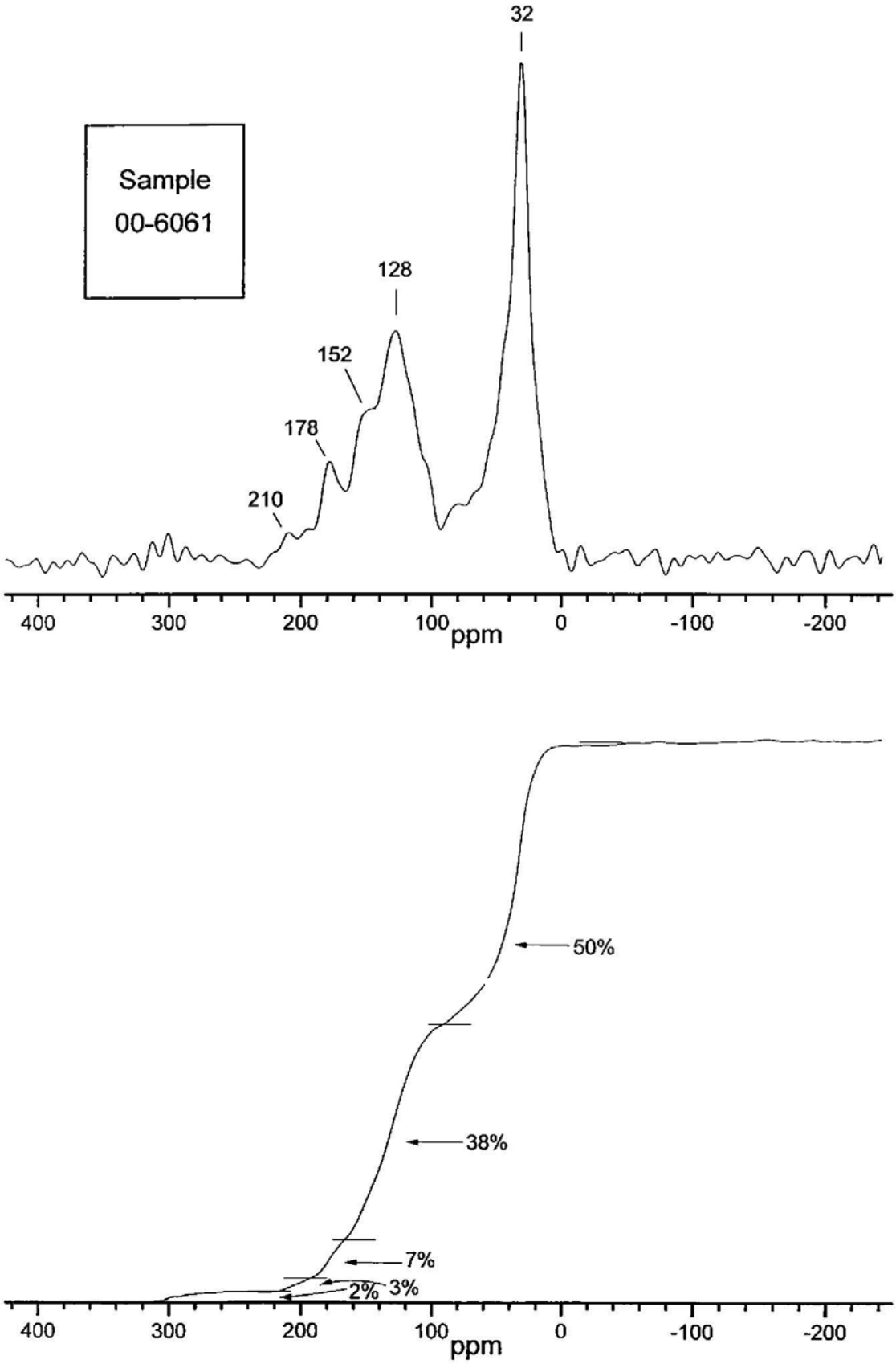

Figure A6.15 **^{13}C NMR spectrum and integrated intensities for sample 00-6062**

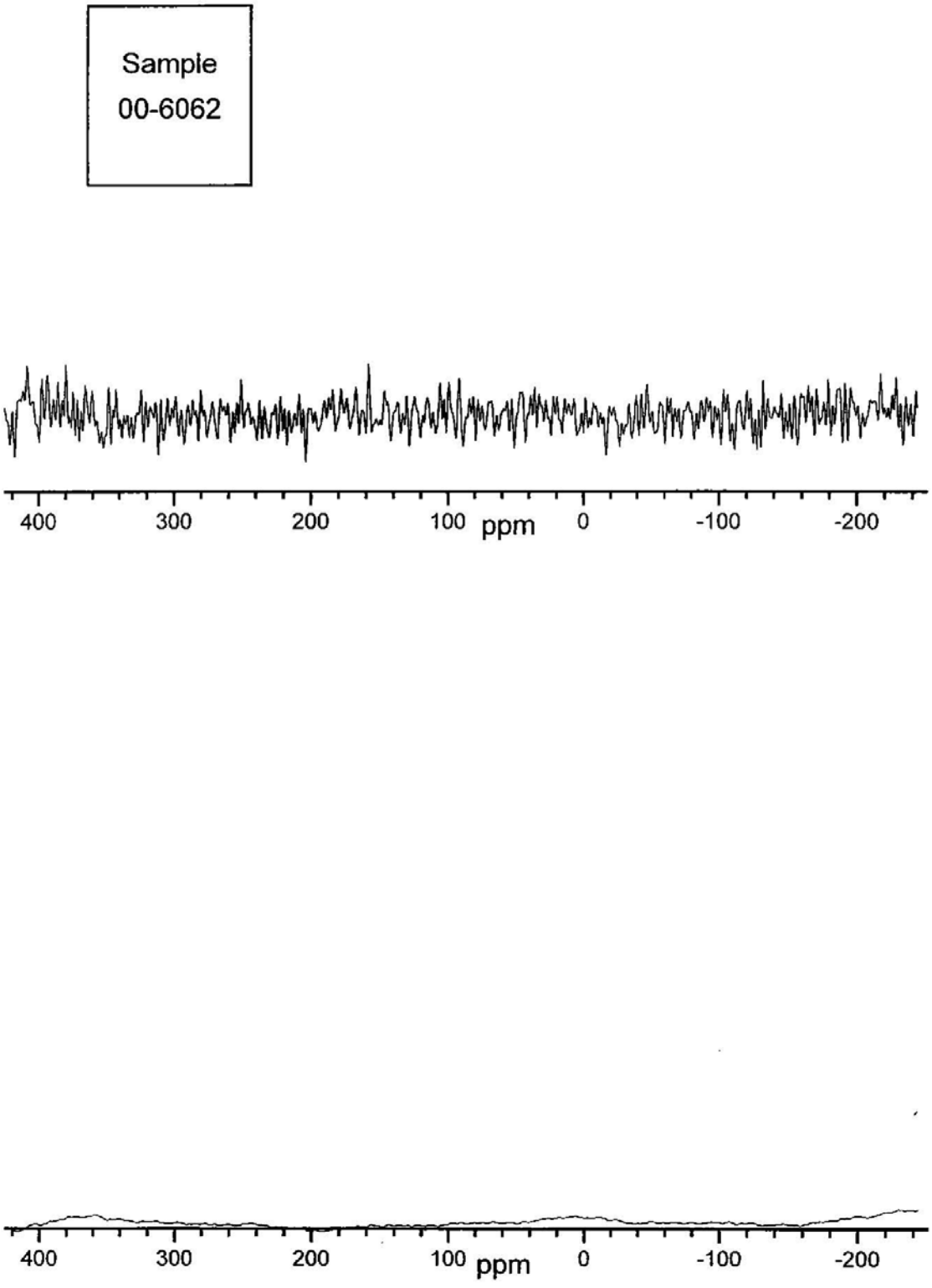

Figure A6.16 ^{13}C NMR spectrum and integrated intensities for sample 00-6063

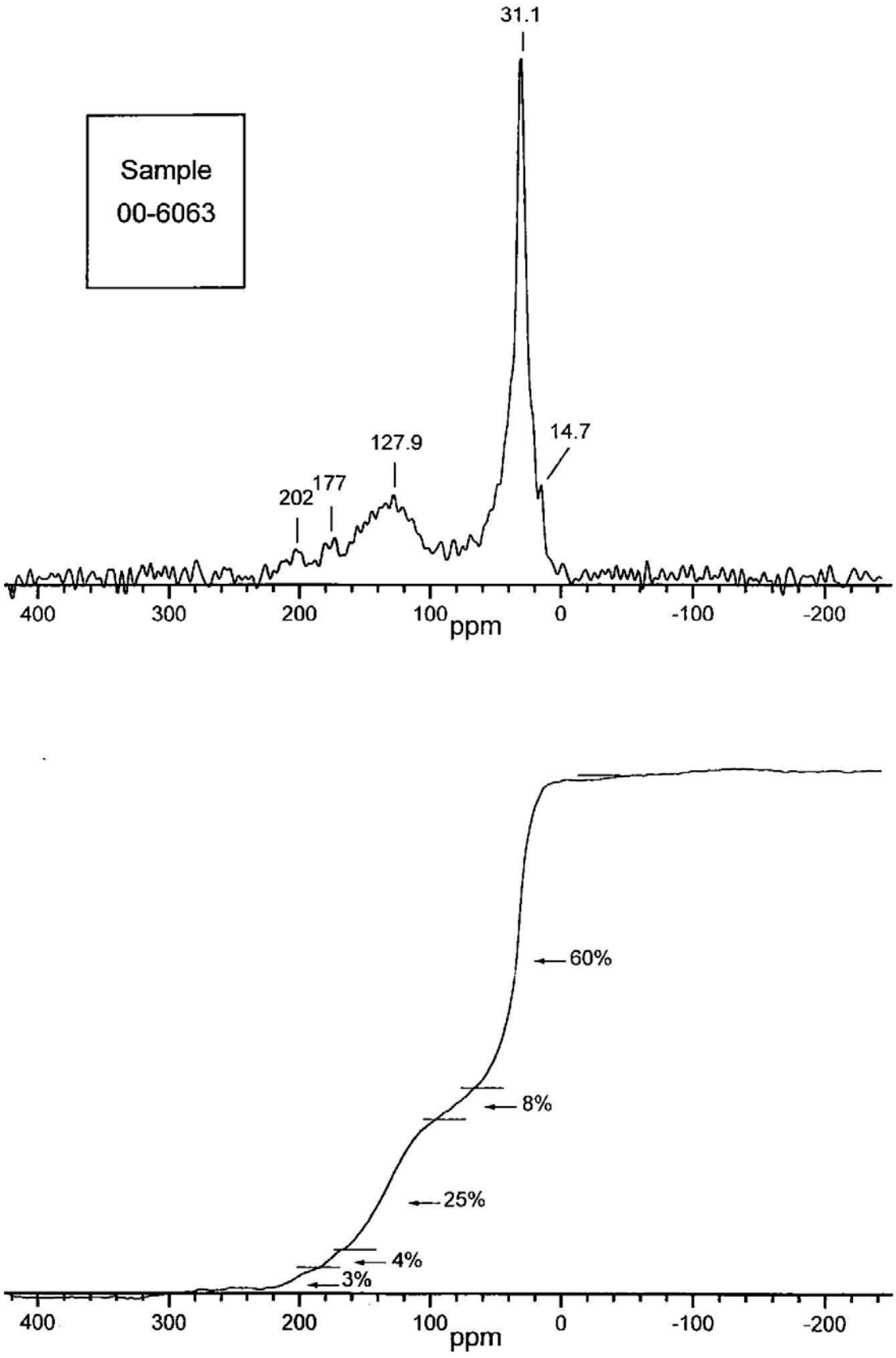

Figure A6.17 ^{13}C NMR spectrum and integrated intensities for sample 00-64

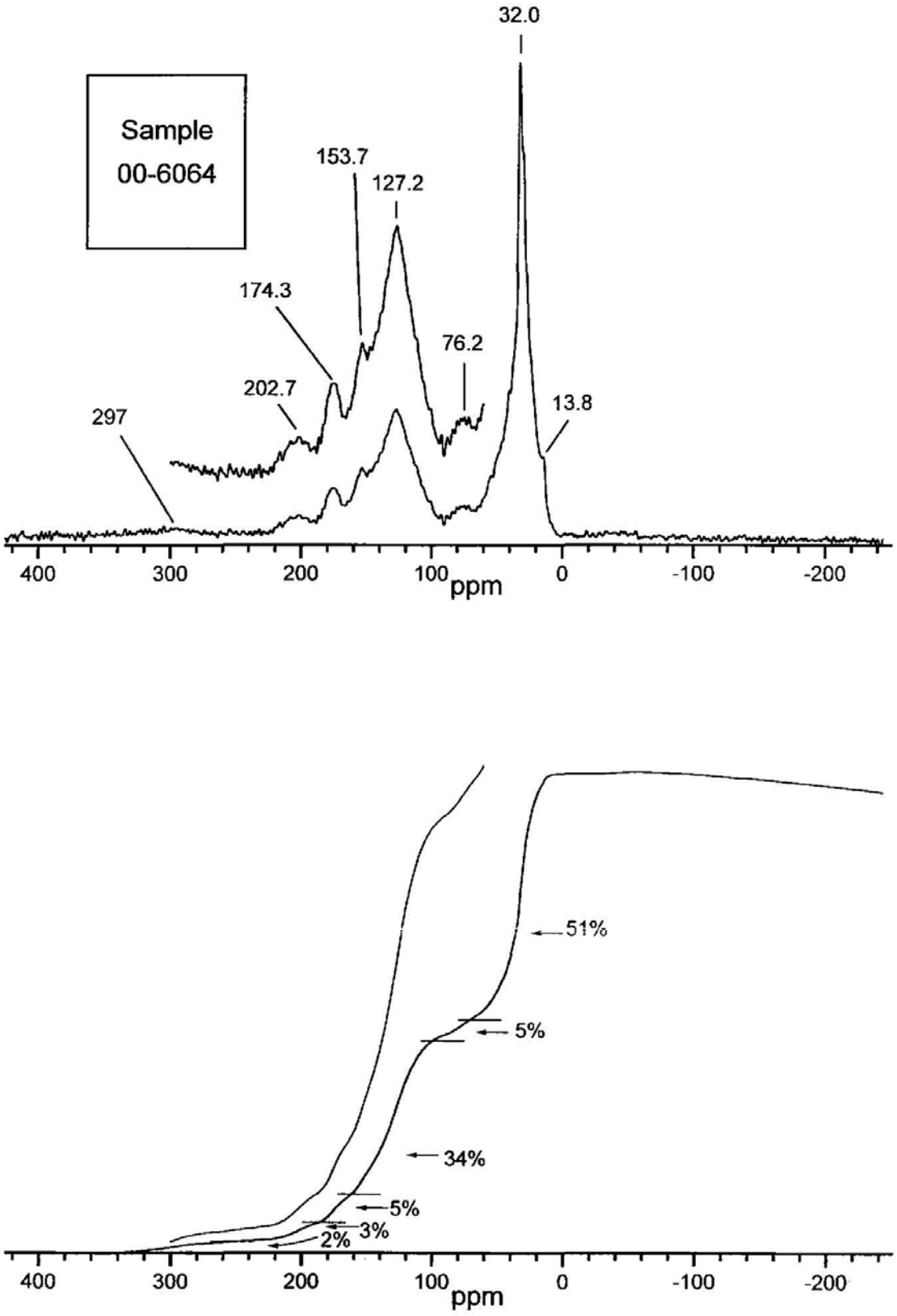

Figure A6.18 ^{13}C NMR spectrum and integrated intensities for sample 00-6070

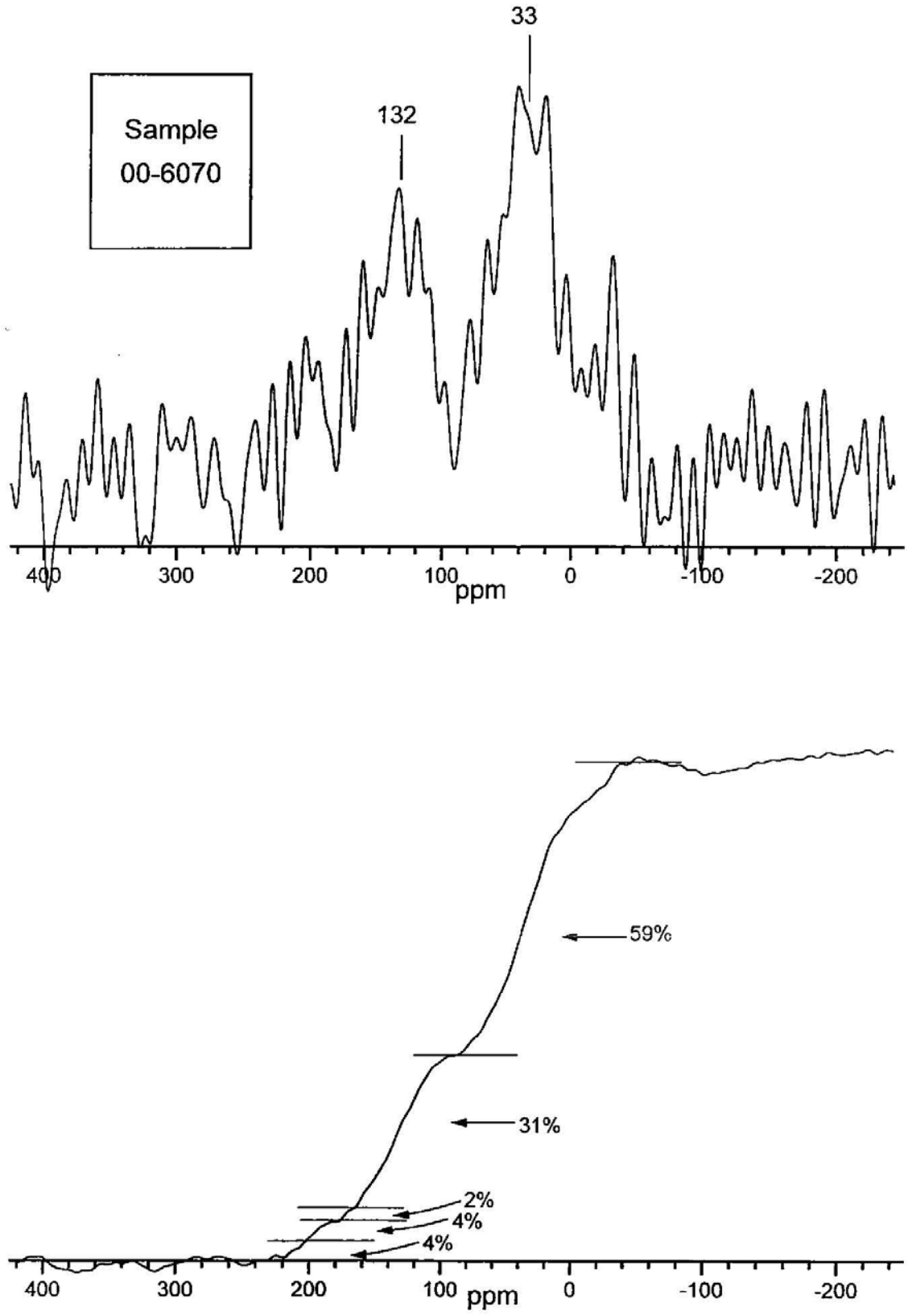

Figure A6.19 ^{13}C NMR spectrum and integrated intensities for sample 00-6071

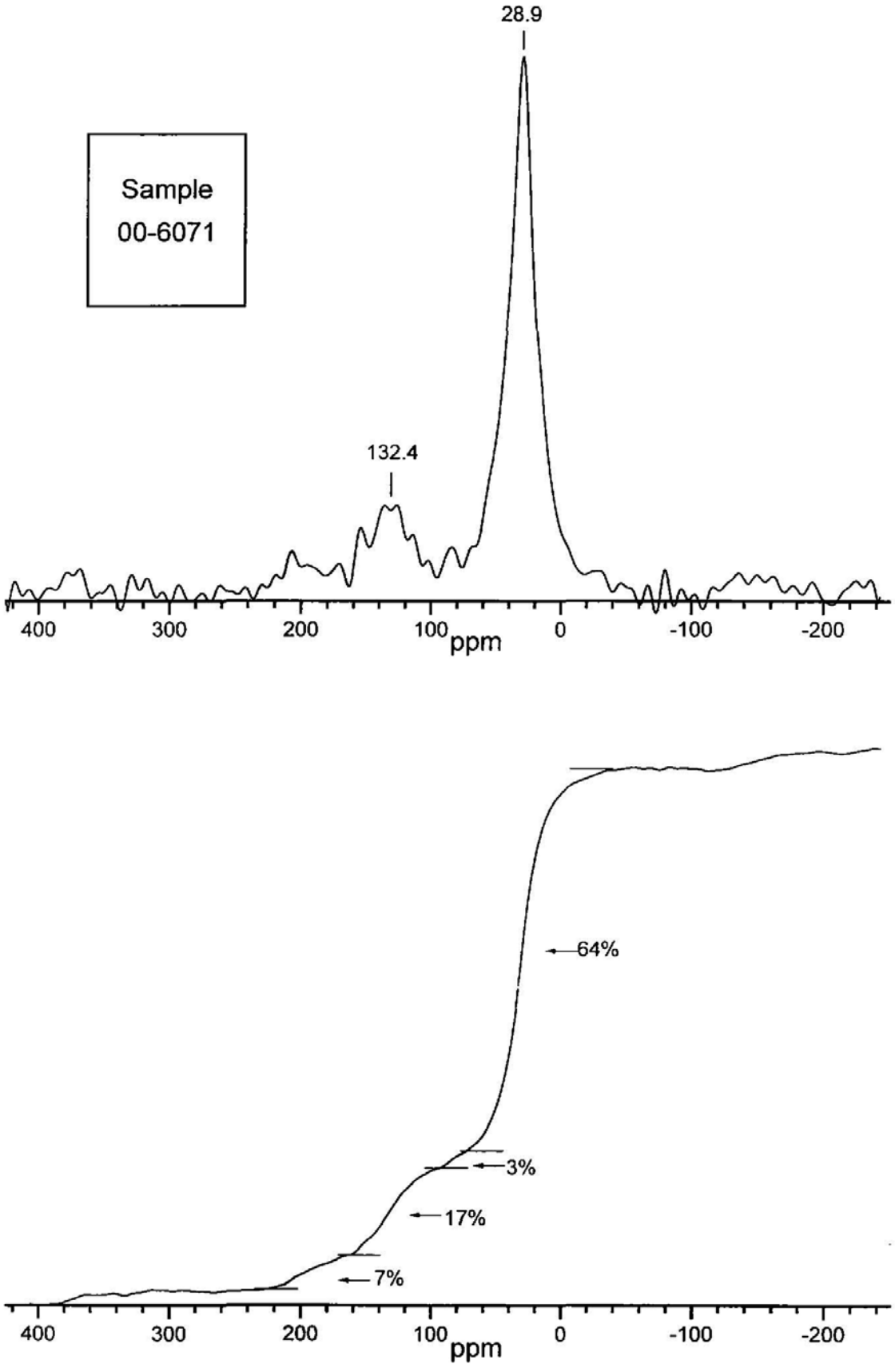

Figure A6.20 ^{13}C NMR spectrum and integrated intensities for sample 00-6072

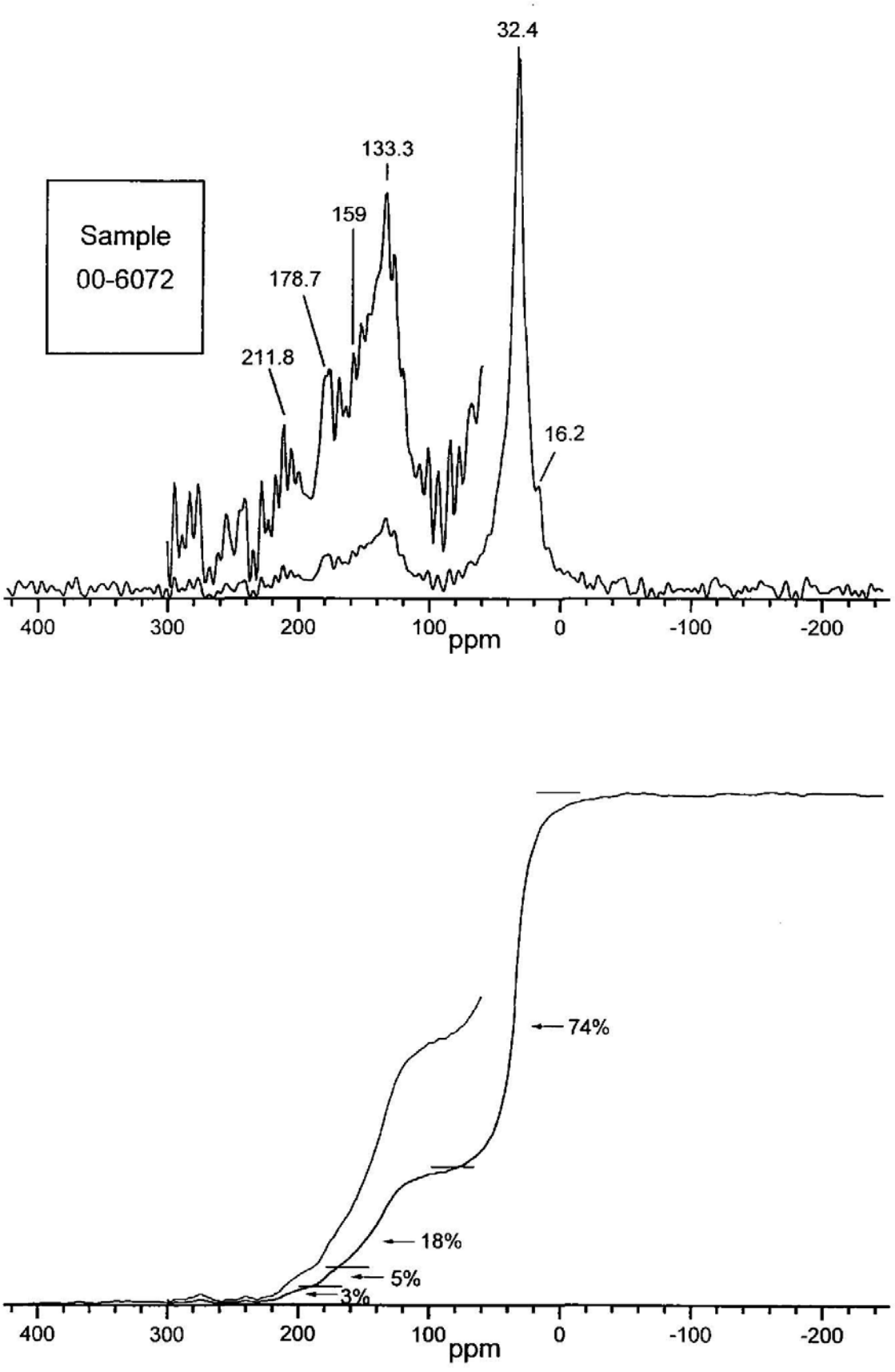

Figure A6.21 ^{13}C NMR spectrum and integrated intensities for sample 00-6074

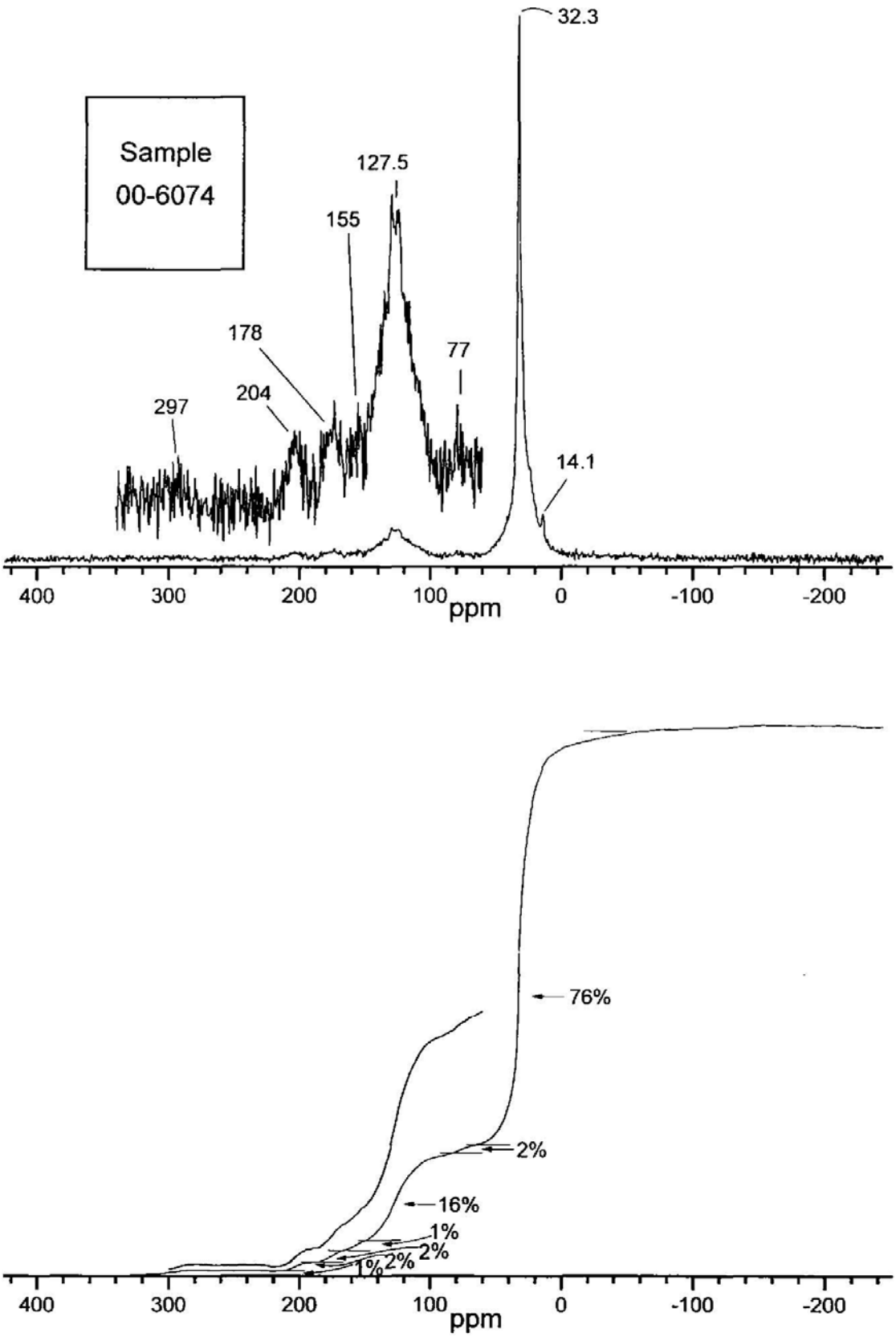

Figure A6.22 ^{13}C NMR spectrum and integrated intensities for sample 00-6076

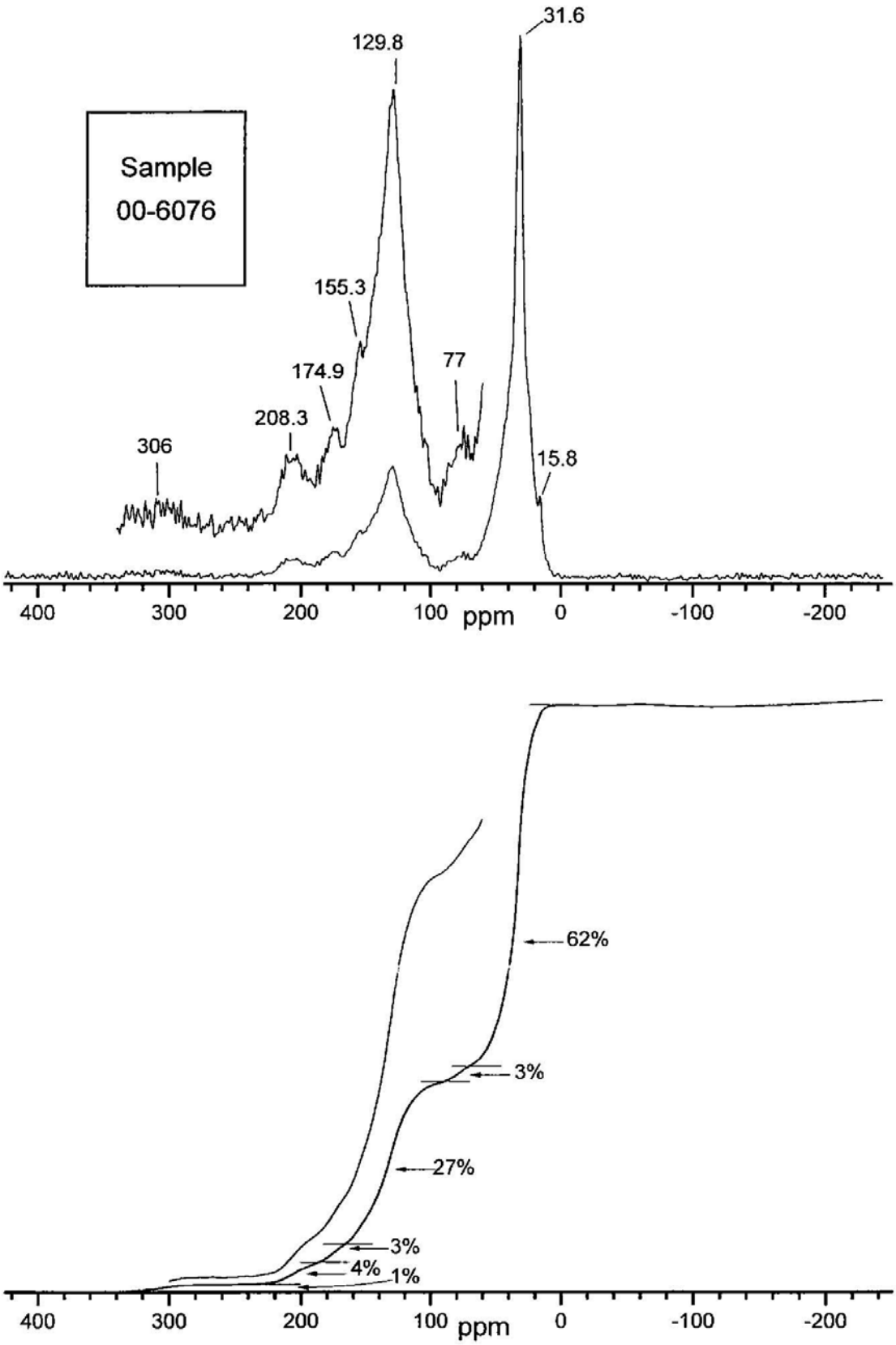

Figure A6.23 ^{13}C NMR spectrum and integrated intensities for sample 00-6077

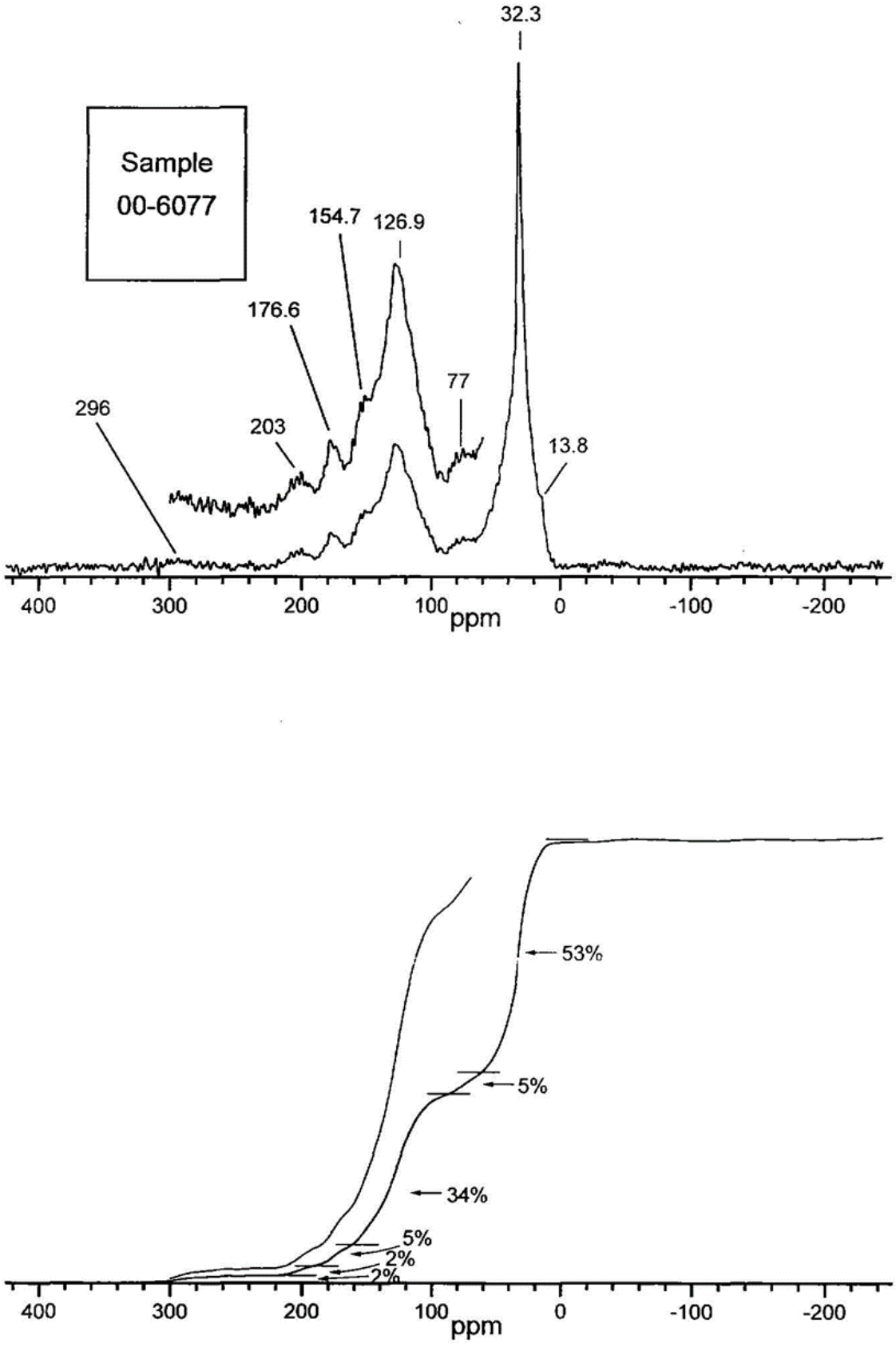

Figure A6.24 ^{13}C NMR spectrum and integrated intensities for sample 00-6079

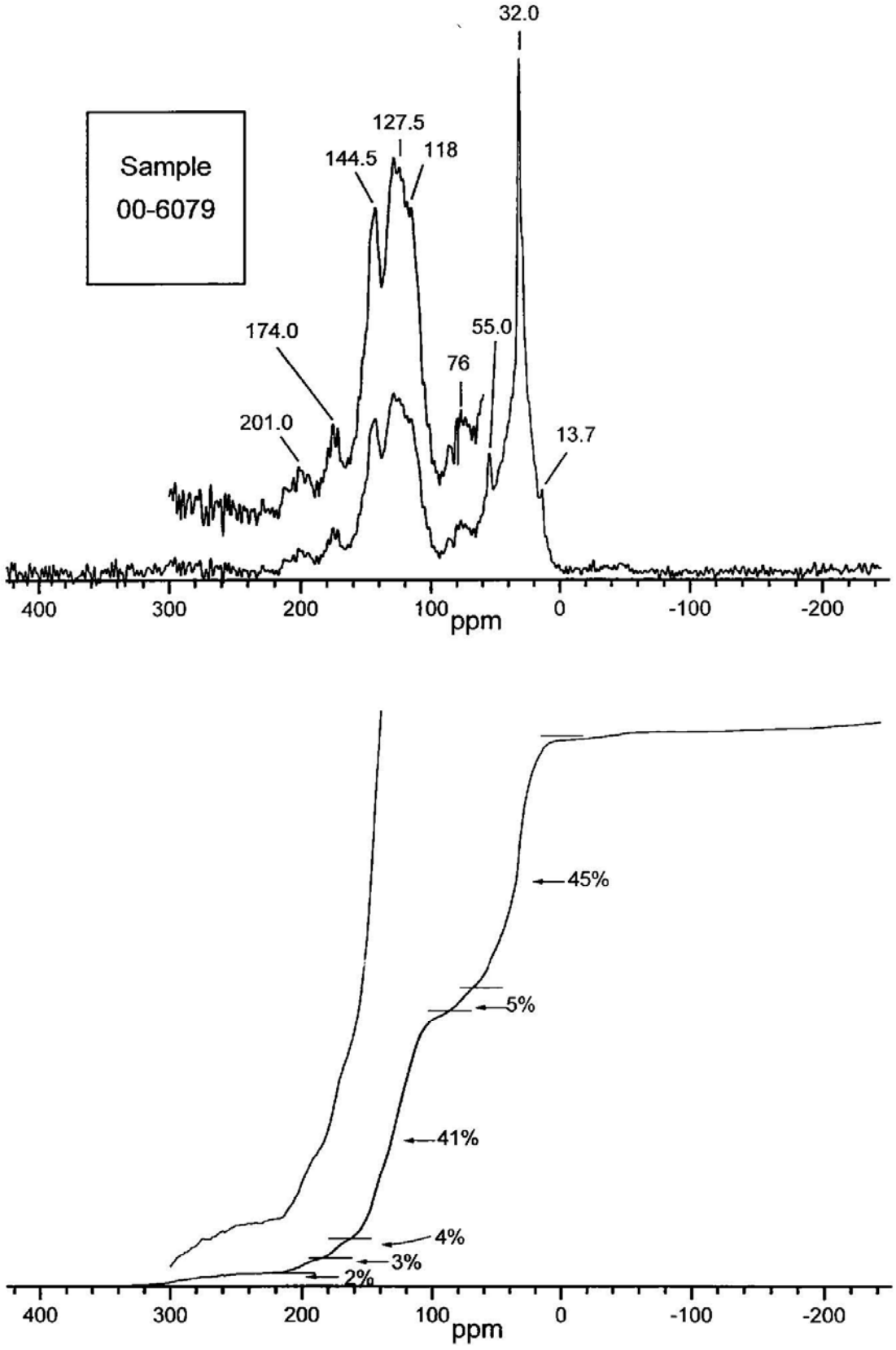

Figure A6.25 **^{13}C NMR spectrum and integrated intensities for sample 00-6080**

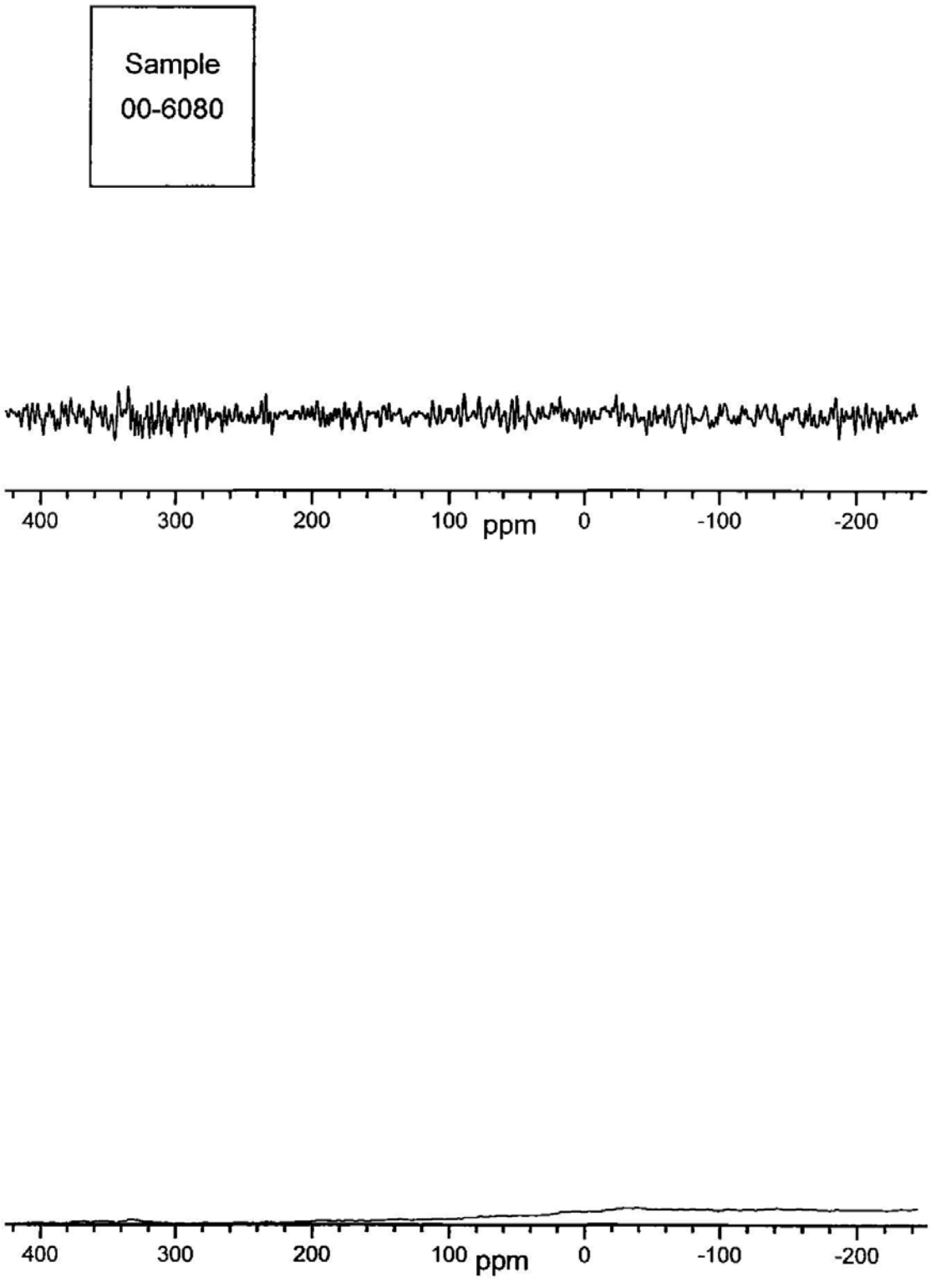

Figure A6.26 **^{13}C NMR spectrum and integrated intensities for sample 00-6081**

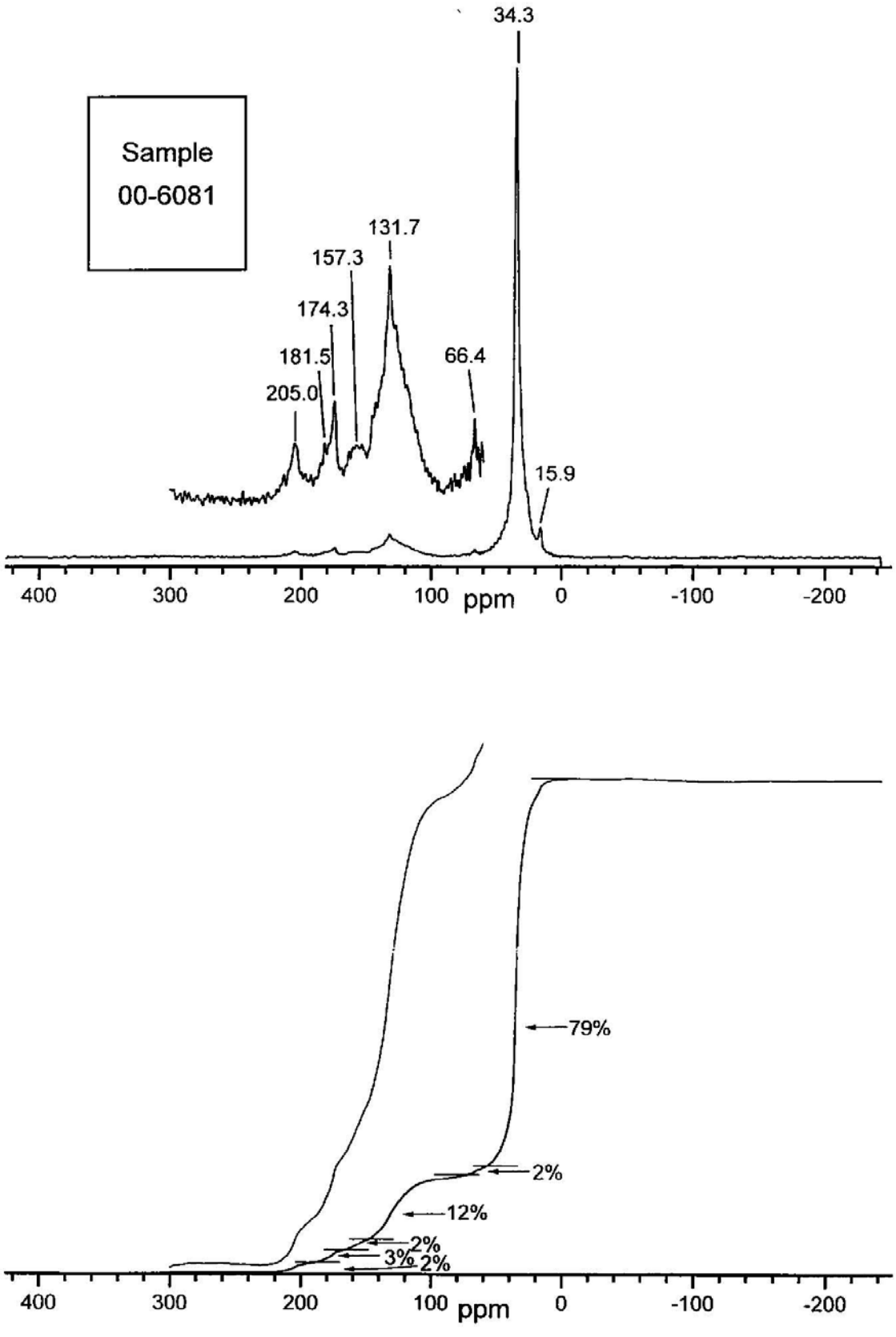

Figure A6.27 ^{13}C NMR spectrum and integrated intensities for sample 00-6085

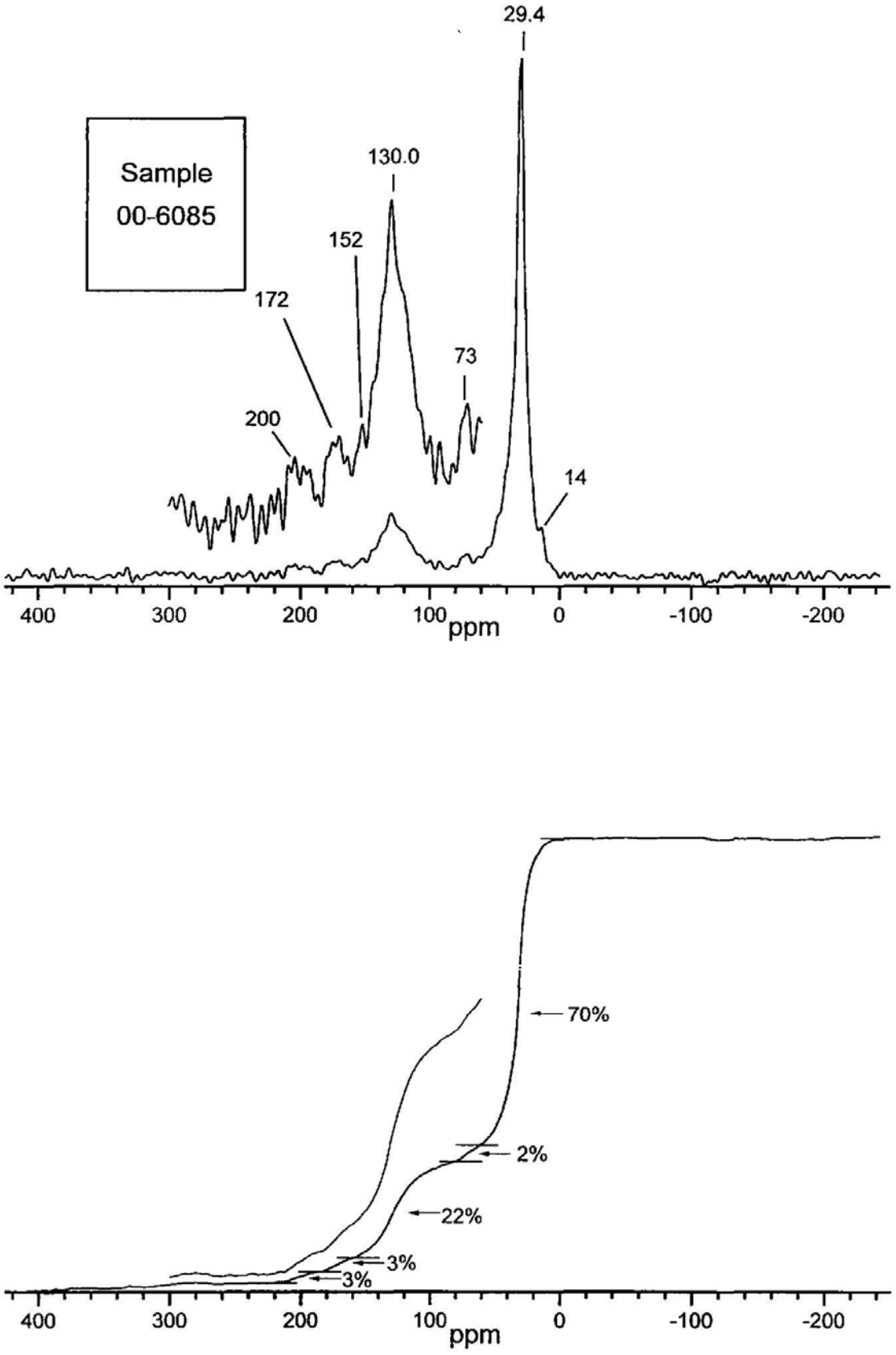

Figure A6.28 **^{13}C NMR spectrum and integrated intensities for sample 00-6086**

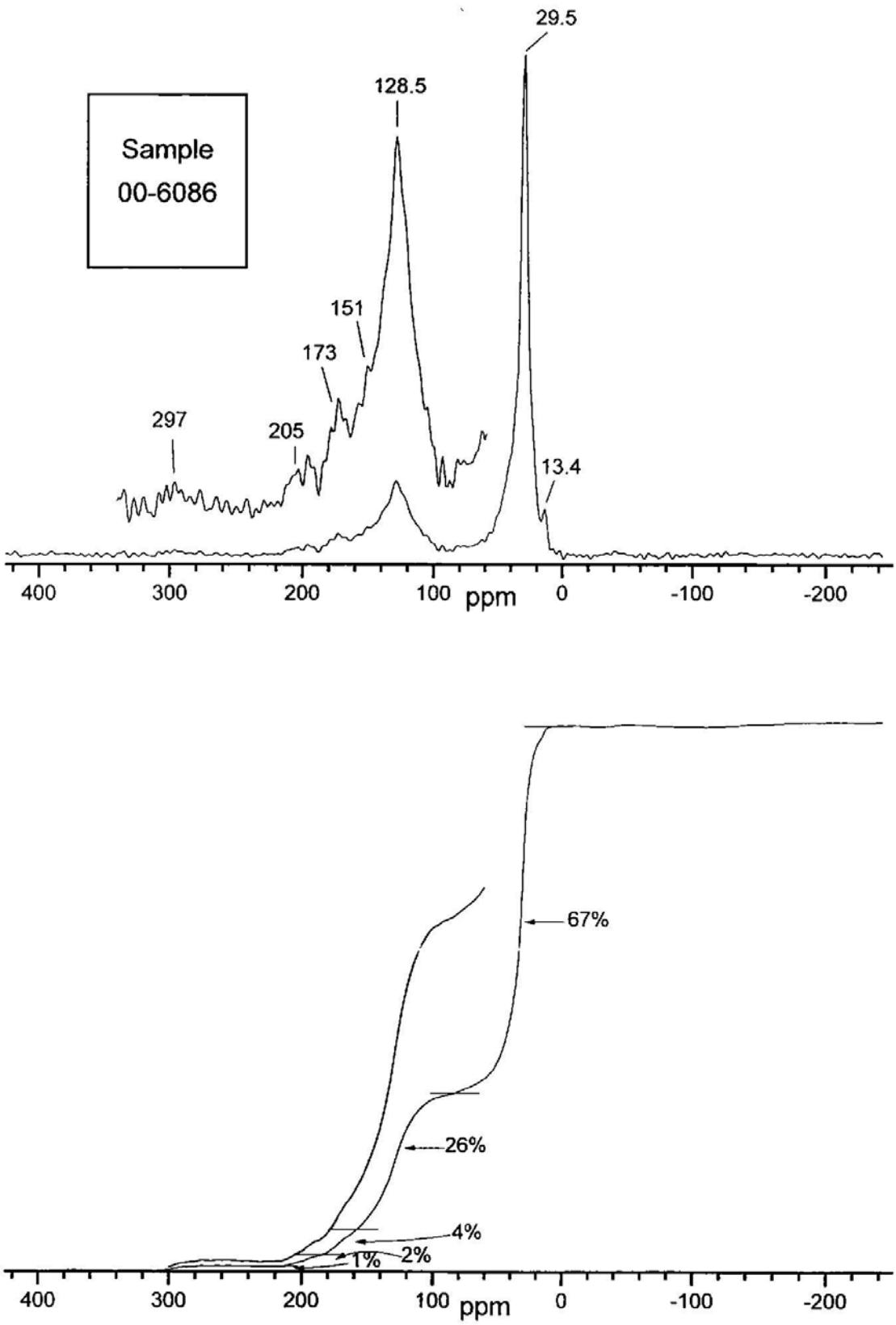

Figure A6.29 **^{13}C NMR spectrum and integrated intensities for sample 00-6088**

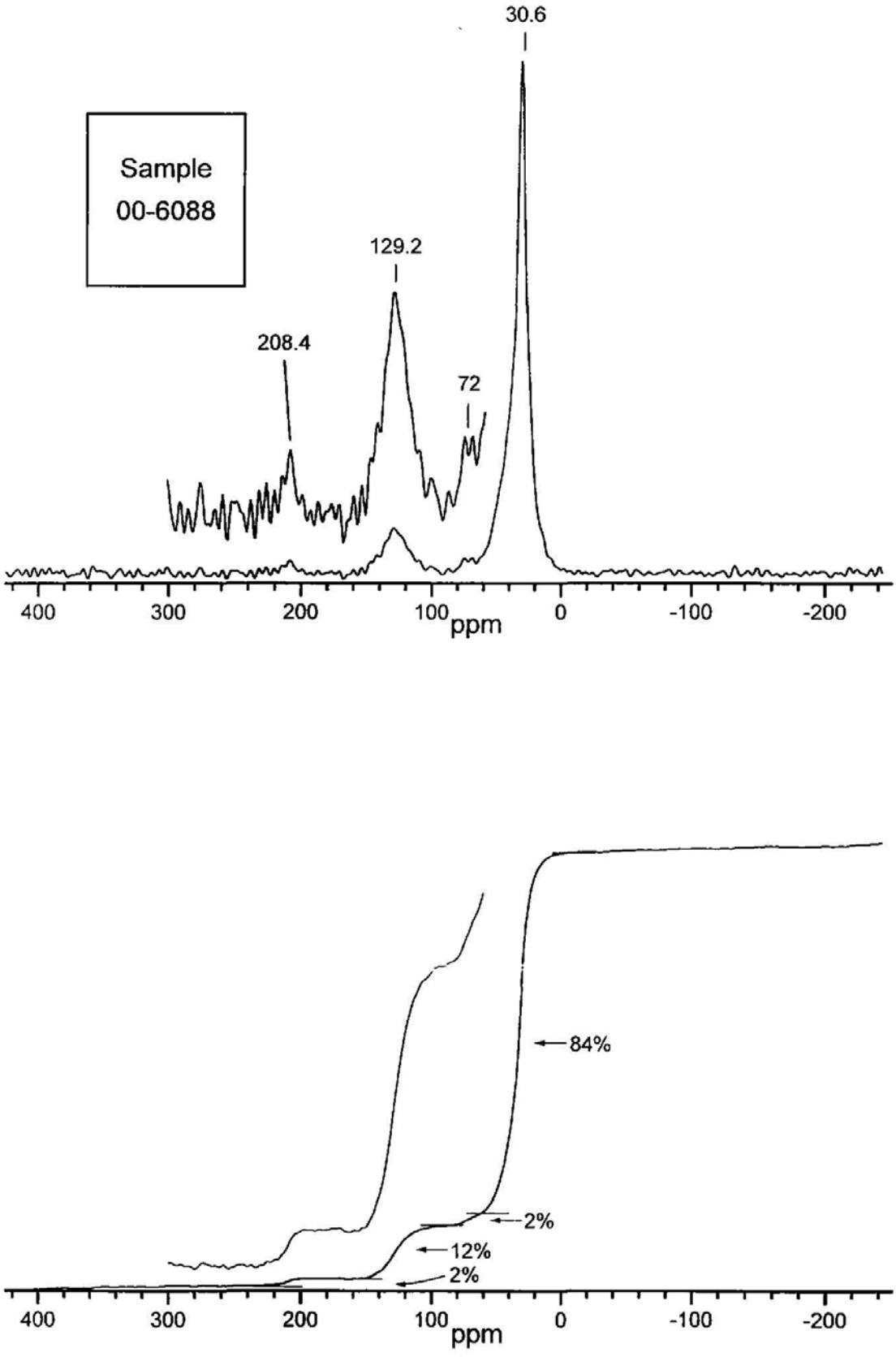

Figure A6.30 ^{13}C NMR spectrum and integrated intensities for sample 00-6089

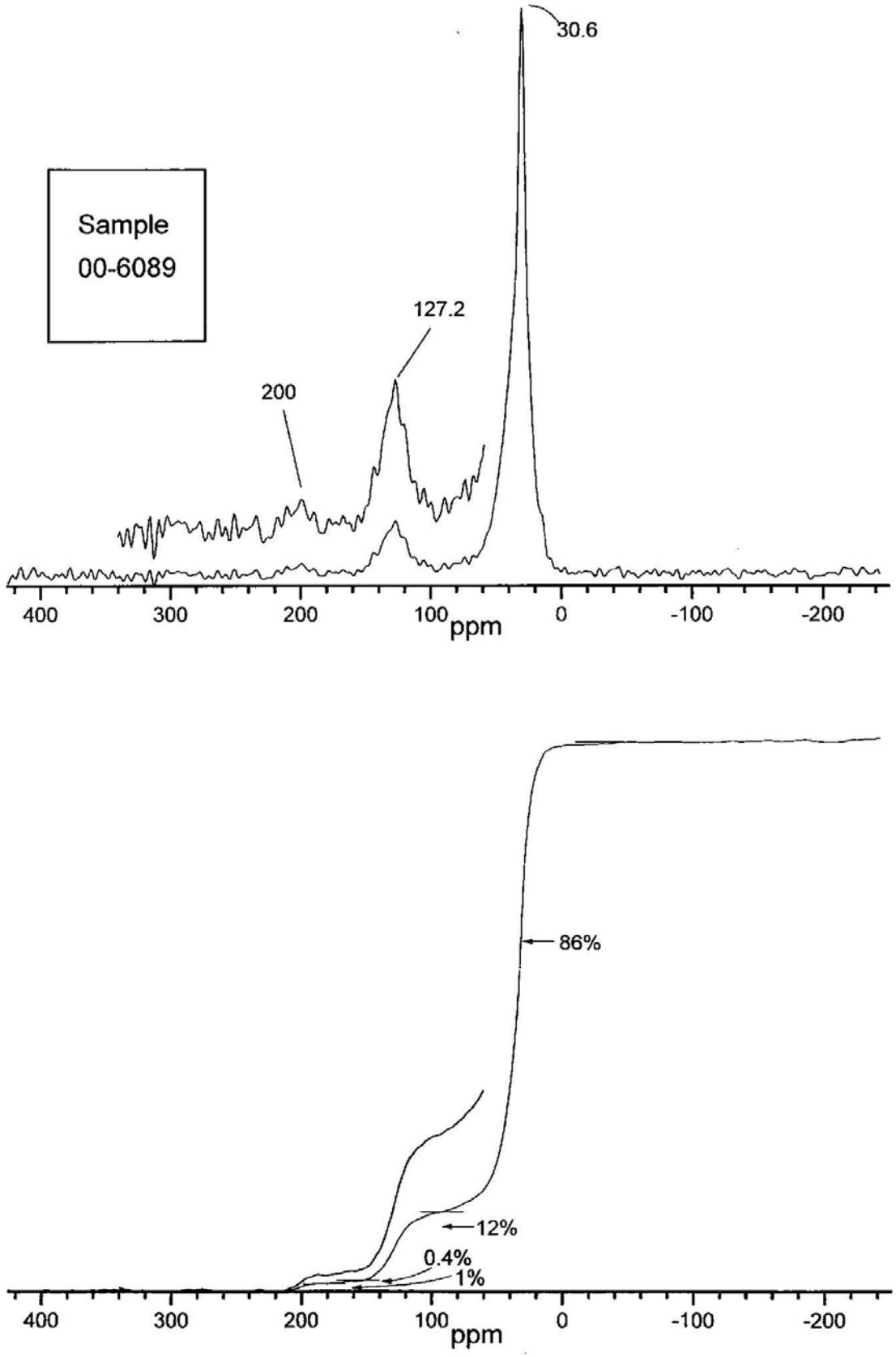

Figure A6.31 ^{13}C NMR spectrum and integrated intensities for sample 00-6091

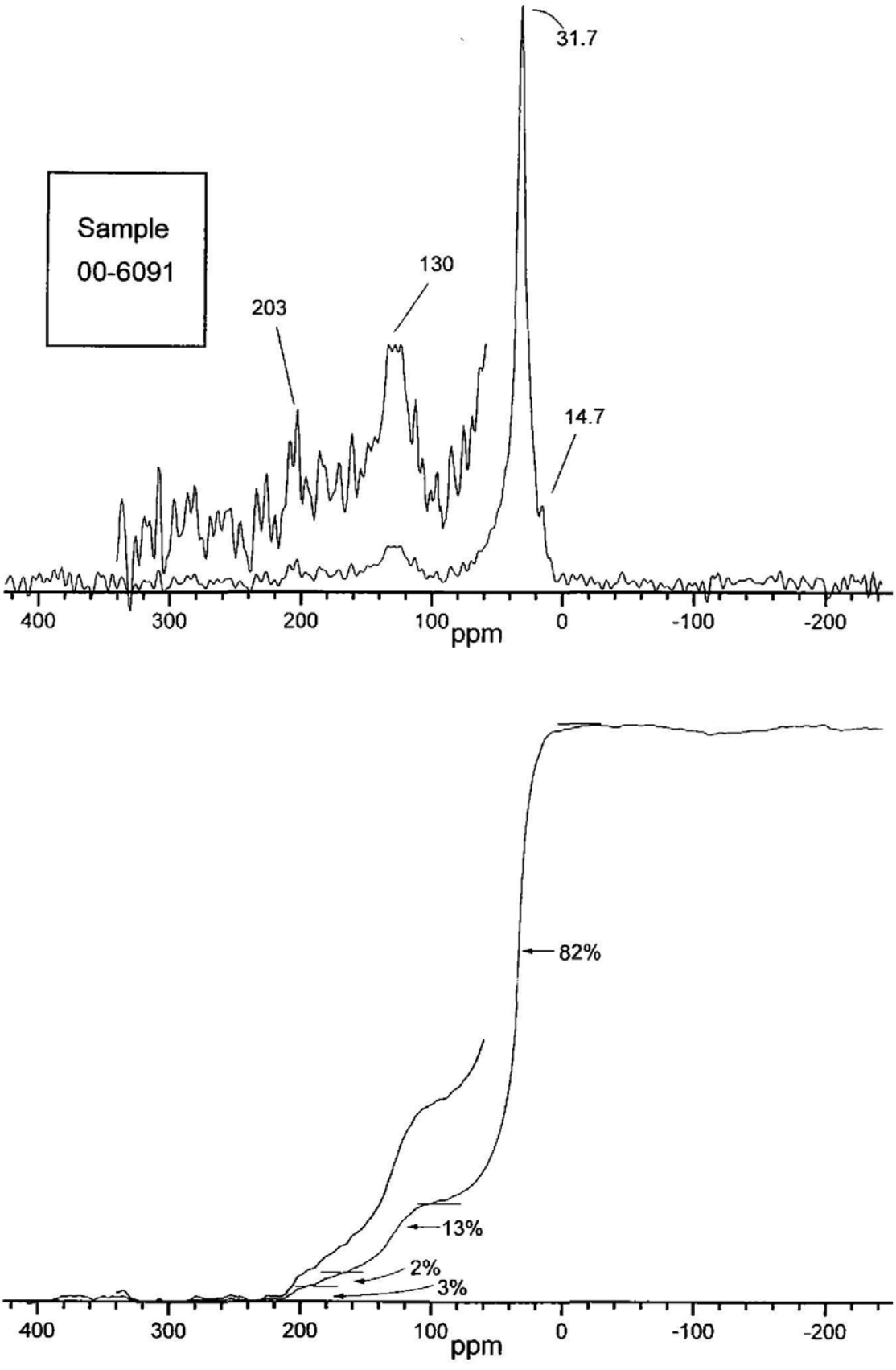

Figure A6.32 ^{13}C NMR spectrum and integrated intensities for sample 00-6093

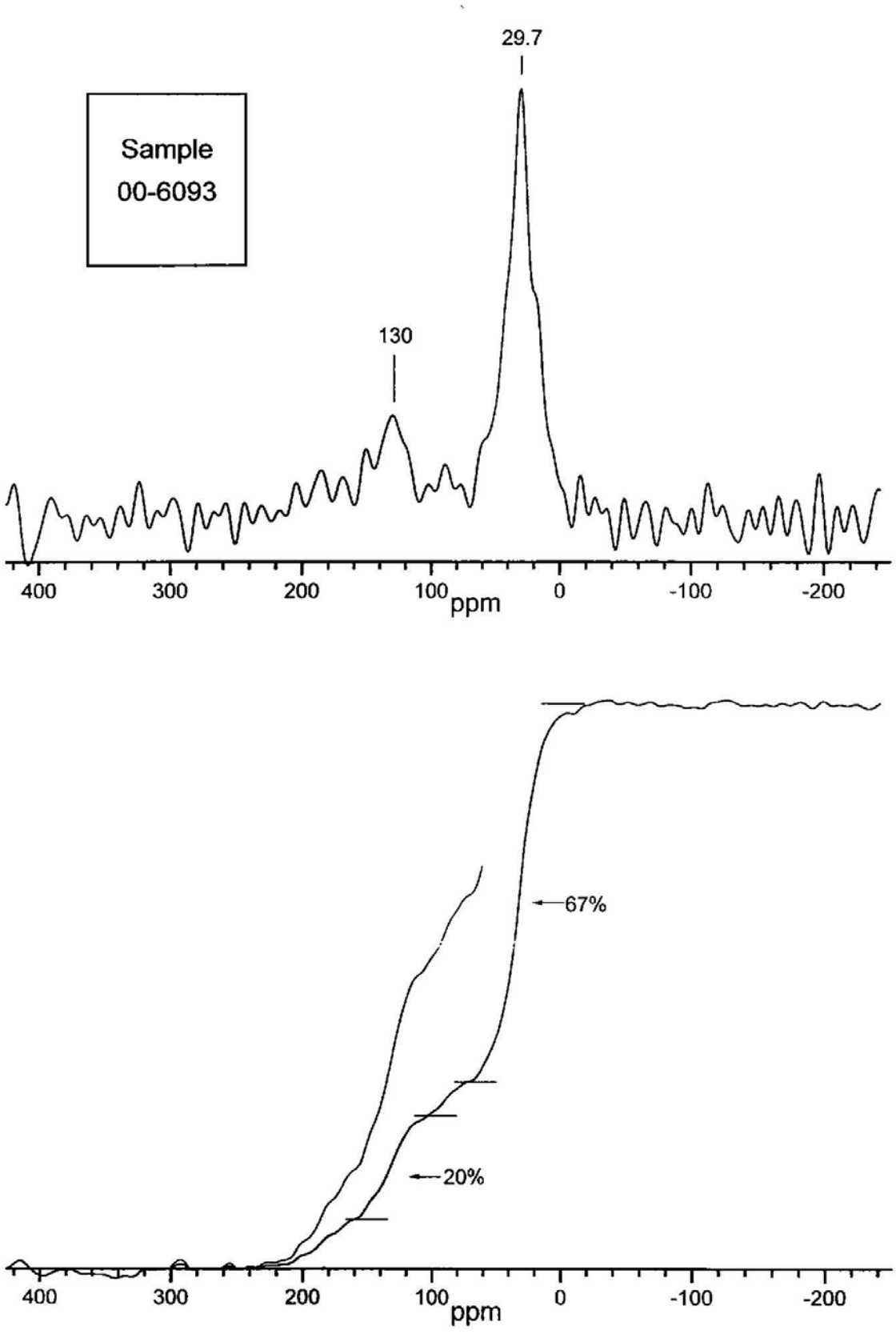

Figure A6.33 **^{13}C NMR spectrum and integrated intensities for sample 00-6095**

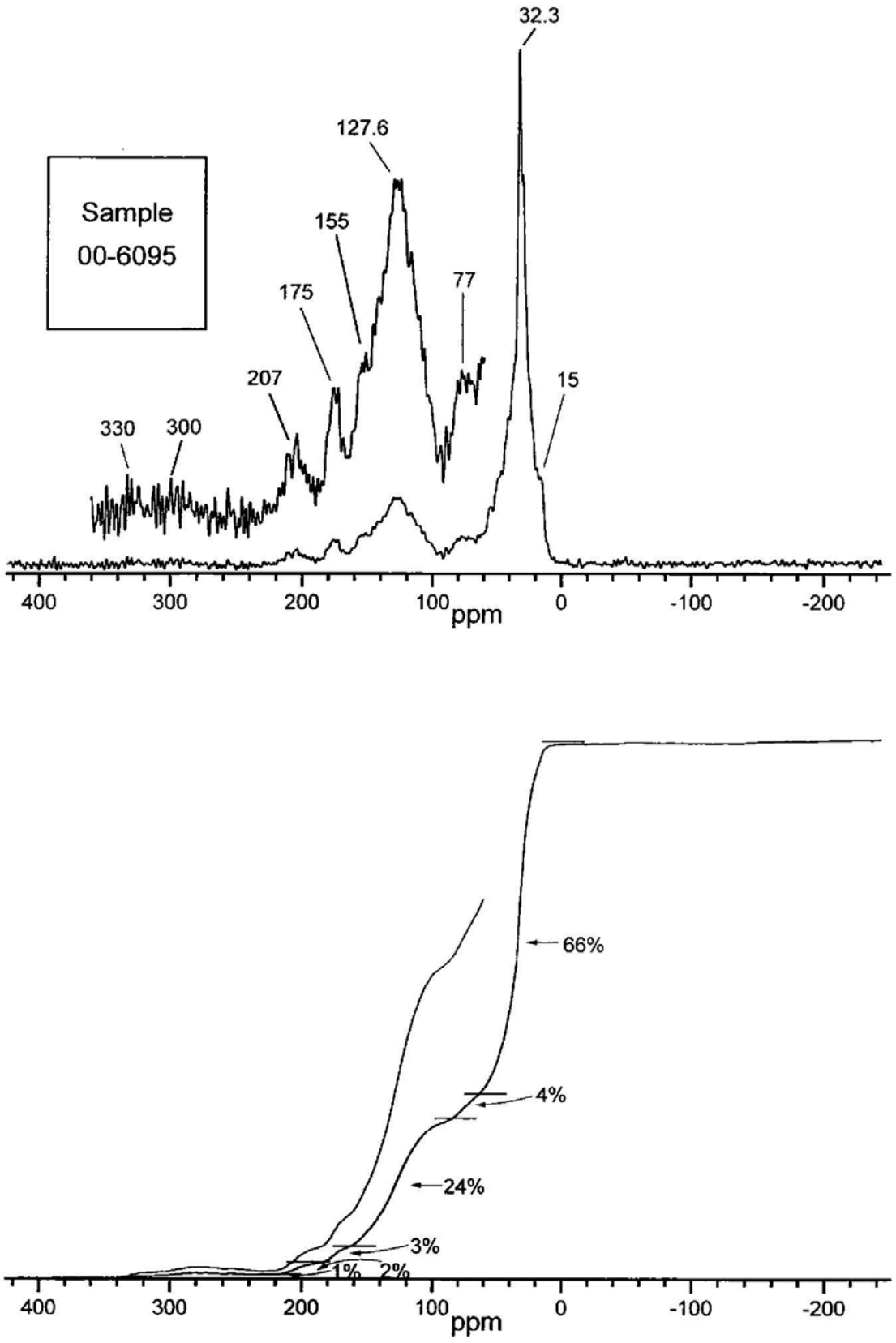

Figure A6.34 ^{13}C NMR spectrum and integrated intensities for sample 00-6096

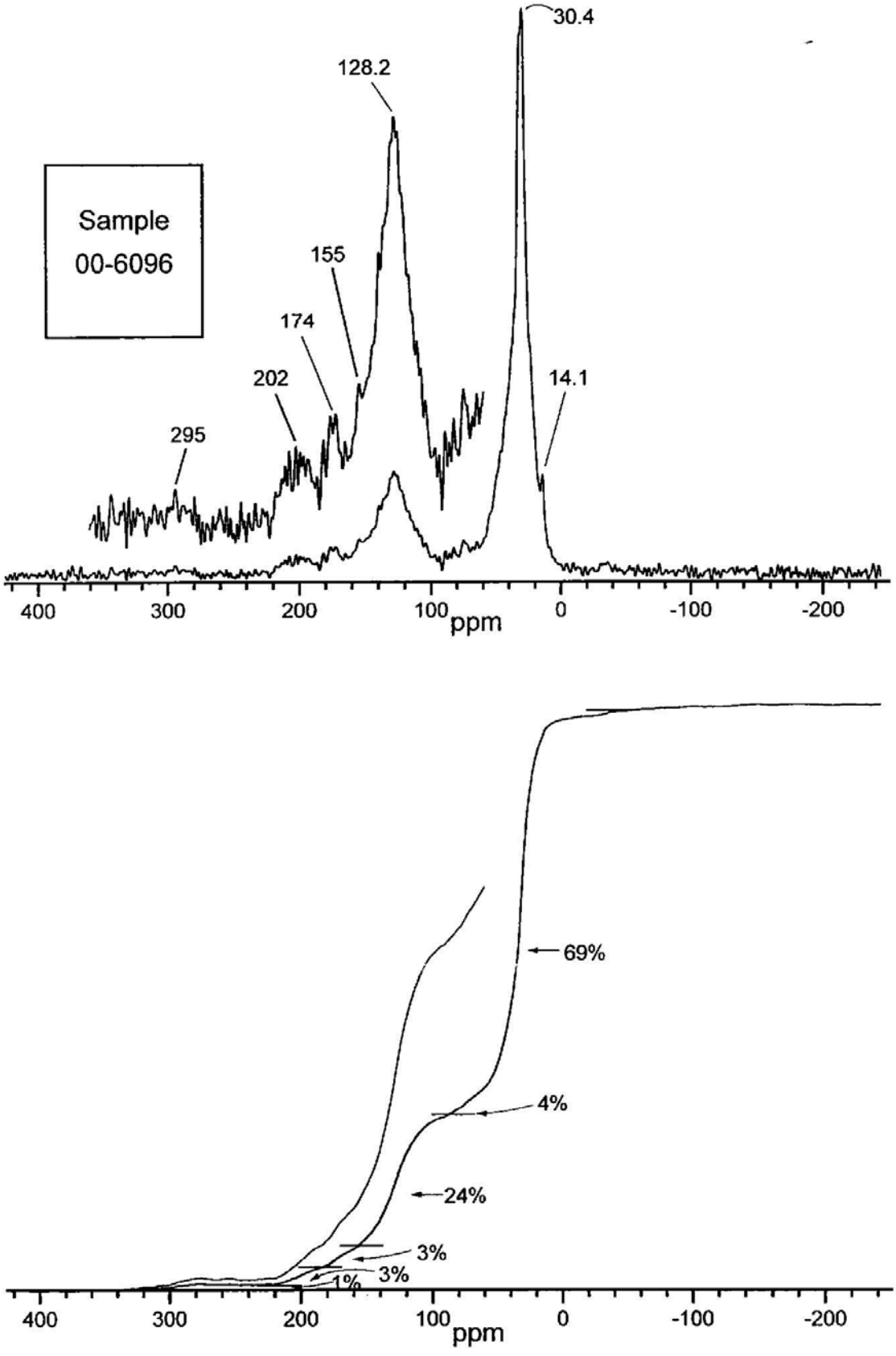

Figure A6.35 ^{13}C NMR spectrum and integrated intensities for sample 00-6097

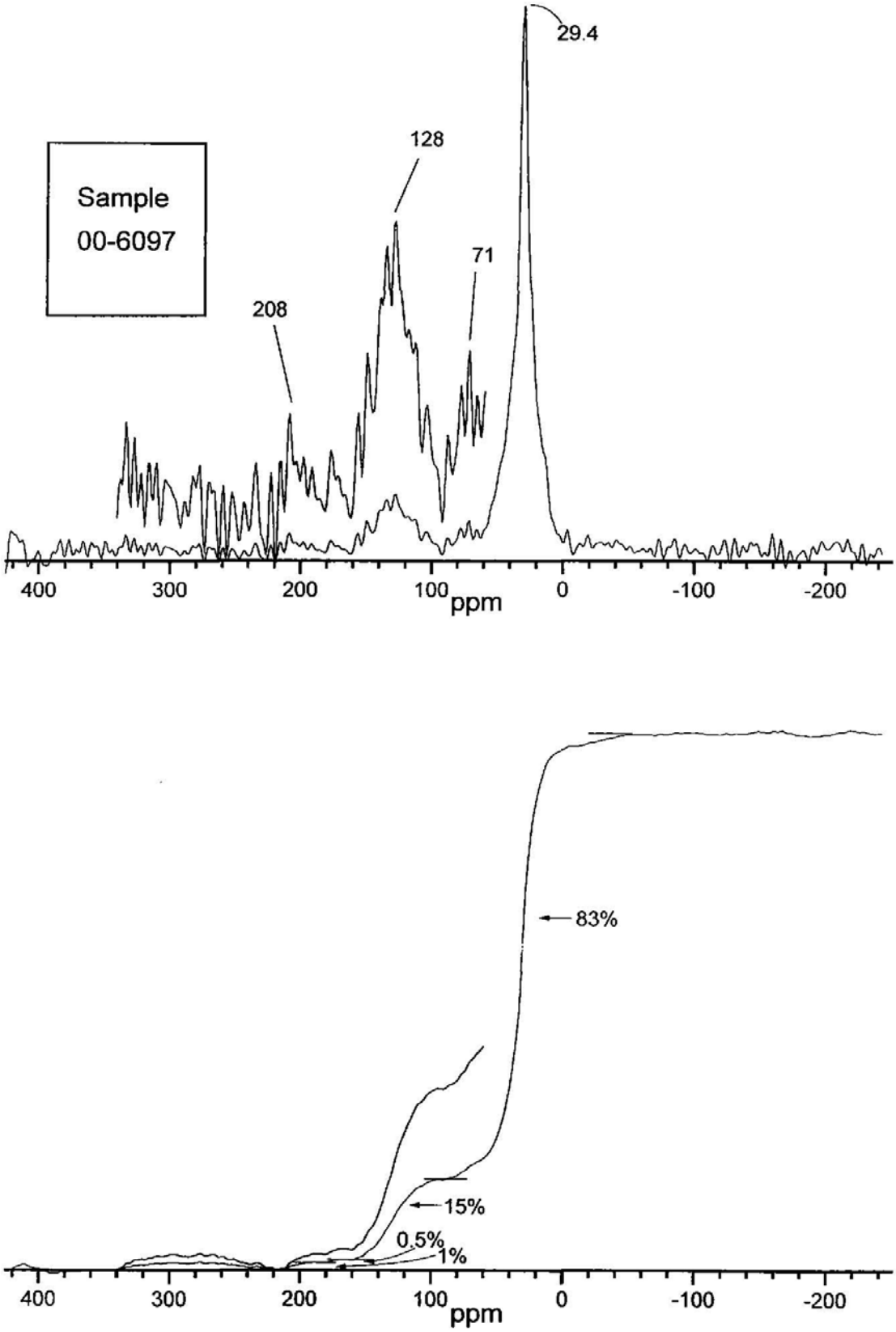

Figure A6.36 ^{13}C NMR spectrum and integrated intensities for sample 00-6099

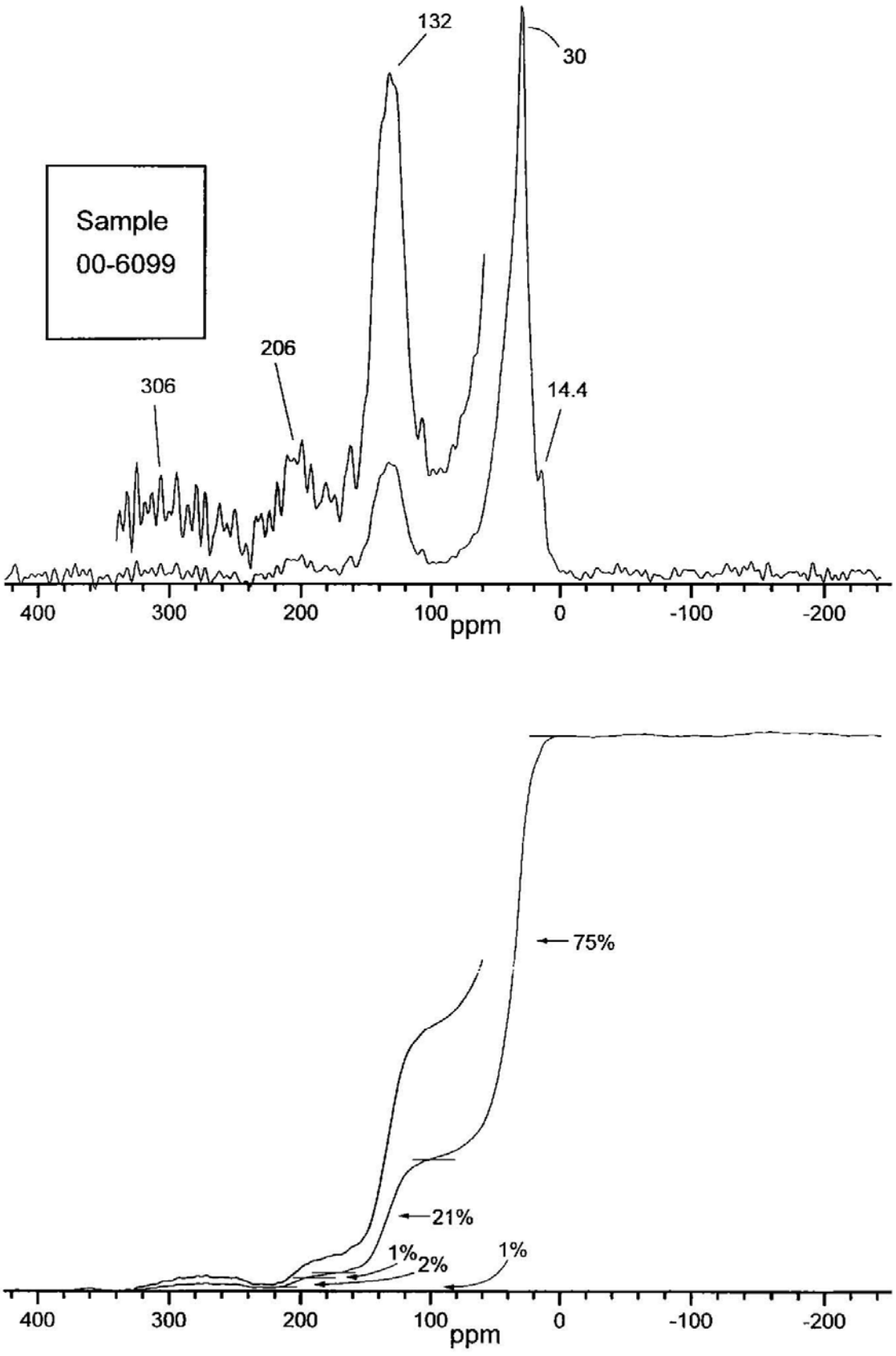

Figure A6.37 ^{13}C NMR spectrum and integrated intensities for sample 00-6114

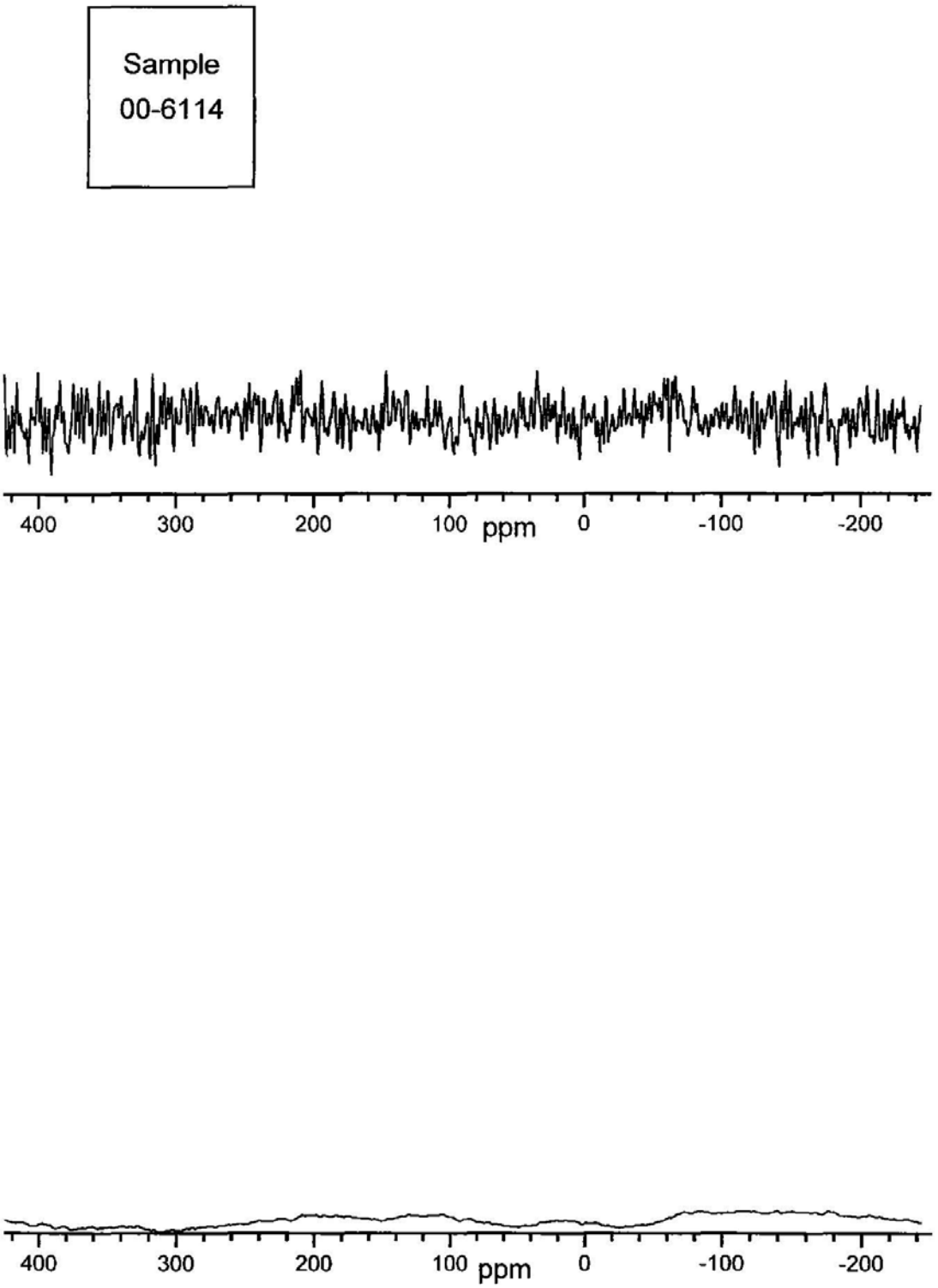

Figure A6.38 ^{13}C NMR spectrum and integrated intensities for sample 00-6116

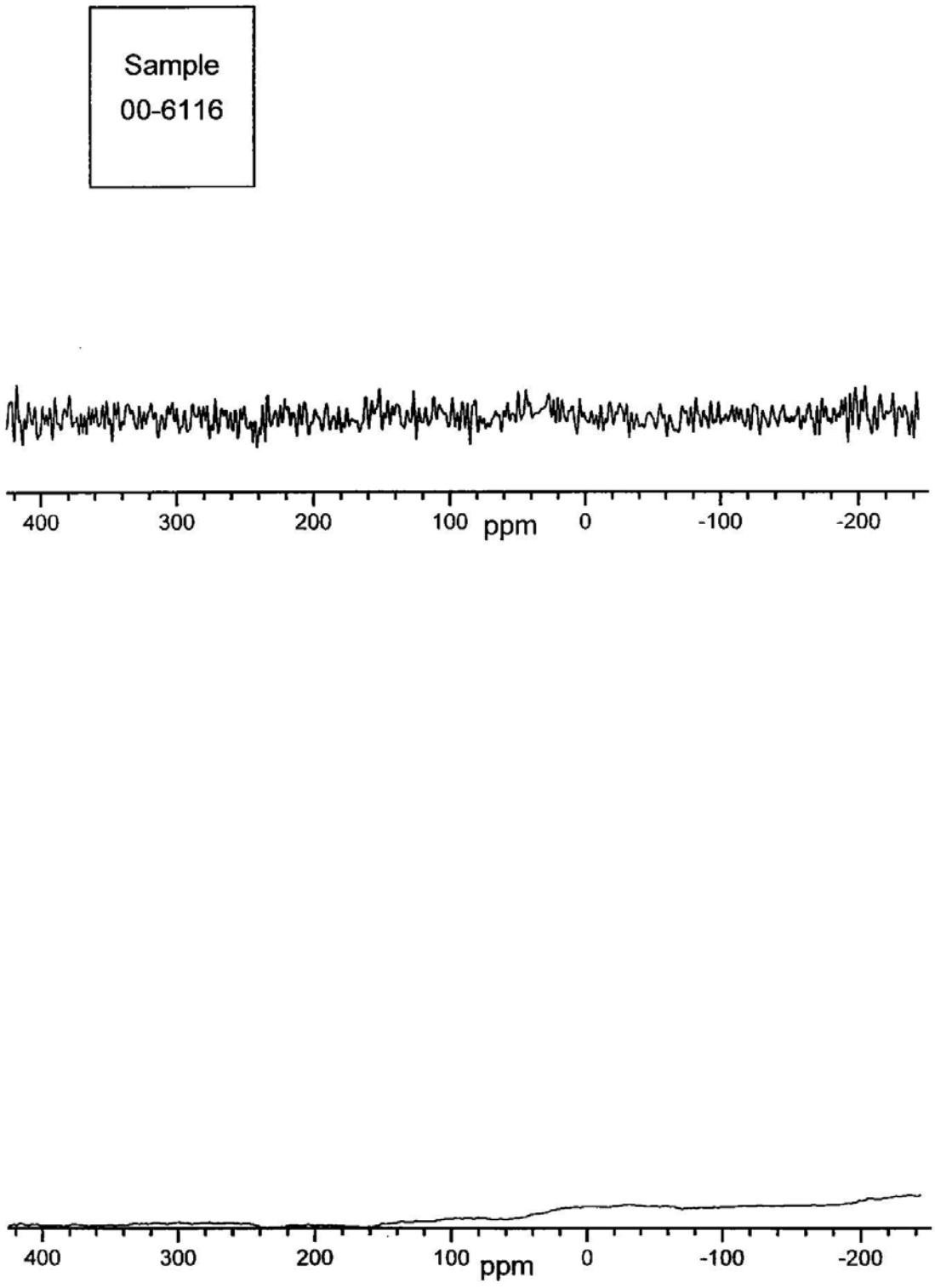

Figure A6.39 **^{13}C NMR spectrum and integrated intensities for sample 00-6117**

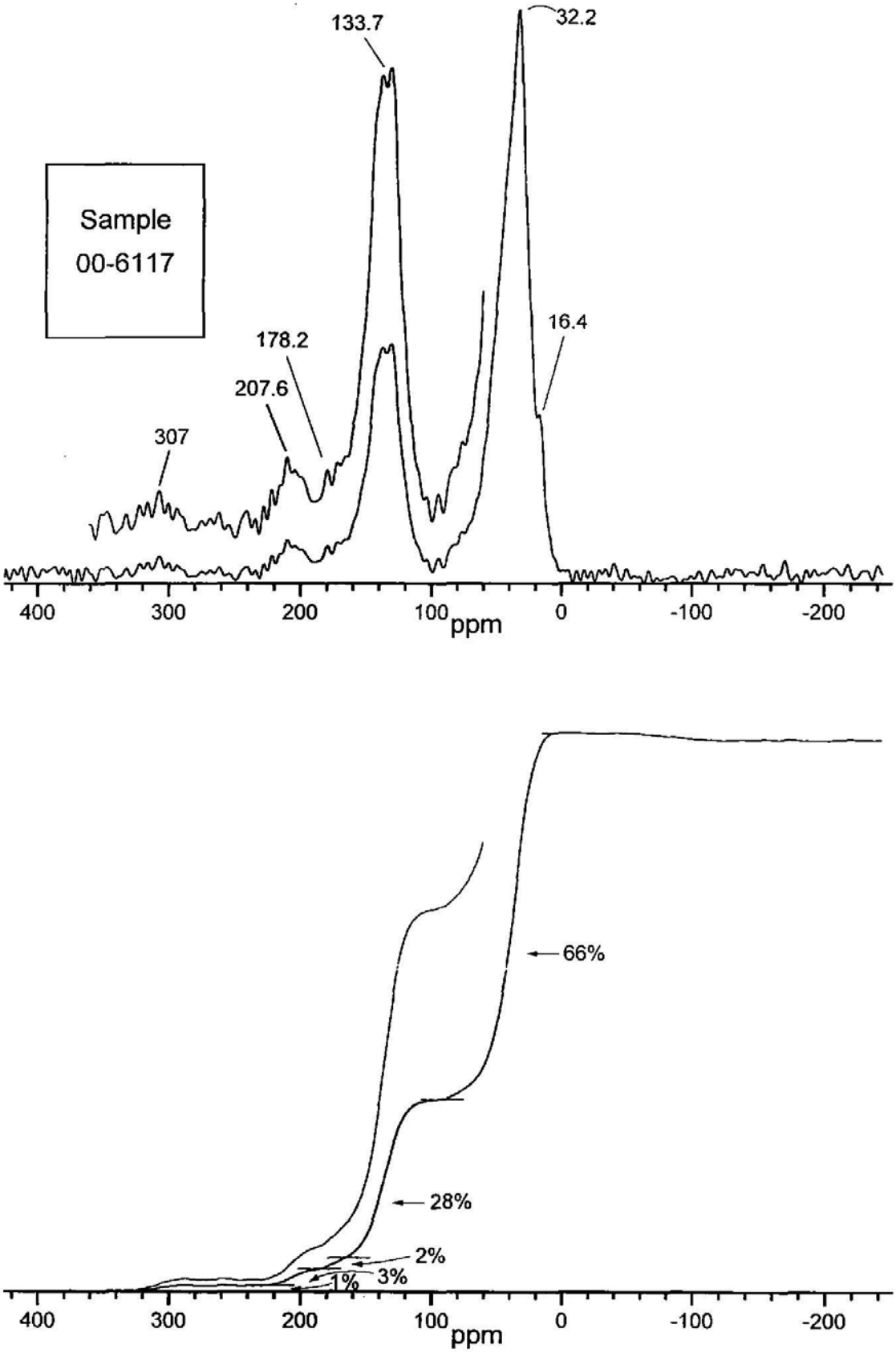

Figure A6.40 ^{13}C NMR spectrum and integrated intensities for sample 00-6165

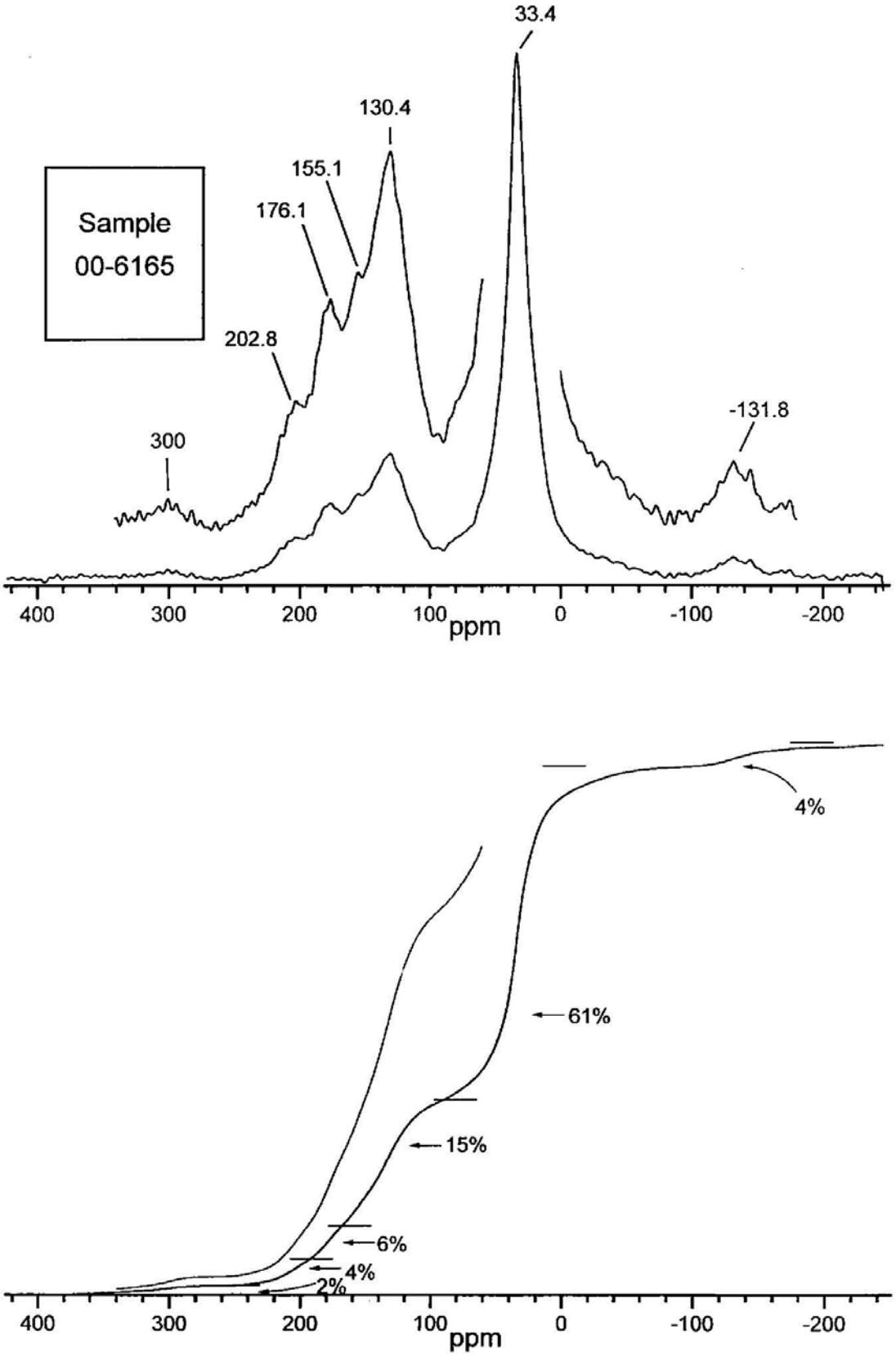

Figure A6.41 ^{13}C NMR spectrum and integrated intensities for sample 00-6167

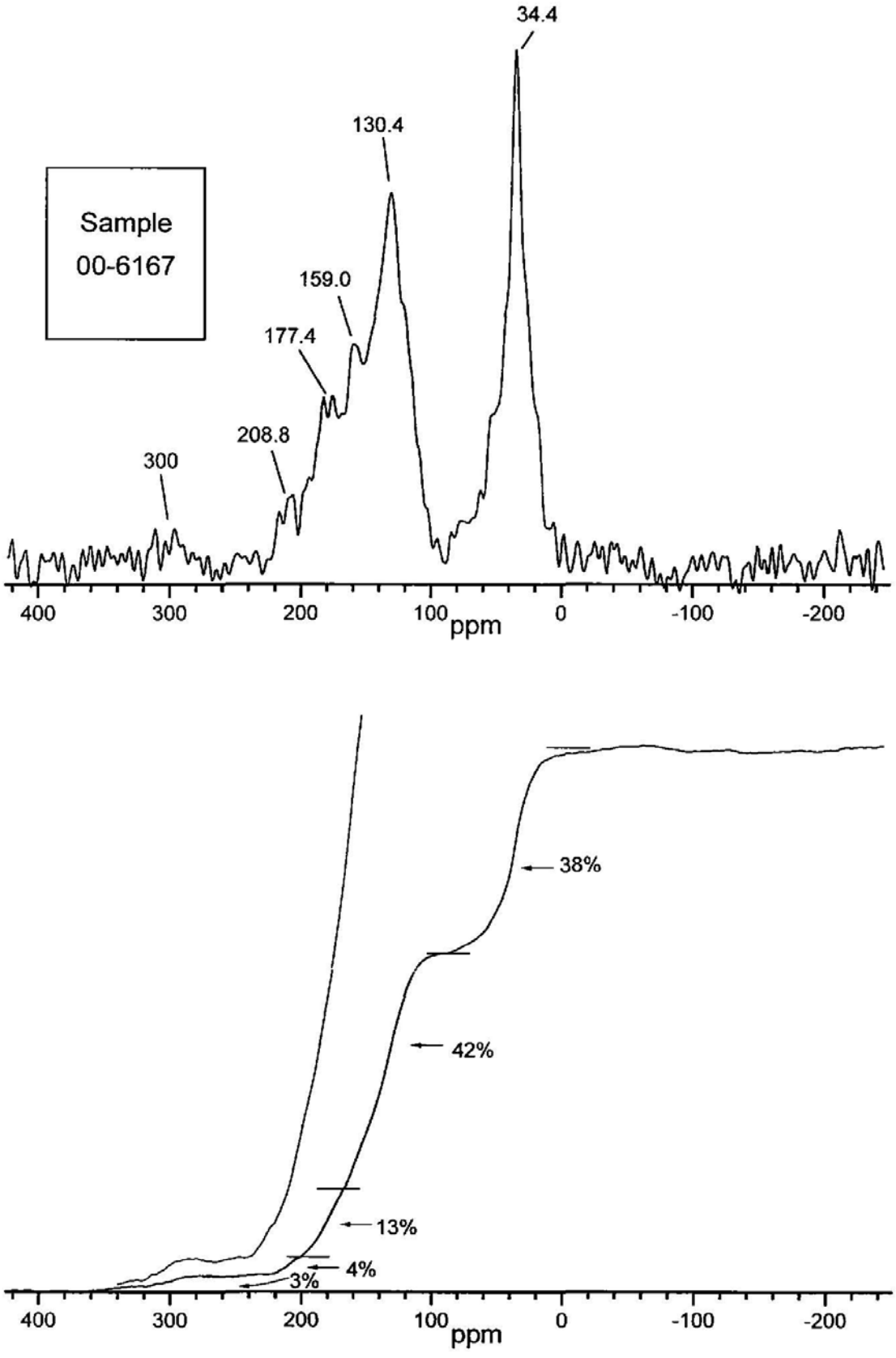

Figure A6.42 **^{13}C NMR spectrum and integrated intensities for sample 00-6172**

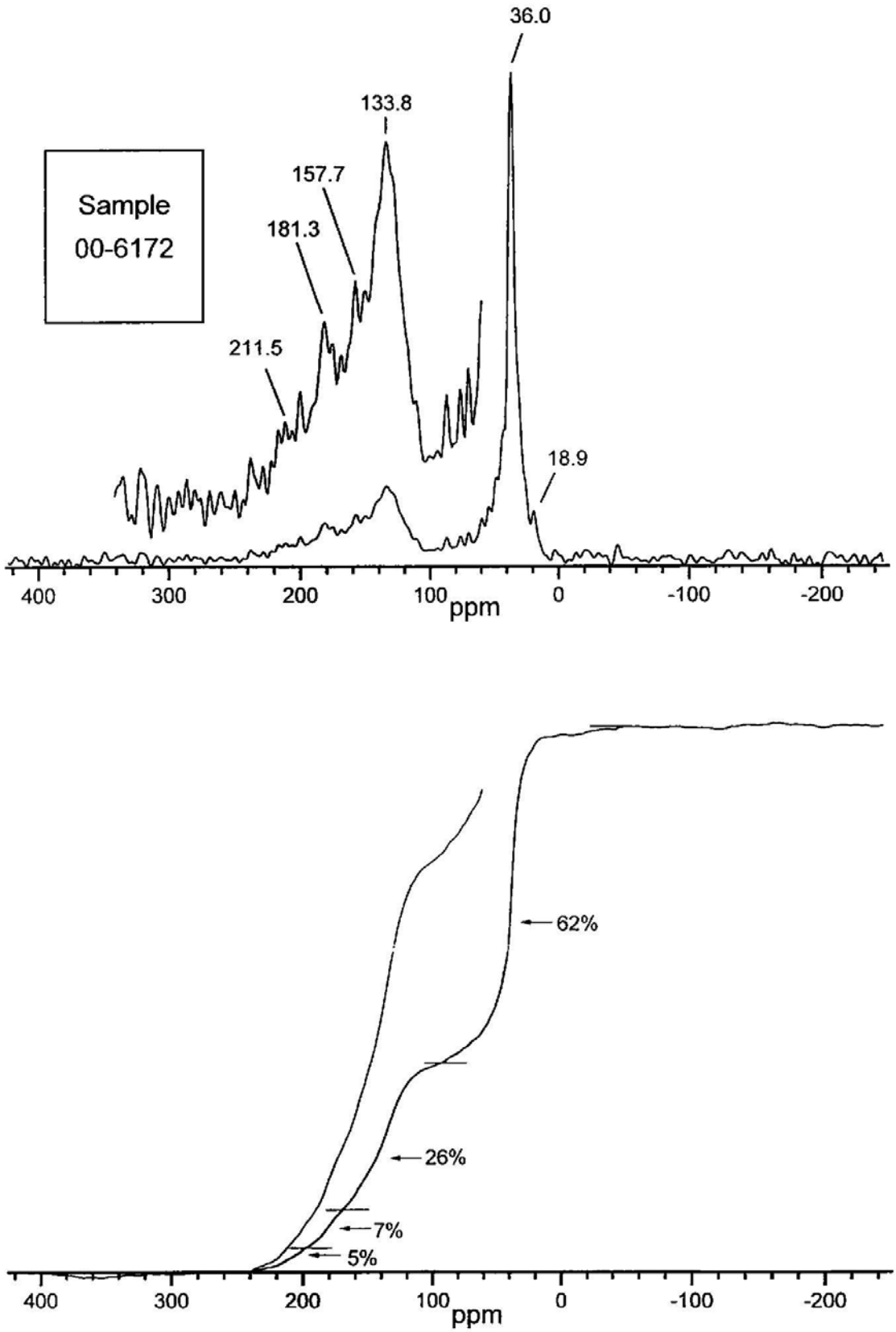

Figure A6.43 ^{13}C NMR spectrum and integrated intensities for sample 00-6178

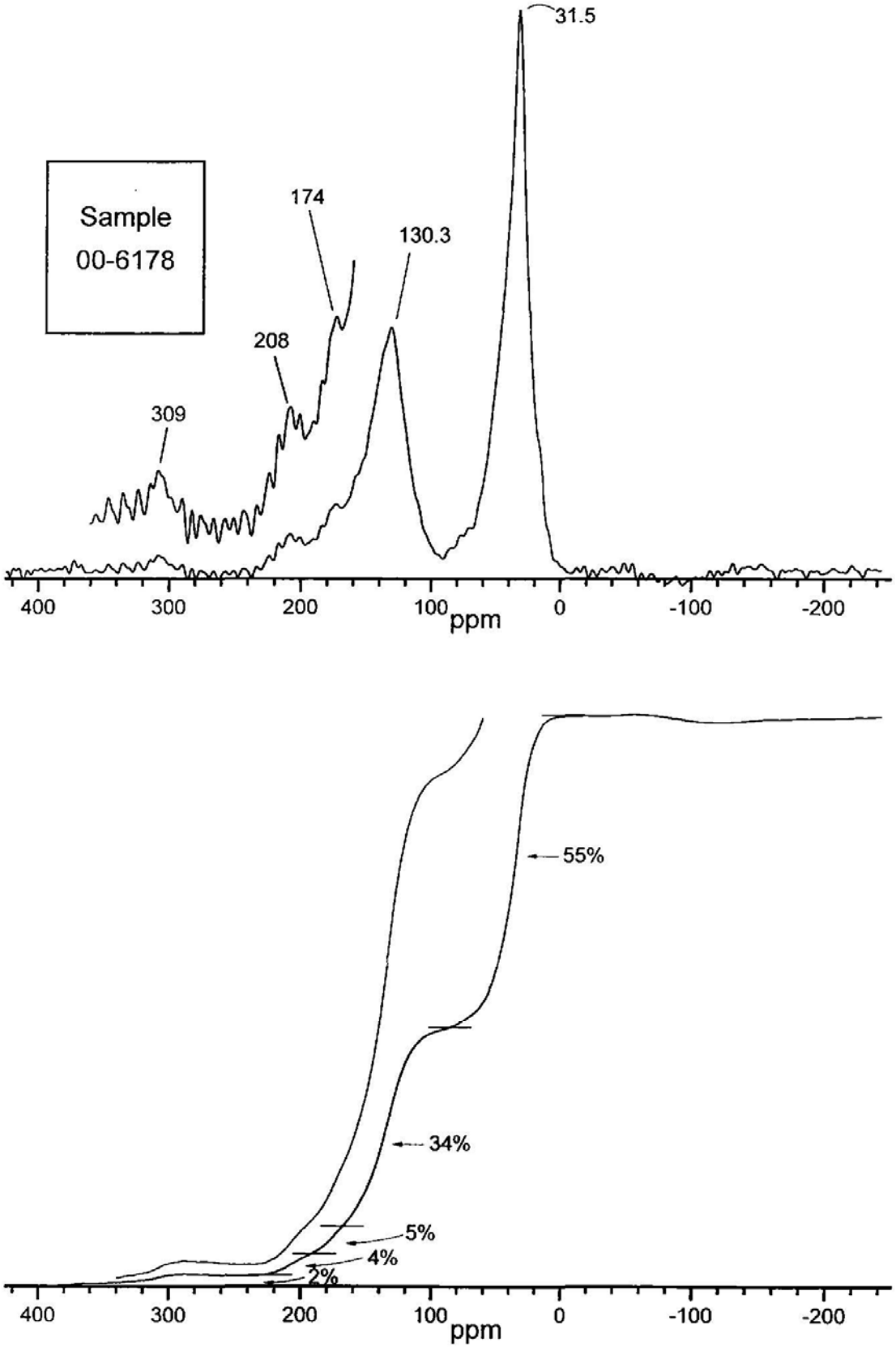

Figure A6.44 **^{13}C NMR spectrum and integrated intensities for sample 00-6186**

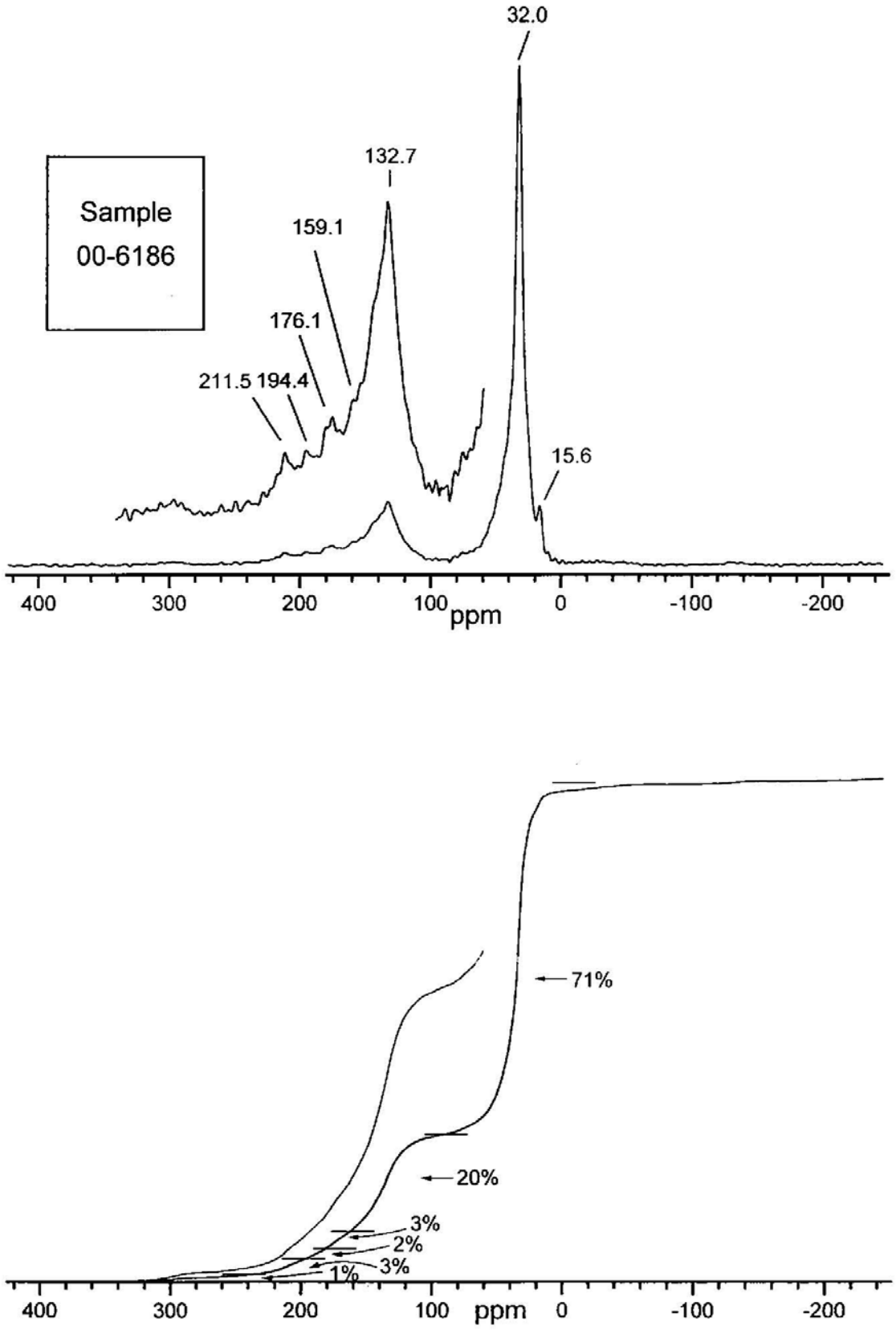

Figure A6.45 ^{13}C NMR spectrum and integrated intensities for sample 00-6187

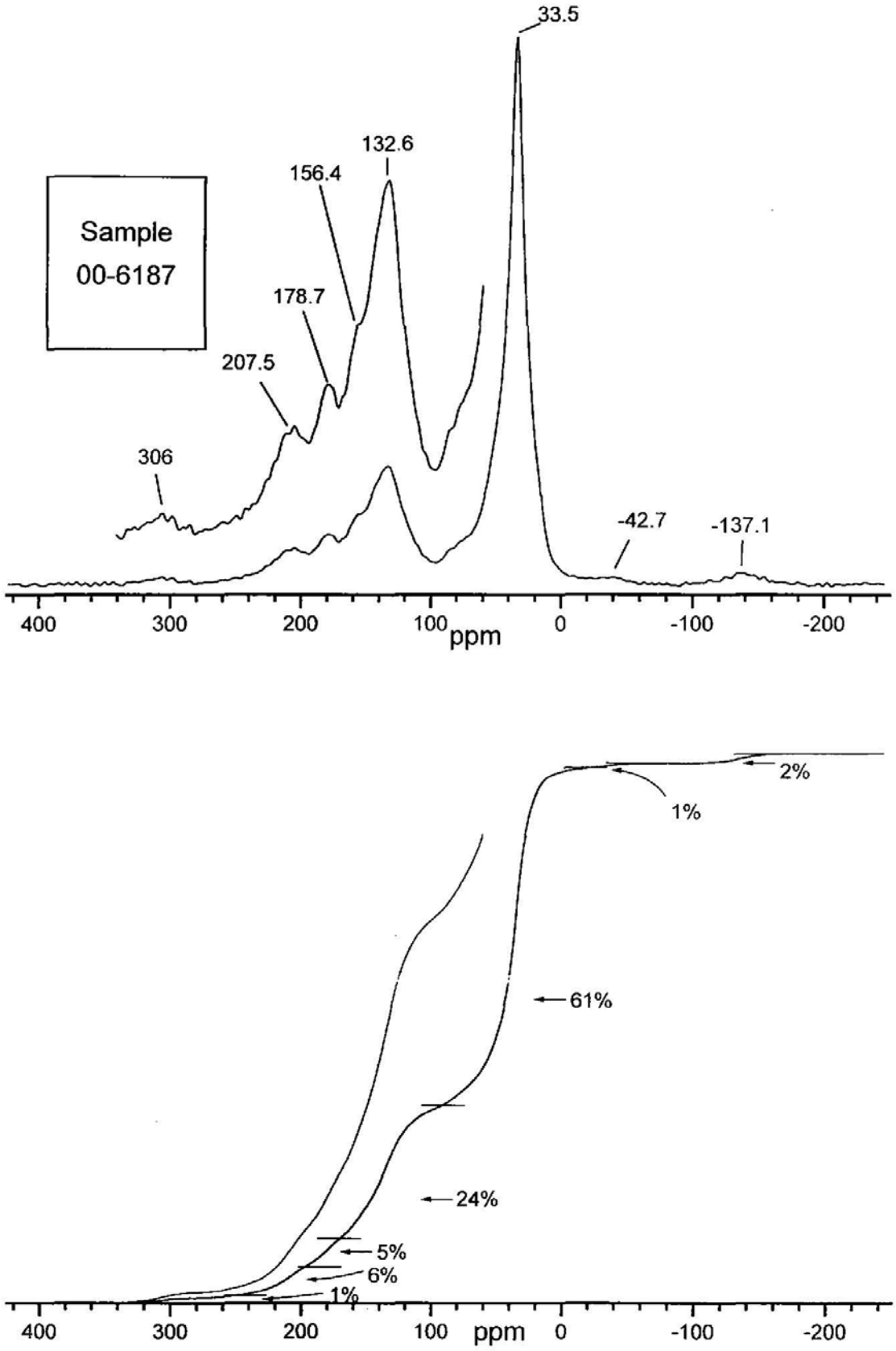

Figure A6.46 ^{13}C NMR spectrum and integrated intensities for sample 00-6197

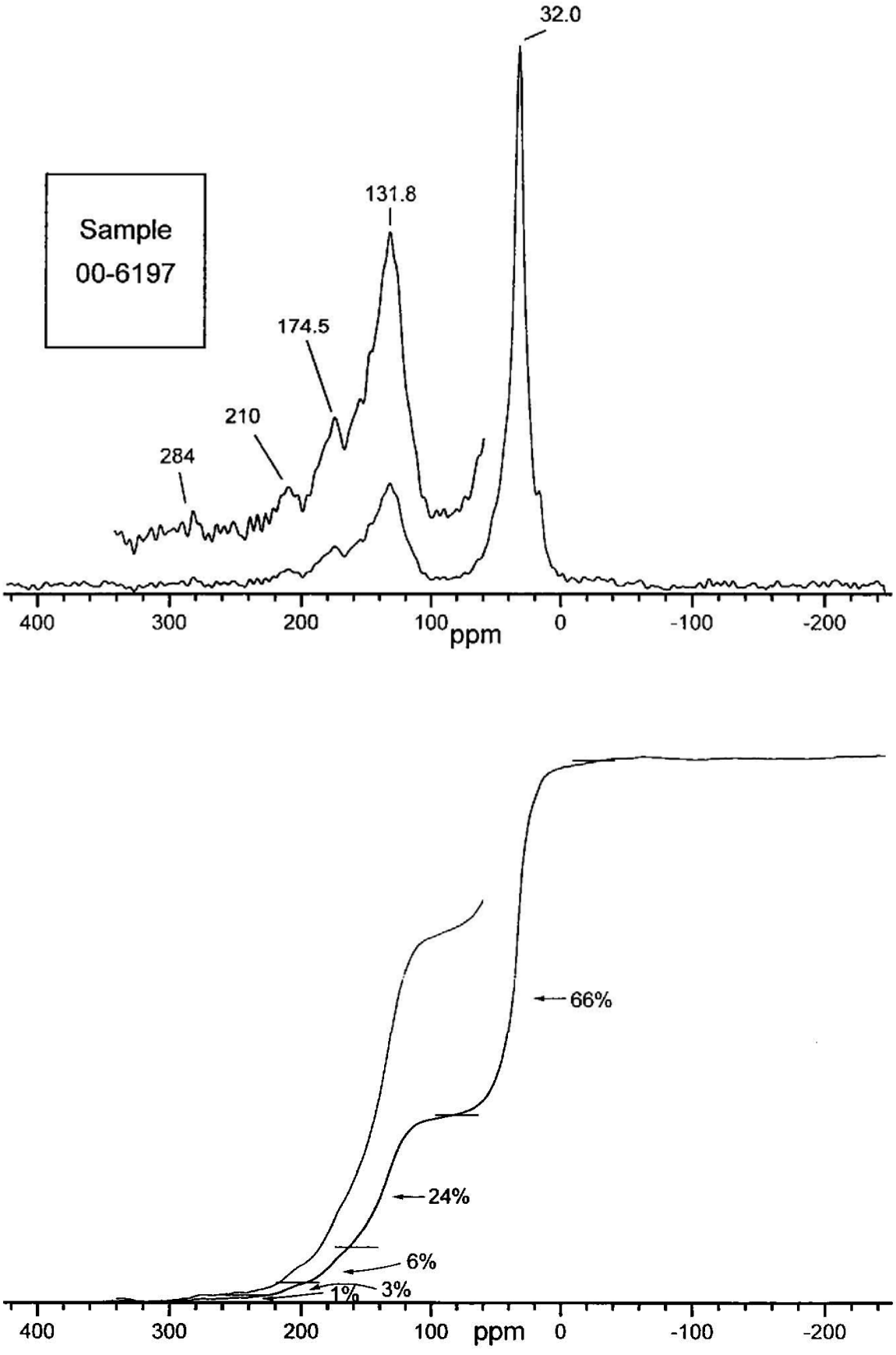

Figure A6.47 ^{13}C NMR spectrum and integrated intensities for sample 00-6198

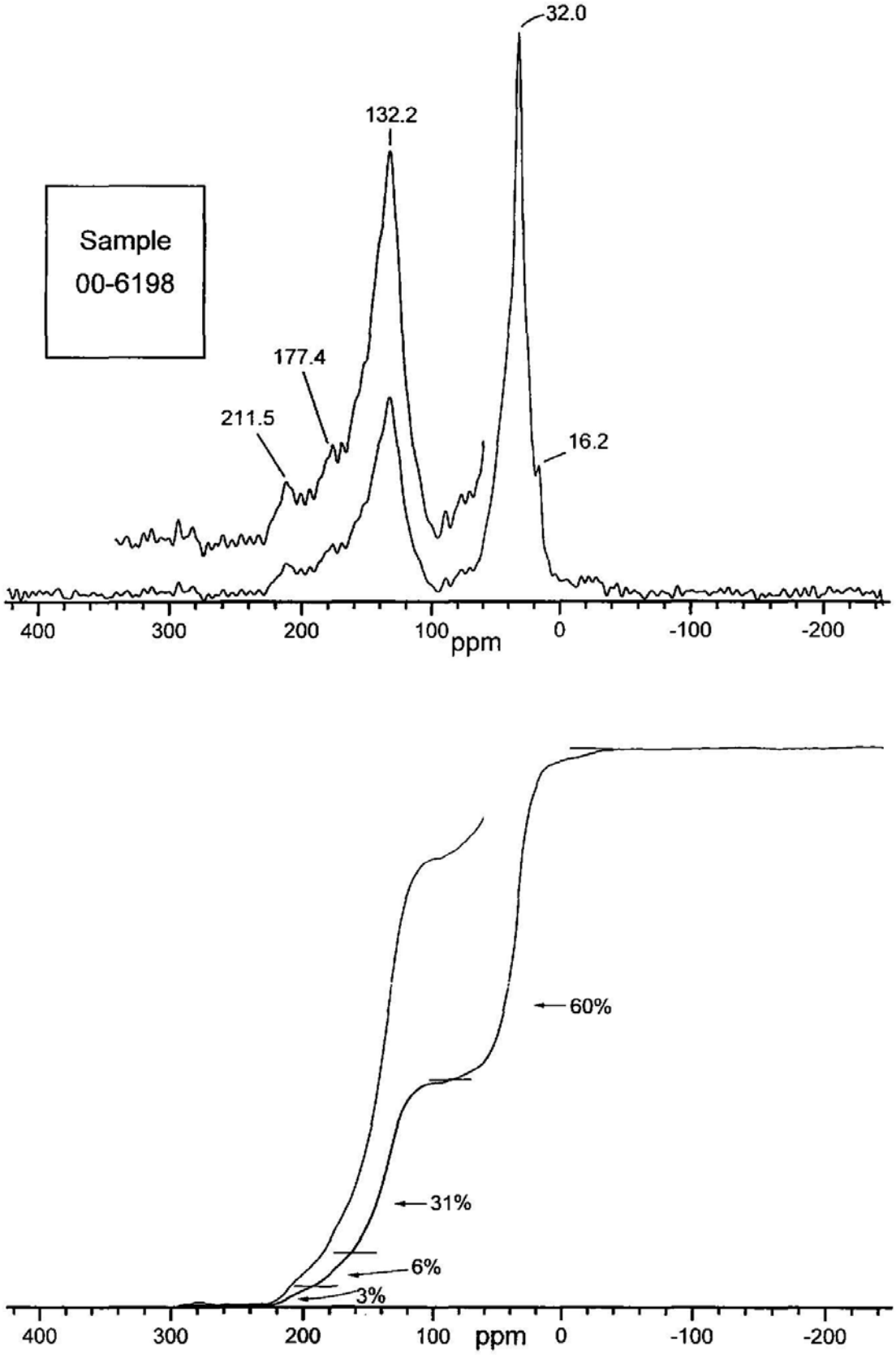

Figure A6.48 ^{13}C NMR spectrum and integrated intensities for sample 00-6199

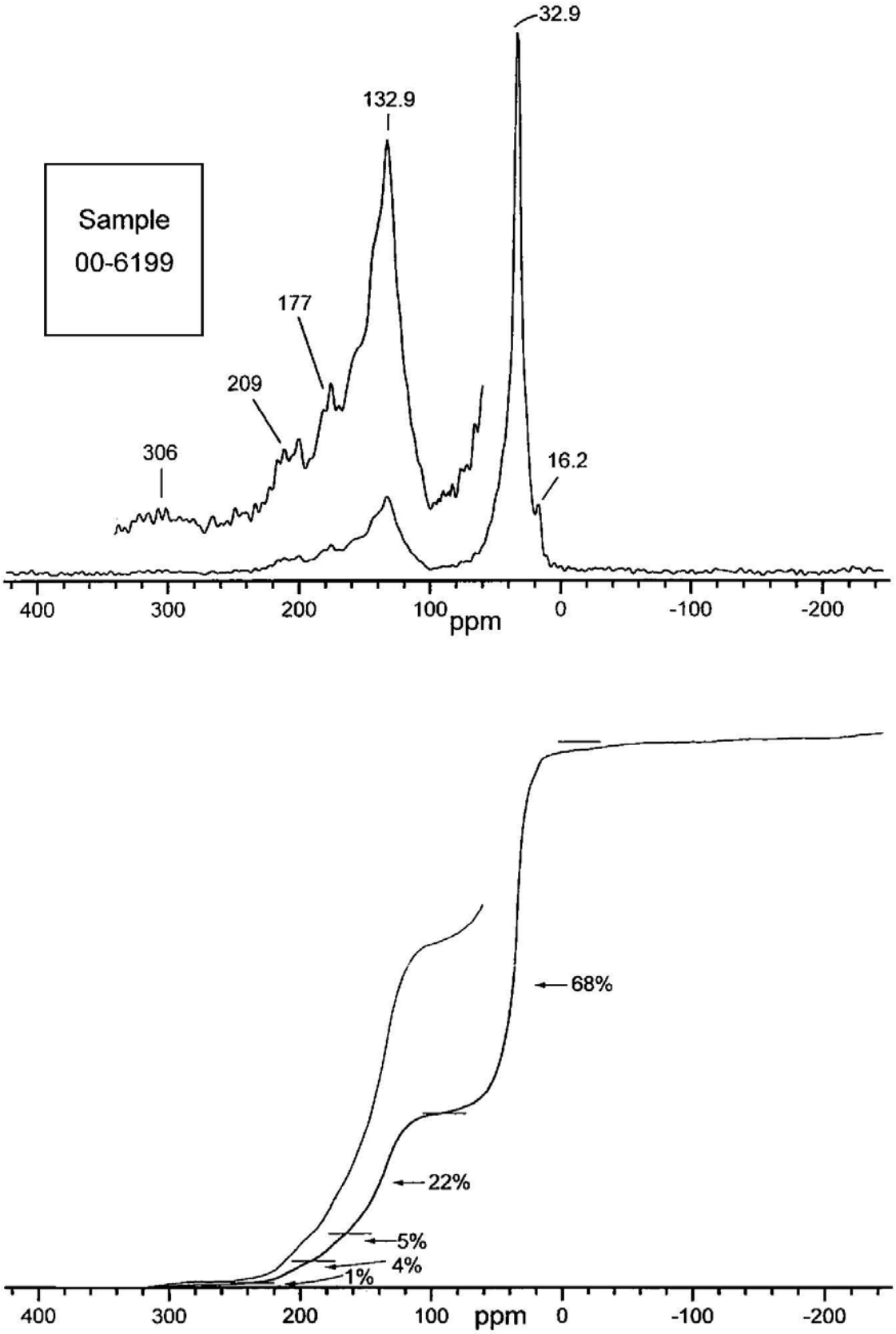

Figure A6.49 ^{13}C NMR spectrum and integrated intensities for sample 00-6210

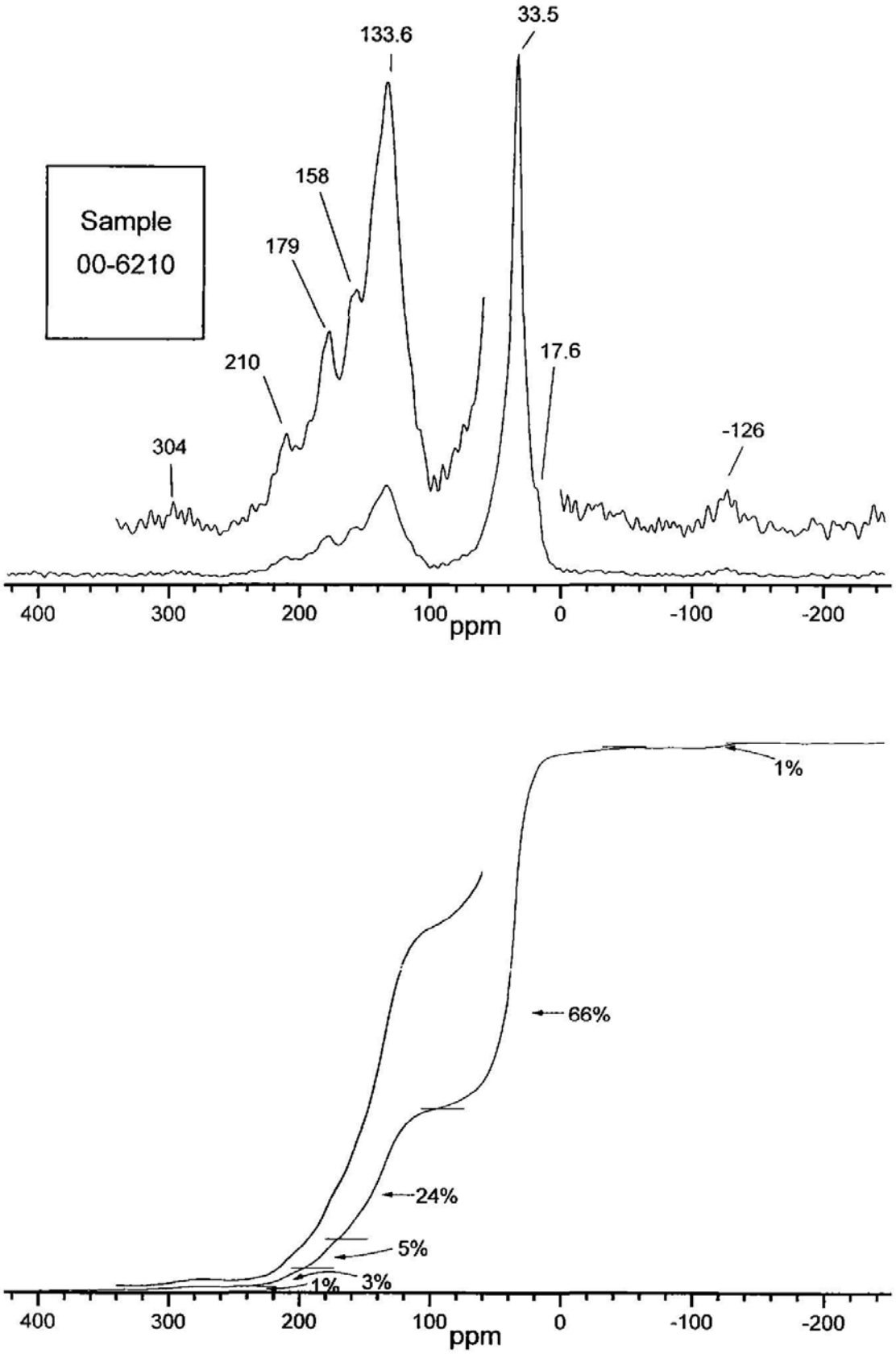

Figure A6.50 ^{13}C NMR spectrum and integrated intensities for sample 00-6211

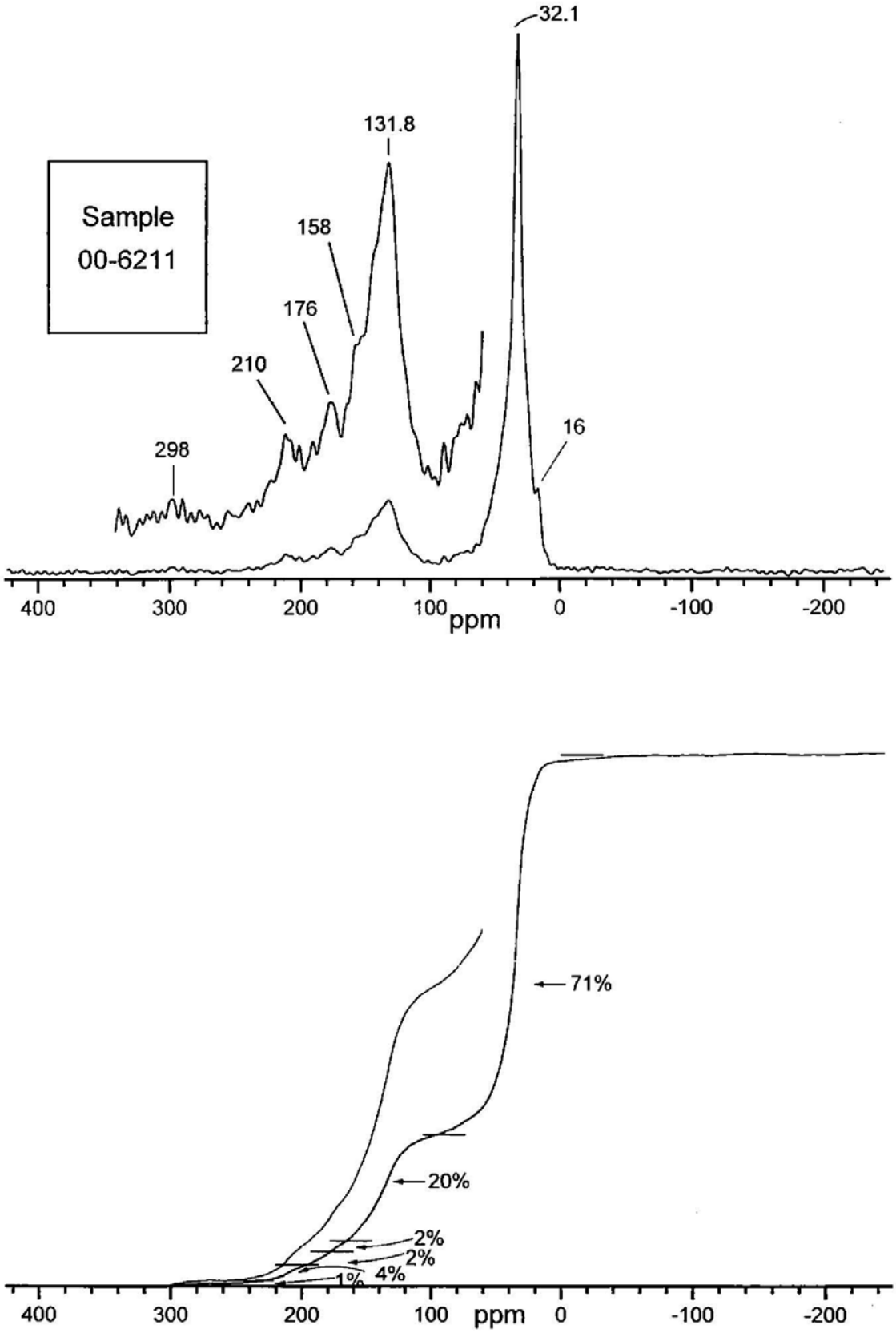

Figure A6.51 ^{13}C NMR spectrum and integrated intensities for sample 00-6212

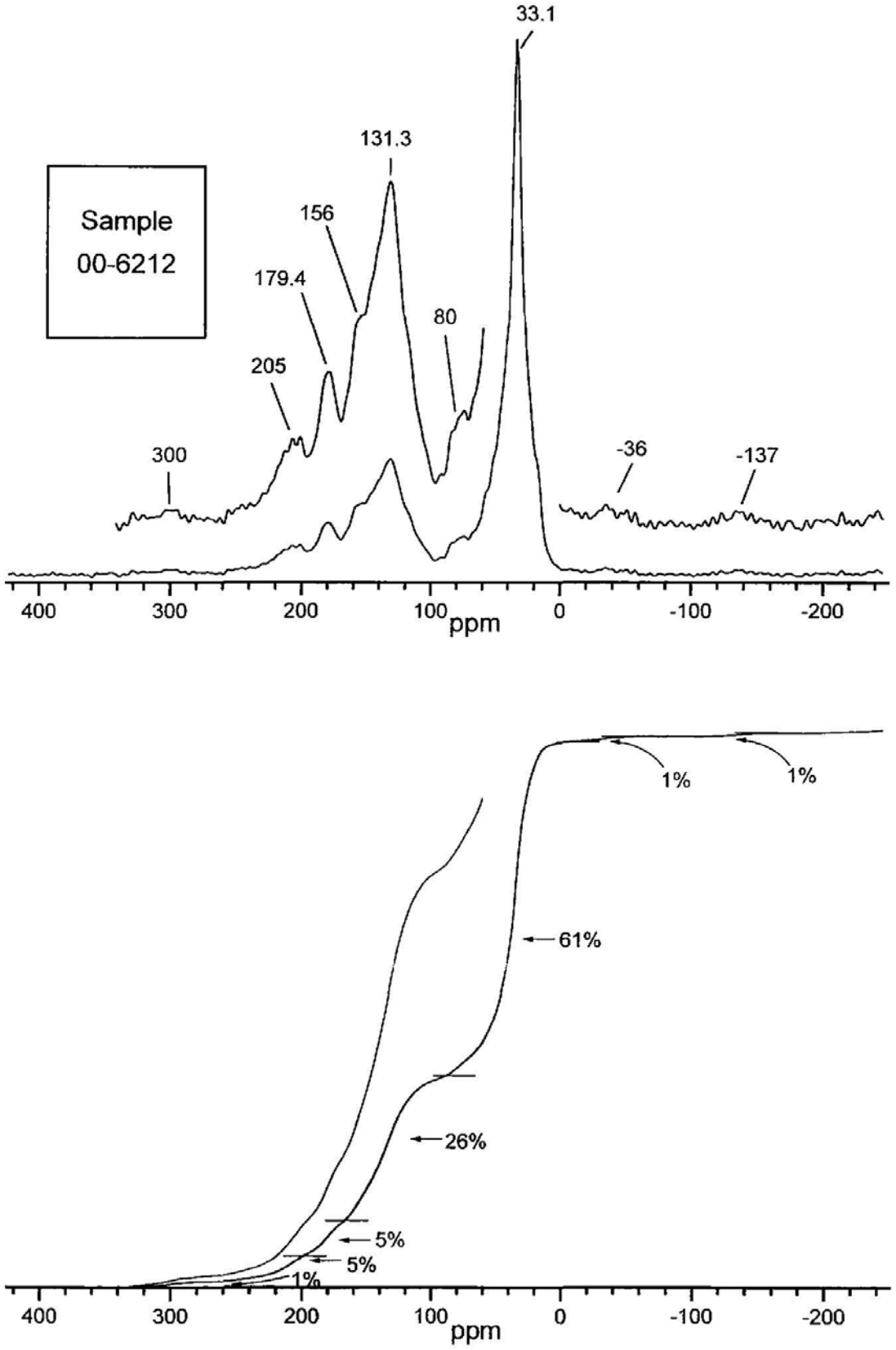

Figure A6.52 ^{13}C NMR spectrum and integrated intensities for sample 00-6213

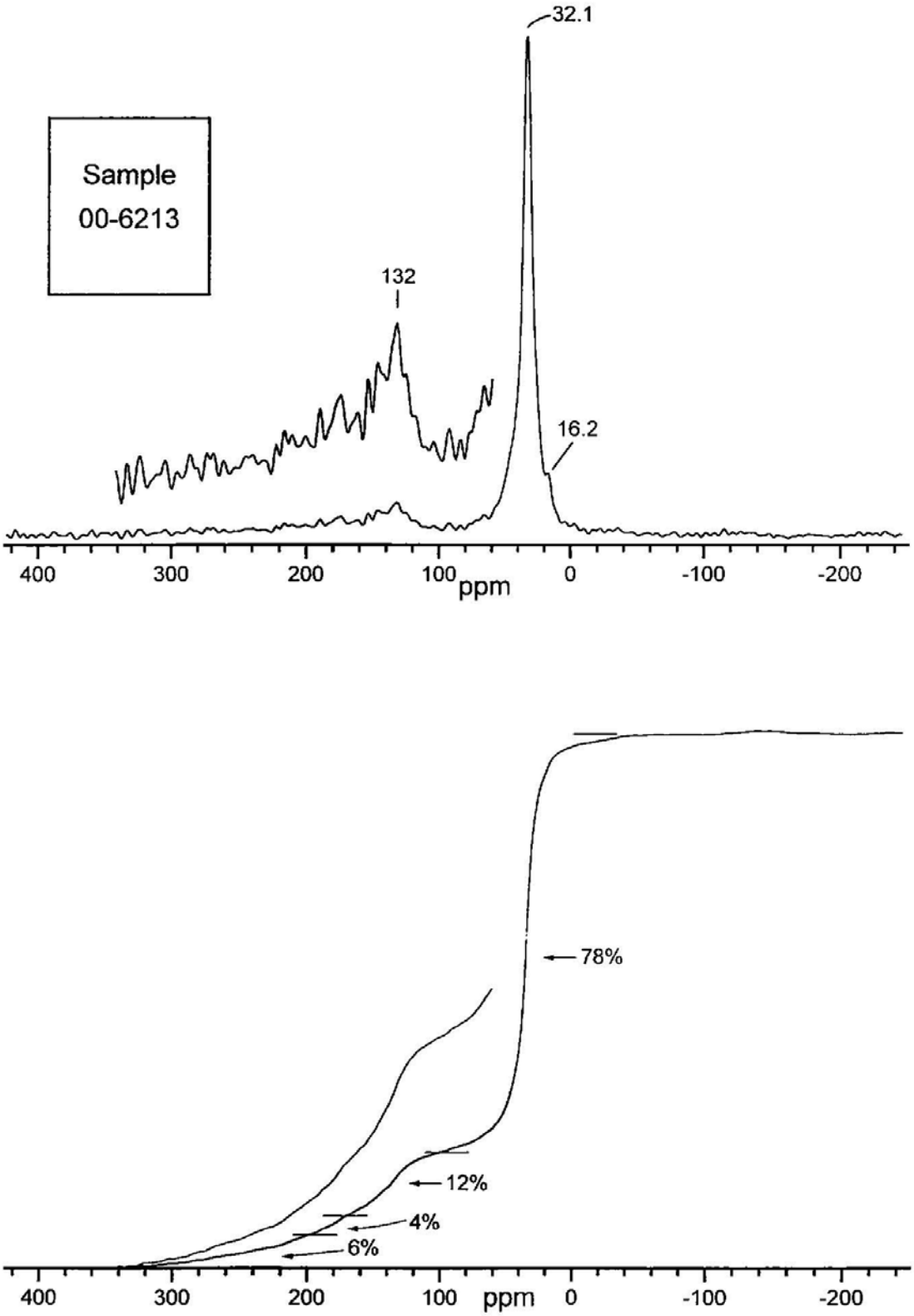

Figure A6.53 Distribution of LOI for the Ambassador deposit, Mulga Rock

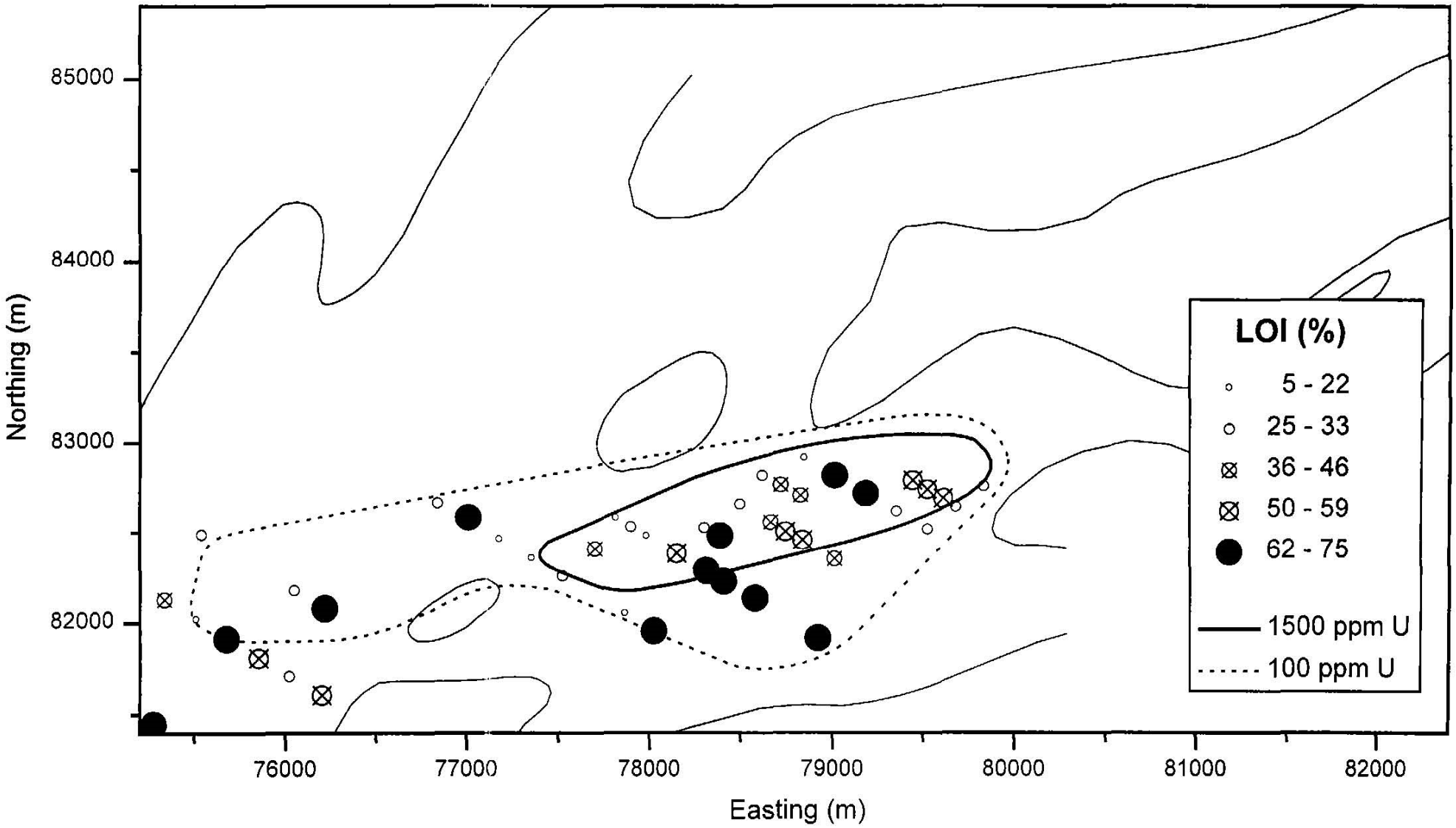

Figure A6.54 Distribution of U for the Ambassador deposit, Mulga Rock

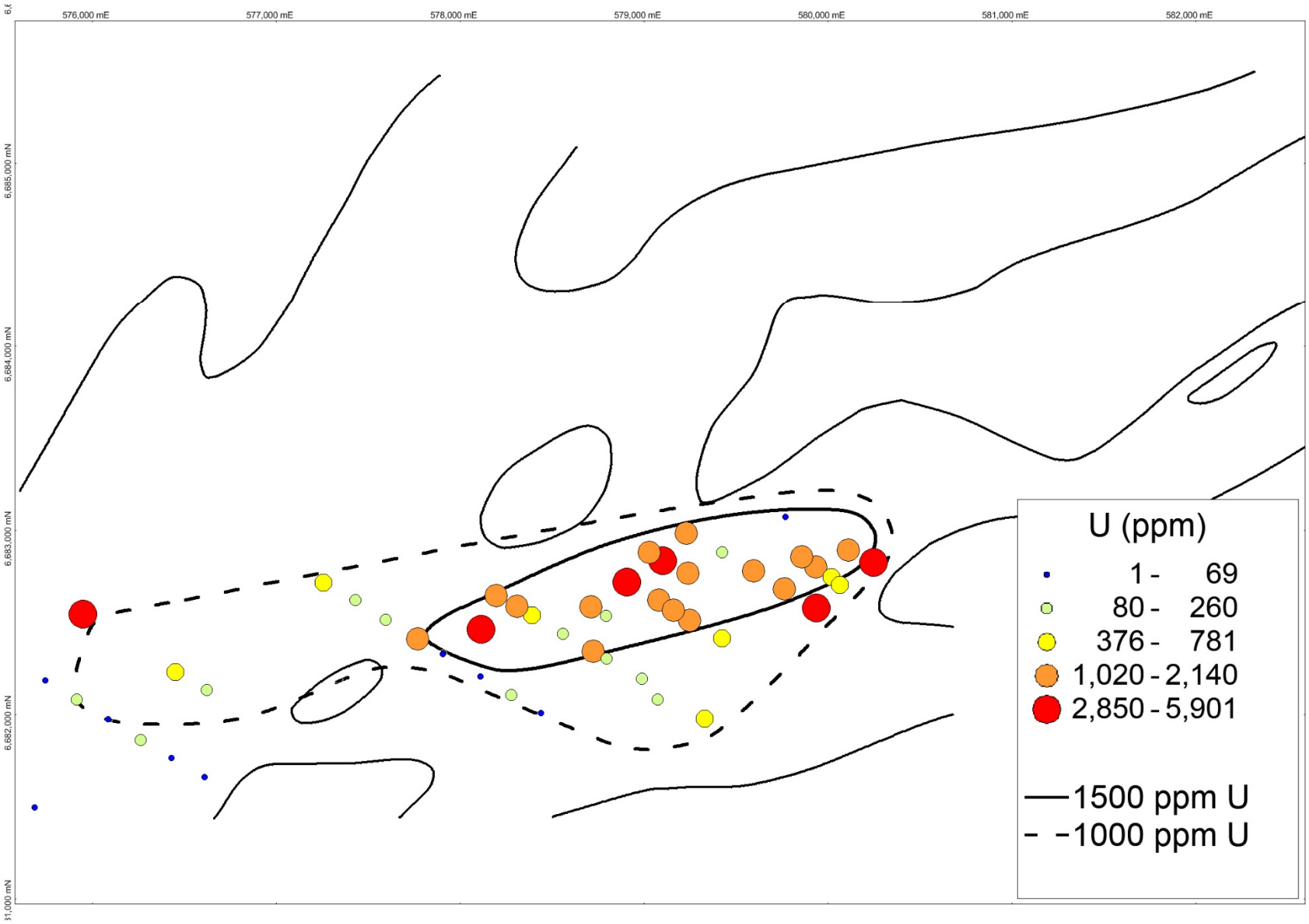

Figure A6.55 Distribution of aliphatic C in Organic matter for the Ambassador deposit, Mulga Rock

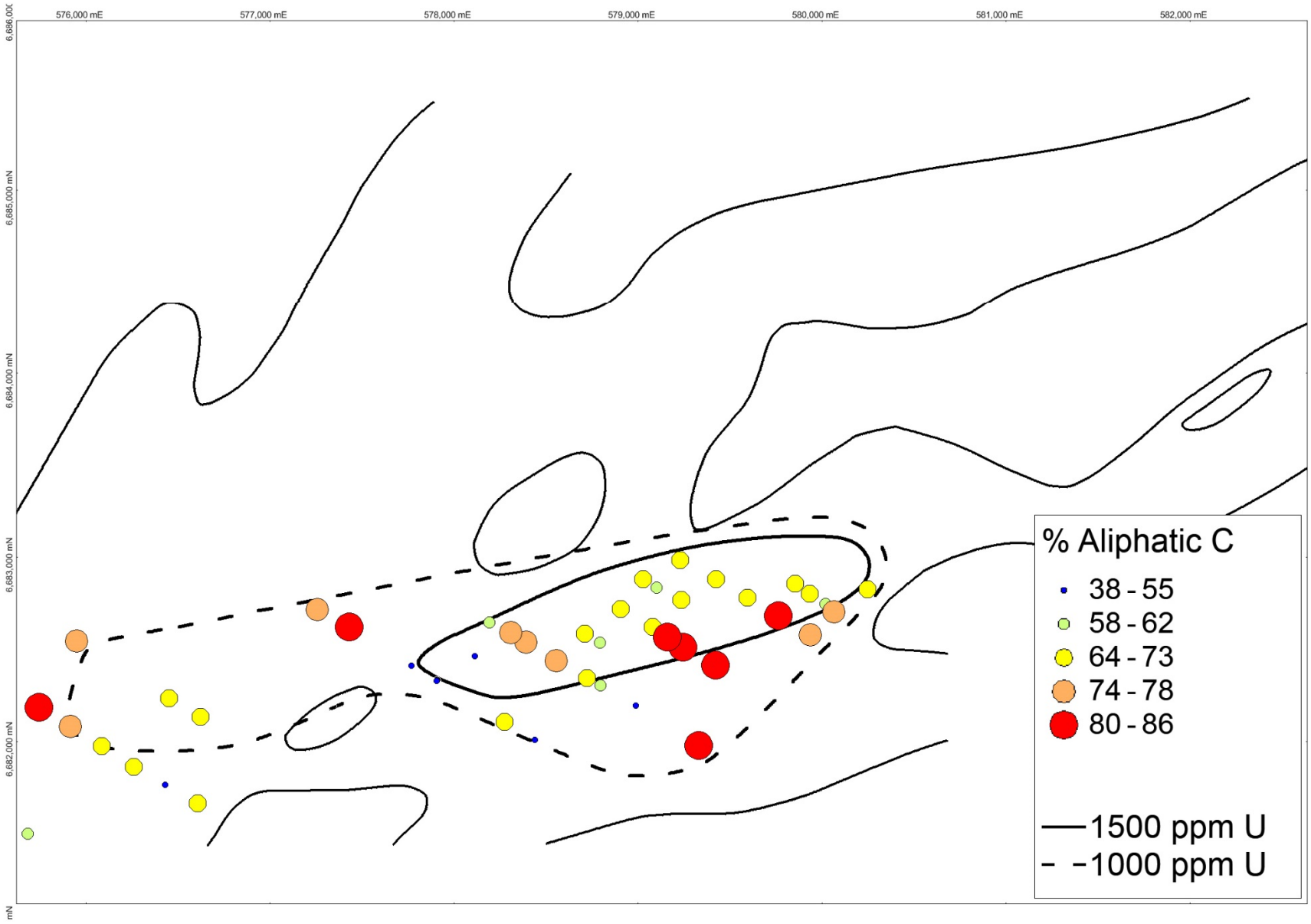

Figure A6.56 Distribution of the Aliphatic Peak Position for the Ambassador deposit, Mulga Rock

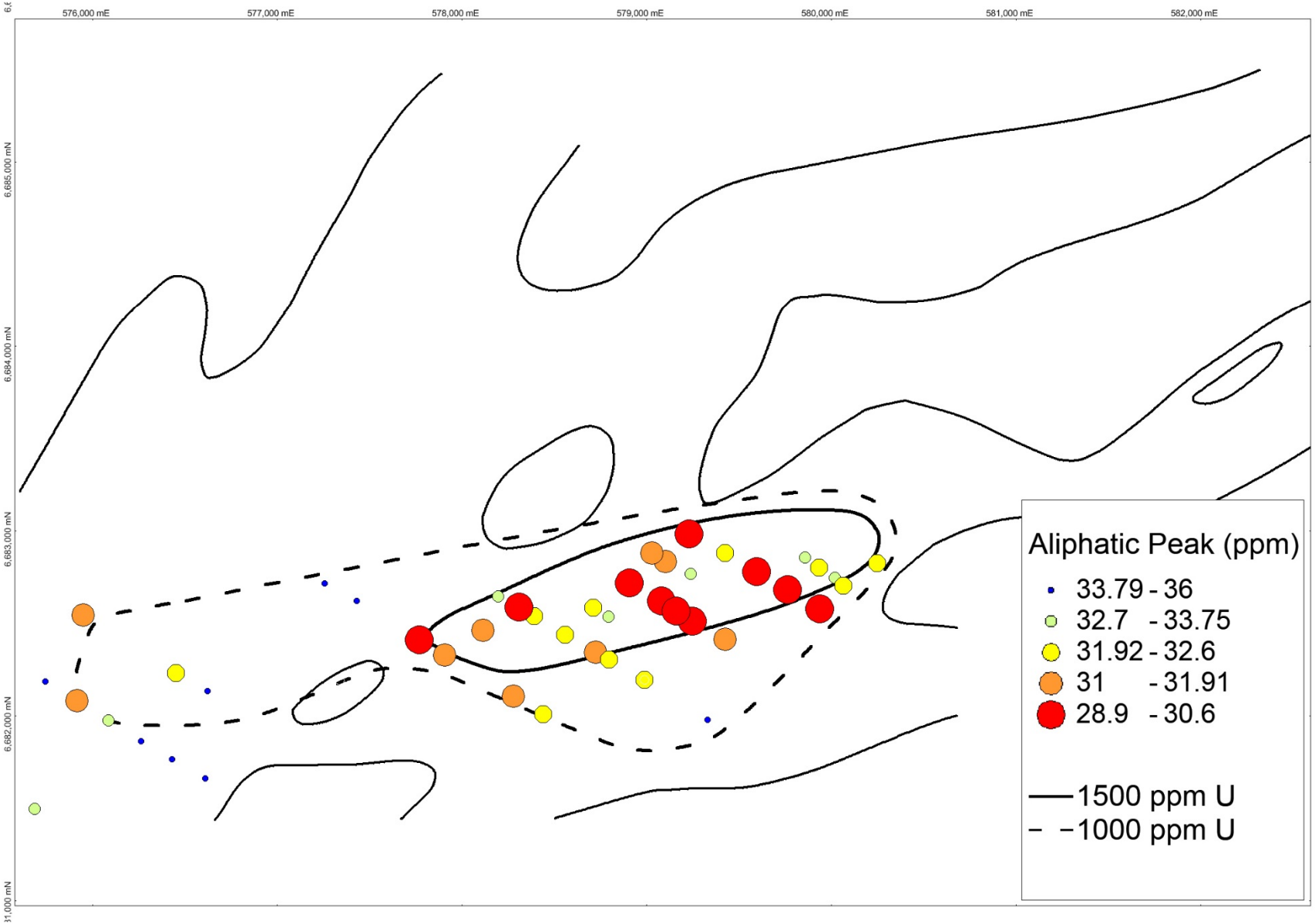

Figure A6.57 Distribution of Aromatic content for the Ambassador deposit, Mulga Rock

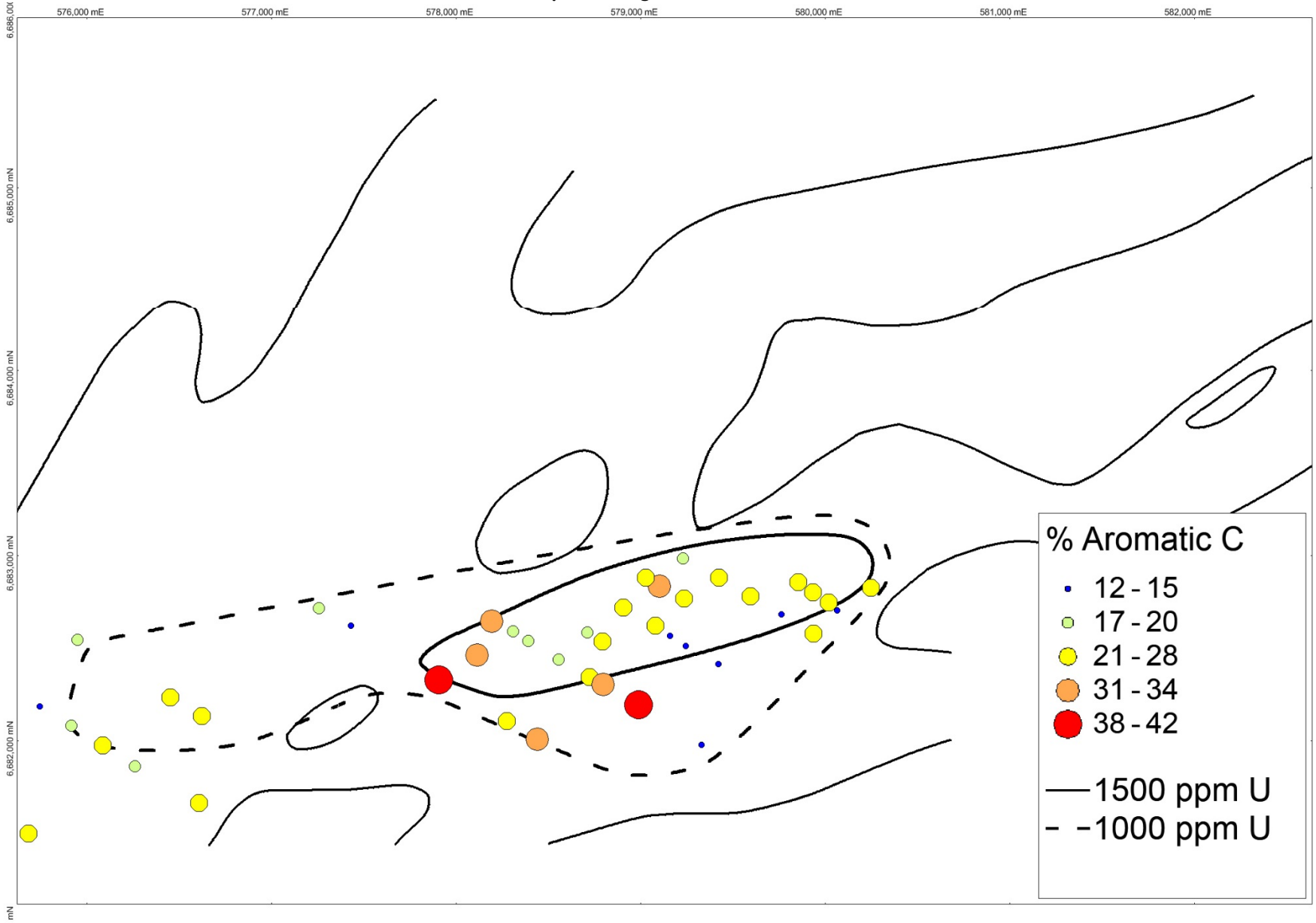

Figure A6.58 Distribution of the Aromatic Peak Position for the Ambassador deposit, Mulga Rock

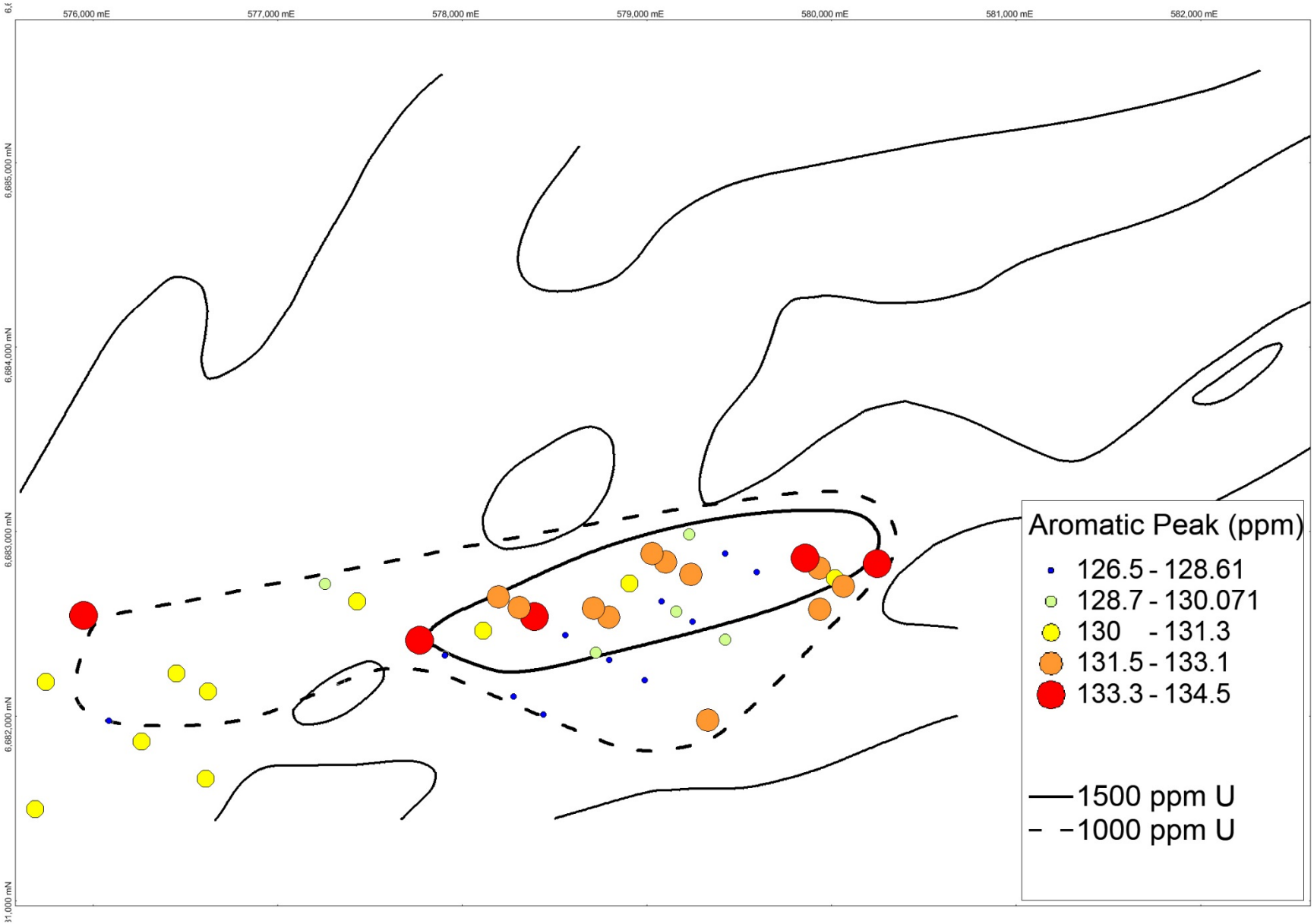

Figure A6.59 Distribution of carboxylic +carbonyl content for the Ambassador deposit, Mulga Rock

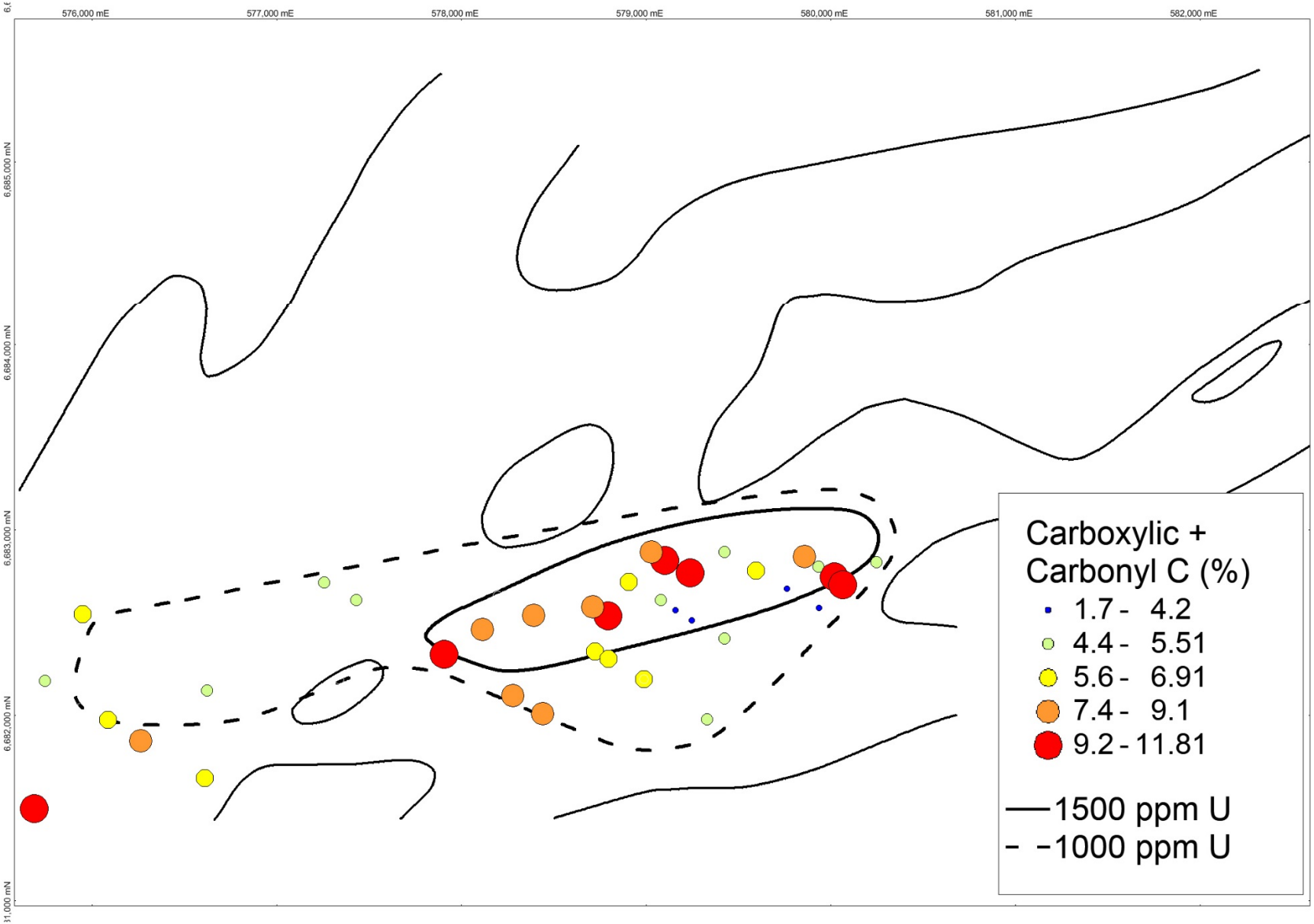

Figure A6.60 Distribution of %C in organic matter for the Ambassador deposit, Mulga Rock

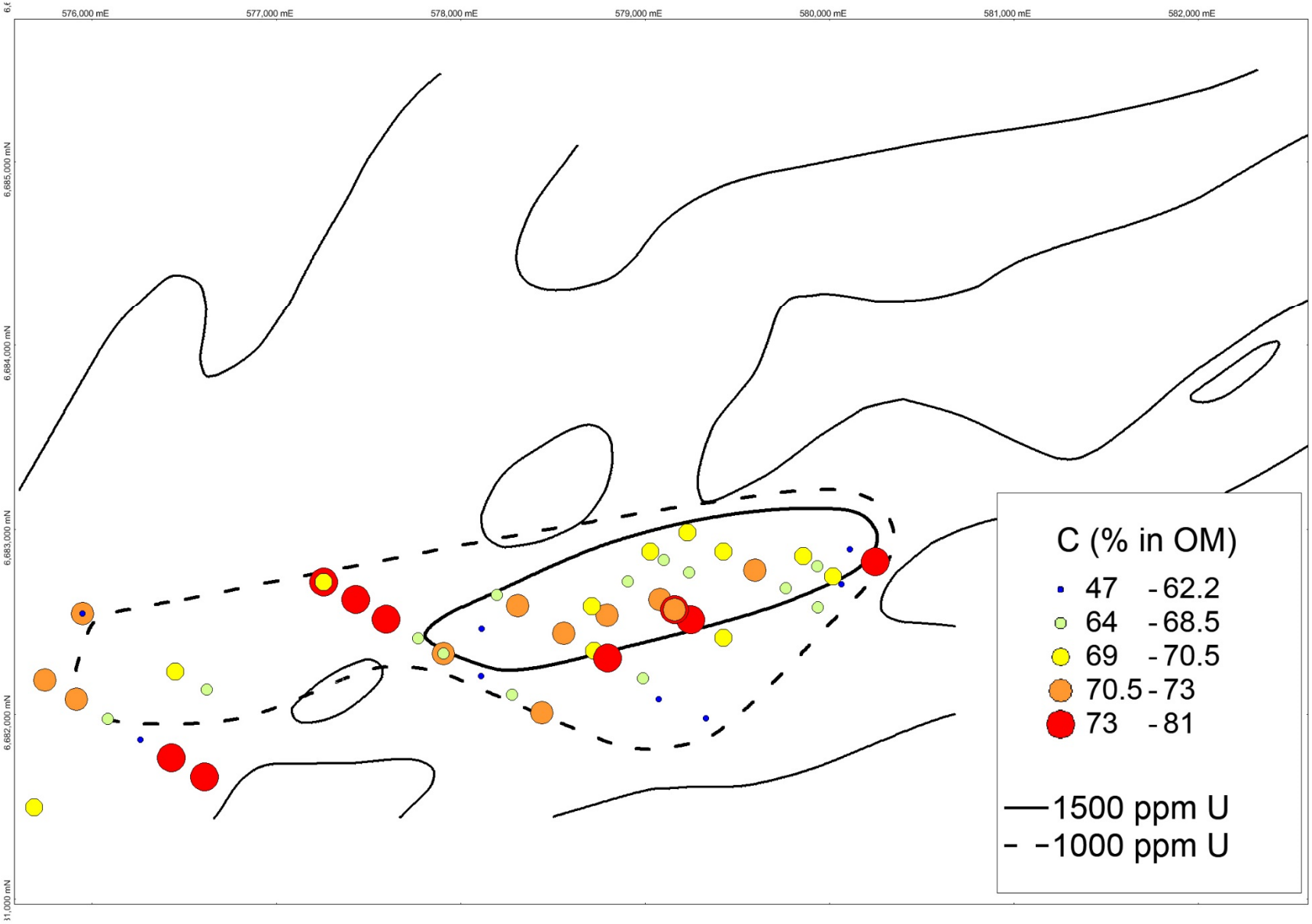

Figure A6.61 Distribution of Atomic H/C in organic matter for the Ambassador deposit, Mulga Rock

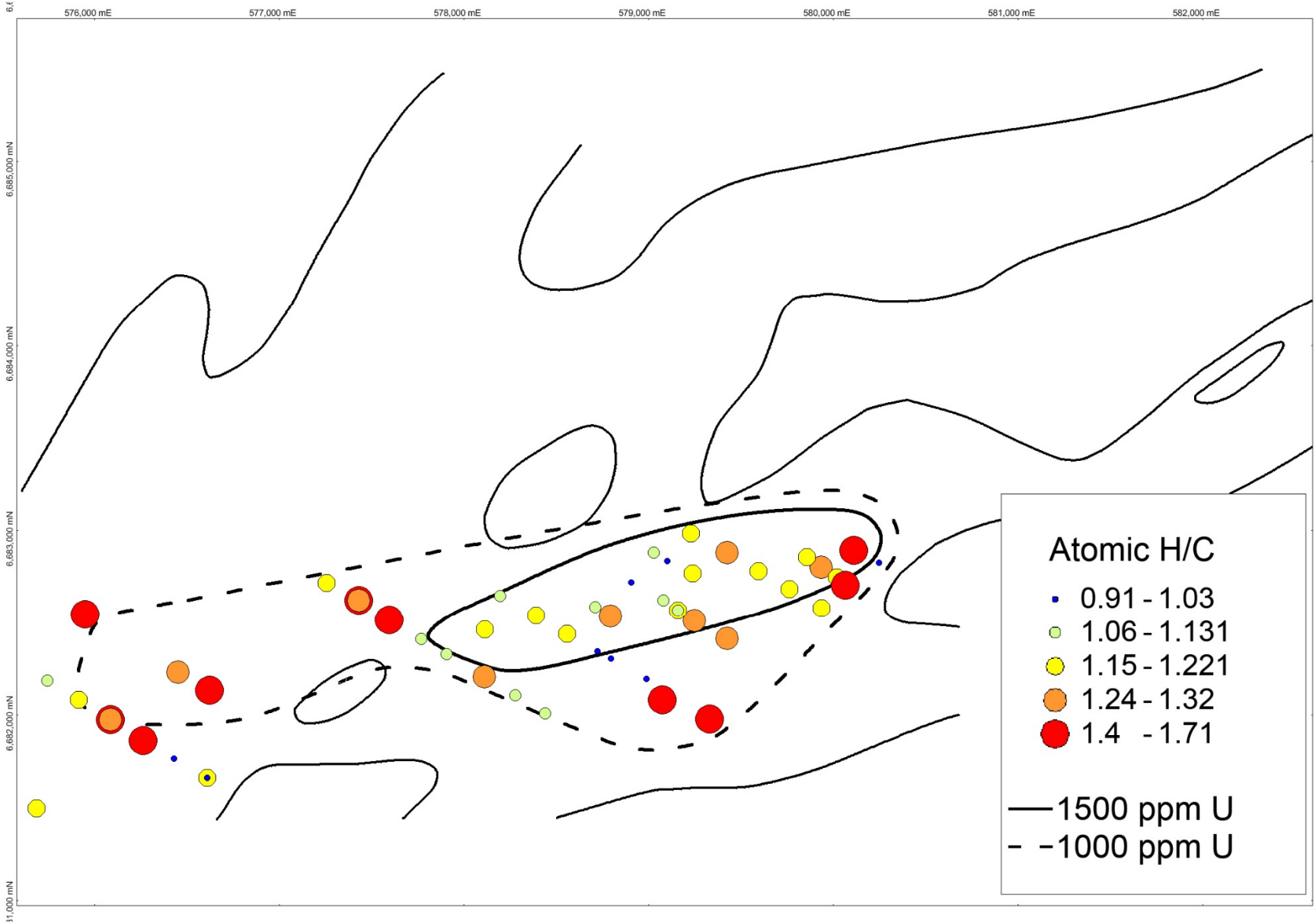

Figure A6.62 Distribution of Atomic O/C in organic matter for the Ambassador deposit, Mulga Rock

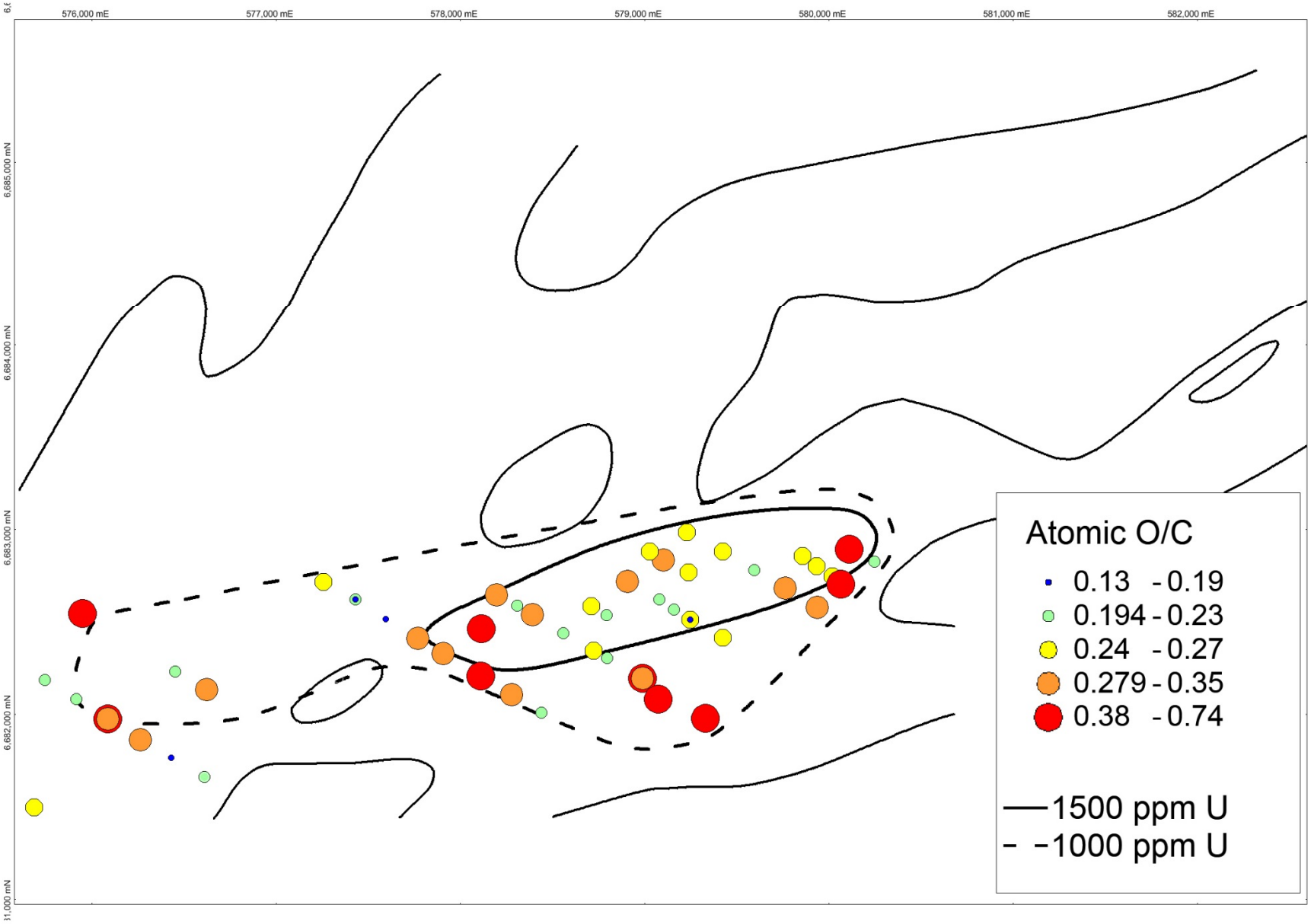

Figure A6.63 Distribution of Atomic N/C for the Ambassador deposit, Mulga Rock

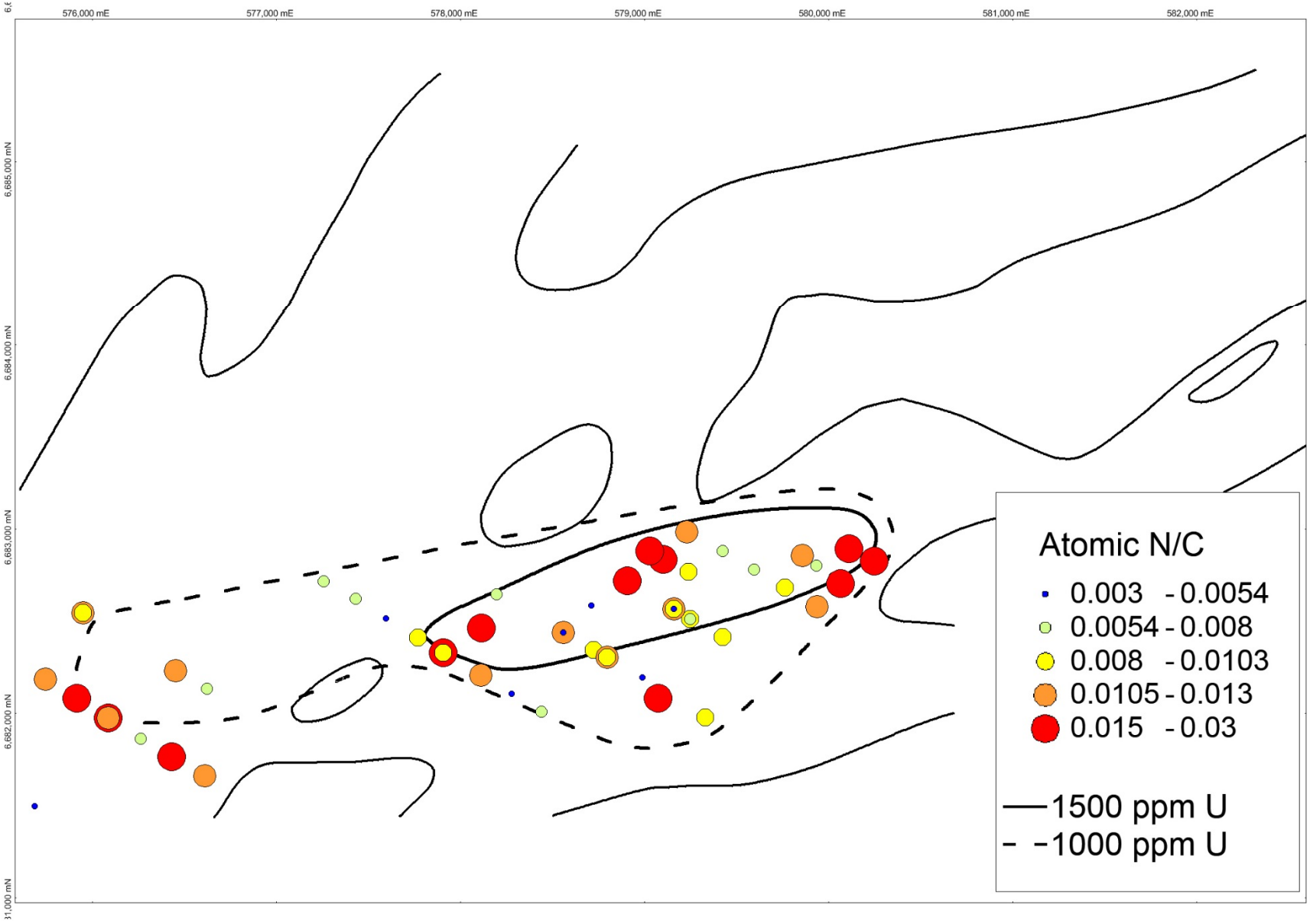

Figure A6.64 **Distribution of calculated vitrinite concentration for the Ambassador deposit, Mulga Rock**

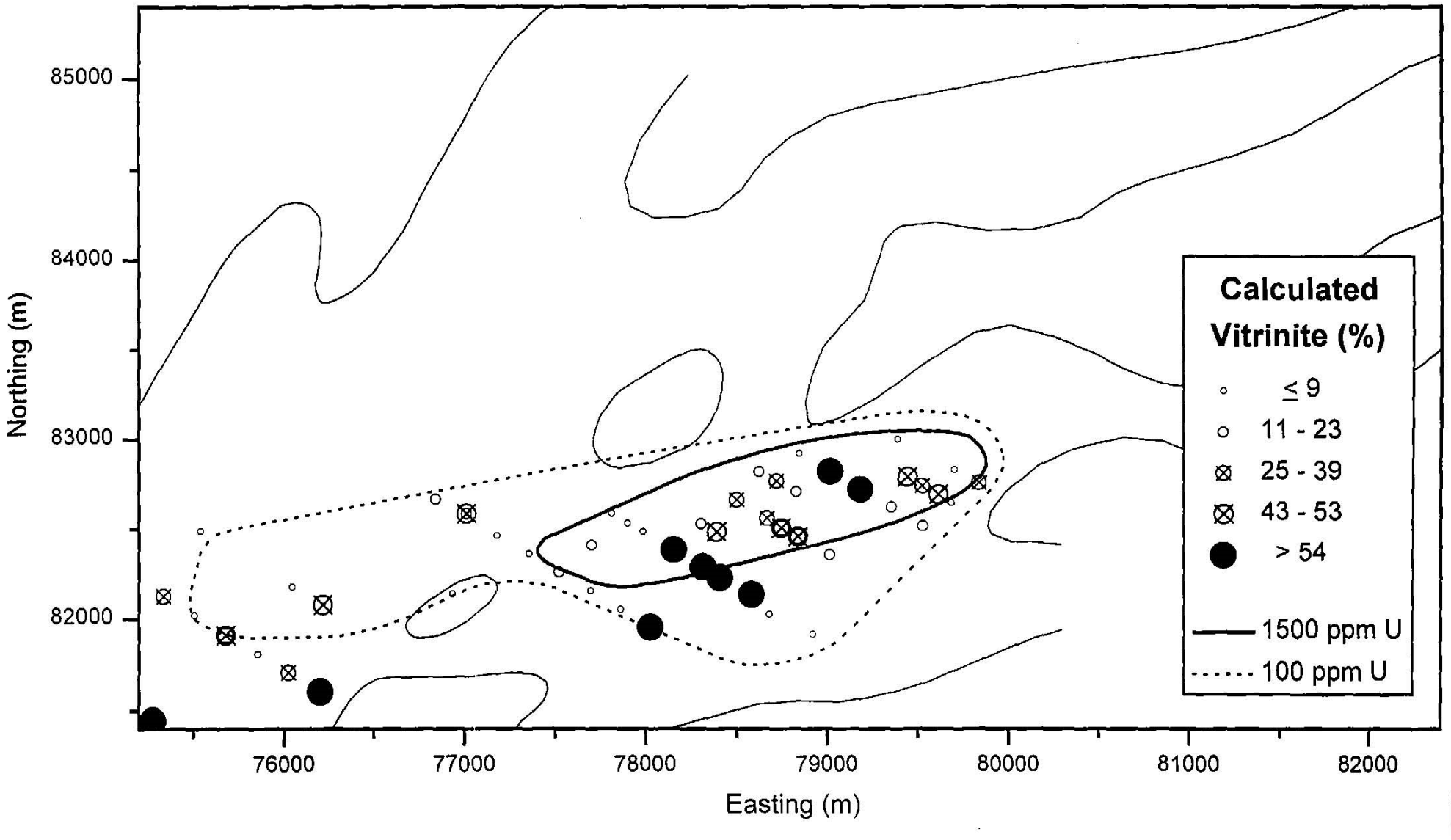

Figure A6.65 **Distribution of calculated mineral/organic matter concentration for the Ambassador deposit, Mulga Rock**

